Ice-related environmental changes in Arctic fjords : new insights from benthic foraminifera

Eleonora Fossile

DOCTORAT SCIENCES BRETAGNE DE LA MER LOIRE ET DU LITTORAL

université angers

THESE DE DOCTORAT DE

L'UNIVERSITE D'ANGERS

ECOLE DOCTORALE N° 598
Sciences de la Mer et du littoral
Spécialité : Ecologie Marine

Par

Eleonora FOSSILE

Ice-related environmental changes in Arctic fjords: new insights from benthic foraminifera

Thèse présentée et soutenue à Angers, le 4 mai 2022
Unité de recherche : LPG UMR CNRS 6112 - Université d'Angers

Rapporteurs avant soutenance :

Jacques GIRAUDEAU	Directeur de Recherche CNRS, Université de Bordeaux
Marit-Solveig SEIDENKRANTZ	Professeure, Aarhus University

Composition du Jury :

Examinateurs :

Elisabeth ALVE	Professeure, University of Oslo
Morten HALD	Professeur, The Arctic University of Norway

Dir. de thèse :

Hélène HOWA	Professeure, Université d'Angers

Co-dir. de thèse :

Meryem MOJTAHID	Maîtresse de Conférence, Université d'Angers

Co-encadrante de thèse :

Maria Pia NARDELLI	Maîtresse de Conférence, Université d'Angers

Invité(s) :

Bruno LANSARD	Maître de Conférence, Université de Versailles Saint-Quentin-en-Yvelines
Caterina MORIGI	Professeure associée, University of Pisa

Ice-related environmental changes in Arctic fjords: new insights from benthic foraminifera

Grazie ❄ Merci ❄ Thanks

Un grand merci va à Hélène, Meryem et Pia. C'est grâce à vous que j'ai eu l'opportunité de faire cette expérience de thèse et de vie inoubliable, qui m'a marqué profondément comme personne et que je porterai avec moi pour toute ma vie. Je vous remercie pour avoir vu du potentiel en moi et pour m'avoir choisi pour porter ce projet de recherche. Merci pour votre encadrement, vous m'avez conseillé, guidé, supporté, encouragé, professionnellement, mais pas que. Merci pour m'avoir laissé choisir mon chemin en autonomie et avoir toujours encouragé mes idées. Vous êtes des encadrantes formidables, sur lesquelles j'ai toujours pu compter et de ma part j'espère d'avoir été une bonne étudiante à la hauteur de vos attentes. Grazie Pia per la tua accoglienza e gentilezza. Grazie per avermi aiutata al mio arrivo in Francia, sei stata sempre disponibile e pronta ad aiutarmi nei momenti di difficoltà. Grazie per aver creduto in me fin dall'inizio. Merci Meryem pour ton optimisme et ta capacité de voir toujours du positif dans les choses. Merci Hélène pour être parfois sévère mais toujours juste, un grand merci pour m'avoir poussé à donner le meilleur de moi-même pendent toutes ces 3 années, merci d'avoir été présent jusqu'à la fin.

Thanks to all the members of the jury, who kindly accepted to be part of it. A particular thanks goes to the two reviewers Jacques Giraudeau and Marit-Solveig Seidenkrantz who accepted to read and evaluate this (too much long) thesis. Thanks to the two examiners Elisabeth Alve and Morten Hald. Thanks to the two invited members Bruno Lansard and Caterina Morigi, who I want to thank also for precious advices during our CSI meetings.

I also would like to thank Katrine Husum, for your kindness and interesting scientific discussions during my stay in Tromsø.

Merci à vous tous, le BIAF, une vraie famille pendant la durée de cette thèse. Je me suis senti tout de suite parti de cette équipe unique et spéciale dans laquelle tout le monde est prêt pour s'aider. Merci pour tous les moments de convivialité, des fois à parler de sciences comme de tout le reste, de fois à faire plein de blagues (que tout le monde n'arrive pas à comprendre, mais Edouard, Julien et moi on s'est toujours bien compris !). J'ai adoré faire cette aventure de thèse avec vous ! Merci à tous les chercheurs du labo pour toutes les looooonge discussions scientifique, merci à Christine (merci pour notre super aventure IMPEC ainsi que tous les moments à rigoler ensemble !), Edouard (merci pour les matchs de volley ensemble et encore tes super blagues !), Aurélia, Frans, Magalie, Erica, Manue, Fabrice, et Grégoire. Merci à toute l'équipe technique Éric, Sophie Q., Sophie S. pour avoir été toujours prêts à m'aider quand j'en avais besoins. Merci également à Luzia e Sophie V. pour m'avoir aidé à traiter avec la bureaucratie française !

Merci aux vieux thésards qui m'ont accueilli à bras ouverts, pour vos conseils sur comment affronter ou mieux, survivre à une thèse ! Merci Constance, Julien, Briz et JB. Merci à tous les thésards qui sont arrivés au cours de mon aventure, à Marie, Pauline, Corentin, et ceux qui

sont arrivés quand j'étais presque à la fin, Maxime, Nour et Mohamed. Merci aussi à Serena, Juliette et Anaëlle qui m'ont aidé pendent leurs stages et merci à Fatima. Merci aux jeunes docteurs qui sont toujours de bons conseils, Aurélie, David, Vivien, Julia, Inge, Sandrine, Christiane, et Yohann. Merci à vous tous pour tous les moments de bonheur et convivialité qui nous avons vécu ensemble, merci pour toutes les sorties, les bons et grands repas organisés ensemble !

Un merci spécial à Aurélie, Constance, Julia, et Marie, à nos soirée-filles, à nos moments et weekends passés ensemble. Merci pour votre gentillesse, sincérité, altruisme. Merci pour être venue jusqu'en Italie pour mon mariage. Je suis ravie de vous avoir dans ma vie. Marie, tu as pris un poste spécial dans mon cœur, je ne sais pas par où commencer. Merci pour tous les trajets à vélo ensemble, merci pour m'avoir fait découvrir la couture (ce n'est jamais trop tard), pour avoir été toujours à mon côté pendent la thèse, merci pour m'avoir soutenue dans les moments difficiles. Merci pour ta générosité, tous les cadeaux fait à la main, les repas préparés quand je rentrais de longs voyages. Merci pour les weekends passés à bricoler-coudre-manger ensemble. Merci pour tous les restos et toutes les soirées à l'escalade avec Chris (que je remercie pour ses super blagues, nous oui on se comprends vraiment !) et Mattia. Merci pour les journées spéciales passé avec nous en Italie. Je porterai tous ces beaux souvenirs avec moi, dans mon cœur.

Ringrazio i miei amici di sempre, per aver sempre creduto in me e per avermi sempre detto che quello che facevo era meraviglioso. Un grazie speciale alla mia Martina, anche se i nostri percorsi ci hanno portato lontane fisicamente, noi ci saremo sempre l'una per l'altra. Coraggio, adesso tocca a te!

Grazie mamma e papà per avermi sempre sostenuto nelle mie scelte anche se spesso controcorrente e che mi hanno portata lontana da casa. Grazie per essere un punto fermo nella mia vita. Grazie per esserci sempre. Grazie alla mia famiglia, grazie per essere sempre entusiasti quando vi racconto di me, delle mie passioni, del mio lavoro.

Grazie al compagno che ho scelto per la vita, mio marito, Mattia. Grazie per aver creduto sempre in me ma soprattutto grazie per avermi insegnato a credere in me. Mi hai insegnato l'importanza del coltivare le mie passioni e ambizioni senza aver paura. Grazie per avermi spinta a inseguire i miei sogni, anche se ciò ci ha portato a vivere lontani. Hai tirato fuori il coraggio che c'era in me, quello che mi serviva per spiccare il volo. Grazie per essere sempre lì al mio fianco pronto ad aiutarmi e grazie perché so che ci sarai per sempre. Grazie per essere riusciti a lavorare l'uno al fianco dell'altra. Entrambi stiamo inseguendo un sogno, e la cosa più incredibile è che abbiamo deciso di percorrere questa strada insieme guardando nella stessa direzione. E lo stiamo facendo come due persone distinte ognuna con le sue passioni ma un obiettivo in comune e il desiderio di condividere con l'altro questo viaggio che si chiama vita. Grazie per i nostri sogni, che sembrano lontani e difficili da realizzare ma che un passo alla volta si stanno concretizzando. Per ora ci hanno portato qui, ma cosa ha in serbo il futuro? Chi lo sa, ma di una cosa sono certa, lo scopriremo insieme!

"From the freedom to explore comes the joy of learning. From knowledge acquired by personal initiative arises the desire for more knowledge. And from mastery of the novel and beautiful world awaiting every child comes self-confidence"

Edward O. Wilson
in *The Creation: An Appeal to Save Life on Earth*

Résume étendu en français de la thèse de doctorat intitulée :

Changements environnementaux liés à la dynamique de la glace dans les fjords de l'Arctique : nouvelles connaissances apportées par les foraminifères benthiques

Le changement climatique menace les régions polaires avec des conséquences majeures sur la dynamique des glaces et les écosystèmes associés. Les simulations de fonte glaciaire reposent sur des reconstitutions paléo-environnementales, qui complètent les mesures directes sur la période actuelle pour réduire l'incertitude des prévisions. L'objectif scientifique principal de cette thèse était d'étudier, de comprendre, et développer des proxies de la dynamique des glaces dans les fjords de l'Arctique, basés sur les communautés de foraminifères benthiques. Plus précisément, les foraminifères benthiques ont été utilisés comme indicateurs pour estimer l'influence des cycles de la glace de mer et de la fonte des glaciers sur les écosystèmes benthiques. Des proxies basés sur l'écologie des foraminifères benthiques ont été développés dans cette thèse pour suivre la dynamique des glaces de mer et le retrait des glaciers côtiers. Cette thèse s'est concentrée sur deux fjords contrastés de l'archipel de Svalbard, en termes de dynamique liée à la glace :

- **Storfjorden :** un fjord affecté par la production et le plongement de saumure (i.e., des eaux froides, salées et corrosives) pendant les phases de production de glace de mer saisonnière. A certains endroits du fjord, ces eaux enrichies en saumure persistent toute l'année dans les eaux de fond. Ce fjord est présenté dans les Chapitres 1 et 2;
- **Kongsfjorden :** un fjord affecté par les rejets massifs d'eau douce et de sédiments des glaciers côtiers (i.e., producteur d'iceberg) pendant la saison estivale. Ce fjord est le sujet des Chapitres 3, 4 et 5.

Les objectifs de cette thèse ont été abordés à travers cinq chapitres dont les principaux résultats sont décrits dans le texte ci-dessous.

Chapitre 1 : Les foraminifères benthiques comme traceurs de la production de saumure dans "l'usine de glace de mer" du Storfjorden

En juillet 2016, la mission océanographique STeP (Storfjorden Polynya Multidisciplinary Study) a été organisée dans le plus grand fjord du Svalbard, Storfjorden, autrement appelé " fabrique de glace de mer ". Le Storfjorden est caractérisé par la formation récurrente d'une polynie à chaleur latente contribuant à la formation d'eau dense dans la région arctique. Une polynie à chaleur latente c'est une zone côtière qui, malgré la production continue de nouvelle

glace (i.e., frazil) en hiver, est maintenue libre de glace de mer (i.e., banquise) grâce à de vents très forts et froids ; cela détermine par conséquence une intense production de saumures, eaux très denses dû à leur très basse température et très haute salinité. Le Chapitre 1 de cette thèse analyse les réponses des foraminifères vivants aux variations de plusieurs paramètres environnementaux (e.g., les caractéristiques des sédiments, la quantité et la qualité de la matière organique, profils d'oxygène et pH des sédiments de surface), afin de comprendre si et comment leur distribution le long du fjord est affectée par les saumures, et de suggérer un proxy témoignant de la production de saumure.

Pour atteindre cet objectif, les sédiments de sept stations ont été échantillonnées le long d'un transect N-S suivant la topographie du Storfjorden : *(i)* trois stations ont été placées dans la zone intérieure du fjord, près des eaux de la polynie, libres de glace, et probablement affectées de façon intermittente par les saumures, *(ii)* deux stations dans les bassins profonds, où les saumures sont piégées et persistent toute l'année, *(iii)* une station au sommet du seuil sous-marin, influencée par le débordement des saumures pendant la saison de production de la glace de mer et *(iv)* la dernière dans la zone extérieure du fjord, potentiellement touchée de façon épisodique par les saumures sortant du fjord.

Les résultats de nos analyses montrent que les foraminifères benthiques vivants échantillonnés pendant la saison estivale se répartissent en trois biozones. Dans la zone " fjord interne ", des espèces calcaires typiques des zones proximales des têtes des fjords en Arctique (i.e., *Cassidulina reniforme* et *Elphidium clavatum*) dominent les assemblages des sédiments de surface, et sont accompagnées par *Nonionellina labradorica*, qui occupe surtout l'habitat endofaunique (i.e. dans le sédiment, sous la surface). Ces espèces ne montrent pas de marque de dissolution sévère, qui aurait pu indiquer l'influence des eaux corrosives des saumures. La présence de juvéniles de ces trois espèces, prouvent des événements reproductifs récents. Les abondances de *C. reniforme* et *E. clavatum* semblent être la réponse opportuniste à des apports de matière organique fraîche, provenant de la prolifération d'algues en été, dont de fortes concentrations ont été mesurées dans cette zone. L'abondance de l'espèce *N. labradorica*, connue pour se nourrir principalement de phytodétritus, étaye cette hypothèse. Cette dernière espèce est particulièrement dominante dans le micro-habitat intermédiaire, peut-être en raison d'une compétition réduite par l'utilisation de différentes voies métaboliques (e.g., l'assimilation de N et S).

La zone "fjord extérieur" est caractérisée par la cohabitation d'espèces polaires, typiques des milieux arctiques, avec des espèces typiques des zones atlantiques (i.e., *Melonis barleeanus*,

Globobulimina auriculata), favorisées par l'intrusion occasionnelle des masses d'eau Atlantique dans le Storfjordrenna.

Entre ces deux zones, la zone " bassins profonds et seuil sous-marin " est principalement caractérisée par des taxons agglutinés typiques de la partie distale des fjords (i.e., *Reophax scorpiurus*, *Reophax fusiformis*, *Recurvoides turbinatus* et *Spiroplectammina biformis*), probablement plus tolérants à une large gamme de conditions, et probablement plus compétitifs lorsque de la matière organique présente est plutôt réfractaire. Sur le seuil sous-marin, l'assemblage est similaire à celui des bassins profonds, bien que des espèces supplémentaires, telles que *Adercotryma glomeratum* et *Textularia torquata*, présentent des abondances relativement importantes, très probablement en raison de l'influence plus importante des eaux atlantiques dans cette zone du fjord. La dominance des faunes agglutinées dans la zone " bassins profonds et seuil sous-marin " peut être associée, en partie, à la qualité de la matière organique, plutôt réfractaire en zone distale. Cependant l'observation de plusieurs degrés de dissolution des foraminifères calcaires, surtout dans les bassins profonds, peut expliquer la dominance des agglutinés. Notre hypothèse est que la persistance toute l'année d'eaux corrosives sur les fonds, due au piégeage des saumures produites en hiver, favorise le développement de taxons agglutinés au détriment des espèces calcaires.

Sur la base de ces résultats, nous avons proposé l'utilisation du ratio agglutinés / calcaires (A/C) comme indicateur de la présence continue de saumure sur les fonds, pour décrypter les archives sédimentaires historiques.

Message essentiel - Chapitre 1

Dans le Storfjorden, les foraminifères benthiques montrent une réponse aux saumures enrichies en CO_2 libérées pendant les processus de formation de glace de mer. Le rapport entre les foraminifères benthiques agglutinés et calcaires (A/C) est proposé comme proxy de la persistance sur les fonds de ces saumures qui provoquent la dissolution des tests calcaires des foraminifères benthiques ou entrave leur production.

Chapitre 2 : Taphonomie précoce des foraminifères benthiques dans "l'usine de glace de mer" du Storfjorden : le rapport agglutiné/calcaire comme indicateur de la persistance des saumures

Sur la base d'une étude écologique solide, le Chapitre 1 a démontré que le rapport A/C dans les faunes vivantes est un indicateur de la persistance et de la circulation de saumure dans le Storfjorden. Dans des études précédentes, la forte proportion d'espèces agglutinées, trouvées dans un état de préservation étonnamment élevé dans les archives sédimentaires, avait été

suggérée comme un signal possible (non calibré) de la présence de saumure dans le Storfjorden, au cours du dernier post-glaciaire. Le Chapitre 2 se focalise sur l'étude des effets de la taphonomie précoce sur les assemblages de foraminifères et donc de tester la fiabilité du proxy A/C mesuré sur les faunes fossiles dans les archives sédimentaires. À cette fin, les assemblages vivants de foraminifères du Chapitre 1 ont été comparés aux faunes fossiles trouvées sous la TAZ (*taphonomically active zone* : zone où ont lieu les processus taphonomiques) des mêmes carottes, afin de mettre en évidence la sélectivité potentielle de la perte taphonomique de certaines espèces. De plus, le rapport A/C de ces faunes fossiles a été comparé celui des faunes vivantes des sept stations pour estimer l'étendue de la perte taphonomique et son effet sur la fiabilité de l'indicateur A/C.

Les zones " fjord interne " et " bassins profonds et seuil sous-marin" sont caractérisées par des densités plus faibles d'individus tout juste morts trouvés dans les sédiments de surface, et de foraminifères fossiles trouvés sous la TAZ, par rapport à la faune vivante. Cette observation met en évidence le fonctionnement d'un fort filtre taphonomique dans toute la zone du fjord. Cependant, dans le " fjord interne ", la composition spécifique est similaire entre les faunes vivantes, les faunes mortes et fossiles (i.e., dominance de *Elphidium clavatum*, *Cassidulina reniforme* et *Nonionellina labradorica*), ce qui suggère que la perte taphonomique n'est pas sélective. Dans la zone des " bassins profonds et seuil sous-marin", un changement spécifique entre les faunes vivantes et fossiles a été observé, avec une perte taphonomique sélective de certains taxons agglutinés plus fragiles (i.e., *Reophax* spp.) accompagnée d'une présence accrue de certaines espèces calcaires (e.g., *E. clavatum*, *Cibicidoides lobatulus*). Ces dernières espèces, peut être allochtones, indiqueraient un transport depuis l'intérieur du fjord via l'écoulement de saumure. Ces changements dans les faunes fossiles et la perte taphonomique sélective ont entraîné une augmentation des proportions de foraminifères calcaires par rapport aux faunes vivantes. Dans le "fjord extérieur", certaines différences dans la composition des assemblages ont été observées avec la disparition du fragile *Globobulimina auriculata* et l'augmentation des abondances relatives d'autres espèces calcaires (e.g., *Buccella frigida*, *E. clavatum*). Cependant, la perte taphonomique est beaucoup plus faible à l'extérieur qu'à l'intérieur du fjord (i.e., " fjord interne " et " bassins profonds et seuil sous-marin"), et n'est pas sélective envers les taxons calcaires ou agglutinés.

Malgré les changements faunistiques dus à la perte taphonomique à l'intérieur du fjord, les différences dans les rapports A/C entre la zone du fjord seulement périodiquement influencée par les saumures (i.e., " fjord interne ") et la zone constamment affectée par les saumures (i.e., " bassins profonds ") où le débordement (i.e., " seuil ") sont encore clairement visibles, avec

des valeurs de rapports A/C jusqu'à trois fois plus élevées. Ces résultats valident l'utilisation du rapport A/C dans les archives sédimentaires pour étudier la présence-absence de saumure dans les eaux du fond et comme indicateur indirect de la production de glace de mer dans les polynies côtières de l'Arctique.

Message essentiel - Chapitre 2

Bien que le signal A/C soit affecté par des processus taphonomiques, il permet de souligner les différences entre les zones affectées par la persistance de saumures et celles sous influence intermittente.

Chapitre 3 : Influence des gradients environnementaux actuels sur le faunes de foraminifères dans la partie interne du Kongsfjorden (Svalbard)

En août 2018, la mission KING18 a été menée dans le Kongsfjorden, un fjord du Svalbard situé sur la côte nord-ouest du Spitzberg. Ce fjord, comme les autres fjords de l'ouest du Svalbard, est largement influencé par les eaux relativement chaudes et salées de l'Atlantique qui remontent vers le nord, et il connaît actuellement un réchauffement particulièrement intense. Pendant l'été, l'entrée des eaux de l'Atlantique dans le fjord favorise la fonte des glaciers côtiers. Les rejets d'eau douce chargées de sédiments, associés à la fonte de ces glaciers créent des gradients de salinité et de turbidité abrupts sur des échelles spatiales relativement petites (moins de 10 km). Outre les effets environnementaux directs, ces décharges influencent également la production primaire et les flux de matières organiques vers les fonds du fjord. Dans le Chapitre 3, nous discutons la distribution des foraminifères en réponse à ces forts gradients environnementaux qui s'établissent au plus fort de la saison estivale. Dans ce cadre, des carottes d'interface provenant de neuf stations ont été échantillonnées en août 2018, le long d'un transect d'environ 10 km commençant près du front du glacier côtier Kronebreen situé au fond du Kongsfjorden.

Nos résultats montrent que les foraminifères réagissent aux gradients environnementaux créés par la dynamique du glacier côtier et l'afflux des eaux Atlantiques, en établissant différents assemblages identifiés en trois biozones : proximale, médiale et distale. La biozone proximale est largement influencée par la dynamique des glaciers côtiers et donc soumise à une forte sédimentation à partir du panache turbide des eaux de fonte. Les assemblages proximaux ne sont composés que de quelques espèces, limitées au microhabitat de surface des sédiments (e.g., *Capsammina bowmanni*, *Cassidulina reniforme* et *Textularia earlandi*). Ces espèces opportunistes, avec leur préférence d'habitat, répondent aux conditions stressantes que sont les

faibles apports organiques ainsi que les perturbations physiques récurrentes qui exigent une recolonisation rapide des habitats.

La biozone médiane montre un assemblage transitoire avec certaines espèces communes avec la biozone proximale, ainsi que plusieurs autres espèces comprenant des indicateurs d'apport de matière organique fraîche, comme *Nonionellina labradorica* et *Stainforthia feylingi*. Ces observations correspondent à la turbidité réduite de l'eau dans cette zone située à environ 6-8 km du front du glacier, ce qui favorise la productivité primaire locale. Les foraminifères ne se limitent pas aux habitats de surface des sédiments et certaines espèces typiques de l'endofaune ont été observées (e.g., *N. labradorica*, *G. auriculata*), ce qui suggère un environnement plus stable et une plus grande diversité des niches fonctionnelles.

Dans la biozone distale, une espèce agglutinée associée aux eaux Atlantique, *Adercotryma glomeratum*, est l'espèce la plus abondante, accompagnée de *N. labradorica*. Comme cela a également été observé dans la zone médiane, l'occupation des micro-habitats endofauniques par ces deux espèces est le résultat de l'exploitation de niches écologiques différentes. L'augmentation de la diversité observée dans la biozone distale est attribuée d'une part à la baisse du stress environnemental liée à l'éloignement du front du glacier côtier, et d'autre part à la forte influence des eaux Atlantiques qui pénètrent jusque dans cette partie du fjord.

Les gradients environnementaux mesurés, directement ou indirectement liés à la dynamique du glacier côtier, sont principalement corrélés à la distance du front du glacier. En parallèle, l'augmentation remarquable de la diversité des foraminifères des biozones proximales aux biozones distales suggère que les paramètres de diversité pourraient être des indicateurs de la position du front glaciaire, et que l'étude de leurs variations serait un indicateur potentiel du recul des glaciers.

Message essentiel - Chapitre 3

Dans le Kongsfjorden, des gradients environnementaux abrupts (e.g., salinité, turbidité de l'eau, flux organiques) sont provoqués par la dynamique des glaciers côtiers. En été, différents assemblages de foraminiféres benthiques s'installent en fonction de l'éloignement au front du glacier et à la réduction du stress environnemental associée.

Chapitre 4 : La diversité taxonomique et fonctionnelle des foraminifères diminue à l'approche d'un front de glacier côtier : un proxy potentiel pour le recul des glaciers

Dans le Chapitre 4, nous montrons comment différents descripteurs de la biodiversité des foraminifères benthiques vivants (i.e., l'abondance, la structure de taille, la composition de la

communauté, la diversité taxonomique et fonctionnelle) varient en fonction de la distance au front du glacier côtier Kronebreen, situé au fond du Kongsfjorden.

L'abondance des populations de foraminifères et la taille des individus ne semblent pas affectées par les perturbations induites par le glacier, alors que tous les autres descripteurs des foraminifères sont corrélés avec la distance du lieu de vie au front du glacier. Une augmentation globale de la biodiversité est observée en s'éloignant du front. La richesse taxonomique et fonctionnelle ainsi que l'indice de Shannon montrent une augmentation rapide sur quelques kilomètres jusqu'à atteindre un plateau à environ 8 km de distance. Cependant, l'uniformité taxonomique et fonctionnelle et l'entropie quadratique de Rao (i.e., indice de dissimilarité fonctionnelle) montrent une augmentation linéaire avec la distance du glacier. La réduction progressive des perturbations induites par le glacier provoque très probablement l'établissement de communautés plus diversifiées et équilibrées. L'occupation croissante de l'espace fonctionnel le long du gradient est possible en raison de la disponibilité accrue de niches écologiques diversifiées suite à la réduction des perturbations induites par le glacier. Près du front du glacier, la faible valeur des mesures de régularité (i.e., équitabilité taxonomique et fonctionnelle) suggère la dominance de quelques espèces opportunistes capables d'occuper seulement une région restreinte de l'espace fonctionnel. L'augmentation de l'équitabilité en s'éloignant du front, ainsi que l'augmentation de l'entropie quadratique de Rao, amènent à une probabilité plus élevée de rencontrer des individus occupant des niches différentes.

Tous les modèles de biodiversité, étudiés à différentes résolutions de taille (i.e., les fractions de taille : >63, >100, >125, et >150 µm), ont permis de trouver le meilleur compromis entre l'effort analytique et l'information écologique. Si les modèles spatiaux d'abondance et de composition des communautés sont maintenus à chaque résolution, en revanche, certains modèles de biodiversité n'ont pas été complètement observés avec la résolution la plus basse (i.e., >150 µm). Plus précisément, les composantes d'équitabilité (taxonomique et fonctionnelle) ne parviennent pas à reproduire correctement les modèles de biodiversité, tandis que l'indice de Shannon et Rao reproduisent partiellement les tendances observées à plus haute résolution.

L'objectif final de cette étude était d'identifier et de proposer un indicateur potentiel du recul des glaciers basé sur les foraminifères benthiques. Sur la base de nos résultats, nous suggérons l'utilisation de quatre mesures de diversité taxonomique et fonctionnelle (i.e., la richesse taxonomique et fonctionnelle, l'indice de Shannon et l'entropie quadratique de Rao) comme indicateurs qualitatifs et semi-quantitatifs de la distance par rapport au front des glaciers et, par conséquent, comme indicateurs du recul des glaciers dans les reconstitutions historiques et

paléo-environnementales. De plus, nous suggérons d'appliquer ces indicateurs en utilisant la fraction de taille des foraminifères >125 µm comme le meilleur compromis pour obtenir un aperçu représentatif des modèles de biodiversité tout en maintenant un effort analytique minimal.

Message essentiel - Chapitre 4

Une augmentation de la diversité taxonomique et fonctionnelle a été mesuré en s'éloignant du front d'un glacier côtier en Arctique. Un indicateur combinant plusieurs mesures de diversité a donc été proposé comme outil de reconstruction du recul des glaciers côtiers des fjords arctiques.

Chapitre 5 : Les foraminifères comme outil de reconstitution le recul des glaciers côtiers : Une étude de cas de Kongsfjorden (Svalbard)

Sur la base de la réponse des faunes de foraminifères benthiques vivants aux gradients environnementaux liés à la distance du front glaciaire, des paramètres de diversité ont été proposées, dans le Chapitre 4, comme proxy potentiel pour le retrait des glaciers. Dans le Chapitre 5, nous avons testé la validité de l'indicateur proposé le long d'une archive sédimentaire influencée par le retrait rapide d'un glacier. La carotte sédimentaire, échantillonnée dans le Kongsfjorden en 2010, a enregistré le recul du complexe glaciaire Kronebreen sur six décennies après le dernier événement de crue (i.e., surge) glaciaire en 1948. Nous avons utilisé les 11 positions connues du front du glacier depuis 1948 (obtenues à partir de publications précédentes) pour calculer l'augmentation de la distance linéaire entre le front du glacier et le site de la carotte, tout au long de la série chronologique. Les modèles de communautés de foraminifères et quatre paramètres de diversité en fonction de la distance du front du glacier ont été étudiés. En parallèle, différents proxys géochimiques (rapport calcium élémentaire) ont été mesurés sur deux espèces de foraminifères.

Des abondances de foraminifères faibles ont été observées dans la première partie de la carotte, en conséquence de taux d'accumulation élevés et d'une forte perturbation physique sur le fond marin, liés au retrait rapide pendant ~30 ans après la crue glaciaire de 1948. Après 1982, certaines variations dans les flux de foraminifères ont été observées et attribuées à la variabilité saisonnière ou interannuelle. Les proxies géochimiques mesurés sur la calcite des foraminifères n'ont pas montré de modèles clairs en fonction de la distance du front, mais un signal généralement plus stable a été observé pour une faune vivant loin du front du glacier.

Des relations positives entre les paramètres de diversité et la distance du front glaciaire ont été observées. Plus précisément, la richesse taxonomique et fonctionnelle est restée faible entre

2 et 5 km du front, puis a augmenté de manière exponentielle par la suite, tandis que l'indice de Shannon et l'entropie quadratique de Rao ont montré une augmentation linéaire avec la distance du front. Ces observations sont cohérentes avec les modèles observés pour les assemblages vivants le long d'un gradient spatial, comme détaillé dans le Chapitre 4. L'augmentation mesurée de la diversité est liée à la réduction de la perturbation induite par le glacier sur le site de carottage avec l'éloignement progressif du front du glacier. Lorsque le site de carottage était proche du front, l'espèce *Cassidulina reniforme*, typiquement tolérante au stress lié à la dynamique du glacier côtier, dominait. Lorsque la perturbation induite par le glacier a diminué, l'assemblage s'est enrichi avec *Elphidium clavatum* et *Quinqueloculina stalkeri* puis avec d'autres espèces mineures dans les assemblages les plus récents. Ces résultats semblent valider l'utilisation des modèles de diversités comme indicateurs qualitatifs et semi-quantitatifs du recul progressif des glaciers côtiers sur une échelle spatiale kilométrique.

Message essentiel - Chapitre 5

L'efficacité de l'indicateur combinant plusieurs mesures de diversité a été testée comme proxy du recul des glaciers côtiers sur une archive sédimentaire des 60 dernières années. Cette étude a validé l'utilisation de ce proxy pour reconstruire le recul des glaciers côtiers en Arctique.

Synthèse - conclusion

Les préférences écologiques spécifiques des foraminifères sont souvent déduites de bonnes corrélations entre leur abondance et les paramètres environnementaux mesurés dans leur milieu de vie. Les proxys écologiques peuvent être définis soit par des espèces indicatrices (i.e., des espèces dominantes dans certaines conditions précises), soit par des paramètres particuliers décrivant les communautés (i.e., différentes mesures telles que, abondance, taille, biomasse, diversité taxonomique et fonctionnelle). Dans cette thèse, nous proposons des proxys axés sur la réponse globale des communautés de foraminifères à un phénomène spécifique.

- **Proxy pour les saumures, expulsées des zones de formation de glace de mer.** Nous avons d'abord observé que la persistance de saumure sur les fonds de fjords avait un effet physico-chimique sur les foraminifères calcaires provoquant leur dissolution ou entravant leur croissance. Ceci, parallèlement à leur adaptabilité potentielle à une matière organique plus réfractaire, a entraîné la prédominance des foraminifères agglutinés dans les zones de persistance de saumure. Ces observations ont abouti à la proposition du rapport entre abondance de foraminifères à tests agglutinés et de foraminifères à tests calcaires (A/C) comme indicateur

de la persistance des eaux enrichies en saumures et indirectement de la formation de glace de mer.

- **Indicateur du recul des glaciers.** Nous avons d'abord observé que la dynamique liée aux glaciers côtiers était responsable de perturbations environnementales à différents niveaux (physiques, chimiques, biologiques) définis à l'échelle mondiale comme des perturbations induites par les glaciers (GID). Le GID a un impact direct sur les microhabitats des foraminifères et conduit à l'établissement de différents assemblages de foraminifères qui se succèdent le long du gradient de proximité par rapport au front d'une glacier côtier. La plupart des caractéristiques des communautés de foraminifères, en plus de la composition des assemblages, se sont révélées être liées à la distance du front glaciaire. Plusieurs paramètres de diversité taxonomique (indice de Shannon) et fonctionnelle (indice de dissimilarité fonctionnelle Rao), ayant montré des relations positives claires avec l'augmentation de la distance du front du glacier, sont proposés comme indicateur du recul des glaciers.

Ces indicateurs d'intensité de formation de glace de mer et de retrait des glaciers côtiers ont été élaborés dans des environnements arctiques spécifiques. Dans l'état actuel des connaissances, leur application semble fiable dans les fjords où ils ont été développés, mais on pourrait envisager d'étendre leur utilisation à d'autres zones caractérisées (ou ayant peut-être été caractérisées dans le passé) par des conditions environnementales similaires. Nos tests de validation et d'applicabilité se sont limités à des faunes fossiles assez récentes, correspondant à une époque historique (<100 ans). Par conséquent, à l'heure actuelle, nous recommandons leur application sur des échelles de temps comparables. La fiabilité de ces proxys pourrait être, dans un futur proche, mise à l'épreuve par leur application sur des reconstructions existantes basées sur d'autres indicateurs.

Les deux proxys proposés dans cette thèse sont basés sur les caractéristiques de l'ensemble des communautés de foraminifères, témoignant ainsi d'un large signal écologique, sans surinterpréter ni négliger les espèces mineures. Un autre avantage majeur est que la quantification de ces proxys ne repose pas sur l'identification d'espèces qui pourrait varier en fonction du domaine d'étude ou du taxonomiste, évitant ainsi un biais potentiel lié à la méthodologie de l'étude. De plus ces proxys devraient être plus facilement utilisée par les non-experts en taxonomie des foraminifères.

Table of Contents

Introduction 1

Preface 2

1. A global changing climate 3

1.1 The Arctic in a changing climate 5

1.2 A sensitive spot to climate change: the Svalbard archipelago 7

2. Fjords 9

2.1 Generalities about fjords 9

2.2 Fjord hydrography and seasonality 9

2.3 Sedimentological processes 11

3. The ice in different forms 12

3.1 The sea ice 12

3.2 The continental ice 15

4. Benthic foraminifera 18

4.1 Powerful tools for current and past environmental survey 18

4.2 Drivers of regional to small-scale patterns 20

4.3 Foraminifera in Arctic fjords 21

5. Objectives 23

6. Context of the PhD thesis 25

References 26

Chapter 1 35

Abstract 36

1. Introduction 37

2. Oceanographic and environmental settings 39

3. Material and methods 42

3.1 Interface sediment sampling and CTD profiles 42

3.2 Geochemical analyses 42

3.3 Grain size analysis and ^{210}Pb dating 43

3.4 Organic matter quantity and biochemical composition 44

3.5 Living foraminiferal fauna sampling and analyses 45

3.6 Multivariate analyses 45

3.7 Visual characterisation of test dissolution 46

4. Results 46

4.1 Bottom water properties 46

4.2 Grain size analysis and sedimentation rate *47*
4.3 Biogeochemical analyses of the sediment *47*
4.4 Foraminiferal assemblages of the 0–5cm sediment layer (>150µm fraction) *49*
4.5 Comparison between the 63-150 and >150µm size fractions (0–1 cm) *54*
4.6 Visual characterisation of test dissolution *58*
5. Discussion 58
5.1 Environmental characteristics of the study area *58*
5.2 Distribution of foraminiferal species in response to environmental conditions *60*
5.3 Agglutinated vs. calcareous taxa: the premise of a paleo-proxy of brine formation *62*
5.4 Insights from the small size fraction *64*
6. Conclusions 65
References 67
Supplement Chapter 1 74
Chapter 2 83
Abstract 84
1. Introduction 85
2. Materials and Methods 87
2.1 Study area *87*
2.2 Sediment sampling *88*
2.3 Sedimentation rates *89*
2.4 Foraminiferal analyses *90*
3. Results 91
3.1 Sediment accumulation rate and determination of the taphonomically active zone *91*
3.2 Taphonomic loss *93*
3.3 Agglutinated/calcareous ratio (A/C) *98*
4. Discussion 99
4.1 Ecological and taphonomic processes affecting foraminiferal standing stocks *99*
4.2 Species preservation in the fossil record *100*
4.3 The A/C ratio as a proxy for historical reconstructions of brine persistence *103*
5. Conclusions 104
References 107
Supplement Chapter 2 112

Chapter 3 113
Abstract 114
1. Introduction 115
2. Study area 117
2.1. Geographical and geological setting 117
2.2. Oceanographic and hydrological setting 118
2.3. Productivity and organic matter export in Kongsfjorden 121
3. Material and methods 121
3.1 Environmental parameters 121
3.2 Foraminiferal analyses 124
4. Results 127
4.1 Environmental parameters 127
4.2 Foraminiferal assemblages in the upper 5 cm sediment (>150 µm fraction) 129
4.3 Comparison between the 63-150 µm and > 150 µm size fractions (in the 1 cm core top) 134
5. Discussion 137
6. Conclusions 143
References 147
Supplement Chapter 3 154
Chapter 4 165
Abstract 166
1. Introduction 167
2. Study area 169
3. Material and methods 170
3.1 Sediment sampling and processing 170
3.2 Foraminiferal analyses 171
3.3 Statistical analyses 178
4. Results 172
4.1 Foraminiferal abundance and size structure 172
4.2 Community composition 173
4.3 Correlations between diversity metrics calculated at different resolution 174
4.4 Relationship between diversity metrics and distance from tidewater glacier front 175
5. Discussion 179
5.1 Foraminiferal responses to glacier induced disturbance 179

5.2 Effect of sampling resolution on biodiversity patterns *181*
5.3 Foraminiferal biodiversity as potential proxy for glacier retreat *182*
6. Conclusions 183
References 185
Supplement Chapter 4 192
Chapter 5 201
Abstract 202
1. Introduction 203
2. Study area 205
3. Material and methods 207
3.1 Core sampling *207*
3.2 Sedimentological analyses and age model *208*
3.3 Foraminiferal analyses *209*
3.4 Laser ablation analysis *210*
3.5 Reconstruction of the distance from the glacier front *213*
3.6 Relationship between diversity metrics and distance from tidewater glacier front *214*
3.7 Foraminiferal communities in relation to the distance from the front *214*
4. Results 214
4.1 Sedimentological parameters *214*
4.2 Foraminiferal changes through time *217*
5. Discussion 220
5.1 Glacier retreat and foraminiferal fluxes *220*
5.2 Foraminiferal diversity patterns *222*
5.3 Validation of diversity metrics as proxies for glacier retreat *223*
5.4 Foraminiferal community changes through time *226*
6. Conclusions 227
References 230
Supplement Chapter 5 236
Synthesis & Perspectives 245
1. Chapters' overview 246
2. Two contrasted glaciated fjords 256
2.1 Environmental differences and major ice-related dynamics *256*
2.2 Analogies in ecological responses of benthic foraminifera *257*
3. Proxies for ice-related dynamics 259

3.1 Proxy development *259*
3.2 Proxy application *260*
4. Concluding remarks 262
5. Perspectives 263
5.1 Overcoming the spatial scale limitations *263*
5.2 Improving the trait-function relationship in foraminifera *263*
5.3 Disentangling the environmental factors *264*
5.4 Linking the recent observed changes to past climatic periods *264*
References 268
Besides Research 273

Introduction

Preface

"The polar regions are losing ice, and their oceans are changing rapidly. The consequences of this polar transition extend to the whole planet, and are affecting people in multiple ways" (IPCC, 2019).

The ongoing climate change is threatening the polar regions at faster rate compared to lower latitudes (Meredith et al., 2019). The Arctic surface air temperature has increased at more than double the global average, a phenomenon known as Arctic Amplification (Holland and Bitz, 2003; Dai et al., 2019). Glacier mass loss together with sea ice cover decrease and its consequent modification of brine production within fjords, are two major effects of climate change. These abrupt modifications have implications for the Arctic marine ecosystems on different trophic levels (Fox-Kemper et al., 2021). Therefore, there is the need to extend our knowledge of the various marine compartments (i.e., benthic, pelagic or sympagic), and to understand the effects of ice-related changes by developing appropriate proxies to follow and reconstruct recent modifications.

Benthic foraminifera are amongst the most effective bioindicators in marine ecosystems. Their success relies upon a quick turnover and a good fossilisation potential. The present PhD thesis investigates living benthic foraminiferal assemblages in two contrasted Svalbard fjords in terms of different ice-related dynamics and further proposes and tests potential ecological proxies (i.e., for sea ice formation and glacier retreat). Firstly, we focus on living foraminiferal assemblages in a typical "sea ice factory" (Storfjorden) still affected by the production and the persistence of brines (*Chapter 1*) and we test whether the signal of brine persistence is preserved after taphonomic processes (*Chapter 2*). Secondly, we investigate foraminiferal distribution in response to steep environmental gradients mainly related to meltwater discharges from glaciers (*Chapter 3*) and we further study diversity patterns as potential proxies for glacier retreat (*Chapter 4*) in a fjord characterised by decreasing ice cover in the last decades (Kongsfjorden). Finally, we test the effectiveness of the ecological proxy for glacier retreat on an historical record of about 60 years from Kongsfjorden (*Chapter 5*).

1. A global changing climate

Earth's climate has been always subjected to natural climatic fluctuations due to internal (e.g., ocean, atmosphere, and cryosphere connexions; Hegerl et al., 2007) and external forcings (e.g., orbital variations, solar radiation, volcanism; Jansen et al., 2007). These forcing factors led to a great variability of the Earth's global temperature over time, concomitantly to changes in the concentration of greenhouse gases, especially the carbon dioxide (CO_2) (e.g., Jansen et al., 2007). This is particularly spectacular during the most recent geological period, the Quaternary (last ~2.6 Ma), characterized by alternating glacial and interglacial conditions that are strongly correlated with CO_2 atmospheric concentrations (800 kyrs; Lüthi et al., 2008) (Fig. 1).

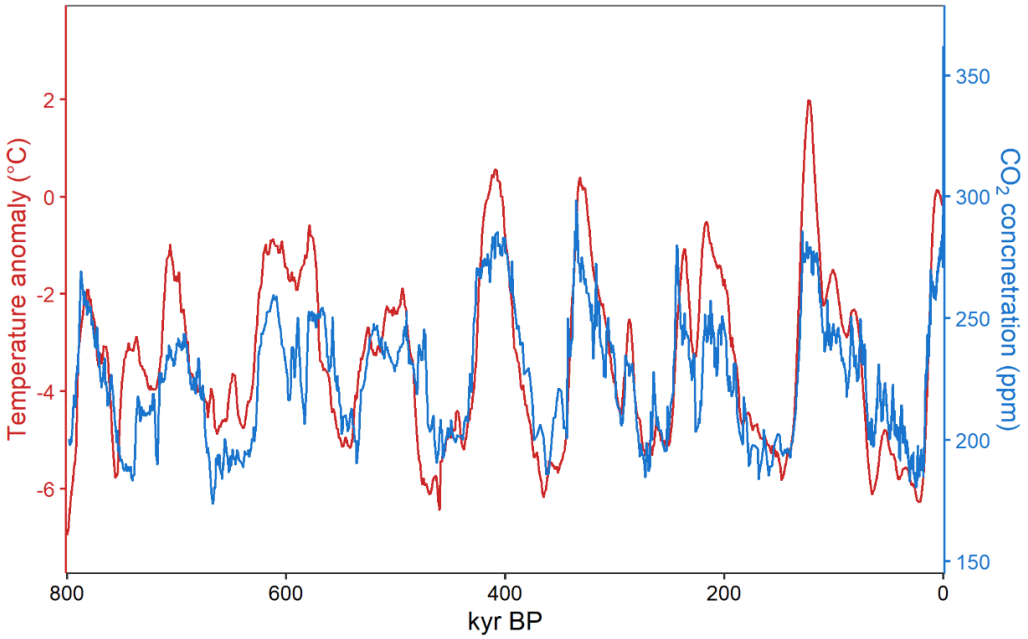

Figure 1. Global average surface temperature as temperature deviation (°C) from present in red and CO_2 concentration (ppm) in blue across the last 800 kyrs BP. Data about temperature are from Snyder (2016). Data about CO_2 are from Bereiter et al. (2015) (online source: http://ncdc.noaa.gov/paleo/study/17975). Figure prepared with R software (R core Team, 2020).

On the geological time scale and compared to glacial–interglacial fluctuations, our current interglacial (the Holocene; past 11,700 years) is a period of fairly stable climate (Rose, 2010). Still, this stable and warm climate has undergone a series of climate oscillations and reorganizations (e.g., 4.2 kyrs BP event, Medieval Warm Period, Little Ice Age) that were sufficient to significantly disturb natural systems (e.g., Green Sahara) (Bradley et al., 2003; Tierney et al., 2017; Bradley and Bakke, 2019). More recently, and superimposed on this natural variability, the anthropogenic forcing factor has become critical in controlling Earth's climate. Allen et al. (2018) reported that the global temperature is rising by 0.2°C per decade

compared to pre-industrial levels (i.e., mean in the 1850-1900 period) (Fig. 2a, 2b). A warming of 1.07°C (mean 2010-2019) since the pre-industrial time is of anthropogenic origin (IPCC, 2021). Since the industrial revolution (mid-18th century) greenhouse gas concentrations in the atmosphere have started to increase at unprecedented rate (IPCC, 2021). The atmospheric CO_2 concentration has increased of about 20 ppm per decade since the year 2000, which is 10 times faster than any increase undergone during the past 800 kyrs (Lüthi et al., 2008; Bereiter et al., 2015; IPCC, 2021). Pre-industrial levels of CO_2 were about 280 ppm whereas today concentrations are more than 410 ppm (Fig. 2c). If CO_2 is the largest contributor to current global warming, all other greenhouse gases (e.g., methane and nitrous oxide), emitted by human activities in smaller quantities, have also increased their atmospheric concentrations since the pre-industrial time (IPCC, 2021).

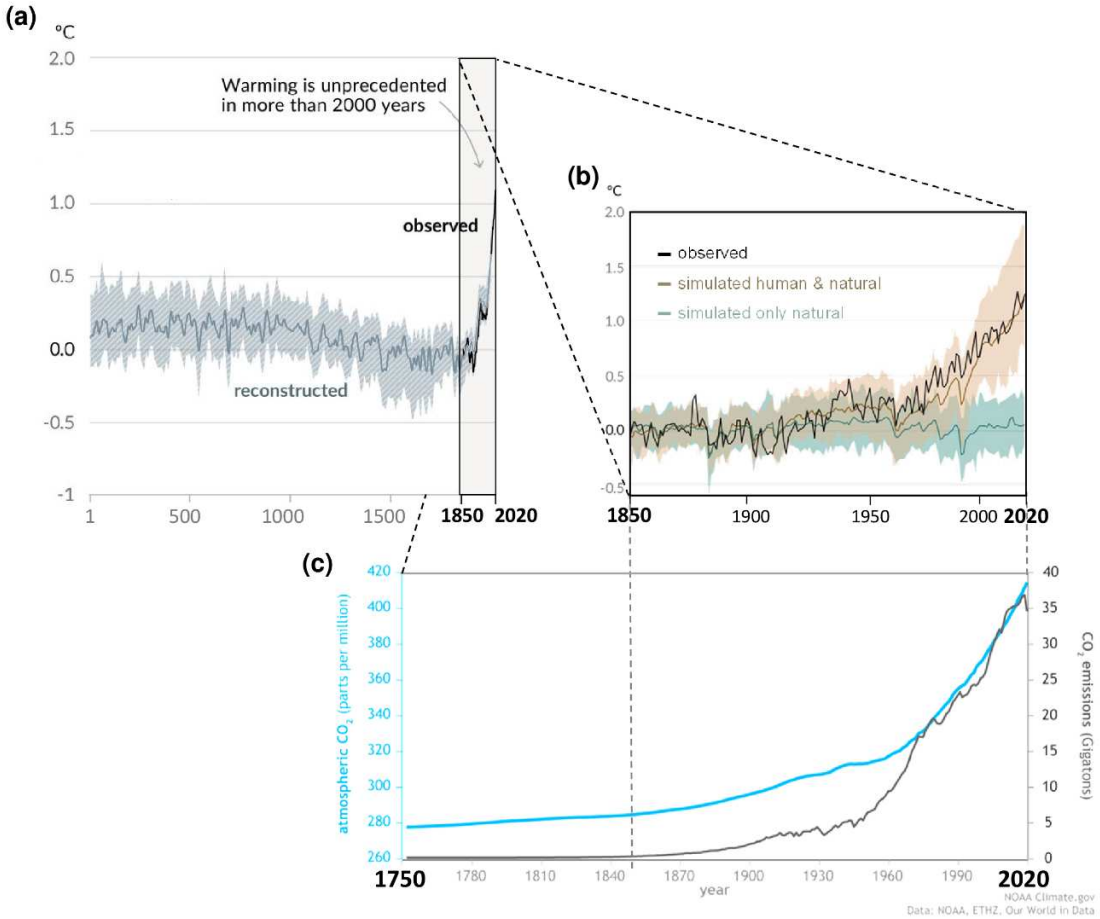

Figure 2. (a) Temperature anomaly in °C (relative to 1850-1900 on ten years average) reconstructed from paleoclimate archives (grey line and error interval) and direct observations (black line); figure modified after IPCC (2021). **(b)** Temperature anomaly as observed (annual average, black line) and simulated including human and natural factors (brown line) and including only natural factors (green line); figure modified after IPCC (2021). **(c)** Atmospheric CO_2 concentrations in ppm (blue line) and CO_2 emissions in Gt; figure modified after NOAA Climate.gov graph (https://www.climate.gov).

The present global warming affects the entire planet, with direct and indirect impacts on the ocean and the cryosphere and important consequences on ecosystems. A schematic overview of these changes is given in Figure 3. Ocean warming, acidification, oxygen loss and sea level rising, are among the major ocean-related effects. In response, nutrient cycles are perturbated, biogeography changes are observed (from primary producers to mammals) as well as alteration in ecosystem structures (Bindoff et al., 2019). Coastal areas are the most sensitive to these changes and are predicted to undergone enlarged biodiversity and functionality loss (Bindoff et al., 2019). The biodiversity loss may already have transgressed a boundary where current rates of extinction put the Earth system furthest outside the safe operating space (Mace et al., 2014). Additionally, the cryosphere is particularly sensitive to global warming: glaciers and ice sheets are losing mass, the Arctic sea ice extent and snow cover are decreasing, and permafrost temperatures are rising (Fig. 3; IPCC, 2019). The rapid changes affecting the cryosphere extends to the whole planet.

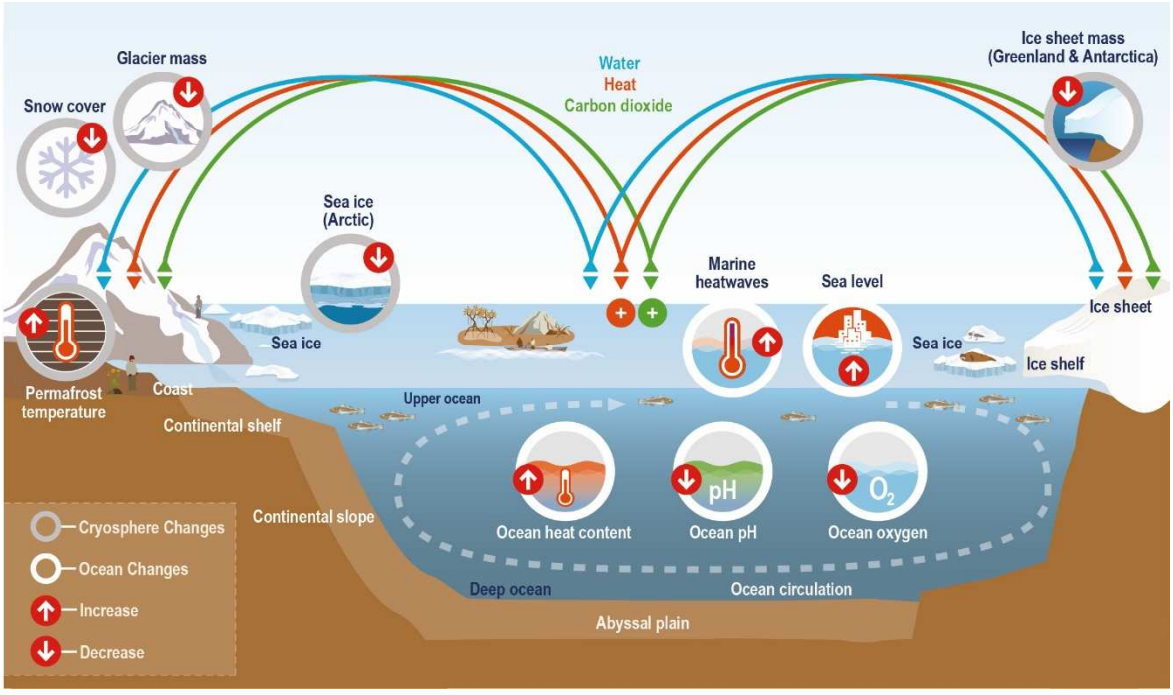

Figure 3. Schematic illustration of environmental changes related to the ocean (white circles) and to the cryosphere (grey circles) and their linkages in the through heat, water, and carbon exchanges. Figure modified after IPCC (2019).

1.1 The Arctic in a changing climate

The Arctic is a real hotspot for climate warming. It is warming two/four times faster than the rest of the planet, a phenomenon known as Arctic Amplification (AA) (e.g., Holland and Bitz, 2003; Dai et al., 2019). Although the exact causes of the AA are still debated, the scientific

community agrees that it is mainly the result of both local feedbacks (e.g. positive ice-albedo feedback; Screen and Simmonds, 2010; Stuecker et al., 2018) and climatic/oceanographic forcing (e.g., increased intensity and course changes in poleward heat transport; Graversen et al., 2008; Screen et al., 2012).

Over the last 40 years, the sea ice cover reduced both in terms of thickness and duration of its extent (Fig. 4a) and model simulations predict a further decrease under all scenarios (Fig. 4b) (Fox-Kemper et al., 2021). The observed sea ice cover reduction is strongly correlated with global mean temperature as well as CO_2 concentrations and cumulative emissions of anthropogenic origin (Fox-Kemper et al., 2021). The reduced sea ice cover implies a reduced surface albedo (i.e., power of reflection) which in turn leads to increased absorption of solar radiation by the ocean, further warming the system and reducing the sea ice cover, as positive feedback.

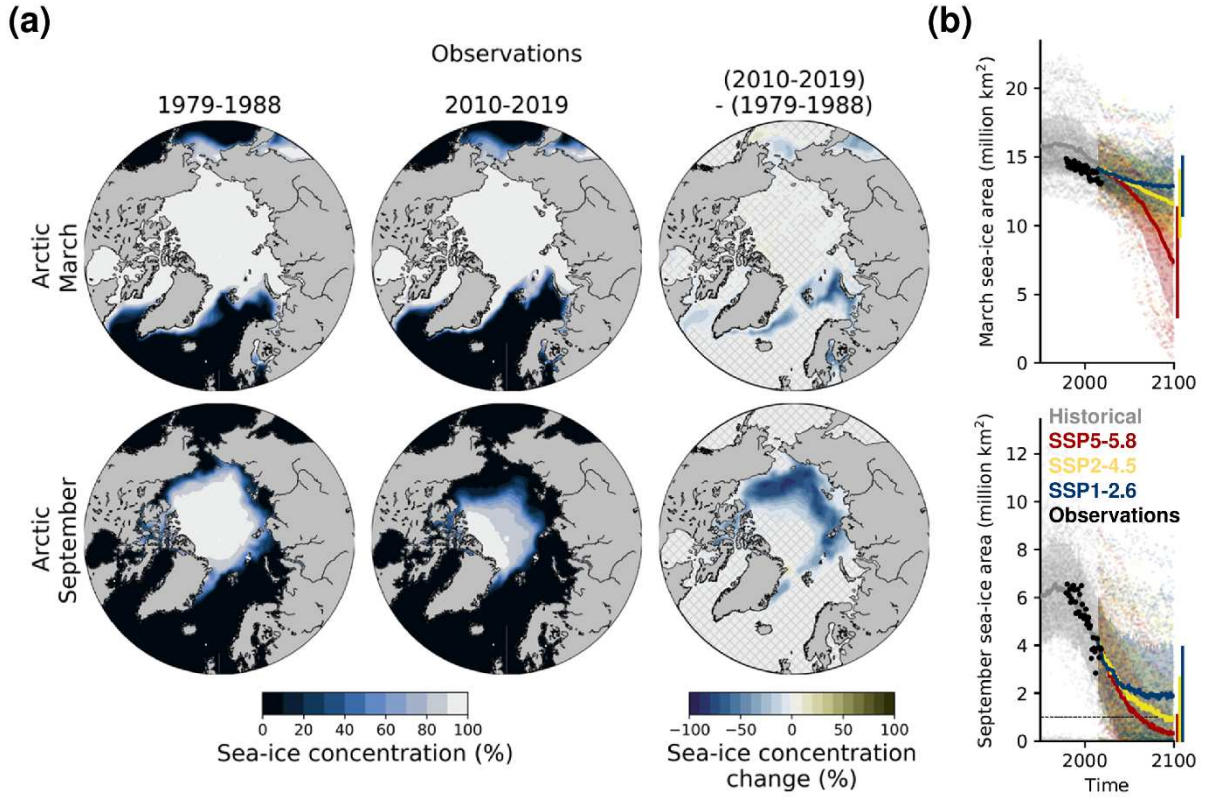

Figure 4. (a) Maps of Arctic sea ice concentrations for March and September (i.e., usually the months of maximum and minimum sea ice extent, respectively) considering satellite-retrieved mean sea ice concentration during the 1979-1988 and 2010-2019 periods, and absolute changes between these two decades; grid lines represent non-significant differences. **(b)** Monthly mean for March and September of sea ice area as a function of time in Coupled Model Intercomparison Project Phase 6 model simulations for historical simulation (grey), and the Representative Concentration Pathway projections corresponding to Shared Socio-economics Pathway SSP1-RCP2.6 (blue), SSP2-RCP4.5 (yellow) and SSP5-RCP8.5. Black dots represent observation data. Figures modified from Fox-Kemper et al. (2021).

The effects of the AA are not limited to the Arctic cercle and extend to lower latitudes, via complex feedback processes and natural internal climate forcing factors (Overland et al., 2016). Indeed, the climate in the Arctic region is subjected to a natural climatic variability. Specifically, on short time scales (i.e., monthly and annually), the Arctic climate is linked to mid-latitude conditions through the Arctic Oscillation (AO; Deser, 2000) and the North Atlantic Oscillation (NAO; Hurrell et al., 2003), both being atmospheric patterns of sea-level pressure anomalies in the northern hemisphere.

1.2 A sensitive spot to climate change: the Svalbard archipelago

The Svalbard archipelago, located north of the Arctic circle (74-81°N and 10-35°E), is extremely sensitive to climate change and to the AA phenomenon (e.g., Adakudlu et al., 2019; Moreno-Ibáñez et al., 2020). The Fram Strait, running west of Svalbard, is the only deep-sea gateway connecting the Atlantic and Arctic Oceans. Active water masses exchanges occur between these two Oceans, which are essential for climate modulation at various time scales (Dickson et al. 2008). Through the Fram Strait circulates warm Atlantic Water (AW) carried northwards by the West Spitsbergen Current (WSC), a branch of the North Atlantic Current (Schauer et al., 2004), the northernmost extension of the Gulf Stream. As such, the Fram strait channels the inflow of the dominant heat source for the Arctic Ocean. The Svalbard archipelago is under the influence of the WSC, but also of the East Spitsbergen current (ESC) that carries colder and fresher Arctic Water (ArW) (Svendsen et al., 2002). On the western margin of Svalbard, the WSC flows northwards along the continental slope whereas the Spitsbergen Polar Current (SPC; an extension of ESC) transports ArW parallel to the continental shelf of Spitzbergen (Tverberg et al., 2019). Cold and fresh ArW carried by SPC is separated from the warm and saline AW by the Arctic front (Fig. 1).

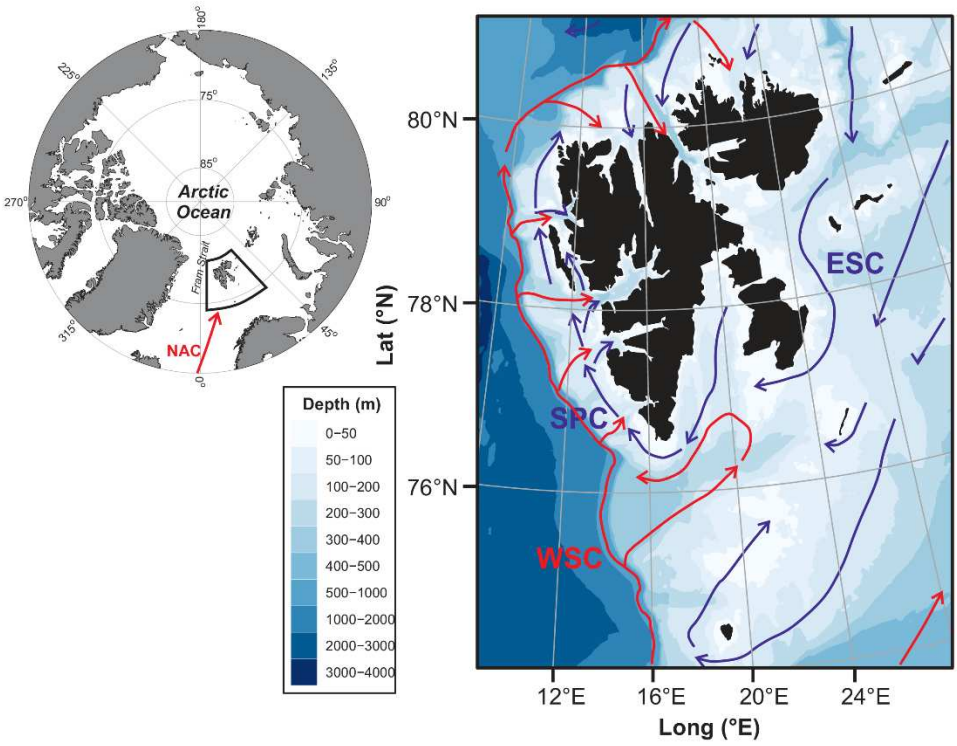

Figure 5. Left panel: Map of the Arctic Ocean with the location of the Svalbard archipelago on the main path of the continuation of the North Atlantic Current (NAC). Right panel: Detailed map of the Svalbard archipelago with the main influencing currents. The West Spitsbergen Current (WSC), the East Spitsbergen Current (ESC) and the Spitsbergen Polar Current (SPC). Currents displayed in red transport warm Atlantic water while currents displayed in blue transport cold Arctic waters. The map was performed with the R package *PlotSvalbard* (Vihtakari, 2020).

The archipelago is experiencing one among the fastest warming rate of the Arctic (e.g., (Descamps et al., 2017). A air temperature warming of 0.32°C per decade (i.e., 3.5 times the global mean over the same period) was observed between 1898 and 2018, but a warming of 1.7°C per decade (i.e., 7 times the global mean over the same period) per decade was measured since 1991 (Descamps et al., 2017; Nordli et al., 2020). Not only the atmosphere, but also the maximum annual sea surface temperature in the Fram Strait has warmed (0.04°C yr^{-1} between 1975-2013) (Descamps et al., 2017). Air and ocean warming have determined glacier mass loss, snow cover reduction, as well as sea ice cover loss. Such changes are affecting the biosphere at multiple levels.

2. Fjords

2.1 Generalities about fjords

Fjords, the focus of this thesis, are semi-enclosed marine basins characteristic of high latitude coasts (i.e., above the fjord belts in both hemispheres), which are the result of the submergence of an over-deepened glaciated valley (Howe et al., 2010). Due to former glacial erosion, fjord topography is often characterised by the presence of a shallow sill at the fjord mouth that limits the exchanges between fjord and shelf waters (e.g., Howe et al., 2010; Bianchi et al., 2020). Fjords, being the link between land and ocean, are places where cross-shelf exchanges occur, between an inshore dominated by local waters and an offshore dominated by oceanic waters (Cottier et al., 2010).

Because of their location at the transition between terrestrial and marine systems, high latitude glaciated fjords are sensitive spots to environmental climate changes (e.g., modifications in meltwater fluxes, terrestrial organic carbon, primary production linked to climate-mediated glacier retreat and altered sea ice cover; Bianchi et al., 2020). As such, fjords are suitable areas to study biological processes such as trophic linkages, pelagic-benthic coupling, and response to abiotic changes (Cottier et al., 2010).

Fjords are classified as polar, subpolar and temperate based on the climatic conditions and as glaciated or non-glaciated based on glacier presence (Howe et al., 2010). Different oceanographic and sedimentological processes characterise these fjords, and here we will focus on the subpolar and glaciated Svalbard fjords.

2.2 Fjord hydrography and seasonality

Fjord hydrography is essential to understand local biological processes. Several forcings, above the air temperature and its seasonal fluctuations, need to be considered to understand oceanographical processes in fjord. Among those we find *(i)* wind stress and its seasonal characteristics that influence the vertical mixing of the water column, and *(ii)* the Coriolis effect that influences surface freshwater distribution as well as inflow of oceanic water masses in the fjord (Cottier et al., 2010). Nonetheless, the fjord bathymetry is of primary importance in controlling water and sediment exchanges between ocean and fjords (e.g., reduced water exchanges because of a sill).

Usually, water masses within fjords (with or without a defined sill; e.g., Cottier et al., 2005; Nilsen et al., 2008) are well stratified and two or three layers can be distinguished depending

on the season (Cottier et al., 2010). Figure 6 represents seasonal hydrological changes occurring typically in Svalbard fjords. During summer, the system is fully stratified with a freshwater surface layer (originating from glaciers, snowmelt, and rivers), an intermediate layer composed of advected oceanic waters, and a deep layer composed of dense water masses formed during the previous winter (i.e., through sea ice formation processes or cooling of intermediate waters). During autumn, the surface water cooling triggers thermal convections to form the Local Water (Svendsen et al., 2002; Nilsen et al., 2008) overlying the more dense old winter waters. During winter, surface cooling continues until sea ice formation with consequent release of saline and cold brines (Haarpaintner et al., 2001). The downwelling of these dense brines leads to halocline convection and formation of homogeneous Winter Water (Svendsen et al., 2002; Nilsen et al., 2008). During late spring, sea ice breaks up followed by surface water warming; surface water salinity decreases, and a stratification is re-established.

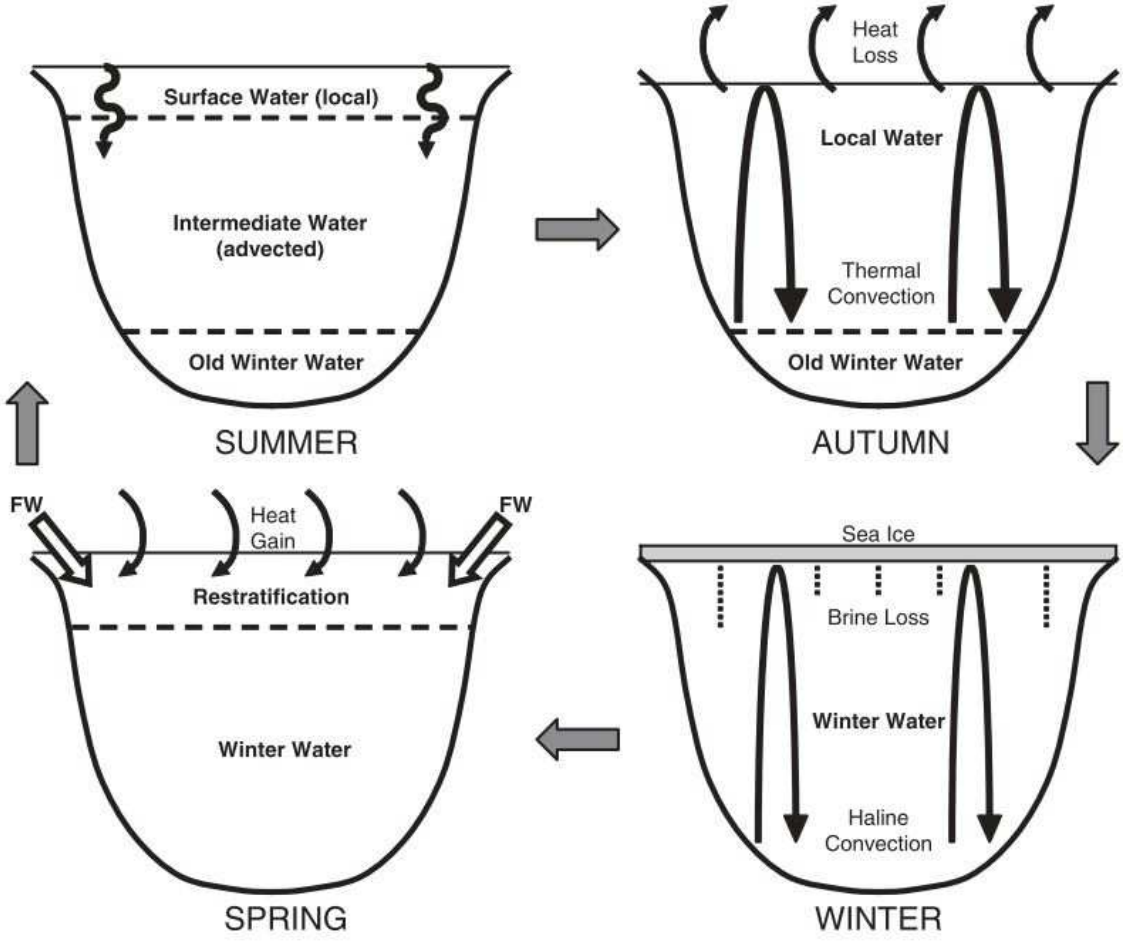

Figure 6. Seasonal cycle of stratification and major water masses characterising a typical Svalbard fjord. Figure modified from Cottier et al. (2010).

2.3 Sedimentological processes

In Arctic fjords, sedimentation is mainly of glacial origin (Howe et al., 2010). Two types of glaciers, marine- and land-terminating, carry particles of different sizes eroded from the substratum of their catchment area. During glacier flowing, sediment from the glacier substratum is incorporated at its base (i.e., basal debris) as well as on its surface (i.e., supra-glacial debris) (Fig. 7).

However, the sedimentary dynamics occurring at the marine- and land-terminating terminus differs. In Svalbard, the land-terminating glaciers are separated from the sea (open sea or adjacent fjord) by a plus/minus large coastal plain occupied by braided fluvial systems. Coarser sediment is stopped on the plain to build coastal deltas, whereas the finer fraction reaches the coast and is dispersed into the fjord through buoyant turbid plumes. In parallel mode, tidewater glaciers transport and discharge a major part of their sediment (from clay to boulder) load directly to the fjord where submarine melting occurs. Sediment may also be ice-driven from active calving and deposited far away from the tidewater glacier front (i.e., ice-rafting; Fig. 7).

Hydrography is important in sediment distribution within fjords. The Coriolis force deviates both meltwater plume trajectory and inflow of oceanic waters, and wind stress drives surface currents that control iceberg rafting. This leads to the shift of the associated sedimentary depot centre (Howe et al., 2010). As a result, different depositional environments can produce different types of deposits which are subjected to seasonality. During summer, meltwater turbid plumes transport the fine sediment away from the coast (riverine delta or glacier terminus) and a large part of this suspension load settles further within the fjord (Bianchi et al., 2020). The coarse sediment, on the contrary, is either immediately deposited at the coast in thick gravel layers or transported by icebergs (ice rafting) produced through calving at the tidewater glacier terminus and deposited further away as dropstones (Fig. 7).

Because of these sedimentation processes linked to glacier dynamics, high sediment accumulation rates are measured in glaciated fjords, especially in the proximity of glacier termini (e.g., Zajączkowski et al., 2004; Zaborska et al., 2006; Howe et al., 2010; Streuff et al., 2015; Bianchi et al., 2020). Indeed, fjord are in general characterised by a thick layer of unconsolidated Late Quaternary sediments and their stratigraphic records preserve sediments accumulated during paraglacial and postglacial phases. As such, they constitute optimal sedimentary archives for past marine and glacial environments (Cottier et al., 2010; Bianchi et al., 2020).

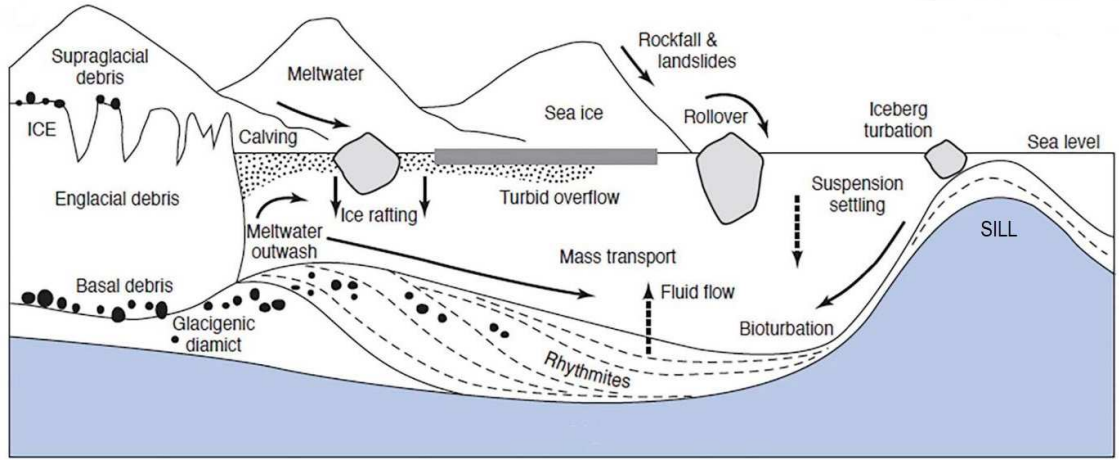

Figure 7. Principal physical processes occurring in a typical glaciated fjord. Figure modified from Bianchi et al. (2020) adapted from Howe et al. (2010).

3. The ice in different forms

In order to evaluate current environmental changes in the Arctic, it is essential to understand ice-related dynamics and their interaction with the biosphere. There are two types of ice based on their formation origin: sea ice formed through seawater freezing and continental ice formed from compacted snow (freshwater).

3.1 The sea ice

3.1.1 Sea ice formation processes

Sea ice is frozen seawater, that grows during winter, and melts in summer. Even though sea ice formation is restricted to Polar regions, its presence has an influence on the global climate through different processes (e.g., albedo effect, oceanic circulation). Sea ice forms at the ocean surface when the temperature reaches the freezing point (i.e., -1.8°C, at salinity 32). Once this point reached, the first stage of sea ice growth begins forming small ice crystals (i.e., millimetric size) called frazil ice. When frazil ice forms, the salt accumulates in brine droplets, and due to the high permeability at this stage, brines absorb and concentrate CO_2 from the atmosphere (Rysgaard et al., 2011). As ice-growth continues, brines are drained and expelled to the under-ice water determining a salinity increase and therefore an increased water density. These dense brine waters, enriched in dissolved CO_2 (i.e., low pH waters) sink and contribute to intermediate and deep-water masses (e.g., Ivanov et al., 2004) (Fig. 8). The sea ice sheet is then formed when frazil ice crystals bond together, through different processes depending on weather conditions (i.e., pancake cycle in rough ocean or congelation growth in a calm ocean). The sea ice sheets

can be of two different types, fast ice when they are attached to the land and pack ice when it is free floating.

3.1.2 Sea ice factories

Even during winter, the ice cover is not uniform over the Arctic Ocean. There are persistent ice-free areas called polynyas which determine the formation of brine enriched dense waters. (Martin, 2019). These could be of two different types:

1. *Coastal latent heat polynyas:* coastal ice-free area formed and maintained by advection of ice by offshore winds and tidal and ocean currents (Fig. 8). When cold and strong winds blow persistently off-shoreward, they push away from the coast the new formed sea ice, thus maintaining an ice-free area. The open water, in contact with the cold atmosphere loses latent heat and this intensive heat loss to the atmosphere lead to a persistent ice formation.
2. *Open-ocean sensible heat polynyas:* ice-free areas in the open ocean formed by upwelling of warm ocean waters maintaining the opening in the pack ice. They are called sensible-heat because the atmospheric heat-loss cools the water column.

In the Arctic, most polynyas are coastal latent heat polynyas (Fig. 8a). Arctic polynyas were estimated to produce 0.2-1.2 Sv (1 Sv = 10^6 m^3 s^{-1}) of dense waters depending on the estimates (e.g., Cavalieri and Martin, 1994; Winsor and Bjork, 2000), which contribute to transformation of intermediate and deep water masses and to the oceanic circulation. The importance of polynyas is not limited to their contribution to the ocean circulation. They have a large biological importance for the winter survival of some arctic mammals and birds who forage in these areas (Martin, 2019).

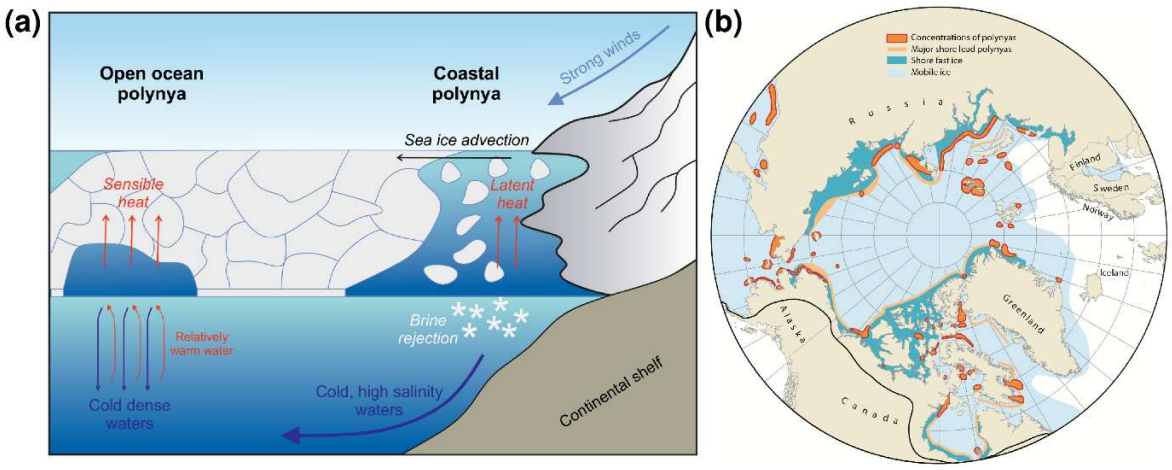

Figure 8. (a) Scheme of typical functioning of a coastal latent heat polynya and an open ocean sensible heat polynya. **(b)** Circumpolar map of known polynyas locations in the Arctic (figure modified from Meltofte (2013) based on Barber and Massom (2007)).

Arctic sea ice cover changes through seasons, expanding in autumn-winter, and shrinking in spring-summer. The seasonal (or first-year) sea ice melts or forms every year, whereas the sea ice persisting all year round in the Arctic Ocean takes the name of perennial (or multi-year) sea ice. The seasonal ice zone (SIZ) is the area of the ocean extending between the perennial sea ice offshore limit and the boundary of maximum winter sea ice extension (Wadhams, 1986).

3.1.3 Seasonality of primary production in the sea ice zone

The extreme seasonality characterising the Arctic Ocean primary production (PP) is the consequence of the alternation between polar night and day, short growing seasons, and the presence of sea ice cover. PP is highly controlled by both light and nutrient availability. Two major primary producers provide energy to the Arctic Ocean food web: sympagic ice algae (algal communities found in first- and multi-year sea ice) and phytoplankton (autotrophic components of the plankton community). The light limits the production period through time, whereas nutrients drive the intensity of productivity determining differences in the trophic status (oligotrophic or eutrophic) through space (e.g., Tremblay et al., 2015).

As detailed by Wassmann (2011), during late spring, as light availability increases, the sea ice thins out and the snow cover disappears, allowing occurrence of ice algae blooms in the SIZ (Fig. 9). Such event is then followed by intense phytoplankton bloom thanks to newly availability of nutrients. As the autotrophic productive period continues all over the summer season, nutrient availability decreases. This determines a progressive switch towards more heterotrophic processes. Such processes are associated with export fluxes of different natures: pulses of fresh phytodetritus in spring and early summer, and more refractory organic matter (e.g., fecal pellets, detritus) the rest of summer and early autumn (Wassmann, 2011). During autumn and winter, the polar night and extensive sea ice cover reduce drastically autotrophic processes and the export fluxes are reduced to minimal levels of detritus (e.g., Dybwad et al., 2021). Vertical carbon exports provide fundamental food resources to the benthic ecosystems (e.g., Boyd and Trull, 2007). The pelagic-benthic coupling in the Arctic is linked to sea ice cover dynamics (extend, thickness).

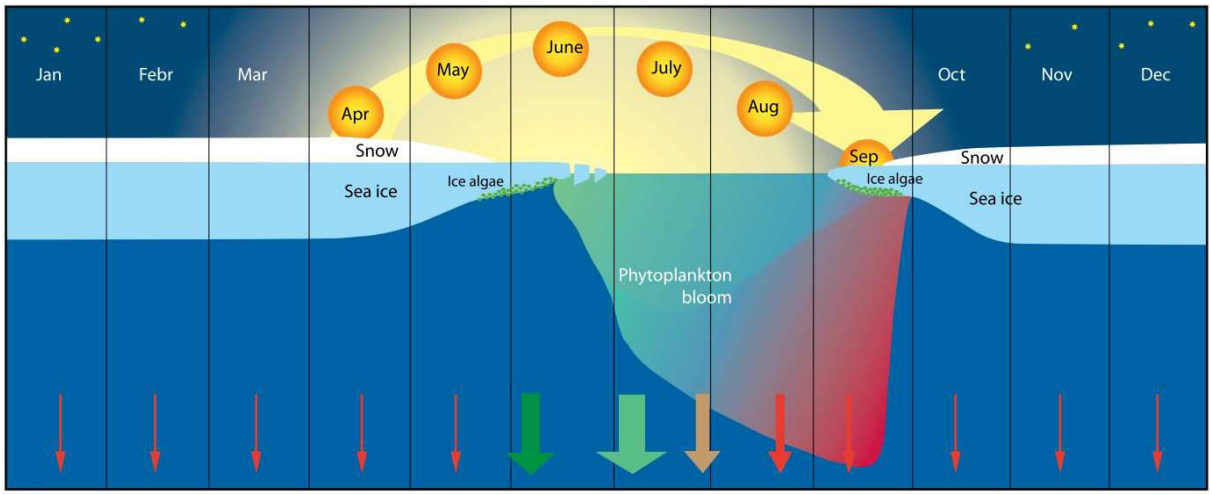

Figure 9. Schematic illustration of biogeochemical processes undergoing in the seasonal ice zone (SIZ) all over the year. In green are indicated autotrophic processes, gradually replaced by heterotrophic processes displayed in red. The coloured arrows indicate the different nature of vertical exports (i.e., fresh phytodetritus in green, faecal pellets and detritus from zooplankton in brown-red). Figure modified from Wassmann and Reigstad (2011).

2.1.4 Climate change influence on sea ice

Climate warming is affecting the temporality of sea ice formation by increasing the duration of sea ice free period thus inducing earlier spring blooms and longer heterotrophic processes (e.g., Wassmann, 2011; Wassmann and Reigstad, 2011). Ice algae and phytoplankton are at the base of the ocean food web, and have a bottom-up control on the trophic chain. Therefore, temporal changes in PP would have repercussion on higher trophic levels (Wassmann, 2011; Wassmann and Reigstad, 2011). Copepods *Calanus* spp., for instance, are the primary consumers of ice algae, and they are able to accumulate large lipid deposits for their winter survival (e.g., Lee et al., 2006). These grazers, as secondary producers, are responsible for the energy transfer to higher trophic levels. Therefore changes in PP timing can determine a mismatch between these two trophic levels with consequences on the lipid-based Arctic marine food web (e.g., Leu et al., 2011). These changes imply modifications in the timing of vertical exports and consequent pelagic-benthic coupling.

3.2 The continental ice

3.2.1 Glacier dynamics

At present, glacial ice (i.e., glaciers, ice caps and ice sheets) occupy about 10% of the land area (most of it is found in Antarctica and Greenland) according to the National Snow and Ice Data Center (NSIDC). Glaciers form through the accumulation and compression of snow for several

years and its freezing. They are not static but instead subjected to natural movements. Indeed, because of their own weight glaciers flow under gravity force.

Glacier's movements can shape landscapes over hundreds and thousands of years, for example forming U-shaped, over-deepened or hanging valleys. The flow of a glacier (i.e., retreat or advance) depends on its mass-balance. Glacier growth and/or retreat is influenced by seasons. During winter, glaciers gain weight thanks to snow accumulation, whereas during summer they lose mass through melting and ablation processes in their downstream parts (Nesje, 2007). Over one year the mass balance of a glacier could remain stable if mass gain and mass loss were equal, while would be positive (advance) or negative (retreat) if mass gain and mass-loss was the dominant process, respectively.

Glacier mass balance is controlled by different processes that can be atmospheric and/or marine-related depending on the glacier's type (Fig. 10). Surface melting, the dominating mass loss process in land-terminating continental glacier (e.g., Zwally et al., 2002; Tedstone et al., 2015), is accompanied by frontal ablation (i.e., calving and submarine melting) in marine-terminating tidewater glaciers (Cogley et al., 2011).

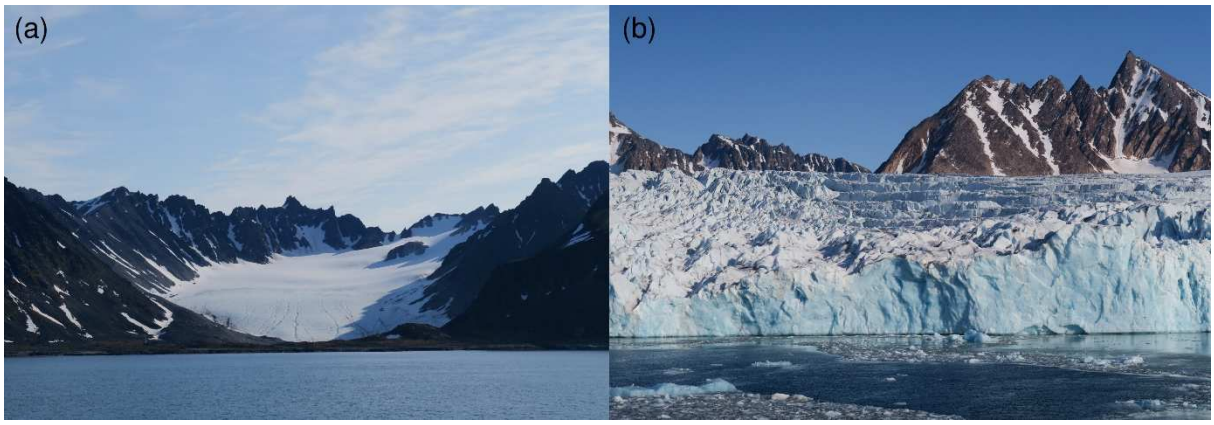

Figure 10. Example of **(a)** land-terminating continental glacier and **(b)** marine-terminating tidewater glacier from Svalbard (west Spitsbergen). Pictures taken by Eleonora Fossile.

3.2.2 Glacier-driven biogeochemical gradient in fjords

Glacier mass budgets/balances are linked to strong seasonality, and glacier's influence on the surrounding environment can extend for several kilometres. Specifically, marine-terminating glaciers are responsible for the creation of environmental gradients at the interface with the ocean with consequences on associated ecosystems (e.g., Hopwood et al., 2020). These gradients are refereed to water physical (i.e., temperature, salinity, turbidity) and chemical (i.e., nutrients) properties (Fig. 11).

Specifically, during the melting season, tidewater glaciers discharge high amounts of meltwater and associated sediment through subglacial discharges and surface runoff (e.g., Meslard et al., 2018). These discharges of freshwaters exit from the base of the glacier and supply a buoyant turbid plume spreading from the terminus (e.g., How et al., 2017). Therefore, at a local scale, within hundreds of meters to few kilometres from tidewater glacier fronts, light is the ultimate limiting factor controlling PP (Hopwood et al., 2020). Glacial meltwaters have generally low concentrations in macronutrients (i.e., nitrate, phosphate) important for PP (e.g., Hopwood et al., 2018; Halbach et al., 2019). However, the upwelling system created at the glacier terminus, enhance vertical fluxes of macronutrient-rich bottom waters to the surface, which can drive PP away from the terminus where light is not anymore a limiting factor (e.g., Hopwood et al., 2018; Halbach et al., 2019).

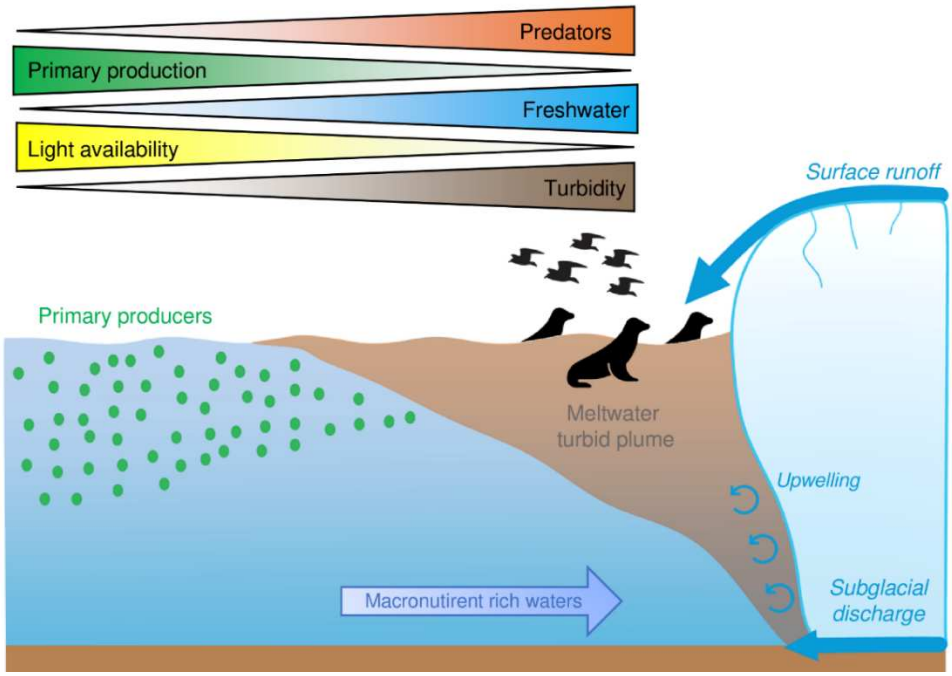

Figure 11. Conceptual model showing the dynamics associated to tidewater glaciers with the principal environmental gradients created.

Areas in proximity of tidewater glaciers are important foraging hotspots. Indeed, in proximity of fronts, strong salinity gradients and suspended particles are fatal for zooplankton and some fish species (Lydersen et al., 2014). Consequently, mammals and birds adapt their feeding strategies locating in the glacier proximal areas to feed on zooplankton and fishes (e.g., Hop et al., 2002; Lydersen et al., 2014).

3.2.3 Climate change influence on glaciers

Tidewater glaciers, located at the interface between terrestrial and marine environments, are particularly sensitive to recent climate warming. Indeed, warmed air and ocean temperatures play an important role in their mass loss and front variations (Luckman et al., 2015). More than half of the land area of the Svalbard archipelago is covered with glaciers and about 15% are tidewater glaciers (Fig. 12). Since 1960, glaciers of Svalbard have started to lose mass and a negative mass balance has been documented since the year 2000 (Fox-Kemper et al., 2021). When predicting the impact on the marine environment of future changes, it is fundamental to consider the different influences of land-terminating vs marine-terminating glaciers on the coastal environments (e.g., nutrient supply, sediment inputs).

Meredith et al. (2019) underlined that the retreat of tidewater glaciers and the associated landward progression of the front may lead to a transition from marine- to land-terminating glaciers. Sediment and nutrient supply areas will shift from the coastal waters to the coastal plain. These shifts have large ecological implications with repercussions at different trophic levels (Meredith et al., 2019).

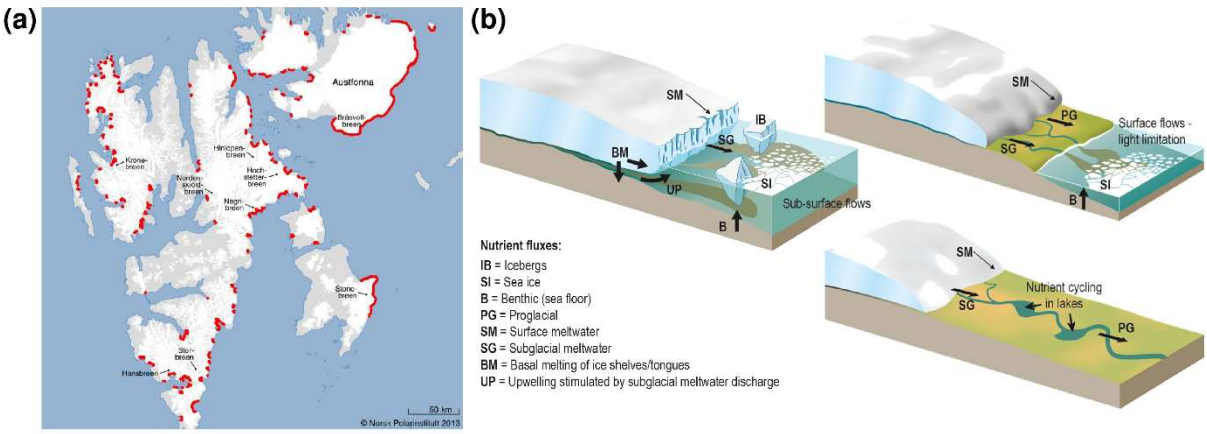

Figure 12. (a) Map of Svalbard with tidewater glacier fronts highlighted in red. Figure modified after Lydersen et al. (2014). **(b)** Transition from a marine- to a land-terminating glacier as progressive landward retreat occurs. Figure modified from Meredith et al. (2019).

4. Benthic foraminifera

4.1 Powerful tools for current and past environmental survey

Counting over 10,000 extant species (Adl et al., 2007), foraminifera are single-celled protists (eukaryotic microorganisms belonging to the Rhizaria group; Adl et al., 2012) worldwide distributed in all marine environments, from the equator to high latitudes, from coastal areas to abyssal plains (Murray, 2006), but also present in freshwater and terrestrial habitats (Holzmann

et al., 2021). Most species inhabit benthic environments, and only about 50 species are planktonic (Schiebel and Hemleben, 2017). Because of their small size (i.e., included in the meiofauna, 0.06-1.0 mm of dimensions, with several exceptions), benthic foraminifera are present with high densities in small sediment volumes.

Benthic foraminifera are separated and protected from the surrounding environment by a shell called test, which can be composed of different materials (i.e., calcareous hyaline and porcelaneous, agglutinated, organic; Fig. 13) and can have several morphologies. Even though there are some limitations (e.g., identification of cryptic species; Pawlowski and Holzmann, 2002), test morphology and composition are extensively used to identify foraminiferal species.

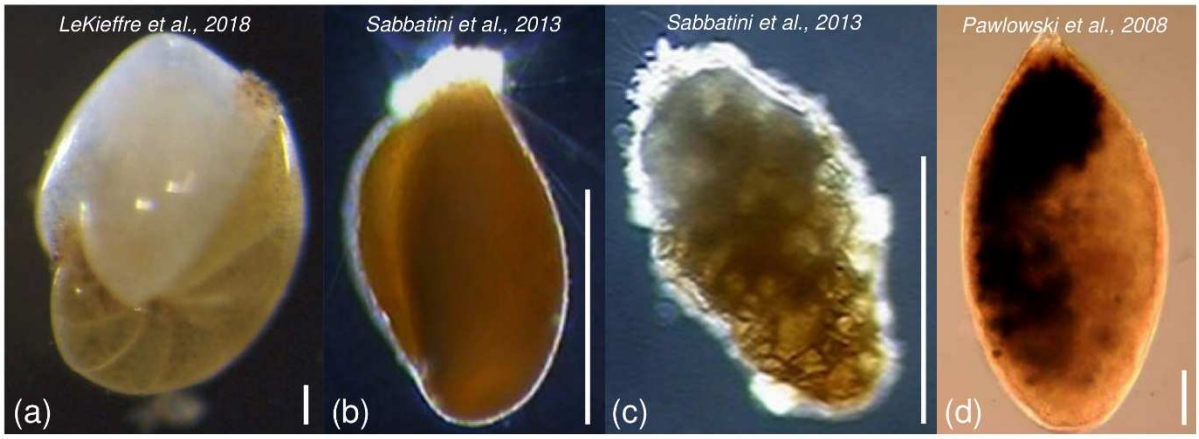

Figure 13. Light micrographs of living foraminifera with different test materials. **(a)** calcareous hyaline (modified from LeKieffre et al., 2018), **(b)** calcareous porcelaneous (modified from Sabbatini et al., 2013), **(c)** agglutinated (modified from Sabbatini et al., 2013), **(d)** organic (modified from Pawlowski et al., 2008). Scales bars are 100 µm.

Besides the high densities and diversity in marine sediments, foraminifera's short life cycles, and specific ecological requirements allow them to respond rapidly to environmental changes. These advantages, in combination with their fossilisation potential, make them powerful tools in different research fields. They are used in biomonitoring studies to evaluate pristine and current environmental conditions (e.g., Hallock et al., 2003; Koukousioura et al., 2011; Bouchet et al., 2012, 2018; Hallock, 2012; Schönfeld et al., 2012; Dimiza et al., 2016; Jorissen et al., 2018), as well as in historical and paleoenvironmental reconstructions to trace past climatic and oceanographic changes (e.g., Murray, 1991, 2006; Schmiedl, 2019).

To reconstruct past environmental conditions, two types of foraminiferal-based proxies exist: ecological (i.e., density, diversity, species composition; e.g., Murray, 2001) and geochemical (i.e., isotopic and trace element composition of the test; e.g., Katz et al., 2010). The first is based on foraminiferal response to different environmental parameters, the latter on the elemental incorporation during the calcification processes. The use of foraminiferal-based

proxies along sedimentary archives relies on the understanding of their ecological requirements and responses to physico-chemical parameters, as well as on experimental calibration under controlled conditions for geochemical proxies. Therefore, it is fundamental to study living benthic foraminifera assemblages in relation to *in situ* measured environmental parameters to develop trustfully ecological proxies.

4.2 Drivers of regional to small-scale patterns

The understanding of benthic foraminiferal ecology is based on observations conducted at small spatial scales (i.e., millimetres for microhabitat distribution) to large spatial scales (i.e., thousands of kilometres for regional distribution) (Gooday, 2003). Foraminiferal distribution at regional scale is influenced by several environmental factors, such as type of sediment (grain-size), water properties (i.e., temperature, salinity), hydrodynamics, food and oxygen availability (Murray, 1991; Gooday, 2003), which are subjected to spatial and temporal variability, especially in dynamic environments (e.g., coastal areas).

While considering foraminiferal distribution at small spatial scales, it is important to consider that benthic foraminifera migrate in sediment thanks to their pseudopodia (i.e., extension of the cytoplasm extruded through the apertures of the test; see Fig. 3) and therefore can occupy different microhabitats depending on the surrounding conditions. They generally live in the surface sediment, but their microhabitat vertical distribution can vary from few millimetres to about 10 centimetres, depending on the succession of redox layers (Jorissen et al., 2021). In the 90's, the TROX-model was proposed to explain foraminiferal microhabitat distribution through two limiting factors: food and oxygen availability (Jorissen et al., 1995) (Fig. 14a). Generally, in oligotrophic conditions the limiting factor would be food availability, whereas under eutrophic conditions the oxygen concentration would be limiting.

Different species have specific requirements in terms of diet and metabolism, and this allow the occupation of species-specific microhabitats (Jorissen, 1999). Foraminifera have shown several feeding strategies (e.g., herbivory, bactivory, mixotrophy, passive suspension feeding, detritivory, carnivory, omnivory, parasitism; e.g., Murray, 2006; Jauffray et al., 2016) as well as different metabolic pathways such as denitrification (e.g., Risgaard-Petersen et al., 2006; Piña-Ochoa et al., 2010) or kleptoplastidy (e.g., Lopez, 1979; Pillet et al., 2011; Jauffrais et al., 2016). The development of different strategies and metabolic adaptations allows foraminifera to survive in all kinds of marine environments and tolerate different stressful conditions.

For these reasons, the TROX model was recently updated by adding nitrate as the third limiting factor for foraminiferal microhabitat distribution (Xu et al., 2021) (Fig. 14b). These limiting factors are intrinsically linked. The organic matter flux (quality and quantity), for instance, affect oxygen demand and redox conditions in the sediment (Jorissen et al., 2021). Indeed, the newly developed 4GFOR model highlights the importance to also consider the quality of food particles, in parallel to organic matter quantity while explaining foraminiferal microhabitat distribution (Jorissen et al., 2021).

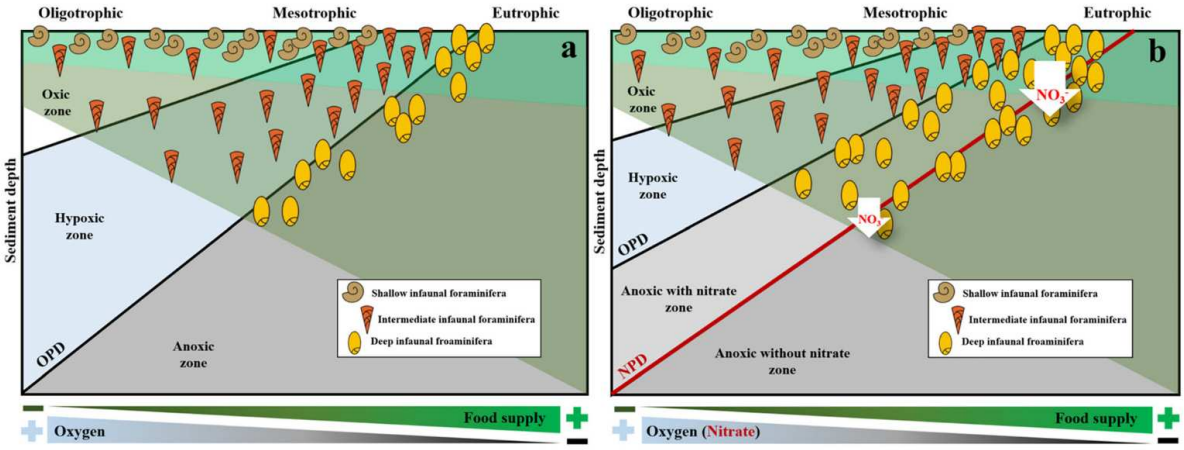

Figure 14. (a) Scheme of the original TROX model (Jorissen et al., 1995) explaining foraminiferal microhabitat distribution in function of oxygen concentrations and food supply with the oxygen penetration depth (OPD). **(b)** Scheme of the modified TROX model including nitrate concentration with the nitrate penetration depth (NPD). Figure modified from Xu et al., (2021).

While investigating foraminiferal distribution within and on the sediment, it is also important to consider biological interactions (i.e., competition, predation). One species, for instance, can feed on different food resources to reduce interspecific competition (Murray, 2006). In general, the environmental parameters influencing foraminiferal microhabitat are linked to the organic flux and to the pelagic-benthic coupling (e.g., Jorissen et al., 1995; Xu et al., 2021).

4.3 Foraminifera in Arctic fjords

In polar regions, as the whole benthic compartment, foraminifera are subjected to a strong seasonality related to biological and physico-chemical processes. In particular, the organic fluxes to the seafloor are not constant all over the year but subjected to pulses. Thus, the benthic system needs to adapt using different feeding strategies. Species may feed on different food resources depending on the season, others may have specific ecological requirements and consequently constrained to specific seasons (e.g., Korsun and Hald, 2000; Bubenshchikova et al., 2008; Skirbekk et al., 2016; Kucharska et al., 2019).

Living benthic foraminifera have been studied in several Arctic fjords of Svalbard archipelago (Korsun et al., 1995; Zajaczkowski et al., 2010; Mackensen and Schmiedl, 2016; Mackensen et al., 2017; Szymańska et al., 2017; Jernas et al., 2018; Saraswat et al., 2018; Kniazeva and Korsun, 2019; Fossile et al., 2020; Kujawa et al., 2021). Recently, Jima et al. (2021) compiled all the literature around Svalbard published between 1984 and 2020. More than 300 species have been identified in Svalbard fjords and foraminiferal gradients have been observed along the main fjord axis going from a shallow glacier proximal inner fjord to a deeper outer fjord. In general, some species are found dominant in outer and middle fjord in a glacier-distal environment (e.g., *Adercotryma glomeratum*) whereas, some other species are commonly found far inside fjords, such as the calcareous *Cassidulina reniforme* and *Elphidium clavatum* in a glacier-proximal environment, or found at variable locations (e.g., *Nonionellina labradorica*) (Jima et al., 2021).

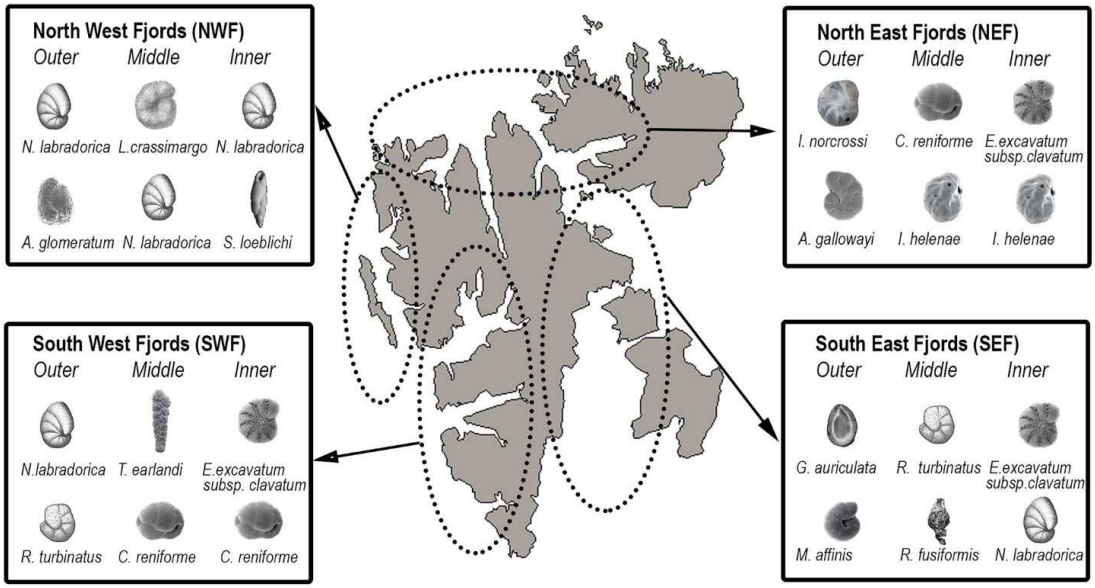

Figure 15. Svalbard map showing the distribution along fjords of the main common species. Figure modified from Jima et al. (2021).

As explained previously, the Svalbard archipelago is under the influence of cold Arctic water as well as warm Atlantic water and often foraminiferal species have been associated to these water masses (e.g., Melis et al., 2018), considered as a whole combination of physico-chemical parameters. The idea that a benthic species or a foraminiferal assemblage is related to certain water mass has long been debated and criticized (e.g., Schnitker, 1974; Mackensen et al., 1993; Schmiedl et al., 1997). There is evidence that water masses (via currents) transport propagules that ultimately settle, grow and reproduce when they reach a suitable environment (e.g., Alve and Goldstein, 2002, 2010). However, as detailed in the previous paragraph, it is well known

that one of the strongest driving parameters for foraminifera distribution is the quantity and quality of organic matter (e.g., Jorissen et al., 1995, 2021), while other water parameters such as temperature or salinity may have a lower influence. The association of specific assemblages to the water masses present in the studied area, therefore, should be interpreted as the ecological response to changing characteristics of the organic matter linked to the different water masses occurring around Svalbard (e.g., Knudsen et al., 2012).

5. Objectives

Sea ice cycles and glacier dynamics are major controlling factors of marine ecology in the Arctic, particularly in coastal areas such as fjords. On the one hand, sea ice cycles influence primary production and water properties through the release of nutrients and fresh water during the melting phase, and through the production of brines during sea ice formation processes. On the other hand, glaciers influence primary production and the pelagic-benthic ecosystem through meltwater discharges and associated sediment loads, inducing a disturbance in proximal environments and physico-chemical gradients in coastal environments. Current climate-induced modifications already impacted sea ice cycles and glaciers and the projected Arctic warming will likely result in continued loss of sea ice and reduction in the mass of glaciers (IPCC, 2019). This has important implications for Arctic marine ecosystems with consequences at different trophic levels in the pelagic and benthic realms (IPCC, 2019).

To predict the potential response of the biosphere to these changes, there is the need to focus on different trophic levels and to understand the major drivers of communities' shifts. It was previously explained that ice-related changes have temporal and spatial influence on physico-chemical parameters (i.e., water and sediment properties) and PP, and thus on organic fluxes to the benthic compartment. In this PhD thesis, we focus on powerful bioindicators, benthic foraminifera, of which the distribution and species composition are strongly influenced by these drivers. The identification of specific foraminiferal ecological responses, so called proxies, to ice-related dynamics such as brine persistence and glacier retreat would help understanding the biosphere response on longer time scales. Indeed, the fossilisation potential of benthic foraminifera, would allow to reconstruct indirectly ice-related changes where direct measurements were not yet established through the application of specific ecological proxies. Historical reconstructions on longer time scales than the current direct observations would allow to obtain better predictions of future changes.

Considering these assumptions, here we use benthic foraminifera as tools to pursue three main objectives:

1. Extend our knowledge on benthic responses to chronical stresses in high latitude environments (i.e., fjords) influenced by different ice-related dynamics;
2. Propose reliable ecological proxies to chronicle recent changes in benthic environments related to ice dynamics;
3. Test the effectiveness of the proposed proxies.

To achieve the first two objectives, living benthic foraminiferal assemblages were analysed in relation to several environmental parameters (i.e., organic inputs, sediment grain size, water masses properties) in two contrasted Svalbard fjords differently influenced by ice-related dynamics and climate-induced modifications (Fig. 16). One is Storfjorden, a fjord affected by strong persistence of brines produced during sea ice formation processes (*Chapter 1*), the other is Kongsfjorden affected by meltwater discharges and the associated transported sediments from tidewater glaciers creating steep environmental gradients (*Chapter 3*). Based on foraminiferal responses to ice-related dynamics in Storfjorden, we propose an ecological proxy for brine persistence and indirectly for sea ice production: the ratio between Agglutinated and Calcareous foraminifera (A/C) (*Chapter 1*). Similarly, we suggest the use of taxonomic and functional diversity metrics as proxies for the distance from tidewater glacier termini and consequently for tidewater glacier retreat (*Chapter 4*). Furthermore, to achieve the third objective, we tested the applicability of the A/C proxy proposed for brine persistence after undergoing taphonomic processes by analysing dead and fossil faunas in comparison with the living faunas at the same Storfjorden locations (*Chapter 2*). In parallel, we test the effectiveness of diversity metrics as proxy for glacier retreat by analysing fossil foraminiferal assemblages along an historical record covering 60 years of retreat in Kongsfjorden (*Chapter 5*).

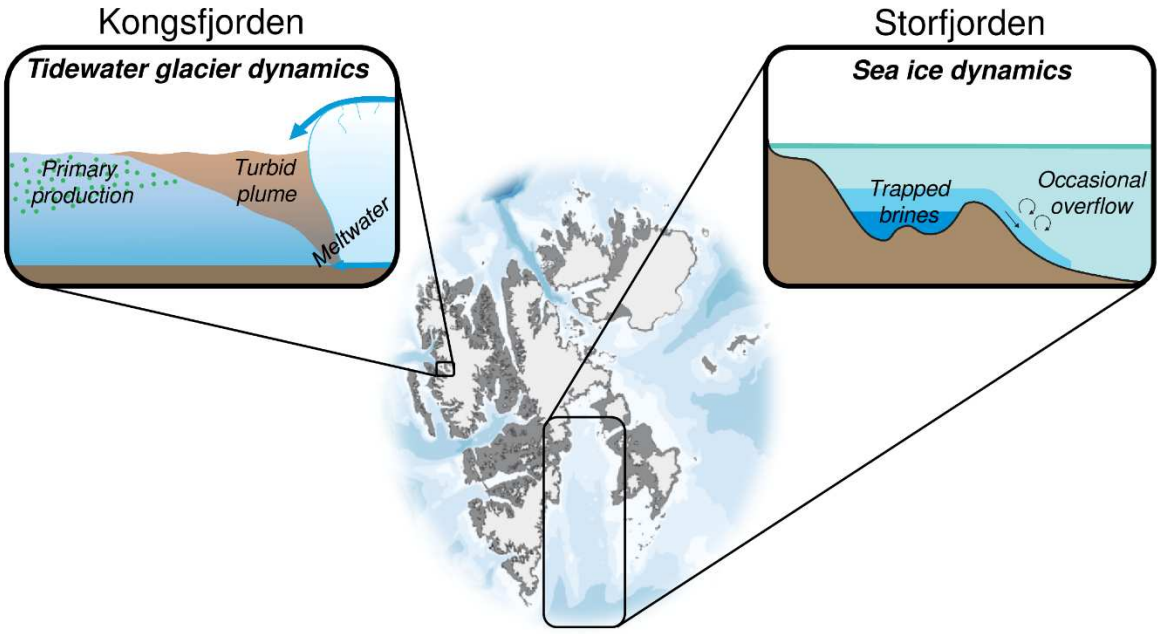

Figure 16. Map of the Svalbard archipelago with focus on the two investigated fjords and the major ice-related dynamics influencing the systems during summer.

6. Context of the PhD thesis

This PhD thesis was co-funded by the first call of the French initiative "Make Our Planet Great Again" (MOPGA) and the University of Angers. The MOPGA program was implemented by France's ministries of Europe and foreign affairs (MEAE) and of higher education, research, and innovation (MESRI). The call was addressed to foreign doctoral candidates wishing to complete a PhD in France on a topic related to earth systems, climate change and sustainability, or the energy transition. In 2018, Pr. Hélène Howa succeed to obtain the funding for the PhD project intitled "*Marine bio-indicators for freeze-thaw cycles of Arctic sea ice; chronicle of recent changes"*. The fees for the analyses associated to the project were sustained by the three projects managed by the associate PhD supervisors Dr. Meryem Mojtahid (ARTICORE – OSUNA, and STING - INSU) and Dr. Maria Pia Nardelli (BI-SMART - Jeunes chercheurs, Université d'Angers). The sampling in Svalbard was organised thanks to the support of IPEV (C3 project, P.I. Pr. Agnès Baltzer).

References

Allen, M.R., O.P. Dube, W. Solecki, F. Aragón-Durand, W. Cramer, S. Humphreys, M. Kainuma, J. Kala, N. Mahowald, Y. Mulugetta, R. Perez, M. Wairiu, and K. Zickfeld: Framing and Context. In: Global Warming of 1.5°C. An IPCC Special Report on the impacts of global warming of 1.5°C above pre-industrial levels and related global greenhouse gas emission pathways, in the context of strengthening the global response to the threat of climate change, sustainable development, and efforts to eradicate poverty [Masson-Delmotte, V., P. Zhai, H.-O. Pörtner, D. Roberts, J. Skea, P.R. Shukla, A. Pirani, W. Moufouma-Okia, C. Péan, R. Pidcock, S. Connors, J.B.R. Matthews, Y. Chen, X. Zhou, M.I. Gomis, E. Lonnoy, T. Maycock, M. Tignor, and T. Waterfield (eds.)]. In Press, 2018.

Adakudlu, M., Andresen, J., Bakke, J., Beldring, S., Benestad, R., Bilt, W., Bogen, J., Borstad, C., Breili, K., Breivik, Ø., Børsheim, K. Y., Christiansen, H. H., Dobler, A., Engeset, R., Frauenfelder, R., Gerland, S., Gjelten, H. M., Gundersen, J., Isaksen, K., Jaedicke, C., Kierulf, H., Kohler, J., Li, H., Lutz, J., Mezghani, A., Nilsen, F., Nilsen, I. B., Nilsen, J. E. Ø., Pavlova, Ravndal, O., Risebrobakken, B., Saloranta, T., Sandven, S., Schuler, T. V., Simpson, M. J. R., Skogen, M., Smedsrud, L. H., Sund, M., Vikhamar-Schuler, D., Westermann, S. and Wong, W. K.: Climate in Svalbard 2100 – a knowledge base for climate adaptation, NCCS Rep., (1), 1–208, 2019.

Adl, S. M., Leander, B. S., Simpson, A. G. B., Archibald, J. M., Anderson, O. R., Bass, D., Bowser, S. S., Brugerolle, G., Farmer, M. A., Karpov, S., Kolisko, M., Lane, C. E., Lodge, D. J., Mann, D. G., Meisterfeld, R., Mendoza, L., Moestrup, Ø., Mozley-Standridge, S. E., Smirnov, A. V. and Spiegel, F.: Diversity, nomenclature, and taxonomy of protists, Syst. Biol., 56(4), 684–689, https://doi.org/10.1080/10635150701494127, 2007.

Adl, S. M., Simpson, A. G. B., Lane, C. E., Lukeš, J., Bass, D., Bowser, S. S., Brown, M. W., Burki, F., Dunthorn, M., Hampl, V., Heiss, A., Hoppenrath, M., Lara, E., Gall, L. Le, Lynn, D. H., McManus, H., Mitchell, E. A. D., Mozley-Stanridge, S. E., Parfrey, L. W., Pawlowski, J., Rueckert, S., Shadwick, L., Schoch, C. L., Smirnov, A. and Spiegel, F. W.: The revised classification of eukaryotes, J. Eukaryot. Microbiol., 59(5), 429–514, https://doi.org/10.1111/j.1550-7408.2012.00644.x, 2012.

Alve, E. and Goldstein, S. T.: Resting stage in benthic foraminiferal propagules: a key feature for dispersal? Evidence from two shallow-water species, J. Micropalaeontology, 21(1), 95–96, https://doi.org/10.1144/jm.21.1.95, 2002.

Alve, E. and Goldstein, S. T.: Dispersal, survival and delayed growth of benthic foraminiferal propagules, J. Sea Res., 63(1), 36–51, https://doi.org/10.1016/j.seares.2009.09.003, 2010.

Barber, D.G. and Massom, R.A.: Chapter 1: The role of sea ice in Arctic and Antarctic polynyas. In: W.O. Smith Jr. and D.G. Barber (eds.). Polynyas: Windows to the world, Elsevier Oceanography Series, 74, Elsevier Science, pp 1-54, 2007.

Bereiter, B., Eggleston, S., Schmitt, J., Nehrbass-Ahles, C., Stocker, T. F., Fischer, H., Kipfstuhl, S. and Chappellaz, J.: Revision of the EPICA Dome C CO_2 record from 800 to 600-kyr before present, Geophys. Res. Lett., 42(2), 542–549, https://doi.org/10.1002/2014GL061957, 2015.

Bianchi, T. S., Arndt, S., Austin, W. E. N., Benn, D. I., Bertrand, S., Cui, X., Faust, J. C., Koziorowska-Makuch, K., Moy, C. M., Savage, C., Smeaton, C., Smith, R. W. and Syvitski, J.: Fjords as Aquatic Critical Zones (ACZs), Earth-Science Rev., 203(February), 103145, https://doi.org/10.1016/j.earscirev.2020.103145, 2020.

Bindoff, N.L., W.W.L. Cheung, J.G. Kairo, J. Arístegui, V.A. Guinder, R. Hallberg, N. Hilmi, N. Jiao, M.S. Karim, L. Levin, S. O'Donoghue, S.R. Purca Cuicapusa, B. Rinkevich, T. Suga, A. Tagliabue, and P. Williamson, 2019: Changing Ocean, Marine Ecosystems, and Dependent Communities. In: IPCC Special Report on the Ocean and Cryosphere in a Changing Climate [H.-O. Pörtner, D.C. Roberts, V. Masson-Delmotte, P. Zhai, M. Tignor, E. Poloczanska, K. Mintenbeck, A. Alegría, M. Nicolai, A. Okem, J. Petzold, B. Rama, N.M. Weyer (eds.)]. In press.

Bouchet, V. M. P., Alve, E., Rygg, B. and Telford, R. J.: Benthic foraminifera provide a promising tool for ecological quality assessment of marine waters, Ecol. Indic., 23(2012), 66–75, https://doi.org/10.1016/j.ecolind.2012.03.011, 2012.

Bouchet, V. M. P., Goberville, E. and Frontalini, F.: Benthic foraminifera to assess Ecological Quality Statuses in Italian transitional waters, Ecol. Indic., 84(January 2017), 130–139, https://doi.org/10.1016/j.ecolind.2017.07.055, 2018.

Boyd, P. W. and Trull, T. W.: Understanding the export of biogenic particles in oceanic waters: Is there consensus?, Prog. Oceanogr., 72(4), 276–312, https://doi.org/10.1016/j.pocean.2006.10.007, 2007.

Bradley, R. S. and Bakke, J.: Is there evidence for a 4.2 kaBP event in the northern North Atlantic region?, Clim. Past, 15(5), 1665–1676, https://doi.org/10.5194/cp-15-1665-2019, 2019.

Bradley R.S., Briffa K.R., Cole J., Hughes M.K., Osborn T.J. (2003) The Climate of the Last Millennium. In: Alverson K.D., Pedersen T.F., Bradley R.S. (eds) Paleoclimate, Global Change and the Future. Global Change — The IGBP Series. Springer, Berlin, Heidelberg. https://doi.org/10.1007/978-3-642-55828-3_6

Bubenshchikova, N., Nürnberg, D., Lembke-Jene, L. and Pavlova, G.: Living benthic foraminifera of the Okhotsk Sea: Faunal composition, standing stocks and microhabitats, Mar. Micropaleontol., 69(3–4), 314–333, https://doi.org/10.1016/j.marmicro.2008.09.002, 2008.

Cogley, J. G., Hock, R., Rasmussen, L. A., Arendt, A. A., Bauder, A., Braithwaite, R. J., Jansson, P., Kaser, G., Möller, M., Nicholson, L. and Zemp, M.: Glossary of glacier mass balance and related terms, UNESCO/IHP, Paris., 2011.

Cottier, F., Tverberg, V., Inall, M., Svendsen, H., Nilsen, F. and Griffiths, C.: Water mass modification in an Arctic fjord through cross-shelf exchange: The seasonal hydrography of Kongsfjorden, Svalbard, J. Geophys. Res. Ocean., 110(12), 1–18, https://doi.org/10.1029/2004JC002757, 2005.

Cottier, F. R., Nilsen, F., Skogseth, R., Tverberg, V., Skarðhamar, J. and Svendsen, H.: Arctic fjords: a review of the oceanographic environment and dominant physical processes, Geol. Soc. London, Spec. Publ., 344, 35–50, https://doi.org/10.1144/sp344.4, 2010.

Dai, A., Luo, D., Song, M. and Liu, J.: Arctic amplification is caused by sea-ice loss under increasing CO2, Nat. Commun., 10(1), 1–13, https://doi.org/10.1038/s41467-018-07954-9, 2019.

Descamps, S., Aars, J., Fuglei, E., Kovacs, K. M., Lydersen, C., Pavlova, O., Pedersen, Å., Ravolainen, V. and Strøm, H.: Climate change impacts on wildlife in a High Arctic archipelago – Svalbard, Norway, Glob. Chang. Biol., 23(2), 490–502, https://doi.org/10.1111/gcb.13381, 2017.

Deser, C.: On the Teleconnectivity of the "Arctic Oscillation," Geophys. Res. Lett., 27(6), 779–782, https://doi.org/10.1029/1999GL010945, 2000.

Dimiza, M. D., Triantaphyllou, M. V., Koukousioura, O., Hallock, P., Simboura, N., Karageorgis, A. P. and Papathanasiou, E.: The Foram Stress Index: A new tool for environmental assessment of soft-bottom environments using benthic foraminifera. A case study from the Saronikos Gulf, Greece, Eastern Mediterranean, Ecol. Indic., 60, 611–621, https://doi.org/10.1016/j.ecolind.2015.07.030, 2016.

Dybwad, C., Assmy, P., Olsen, L. M., Peeken, I., Nikolopoulos, A., Krumpen, T., Randelhoff, A., Tatarek, A., Wiktor, J. M. and Reigstad, M.: Carbon Export in the Seasonal Sea Ice Zone North of Svalbard From Winter to Late Summer, Front. Mar. Sci., 7(January), 1–21, https://doi.org/10.3389/fmars.2020.525800, 2021.

Fossile, E., Nardelli, M. P., Jouini, A., Lansard, B., Pusceddu, A., Moccia, D., Michel, E., Péron, O., Howa, H. and Mojtahid, M.: Benthic foraminifera as tracers of brine production in the Storfjorden "sea ice factory," Biogeosciences, 17(7), 1933–1953, https://doi.org/10.5194/bg-17-1933-2020, 2020.

Fox-Kemper, B., H.T. Hewitt, C. Xiao, G. Aðalgeirsdóttir, S.S. Drijfhout, T.L. Edwards, N.R. Golledge, M. Hemer, R.E. Kopp, G. Krinner, A. Mix, D. Notz, S. Nowicki, I.S. Nurhati, L. Ruiz, J.-B. Sallée, A.B.A. Slangen, and Y. Yu, 2021: Ocean, Cryosphere and Sea Level Change. In Climate Change 2021: The Physical Science Basis. Contribution of Working Group I to the Sixth Assessment Report of the Intergovernmental Panel on Climate Change [Masson-Delmotte, V., P. Zhai, A. Pirani, S.L. Connors, C. Péan, S. Berger, N. Caud, Y. Chen, L. Goldfarb, M.I. Gomis, M. Huang, K. Leitzell, E. Lonnoy, J.B.R. Matthews, T.K. Maycock, T. Waterfield, O. Yelekçi, R. Yu, and B. Zhou (eds.)]. Cambridge University Press. In Press.

Gooday, A. J.: Benthic foraminifera (protista) as tools in deep-water palaeoceanography: Environmental influences on faunal characteristics, Adv. Mar. Biol., 46, 1–90, https://doi.org/10.1016/S0065-2881(03)46002-1, 2003.

Graversen, R. G., Mauritsen, T., Tjernström, M., Källén, E. and Svensson, G.: Vertical structure of recent Arctic warming, Nature, 451(7174), 53–56, https://doi.org/10.1038/nature06502, 2008.

Haarpaintner, J., Gascard, J. and Haugan, P. M.: Ice production and brine formation in Storfjorden, Svalbard, J. Geophys. Res. Ocean., 106(C7), 14001–14013, https://doi.org/10.1029/1999JC000133, 2001.

Halbach, L., Vihtakari, M., Duarte, P., Everett, A., Granskog, M. A., Hop, H., Kauko, H. M., Kristiansen, S., Myhre, P. I., Pavlov, A. K., Pramanik, A., Tatarek, A., Torsvik, T., Wiktor, J., Wold, A., Wulff, A., Steen, H.

and Assmy, P.: Tidewater Glaciers and Bedrock Characteristics Control the Phytoplankton Growth Environment in a Fjord in the Arctic, Front. Mar. Sci., 6(254), https://doi.org/10.3389/fmars.2019.00254, 2019.

Hallock, P.: The FoRAM Index revisited: uses, challenges, and limitations, Proc. 12th Int. Coral Reef …, (July), 9–13 http://www.icrs2012.com/proceedings/manuscripts/ICRS2012_15F_2.pdf, 2012.

Hallock, P., Lidz, B. H., Cockey-Burkhard, E. M. and Donnelly, K. B.: Foraminifera as bioindicators in coral reef assessment and monitoring: The foram index, Environ. Monit. Assess., 81(1–3), 221–238, https://doi.org/10.1023/A:1021337310386, 2003.

Hegerl, G. C., F. W. Zwiers, Braconnot, P., Gillett, N. P., Luo, Y., Orsini, J. A. M., Nicholls, N., Penner, J. E. and Stott, P. A.: Understanding and Attributing Climate Change, in Climate Change 2007: The Physical Science Basis. Contribution of Working Group I to the Fourth Assessment Report of the Intergovernmental Panel on Climate Change, vol. 80, edited by S. Solomon, D. Qin, M. Manning, Z. Chen, M. Marquis, K. B. Averyt, M. Tignor, and H. L. Miller, pp. 213–238, Cambridge University Press, Cambridge, United Kingdom and New York, NY, USA, https://www.ipcc.ch/pdf/assessment-report/ar4/wg1/ar4-wg1-chapter9.pdf, 2007.

Holland, M. M. and Bitz, C. M.: Polar amplification of climate change in coupled models, Clim. Dyn., 21(3–4), 221–232, https://doi.org/10.1007/s00382-003-0332-6, 2003.

Holzmann, M., Gooday, A. J., Siemensma, F. and Pawlowski, J.: Review: Freschwater and soil foraminifera - A story of long-forgotten relatives, J. Foraminifer. Res., 51(4), 318–331, 2021.

Hop, H., Pearson, T., Hegseth, E. N., Kovacs, K. M., Wiencke, C., Kwasniewski, S., Eiane, K., Mehlum, F., Gulliksen, B., Wlodarska-Kowalezuk, M., Lydersen, C., Weslawski, J. M., Cochrane, S., Gabrielsen, G. W., Leakey, R. J. G., Lonne, O. J., Zajaczkowski, M., Falk-Petersen, S., Kendall, M., Wangberg, S. A., Bischof, K., Voronkov, A. Y., Kovaltchouk, N. A., Wiktor, J., Poltermann, M., di Prisco, G., Papucci, C. and Gerland, S.: The marine ecosystem of Kongsfjorden, Svalbard, Polar Res., 21(1), 167–208, https://doi.org/https://doi.org/10.3402/polar.v21i1.6480, 2002.

Hopwood, M. J., Carroll, D., Browning, T. J., Meire, L., Mortensen, J., Krisch, S. and Achterberg, E. P.: Non-linear response of summertime marine productivity to increased meltwater discharge around Greenland, Nat. Commun., 9(1), https://doi.org/10.1038/s41467-018-05488-8, 2018.

Hopwood, M. J., Carroll, D., Dunse, T., Hodson, A., Holding, J. M., Iriarte, J. L., Ribeiro, S., Achterberg, E. P., Cantoni, C., Carlson, D. F., Chierici, M., Clarke, J. S., Cozzi, S., Fransson, A., Juul-Pedersen, T., Winding, M. H. S. and Meire, L.: Review article: How does glacier discharge affect marine biogeochemistry and primary production in the Arctic?, Cryosphere, 14(4), 1347–1383, https://doi.org/10.5194/tc-14-1347-2020, 2020.

How, P., Benn, D. I., Hulton, N. R. J., Hubbard, B., Luckman, A., Sevestre, H., Pelt, W. J. J. V., Lindbäck, K., Kohler, J. and Boot, W.: Rapidly changing subglacial hydrological pathways at a tidewater glacier revealed through simultaneous observations of water pressure, supraglacial lakes, meltwater plumes and surface velocities, Cryosphere, 11(6), 2691–2710, https://doi.org/10.5194/tc-11-2691-2017, 2017.

Howe, J. A., Austin, W. E. N., Forwick, M., Paetzel, M., Harland, R. E. X. and Cage, A. G.: Fjord systems and archives : a review, Fjord Syst. Arch., 5–15, https://doi.org/10.1144/SP344.2, 2010.

Hurrell, J. W., Kushnir, Y., Ottersen, G. and Visbeck, M.: An overview of the north atlantic oscillation, Geophys. Monogr. Ser., 134, 1–35, https://doi.org/10.1029/134GM01, 2003.

IPCC, 2019: Technical Summary [H.-O. Pörtner, D.C. Roberts, V. Masson-Delmotte, P. Zhai, E. Poloczanska, K. Mintenbeck, M. Tignor, A. Alegría, M. Nicolai, A. Okem, J. Petzold, B. Rama, N.M. Weyer (eds.)]. In: IPCC Special Report on the Ocean and Cryosphere in a Changing Climate [H.- O. Pörtner, D.C. Roberts, V. Masson-Delmotte, P. Zhai, M. Tignor, E. Poloczanska, K. Mintenbeck, A. Alegría, M. Nicolai, A. Okem, J. Petzold, B. Rama, N.M. Weyer (eds.)]. In press, 2019.

IPCC, 2021: Summary for Policymakers. In: Climate Change 2021: The Physical Science Basis. Contribution of Working Group I to the Sixth Assessment Report of the Intergovernmental Panel on Climate Change [Masson-Delmotte, V., P. Zhai, A. Pirani, S.L. Connors, C. Péan, S. Berger, N. Caud, Y. Chen, L. Goldfarb, M.I. Gomis, M. Huang, K. Leitzell, E. Lonnoy, J.B.R. Matthews, T.K. Maycock, T. Waterfield, O. Yelekçi, R. Yu, and B. Zhou (eds.)]. In Press, 2021.

Ivanov, V. V., Shapiro, G. I., Huthnance, J. M., Aleynik, D. L. and Golovin, P. N.: Cascades of dense water around the world ocean., 2004.

Jansen, E., Overpeck, J., Briffa, K. R., Duplessy, J.-C., Joos, F., Masson-Delmotte, V., Olago, D., Otto-Bliesner, B., Peltier, W. R., Rahmstorf, S., Ramesh, R., Raynaud, D., Rind, D., Solomina, O., Villalba, R. and Zhang, D.: Paleoclimate, in Climate Change 2007: The Physical Science Basis. Contribution of Working Group I to

the Fourth Assessment Report of the Intergovernmental Panel on Climate Change, edited by S. Solomon, D. Qin, M. Manning, Z. Chen, M. Marquis, K. B. Averyt, M. Tignor, and H. L. Miller, Cambridge University Press, Cambridge, United Kingdom and New York, NY, USA, https://doi.org/10.1007/978-94-007-5784-4_45, , 2007.

Jauffrais, T., Jesus, B., Metzger, E., Mouget, J. L., Jorissen, F. and Geslin, E.: Effect of light on photosynthetic efficiency of sequestered chloroplasts in intertidal benthic foraminifera (Haynesina germanica and Ammonia tepida), Biogeosciences, 13(9), 2715–2726, https://doi.org/10.5194/bg-13-2715-2016, 2016.

Jernas, P., Klitgaard-Kristensen, D., Husum, K., Koç, N., Tverberg, V., Loubere, P., Prins, M., Dijkstra, N. and Gluchowska, M.: Annual changes in Arctic fjord environment and modern benthic foraminiferal fauna: Evidence from Kongsfjorden, Svalbard, Glob. Planet. Change, 163(November 2017), 119–140, https://doi.org/10.1016/j.gloplacha.2017.11.013, 2018.

Jima, M., Jayachandran, P. R. and Nandan, S. B.: Modern Benthic Foraminiferal Diversity Along the Fjords of Svalbard Archipelago : Diversity Evaluation, Thalass. An Int. J. Mar. Sci., https://doi.org/10.1007/s41208-021-00356-7, 2021.

Jorissen, F., Nardelli, M. P., Almogi-Labin, A., Barras, C., Bergamin, L., Bicchi, E., El Kateb, A., Ferraro, L., McGann, M., Morigi, C., Romano, E., Sabbatini, A., Schweizer, M. and Spezzaferri, S.: Developing Foram-AMBI for biomonitoring in the Mediterranean: Species assignments to ecological categories, Mar. Micropaleontol., 140(January), https://doi.org/10.1016/j.marmicro.2017.12.006, 2018.

Jorissen, F. J.: Benthic foraminiferal microhabitats below the sediment-water interface, in Modern Foraminifera, vol. Chapter 10, edited by B. K. Sen Gupta, pp. 161–179, Kluwer Academic Publisher, Great Bri, , 1999.

Jorissen, F. J., de Stigter, H. C. and Widmark, J. G. V: A conceptual model explaining benthic foraminiferal microhabitats, Mar. Micropaleontol., 26, 3–15, https://doi.org/10.1016/0377-8398(95)00047-X, 1995.

Jorissen, F. J., Meyers, S. R., Kelly-Gerreyn, B. A., Huchet, L., Mouret, A. and Anschutz, P.: The 4GFOR model – Coupling 4G early diagenesis and benthic foraminiferal ecology, Mar. Micropaleontol., 170(December 2021), 102078, https://doi.org/10.1016/j.marmicro.2021.102078, 2021.

Katz, M. E., Cramer, B. S., Franzese, A., Hönisch, B., Miller, K. G., Rosenthal, Y. and Wright, J. D.: Traditional and emerging geochemical proxies in foraminifera, J. Foraminifer. Res., 40(2), 165–192, https://doi.org/10.2113/gsjfr.40.2.165, 2010.

Kniazeva, O. and Korsun, S.: Seasonal data on Rose Bengal stained foraminifera in the head of Kongsfjorden, Svalbard, Data Br., 25, 104040, https://doi.org/10.1016/j.dib.2019.104040, 2019.

Knudsen, K. L., Eiríksson, J. and Bartels-Jónsdóttir, H. B.: Oceanographic changes through the last millennium off North Iceland: Temperature and salinity reconstructions based on foraminifera and stable isotopes, Mar. Micropaleontol., 84–85, 54–73, https://doi.org/10.1016/j.marmicro.2011.11.002, 2012.

Korsun, S. and Hald, M.: Seasonal dynamics of Benthic Foraminifera in a Glacially Fed Fjord of Svalbard, European Arctic, J. Foraminifer. Res., 30(4), 251–271, https://doi.org/10.2113/0300251, 2000.

Korsun, S. A., Pogodina, I. A., Forman, S. L. and Lubinski, D. J.: Recent foraminifera in glaciomarine sediments from three arctic fjords of Novaja Zemlja and Svalbard, Polar Res., 14(1), 15–32, https://doi.org/10.3402/polar.v14i1.6648, 1995.

Koukousioura, O., Dimiza, M. D., Triantaphyllou, M. V. and Hallock, P.: Living benthic foraminifera as an environmental proxy in coastal ecosystems: A case study from the Aegean Sea (Greece, NE Mediterranean), J. Mar. Syst., 88(4), 489–501, https://doi.org/10.1016/j.jmarsys.2011.06.004, 2011.

Kucharska, M., Kujawa, A., Pawłowska, J., Łącka, M., Szymańska, N., Lønne, O. J. and Zajączkowski, M.: Seasonal changes in foraminiferal assemblages along environmental gradients in Adventfjorden (West Spitsbergen), Polar Biol., 42(3), 569–580, https://doi.org/10.1007/s00300-018-02453-5, 2019.

Kujawa, A., Łącka, M., Szymańska, N., Pawłowska, J., Telesiński, M. M. and Zajączkowski, M.: Could Norwegian fjords serve as an analogue for the future of the Svalbard fjords? State and fate of high latitude fjords in the face of progressive "atlantification," Polar Biol., (2016), https://doi.org/https://doi.org/10.1007/s00300-021-02951-z, 2021.

Lee, R. F., Hagen, W. and Kattner, G.: Lipid storage in marine zooplankton, Mar. Ecol. Prog. Ser., 307(1863), 273–306, https://doi.org/10.3354/meps307273, 2006.

LeKieffre, C., Bernhard, J. M., Mabilleau, G., Filipsson, H. L., Meibom, A. and Geslin, E.: An overview of cellular ultrastructure in benthic foraminifera: New observations of rotalid species in the context of existing literature, Mar. Micropaleontol., 138(October 2017), 12–32, https://doi.org/10.1016/j.marmicro.2017.10.005, 2018.

Leu, E., Søreide, J. E., Hessen, D. O., Falk-Petersen, S. and Berge, J.: Consequences of changing sea-ice cover for primary and secondary producers in the European Arctic shelf seas: Timing, quantity, and quality, Prog. Oceanogr., 90(1–4), 18–32, https://doi.org/10.1016/j.pocean.2011.02.004, 2011.

Lopez, E.: Algal chloroplasts in the protoplasm of three species of benthic foraminifera: taxonomic affinity, viability and persistence, Mar. Biol., 53(3), 201–211, https://doi.org/10.1007/BF00952427, 1979.

Luckman, A., Benn, D. I., Cottier, F., Bevan, S., Nilsen, F. and Inall, M.: Calving rates at tidewater glaciers vary strongly with ocean temperature, Nat. Commun., 6, https://doi.org/10.1038/ncomms9566, 2015.

Lüthi, D., Le Floch, M., Bereiter, B., Blunier, T., Barnola, J. M., Siegenthaler, U., Raynaud, D., Jouzel, J., Fischer, H., Kawamura, K. and Stocker, T. F.: High-resolution carbon dioxide concentration record 650,000-800,000 years before present, Nature, 453(7193), 379–382, https://doi.org/10.1038/nature06949, 2008.

Lydersen, C., Assmy, P., Falk-Petersen, S., Kohler, J., Kovacs, K. M., Reigstad, M., Steen, H., Strøm, H., Sundfjord, A., Varpe, Ø., Walczowski, W., Weslawski, J. M. and Zajaczkowski, M.: The importance of tidewater glaciers for marine mammals and seabirds in Svalbard, Norway, J. Mar. Syst., 129, 452–471, https://doi.org/10.1016/j.jmarsys.2013.09.006, 2014.

Mace, G. M., Reyers, B., Alkemade, R., Biggs, R., Chapin, F. S., Cornell, S. E., Díaz, S., Jennings, S., Leadley, P., Mumby, P. J., Purvis, A., Scholes, R. J., Seddon, A. W. R., Solan, M., Steffen, W. and Woodward, G.: Approaches to defining a planetary boundary for biodiversity, Glob. Environ. Chang., 28(1), 289–297, https://doi.org/10.1016/j.gloenvcha.2014.07.009, 2014.

Mackensen, A. and Schmiedl, G.: Brine formation recorded by stable isotopes of Recent benthic foraminifera in Storfjorden, Svalbard: palaeoceanographical implications, Boreas, 45(3), 552–566, https://doi.org/10.1111/bor.12174, 2016.

Mackensen, A., Fütterer, D. K., Grobe, H. and Schmiedl, G.: Benthic foraminiferal assemblages from the eastern South Atlantic Polar Front region between 35° and 57°S: Distribution, ecology and fossilization potential, Mar. Micropaleontol., 22, 33–69, https://doi.org/10.1016/0377-8398(93)90003-G, 1993.

Mackensen, A., Schmiedl, G., Thiele, J. and Damm, E.: Microhabitat preferences of live benthic foraminifera and stable carbon isotopes off SW Svalbard in the presence of widespread methane seepage, Mar. Micropaleontol., 132, 1–17, https://doi.org/10.1016/j.marmicro.2017.04.004, 2017.

Martin, S.: Polynyas, Encycl. Ocean Sci., (August 2018), 175–180, https://doi.org/10.1016/B978-0-12-409548-9.11477-0, 2019.

Melis, R., Carbonara, K., Villa, G., Morigi, C., Bárcena, M. A., Giorgetti, G., Caburlotto, A., Rebesco, M. and Lucchi, R. G.: A new multi-proxy investigation of Late Quaternary palaeoenvironments along the north-western Barents Sea (Storfjorden Trough Mouth Fan), J. Quat. Sci., 33(6), 662–676, https://doi.org/10.1002/jqs.3043, 2018.

Meltofte, H.: Arctic Biodiversity Assessment Status and Trends in Arctic Biodiversity. Conservation of Arctic Flora and Fauna, Akureyri, Iceland, 2013

Meredith, M., M. Sommerkorn, S. Cassotta, C. Derksen, A. Ekaykin, A. Hollowed, G. Kofinas, A. Mackintosh, J. Melbourne-Thomas, M.M.C. Muelbert, G. Ottersen, H. Pritchard, and E.A.G. Schuur: Polar Regions. In: IPCC Special Report on the Ocean and Cryosphere in a Changing Climate [H.-O. Pörtner, D.C. Roberts, V. Masson-Delmotte, P. Zhai, M. Tignor, E. Poloczanska, K. Mintenbeck, A. Alegría, M. Nicolai, A. Okem, J. Petzold, B. Rama, N.M. Weyer (eds.)]. In press, 2019

Meslard, F., Bourrin, F., Many, G. and Kerhervé, P.: Suspended particle dynamics and fluxes in an Arctic fjord (Kongsfjorden, Svalbard), Estuar. Coast. Shelf Sci., 204, 212–224, https://doi.org/10.1016/j.ecss.2018.02.020, 2018.

Moreno-Ibáñez, M., Hagen, J. O., Hübner, C., Lihavainen, H. and Zaborska, A.: SESS REPORT 2020, Svalbard Integrated Arctic Earth Observing System, Longyearbyen., 2020.

Murray, J. W.: Ecology and Palaeoecology of Benthic Foraminifera, Taylor & Francis, New York., 1991.

Murray, J. W.: The niche of benthic foraminifera, critical thresholds and proxies, Mar. Micropaleontol., 41(1–2), 1–7, https://doi.org/10.1016/S0377-8398(00)00057-8, 2001.

Murray, J. W.: Ecology and Application of Benthic Foraminifera, Cambridge University Press, Cambridge, New York., 2006.

Nesje, A.: Paleo-ELAs, in Encyclopedia of Quaternary Science, pp. 882–892, https://doi.org/10.1016/B978-0-444-53643-3.00079-0, , 2007.

Nilsen, F., Cottier, F., Skogseth, R. and Mattsson, S.: Fjord-shelf exchanges controlled by ice and brine production: The interannual variation of Atlantic Water in Isfjorden, Svalbard, Cont. Shelf Res., 28(14), 1838–1853, https://doi.org/10.1016/j.csr.2008.04.015, 2008.

Nordli, Ø., Wyszyński, P., Gjelten, H. M., Isaksen, K., Łupikasza, E., Niedźwiedź, T. and Przybylak, R.: Revisiting the extended svalbard airport monthly temperature series, and the compiled corresponding daily series 1898–2018, Polar Res., 39, 1–15, https://doi.org/10.33265/polar.v39.3614, 2020.

Overland, J. E., Dethloff, K., Francis, J. A., Hall, R. J., Hanna, E., Kim, S. J., Screen, J. A., Shepherd, T. G. and Vihma, T.: Nonlinear response of mid-latitude weather to the changing Arctic, Nat. Clim. Chang., 6(11), 992–999, https://doi.org/10.1038/nclimate3121, 2016.

Pawlowski, J. and Holzmann, M.: Molecular phylogeny of Foraminifera - A review, Eur. J. Protistol., 38(1), 1–10, https://doi.org/10.1078/0932-4739-00857, 2002.

Pawlowski, J., Majewski, W., Longet, D., Guiard, J., Cedhagen, T., Gooday, A. J., Korsun, S., Habura, A. A. and Bowser, S. S.: Genetic differentiation between Arctic and Antarctic monothalamous foraminiferans, Polar Biol., 31(10), 1205–1216, https://doi.org/10.1007/s00300-008-0459-3, 2008.

Pillet, L., de Vargas, C. and Pawlowski, J.: Molecular identification of sequestered diatom chloroplasts and kleptoplastidy in foraminifera, Protist, 162(3), 394–404, https://doi.org/10.1016/j.protis.2010.10.001, 2011.

Piña-Ochoa, E., Høgslund, S., Geslin, E., Cedhagen, T., Revsbech, N. P., Nielsen, L. P., Schweizer, M., Jorissen, F., Rysgaard, S. and Risgaard-Petersen, N.: Widespread occurrence of nitrate storage and denitrification among Foraminifera and Gromiida, Proc. Natl. Acad. Sci. U. S. A., 107(3), 1148–1153, https://doi.org/10.1073/pnas.0908440107, 2010.

R Core Team: R: A language and environment for statistical computing. R Foundation for Statistical Computing, Vienna, Austria. URL https://www.R-project.org/, 2020

Risgaard-Petersen, N., Langezaal, A. M., Ingvardsen, S., Schmid, M. C., Jetten, M. S. M., Op Den Camp, H. J. M., Derksen, J. W. M., Piña-Ochoa, E., Eriksson, S. P., Nielsen, L. P., Revsbech, N. P., Cedhagen, T. and Van Der Zwaan, G. J.: Evidence for complete denitrification in a benthic foraminifer, Nature, 443(7107), 93–96, https://doi.org/10.1038/nature05070, 2006.

Rose, J.: Quaternary climates: a perspective for global warming. Proceedings of the Geologists' Association 121, 334–341, 2010.

Rysgaard, S., Bendtsen, J., Delille, B., Dieckmann, G. S., Glud, R. N., Kennedy, H., Mortensen, J., Papadimitriou, S., Thomas, D. N. and Tison, J. L.: Sea ice contribution to the air-sea CO_2 exchange in the Arctic and Southern Oceans, Tellus, Ser. B Chem. Phys. Meteorol., 63(5), 823–830, https://doi.org/10.1111/j.1600-0889.2011.00571.x, 2011.

Sabbatini, A., Morigi, C., Nardelli, M. P. and Negri, A.: Foraminifera, in The Mediterranean Sea: Its History and Present Challenges, edited by S. Goffredo and Z. Dubinsky, pp. 237–256, Springer, Dordrecht, https://doi.org/10.1007/978-94-007-6704-1, 2013.

Saraswat, R., Roy, C., Khare, N., Saalim, S. M. and Kurtarkar, S. R.: Assessing the environmental significance of benthic foraminiferal morpho-groups from the northern high latitudinal regions, Polar Sci., 18(August), 28–38, https://doi.org/10.1016/j.polar.2018.08.002, 2018.

Schauer, U., Fahrbach, E., Osterhus, S. and Rohardt, G.: Arctic warming through the Fram Strait: Oceanic heat transport from 3 years of measurements, J. Geophys. Res. C Ocean., 109(6), 1–14, https://doi.org/10.1029/2003JC001823, 2004.

Schmiedl, G.: Use of foraminifera in climate science. Oxford Research Encyclopedia of Climate Science, Oxford University Press, doi: 10.1093/acrefore/9780190228620.013.735, 2019

Schiebel, R. and Hemleben, C.: Ecology, in Planktic Foraminifers in the Modern Ocean, Springer Berlin Heidelberg, Berlin, Heidelberg, Germany, 209–230, 2017.

Schmiedl, G., Mackensen, A. and Müller, P. J.: Recent benthic foraminifera from the eastern South Atlantic Ocean: Dependence on food supply and water masses, Mar. Micropaleontol., 32(3–4), 249–287, https://doi.org/10.1016/S0377-8398(97)00023-6, 1997.

Schnitker, D.: West Atlantic abyssal circulation during the past 120,000 years, Nature, 248, 385–387, https://doi.org/10.1038/248385a0, 1974.

Schönfeld, J., Alve, E., Geslin, E., Jorissen, F., Korsun, S., Spezzaferri, S., Abramovich, S., Almogi-Labin, A., du Chatelet, E. A., Barras, C., Bergamin, L., Bicchi, E., Bouchet, V., Cearreta, A., Di Bella, L., Dijkstra, N., Disaro, S. T., Ferraro, L., Frontalini, F., Gennari, G., Golikova, E., Haynert, K., Hess, S., Husum, K., Martins, V., McGann, M., Oron, S., Romano, E., Sousa, S. M. and Tsujimoto, A.: The FOBIMO (FOraminiferal BIo-MOnitoring) initiative-Towards a standardised protocol for soft-bottom benthic foraminiferal monitoring studies, Mar. Micropaleontol., 94–95, 1–13, https://doi.org/10.1016/j.marmicro.2012.06.001, 2012.

Screen, J. A. and Simmonds, I.: The central role of diminishing sea ice in recent Arctic temperature amplification, Nature, 464(7293), 1334–1337, https://doi.org/10.1038/nature09051, 2010.

Screen, J. A., Deser, C. and Simmonds, I.: Local and remote controls on observed Arctic warming, Geophys. Res. Lett., 39(10), 1–5, https://doi.org/10.1029/2012GL051598, 2012.

Skirbekk, K., Hald, M., Marchitto, T. M., Junttila, J., Kristensen, D. K. and Sørensen, S. A.: Benthic foraminiferal growth seasons implied from Mg/Ca-temperature correlations for three Arctic species, Geochemistry, Geophys. Geosystems, 17, 4684–4704, https://doi.org/doi:10.1002/2016GC006505, 2016.

Snyder, C. W.: Evolution of global temperature over the past two million years, Nature, 538(7624), 226–228, https://doi.org/10.1038/nature19798, 2016.

Streuff, K., Forwick, M., Szczuciński, W., Andreassen, K. and Ó Cofaigh, C.: Submarine landform assemblages and sedimentary processes related to glacier surging in Kongsfjorden, Svalbard, Arktos, 1(1), 14, https://doi.org/10.1007/s41063-015-0003-y, 2015.

Stuecker, M. F., Bitz, C. M., Armour, K. C., Proistosescu, C., Kang, S. M., Xie, S. P., Kim, D., McGregor, S., Zhang, W., Zhao, S., Cai, W., Dong, Y. and Jin, F. F.: Polar amplification dominated by local forcing and feedbacks, Nat. Clim. Chang., 8(12), 1076–1081, https://doi.org/10.1038/s41558-018-0339-y, 2018.

Svendsen, H., Beszczynska-Møller, A., Hagen, J. O., Lefauconnier, B., Tverberg, V., Gerland, S., Ørbæk, J. B., Bischof, K., Papucci, C., Zajaczkowski, M., Azzolini, R., Bruland, O., Wiencke, C., Winther, J.-G. and Dallmann, W.: The physical environment of Kongsfjorden – Krossfjorden, an Arctic fjord system in Svalbard, Polar Res., 21(1), 133–166, https://doi.org/10.3402/polar.v21i1.6479, 2002.

Szymańska, N., Pawłowska, J., Kucharska, M., Kujawa, A., Łącka, M. and Zajączkowski, M.: Impact of shelf-transformed waters (STW) on foraminiferal assemblages in the outwash and glacial fjords of Adventfjorden and Hornsund, Svalbard, Oceanologia, 59(4), 525–540, https://doi.org/10.1016/j.oceano.2017.04.006, 2017.

Tedstone, A. J., Nienow, P. W., Gourmelen, N., Dehecq, A., Goldberg, D. and Hanna, E.: Decadal slowdown of a land-terminating sector of the Greenland Ice Sheet despite warming, Nature, 526(7575), 692–695, https://doi.org/10.1038/nature15722, 2015.

Tierney, J. E., Pausata, F. S. R. and De Menocal, P. B.: Rainfall regimes of the Green Sahara, Sci. Adv., 3(1), 1–10, https://doi.org/10.1126/sciadv.1601503, 2017.

Tremblay, J. É., Anderson, L. G., Matrai, P., Coupel, P., Bélanger, S., Michel, C. and Reigstad, M.: Global and regional drivers of nutrient supply, primary production and CO_2 drawdown in the changing Arctic Ocean, Prog. Oceanogr., 139, 171–196, https://doi.org/10.1016/j.pocean.2015.08.009, 2015.

Tverberg V., Skogseth R., Cottier F., Sundfjord A., Walczowski W., Inall M. E., Falck E., Pavlova O., and Nilsen F.: The Kongsfjorden Transect: Seasonal and Inter-annual Variability in Hydrography. In: Hop H., Wiencke C. (eds) The Ecosystem of Kongsfjorden, Svalbard. Advances in Polar Ecology, vol 2. Springer, Cham. https://doi.org/10.1007/978-3-319-46425-1_3, 2019

Vihtakari M.: PlotSvalbard: PlotSvalbard - Plot research data from Svalbard on maps. R package version 0.9.2. https://github.com/MikkoVihtakari/PlotSvalbard, 2020

Wadhams P.:The Seasonal Ice Zone. In: Untersteiner N. (eds) The Geophysics of Sea Ice. NATO ASI Series (Series B: Physics). Springer, Boston, MA. https://doi.org/10.1007/978-1-4899-5352-0_15, 1986.

Wassmann, P.: Arctic marine ecosystems in an era of rapid climate change, Prog. Oceanogr., 90(1–4), 1–17, https://doi.org/10.1016/j.pocean.2011.02.002, 2011.

Wassmann, P. and Reigstad, M.: Future Arctic Ocean seasonal ice zones and implications for pelagic-benthic coupling, Oceanography, 24(3), 220–231, https://doi.org/10.5670/oceanog.2011.74, 2011.

Xu, Z., Liu, S. and Ning, X.: Potential foraminiferal nitrate transport in sediments in contact with oxic overlying water, Limnol. Oceanogr., 66(4), 1510–1530, https://doi.org/10.1002/lno.11701, 2021.

Zaborska, A., Pempkowiak, J. and Papucci, C.: Some Sediment Characteristics and Sedimentation Rates in an Arctic Fjord (Kongsfjorden, Svalbard), Annu. Environ. Prot., 8, 79–96, http://ros.edu.pl/images/roczniki/archive/pp_2006_006.pdf, 2006.

Zajaczkowski, M., Szczuciński, W., Plessen, B. and Jernas, P.: Benthic foraminifera in Hornsund, Svalbard: Implications for paleoenvironmental reconstructions, Polish polar Res., 31(4), 349–375, https://doi.org/10.2478/v10183−010−0010−4, 2010.

Zajączkowski, M., Szczuciński, W. and Bojanowski, R.: Recent changes in sediment accumulation rates in Adventfjorden, Svalbard, Oceanologia, 46(2), 217–231, 2004.

Zwally, H. J., Abdalati, W., Herring, T., Larson, K., Saba, J. and Steffen, K.: Surface Melt – Induced Acceleration of Greenland Ice-Sheet Flow, Science, 297(5579), 218–222, https://doi.org/10.1126/science.1072708,2002

Chapter 1

Benthic foraminifera as tracers of brine production in the Storfjorden "sea ice factory"

Eleonora Fossile[1]*, Maria Pia Nardelli[1], Arbia Jouini[1], Bruno Lansard[2], Antonio Pusceddu[3], Davide Moccia[3], Elisabeth Michel[2], Olivier Péron[4], Hélène Howa[1], and Meryem Mojtahid[1]

[1]*LPG-BIAF UMR-CNRS 6112, UNIV Angers, CNRS, UFR Sciences, 2 bd Lavoisier 49045, Angers CEDEX 01, France*

[2]*LSCE, UMR 8212, IPSL-CEA-CNRS-UVSQ-Université Paris Saclay, 91198 Gif-sur-Yvette, France*

[3]*Department of Life and Environmental Sciences, University of Cagliari, 09126 Cagliari, Italy*

[4]*SUBATECH, UMR 6457, CNRS-Université de Nantes, 4 rue A. Kastler, 44307 Nantes, France*

*Corresponding author: Eleonora Fossile (eleonora.fossile@etud.univ-angers.fr)

This chapter has been published in *Biogeosciences*, 17, 1933-1953, 2020 (https://doi.org/10.5194/bg-17-1933-2020) and its contents have been reformatted here for consistency with the rest of the thesis.

Abstract

The rapid response of benthic foraminifera to environmental factors (e.g., organic matter quality and quantity, salinity, pH) and their high fossilisation potential make them promising bio-indicators for the intensity and recurrence of brine formation in Arctic seas. Such an approach, however, requires a thorough knowledge of their modern ecology in such extreme settings. To this aim, seven stations along a north-south transect across the Storfjorden (Svalbard archipelago) have been sampled using an interface multicorer. This fjord is an area of intense sea ice formation characterised by the production of brine-enriched shelf waters (BSW) as a result of a recurrent latent-heat polynya. Living (rose bengal-stained) foraminiferal assemblages were analysed together with geochemical and sedimentological parameters in the top 5 cm of the sediment. Three major biozones were distinguished. *(i)* The "inner fjord" zone, dominated by typical glacier proximal calcareous species, which opportunistically respond to fresh organic matter inputs. *(ii)* The "deep basins and sill" zone characterised by glacier distal agglutinated fauna; these are either dominant because of the mostly refractory nature of organic matter and/or the brine persistence that hampers the growth of calcareous species and/or causes their dissolution. *(iii)* The "outer fjord" zone characterised by typical North Atlantic species due to the intrusion of the North Atlantic water in the Storfjordrenna. The stressful conditions present in the deep basins and sill (i.e., acidic waters and low food quality) result in a high agglutinated/calcareous ratio (A/C). This supports the potential use of the A/C ratio as a proxy for brine persistence and overflow in Storfjorden.

1. Introduction

The polar regions are particularly sensitive to climate change, as evidenced from the several dramatic alterations in recent decades (Peings, 2018). For instance, Arctic surface temperatures have increased at twice the global rate (i.e., Arctic amplification; Holland and Bitz, 2003; Dai et al., 2019), while sea ice cover has been steadily decreasing over recent decades both in extent and volume (IPCC, 2013; Labe et al., 2018). With less ice present, the ocean surface absorbs considerably more sunlight energy. This leads to further warming of the atmosphere and the ocean, therefore enhancing sea ice melting, which, in turn, affects marine and continental ecosystems (Perovich and Richter-Menge, 2009).

A recent review study compiling several high-resolution terrestrial proxies show that the modern decline in Arctic sea ice is unprecedented compared to at least the last few thou- sand years and is unexplainable by known natural variability (e.g., Kinnard et al., 2011). To better understand how and how much natural and anthropogenic forcing factors control sea ice dynamics, there is a need for more high-resolution marine time series covering the historical period (i.e., hundreds of years) and for robust biological proxies in key areas from the circum-Arctic. Storfjorden, a semi-enclosed bay located in the Svalbard archipelago (Fig. 1a), is one of the Arctic regions particularly suitable for studying first-year sea ice dynamics. Indeed, Skogseth et al. (2004) defined Storfjorden as an "ice factory" because of the presence of a recurrent coastal polynya that contributes to about 5-10% to the total brine waters produced on Arctic shelves (Smedsrud et al., 2006). Brine are salty and CO_2-rich waters (i.e., low pH) (Rysgaard et al., 2011) that are produced when sea ice forms in inner fjords, and for this reason they can be used as proxies for sea ice production. Because of their high density, they cascade after mixing with shelf waters (Skogseth et al., 2005a) and ventilate the deep sea (Rumohr et al., 2001). During cascading, brine may cause sedimentary disturbance as they can release downslope turbidity flows (Rumohr et al., 2001) and, in the meantime, export particulate and dissolved inorganic and organic carbon from the productive surface waters down to the seafloor (Anderson et al., 2004). The brine's contribution to maintaining the halocline of the Arctic Ocean (Aagaard et al., 1985; Cavalieri and Martin, 1994) and its influence on the ocean circulation further underline the need to study brine evolution in recent times in relation to global warming. In fact, the current Arctic amplification will determine a decrease in the production of sea ice in several polynyas from the Arctic region (Tamura and Ohshima, 2011) and, in the future scenario of an ice-free Arctic Ocean during summer (IPCC, 2013), sea ice factories will gradually disappear. However, these predictions are largely based on direct

observations on a short timescale (i.e., satellite data since 1979), which only opens a narrow window on the natural variability of sea ice dynamics. The scientific community is now focusing on longer time series to place the recent trends in a longer-term perspective (i.e., multi-centennial timescale) (Nicolle et al., 2018) and validate these scenarios.

Benthic foraminifera are among the most abundant protists living in marine ecosystems, from brackish waters to abyssal plains (e.g., Murray, 2006). Due to their short life cycle, high diversity and specific ecological requirements, they respond quickly to the physicochemical environmental conditions (e.g., organic inputs, oxygenation, pH) by increasing their density (e.g., Kitazato et al., 2000), changing the faunal composition or modifying their microhabitat (Jorissen et al., 1995; Ohga and Kitazato, 1997). Therefore, benthic foraminifera are potentially good proxies for brine waters that bathe the deep-sea Arctic environments directly and for sea ice production indirectly. The existing benthic foraminiferal-based studies in Storfjorden used fossil fauna to interpret late Quaternary paleoenvironmental changes (Rasmussen and Thomsen, 2009, 2014, 2015). Although highlighting major difficulties in the interpretation of most of these paleo-records without modern proxy calibrations, those studies further suggested the ratio of agglutinated to calcareous benthic foraminifera as a potential proxy for brine changes. Living foraminiferal distributions have been, however, studied in several Svalbard fjords, in particular in relation to the distance from tidewater glaciers and the associated sedimentary supply (Hansen and Knudsen, 1995; Korsun et al., 1995; Hald and Korsun, 1997; Korsun and Hald, 2000; Sabbatini et al., 2007; Ivanova et al., 2008; Forwick et al., 2010; Zajaczkowski et al., 2010; Łacka and Zajaczkowski, 2016; Jernas et al., 2018). To our knowledge, none of these studies targeted the influence of brine-enriched shelf waters (BSW).

To develop a robust biological marine proxy of environmental variation based on communities of benthic fossil foraminifera, it is crucial to understand their modern ecology well in this specific environment beforehand. To provide new insights on this issue, here we investigate living (rose bengal-stained) benthic foraminiferal fauna from Storfjorden and their response to various measured environmental variables (e.g., sediment characteristics, organic matter quantity and composition, sediment oxygen and pH microprofiles) that are further linked with BSW. Furthermore, the interpretation of our results integrates the extended literature of the physical oceanography in this specific semi-enclosed bay (e.g., Haarpaintner et al., 2001a, b, c; Omar et al., 2005; Skogseth et al., 2004, 2005a, b, 2008; Geyer et al., 2009; Jardon et al., 2014).

2. Oceanographic and environmental settings

The Svalbard archipelago, located north of the Arctic circle, extends from 74 to 81°N and 10 to 35°E (Fig. 1a). It is surrounded by the Arctic Ocean to the north, the Barents Sea to the south and east, and the Norwegian and Greenland seas to the west. Storfjorden, the biggest fjord in the Svalbard archipelago, is approximately 190km long with a maximum water depth of ~190m present in a central deep glacial trough (referred to as deep basins in Fig. 1b). The northern part of Storfjorden (i.e., inner fjord; Fig. 1b) is connected with the northwestern Barents Sea by two sounds (Heleysundet and Freemansundet) through where relatively energetic tidal exchanges occur (McPhee et al., 2013). To the south, a sill (77°N-19°E) about 120m deep separates the inner Storfjorden and the deep basins from the outer Storfjorden trough (Storfjordrenna) (Fig. 1a), a 200-300m deep glacial paleo-valley that incised the western Barents Sea continental margin during previous sea level low stands (Pedrosa et al., 2011).

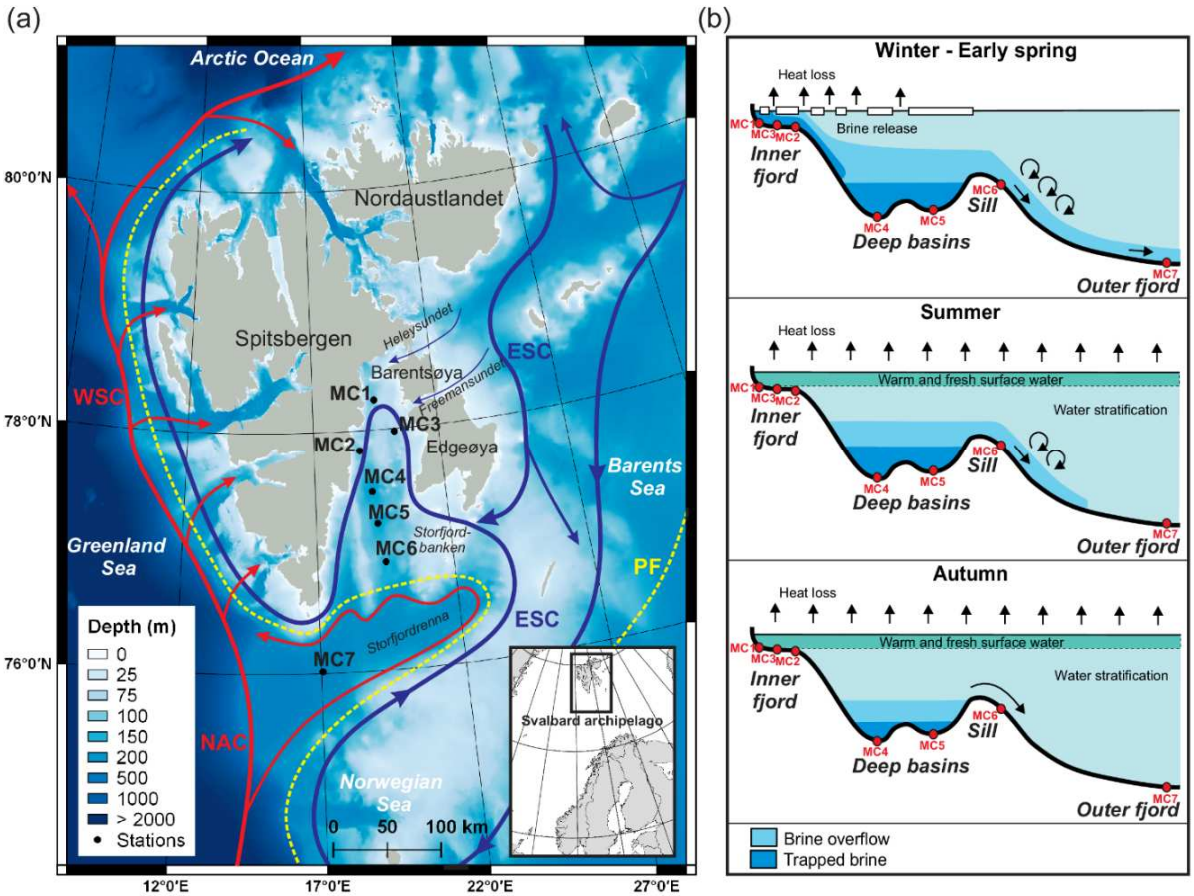

Figure 1. (a) Bathymetric map showing the main current circulations around the Svalbard archipelago (currents from Skogseth et al., 2005b and Misund et al., 2016) and locations of the sampling stations. The red lines represent the warm North Atlantic waters carried by the Norwegian Atlantic Current (NAC) and West Spitsbergen Current (WSC). The blue lines represent the cold Arctic waters carried by the East Spitsbergen Current (ESC). The dotted yellow line represents the polar front (PF). Bathymetry was obtained from EMODnet

(http://portal.emodnet-bathymetry.eu, last access: 24 January 2019), and the map was elaborated with QGIS (made with Natural Earth). **(b)** Longitudinal bathymetric profile sketches showing seasonal formation and flow of brine in inner and outer Storfjorden (modified from Skogseth et al., 2005a and Rasmussen and Thomsen, 2015) and the indicative location of the sampling stations (red dots).

The Svalbard archipelago is influenced by two major water masses. Along the eastern and southern margin of Svalbard, cold and relatively low saline Arctic waters flow out from the Barents Sea via the East Spitsbergen Current (ESC) (Fig. 1a). In the eastern Norwegian and Greenland seas, the main stream of Atlantic Water, which is the most important source of heat and salty water into the Arctic Ocean, is carried northwards by the Norwegian Atlantic Current (NAC) (Fig. 1a). North of Norway, the NAC splits into two branches: *(i)* the Norwegian Current (NC, or Norwegian Coastal Current), which enters the Barents Sea eastward around 70°N (not shown in Fig. 1a) along the northern coast of Norway, and *(ii)* the West Spitsbergen Current (WSC), which flows northwards along the western Svalbard coast towards the Fram Strait (Schauer, 1995). Recent studies report fluctuations in heat transport to the Arctic Ocean by the WSC in particular that are linked with global climate change (e.g., Holliday et al., 2008; Piechura and Walczowski 2009; Beszczynska-Moller et al., 2012). This current is playing a significant role in the process of recent Arctic warming by influencing sea ice distribution and cover in Svalbard (Polyakov et al., 2012).

The water masses in Storfjorden have two main origins: warm Atlantic waters and cold Arctic waters. These are mostly separated by the location of the polar front, which shifts seasonally and therefore influences the northward or southward position of these water masses (Loeng, 1991) (Fig. 1a). The warm Atlantic surface waters carried by the NAC enter the Storfjordrenna from the southwest (Wekerle et al., 2016) (Fig. 1a). During spring-summer, this latter flows into Storfjorden along its eastern margin following a cyclonic circulation (Nielsen and Rasmussen, 2018; Piechura and Walczowski, 2009). The cold Arctic waters derived from the ESC enter Storfjorden from the east through narrow topographic gateways (Heleysundet and Freemansundet sounds) and the topographic depression north of Storfjordbanken (Fig. 1a). This Arctic water circulates cyclonically through the fjord, flowing southwards along the western Storfjorden coast and continuing northwards as a coastal current along the west Spitsbergen coast (Nielsen and Rasmussen, 2018; Rasmussen and Thomsen, 2015). Vertically, water masses are usually arranged in three main layers within an Arctic fjord with a sill (Farmer and Freeland, 1983): a relatively fresh surface layer, a deep and saline layer below the sill depth, and an intermediate layer in between (Fig. 1b). Profiles from late summer in Storfjorden show a well-mixed fresh surface layer extending down to 40m depth separated from the intermediate

layer (comprising advected Atlantic Water) by a steep halocline. The deepest layer, which sits below the sill depth, is a cold and saline water mass derived from trapped brine (e.g., Skogseth et al., 2005a; Cottier et al., 2010; Rasmussen and Thomsen, 2015).

The shelf sea in the Storfjorden is characterised by an extended winter first-year sea ice cover due to the presence of a recurrent winter coastal latent-heat polynya mostly located in the northeastern part (Skogseth et al., 2004). Polynyas are ice-free areas formed and maintained by advection of ice by offshore winds and tidal and ocean currents. The presence of northerly winds allows for the development of the polynya, while southerly winds cause the polynya to shrink, which makes the extension and the position of the polynya highly variable (Haarpaintner et al., 2001b). The opening of a latent-heat polynya determines an intensive heat loss to the atmosphere that can lead to a persistent ice formation (Fer et al., 2004; Skogseth et al., 2005a). Polynya particularly occurs when northeasterly winds intensify in winter (Skogseth et al., 2004). The continuous production of thin, first-year sea ice, which generally starts in December (Smedsrud et al., 2006), leads to a subsequent formation of brine waters in Storfjorden. Brines are cold, dense and well-oxygenated waters, enriched in salt and total dissolved inorganic carbon (DIC) (i.e., low pH), that are rejected in undersea ice waters when sea ice is formed (Rysgaard et al., 2011; Anderson et al., 2004). The shelf convection promotes the mixing of brine with shelf waters, leading to the formation of brine-enriched shelf waters (BSW). In the early winter freezing period, the extremely dense BSW sink, filling the deeper basins and pushing the less dense waters above the sill level, causing a weak overflow (Skogseth et al., 2005a) (Fig. 1b). During winter the low temperature causes a brine volume contraction and a decrease in the sea ice permeability that prevents the air-sea ice gas exchange; brine volume contraction causes a further increase in brine salinity and $CO_{2(aq)}$ (Rysgaard et al., 2011). The continuous freezing in spring causes the accumulation of BSW in the deep basins and a strong steady overflow period over the sill. Although weaker, the overflow continues even in summer after the end of the freezing period. In the meantime, the fresh melting surface water is warmed by surface heating (Skogseth et al., 2005a). During spring and summer, the ice melting reduces $CO_{2(aq)}$ (Rysgaard et al., 2011) and the increase in light availability (Horner and Schrader, 1982) triggers ice algae photosynthetic activity, which further reduces DIC concentrations of surface waters (Gleitz et al.,1995). In autumn, surface waters lose heat and become colder. At this time, the old BSW are trapped in the deep basins, but strong wind events cause occasional discharges over the sill (Skogseth et al., 2005a) (Fig. 1b). All Arctic coastal polynyas together produce about 0.7-1.2 Sv ($1Sv = 10^6\ m^3\ s^{-1}$) of BSW (Cavalieri and Martin, 1994), providing about 10% of the deep water formed in the Arctic Ocean and Barents Sea today (Smethie et al., 1986;

Quadfasel et al., 1988; Rudels and Quadfasel, 1991). Storfjorden is a major supplier of BSW, alone producing 5-10% of the dense water in the Arctic Ocean (Quadfasel et al., 1988; Smedsrud et al., 2006).

Spitsbergen is characterised by the presence of several tidewater glaciers influencing the head of the Storfjorden (see Fig. 9 in Lydersen et al., 2014). Ongoing climate warming has been causing the retreat of several glaciers present on Svalbard over the last 100 years, increasing sediment supply and accumulation (Zajaczkowski et al., 2004). In this context, Winkelmann and Knies (2005) classified the inner Storfjorden as a low-energy environment characterised by high sedimentation rates and organic-rich sediments (total organic carbon content (TOC) > 2%) with a high proportion of terrestrial components.

3. Material and methods

3.1 Interface sediment sampling and CTD profiles

In July 2016, seven stations were sampled along a north-south transect in Storfjorden (Fig. 1a, Table 1) during the STeP (Storfjorden Polynya Multidisciplinary Study) cruise on board the R/V L'Atalante (IFREMER). Stations MC1 to MC3 are positioned on the continental shelf at the head of the fjord, stations MC4 and MC5 are located in the deep central basins, station MC6 is located on the sill, and station MC7 is located in the Storfjordrenna (Fig. 1a, Table 1). At each station, 10 to 40 cm long sediment cores were sampled using a multi-corer (10 cm inner diameter) in order to get undisturbed sediment–water interfaces. Three replicate cores were sampled at each station (except for station MC3 where only two cores were collected): the first core for geochemical analysis (oxygen, pH and porosity profiles); the second for $^{210}Pb_{xs}$ dating, grain size, phytopigment, and organic matter analyses; and the third for foraminiferal analysis. In order to determine the main environmental characteristics of each site, hydrographic casts were performed with a conductivity-temperature-depth sensor (Seabird 911 plus CTD) equipped with a fluorometer. A rosette sampler supplied with 22×12L Niskin bottles was used for water column sampling. Bottles were fired at standard depths to measure oxygen, nutrients and Chlorophyll *a*.

3.2 Geochemical analyses

Immediately after the recovery of sediment cores, oxygen and pH microprofiles were measured at the sediment-water interface. We used a micromanipulator that can drive O_2 and pH microelectrodes (Unisense®) at the same time with a 200 µm vertical resolution. Oxygen

profiles were performed using Clark-type microelectrodes with a 100 µm thick tip (Revsbech 1989), while pH profiles were measured using a glass microelectrode with a 200 µm thick tip. The O_2 concentration of bottom water was analysed by Winkler titration (Grasshoff et al., 1983). At each station, triplicate samples were analysed with a reproducibility of ±2 µmolL^{-1}. The pH microelectrodes were calibrated using National Bureau of Standards (NBS) buffer solutions (pH 4, 7 and 10). The pH of bottom water was also determined by spectrophotometry using m-Cresol Purple as dye (Dickson et al., 2007). All pH measurements were recalculated at in situ temperature, salinity and depth using CO2SYS (Pierrot et al., 2006) and were reported on the total proton scale (pH_T). The measurements for both O_2 and pH profiles, were repeated many times in order to assess the reproducibility of the measurements and the natural heterogeneity of these parameters in the sediment.

Sampling date	Station	Latitude (N)	Longitude (E)	Depth (m)	Temp (°C)	Salinity	Density (kg m^{-3})	pH_T	O_2 (µmol.L^{-1})
13/07/2016	MC1	78°15.0	19°30.0	108.0	-1.74	34.89	1028.59	8.00	341
14/07/2016	MC2	77°50.0	18°48.0	117.0	-1.59	34.79	1028.52	7.95	317
14/07/2016	MC3	77°58.6	20°14.6	99.0	1.10	34.74	1028.29	8.12	350
15/07/2016	MC4	77°29.2	19°10.6	191.5	-1.78	34.92	1029.01	7.92	319
17/07/2016	MC5	77°13.2	19°17.9	171.0	-1.78	34.93	1028.91	7.91	317
18/07/2016	MC6	76°53.9	19°30.3	157.0	-1.13	34.80	1028.72	7.97	317
19/07/2016	MC7	76°00.9	17°03.4	321.0	3.53	35.05	1029.33	8.04	305

Table 1. Geographic coordinates, depths of the seven studied stations and bottom water parameters (temperature and salinity are measured in situ by the CTD, O_2 (dissolved oxygen) and pH_T are measured from Niskin bottles).

3.3 Grain size analysis and ^{210}Pb dating

At each station (except for the MC3), one core was sliced on board, collecting five sediment layers (0-0.5, 0.5-1, 1-2, 2-5 and 5-10 cm), then stored at -20°C. In the land-based laboratory, an aliquot of sediment was sampled for grain size analyses and the rest was lyophilised for the $^{210}Pb_{xs}$ analyses. Grain size analyses were performed using the laser diffraction particle size analyser Malvern Mastersizer 3000. The particle size distributions were analysed with GRADISTAT 8.0 software program (Blott and Pye, 2001). Replicated analyses were run for each sample aliquot and the most representative was selected. For the analysis of fauna in response to environmental parameters, the grain size of the superficial sediment layer (0.0-0.5 cm depth) was considered representative of the sediment-water interface characteristics. Another aliquot of sediment was freeze-dried for gamma spectrometry measurements in order to determine the apparent sedimentation rate by the $^{210}Pb_{xs}$ method (Appleby and Oldfield, 1978). The ^{210}Pb dating was conducted using a gamma spectrometer Canberra® HPGe GX4520

coaxial photon detector. The homogenised samples were weighed and sealed in a defined geometry for at least 3 weeks to ensure ^{222}Rn-^{226}Ra-^{214}Pb equilibration. Sedimentation rate was based on the determination of the excess or unsupported activity ^{210}Pb (^{210}Pb$_{xs}$) and performed through constant flux-constant sedimentation (CFCS) model (Sanchez-Cabeza and Ruiz-Fernández, 2012). The ^{210}Pb$_{xs}$, incorporated rapidly into the sediment from atmospheric fallout and water column scavenging, was calculated as the difference between the total measured ^{210}Pb activity (supported + excess) at 46.54 keV and ^{214}Pb at 351.93 keV.

3.4 Organic matter quantity and biochemical composition

To assess the quantity and biochemical composition of the organic matter, the top 0.5 cm of the sediment cores was sliced on board and immediately stored at -20°C until analysis. As the redox fronts and foraminiferal microhabitats in the sediment are strictly driven by the organic matter supply at the sediment–water interface (e.g., Jorissen et al., 1995), only the organic matter data for the upper 0.5 cm were used to interpret the faunal distribution.

In the laboratory, chlorophyll *a* (Chl *a*), phaeopigment, lipid (LIP), carbohydrate (CHO) and protein (PRT) contents were determined on three pseudo-replicates (ca. 1 g wet sediment). Chlorophyll *a* and phaeopigment analyses were carried out according to Lorenzen and Jeffrey (1980). Briefly, pigments were extracted with 90% acetone (12 h in the dark at 4°C). After the extraction, the pigments were fluorometrically analysed to estimate the quantity of Chl *a* and, after acidification (20 s) with 0.1N HCl (Plante-Cuny, 1974), to estimate the amount of phaeopigments. Chloroplastic pigment equivalents (CPE) were calculated as sum of Chl *a* and phaeopigment contents, and carbon associated with CPE (C-CPE) was calculated by converting CPE contents into carbon equivalents using a factor of 30 µgC per µg of phytopigment (de Jonge, 1980). Protein, carbohydrate and lipid sedimentary contents were determined by spectrophotometry (Danovaro, 2009) and concentrations reported as bovine serum albumin, glucose and tripalmitin equivalents (mg per gram of dry weight sediment), respectively. Protein, carbo- hydrate and lipid concentrations were converted into carbon equivalents using the conversion factors 0.49, 0.40 and 0.75 gCg^{-1}, respectively (Fabiano et al., 1995). The sum of protein, carbohydrate and lipid carbon was referred to as biopolymeric carbon (BPC; Tselepides et al., 2000) that represents the semi-labile fraction of the total organic carbon (Pusceddu et al., 2009; Van Oevelen et al., 2011). The algal fraction of biopolymeric C, a proxy for the most labile fraction of sedimentary organic matter (Pusceddu et al., 2003, 2010) was calculated as the percentage ratio of C-CPE in BPC.

3.5 Living foraminiferal fauna sampling and analyses

Immediately after sampling, interface cores were sliced horizontally every 0.5 cm between 0 and 2 cm, every 1cm from 2 down to 6 cm, and every 2cm from 6 to 10 cm depth. Each slice was stored in a 500 cm^3 plastic bottle filled with 95% ethanol containing 2 gL^{-1} of rose bengal stain (in order to label living foraminifera) following the FOBIMO directive (Schönfeld et al., 2012). In the laboratory, sediment samples were sieved through 63, 125 and 150 µm meshes, and the resulting fractions were stored in 95% ethanol. All living (rose bengal-stained) specimens from the >150 µm fraction were hand-picked in water from the surface layer down to 5 cm depth. Additionally, the living foraminifera of the 63-150 µm fraction were picked only for the first centimetre of sediment, in order to investigate the potential use of this size fraction for ecological consideration. We counted only the specimens with bright rose staining (assessing the colouration intensity of living specimens for every individual species, as recommended by Schönfeld et al., 2012) as living foraminifera.

Samples of the smallest size fraction, showing very high benthic foraminiferal abundance, were dried at 50°C and split with an Otto Microsplitter. Then foraminifera were hand-sorted from an entire split containing a minimum of 300 individuals and the counts were extrapolated for the total sample. Foraminiferal biodiversity was estimated using different diversity indices: species richness measured as the number of species, species diversity measure using the Shannon-Wiener Index (H') and species equitability (J) measured using the "Pielou Index (1975)". All indices were calculated using the Paleontological Statistics Data Analysis (PAST) software (version 2.17c; Hammer et al., 2001). Foraminiferal densities are expressed per 50 cm^2 (when considering total densities) and per 50 cm^3 (when considering layers of different thickness). The agglutinated species *Spiroplectammina earlandi* and *Spiroplectammina biformis* were not distinguished because these are morphotypes of the same species according to Korsun and Hald (2000).

3.6 Multivariate analyses

A canonical correspondence analysis (CCA) was used to investigate the relationships between the environmental parameters (depth, bottom water temperature, salinity, oxygen penetration depth or OPD, sediment porewater pH, sediment grain size, and organic matter) and the fauna (>150 µm, 0-5 cm) of all stations considering only the absolute densities (ind. 50 cm^{-2}) of the species which contribute with > 5% to the assemblage. We used the grain size characteristics and the organic matter contents and composition of the uppermost sediment layer (0.0-0.5 cm).

Values of different environmental variables and different orders of magnitude were homogenised using the following standardisation: (*x*-mean *x*)/*sd*, in which x is the value of the variable at one station, mean *x* is the mean of the same variable among the stations and *sd* is the corresponding standard deviation. Non-metric multidimensional scaling (nMDS) bi-plot and cluster analyses (Bray-Curtis dissimilarity) were used to visualise the differences among stations and size fractions. The analyses were conducted on the foraminiferal assemblages of the topmost centimetre of sediment separately considering the smaller fraction 63-150 µm, the >150 µm fraction and the total assemblage (>63 µm fraction). The densities of the foraminiferal fauna were normalised using the following transformation: $\log_{10}(x+1)$, where *x* is the density expressed in ind. 50 cm^{-2} (considering the 0–5 cm sediment interval for the CCA and the 0-1 cm interval for the nMDS and cluster analysis). All analyses were performed using the PAST software (version 2.17c; Hammer et al., 2001).

3.7 Visual characterisation of test dissolution

Using high-resolution scanning electron microscope (SEM) images of specimens from the >150 µm size fraction (Fig. S2 in the Supplement), we qualitatively distinguish four dissolution stages from weak to severe, following the classification of Gonzales et al. (2017): (I) no sign of dissolution, transparent tests and smooth surfaces; (II) whitish tests with visible pores, where frequently the last chamber is lost in addition to the first calcite layers; (III) several chambers are dissolved and the remaining ones present opaque wall tests; and (IV) nearly complete dissolution of the tests, and only the organic material remains. The percentage of specimens belonging to each of the four stages in all samples was not quantified because of the potential loss of information due to the bad preservation characterising the two most severe dissolution stages.

4. Results

4.1 Bottom water properties

In July 2016, bottom waters at the inner fjord stations MC1 and MC2 are cold (below −1.5°C) and relatively salty (34.89 and 34.79, respectively), while station MC3 presents a positive bottom water temperature (1.10°C), the lowest salinity (34.74), and the highest pH_T (8.12) and O_2 (350 $\mu molL^{-1}$) of the fjord transect (Table 1). The two deep basin stations (MC4 and MC5) display the lowest bottom water temperature (both −1.78°C), the lowest pH_T (7.92 and 7.91, respectively) and the highest salinity (34.92 and 34.93, respectively) (Table 1). The sill station

MC6 shows the same range of salinity than in the inner fjord (34.80) with a slightly higher temperature (−1.13°C). The outer fjord station MC7 records the highest temperature (3.53°C) and salinity (35.05) of the sampled transect. The shallowest stations (MC1 and MC3) are well ventilated, with O_2 concentrations higher than 340 $\mu molL^{-1}$. Stations MC2, MC4, MC5 and MC6 show the same bottom water O_2 concentration (318±2 $\mu molL^{-1}$). The deepest station (MC7), located outside Storfjorden, shows a lower O_2 concentration (305 $\mu molL^{-1}$).

4.2 Grain size analysis and sedimentation rate

The ^{210}Pb age models show a relatively high sedimentation rate at all stations, with an average of 3.6±0.4 mm yr^{-1} (see Supplement, Table S1 for more details), except at the outer fjord station MC7 where sedimentation rate is much lower (1.3±0.6 mm yr^{-1}; Table S1). Grain size analyses of the topmost 0.5 cm of the sediment indicate the dominance of silt sediments at all stations (around 84% to 89 %, Table S1). Slight differences are, however, noted in terms of the mode: in the fjord fine silt (~10 µm) is dominant, while in the outer station MC7 the mode corresponds to medium silt (~20 µm). Moreover, the percentage of sand increases from approximately 4.0% at MC1 to 10.4% at station MC6 and declines to 6.8% at MC7.

4.3 Biogeochemical analyses of the sediment

The sediment oxygen profiles (Fig. S1a) at the inner fjord stations (MC1 to MC3) display an average oxygen penetration depth (OPD) of 7.7±1.0 mm (n = 3), 4.9±0.4 mm (n = 4) and 4.8±1.9mm (n = 6), respectively. The OPD at the deep basin stations (MC4 and MC5) and at the sill station (MC6), are 5.7±1.1 mm (n = 3), 6.2±0.9 mm (n = 10) and 8.6±3.8 mm (n = 6), respectively. The outer fjord station (MC7) shows the highest OPD of the sampled transect (15.6±1.0 mm, n = 6).

The porewater pH_T at the sediment–water interface (pH profiles in Fig. S1b) is significantly different among the stations (one-way ANOVA, $F = 128.8$, $p < 0.001$). The inner fjord stations (MC1 to MC3), the sill (MC6) and outer fjord (MC7) have pH_T values generally above 7.95, significantly different (Tukey's HSD post hoc test, $p < 0.001$) from the deep basin stations which have pH_T values less than or equal to 7.90. When considering the entirety of the profiles, pH strongly decreases in the topmost part of the sediment (0-5 mm) at all stations but with different slopes. The gradients of the two extremes are −0.2 pH unit per millimetre at station MC3 and −0.1 pH unit mm^{-1} at MC7 (see Fig. S1b).

Concerning the organic matter, the results for BPC, PRT, CHO, LIP, and CPE content and algal fraction of BPC (C-CPE/BPC) are presented in Fig. 2. The complete dataset is reported as average ± standard deviation (n = 3) in Table S2 of the Supplement. The BPC (Fig. 2a) varies significantly among the stations (one-way ANOVA, $F = 21.72$, $p < 0.001$). Stations MC1 and MC7 have values of BPC significantly lower (5.49±0.49 and 4.71±0.07 $mgCg^{-1}$, respectively, Tukey's HSD $p < 0.05$) than at all other stations. In the latter, the average BPC varies between 6.86±0.45 and 7.38±0.21 $mgCg^{-1}$. The PRT contents (%) (Fig. 2a) of the BPC varies significantly among the stations (one-way ANOVA, $F = 6.94$, $p < 0.01$). In particular, the deep basins present significantly lower percentages of PRT compared to all the other stations (32.12±4.42% at MC4 and 30.75± 4.58 % at MC5; Tukey's HSD $p < 0.01$). The CHO contents (%) (Fig. 2a) change significantly among the stations (one-way ANOVA; $F = 46.6$; $p < 0.001$), displaying the highest scores in the deep basins (33.79±1.71 % and 36.08±2.52 % at MC4 and MC5, respectively). The CPE (Fig. 2b) varies significantly among the stations (one-way ANOVA, $F = 52.03$, $p < 0.001$). CPE content is considerably lower in the outer fjord station MC7 (6.43±0.45 $\mu g g^{-1}$) compared to all other stations ($p < 0.001$). Inside the fjord, station MC1 differs from MC2, with values of 24.04±3.69 and 41.19± 9.62 $\mu g g^{-1}$, respectively (Tukey's HSD $p = 0.02$), whereas all other CPE contents present intermediate values. The C-CPE/BPC (Fig. 2b) in the uppermost 0.5 cm varies significantly among the stations (one-way ANOVA, $F = 76.82$, $p < 0.001$). In particular, the algal fraction is significantly lower in the outer fjord station MC7 (4.09±0.33 %) compared to all other stations (Tukey's HSD $p < 0.001$). On the contrary, all the stations inside the fjord do not differ significantly and have values between 13% and 17%.

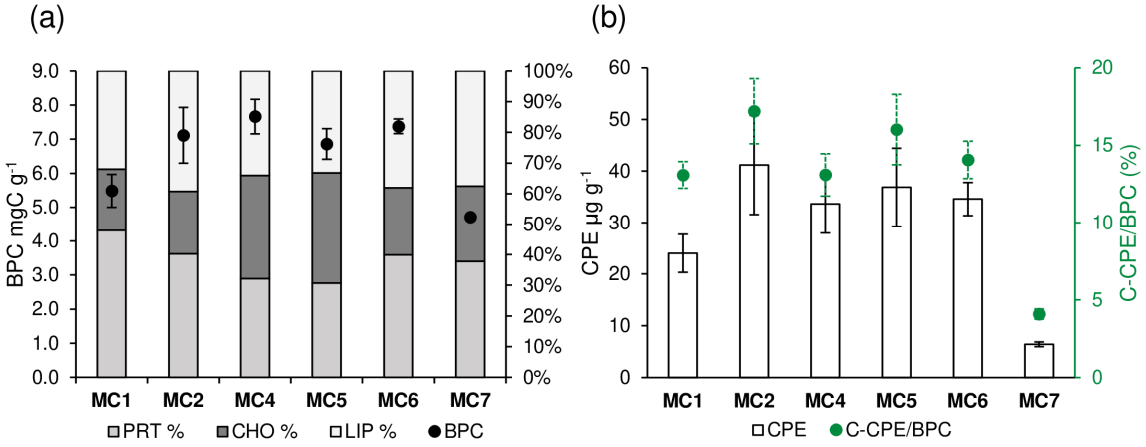

Figure 2. For each sampling station the following information is shown (data are not available at station MC3): **(a)** content of biopolymeric carbon (BPC, black dots) and percentage of protein, carbohydrate, and lipid content (cumulative bars) and **(b)** the content of chloroplastic pigment equivalents (CPE, white bars) and algal fraction of BPC (C-CPE/BPC, green dots).

4.4 Foraminiferal assemblages of the 0–5cm sediment layer (>150 µm fraction)

4.4.1 Abundances and diversity

Considering the total foraminiferal fauna in the 0-5 cm sediment interval (Table 2), the highest absolute abundance is displayed at the inner fjord station MC2 (2249 ind. 50 cm^{-2}), whereas it is reduced by about half at the other two inner fjord stations (1104 and 1353 ind. 50 cm^{-2} at MC1 and MC3, respectively). The absolute abundance increases at the deep basin stations (1861 and 1439 ind. 50 cm^{-2} at MC4 and MC5, respectively) and drastically declines at the sill station MC6, reaching the lowest abundance detected in the transect (940 ind. 50 cm^{-2}). At the outer fjord station MC7, the total absolute abundance is 1238 ind. 50 cm^{-2}.

The inner fjord stations MC1 and MC2 present the same number of species (27) (Table 2) and similar Shannon-Wiener index (H' = 1.61 and 1.48) and equitability (J = 0.49 and 0.45). The third inner fjord station MC3 is characterised by the lowest diversity (19 species and H' = 0.92) and the lowest equitability (J = 0.31), whereas the deep basin stations MC4 and MC5 show relative high H' (2.25 and 2.35, respectively) and J values (0.62 and 0.70, respectively). The sill station MC6 shows similar H' and J values compared to the deep basin stations (2.18 and 0.65, respectively). The outer fjord station MC7 shows the highest number of species (44) and H' index (2.40).

Stations	MC1	MC2	MC3	MC4	MC5	MC6	MC7
Abundance (ind. 50 cm^{-2})	1104	2249	1353	1861	1439	940	1238
Species Richness	27	27	19	37	29	29	44
Shannon-Wiener (H')	1.61	1.48	0.92	2.25	2.35	2.18	2.40
Equitability (J)	0.49	0.45	0.31	0.62	0.70	0.65	0.64

Table 2. Foraminiferal total abundances (in number of individuals per 50 cm^2) and diversity indexes, considering the total living fauna (>150 µm size fraction) in the 0 to 5cm core top sediment.

In terms of species composition (Fig. 3a), the inner fjord stations are mainly dominated by two calcareous species: *Elphidium clavatum*, contributing 22%, 47%, and 75% of the total fauna, and *Nonionellina labradorica*, contributing 51%, 31%, and 13% at MC1, MC2, and MC3, respectively. *Cassidulina reniforme* is a secondary species at station MC1 (10%), and *Elphidium bartletti* is a secondary species at station MC2 (8%). The deep basin stations (MC4 and MC5) are dominated by various agglutinated species that contribute differently to the total assemblages. The most abundant are *Recurvoides turbinatus* (12% and 18%, respectively, at MC4 and MC5), *Reophax fusiformis* (13% and 10%) and *Reophax scorpiurus* (27% and 17%). *Ammotium cassis* and *Labrospira crassimargo* are less abundant at MC4 compared to MC5

(2% and 11% for *A. cassis* and 6% and 11% for *L. crassimargo*, respectively). Additionally, the calcareous *N. labradorica* is still quite abundant (20% at MC4 and 8% at MC5). The sill station MC6 shows similarity with the deep basin stations because of the presence of the agglutinated *R. turbinatus* (10%) and *R. fusiformis* (24%) but it differs by the presence of the agglutinated *Adercotryma glomeratum* (29%). The outer fjord station (MC7) can be distinguished from all other stations by the exclusive presence of the two calcareous species *Globobulimina auriculata* and *Melonis barleeanus* (9% and 12%, respectively) and by the major contribution of the agglutinated species *Lagenammina difflugiformis* (14%). Nevertheless, some species that are abundant inside the fjord are also present at station MC7 (e.g., *N. labradorica* 25%, *R. fusiformis* 6% and *R. scorpiurus* 15%).

4.4.2 Agglutinated vs. calcareous foraminifera (0–5 cm, >150 µm)

The comparison between the relative abundances of calcareous and agglutinated species, considering the total living fauna in the 0-5 cm sediment interval (Fig. 3b) shows the strong dominance of calcareous species (between 91 and 94 %) at the inner fjord stations (MC1, MC2 and MC3). The opposite is observed at the two deep basin stations (MC4 and MC5) and at the sill station (MC6), where the relative abundances of agglutinated foraminifera vary from 65% to 77%. At the outer fjord station, MC7, calcareous species have higher proportions (60%), although they are not as dominant as at the inner fjord stations.

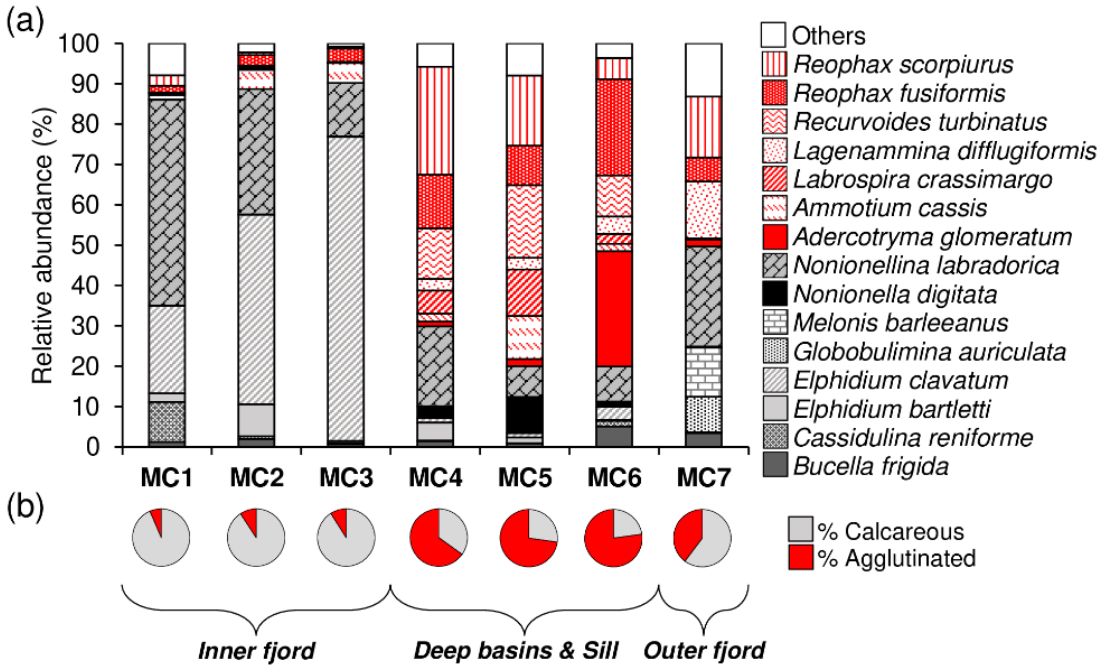

Figure 3. (a) Species relative abundances of the total living fauna (> 150 µm fraction) in the 0 to 5 cm core top sediment at each station and **(b)** the agglutinated species (in red) vs. calcareous species (in grey) ratio.

4.4.3 Vertical distribution

The foraminiferal absolute density displays an overall decreasing trend from the surface sediment down to 5 cm depth at all stations (Fig. 4). The superficial layers (0-1 cm) of the inner fjord stations (MC1, MC2, MC3; Fig. 4a) are mostly represented by *Elphidium clavatum*, *Cassidulina reniforme* (especially at MC1), *Nonionellina labradorica* and other accessory species (e.g., *Triloculina oblonga*, *Elphidium bartletti*, *Ammotium cassis*). The deeper layers (down to 5 cm) show much lower abundances and are increasingly occupied by *Nonionellina labradorica*.

In the two deep basins (MC4 and MC5; Fig. 4b), four agglutinated species are dominant in the first centimetre of sediment: *Reophax scorpiurus*, *Reophax fusiformis*, *Recurvoides turbinatus* and *Labrospira crassimargo*. At both stations, the infaunal species *N. labradorica* is present in high relative abundance in the 1-3 cm sediment intervals, together with *Nonionella digitata*. In the deepest sediment layers (3-5 cm), *L. crassimargo*, *R. scorpiurus* and *R. turbinatus* are dominant. At the sill station MC6, the dominant species present in the uppermost centimetre are *R. fusiformis*, *R. turbinatus* and *Adercotryma glomeratum* (Fig. 4b). These species are also present with important abundances in the deeper layers where they are accompanied by *N. labradorica* at the 1-3 cm depth intervals. At the outer fjord station MC7, the 0-1 cm sediment interval show a dominance of *R. scorpiurus*, *R. fusiformis* and *L. difflugiformis* (Fig. 4c). In the deeper layers, these species are accompanied and gradually replaced by significant abundances of the calcareous species *Melonis barleeanus* and *Globobulimina auriculata*.

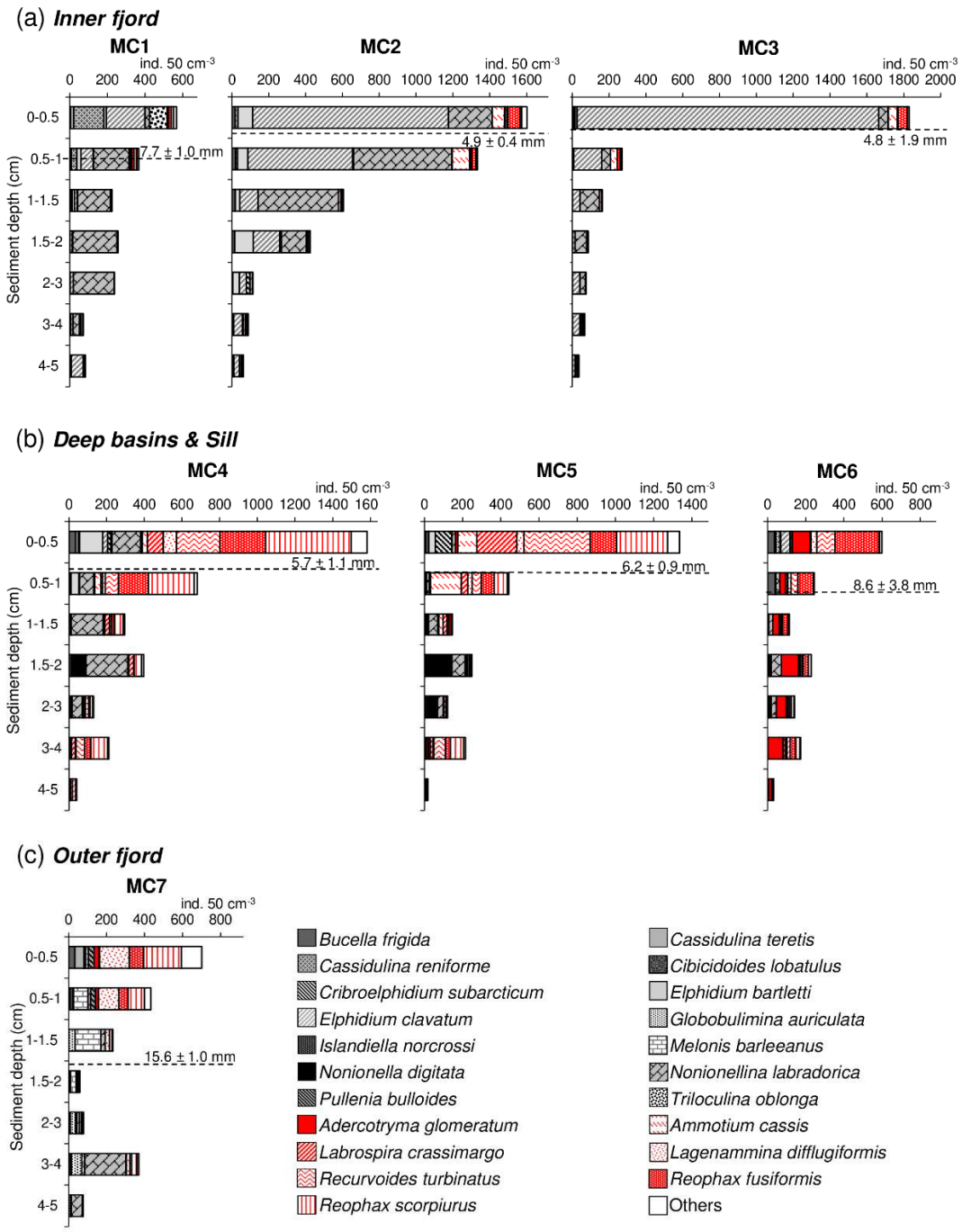

Figure 4. Foraminiferal vertical distribution from 0 to 5cm sediment depth (> 150 µm fraction) for **(a)** the inner fjord (stations MC1 to MC3) **(b)** deep basins (stations MC4 and MC5) and sill (station MC6), and **(c)** outer fjord (station MC7). Calcareous species are shown using different grey textures, whereas agglutinated species are shown using different red textures. The dashed black line represents the average oxygen penetration depth (OPD) at each station.

4.4.4 Multivariate analysis

The CCA analysis based on the foraminiferal data (0-5 cm, >150 µm, total absolute densities of 15 species, with a relative abundance >5%) and 15 measured environmental variables is presented in Fig. 5. Axes 1 and 2 explain nearly 90% of the total variance. This multivariate

analysis clearly divides the stations into three groups based on the differences determined by the foraminiferal assemblages and the environmental variables. Axis 1 strongly separates station MC7 from the rest of the stations. This difference is mainly determined by bottom water parameters (T, S, pH), OPD, percentage of silt and water depth. The negative correlation between the outer fjord station MC7 and the CPE content and algal fraction distinguishes it from all other stations. Axis 2 clearly divides the other six stations into two groups: the inner fjord group (composed of stations MC1, MC2 and MC3) and the deep basins and sill group (stations MC4 and MC5 and station MC6). This separation is mainly based on the organic matter composition of the sediment. The inner fjord group of stations is positively correlated with the percentage of proteins, whereas the deep basins and sill group is mainly correlated with the percentage of carbohydrates and the biopolymeric carbon content. This group of stations MC4 to MC6 is also positively correlated with the CPE content and the algal fraction of BPC. These three groups are characterised by different foraminiferal assemblages. The calcareous species *Cassidulina reniforme*, *Elphidium clavatum*, *Nonionellina labradorica*, and *Elphidium bartletti* characterise the inner fjord, whereas three agglutinated species, *Labrospira crassimargo*, *Adercotryma glomeratum*, and *Recurvoides turbinatus*, and one calcareous species, *Nonionella digitata*, define the deep basins and sill group. Finally, the exclusive presence of the two species, *Melonis barleeanus* and *Globobulimina auriculata*, characterise the outer fjord station MC7.

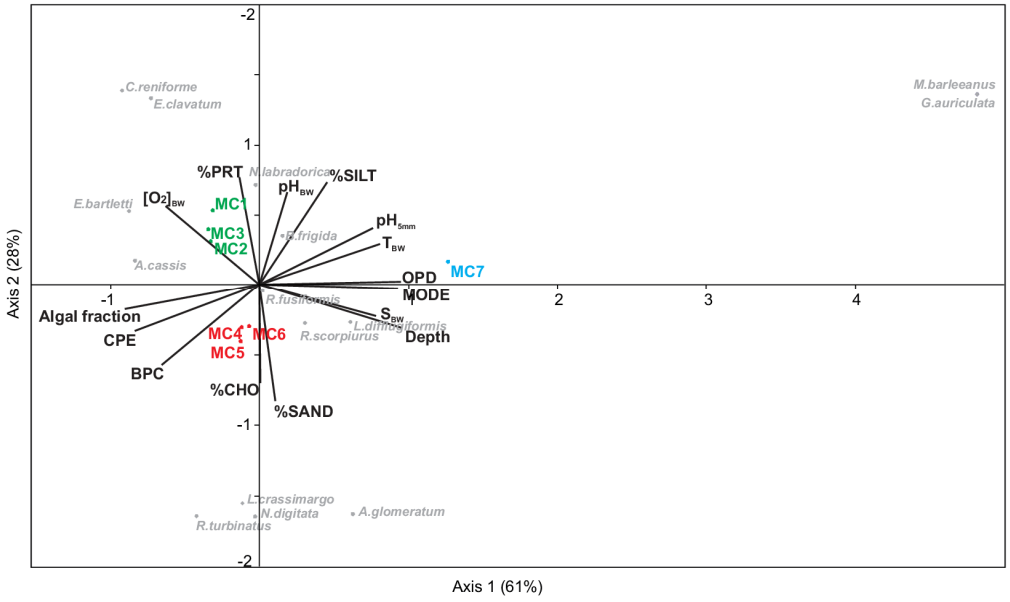

Figure 5. Canonical correspondence analysis based on real abundances (ind. 50 cm−2) of the living fauna in the 0–5 cm sediment layer (> 150 µm size fraction) considering the major species (> 5 %) vs. environmental variables described in Tables 1, S1 and S2.

4.5 Comparison between the 63-150 and >150 µm size fractions (0–1 cm)

4.5.1 Abundances and diversity

Foraminiferal abundances considering the entire > 63 µm fraction (63-150 + >150 µm fractions) in the topmost centimetre of the sediment are maximal at MC2 and MC4 (4610 and 3936 ind. 50 cm^{-2}, respectively), while all other stations present lower values (<3000 ind. 50 cm^{-2}) (Fig. 6a). When considering only the largest fraction (>150 µm) at the first centimetre, MC2 (1467 ind. 50 cm^{-2}) and MC4 (1132 ind. 50 cm^{-2}) still shows the highest abundances followed by MC3 and MC5 (1050 and 889 ind. 50 cm^{-2}). For the rest, values are lower than 600 ind. 50 cm^{-2}. The small fraction (63-150 µm) is dominant at all stations, contributing with values between 59% (at MC2) and 83% (at MC6) to the total abundances.

Regarding diversity values, at MC1 and MC7 no significant differences in the H' and J indices are found between the two size fractions (Fig. 6b, c). At stations MC2, MC3 and MC6, H' and J values are lower for the >150 µm fraction, whereas the opposite is observed for stations MC4 and MC5, where small size fractions show lower diversity.

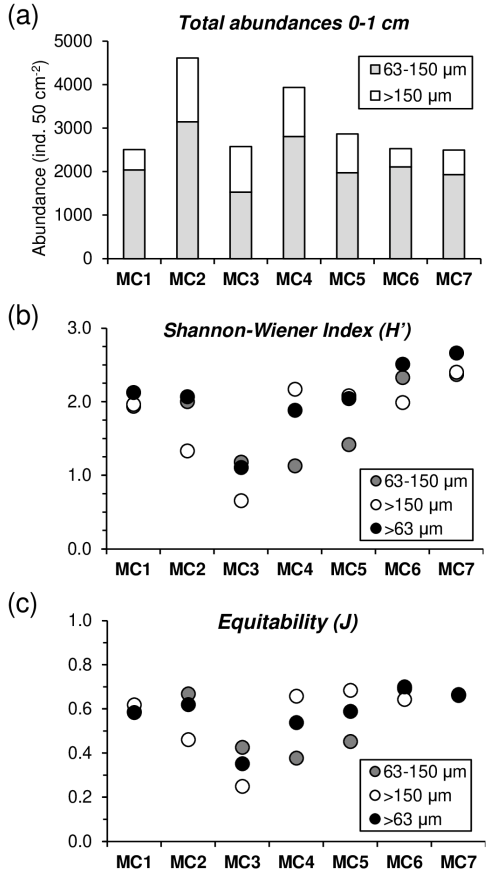

Figure 6. (a) Foraminiferal cumulative abundances (ind. 50 cm^{-2}) for two size fractions (63-150 µm, grey, and >150 µm, white) of the 0-1 cm sediment layer. **(b)** Shannon–Wiener (H') and **(c)** equitability (J) indexes comparison among the 63-150µm, >150µm and >63µm (black) fractions.

In terms of species composition (Fig. 7), the higher diversity of the 63-150 µm fraction at stations MC2 and MC3 is due to the additional presence of Stainforthia feylingi, *Spiroplectammina biformis* and *Textularia torquata*. However, at this size fraction, as in the > 150 µm fraction, the fauna at the three inner fjord stations (MC1, MC2, MC3) is also largely represented by *Elphidium clavatum* (juveniles) (16%, 30% and 66%, respectively). Similarly, juveniles of *Cassidulina reniforme* are observed in the small fraction at station MC1 (38%). At stations MC4 and MC5, the lower diversity of the 63-150 µm fraction is due to the strong dominance of *S. biformis* (75% and 65 %, respectively), which is nearly absent in the large size fraction. At station MC7, the small size fraction is characterised by the presence of juveniles of *Cassidulina teretis* (11%) and *Melonis barleeanus* (8%), species that are also present in the > 150 µm fraction (5% and 8%, respectively). These species are accompanied by *C. reniforme* (21%) and *Alabaminella weddellensis* (27%) that are only present in the small size fraction at this site.

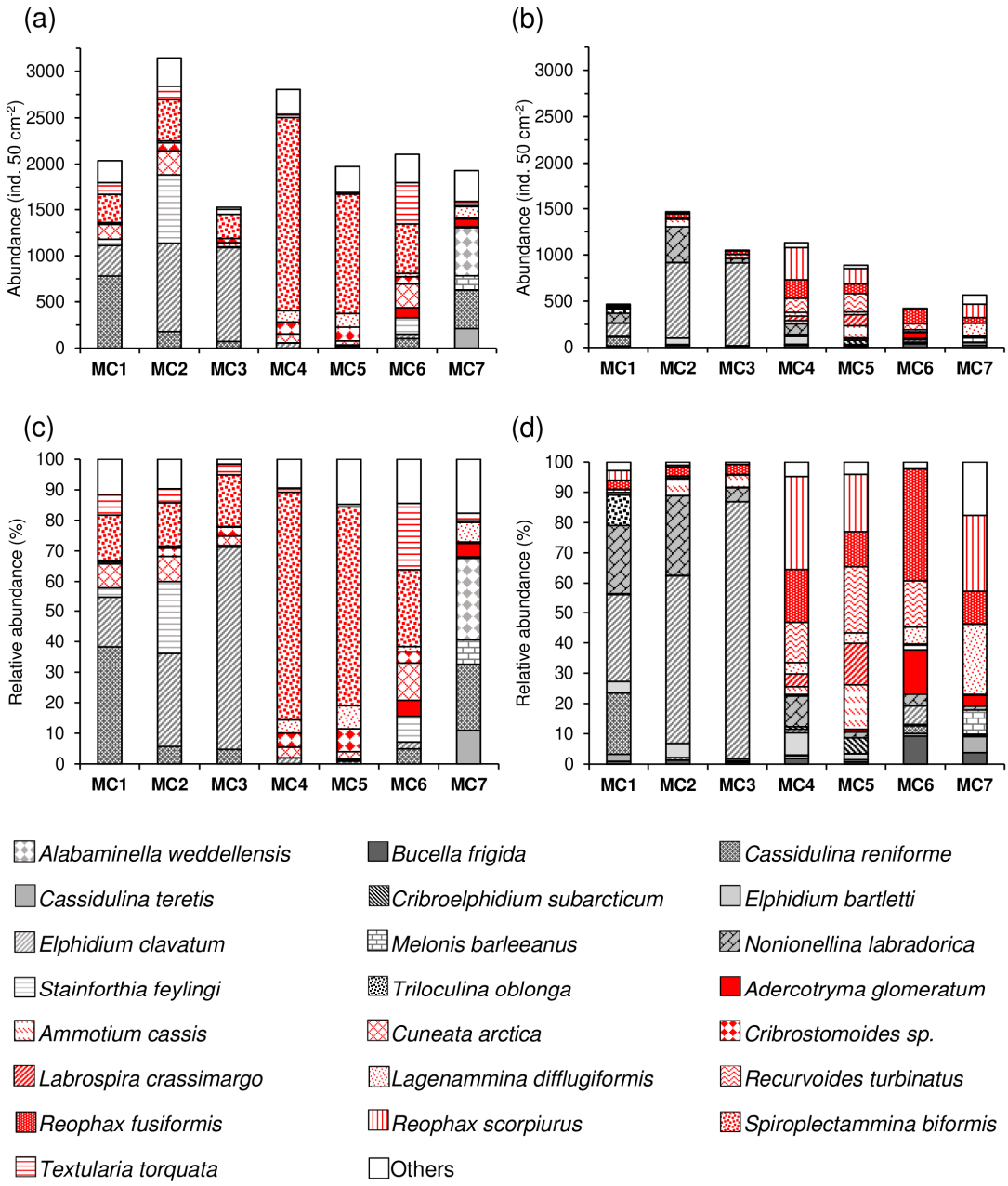

Figure 7. Total abundances (ind. 50 cm^{-2}) and correspondent relative abundances (%) of the dominant species (>5% for at least one station) of the 0-1 cm sediment layer for the 63-150 µm fraction **(a, c)** and the >150 µm fraction **(b, d)**. The calcareous species are shown using different grey textures, whereas agglutinated species are shown using different red textures.

4.5.2 Agglutinated vs. calcareous foraminifera

The percentage of agglutinated forms is systematically higher in the entire fraction >63 µm compared to the >150 µm at stations MC1 to MC6 (Fig. 8). This is explained by the presence of the small-sized agglutinated species *Spiroplectammina biformis* and other minor agglutinated species (*Cuneata arctica*, *Textularia torquata*, *Cribrostomoides* sp.). Conversely, the outer fjord station MC7 shows the opposite pattern, mainly because of the presence in the

small fraction of calcareous species that are absent in the >150 µm size fraction (i.e., *Cassidulina teretis*, *Cassidulina reniforme*, *Alabaminella weddellensis*).

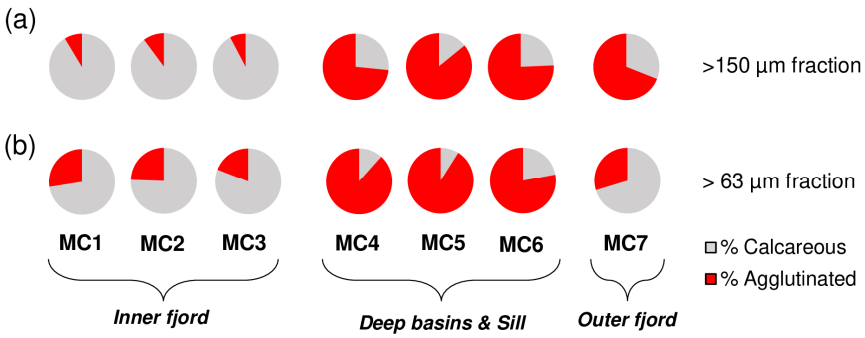

Figure 8. Relative abundances of calcareous foraminifera (in grey) and agglutinated foraminifera (in red) considering the >150 µm size fraction **(a)** and the > 63 µm size fraction **(b)**.

4.5.3 Multivariate analyses

Coordinate 2 of the nMDS analysis separates the >150 µm fraction from the 63 to 150 and >63 µm fractions (Fig. 9a), and the cluster (Bray-Curtis dissimilarity) analysis shows less than 50% similarity between the two groups (Fig. 9b). However, nMDS coordinate 1 groups all fractions into the same three stations' groups (Fig. 9a) as those previously determined by the CCA analysis based on the >150 µm fraction (Fig. 5).

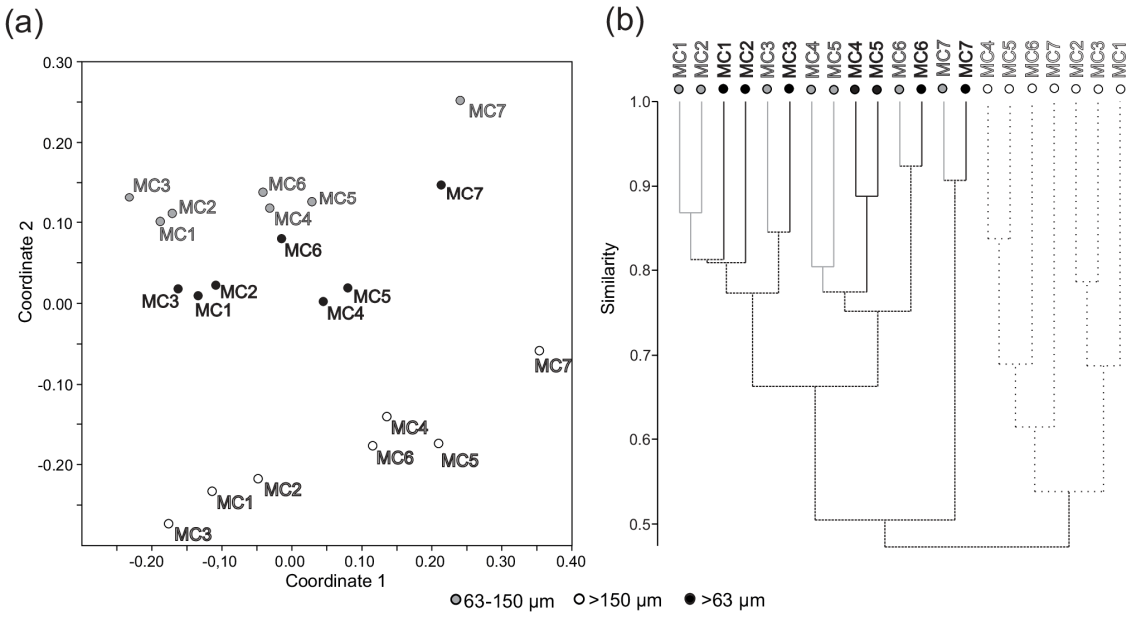

Figure 9. (a) Non-metric multidimensional scaling analysis and **(b)** cluster analysis (Bray-Curtis dissimilarity measure) considering the densities (ind. 50 cm^{-2}) of the major foraminiferal species (relative abundance >5% in at least one station in one size fraction) for the 63-150 µm fraction, the >150 µm fraction and the >63 µm total fraction.

4.6 Visual characterisation of test dissolution

At all stations inside the fjord (from MC1 to MC6) most of the calcareous species display different degrees of dissolution, including for small sized specimens. As visualised in Fig. S2 of the Supplement, the species *Elphidium clavatum*, *Elphidium bartletti*, *Triloculina oblonga* and *Robertinoides* sp. show the most severe degree of dissolution, whereas *Nonionellina labradorica* seems to be less sensitive to dissolution (individuals classified at stage I or II of dissolution). Interestingly, the highest degree of dissolution (stage IV) is exclusively observed in the deep basin and the sill stations.

5. Discussion

5.1 Environmental characteristics of the study area

According to the topography of the fjord, distribution of the main water masses and physicochemical characteristics of the sediments, we can separate the fjord into three main areas: the inner fjord (i.e., stations MC1 to MC3), the central deep basins (i.e., stations MC4 and MC5) constrained by the sill (i.e., station MC6) and the outer fjord Storfjordrenna (i.e., station MC7) (Fig. 1b).

In July 2016, the inner fjord sea surface water temperatures and salinities (Fig. S3 of the Supplement) are indicative of a mixture between meltwaters and Storfjorden surface water, as previously indicated by Skogseth et al. (2005b). On the contrary, the recorded inner fjord bottom water parameters are not homogeneous (Table 1). In fact, stations MC1 and MC2, on the western side of the fjord, are characterised by salinity and temperature within the range of BSW (Skogseth et al., 2005b). The location of these stations in small topographic depressions on the shelf may explain the presence of these cold and salty waters. The shallowest station MC3 (99m depth), located on the eastern side of the inner fjord, seems influenced by modified Atlantic water (as defined Skogseth et al., 2005b).

The bottom water values of salinity and temperature measured in July 2016 in the deep basins, still allow us to identify the presence of trapped residual BSW a long time after the season of sea ice formation, as previously hypothesised by Skogseth et al. (2005b). The bottom water properties at the sill fall into the range of Arctic water (Skogseth et al., 2005b). In contrast to the inner fjord and the deep basins, the outer fjord water column displays typical values of North Atlantic Water (NAW) from the surface to the bottom (Skogseth et al., 2005b).

The summer melting of tidewater glaciers flowing in Storfjorden produces an important supply of terrigenous materials to the head of the fjord (Winkelmann and Knies, 2005). This sedimentary dynamic results in relatively high sedimentation rates of about 3.6 ± 0.4 mm yr^{-1} recorded in the fjord (stations MC1 to MC6, Table S1), which is lower than in other Svalbard fjords (e.g., Kongsfjorden 5-10 mm yr^{-1}; Zaborska et al., 2006). Associated with this terrigenous flux, organic matter supply is high in the internal fjord. In contrast, low sedimentation rate (1.3 ± 0.6 mm yr^{-1}, Table S1) and low organic matter supply are recorded in the outer fjord. This clearly indicates a lower influence of tidewater glacier inputs in Storfjordrenna (station MC7) compared to the internal fjord (stations MC1 to MC6).

Regarding the organic supply, the high concentrations of organic matter at all our stations, and particularly in the deep basins, confirm the sedimentary organic-rich character of Storfjorden, as previously reported in the literature (Winkelmann and Knies, 2005; Mackensen et al., 2017). The higher CHO (%) associated with lower PRT (%) in the deep basins (station MC4 and MC5) compared to the other stations is indicative of the presence of older and more refractory organic matter (Pusceddu et al., 2000). This could either be related to higher continental supplies of more refractory organic matter, higher heterotrophic consumption, or the presence of long-residence water masses, influenced by BSW and isolated by a strong chemocline during periods of sea ice melting (Rysgaard et al., 2011). In contrast, the higher contents of PRT (%) and CPE in the inner fjord (stations MC1 to MC3) and at the sill (MC6) could be the result of a recent (summer) phytoplankton bloom. Compared to the inner fjord, the CPE contents in the Storfjordrenna are much lower (Fig. 2b), indicating a less fresh algal input to the bottom, which is consistent with the greater water depth (> 300 m) at this outer fjord site.

The oxygen profiles and the OPD in particular (Fig. S1a) reflect the quantity of organic matter supplies. Indeed, the organic carbon accumulation depends on its reactivity with available oxygen (Dauwe et al., 2001) and vice versa, the oxygen consumption is proportional to the organic matter mineralisation rate. Except for the outer fjord, all stations (MC1 to MC6) present shallow OPD values (<10 mm) consistent with the high contents of available organic matter (i.e., BPC) (Fig. 2). Organic matter aerobic respiration is also the reason for the rapid pH decrease in the first millimetre of the sediment column at these stations (Fig. S1b). At the outer fjord, the slower pH decrease and the higher OPD (>15 mm) would therefore be attributed to lower BCP content at this station.

5.2 Distribution of foraminiferal species in response to environmental conditions

According to the topography and physical characteristics of the fjord, the foraminiferal distribution and the measured environmental parameters also define three biozones: *(i)* the inner fjord, *(ii)* the deep basins and sill, and *(iii)* the outer fjord. The CCA analysis (Fig. 5) shows that the inner fjord faunas are positively correlated to PRT (%) and negatively correlated to CHO (%), meaning that they favourably respond to the availability of fresh and labile organic matter.

Elphidium clavatum dominates the innermost fjord stations, where it preferentially occupies the superficial microhabitats. The high dominance of this species in the inner fjord is consistent with previous findings from other glacier-proximal inner Svalbard fjords (Hald and Korsun, 1997; Korsun and Hald, 2000) and Arctic domains (e.g., Iceland; Jennings et al., 2004). *Elphidium clavatum* is also often described as being able to adapt to harsh environments, such as near tidewater glacier fronts and riverine estuaries (e.g., Hald and Korsun 1997; Korsun and Hald, 1998; Forwick et al., 2010). The presence of this species therefore suggests quite stressful conditions.

The station MC1, at the fjord head, is additionally characterised by the presence of *Cassidulina reniforme*. This species tolerates high concentrations of suspended particulate organic matter (Schäfer and Cole, 1986) and prefers cold water environments (Jernas et al., 2018). Korsun and Hald (1998) hypothesised that *C. reniforme* becomes dominant when glacier-driven turbidity is lower and phytoplankton production is higher. According to our findings, fauna at stations MC2 and MC3 potentially reflect a more stressful environment than station MC1. The strong dominance of these two species is also visible in the small size fraction, suggesting recent reproductive events, probably in response to fresh organic matter inputs to the seafloor. This hypothesis also matches with the dominance of *Nonionellina labradorica* in the intermediate microhabitats. In fact, this species is often reported in highly productive areas (Lloyd, 2006) because of its preference for feeding on fresh phytodetritus and on diatoms in particular (Cedhagen, 1991). Korsun and Hald (2000) suggest that this species may start reproducing during spring in glaciomarine environments, possibly following the diatom bloom starting in March under the sea ice (Rysgaard et al., 2011). Therefore, we instead interpret its presence as a response to meltwater discharge and consequent phytoplanktonic bloom. Additionally, *Elphidium bartletti* that occurs as an accessory species (especially at station MC2) was previously reported in river-affected habitats of the southern Kara Sea, characterised by

highly variable environmental conditions (Polyak et al., 2002), further supporting our interpretations.

The CCA analysis (Fig. 6) shows a negative correlation of the deep basins and sill fauna with proteins and a positive correlation with carbohydrates, highlighting a response of the fauna to old (refractory) organic matter. The assemblages in the two deep basin stations (MC4 and MC5) display similar diversities, which are in both cases higher than in the inner fjord. Agglutinated species dominate the topmost centimetre of the sediment, in particular *Reophax scorpiurus*, *Reophax fusiformis*, and *Recurvoides turbinatus*, occasionally accompanied by *Labrospira crassimargo* and *Ammotium cassis*. These species are often found in the distal part of other Svalbard fjords (e.g., Hald and Korsun, 1997; Murray and Alve, 2011; Jernas et al., 2018) and widely distributed in areas covered with seasonal sea ice in the Arctic Ocean (e.g., Wollenburg and Kuhnt, 2000; Wollenburg and Mackensen, 1998). They are considered as tolerating low food quality, high sedimentation rates, and a wide range of salinities, temperatures, and organic matter fluxes (Hald and Korsun, 1997; Murray, 2006; Jernas et al., 2018). This capacity for adaptation may explain the abundance of all these agglutinated species in the deep basins where residual BSW (with high S, low T and pH) and high concentrations of refractory carbohydrates are recorded in the top sediment. At station MC4, *N. labradorica* also lives in a subsurface microhabitat (from 1 down to 3 cm depth), probably profiting from the phytodetritus supply, as testified by the high CPE contents.

The assemblage composition at the sill (station MC6) is close to those found in the deep basins, except for the dominant presence of *Adercotryma glomeratum*. The similarities with the deep basin's assemblages are interpreted as the result of intermittent pulses of BSW outflowing the fjord and bypassing the sill during some periods of the year and therefore influencing this station. The opportunist *A. glomeratum* (e.g., Gooday and Rathburn, 1999; Heinz et al., 2002) has been reported as being positively related to increasing distance from glaciers and from the fjord head (Hald and Korsun, 1997). Its dominance at this station suggests a positive relationship with an increase in salinities and temperatures and consequently with Transformed Atlantic Water (TAW) during summer, according to existing literature (e.g., Hald and Korsun, 1997; Jernas et al., 2018). It has therefore been interpreted as the consequence of seasonal influence of Atlantic waters on the sill, when BSW overflow is weakened or absent. In addition to the assemblage composition, the presence of very badly preserved calcareous foraminifera tests and the dominance of agglutinated species in the deep basins plus the sill, strongly suggest that corrosive BSW has a primary control on the benthic ecology in this sector of the fjord.

The outer fjord biozone (station MC7) is characterised by a thicker overlying water column (> 300 m), and higher bottom water salinity and temperature compared to the rest of the studied sites. The presence at this station of agglutinated species shared with the deep basin stations is probably due to the widespread character of these species. However, the clear influence of the NAW at this site is indicated by the presence of typical Atlantic species such as *Melonis barleeanus* and *Globobulimina auriculata*. In the North Atlantic Ocean, *M. barleeanus* is described as infaunal and opportunist toward good-quality organic matter (e.g., Caralp et al., 1989; Nardelli et al., 2010). At high latitudes, its presence suggests the influence of relatively warm Atlantic Water (AW) (Caralp, 1989; Polyak et al., 2002; Jennings et al., 2004; Knudsen et al., 2012; Melis et al., 2018). This interpretation is further confirmed by the presence of the deeper dwelling *Globobulimina auriculata*, presumed to be related to increasing bottom water salinity (Williamson et al., 1984; Jernas et al., 2018) and often associated with buried organic matter (e.g., Alve, 2010).

5.3 Agglutinated vs. calcareous taxa: the premise of a paleo-proxy of brine formation

In both size fractions (63–150 and > 150 µm), low agglutinated / calcareous (A/C) ratios characterise the inner fjord, in contrast to the high values observed at the deep basin and sill stations (Figs. 3b and 8). The exclusive presence of some agglutinated species in the smaller fraction (e.g., *Cuneata arctica*, *Spiroplectammina biformis* and *Textularia torquata*) results in relatively high A/C ratios for the > 63 µm fraction compared to the > 150 µm fraction. It is worth mentioning that in the Storfjordrenna (station MC7) the A/C ratio in the > 63 µm fraction is lowered by the presence of several small calcareous species (e.g., *Stainforthia feylingi*, *Cassidulina teretis*, *Alabaminella weddellensis*, *Cassidulina reniforme*) that are not present in the larger fraction (Fig. 8).

Several hypotheses, which are eventually not exclusive, arise to explain the dominance of agglutinated species at the deep basins and sill stations.

i. *The influence of organic matter quality*. Jernas et al. (2018) suggest that agglutinated species may be more tolerant or less sensitive to the lower quality and/or quantity of food than the calcareous fauna. Following this idea, the dominance of agglutinated species in the deep basins is coherent with the more refractory organic matter (higher CHO %) measured in July 2016 (Fig. 2). However, the lower percentage of CHO observed at the sill station MC6 seems to contradict this hypothesis.

ii. *The brine-related calcareous test dissolution.* Low relative abundances of calcareous taxa found in the sediment in the deep basins could be attributed either to hampered growth, limited reproduction, or test dissolution. Indeed, at the deep basins and sill stations we observe the most severe degree of dissolution on *Elphidium clavatum*, *Elphidium bartletti*, *Triloculina oblonga* and *Robertinoides* spp. in particular (Fig. S2). The most obvious explanation for that is the corrosive effect of brine waters that persist all year round at stations MC4 and MC5 and may impact station MC6 through episodes of overflow from autumn to spring. In the inner fjord stations, these species also present some dissolution, but this is largely less severe (Fig. S2). In our opinion the dissolution at these sites can but either related to early cascading of BSW during winter or to the high seasonal input of meltwater as a factor affecting the preservation of carbonate (Schröder-Adams et al., 1990).

iii. *The combined effect of brine and organic matter mineralisation.* As an alternative (or in parallel) calcareous test dissolution may result from decaying organic matter. Indeed, test dissolution of E. clavatum species was previously observed in the Adventfjorden (west Svalbard) and was attributed to low pH in the pore waters of upper sediments due to organic matter decay (Majewski and Zajagczkowski, 2007), whereas in the Barents-Kara shelf this process was associated with sinking of brine (Hald and Steinsund, 1992; Steinsund and Hald, 1994). The coupled effect of corrosive brine and organic matter remineralisation probably simultaneously contributes to the dissolution of the calcareous fauna. It is difficult to decouple the effects of both these factors. However, we observe the most severe degree of dissolution in the deep basins, where organic matter is less available. This lets us conclude that the persistence of brine is the main factor responsible for the dissolution. This conclusion supports some previous paleoceanographical studies from the Arctic, which proposed that the high proportion of agglutinated taxa in sediment cores is dependent on bottom water hydrographical condition (Seidenkrantz et al., 2007) and on corrosive brine production specifically (Rasmussen and Thomsen, 2015).

In light of these arguments, we propose the A/C ratio as a proxy for brine persistence and/or overflow in historical sedimentary archives. Rasmussen and Thomsen (2014, 2015) reported an exceptional fossilising potential of agglutinated species in this area on records back to 10 ka, therefore it is most likely that the ratio is not affected on a timescale of hundreds of years.

5.4 Insights from the small size fraction

The additional observation of the small size fraction (63-150 µm) results in the definition of the same three biozones and similar A/C ratios as for the larger fraction (except for the outer fjord station where the ratio changes) (Figs. 8 and 9a). The cluster analysis (Fig. 9b) further shows that the consideration of the 63-150 µm fraction increases the percentage of similarity among stations belonging to the same biozone and it increases the dissimilarity between the stations inside the fjord (from MC1 to MC6) and outside the fjord (MC7). Nonetheless, the study of the 63-150 µm fraction provides new insights into the benthic foraminiferal ecology of Storfjorden.

At the inner fjord stations MC2 and MC3, the exclusive presence of the calcareous species *Stainforthia feylingi* and the three agglutinated species *Cuneata arctica*, *Spiroplectammina biformis*, and *Textularia torquata* in the 63-150 µm fraction increases the overall diversity compared to the larger fraction. These four species, with individuals of small size, are typical of Arctic and cold boreal environments and show an opportunistic behaviour in response to a wide range of environmental conditions (e.g., Schäfer and Cole, 1986; Hald and Korsun, 1997; Korsun and Hald, 1998, 2000; Lloyd et al., 2007; Leduc et al., 2002; Pawlowska et al., 2016; Jernas et al., 2018). The presence of numerous juveniles (63-150 µm) of *Elphidium clavatum* and *Cassidulina reniforme* in the inner fjord also confirms recent reproductive events, possibly related to phytoplanktonic bloom and associated fresh organic matter inputs in the benthic system, in agreement with the high percentages of PRT measured in the sediment (Fig. 2).

On the contrary, in the deep basins, the diversity decreases when the small fraction is considered, due to the strong dominance of the agglutinated species *S. biformis*. In the literature, this is an opportunistic species in glaciomarine habitats, indicative of the presence of cold Arctic waters (Hald and Korsun, 1997; Korsun and Hald, 1998, 2000; Schäfer and Cole, 1986). The high numbers of small individuals found in the deep basins, coupled with the high percentages of CHO, may suggest an eventual positive response of *S. biformis* to refractory organic matter. The relatively high abundances of *T. torquata* at the sill station MC6 suggests high salinity fluctuations (Wollenburg and Kuhnt, 2000), which could be consistent with occasional or seasonal overflow of BSW at this site, further confirming our hypothesis based on the >150 µm assemblages.

In the Storfjordrenna, *Cassidulina teretis* and *Alabaminella weddellensis* are exclusively present in the 63-150 µm fraction. These two species, usually associated with AW (Wollenburg and Mackensen, 1998), further give evidence of the influence of this water mass in the outer fjord area. The presence of *C. reniforme* at this station exclusively as juveniles is less easy to

interpret. Because of its preference for cold waters (e.g., Jernas et al., 2018), its presence could be the result of an occasional influence of Arctic waters on this station.

Taking into consideration the comparison between the 63-150 and >150 µm data, the additional information from the small fauna is limited to a slightly more precise estimation of biodiversity and the confirmation of ecological speculations based on the large fauna (e.g., recent blooming events at inner stations). Therefore, regarding the high time-consuming character inherent to the investigation of the 63-150 µm fraction, we propose that the small fraction could be neglected in comparable future studies in Storfjorden unless it is studied with the aim of answering some very specific questions.

6. Conclusions

Living benthic foraminiferal fauna from the Storfjorden "sea ice factory" were studied in order to determine the response of foraminiferal communities to the major driving factors controlling the sea bottom ecology in this area. The benthic ambient conditions were further connected to brine-enriched shelf waters (BSW) production and persistence and indirectly to first-year sea ice formation. The influence of the BSW persistence on benthic foraminiferal assemblages was identified on the basis of characteristic fauna inhabiting the two deep basins and the sill of the fjord. At these sites, BSW are, respectively, trapped for a long part of the year or overflow during the maximum production period. The assemblages at these stations are dominated by agglutinated taxa, resulting in high agglutinated/calcareous ratio (A/C). The presence of heavily dissolved calcareous tests supports the hypothesis that one of the main factors responsible for this result is the corrosive character of BSW. Additionally, the chemocline related to BSW presence at the bottom could limit the fresh organic matter flux to the seabed and indirectly influence the assemblages. In light of these results, we propose the application of the A/C ratio as a proxy for brine persistence and overflow on historical sedimentary records from Storfjorden, in order to reconstruct past changes in BSW intensity and, by extension, in first-year sea ice production.

Data availability. Raw data are available from the following link: https://doi.org/10.1594/PANGAEA.907687 (Fossile et al., 2019).

Supplement. Tables S1 and S2 and Figs. S1, S2, and S3 can be found in the Supplement. Scanning electron micrographs (plates) of the most relevant species are shown in Figs. S4 and S5 in the Supplement section.

Author contributions. EF, MM, MPN and HH wrote the manuscript, which was commented by all co-authors. EM was the cruise leader, and field work was performed by HH and BL. EF, MPN, MM, HH, AJ, BL and DM collected the data. EF, MPN, MM, HH, AJ, BL and AP analysed and interpreted the data.

Acknowledgements. We are grateful to the captain and crew of R/V L'Atalante, which was chartered by IFREMER (French Research Institute for Exploitation of the Sea); Frédéric Vivier (co-chief of the cruise); and all participants who contributed to the success of to the STeP cruise. We particularly thank Bruno Bombled for his technical assistance during the cruise. Original SEM micrographs of foraminiferal species (Figs. S2, S4, S5) were realised by Romain Mallet at SCIAM (Université d'Angers). We fully acknowledge the efficient technical help provided by Sophie Quinchard and Raphäel Hubert-Huard, and we thank Benedicte Ferré for the useful discussions about the oceanography of the study area. We are grateful to Shungo Kawagata and one anonymous reviewer for their constructive comments. This research is part of the PhD thesis of Eleonora Fossile, which is co-funded by French National Program MOPGA (Make Our Planet Great Again) and the University of Angers.

Financial support. The research was funded by the ABBA (Observatoire des Sciences de l'Univers de Nantes Atlantique), Bi-SMART (University of Angers) and TANDEM (Région Pays de la Loire) projects.

Competing interests. The authors declare that they have no conflict of interest.

Review statement. This paper was edited by Hiroshi Kitazato and reviewed by Shungo Kawagata and one anonymous referee.

References

Aagaard, K., Swift, J. H., and Carmack, E. C.: Thermohaline circulation in the Arctic Mediterranean Seas, J. Geophys. Res., 90, 4833, https://doi.org/10.1029/JC090iC03p04833, 1985.

Alve, E.: Benthic foraminiferal responses to absence of fresh phytodetritus: A two-year experiment, Mar. Micropaleontol., 76, 67– 75, https://doi.org/10.1016/j.marmicro.2010.05.003, 2010

Anderson, L. G., Falck, E., Jones, E. P., Jutterström, S., and Swift, J. H.: Enhanced uptake of atmospheric CO_2 during freezing of seawater: A field study in Storfjorden, Svalbard, J. Geophys. Res., 109, C06004, https://doi.org/10.1029/2003JC002120, 2004.

Appleby, P. G. and Oldfield, F.: The calculation of lead-210 dates assuming a constant rate of supply of unsupported 210Pb to the sediment, Catena, 5, 1–8, https://doi.org/10.1016/S0341- 8162(78)80002-2, 1978.

Beszczynska-Moller, A., Fahrbach, E., Schauer, U., and Hansen, E.: Variability in Atlantic water temperature and transport at the entrance to the Arctic Ocean, 1997–2010, ICES J. Mar. Sci., 69, 852–863, https://doi.org/10.1093/icesjms/fss056, 2012.

Blott, S. J. and Pye, K.: GRADISTAT: a grain size distribution and statistics package for the analysis of unconsolidated sediments, Earth Surf. Proc. Land., 26, 1237–1248, https://doi.org/10.1002/esp.261, 2001.

Caralp, M. H.: Abundance of Bulimina exilis and *Melonis barleeanum*: Relationship to the quality of marine organic matter, Geo-Mar. Lett., 9, 37–43, https://doi.org/10.1007/BF02262816, 1989.

Cavalieri, D. J. and Martin, S.: The contribution of Alaskan, Siberian, and Canadian coastal polynyas to the cold halocline layer of the Arctic Ocean, J. Geophys. Res., 99, 18343–18362, https://doi.org/10.1029/94JC01169, 1994.

Cedhagen, T.: Retention of chloroplasts and bathymetric distribution in the sublittoral foraminiferan *Nonionellina Labradorica*, Ophelia, 33, 17–30, https://doi.org/10.1080/00785326.1991.10429739, 1991.

Cottier, F. R., Nilsen, F., Skogseth, R., Tverberg, V., Skarðhamar, J. and Svendsen, H.: Arctic fjords: a review of the oceanographic environment and dominant physical processes, Geol. Soc. Spec. Publ., 344, 35–50, https://doi.org/10.1144/sp344.4, 2010.

Dai, A., Luo, D., Song, M., and Liu, J.: Arctic amplification is caused by sea-ice loss under increasing CO_2, Nat. Commun., 10, 1–13, https://doi.org/10.1038/s41467-018-07954-9, 2019.

Danovaro, R.: Methods for the Study of Deep-Sea Sediments, Their Functioning and Biodiversity, CRC Press, Boca Raton, 2009.

Dauwe, B., Middelburg, J. J., and Herman, P. M. J., Effect of oxygen on the degradability of organic matter in subtidal and intertidal sediments of the North Sea area, Mar. Ecol.-Prog. Ser., 215, 13– 22, https://doi.org/10.3354/meps215013, 2001.

de Jonge, V. N.: Fluctuations in the Organic Carbon to Chlorophyll- a Ratios for Estuarine Benthic Diatom Populations, Mar. Ecol.- Prog. Ser., 2, 345–353, https://doi.org/10.3354/meps002345, 1980.

Dickson, A. G., Sabine, C. L., and Christian, J. R.: Guide to best practices for ocean CO_2 measurements, PICES Special Publica- tion 3, 191 pp., 2007.

Fabiano, M., Danovaro, R., and Fraschetti, S.: A three-year time series of elemental and biochemical composition of organic matter in subtidal sandy sediments of the Ligurian Sea (northwestern Mediterranean), Cont. Shelf Res., 15, 1453–1469, https://doi.org/10.1016/0278-4343(94)00088-5, 1995.

Farmer, D. M. and Freeland, H. J.: The physical oceanography of Fjords, Prog. Oceanogr., 12, 147–220, https://doi.org/10.1016/0079-6611(83)90004-6, 1983.

Fer, I., Skogseth, R., and Haugan, P. M.: Mixing of the Storfjorden overflow (Svalbard Archipelago) inferred from density overturns, J. Geophys. Res., 109, C01005, https://doi.org/10.1029/2003JC001968, 2004.

Forwick, M., Vorren, T. O., Hald, M., Korsun, S., Roh, Y., Vogt, C., and Yoo, K.-C.: Spatial and temporal influence of glaciers and rivers on the sedimentary environment in Sassenfjorden and Tempelfjorden, Spitsbergen, Geol. Soc. Spec. Publ., 344, 163– 193, https://doi.org/10.1144/SP344.13, 2010.

Fossile, E., Nardelli, M. P., and Mojtahid, M.: STEP2016 living foraminifera in surface sediments of a N-S transect in the Storfjorden, PANGAEA, https://doi.org/10.1594/PANGAEA.907687, 2019.

Geyer, F., Fer, I., and Eldevik, T.: Dense overflow from an Arctic fjord: Mean seasonal cycle, variability and wind influence, Cont. Shelf Res., 29, 2110–2121, https://doi.org/10.1016/j.csr.2009.08.003, 2009.

Gleitz, M., Rutgers v.d. Loeff, M., Thomas, D. N., Dieckmann, G. S., and Millero, F. J.: Comparison of summer and winter inorganic carbon, oxygen and nutrient concentrations in Antarctic sea ice brine, Mar. Chem., 51, 81–91, https://doi.org/10.1016/0304-4203(95)00053-T, 1995.

Gonzales, M. V., De Almeida, F. K., Costa, K. B., Santarosa, A. C. A., Camillo, E., De Quadros, J. P., and Toledo, F. A. L.: Help Index: Hoeglundina Elegans Preservation Index for Marine Sediments in the Western South Atlantic, J. Foramin. Res., 47, 56–69, https://doi.org/10.2113/gsjfr.47.1.56, 2017.

Gooday, A. J. and Rathburn, A. E.: Temporal variability in living deep-sea benthic foraminifera: a review, Earth Sci. Rev., 46, 187– 212, https://doi.org/10.1016/S0012-8252(99)00010-0, 1999.

Grasshoff, K., Ehrhardt, M., and Kremling, K.: Methods of seawater analysis, second revised and extended edition, Academia press, London, New York, 1983.

Haarpaintner, J., Gascard, J., and Haugan, P. M.: Ice production and brine formation in Storfjorden, Svalbard, J. Geophys. Res.-Oceans, 106, 14001–14013, https://doi.org/10.1029/1999JC000133, 2001a.

Haarpaintner, J., Haugan, P. M., and Gascard, J. C.: Interannual variability of the Storfjorden (Svalbard) ice cover and ice pro- duction observed by ERS-2 SAR, Ann. Glaciol., 33, 430–436, 2001b.

Haarpaintner, J., O'Downer, J., Gascard, J. C., Haugan, P. M., Schauer, U. and Øterhus, S.: Seasonal transformation of water masses, circulation and brine formation observed in Storfjorden, Svalbard, Ann. Glaciol., 33, 437–443, https://doi.org/10.3189/172756401781818635, 2001c.

Hald, M. and Korsun, S.: Distribution of modern benthic foraminifera from fjords of Svalbard, European Arctic, J. Foramin. Res., 27, 101–122, https://doi.org/10.2113/gsjfr.27.2.101, 1997.

Hald, M. and Steinsund, P. I.: Distribution of surface sediment benthic foraminifera in the southwestern Barents Sea, J. Foramin. Res., 22, 347–362, https://doi.org/10.2113/gsjfr.22.4.347, 1992.

Hammer, Ø., Harper, D., and Ryan, P. D.: PAST: Palaeontological statistics software package for education and data analysis, Palaeontol. Electron., 4, 1–9, 2001.

Hansen, A. and Knudsen, K. L.: Recent foraminiferal dis- tribution in Freemansundet and Early Holocene stratigraphy on Edgeøya, Svalbard, Polar Res., 14, 215–238, https://doi.org/10.3402/polar.v14i2.6664, 1995.

Heinz, P., Hemleben, C., and Kitazato, H.: Time-response of cultured deep-sea benthic foraminifera to different algal diets, Deep-Sea Res. Pt. I, 49, 517–537, https://doi.org/10.1016/S0967- 0637(01)00070-X, 2002.

Holland, M. M. and Bitz, C. M.: Polar amplification of cli- mate change in coupled models, Clim. Dynam., 21, 221–232, https://doi.org/10.1007/s00382-003-0332-6, 2003.

Holliday, N. P., Hughes, S. L., Bacon, S., Beszczynska-Möller, A., Hansen, B., Lavín, A., Loeng, H., Mork, K. A., Østerhus, S., Sherwin, T., and Walczowski, W.: Reversal of the 1960s to 1990s freshening trend in the northeast North Atlantic and Nordic Seas, Geophys. Res. Lett., 35, 1–5, https://doi.org/10.1029/2007GL032675, 2008.

Horner, R. and Schrader, G. C.: Relative Contributions of Ice Algae, Phytoplankton, and Benthic Microalgae to Primary Production in Nearshore Regions of the Beaufort Sea, Arctic, 35, 485–503, 1982.

IPCC: Climate Change 2013: The Physical Science Basis. Contribution of Working Group I Contribution to the Fifth Assessment Report of the Intergovernmental Panel on Climate Change, edited by: Stocker, T. F., Qin, D. Plattner, G.- K., Tignor, M., Allen, S. K., Boschung, J., Nauels, A., Xia, Y., Bex, V., and Midgley, P. M., Cambridge Univ. Press, Cambridge, UK, New York, NY, USA, 1535 pp., https://doi.org/10.1017/CBO9781107415324, 2013.

Ivanova, E. V., Ovsepyan, E. A., Risebrobakken, B., and Vetrov, A. A.: Downcore distribution of living calcareous foraminifera and stable isotopes in the West- ern Barents Sea, J. Foramin. Res., 38, 337–356, https://doi.org/10.2113/gsjfr.38.4.337, 2008.

Jardon, F. P., Vivier, F., Bouruet-Aubertot, P., Lourenço, A., Cuypers, Y., and Willmes, S.: Ice production in Storfjorden (Svalbard) estimated from a model based on AMSR-E observa- tions: Impact on water mass properties, J. Geophys. Res.-Oceans, 119, 377–393, https://doi.org/10.1002/2013JC009322, 2014.

Jennings, A. E., Weiner, N. J., Helgadottir, G., and Andrews, J. T.: Modern Foraminiferal Faunas of the Southwestern To Northern Iceland Shelf: Oceanographic and Environmental Controls, J. Foramin. Res., 34, 180–207, https://doi.org/10.2113/34.3.180, 2004.

Jernas, P., Klitgaard-Kristensen, D., Husum, K., Koç, N., Tverberg, V., Loubere, P., Prins, M., Dijkstra, N., and Glu- chowska, M.: Annual changes in Arctic fjord environment and modern benthic foraminiferal fauna: Evidence from Kongsfjorden, Svalbard, Global Planet. Change, 163, 119–140, https://doi.org/10.1016/j.gloplacha.2017.11.013, 2018.

Jorissen, F. J., de Stigter, H. C., and Widmark, J. G. V: A conceptual model explaining benthic foraminiferal microhabitats, Mar. Micropaleontol., 26, 3–15, https://doi.org/10.1016/0377- 8398(95)00047-X, 1995.

Kinnard, C., Zdanowicz, C. M., Fisher, D. A., Isaksson, E., de Vernal, A., and Thompson, L. G.: Reconstructed changes in Arctic sea ice over the past 1450 years, Nature, 479, 509–512, https://doi.org/10.1038/nature10581, 2011.

Kitazato, H., Shirayama, Y., Nakatsuka, T., Fujiwara, S., Shimanaga, M., Kato, Y., Okada, Y., Kanda, J., Yamaoka, A., Masuzawa, T., and Suzuki, K.: Seasonal phytodetritus deposition and responses of bathyal benthic foraminiferal populations in Sagami Bay, Japan: preliminary results from "Project Sagami 1996–1999", Mar. Micropaleontol., 40, 135– 149, https://doi.org/10.1016/S0377-8398(00)00036-0, 2000.

Knudsen, K. L., Eiríksson, J., and Bartels-Jónsdóttir, H. B.: Oceanographic changes through the last millennium off North Iceland: Temperature and salinity reconstructions based on foraminifera and stable isotopes, Mar. Micropaleontol., 84–85, 54–73, https://doi.org/10.1016/j.marmicro.2011.11.002, 2012.

Korsun, S. and Hald, M.: Modern benthic foraminifera off Novaya Zemlya tidewater glaciers, Russian Arctic, Arct. Antarct. Alp. Res., 30, 61–77, https://doi.org/10.2307/1551746, 1998.

Korsun, S. and Hald, M.: Seasonal dynamics of Benthic Foraminifera in a Glacially Fed Fjord of Svalbard, European Arctic, J. Foramin. Res., 30, 251–271, https://doi.org/10.2113/0300251, 2000.

Korsun, S. A., Pogodina, I. A., Forman, S. L., and Lubinski, D. J.: Recent foraminifera in glaciomarine sediments from three arctic fjords of Novaja Zemlja and Svalbard, Polar Res., 14, 15–32, https://doi.org/10.3402/polar.v14i1.6648, 1995.

Labe, Z., Magnusdottir, G., and Stern, H.: Variability of Arctic sea ice thickness using PIOMAS and the CESM large ensemble, J. Climate, 31, 3233–3247, https://doi.org/10.1175/JCLI-D- 17-0436.1, 2018.

Łacka, M. and Zaja¸czkowski, M.: Does the recent pool of benthic foraminiferal tests in fjordic surface sediments reflect interannual environmental changes? The resolution limit of the foraminiferal record, Ann. Soc. Geol. Pol., 86, 59–71, https://doi.org/10.14241/asgp.2015.019, 2016.

Leduc, J., Bilodeau, G., De Vernal, A., and Mucci, A.: Distribution of benthic foraminiferal populations in surface sediments of the Saguenay Fjord, before and after the 1996 flood, Palaeogeogr. Palaeoclimatol. Palaeoecol., 180, 207–223, https://doi.org/10.1016/S0031-0182(01)00429-1, 2002.

Lloyd, J., Kuijpers, A., Long, A., Moros, M., and Park, L. A.: Foraminiferal reconstruction of mid- to late-Holocene ocean circulation and climate variability in Disko Bugt, West Greenland, Holocene, 8, 1079–1091, https://doi.org/10.1177/0959683607082548, 2007.

Lloyd, J. M.: Modern Distribution of Benthic Foraminifera From Disko Bugt, West Greenland, J. Foramin. Res., 36, 315–331, https://doi.org/10.2113/gsjfr.36.4.315, 2006.

Loeng, H.: Features of the physical oceanographic conditions of the Barents Sea, Polar Res., 10, 5–18, https://doi.org/10.3402/polar.v10i1.6723, 1991. Lorenzen, C. J. and Jeffrey, S. W.: Determination of chlorophyll in seawater, Unesco Tech. Pap. Mar. Sci., 35, 1–20, 1980.

Lydersen, C., Assmy, P., Falk-Petersen, S., Kohler, J., Ko- vacs, K. M., Reigstad, M., Steen, H., Strøm, H., Sund-fjord, A., Varpe, Ø., Walczowski, W., Weslawski, J. M., and Zaja¸czkowski, M.: The importance of tidewater glaciers for marine mammals and seabirds in Svalbard, Norway, J. Marine Syst., 129, 452–471, https://doi.org/10.1016/j.jmarsys.2013.09.006, 2014.

Mackensen, A., Schmiedl, G., Thiele, J., and Damm, E.: Mi- crohabitat preferences of live benthic foraminifera and stable carbon isotopes off SW Svalbard in the presence of widespread methane seepage, Mar. Micropaleontol., 132, 1–17, https://doi.org/10.1016/j.marmicro.2017.04.004, 2017.

Majewski, W. and Zaja˛czkowski, M.: Benthic Foraminifera in Adventfjorden, Svalbard: Last 50 Years of Local Hy- drographic Changes, J. Foramin. Res., 37, 107–124, https://doi.org/10.2113/gsjfr.37.2.107, 2007.

McPhee, M. G., Skogseth, R., Nilsen, F., and Smedsrud, L. H.: Creation and tidal advection of a cold salinity front in Storfjorden: 2. Supercooling induced by turbulent mixing of cold water, J. Geophys. Res.-Oceans, 118, 3737–3751, https://doi.org/10.1002/jgrc.20261, 2013.

Melis, R., Carbonara, K., Villa, G., Morigi, C., Bárcena, M. A., Giorgetti, G., Caburlotto, A., Rebesco, M., and Lucchi, R. G.: A new multi-proxy investigation of Late Quaternary palaeoenvironments along the north-western Barents Sea (Storfjorden Trough Mouth Fan), J. Quaternary Sci., 33, 662–676, https://doi.org/10.1002/jqs.3043, 2018.

Misund, O. A., Heggland, K., Skogseth, R., Falck, E., Gjøsæter, H., Sundet, J., Watne, J., and Lønne, O. J.: Norwegian fisheries in the Svalbard zone since 1980. Regulations, profitability and warming waters affect landings, Polar Sci., 10, 312–322, https://doi.org/10.1016/j.polar.2016.02.001, 2016.

Murray, J. W.: Ecology and Application of Benthic Foraminifera, Cambridge University Press, Cambridge, New York, https://doi.org/10.1017/CBO9780511535529, 2006.

Murray, J. W. and Alve, E.: The distribution of agglutinated foraminifera in NW European seas: Baseline data for the interpretation of fossil assemblages, Palaeontol. Electron., 14, 1–41, 2011.

Nardelli, M., Jorissen, F., Pusceddu, A., Morigi, C., Dell'Anno, A., Danovaro, R., De Stigter, H. C., and Negri, A.: Living benthic foraminiferal assemblages along a latitudinal transect at 1000m depth off the Portuguese margin, Micropaleontology, 56, 323– 344, 2010.

Nicolle, M., Debret, M., Massei, N., Colin, C., deVernal, A., Di- vine, D., Werner, J. P., Hormes, A., Korhola, A., and Linder- holm, H. W.: Climate variability in the subarctic area for the last 2 millennia, Clim. Past, 14, 101–116, https://doi.org/10.5194/cp- 14-101-2018, 2018.

Nielsen, T. and Rasmussen, T. L.: Reconstruction of ice sheet retreat after the Last Glacial maximum in Storfjorden, southern Svalbard, Mar. Geol., 402, 228–243, https://doi.org/10.1016/j.margeo.2017.12.003, 2018.

Ohga, T. and Kitazato, H.: Seasonal changes in bathyal foraminiferal populations in response to the flux of organic matter (Sagami Bay, Japan), Terra Nova, 9, 33–37, https://doi.org/10.1046/j.1365-3121.1997.d01-6.x, 1997.

Omar, A., Johannessen, T., Bellerby, R. G. J., Olsen, A., Ander- son, L. G., and Kivimae, C.: Sea-Ice and Brine Formation in Storfjorden: Implications for the Arctic Wintertime Air-Sea CO_2 Flux, in: The Nordic Seas: An Integrated Perspective, edited by: Drange, H., Dokken, T., Furevik, T., Gerdes, R., and Berger, W., Geophysical Monograph 158, American Geophysical Union, Washington, DC, 117–187, https://doi.org/10.1029/158GM12, 2005.

Pawłowska, J., Zaja˛czkowski, M., Ła˛cka, M., Lejzerowicz, F., Es- ling, P., and Pawlowski, J.: Palaeoceanographic changes in Horn- sund Fjord (Spitsbergen, Svalbard) over the last millennium: new insights from ancient DNA, Clim. Past, 12, 1459–1472, https://doi.org/10.5194/cp-12-1459-2016, 2016.

Pedrosa, M. T., Camerlenghi, A., De Mol, B., Urgeles, R., Rebesco, M., and Lucchi, R. G.: Seabed morphology and shallow sedimentary structure of the Storfjorden and Kveithola trough- mouth fans (north west Barents Sea), Mar. Geol., 286, 65–81, https://doi.org/10.1016/j.margeo.2011.05.009, 2011.

Peings, Y.: The atmospheric response to sea-ice loss, Nat. Clim. Chang., 8, 664–665, https://doi.org/10.1038/s41558-018-0243-5, 2018.

Perovich, D. K. and Richter-Menge, J. A.: Loss of Sea Ice in the Arctic, Annu. Rev. Mar. Sci., 1, 417–441, https://doi.org/10.1146/annurev.marine.010908.163805, 2009.

Piechura, J. and Walczowski, W.: Warming of the West Spitsbergen Current and sea ice north of Svalbard, Oceanologia, 51, 147–164, https://doi.org/10.5697/oc.51-2.147, 2009.

Pierrot, D., Lewis, E., andWallace, D.W. R.: MS Excel program developed for CO_2 system calculations, ORNL/CDIAC-105a, Car- bon Dioxide Information Analysis Center, Oak Ridge National Laboratory, US Department of Energy, Oak Ridge, Tennessee, 2006.

Plante-Cuny, M. R.: Evaluation par spectrophotométrie des teneurs en chlorophylle-a fonctionnelle et en phéopigments des substrats meubles marins, Doc. Sci. la Mission l'O.R.S.T.O.M. à Nosy-Bé, 45, 76, 1974.

Polyak, L., Korsun, S., Febo, L. A., Stanovoy, V., Khusid, T., Hald, M., Paulsen, B. E., and Lubinski, D. J.: Benthic foraminiferal assemblages from the Southern Kara Sea, a river-influenced Arctic marine environment, J. Foramin. Res., 32, 252– 273, 2002.

Polyakov, I. V., Walsh, J. E., and Kwok, R.: Recent changes of Arc- tic multiyear sea ice coverage and the likely causes, B. Am. Meteorol. Soc., 93, 145–151, https://doi.org/10.1175/BAMS-D-11- 00070.1, 2012.

Pusceddu, A., Dell'Anno, A., and Fabiano, M.: Organic mat- ter composition in coastal sediments at Terra Nova Bay (Ross Sea) during summer 1995, Polar Biol., 23, 288–293, https://doi.org/10.1007/s003000050446, 2000.

Pusceddu, A., Dell'Anno, A., Danovaro, R., Manini, E., Sarà, G., and Fabiano, M.: Enzymatically hydrolyzable protein and carbohydrate sedimentary pools as indicators of the trophic state of detritus sink systems: A case study in a mediterranean coastal lagoon, Estuaries, 26, 641–650, https://doi.org/10.1007/BF02711976, 2003.

Pusceddu, A., Dell'Anno, A., Fabiano, M., and Danovaro, R.: Quantity and bioavailability of sediment organic matter as signatures of benthic trophic status, Mar. Ecol.-Prog. Ser., 375, 41–52, https://doi.org/10.3354/meps07735, 2009.

Pusceddu, A., Bianchelli, S., Canals, M., Sanchez-Vidal, A., Dur- rieu De Madron, X., Heussner, S., Lykousis, V., de Stigter, H., Trincardi, F., and Danovaro, R.: Organic matter in sediments of canyons and open slopes of the Portuguese, Catalan, Southern Adriatic and Cretan Sea margins, Deep-Sea Res. Pt. I, 57, 441– 457, https://doi.org/10.1016/j.dsr.2009.11.008, 2010.

Quadfasel, D., Rudels, B., and Kurz, K.: Outflow of dense water from a Svalbard fjord into the Fram Strait, Deep-Sea Res. Pt. I, 35, 1143–1150, https://doi.org/10.1016/0198-0149(88)90006-4, 1988.

Rasmussen, T. L. and Thomsen, E.: Stable isotope signals from brines in the Barents Sea: Implications for brine formation during the last glaciation, Geology, 37, 903–906, https://doi.org/10.1130/G25543A.1, 2009.

Rasmussen, T. L. and Thomsen, E.: Brine formation in relation to climate changes and ice retreat during the last 15 000 years in Storfjorden, Svalbard, 76–78◦ N, Paleoceanography, 29, 911– 929, https://doi.org/10.1002/2014PA002643, 2014.

Rasmussen, T. L. and Thomsen, E.: Palaeoceanographic development in Storfjorden, Svalbard, during the deglaciation and Holocene: Evidence from benthic foraminiferal records, Boreas, 44, 24–44, https://doi.org/10.1111/bor.12098, 2015.

Revsbech, N. P.: An oxygen microsensor with a guard cathode, Limnol. Oceanogr., 34, 474–478, https://doi.org/10.4319/lo.1989.34.2.0474, 1989.

Rudels, B. and Quadfasel, D.: Convection and deep water formation in the Arctic Ocean-Greenland Sea System, J. Marine Syst., 2, 435–450, https://doi.org/10.1016/0924-7963(91)90045-V, 1991.

Rysgaard, S., Bendtsen, J., Delille, B., Dieckmann, G. S., Glud, R. N., Kennedy, H., Mortensen, J., Papadimitriou, S., Thomas, D. N., and Tison, J. L.: Sea ice contribution to the air- sea CO_2 exchange in the Arctic and Southern Oceans, Tellus B, 63, 823–830, https://doi.org/10.1111/j.1600-0889.2011.00571.x, 2011.

Rumohr, J., Blaume, F., Erlenkeuser, H., Fohrmann, H., Hollen-der, F.-J., Mienert, J., and Schäfer-Neth, C.: Records and processes of near-bottom sediment transport along the Norwegian- Greenland Sea margins during Holocene and late Weichselian (Termination I) times, in: The Northern North Atlantic: A Changing Environment, edited by: Schäfer, P., Ritzau, W., Schlüter, M., and Thiede, J., Springer, Berlin, Heidelberg, 155– 178, https://doi.org/10.1007/978-3-642-56876-3_10, 2001.

Sabbatini, A., Morigi, C., Negri, A., and Gooday, A. J.: Distribution and biodiversity of stained monothalamous foraminifera from Tempelfjord, Svalbard, J. Foramin. Res., 37, 93–106, https://doi.org/10.2113/gsjfr.37.2.93, 2007.

Sanchez-Cabeza, J. A. and Ruiz-Fernández, A. C.: ^{210}Pb sediment radiochronology: An integrated formulation and classification of dating models, Geochim. Cosmochim. Ac., 82, 183–200, https://doi.org/10.1016/j.gca.2010.12.024, 2012.

Schäfer, C. T. and Cole, F. E.: Reconnaissance Survey of Benthonic Foraminifera from Baffin Island Fiord Environments, Arctic, 39, 232–239, 1986.

Schauer, U.: The release of brine-enriched shelf water from Storfjord into the Norwegian Sea, J. Geophys. Res., 100, 16015– 16028, https://doi.org/10.1029/95JC01184, 1995.

Schönfeld, J., Alve, E., Geslin, E., Jorissen, F., Korsun, S., Spezza- ferri, S., Abramovich, S., Almogi-Labin, A., du Chatelet, E. A., Barras, C., Bergamin, L., Bicchi, E., Bouchet, V., Cear- reta, A., Di Bella, L., Dijkstra, N., Disaro, S. T., Ferraro, L., Frontalini, F., Gennari, G., Golikova, E., Hayn- ert, K., Hess, S., Husum, K., Martins, V., McGann, M., Oron, S., Romano, E., Sousa, S. M., and Tsujimoto, A.: The FOBIMO (FOraminiferal BIo-MOnitoring) initiative – Towards a standardised protocol for soft-bottom benthic foraminiferal monitoring studies, Mar. Micropaleontol., 94–95, 1–13, https://doi.org/10.1016/j.marmicro.2012.06.001, 2012.

Schröder-Adams, C. J., Cole, F. E., Medioli, F. S., Mudie, P. J., Scott, D. B., and Dobbin, L.: Recent Arctic shelf foraminifera: seasonally ice covered vs. perennially ice covered areas, J. Foramin. Res., 20, 8–36, https://doi.org/10.2113/gsjfr.20.1.8, 1990.

Seidenkrantz, M. S., Aagaard-Sørensen, S., Sulsbrück, H., Kui- jpers, A., Jensen, K. G., and Kunzendorf, H.: Hydrography and climate of the last 4400 years in a SW Greenland fjord: Implica- tions for Labrador Sea palaeoceanography, Holocene, 17, 387– 401, https://doi.org/10.1177/0959683607075840, 2007.

Skogseth, R., Haugan, P. M., and Haarpaintner, J.: Ice and brine production in Storfjorden from four winters of satellite and in situ observations and modeling, J. Geophys. Res.-Oceans, 109, 1–15, https://doi.org/10.1029/2004JC002384, 2004.

Skogseth, R., Fer, I., and Haugan, P. M.: Dense-water pro- duction and overflow from an arctic coastal polynya in Storfjorden, Geophys. Monogr. Ser., 158, 73–88, https://doi.org/10.1029/158GM07, 2005a.

Skogseth, R., Haugan, P. M., and Jakobsson, M.: Watermass transformations in Storfjorden, Cont. Shelf Res., 25, 667–695, https://doi.org/10.1016/j.csr.2004.10.005, 2005b.

Skogseth, R., Smedsrud, L. H., Nilsen, F., and Fer, I.: Observations of hydrography and downflow of brine-enriched shelf water in the Storfjorden polynya, Svalbard, J. Geophys. Res.-Oceans, 113, 1–13, https://doi.org/10.1029/2007JC004452, 2008.

Smedsrud, L. H., Budgell, W. P., Jenkins, A. D., and Ådlandsvik, B.: Fine-scale sea-ice modelling of the Storfjorden polynya, Svalbard, Ann. Glaciol., 44, 73–79, https://doi.org/10.3189/172756406781811295, 2006.

Smethie, W. M., Ostlundt, H. G., and Loosli, H. H.: Ventilation of the deep Greenland and Norwegian seas: evidence from krypton- 85, tritium, carbon-14 and argon-39, Deep-Sea Res., 33, 675– 703, 1986.

Steinsund, P. I. and Hald, M.: Recent calcium carbonate dissolution in the Barents Sea: Paleoceanographic applications, Mar. Geol., 117, 303–316, https://doi.org/10.1016/0025-3227(94)90022-1, 1994.

Tamura, T. and Ohshima, K. I.: Mapping of sea ice production in the Arctic coastal polynyas, J. Geophys. Res. - Oceans, 116, 1– 20, https://doi.org/10.1029/2010JC006586, 2011.

Tselepides, A., Polychronaki, T., Marrale, D., Akoumianaki, I., Dell'Anno, A., Pusceddu, A., and Danovaro, R.: Organic matter composition of the continental shelf and bathyal sediments of the Cretan Sea (NE Mediterranean), Prog. Oceanogr., 46, 311–344, https://doi.org/10.1016/S0079-6611(00)00024-0, 2000.

van Oevelen, D., Soetaert, K., Garcia, R., de Stigter, H. C., Cunha, M. R., Pusceddu, A., and Danovaro, R.: Canyon conditions impact carbon flows in food webs of three sections of the Nazaré canyon, Deep-Sea Res. Pt. II, 58, 2461–2476, https://doi.org/10.1016/j.dsr2.2011.04.009, 2011.

Wekerle, C., Wang, Q., Danilov, S., Schourup-Kristensen, V., von Appen, W.-J., and Jung, T.: Atlantic Water in the Nordic Seas: Locally eddy-permitting ocean simulation in a global setup, J. Geophys. Res.-Oceans, 122, 914–940, https://doi.org/10.1002/2016JC012121, 2016.

Williamson, M. A., Keen, C. E., and Mudie, P. J.: Foraminiferal distribution on the continental margin off Nova Scotia, Mar. Micropaleontol., 9, 219–239, 1984.

Winkelmann, D. and Knies, J.: Recent distribution and accumulation of organic carbon on the continental margin west off Spitsbergen, Geochem. Geophys. Geosy., 6, Q09012, https://doi.org/10.1029/2005GC000916, 2005.

Wollenburg, J. E. and Kuhnt, W.: The response of benthic foraminifers to carbon flux and primary production in the Arctic Ocean, Mar. Micropaleontol., 40, 189–231, https://doi.org/10.1016/S0377-8398(00)00039-6, 2000.

Wollenburg, J. E. and Mackensen, A.: Living benthic foraminifers from the central Arctic Ocean: Faunal composition, standing stock and diversity, Mar. Micropaleontol., 34, 153–185, https://doi.org/10.1016/S0377-8398(98)00007-3, 1998.

Zaborska, A., Pempkowiak, J., and Papucci, C.: Some Sediment Characteristics and Sedimentation Rates in an Arctic Fjord (Kongsfjorden, Svalbard), Annu. Environ. Prot., 8, 79–96, 2006.

Zaja¸czkowski, M., Szczuci´nski, W., and Bojanowski, R.: Recent changes in sediment accumulation rates in Adventfjorden, Sval- bard, Oceanologia, 46, 217–231, 2004.

Zaja¸czkowski, M., Szczuci´nski, W., Plessen, B., and Jernas, P.: Benthic foraminifera in Hornsund, Svalbard: Implications for paleoenvironmental reconstructions, Pol. Polar Res., 31, 349–375, 2010.

Supplement Chapter 1

Table S1. Sedimentation rate and sediment grain size characteristics (percentage of sand and silt, distribution mean and mode) of the topmost centimetre of sediment (0.0-0.5 and 0.5-1.0 cm sediment layers separately) for each sampling station (data are not available for station MC3).

Station	Depth (m)	Sedimentation rate (mm yr^{-1})	Grain size characteristics				
			Layer (cm)	% SAND	% SILT	Mean (µm)	Mode (µm)
MC1	108	3.1 ± 2.5	**0.0-0.5**	4.0	87.3	8.7	10.5
			0.5-1.0	3.5	87.4	8.1	9.3
MC2	117	3.9 ± 0.3	**0.0-0.5**	4.8	87.0	9.3	9.3
			0.5-1.0	5.9	82.6	7.6	7.2
MC4	191.5	3.2 ± 0.5	**0.0-0.5**	7.3	86.2	10.9	12.0
			0.5-1.0	6.7	85.1	9.1	9.3
MC5	171	2.6 ± 0.9	**0.0-0.5**	9.0	83.8	10.8	10.5
			0.5-1.0	8.2	85.1	10.8	10.5
MC6	157	5.0 ± 3.2	**0.0-0.5**	10.4	84.8	14.2	13.6
			0.5-1.0	4.3	88.9	10.0	12.0
MC7	321	1.3 ± 0.6	**0.0-0.5**	6.8	88.2	14.3	19.9
			0.5-1.0	6.2	88.9	14.1	19.9

Table S2. For each sampling station (data are not available for station MC3), biochemical parameters are reported as average ± sd (n = 3). Starting from left: total amount of proteins (PRT), carbohydrates (CHO), lipids (LIP), relative contribution of PRT, CHO and LIP to the BPC, the biopolymeric carbon contents (BPC), chlorophyll-*a* (Chl-*a*) and phaeopigment (Phaeo) contents, the chloroplastic pigment equivalent (CPE), the autotrophic Carbon (C-CPE) and the algal fraction of BPC (C-CPE/BPC).

Stations	PRT mg g^{-1}		CHO mg g^{-1}		LIP mg g^{-1}		PRT %		CHO %		LIP %	
	avg	*sd*	*avg*	*sd*	*avg*	*sd*	*avg*	*sd*	*avg*	*sd*	*avg*	*sd*
MC1	5.39	0.74	2.75	0.32	2.33	0.01	47.95	2.41	20.03	0.53	32.03	2.94
MC2	5.85	0.76	3.64	0.28	3.72	0.44	40.23	0.62	20.52	0.80	39.24	0.18
MC4	5.06	1.01	6.47	0.31	3.47	0.08	32.12	4.42	33.79	1.71	34.09	3.00
MC5	4.33	0.92	6.21	0.84	3.01	0.45	30.75	4.58	36.08	2.52	33.16	7.11
MC6	6.01	0.26	4.07	0.57	3.75	0.09	39.91	1.69	22.02	2.77	38.07	1.15
MC7	3.62	0.50	2.91	0.06	2.36	0.40	37.76	5.76	24.71	0.35	37.53	5.87
Stations	**BPC mgC g^{-1}**		**Chl-a µg g^{-1}**		**Phaeo µg g^{-1}**		**CPE µg g^{-1}**		**C-CPE mgC g^{-1}**		**C-CPE/BPC %**	
	avg	*sd*	*avg*	*sd*	*avg*	*sd*	*avg*	*sd*	*avg*	*sd*	*avg*	*sd*
MC1	5.49	0.49	4.08	0.19	19.96	3.50	24.04	3.69	0.72	0.11	13.09	0.87
MC2	7.12	0.82	6.08	0.47	35.12	9.15	41.19	9.62	1.24	0.29	17.21	2.10
MC4	7.67	0.51	5.27	0.33	28.35	5.30	33.62	5.63	1.01	0.17	13.10	1.37
MC5	6.86	0.45	6.41	0.44	30.45	7.13	36.86	7.58	1.11	0.23	16.02	2.27
MC6	7.38	0.21	6.82	0.76	27.78	2.46	34.60	3.22	1.04	0.10	14.06	1.20
MC7	4.71	0.07	0.02	0.04	6.40	0.48	6.43	0.45	0.19	0.01	4.09	0.33

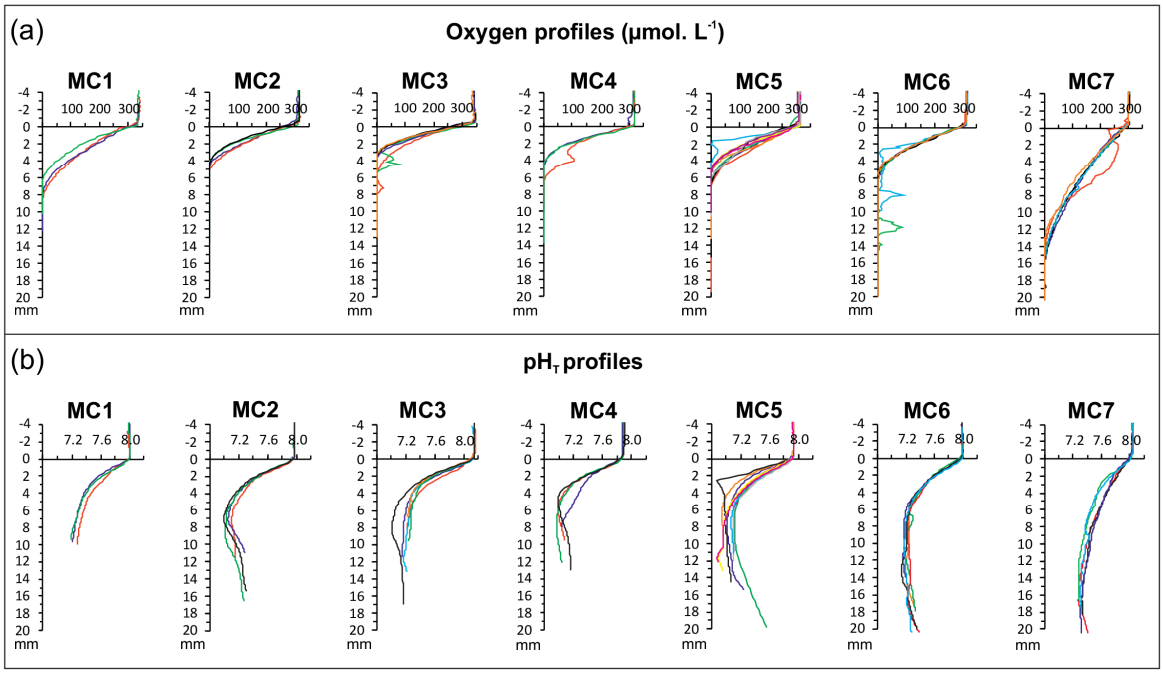

Figure S1. Replicated measurements of sediment oxygen **(a)** and pH_T microprofiles **(b)** in interface cores sampled at each station. Level 0 is the position of the sediment-water interface. Different colours represent different replicates of profiles.

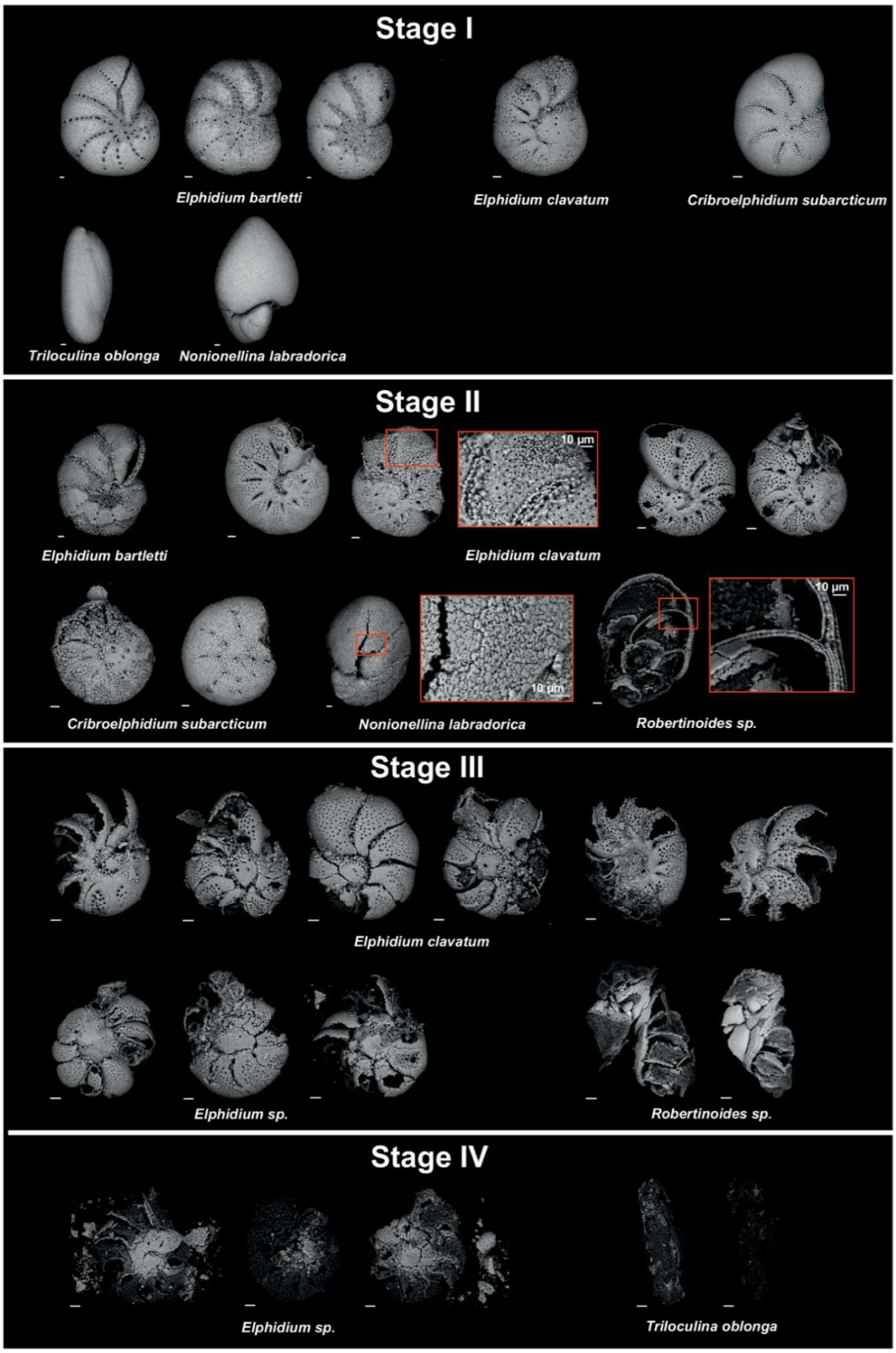

Figure S2. High-resolution SEM images of specimens (from the >150 µm size fraction) classified into four dissolution stages from weak (stage I) to severe (stage IV) following the classification of Gonzales et al. (2017). Scale bars 20 µm.

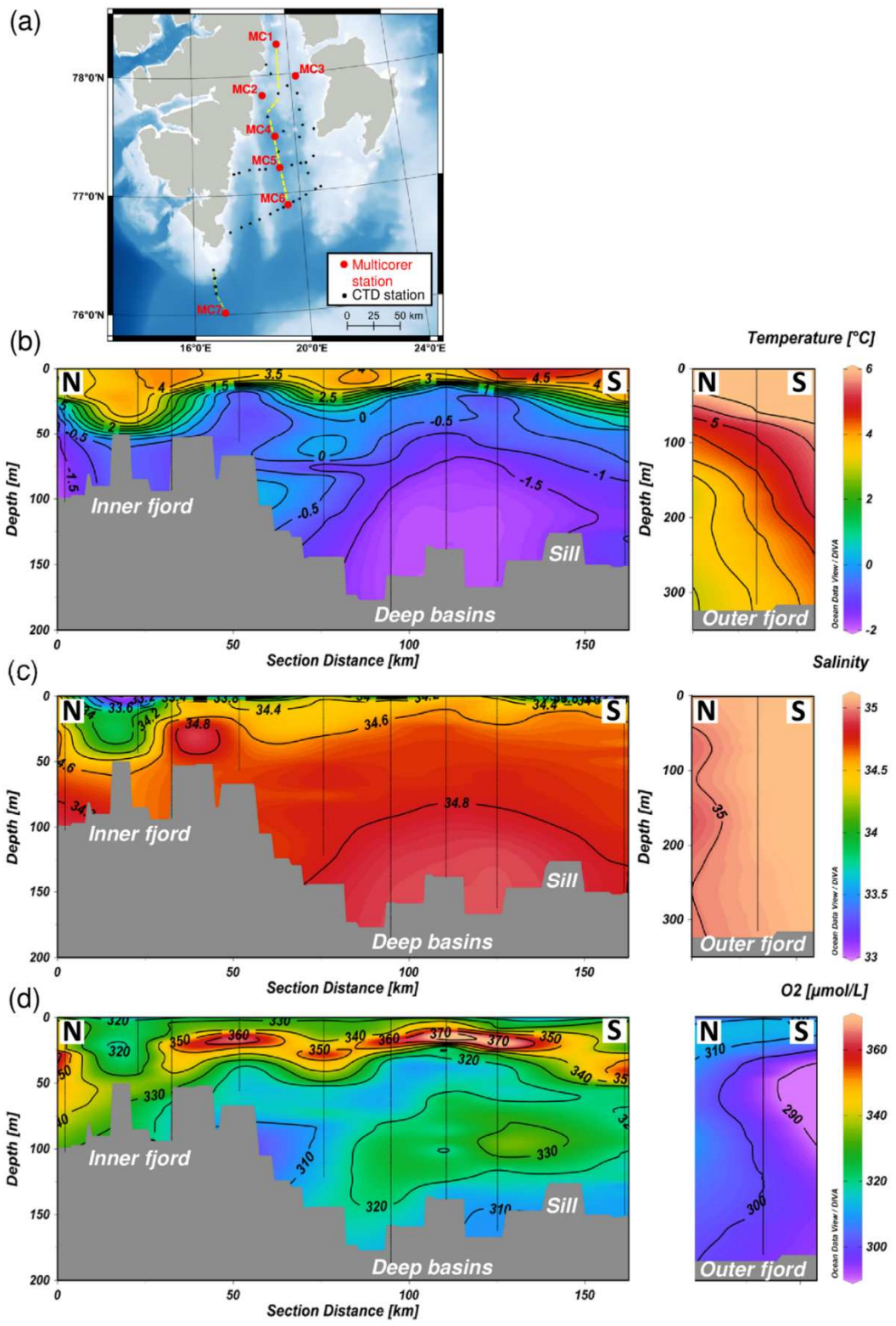

Figure S3. (a) Map with the location of all CTD stations from the STeP cruise (black dots) and of the interface multicorer stations analysed in the present study (red dots). The dashed yellow line is the N-S transect used for the ODV interpolations shown on the left panels and the dashed green line the one shown on the right panels. Bathymetry obtained from EMODnet (http://portal.emodnet-bathymetry.eu) and map elaborated with QGIS (made with Natural Earth). Ocean Data View interpolation for temperature **(b)** salinity **(c)** and oxygen **(d)** of CTD profiles.

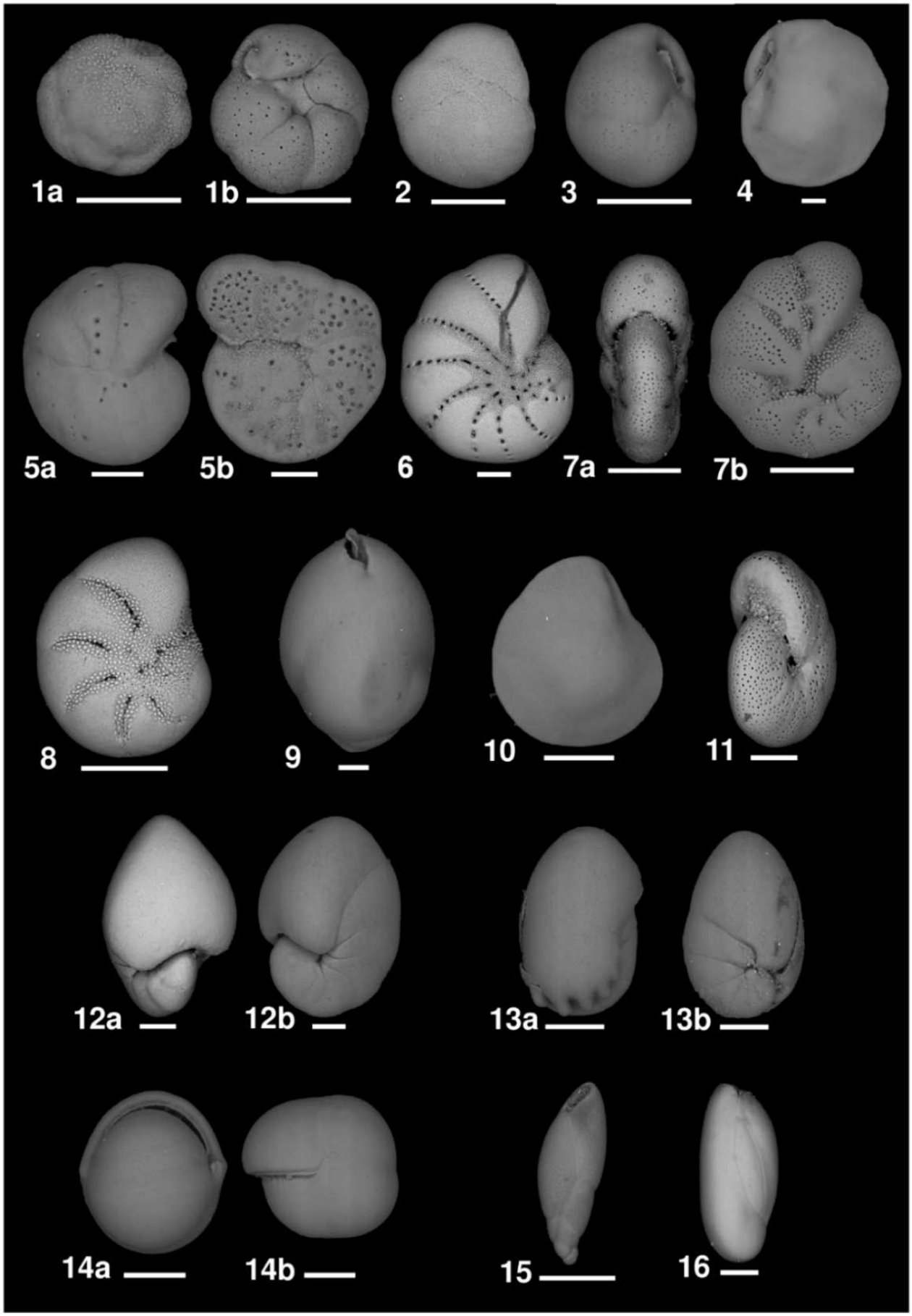

Figure S4. Please see caption in the next page.

Figure S4. Scanning electron micrographs of the most relevant calcareous benthic species from Storfjorden (scale bars = 100 μm). **1a, 1b.** *Alabaminella weddellensis* (Earland, 1936). **2.** *Buccella frigida* (Cushman, 1922). **3.** *Cassidulina reniforme* Nørvang, 1945. **4.** *Cassidulina teretis* Tappan, 1951. **5a, 5b** *Cibicidoides lobatulus* (Walker & Jacob, 1798). **6.** *Elphidium bartletti* Cushman, 1933. **7a, 7b**. *Elphidium clavatum* Cushman, 1930. **8.** *Cribroelphidium subarcticum* (Cushman, 1944). **9.** *Globobulimina auriculata* (Bailey, 1894). 10. *Islandiella norcrossi* (Cushman, 1933). **11.** *Melonis barleeanus* (Williamson, 1858). **12a, 12b.** *Nonionellina labradorica* (Dawson, 1860). **13a, 13b.** *Nonionella digitata* Nørvang, 1945. **14a, 14b.** *Pullenia bulloides* (d'Orbigny, 1846). **15.** *Stainforthia feylingi* Knudsen & Seidenkrantz, 1994. **16.** *Triloculina oblonga* (Montagu, 1803).

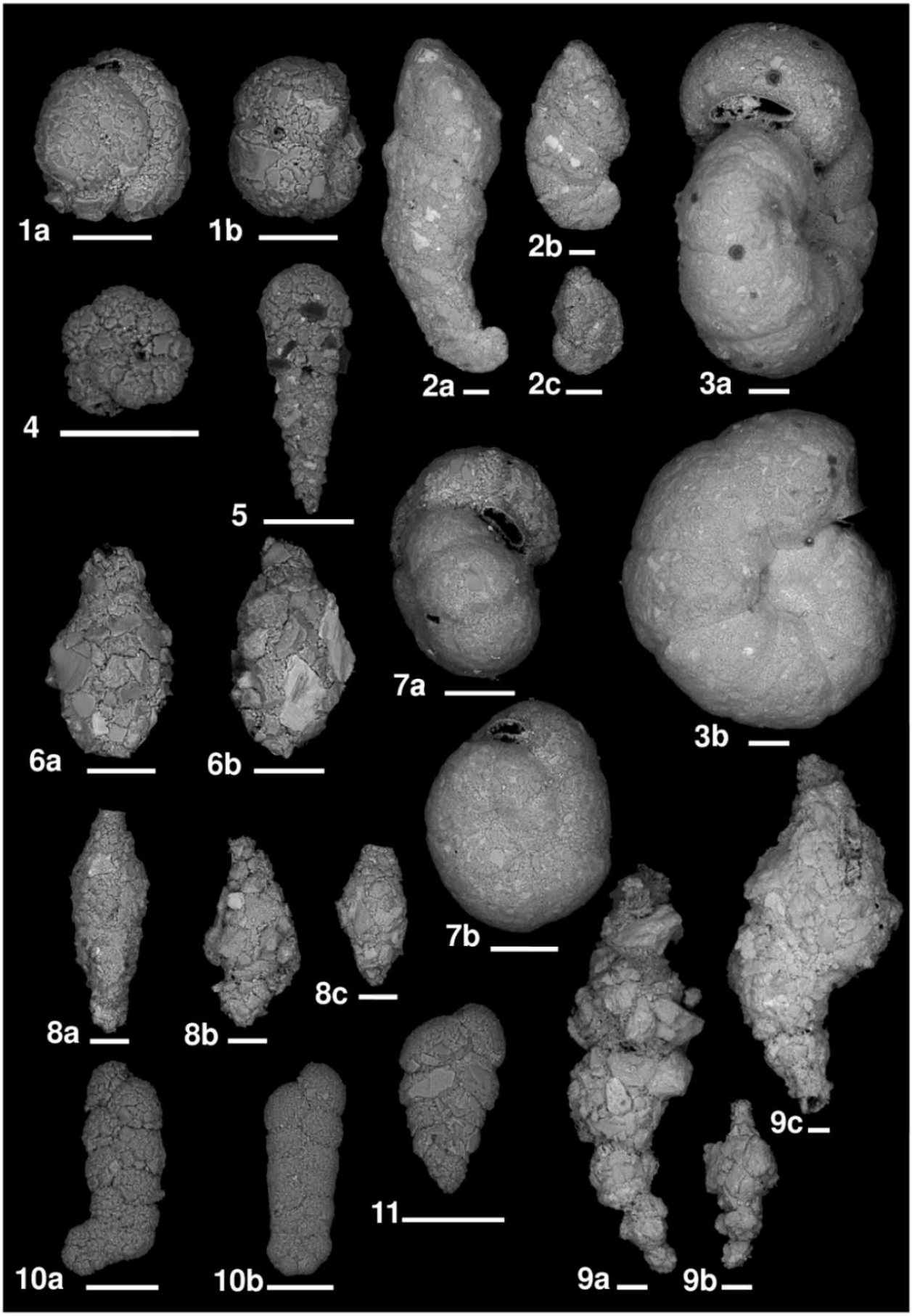

Figure S5. Please see caption in the next page.

Figure S5. Scanning electron micrographs of the most relevant agglutinated benthic species from Storfjorden (scale bars = 100 μm). **1a, 1b.** *Adercotryma glomeratum* (Brady, 1878). **2a, 2b, 2c.** *Ammotium cassis* (Parker, 1870). **3a, 3b.** *Labrospira crassimargo* (Norman, 1892). **4.** *Cribrostomoides sp.* Cushman, 1910. **5.** *Cuneata arctica* (Brady, 1881). **6a, 6b.** *Lagenammina difflugiformis* (Brady, 1879). **7a, 7b.** *Recurvoides turbinatus* (Brady, 1881). **8a, 8b, 8c.** *Reophax fusiformis* (Williamson, 1858). **9a, 9b, 9c.** *Reophax scorpiurus* Montfort, 1808. **10a, 10b.** *Spiroplectammina biformis* (Parker & Jones, 1865). **11.** *Textularia torquata* Parker, 1952.

Erratum

The paper presented here as Chapter 1 of the thesis is the same version published on *Biogeosciences* (doi:10.5194/bg-17-1933-2020). After the acceptance and publication of the manuscript, the authors realised that the inner diameter of the collected sediment cores, used to standardise foraminiferal densities, was 9.6 cm instead of 10 cm as reported in the published manuscript (which changes the radius of the core by 0.2 cm). We did not publish an erratum of the paper because this error determines a consistent underestimation of absolute foraminiferal densities by 7.84% (calculated as $1-(r_2^2/r_1^2) *100$; where r_2 is 4.8 cm and r_1 is 5 cm). Therefore, the relative differences among stations, as well as the relative foraminiferal abundances, do not change after the correction, and the ensuing discussion and the main findings of the paper are not affected. Data of foraminiferal densities were corrected for this error on the PANGAEA online repository.

Chapter 2

Early taphonomy of benthic foraminifera in Storfjorden "sea ice factory": the agglutinated/calcareous ratio as a proxy for brine persistence

Maria Pia Nardelli[1]*[#], Eleonora Fossile[1#], Olivier Péron[2], Hélène Howa[1] and Meryem Mojtahid[1]

[1] *LPG UMR CNRS 6112, Université d'Angers, Nantes Université, Le Mans Univ, 2 bd Lavoisier 49045, Angers CEDEX 01, France*

[2] *SUBATECH, UMR 6457, CNRS-Université de Nantes, 4 rue A. Kastler, 44307 Nantes, France*

[#]These authors contributed equally to this work

*Corresponding author: Maria Pia Nardelli (mariapia.nardelli@univ-angers.fr)

An updated version of this chapter including minor revisions has been published in *Boreas* (https://doi.org/10.1111/bor.12592).

Abstract

The recurrent latent-heat polynya characterising the Storfjorden (Svalbard, Norway) triggers seasonal formation of thin first-year sea ice. This leads to the production of dense, salty, and corrosive brines that cascade towards the seafloor and mix with shelf waters. The bottom topography of the fjord is responsible for the retention of these dense waters in two central deep basins all over the year. Recent studies show that living benthic foraminifera in the Storfjorden are particularly affected by the persistence of brines on the seafloor, with a strong dominance of agglutinated (A) species and high dissolution degrees of calcareous (C) faunas. Therefore, the A/C ratio, calculated on living faunas, was proposed as a proxy for brine persistence. In the present study we analyse the fossil faunas, found below the taphonomically active zone, to investigate the residual signal of the A/C proxy after the early intense taphonomic processes and challenge its applicability in sedimentary archives. Our results show that despite the generally high taphonomic loss inside the fjord, the high proportion of agglutinated species is still visible in fossil faunas at the stations under regular and/or persistent presence of brine-enriched shelf waters. These results support the application of the A/C ratio in historical records to reconstruct the persistence of brines and indirectly of the first-year thin sea ice formation in the Storfjorden. This can be further applied to other Arctic fjords with similar settings and characterised by the production of brines during the winter-early spring season.

Keywords: Arctic, polynya, brine-enriched shelf waters, fjord, climate, diagenesis, fossilisation, dissolution

1. Introduction

The world ocean thermohaline circulation depends on the formation of deep waters in Polar Regions. In the Arctic, deep waters are mainly formed by the densification of surface waters through cooling and salinity increase due to brine release in sea ice production areas (e.g., Rudels and Quadfasel, 1991). The Storfjorden, in the Svalbard archipelago, is a major supplier of brine-enriched shelf waters, contributing for up to 5-10 % of dense water production in the Arctic Ocean (Quadfasel et al., 1988; Smedsrud et al., 2006).

The release of brines is strictly related to the production of sea ice (Rysgaard et al., 2011) and therefore indirectly connected to climate forcings. The polynya regions (i.e., sea ice free areas formed and maintained by advection of ice by offshore winds and currents) are the main zones where the production of brines occurs. Due to their largely ephemeral nature, polynyas have been suggested as sentinel regions for temporal large-scale climate-related sea ice changes in polar marine environments (Smith and Barber, 2007). At present, there are solid observations about the fact that ongoing climate change strongly affects sea ice growth and extension in the Arctic (e.g., Meredith et al., 2019) and in this context vulnerability of polynyas has been highlighted by several studies (e.g., Vincent, 2019; Ribeiro et al., 2021). Among other possible consequences, the reduction of first-year sea ice production in polynyas could lead to reduced brine-enriched shelf waters (BSW) production with potential consequences on global deep water circulation (e.g., Ohshima et al., 2016). The high natural variability of sea ice dynamics in polynya regions, however, complicates the long-term prediction based on direct present-day observations, based on satellite images. The main challenge is to understand the significance of the observed present-day sea ice trends on longer time scales (i.e., hundreds of years) to trustfully predict their potential consequences on global ocean circulation.

The solely short-term information about interactions between the climate, the cryosphere and the oceans has motivated the development and calibration of geochemical and biological tracers preserved in the sediments. These proxies are the potential key to reconstruct historical sea ice changes and to define the environmental variability on an annual or multi-annual resolution (Limoges et al., 2018). Lately, several efforts have been conducted to validate the application of proxies related to sea ice dynamics, and several proxies seem suitable for tracing the presence and variability of sea ice (i.e., dinoflagellate cysts, diatoms, ostracods, and biomarkers; see De Vernal et al., 2013 and references therein). However, each proxy presents some limitations (e.g., see review by De Vernal et al., 2013 for a complete overview), including the most promising ones that preserve well in recent sedimentary archives such as the IP_{25}

(organic lipid produced by sea ice endemic diatoms) (Belt, 2018, 2019; Belt et al., 2007; Belt and Müller, 2013). For instance, the preservation and storage of the sediment samples for IP_{25} analyses are complex (Belt et al., 2007; Belt and Müller, 2013; Müller et al., 2009, 2011) and some missing information further limit its applicability (e.g., absence of the biomarker in the Antarctic, (partially) unknown species responsible for the biomarker production, lack of knowledge about the distribution of the species in question in the Arctic region). All these aspects limit, by the moment, its application for sea ice dynamics reconstruction in the Northern Polar region. This further suggests the necessity of a multi-proxy approach to obtain reliable datasets for sea ice reconstruction.

A previous investigation of benthic foraminiferal faunas under seasonal sea ice cover conditions did not identify any endemic species exclusively related to sea ice presence, and concluded that foraminiferal assemblages cannot be used as direct proxies for sea ice cover (Seidenkrantz, 2013). The recent study of Fossile et al. (2020), based on ecological interpretations from living assemblages in Storfjorden (Svalbard, Norway), suggested the potential use of a benthic foraminiferal-based proxy to reconstruct past brine production in coastal Arctic polynyas. Because the brine-enriched shelf waters cascading strictly depends on first-year sea ice growth (e.g., Skogseth et al., 2004, 2005a, 2008) the proposed proxy has been suggested as indirect indicator of seasonal sea ice production (Fossile et al., 2020). This proxy, based on benthic foraminiferal assemblages, consist of the ratio between agglutinated (A) and calcareous (C) species, with the A/C ratio increasing in the presence of persistent brines at the seafloor (Fossile et al., 2020). Indeed, due to the CO_2 release during sea ice formation and the winter lasting interruption of direct exchanges with the atmosphere, the brines are CO_2-enriched and consequently corrosive (Rysgaard et al., 2011), affecting therefore the mineralization of calcareous shells to the advantage of agglutinated forms. However, Fossile et al. (2020) also suggested that high A/C ratio (i.e., high presence of agglutinated forms) could also be related to high contents of quite refractory organic matter. Most probably, the combined effect of corrosive brines, organic matter remineralisation, and persistence of brine-enriched shelf waters in the deep basins determine the dominance of agglutinated forms. In the deep basins, the organic matter is less labile, compared to the shallower stations where seasonal mixing and phytoplankton blooms favour fresher organic supplies to which calcareous forms respond greatly. A tolerance to less labile organic matter could be an additional competitive advantage for the agglutinated species inhabiting the fjord (Fossile et al., 2020).

Although promising, the possibility to realistically use the A/C proxy in historical records relies on: *(i)* the preservation potential of the agglutinated species dominating the living

assemblages after death and below the taphonomically active zone (TAZ), corresponding to the bioturbated zone beneath the sediment surface where most of early diagenesis occurs (Davies et al., 1989; Berkeley et al., 2007), and *(ii)* the preservation of the residual calcareous specimens after early dissolution events. In fact, agglutinated species, and in particular the species with organic cement, are known to be particularly fragile and to have a bad preservation potential in the fossil faunas (Bizon and Bizon, 1984; Schröder, 1988; Bender, 1995). In the Storfjorden, however, an exceptional preservation of agglutinated foraminifera was reported from relatively recent fossil records (e.g., Late Holocene; Rasmussen and Thomsen, 2014, 2015), probably promoted by low temperatures and high sedimentation rates. Therefore, their preservation in this region should ensure a good representativity of foraminiferal assemblages from historical sedimentary archives.

The aims of the present study are to: *(i)* estimate the information loss due to taphonomy of benthic foraminiferal assemblages and *(ii)* challenge the possibility of using the A/C ratio calculated from fossil faunas as a proxy for brine-enriched shelf waters persistence in the recent past (tenths to hundreds of years). The study of Fossile et al. (2020) investigated living assemblages in Storfjorden (Svalbard, Norway), and provided ecological interpretations of the main benthic foraminiferal species. By comparing living assemblages of the topmost five sediment centimetres (Fossile et al., 2020) with dead and fossil foraminiferal assemblages from the same cores, we further investigate in the present study, the preservation state of foraminiferal assemblages from fossil faunas just below the TAZ and the effect of taphonomic processes on the residual assemblages.

2. Materials and Methods

2.1 Study area

Storfjorden is the largest fjord of the Svalbard archipelago, Norway (74°-81° N and 10°-35° E, Fig. 1). It is characterised by shallow water depth in the innermost area (average depth ~100 m), two central deep basins (average depth ~180 m) and a sill (~120 m water depth) that separates these basins from the outer shelf (>200 m). The inner part of the Storfjorden is characterised by the presence of a latent-heat polynya, where thin first-year sea ice is continuously produced during winter-early spring (Skogseth et al., 2004, 2005a). The sea ice production process leads to the ejection of CO_2 and salt and the formation of dense, cold, salty, and corrosive brines (Anderson et al., 2004; Rysgaard et al., 2011). These waters cascade

towards the seafloor as brine-enriched shelf waters, mixing with shelf Arctic waters (Skogseth et al., 2005a, 2005b).

During the cold seasons, brine-enriched shelf waters fill the deep basins up to the sill level and overflow towards the Barents Sea and the Fram Strait, passing below the Atlantic waters (Fer et al., 2003). The contribution of brine-enriched shelf waters produced in the Storfjorden has been estimated at 5 to 10% of Arctic deep waters (Quadfasel et al., 1988; Skogseth et al., 2004, 2005a; Smedsrud et al., 2006) and their circulation contributes to the ventilation of Arctic deep waters (Schauer and Fahrbach, 1999). During summer, when sea ice production is null, brine overflow over the sill stops, but residual BSW are trapped in the deep central basins all year round (Haarpaintner et al., 2001a, 2001c). The production of BSW and their properties (salinity and density) in the Storfjorden depend on the polynya activity and position, which in turn is influenced by climate variability (North Atlantic Oscillation; Skogseth et al., 2004). Haarpaintner et al. (2001b) report denser BSW formed during milder winters, due to a shallower position of the polynya on the shelf. The topography and the tidal currents also play an important role on brine-enriched shelf waters physical characteristics, by promoting the mixing of water masses and the decrease of brine-enriched shelf waters density (Haarpaintner et al., 2001a, 2001c).

2.2 Sediment sampling

During the STeP (Storfjorden Polynya Multidisciplinary Study) cruise on board the R/V L'Atalante (IFREMER) in July 2016, we sampled interface cores (9.6 cm internal diameter) with a multi-corer at seven stations across an inner-outer fjord transect (Fig. 1). Three stations were sampled in the inner fjord (at ~110 m depth), two in the two central deep basins (at ~180 m), one over the sill (at ~160 m) and one just outside the fjord (at ~320 m). All details relative to the sampling stations are given in Table 1. At each station, except for MC3, two cores were retrieved, one for foraminiferal analyses and one for age models.

Sampling date	Station	Latitude (N)	Longitude (E)	Depth (m)
13/07/2016	MC1	78°15.0	19°30.0	108.0
14/07/2016	MC2	77°50.0	18°48.0	117.0
14/07/2016	MC3	77°58.6	20°14.6	99.0
15/07/2016	MC4	77°29.2	19°10.6	191.5
17/07/2016	MC5	77°13.2	19°17.9	171.0
18/07/2016	MC6	76°53.9	19°30.3	157.0
19/07/2016	MC7	76°00.9	17°03.4	321.0

Table 1. Sampling date, coordinates, and sampling water depth of the nine stations sampled during the STeP mission.

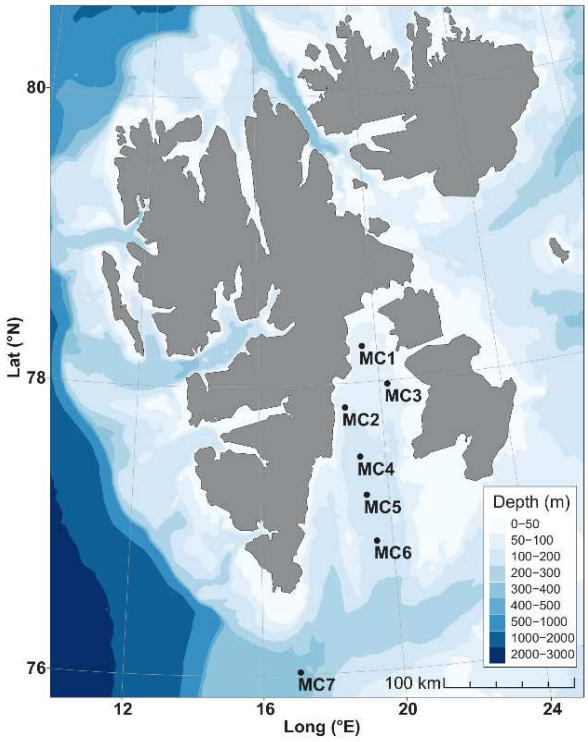

Figure 1. Svalbard map with bathymetry showing the seven sampling stations along an inner-outer transect in Storfjorden. The map was prepared with R package *PlotSvalbard* (Vihtakari, 2020) using R software (R Core Team, 2020).

2.3 Sedimentation rates

At each station (except for the MC3), cores were sliced on board, collecting five sediment layers (0–0.5, 0.5–1, 1–2, 2–5 and 5–10 cm), then stored at −20°C. In the laboratory, sediment samples were lyophilized to perform gamma spectrometry measurements to determine the apparent sedimentation rate by the $^{210}Pb_{xs}$ method (Appleby and Oldfield, 1978). The ^{210}Pb dating was conducted using a gamma spectrometer Mirion Canberra HPGe GX4520 coaxial photon detector at Subatech Laboratory Nantes. The homogenised samples were weighed and sealed in a defined geometry for at least 3 weeks to ensure ^{222}Rn-^{226}Ra-^{214}Pb equilibration. Sedimentation rate was based on the determination of the excess or unsupported activity ^{210}Pb ($^{210}Pb_{xs}$) and performed through constant flux-constant sedimentation (CF-CS) model (Sanchez-Cabeza and Ruiz-Fernández, 2012). The $^{210}Pb_{xs}$, incorporated rapidly into the sediment from atmospheric fallout and water column scavenging, was calculated as the difference between the total measured ^{210}Pb activity (supported + excess) at 46.54 keV and ^{214}Pb at 351.93 keV.

The depth of the surface mixed-layer was established on the base of homogenous $^{210}Pb_{ex}$ activity. This homogeneity is the result of physical (resuspension/deposition) and/or biological

disturbance (e.g., Schmidt et al., 2005). The surface mixed layer does not correspond exactly to the bioturbation depth, because bioturbation can still occur in the deeper incomplete mixing layers (Tomašových et al., 2019). However, below the surface mixed layer, bioturbation coefficients are generally lower (10-20%; Silverberg et al., 1986) up to orders of magnitude (Muñoz et al., 2004) and thus their influence on taphonomic processes is reduced or negligible. The TAZ, defined as the zone of the sediment included between the surface and the bottom of the bioturbated area (Berkeley et al., 2007), was therefore assimilated to the surface mixed layer, where the effects of physical disturbance are recorded in the sediment chemistry (i.e., $^{210}Pb_{ex}$ activity).

2.4 Foraminiferal analyses

Interface sediment cores dedicated to foraminiferal analyses were sliced every 0.5 cm down to 2 cm depth, then 1 cm down to 6 cm depth and 2 cm down to 10 cm depth. Each sediment sample was stained with 2 g L^{-1} Rose Bengal in ethanol to distinguish living and dead specimens. Once in the laboratory, the samples were washed using 63, 125 and 150 µm meshed sieves. The living specimens were hand-picked in water and analysed together with geochemical and sedimentological parameters in the top 5 cm of the sediment by Fossile et al. (2020). For dead (i.e., above the TAZ) and fossil (i.e., below the TAZ) faunal analyses, the residual samples were dried at 50°C. When the densities were high, the dry residues were split using an OTTO microsplitter. A minimum of 300 individuals were picked from a single split and the counts were then standardised to the total sample. These analyses were performed on the >150 µm fraction of the dead assemblage (0-1 cm) and fossil assemblages (3-4 cm and 6-8 cm sediment layers). The size fraction to consider was chosen based on the observations of Fossile et al. (2020), who highlighted that the large size fraction (>150µm) gives similar ecological information as the small size assemblages (63-150 µm) in the study area.

Foraminiferal densities in the 3-4 and 6-8 cm sediment layers are supposed to represent the fossil or preserved fraction of fauna integrating *(i)* foraminifera living at the surface sediment at the time where the layer was located at the water-sediment interface and *(ii)* the infaunal foraminifera that lived in this layer after its burying. These two sediment layers are supposed to lie below the TAZ, where bioturbation can have a strong influence on sediment reworking and early diagenesis (Berkeley et al., 2007, 2014). Therefore, they should contain early fossil assemblages having undergone the first steps of taphonomic processes. The two sediment layers were analysed to eventually detect significant differences that would have indicated strong

diagenetic processes occurring below the TAZ. Fossil foraminifera from both layers were compared to living faunas (in the 0-1 and 0-5 cm sediment layers) and to the dead fauna from the topmost centimetre, to estimate taphonomic loss.

To compare faunas from sediment layers of different volumes and sampled at different depths in the core (i.e., with possible differences in the compaction state), we normalized and expressed foraminiferal absolute abundances as individuals per gram of dry sediment. As the foraminiferal samples were not weighted before the sieving, we estimated the water content of each layer from the analyses of twin cores sampled at each station for other sedimentological analyses. Wet and dry sediment layers of these cores were weighted, and the porosity calculated on the base of the water content. The raw number of picked foraminifera being standardised for 50 cm^3 (wet sediment), the volume of water was subtracted, and the remaining was converted to mass of sediment by multiplying by sediment density (a density of 2.6 $g.cm^{-3}$ was used as an average for clay-silt sediment particles, e.g., Blake, 2008).

To quantitatively estimate the differences between living and fossil assemblages, the L/(L+F) ratio was calculated using the relative abundances of the major species (Jorissen and Wittling, 1999). In the following formula $L_{0-5cm}/(L_{0-5cm}+ F_{6-8cm})$, L indicates the relative abundance of each living species in the 0-5 cm sediment layer whereas F indicates the relative abundance of each fossil species from the 6-8 cm sediment layer. For each species, ratios between 0 and 0.5 indicate that the species is relatively more abundant in the fossil fauna, ratio between 0.5 and 1 in the living faunas, whereas a value of 0.5 means an equal representation.

The A/C ratio is calculated as the ratio of relative abundances of the agglutinated and calcareous (miliolids and hyaline) species. As the fossil layers are supposed to integrate the fauna living at all microhabitats (including infaunal) and at all seasons (fauna of the year) we compared the A/C ratio of the whole living assemblages (0-5 cm) and of the annual fauna (total = living + dead, 0-1 cm) with the one of the fossil layer (6-8 cm) to detect possible changes due to taphonomy.

3. Results

3.1 Sediment accumulation rate and determination of the taphonomically active zone

The results of the $^{210}Pb_{xs}$ are reported in Figure 2. The sediment mixed layer (SML), where the sediment is distinctly bioturbated, can be identified through the unvaried ^{210}Pb activity values in the topmost centimetre of the cores. This depth is identified as the limit of the taphonomic active zone. The $^{210}Pb_{xs}$ points included in the surface mixed layer (in red in Fig. 2) are excluded

from the Sediment Accumulation Rate (SAR) estimation. The SAR is particularly high in the inner fjord (0.26 ± 0.09 to 0.39 ± 0.03 cm yr^{-1}; i.e., from 30 to 23 years old on the depths considered, respectively) (MC2 to MC5) and lower at the outer MC7 station (0.13 ± 0.06 cm yr^{-1}). The precision of the SAR obtained for stations MC1 and MC6 is too low to be considered as reliable (error >2σ). The slope of the linear model for $^{210}Pb_{xs}$ measurements in core MC7 is strongly driven by the deepest point, which could be the result of irregular sedimentation at this station.

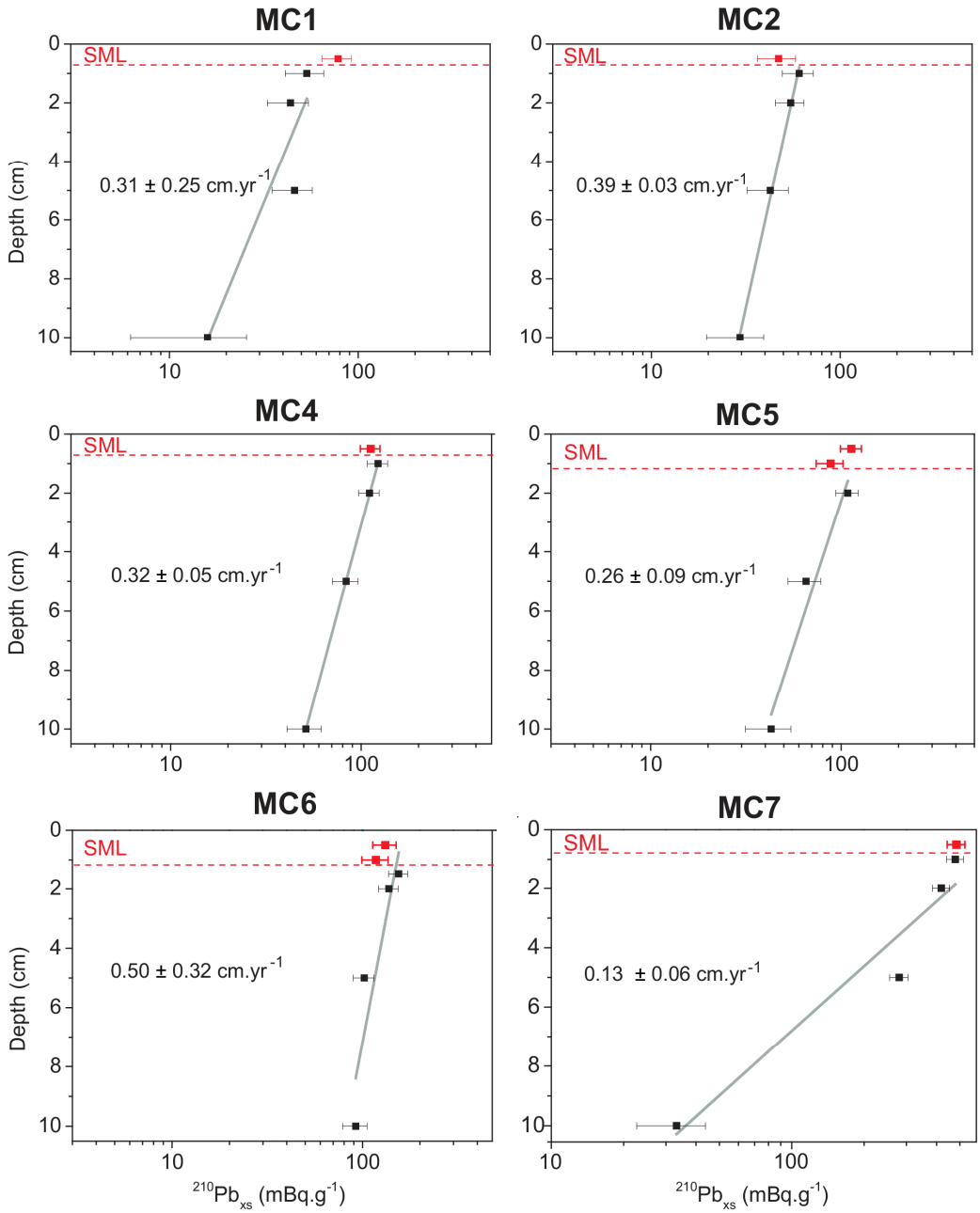

Figure 2. $^{210}Pb_{xs}$ incorporation into sediment from the sediment surface down to 10 cm depth and the correspondent Sediment Accumulation Rates (SAR) expressed as cm yr^{-1}. The dashed lines correspond to the limit of the Sediment Mixed Layer (SML), also identified as the TAZ. In red are reported the $^{210}Pb_{xs}$ points included in the SML.

3.2 Taphonomic loss

3.2.1 Density

The analysis of the total fauna (living + dead foraminifera) in the 0-1 cm layer (Fig. 3a) shows the same order of magnitude in total densities between stations, with MC6 (sill) and MC1 (inner fjord) showing the lowest densities (~20 and 40 ind. g^{-1} respectively), and station MC7 (outer fjord) showing the highest density (85 ind. g^{-1}). However, while inside the fjord (MC1 to MC6) most of the superficial fauna is represented by living specimens (>80%), the high density at the outer fjord MC7 is largely represented by dead faunas (65%).

The comparison of total densities (living + dead 0-1 cm) with the ones of fossil fauna at 3-4 cm (Fig. 3b) and 6-8 cm (Fig. 3c) shows generally lower densities for the stations of the inner fjord (MC1 to MC5). This is particularly striking for station MC3 where fossil faunas are nearly absent (2 ind. g^{-1}). At station MC6 this is true for the 3-4 cm layer (~ 10 ind. g^{-1}) but densities are slighter higher at 6-8 cm (~30 ind. g^{-1}). At station MC7, fossil faunas are denser (~120 ind. g^{-1}) than in the total assemblage of the topmost centimetre (~90 ind. g^{-1}). No major differences are observed between the 3-4 and 6-8 cm layers except for the three times lower densities observed at station MC6 at 3-4 cm depth.

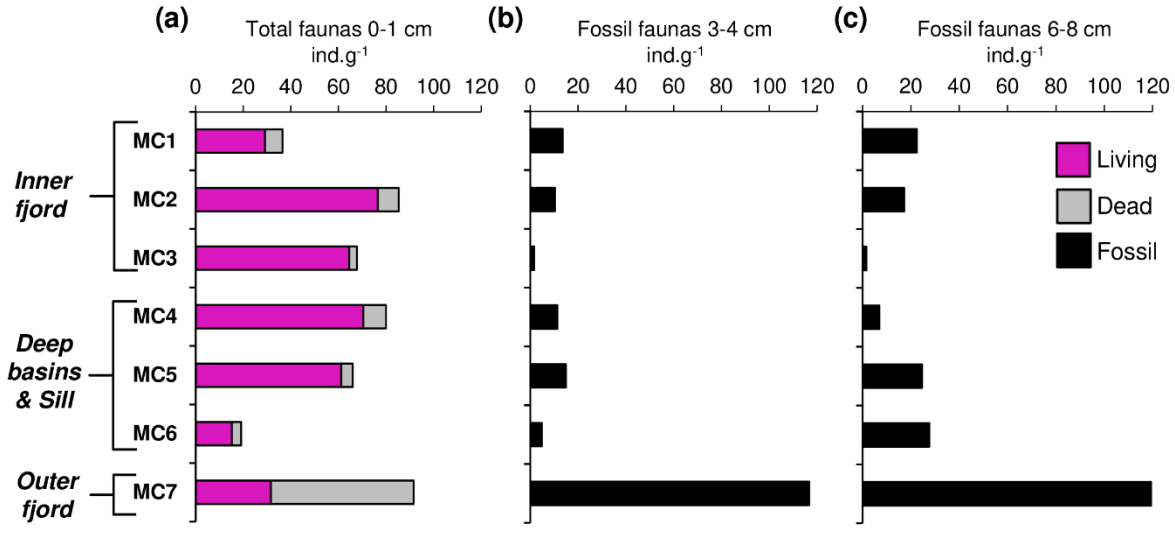

Figure 3. Foraminiferal densities expressed in individuals per gram of dry sediment (ind. g^{-1}) considering the **(a)** total faunas (living + dead) in the 0-1 cm sediment layer, **(b)** the fossil faunas in the 3-4 cm and **(c)** 6-8 cm sediment layers.

3.2.2 Species composition

In Figure 4, the relative abundances of the 21 major species (>5 % in at least one layer) are shown for the living assemblages of the first 5 cm of sediment, living and dead assemblages of the 0-1 cm layer, and the fossil faunas at 3-4 and at 6-8 cm.

In the inner fjord stations (MC1 to MC3), the living (0-1 and 0-5 cm) and the dead faunas (0-1 cm) are mainly represented by the same major species, *Elphidium clavatum* and *Nonionellina labradorica* (this latter is more abundant when subsurface layers are considered). In both the fossil assemblages of these inner fjord stations (at 3-4 and 6-8 cm depths), the same species dominate, with comparable proportions among the two sediment layers. Despite the very low densities observed in the MC3 fossil faunas (i.e., ~2 ind. g^{-1} at both 3-4 and 6-8 cm depth; Fig. 3b and Fig. 3c), the major species are still represented. *Cassidulina reniforme,* limited to the MC1 station*,* is represented at each considered depth. *Elphidium clavatum* at MC3 shows reduced percentages in the fossil faunas (both at 3-4 and 6-8 cm) compared to the living and dead assemblages (~40 vs 80 % respectively). Conversely, *Ammotium cassis* is nearly absent in the living and dead faunas and reaches about 20 % in the fossil assemblages. The calcareous *Buccella frigida* is nearly absent in the living faunas and its relative abundances increase in the dead and fossil assemblages (5-15 %).

In the deep basins (MC4 and MC5) and sill station (MC6), living faunas and dead faunas of the topmost centimetre are largely represented by *Reophax* spp. (30-50 %), *Recurvoides turbinatus* (10 to 25 %) and *Labrospira crassimargo* (5 to 15 %). These agglutinated species are accompanied by 8-10 % of *N. labradorica* in the living assemblages of the 0-5 cm sediment layers. At station MC6, a high proportion of *Adercotryma glomeratum* is also observed (10-30 %). The proportion of *L. crassimargo* and *R. turbinatus* is comparable in both the 3-4 and 6-8 cm fossil assemblages, whereas *Reophax* spp. drastically decreases to reach 0 to 12 %. *Adercotryma glomeratum* reaches only 5 % in the deeper fossil faunas (6-8 cm). Some calcareous species become noticeable only in the fossil faunas, such as *Elphidium clavatum* (about 10-25 %), *Elphidium bartletti* (about 5-13 % in the 6-8 cm) and *C. reniforme* (10 %) at MC4.

The living and dead assemblages at the outer fjord station MC7 show high proportions of *Reophax* spp. (15-35 %), *Lagenammina difflugiformis* (10-25 %), *Melonis barleeanus* (~10%), accompanied with *N. labradorica* in the 0-5 cm (25 %) and in the dead assemblages of 0-1 cm layer (15 %). In the fossil assemblages of both 3-4 and 6-8 cm sediment layers, the agglutinated species are nearly absent, and the relative abundances of *M. barleeanus* remains the same while the proportion of *N. labradorica* decreases to 5-10 %. Furthermore, some calcareous species are only present in the fossil assemblages (e.g., *Cribroelphidium subarcticum,* 10 %) or in both dead and fossil assemblages (e.g., *E. clavatum*, 10-20 %).

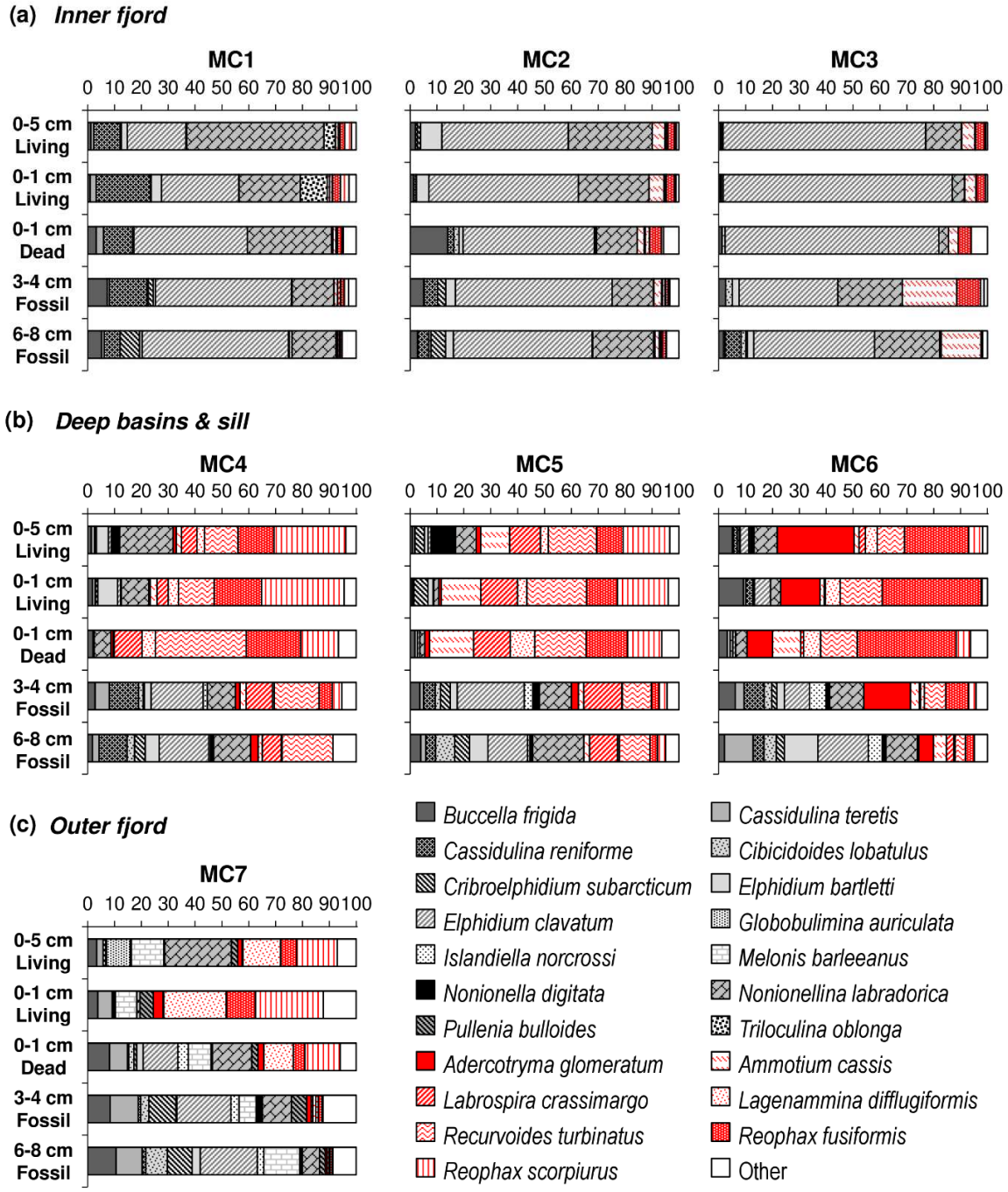

Figure 4. Relative abundances of the 21 major species (>5% in at least one layer) considering the living faunas from the 0-5 cm and 0-1 cm sediment layers, the dead faunas from the 0-1 cm sediment layer and the fossil faunas form the 3-4 cm and 6-8 cm sediment layers for **(a)** the inner fjord, **(b)** the deep basins and sill and **(c)** the outer fjord. Red textures represent agglutinated species whereas grey ones the calcareous. "Other" category includes both agglutinated and calcareous rare species.

3.2.3 Living vs fossil assemblages

To quantitatively estimate the difference between species composition of living and fossil assemblages, the $L_{0\text{-}5cm}/(L_{0\text{-}5cm}+ F_{6\text{-}8cm})$ ratio is calculated for 19 major species (Fig. 5). The $^{210}Pb_{xs}$-based estimation of sedimentation rates shows that both 3-4 and 6-8 cm layers were

below the TAZ. The differences in terms of species composition between the two layers are low at all stations. Since the older layer (6-8 cm) has undergone taphonomic processes for a longer period of time than the 3-4 cm layer, this is regarded as the best representative for the fossil assemblages and therefore presented on Figure 5 for comparison.

In the inner fjord, the ratio for the calcareous *Elphidium clavatum* is about 0.3 at MC1 and it increases to 0.5 and 0.6 respectively at MC2 and MC3. *Nonionellina labradorica* shows a ratio from about 0.6-0.8 at MC1 and MC2 to about 0.4 at MC3. In the inner fjord, the only major agglutinated species is *Ammotium cassis* at MC3, which shows a ratio of 0.3.

In the deep basins (MC4 and MC5) and sill (MC6) stations all the calcareous species show ratios <0.5, except for *N. labradorica* at MC4 (0.6 ratio) and *Nonionella digitata* at MC5 (0.9 ratio). The agglutinated taxa *Reophax* spp., *Recurvoides turbinatus*, *A. cassis* generally have ratios of about 0.6 to 1 in these stations. The exceptions are *R. turbinatus* at MC4, showing a ratio of 0.4, and *Labrospira crassimargo* with 0.4-0.5 ratios at MC4 and MC5. Finally, a ratio of 0.8 is observed for *Adercotryma glomeratum* at the sill station MC6.

In the outer fjord, MC7, *Buccella frigida*, *Cassidulina teretis*, *Cibicidoides lobatulus* *Cribroelphidium subarcticum* and *E. clavatum* have ratios <0.2. *Globobulimina auriculata* and *N. labradorica* show 0.8 to 1 ratios. Concerning the agglutinated taxa, *Reophax* spp. and *Lagenammina difflugiformis* have ratios of 0.9-1.

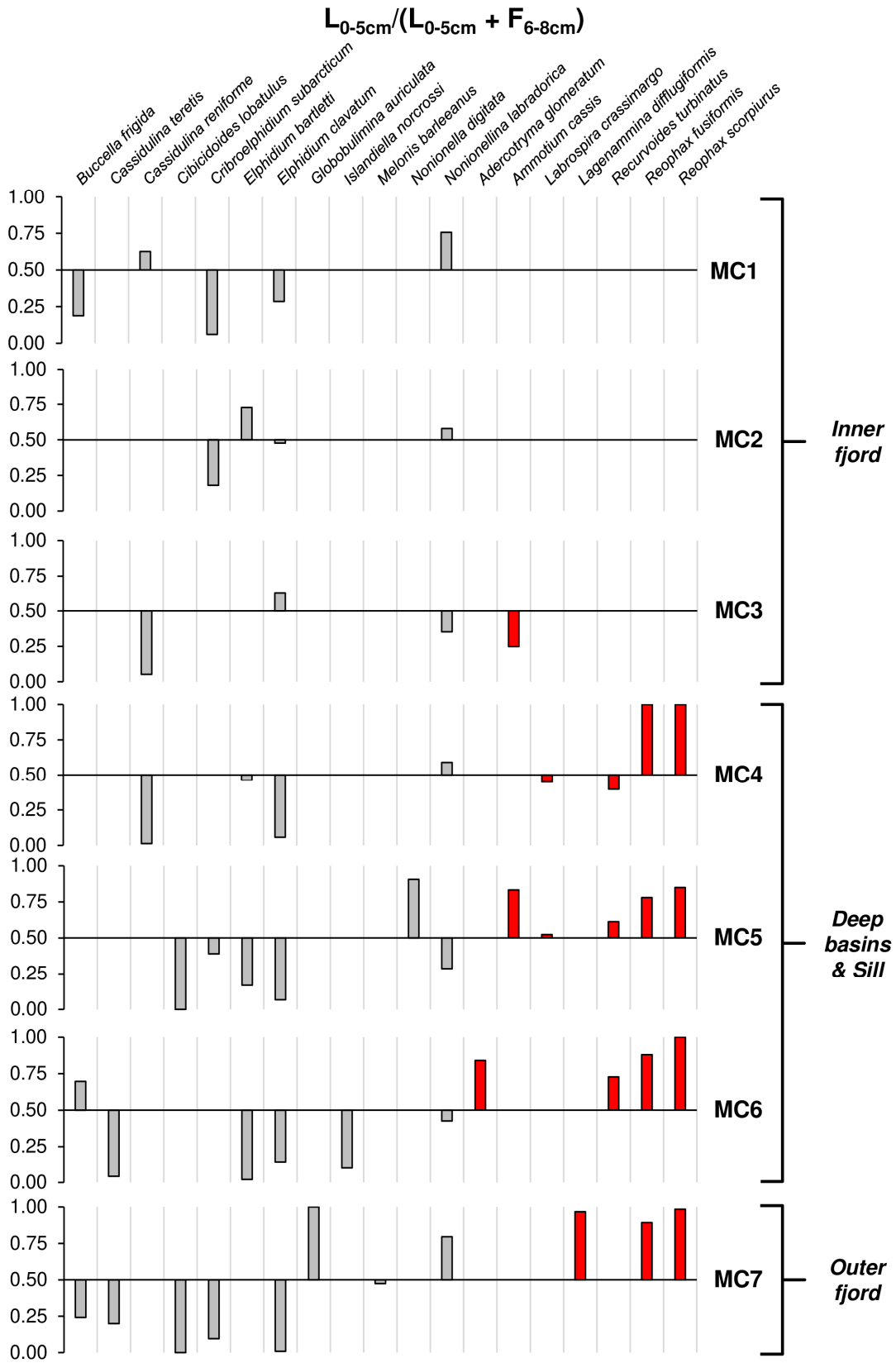

Figure 5. Ratio between living faunas (from the 0-5 cm sediment layer) and the fossil faunas (from the 6-8 cm sediment layer) calculated as: $L_{0\text{-}5cm}/(L_{0\text{-}5cm}+ F_{6\text{-}8cm})$. Ratio >0.5 indicates a relatively higher representation of the actual species in the living faunas, ratio <0.5 a higher representation of the species in the fossil faunas, whereas a value of 0.5 shows an equal representation.

3.3 Agglutinated/calcareous ratio (A/C)

The A/C ratios were calculated from the relative abundances of species from the living faunas (0-5 cm) (Fig. 6a; Fossile et al., 2020), the total faunas (living + dead in the 0-1 cm) (Fig. 6b) and from the fossil faunas at 6-8 cm depth (Fig. 6c).

The A/C ratio at the inner fjord stations (MC1 to MC3) is <0.1 due to high relative abundances of calcareous species (i.e., 89-94 %), in the living (0-5 cm; Fig. 6a), total (living + dead, 0-1 cm; Fig. 6b) and fossil (6-8 cm; Fig. 6c) faunas. The only noticeable difference is the slight increase in the ratio from 0.1 to 0.2 for the fossil assemblages at MC3.

In the deep basin and sill stations (MC4 to MC6) the A/C ratio varies between 1.9 and 3.4 in the living faunas (0-5 cm; Fig. 6a), and it increases up to 3.0-6.2 for the total faunas (living + dead, 0-1 cm; Fig. 6b). This is determined by high percentages of agglutinated species (i.e., 65-86 %). In the fossil faunas (6-8 cm; Fig. 6c), the A/C ratio decreases to values of 0.3-0.5 (agglutinated species about 20-33 %), but it is still two to three times higher than in the inner fjord stations.

In the outer fjord station MC7, the ratio is about 0.7-0.8 in the living (0-5 cm; Fig. 6a) and total faunas (living + dead; Fig. 6b) due to high proportion of calcareous species (about 60%). The ratio decreases to 0.03 in the fossil faunas (6-8 cm; Fig. 6c) due to a stronger dominance of calcareous species (95%).

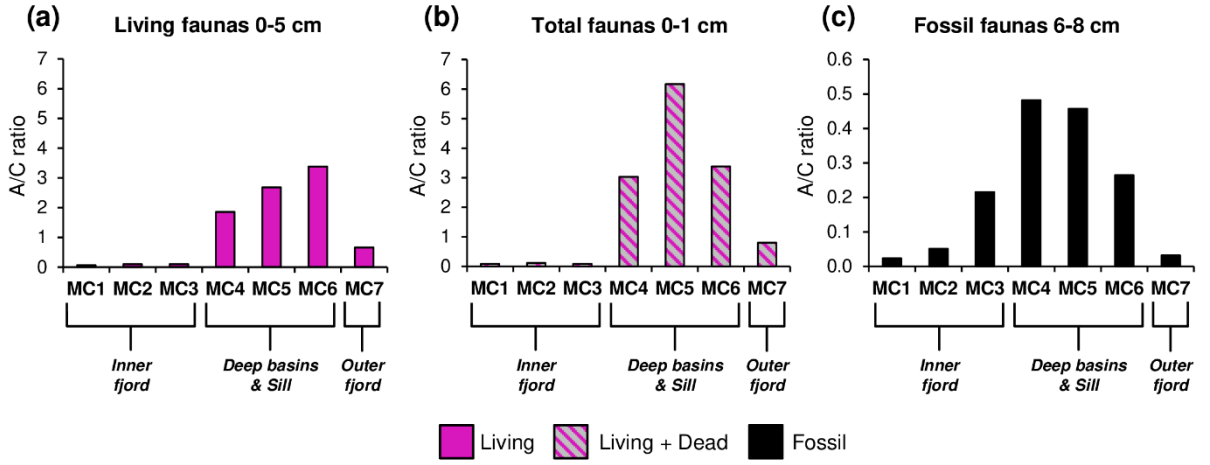

Figure 6. Agglutinated/Calcareous (A/C) ratio calculated for **(a)** living faunas from the 0-5 cm sediment layer, **(b)** total faunas (living + dead) form the 0-1 cm sediment layer and **(c)** fossil faunas from the 6-8 cm sediment layer. Note that the ratio scale is different for the fossil faunas that for the others.

4. Discussion

4.1 Ecological and taphonomic processes affecting foraminiferal standing stocks

Foraminiferal total fauna (dead + living) represents the integration of most of the specimens inhabiting a given place over a certain period of time. According to the estimated sedimentation rates, the total faunas of the 0-1 cm layer integrate approximately 2.5 to 4 years' time period (Fig. 2). The accumulation of dead faunas depends both on species production and taphonomic factors (e.g., Schönfeld et al., 2012). The comparison between living and dead faunas from the topmost centimetre of the sediments in the Storfjorden (Fig. 3a) shows a major difference between the stations inside the fjord (MC1 to MC6) and the outer fjord station (MC7). Inside the fjord, the dead assemblages of the top centimetre account for only 5 to 20% of the total fauna while in the outer station MC7, they represent about 65% of the total assemblage. This difference could be explained either by *(i)* a seasonal contrast in foraminiferal densities between summer (the sampling season) and other seasons, *(ii)* more intense early taphonomic processes inside than outside the fjord, and/or *(iii)* a difference in sedimentation rates.

(i) The winter in the Arctic realm, including in the Storfjorden, is characterised by the scarcity of light and by water stratification (Berge et al., 2015a, 2015b; Howe et al., 2010). This seasonal physical setting controls the timing and rate of primary productivity (PP), and the associated organic fluxes to the seafloor, which largely increase during the spring-summer season. Increased density and diversity of meiofauna and macrofauna were observed in the Adventfjorden (Svalbard), as a response to meltwater discharges and increased PP during the warm season (Pawłowska et al., 2011). As benthic meiofaunal consumers, foraminifera may as well lower their production rate during winter to adapt to low organic matter fluxes (e.g., Pawłowska et al., 2011; Juul-Pedersen et al., 2015) and increase their abundances during the warm season. Such seasonal and interannual variability in living foraminiferal densities was reported recently from the Kongsfjorden, another Svalbard fjord, and was inferred temporal variability in PP (Jernas et al., 2018). In our case study, this would explain the high densities of living foraminifera (i.e., warm-seasonal faunas; Fig. 3) compared to dead assemblages, inside the fjord (MC1 to MC6). The observed dead assemblages would mainly represent the rest of the living faunas of the previous warm seasons, after early taphonomic loss, rather than faunas of other seasons. The higher proportion of dead faunas at MC7 would be therefore due to reduced taphonomy at this station.

(ii) Inside the fjord, the production and cascading of corrosive brine-enriched shelf waters during winter-early spring is a potential cause of early taphonomic processes occurring close to the sediment surface and leading to a partial or total dissolution of calcitic-shelled foraminifera as reported from Fossile *et al.* (2020). Additionally, higher fluxes of organic matter during the warm season, and its enhanced remineralisation can contribute to further lower the pH in the first layers of the sediment column (Fossile *et al.* 2020). As such, the resulting dissolution of calcitic shells may explain the low percentages of dead faunas in the fjord stations. Outside the fjord, the influence of brine-enriched shelf waters is episodic and only related to the seasonal outflow during their production period (Skogseth *et al.* 2005a).

(iii) Outside the fjord, the sedimentation rates are on average three times lower than inside. This, added to reduced BSW influence, promotes the accumulation of dead faunas at MC7 (see Fig. S1).

The difference in the preservation potential observed in the upper centimetre faunas between the stations inside and the one outside the fjord, is also observed in the fossil faunas from the 3-4 and 6-8 cm sediment layers (Fig. 3). Except for the sill station MC6, where standing stock fluctuations among layers are observed, the stations inside the fjord (MC1- MC5) generally show low preservation of fossils (Fig. 3), while an accumulation of specimens is visible outside the fjord (MC7). The higher variability observed at station MC6 highlights the possible influence of natural temporal variability of standing stocks on fossil assemblage accumulation. This could be due to biological reasons (increased reproduction rates at some periods) and/or to physical processes influencing accumulation, including transport over the sill during brines outflow (e.g., Nielsen and Rasmussen, 2018).

The generally high similarity, in terms of standing stocks, between fossil faunas at 3-4 and 6-8 cm depths (Fig. 3) at all stations confirms that: *(i)* the maximum taphonomic loss occurs at the sediment surface (inside the TAZ), *(ii)* both 3-4 and 6-8 cm sediment layers contain fossil faunas that crossed the early taphonomic stages, and *(iii)* there is not a major taphonomic loss occurring between 3-4 cm and 6-8 cm layers.

4.2 Species preservation in the fossil record

Species composition of the living (0-1 and 0-5 cm), dead (0-1 cm) and fossil (3-4 and 6-8 cm) assemblages show different results for calcareous and agglutinated species in terms of preservation potential.

In the innermost fjord stations (MC1 to MC3), all the assemblages (i.e., living, dead and fossils) are largely dominated by the same calcareous species (*Elphidium clavatum*, *Cassidulina reniforme*, and *Nonionellina labradorica*). This indicates a low temporal variability in this part of the fjord. The presence of these species in the living assemblages, which reflect summer conditions, may indicate their tolerance to the potential stressful environmental conditions during the melting season (i.e., high freshwater and sediment inputs from glaciers) and their preference and/or tolerance of high concentrations of (fresh) organic matter fluxes (e.g., Hald and Korsun, 1997; Korsun and Hald, 1998; Forwick et al., 2010; Fossile et al., 2020). The low variability observed between dead and fossil assemblages in the inner fjord (MC1 to MC3) suggests that the fossil faunas mostly reflect, in terms of species composition, the summer foraminiferal assemblages. The alternative hypothesis would be the dissolution of cold season faunas during the phases of intense brine production and cascading. Considering the living assemblages, the low proportion of *E. clavatum* in favour of *N. labradorica* in the 0-5 cm layer compared to the sediment surface (0-1 cm), reiterates the necessity to integrate the infaunal microhabitats in the comparison of living and fossil faunas, to avoid underestimating infaunal species.

In our samples, there is only one calcareous species, *Buccella frigida*, which is abundant only in the dead/fossil assemblages and nearly absent in the living fauna. This species has been previously reported from glacier-proximal areas of Arctic fjords (e.g., Korsun and Hald, 1998; Jernas et al., 2013) and suggested by Szymańska et al. (2017) as an indicator of sea ice formation during winter. Its presence in the dead faunas may suggest its occurrence only during winter season. This corroborates that winter faunas are not completely impacted by taphonomy and that the dead and fossil assemblages reflect most likely a higher foraminiferal production in summer. Another possibility could be that *B. frigida* resists dissolution better than other winter species which would not be preserved in dead and fossil faunas. However, species relative abundances are comparable in the fossil faunas, suggesting no species-specific taphonomic loss. The only exception is *E. clavatum*, which seems to suffer high taphonomic loss in terms of relative abundances (Fig. 4) but it is still well represented in the fossil assemblages.

In the deep basins (MC4 and MC5) and sill (MC6) stations, the living faunas are dominated by agglutinated species, including fragile organic-cemented agglutinated taxa such as *Reophax* spp. (e.g., Schröder 1988). The dead faunas at these stations (MC4-MC6) are similar to the living assemblages, suggesting that the diagenesis of agglutinated tests does not occur rapidly after their death, despite the brine-enriched shelf waters persistence as previously reported by

Fossile et al. (2020). This is in accord with Rasmussen and Thomsen (2015) who reported the presence of *Reophax* spp. in Holocene archives from the central Storfjorden and suggested that the high sedimentation rates of the fjord would be responsible for the exceptional preservation of these species. In our samples, however, the fossil faunas show a clear shift towards the dominance of calcareous species, while the agglutinated taxa, after the loss of fragile species, are mostly represented by more robust agglutinated species *Adercotryma glomeratum*, *Ammotium cassis*, *Recurvoides turbinatus* and *Labrospira crassimargo* (Fig. 4, Fig. 5), which may have a better preservation potential (e.g., Rasmussen and Thomsen 2015). As such, the higher proportion of calcareous species in the fossil faunas at these stations would mainly be the consequence of selective taphonomic loss on some agglutinated species.

Differently from the inner fjord, where the dominant calcareous species do not change among layers, in the deep basins and sill stations, some major changes in calcareous species composition are observed. For instance, *E. clavatum* is nearly absent in the living faunas of the deep basin and, when present, it shows high degrees of dissolution (Fossile et al., 2020). Its higher relative density in the living faunas of the sill station MC6 would be related to the only intermittent influence of BSW over the sill. The quite high relative abundance of *E. clavatum* in the fossil faunas of the stations MC4 to MC6, therefore, would indicate either past conditions with different environmental characteristics in this area of the fjord (i.e., more similar to inner fjord, lower BSW influence) or a possible transport from the inner fjord with BSW cascading or near-bottom currents, followed by a rapid burial. As, according to the literature, deep basins are characterised by constant conditions under year-round persisting BSW (Skogseth et al., 2005a), transport seems the most reliable hypothesis to retain. Moreover, the increased presence of *E. clavatum* in the fossil faunas is coeval with increased abundances of *Cibicidoides lobatulus.* This latter species has been previously reported from glacier-proximal stations in the Storfjorden (e.g., Mackensen and Schmiedl, 2016) and is often associated with coarse sediments and high-energy environments in the outer or threshold area of various Arctic fjords (e.g. Hald & Korsun 1997). Its presence in the fossil faunas would be in accordance with the hypothesis of intermittent transport by near-bottom currents or brine-enriched shelf waters cascading formulated for *E. clavatum.*

Among the calcareous species found in the deep basins (MC4 and MC5) and sill (MC6) stations, *N. labradorica* is largely present in all the assemblages and does not show high degrees of dissolution in the living assemblages directly under the influence of corrosive BSW (Fossile et al., 2020). Although the reason for such a resistance to dissolution is intriguing, this seems to be the only possible explanation of its high preservation potential in the fossil record (Fig. 4,

5). The resistance could be related to a high robustness of the shell or to physiological adaptative patterns. Indeed, the pH values in the first millimetres or centimetre of the sediment are typically lower than at water-sediment interface, due to aerobic respiration of organic matter. As a shallow to deep infaunal species (e.g., Fontanier et al., 2014), *N. labradorica* could be adapted to calcify under low pH conditions, and as such, this might be an advantage for preservation in this kind of environment affected by corrosive BSW.

Finally, we highlight that the outer fjord station MC7 shows very different assemblages when comparing living and fossil faunas. Living faunas is composed of typical Atlantic species, such as *Melonis barleeanus, Cassidulina teretis* and *Globobulimina auriculata* (e.g., Jennings et al., 2004; Knudsen et al., 2012; Jernas et al., 2018). While *M. barleeanus* and *C. teretis* are still well represented in the dead and fossil assemblages, *G. auriculata* is completely absent in the fossil record. This latter species has a very thin and delicate calcareous test, with consequent lower fossilising potential, suggesting a possible selective taphonomy against this species. Fossil faunas show an interesting mix of Atlantic and Arctic species (i.e., *B. frigida, E. clavatum*, *N. labradorica*). This station, located at about 300 m depth in the Storfjordrenna, about 50 km from the southern coast of Spitsbergen, is possibly influenced both by Atlantic waters (during summer) and BSW overflow from Storfjorden during winter-early spring (i.e., the period of intensive sea ice formation). Furthermore, the presence of both Atlantic and Arctic species is representative of the seasonal variability in the assemblage composition at the outer fjord.

4.3 The A/C ratio as a proxy for historical reconstructions of brine persistence

The comparison between recent (living and dead) and fossil assemblages in terms of shell composition shows that the effects of brine persistence in the bottom waters (as observed by Fossile et al., 2020), are still visible after the first phases of taphonomic processes. In fact, despite the considerable loss of foraminifera (e.g., both at 3-4 cm and 6-8 cm depth, Fig. 3), and the selective disappearance of delicate agglutinated taxa (mainly *Reophax* and *Lagenammina* spp.) or fragile calcareous species (e.g., *G. auriculata*), the A/C ratios still reflect the ratios calculated for the living faunas.

In absolute terms, A/C ratios decrease of one order of magnitude when comparing the 0-1 cm total (living and dead) faunas and the 6-8 cm fossil faunas. This is possibly due to the selective loss of agglutinated species under taphonomic processes. Such difference is smoothed when comparing the 0-5 cm living faunas to the fossil faunas (6-8 cm) because of the presence

of calcareous species in the infaunal microhabitat (e.g., *Nonionellina labradorica*). This result underlines that the decrease of the A/C ratio in the fossil faunas is not exclusively related to the preservation potential of agglutinated species but also to the fact that fossil assemblages integrate species from potentially different microhabitats.

Nevertheless, the loss of A/C signal between the recent faunas (total from 0-1 cm and living from 0-5 cm) and the fossil faunas (6-8 cm), does not invalidate the use of this ratio as a proxy for brine persistence. The A/C ratio, calculated on fossil faunas, in the deep basin is two to three times higher than in the inner fjord (Fig. 6). This confirms that the relative difference between the inner fjord stations (MC1-MC3), not impacted by persistent brines, and the deep basin and sill stations (MC4-MC6), influenced by long-term presence of BSW at the seafloor, is still clearly expressed.

Accordingly, our findings suggest that the A/C ratio can be used in historical sedimentary archives to determine the presence or absence of persistent BSW at the seafloor as an indirect proxy for thin first-year sea ice production in coastal polynyas. The plus-value of the A/C ratio as a proxy for sea ice production is its applicability in Arctic coastal settings where the common proxies for sea ice reconstruction in open marine areas are not valuable (e.g., IP_{25}, Ribeiro et al., 2017; Limoges et al., 2018). Although our findings validate the use of the A/C proxy, we recommend its association with other proxies to get a more robust overview of historical sea ice dynamics. For example, Ribeiro et al. (2017) performed a calibration of possible useful proxies in some fjords of Greenland and suggested that organic compounds, biogenic silica and a sea ice-associated biomarker (i.e., HBI III) can well reflect marine influence and sea ice edge position in the fjord system. The complementary application of the A/C ratio would allow the identification of events (or their absence) of thin sea-ice production in the recent past (i.e., hundreds of years) in Arctic coastal/fjord settings.

5. Conclusions

The seasonal formation of sea ice and the consequent production of brine-enriched shelf waters (BSW) undeniably impact the benthic environment in Storfjorden, as shown by foraminiferal assemblages, with clear spatial differences linked to the fjord topography. The persistence of corrosive brines at the seafloor is a major driving factor for foraminiferal distribution, leading to a relative increase of agglutinated species vs calcareous species more sensitive to dissolution in the living assemblages. The present study validates the applicability of the Agglutinated/Calcareous (A/C) ratio as a proxy to reconstruct historical brine production and

BSW persistence at the seafloor, and indirectly, for a semi-quantitative estimation of the first-year thin sea ice formation in the fjord. The *conditio sine qua non* for this validation was the preservation in the fossil records below the TAZ of the signal observed in living and recently dead faunas. Despite a high taphonomic loss in superficial sediment of the Storfjorden in terms of standing stocks, the fossil faunas allow to clearly detect the increased proportion of agglutinated species in the area persistently influenced by BSW (deep basins) compared to the one only influenced (inner fjord). In Storfjorden and similar fjords characterised by the presence of deep basins delimited by a sill, the analyses of cores sampled at or outside the sill would allow to connect the persistence of BSW to intense overflow and therefore to the intense (or not) production of first-year thin sea ice. The possibility to reconstruct sea ice dynamics in polar fjords on a historical time scale is crucial to confirm short time scale tendencies observed by satellite images on present-day ice cover and perform more reliable predictions for the future.

Data availability. Foraminiferal densities for dead (0-1 cm) and fossil (3-4 cm, 6-8 cm) will be available online upon publication of this manuscript in *Boreas*. Foraminiferal densities for the living faunas (0-5 cm) are available from the following link: https://doi.org/10.1594/PANGAEA.907687 (Fossile et al., 2019).

Supplement. Figure S1 can be found in the Supplement section.

Author contributions. MPN, EF: conceptualisation, data curation, formal analysis, investigation, methodology, validation, visualisation, writing-original draft, writing-review and editing. MPN, MM, HH: conceptualisation, funding acquisition, investigation, resources, supervision, validation, writing-review and editing. OP: methodology, writing-review and editing.

Acknowledgements. We thank the captain and crew of R/V L'Atalante, which was chartered by IFREMER (French Research Institute for Exploitation of the Sea); Frédéric Vivier (co-chief of the cruise); and all participants who contributed to the success of to the STeP cruise. We thank Bruno Bombled for his technical assistance during the cruise. We fully acknowledge the efficient technical help provided by Arbia Jouini and we thank Bruno Lansard and Caterina Morigi for the useful discussions about this research.

Financial support. The research was funded by the ABBA (Observatoire des Sciences de l'Univers de Nantes Atlantique), Bi-SMART (University of Angers) and TANDEM (Région Pays de la Loire) projects. This research is part of the PhD thesis of Eleonora Fossile, which is co-funded by French National Program MOPGA (Make Our Planet Great Again) and the University of Angers.

Competing interests. The authors declare that they have no conflict of interest.

References

Anderson, L. G., Falck, E., Jones, E. P., Jutterström, S. and Swift, J. H.: Enhanced uptake of atmospheric CO_2 during freezing of seawater: A field study in Storfjorden, Svalbard, J. Geophys. Res., 109(C06004), https://doi.org/10.1029/2003JC002120, 2004.

Appleby, P. G. and Oldfield, F.: The calculation of lead-210 dates assuming a constant rate of supply of unsupported 210Pb to the sediment, CATENA, 5, 1–8, https://doi.org/10.1016/S0341-8162(78)80002-2, 1978.

Belt, S. T.: Source-specific biomarkers as proxies for Arctic and Antarctic sea ice, Org. Geochem., 125, 277–298, https://doi.org/10.1016/j.orggeochem.2018.10.002, 2018.

Belt, S. T.: What do IP25 and related biomarkers really reveal about sea ice change?, Quat. Sci. Rev., 204, 216–219, https://doi.org/10.1016/j.quascirev.2018.11.025, 2019.

Belt, S. T. and Müller, J.: The Arctic sea ice biomarker IP25: A review of current understanding, recommendations for future research and applications in palaeo sea ice reconstructions, Quat. Sci. Rev., 79, 9–25, https://doi.org/10.1016/j.quascirev.2012.12.001, 2013.

Belt, S. T., Massé, G., Rowland, S. J., Poulin, M., Michel, C. and LeBlanc, B.: A novel chemical fossil of palaeo sea ice: IP25, Org. Geochem., 38(1), 16–27, https://doi.org/10.1016/j.orggeochem.2006.09.013, 2007.

Bender, H.: Test structure and classification in agglutinated foraminifera. In: Proceedings of the 4th international workshop on agglutinated foraminifera, edited by M. A. Kaminski, S. Geroch, and M. A. Gashiski, 3, pp. 27-70, Kraków Poland, 1995.

Berge, J., Renaud, P. E., Darnis, G., Cottier, F., Last, K., Gabrielsen, T. M., Johnsen, G., Seuthe, L., Weslawski, J. M., Leu, E., Moline, M., Nahrgang, J., Søreide, J. E., Varpe, Ø., Lønne, O. J., Daase, M. and Falk-Petersen, S.: In the dark: A review of ecosystem processes during the Arctic polar night, Prog. Oceanogr., 139, 258–271, https://doi.org/10.1016/j.pocean.2015.08.005, 2015a.

Berge, J., Daase, M., Renaud, P. E., Ambrose, W. G., Darnis, G., Last, K. S., Leu, E., Cohen, J. H., Johnsen, G., Moline, M. A., Cottier, F., Varpe, O., Shunatova, N., Bałazy, P., Morata, N., Massabuau, J. C., Falk-Petersen, S., Kosobokova, K., Hoppe, C. J. M., Węsławski, J. M., Kukliński, P., Legeżyńska, J., Nikishina, D., Cusa, M., Kędra, M., Włodarska-Kowalczuk, M., Vogedes, D., Camus, L., Tran, D., Michaud, E., Gabrielsen, T. M., Granovitch, A., Gonchar, A., Krapp, R. and Callesen, T. A.: Unexpected levels of biological activity during the polar night offer new perspectives on a warming arctic, Curr. Biol., 25(19), 2555–2561, https://doi.org/10.1016/j.cub.2015.08.024, 2015b.

Berkeley, A., Perry, C. T., Smithers, S. G., Horton, B. P. and Taylor, K. G.: A review of the ecological and taphonomic controls on foraminiferal assemblage development in intertidal environments, Earth-Science Rev., 83(3–4), 205–230, https://doi.org/10.1016/j.earscirev.2007.04.003, 2007.

Berkeley, A., Perry, C. T., Smithers, S. G. and Hoon, S.: Towards a formal description of foraminiferal assemblage formation in shallow-water environments: Qualitative and quantitative concepts, Mar. Micropaleontol., 112, 27–38, https://doi.org/10.1016/j.marmicro.2014.08.005, 2014.

Bizon, G., Bizon, J.J. Méthode d'études et mode de prélèvement des sédiments d"ECOMED. In: Ecologie des microorganismes en Méditerranée occidentale "ECOMED". Bizon, J.J., Burollet, P.F. (Eds.), Association Française des Techniciens du Pétrole, Paris, pp. 81-83, 1984.

Blake, G. R.: Particle density. In: Encyclopedia of Soil Science. Chesworth W. (Ed.), Springer, Netherlands, 2008.

Davies, D., Powell, E., Stanton, R.: Relative rates of shell dissolution and net sediment accumulation - a commentary: can shell beds form by the gradual accumulation of biogenic debris on the sea floor?, Lethaia 22, 207-212, 1989.

Fer, I., Skogseth, R., Haugan, P. M. and Jaccard, P.: Observations of the Storfjorden overflow, Deep. Res. Part I Oceanogr. Res. Pap., 50(10–11), 1283–1303, https://doi.org/10.1016/S0967-0637(03)00124-9, 2003.

Fontanier, C., Duros, P., Toyofuku, T., Oguri, K., Koho, K. A., Buscail, R., Grémare, A., Radakovitch, O., Deflandre, B., De Nooijer, L. J., Bichon, S., Goubet, S., Ivanovsky, A., Chabaud, G., Menniti, C., Reichart, G. J. and Kitazato, H.: Living (stained) deep-sea foraminifera off hachinohe (NE Japan, western Pacific): Environmental interplay in oxygen-depleted ecosystems, J. Foraminifer. Res., 44(3), 281–299, https://doi.org/10.2113/gsjfr.44.3.281, 2014.

Forwick, M., Vorren, T. O., Hald, M., Korsun, S., Roh, Y., Vogt, C. and Yoo, K.-C.: Spatial and temporal influence of glaciers and rivers on the sedimentary environment in Sassenfjorden and Tempelfjorden, Spitsbergen, Geol. Soc. London, Spec. Publ., 344, 163–193, https://doi.org/10.1144/SP344.13, 2010.

Fossile, E., Nardelli, M. P., and Mojtahid, M. STEP2016 living foraminifera in surface sediments of a N-S transect in the Storfjorden, PANGAEA, https://doi.org/10.1594/PANGAEA.907687, 2019.

Fossile, E., Nardelli, M. P., Jouini, A., Lansard, B., Pusceddu, A., Moccia, D., Michel, E., Péron, O., Howa, H. and Mojtahid, M.: Benthic foraminifera as tracers of brine production in the Storfjorden "sea ice factory," Biogeosciences, 17(7), 1933–1953, https://doi.org/10.5194/bg-17-1933-2020, 2020.

Haarpaintner, J., Gascard, J. and Haugan, P. M.: Ice production and brine formation in Storfjorden, Svalbard, J. Geophys. Res. Ocean., 106(C7), 14001–14013, https://doi.org/10.1029/1999JC000133, 2001a.

Haarpaintner, J., Haugan, P. M. and Gascard, J. C.: Interannual variability of the Storfjorden (Svalbard) ice cover and ice production observed by ERS-2 SAR, Ann. Glaciol., 33, 430–436, 2001b.

Haarpaintner, J., O'Downer, J., Gascard, J. C., Haugan, P. M., Schauer, U. and Øterhus, S.: Seasonal transformation of water masses, circulation and brine formation observed in Storfjorden, Svalbard, Ann. Glaciol., 33, 437–443, https://doi.org/doi:10.3189/172756401781818635, 2001c.

Hald, M. and Korsun, S.: Distribution of modern benthic foraminifera from fjords of Svalbard, European Arctic, J. Foraminifer. Res., 27(2), 101–122, https://doi.org/10.2113/gsjfr.27.2.101, 1997.

Howe, J. A., Austin, W. E. N., Forwick, M., Paetzel, M., Harland, R. E. X. and Cage, A. G.: Fjord systems and archives: a review, Fjord Syst. Arch., 5–15, https://doi.org/10.1144/SP344.2, 2010.

Jennings, A. E., Weiner, N. J., Helgadottir, G. and Andrews, J. T.: Modern foraminiferal faunas of the southwestern to northern Iceland shelf: Oceanographic and environmental controls, J. Foraminifer. Res., 34(3), 180–207, https://doi.org/10.2113/34.3.180, 2004.

Jernas, P., Klitgaard Kristensen, D., Husum, K., Wilson, L. and Koç, N.: Palaeoenvironmental changes of the last two millennia on the western and northern Svalbard shelf, Boreas, 42(1), 236–255, https://doi.org/10.1111/j.1502-3885.2012.00293.x, 2013.

Jernas, P., Klitgaard-Kristensen, D., Husum, K., Koç, N., Tverberg, V., Loubere, P., Prins, M., Dijkstra, N. and Gluchowska, M.: Annual changes in Arctic fjord environment and modern benthic foraminiferal fauna: Evidence from Kongsfjorden, Svalbard, Glob. Planet. Change, 163, 119–140, https://doi.org/10.1016/j.gloplacha.2017.11.013, 2018.

Jorissen, F. J. and Wittling, I.: Ecological evidence from live-dead comparisons of benthic foraminiferal faunas off Cape Blanc (Northwest Africa), Palaeogeogr. Palaeoclimatol. Palaeoecol., 149(1–4), 151–170, https://doi.org/10.1016/S0031-0182(98)00198-9, 1999.

Juul-Pedersen, T., Arendt, K. E., Mortensen, J., Blicher, M. E., Søgaard, D. H. and Rysgaard, S.: Seasonal and interannual phytoplankton production in a sub-Arctic tidewater outlet glacier fjord, SW Greenland, Mar. Ecol. Prog. Ser., 524, 27–38, https://doi.org/10.3354/meps11174, 2015.

Knudsen, K. L., Eiríksson, J. and Bartels-Jónsdóttir, H. B.: Oceanographic changes through the last millennium off North Iceland: Temperature and salinity reconstructions based on foraminifera and stable isotopes, Mar. Micropaleontol., 84–85, 54–73, https://doi.org/10.1016/j.marmicro.2011.11.002, 2012.

Korsun, S. and Hald, M.: Modern benthic foraminifera off Novaya Zemlya tidewater glaciers, Russian Arctic, Arct. Alp. Res., 30(1), 61–77, https://doi.org/10.2307/1551746, 1998.

Limoges, A., Massé, G., Weckström, K., Poulin, M., Ellegaard, M., Heikkilä, M., Geilfus, N. X., Sejr, M. K., Rysgaard, S. and Ribeiro, S.: Spring succession and vertical export of diatoms and ip25 in a seasonally ice-covered high Arctic fjord, Front. Earth Sci., 6, 1–15, https://doi.org/10.3389/feart.2018.00226, 2018.

Mackensen, A. and Schmiedl, G.: Brine formation recorded by stable isotopes of Recent benthic foraminifera in Storfjorden, Svalbard: palaeoceanographical implications, Boreas, 45(3), 552–566, https://doi.org/10.1111/bor.12174, 2016.

Meredith, M., Sommerkorn, M., Cassotta, S., Derksen, C., Ekaykin, A., Hollowed, A., Kofinas, G., Mackintosh, A., Melbourne-Thomas, J., Muelbert, M. M. C., Ottersen, G., Pritchard, H. and Schuur, E. A. G.: Polar Regions, in IPCC Special Report on the Ocean and Cryosphere in a Changing Climate, pp. 203–320, , 2019.

Müller, J., Massé, G., Stein, R. and Belt, S. T.: Variability of sea-ice conditions in the Fram Strait over the past 30,000 years, Nat. Geosci., 2(11), 772–776, https://doi.org/10.1038/ngeo665, 2009.

Müller, J., Wagner, A., Fahl, K., Stein, R., Prange, M. and Lohmann, G.: Towards quantitative sea ice reconstructions in the northern North Atlantic: A combined biomarker and numerical modelling approach, Earth Planet. Sci. Lett., 306(3–4), 137–148, https://doi.org/10.1016/j.epsl.2011.04.011, 2011.

Muñoz, P., Lange, C. B., Gutiérrez, D., Hebbeln, D., Salamanca, M. A., Dezileau, L., Reyss, J. L. and Benninger, L. K.: Recent sedimentation and mass accumulation rates based on 210Pb along the Peru-Chile continental margin, Deep. Res. Part II Top. Stud. Oceanogr., 51(20–21), 2523–2541, https://doi.org/10.1016/j.dsr2.2004.08.015, 2004.

Nielsen, T. and Rasmussen, T. L.: Reconstruction of ice sheet retreat after the Last Glacial maximum in Storfjorden, southern Svalbard, Mar. Geol., 402, 228–243, https://doi.org/10.1016/j.margeo.2017.12.003, 2018.

Ohshima, K. I., Nihashi, S. and Iwamoto, K.: Global view of sea-ice production in polynyas and its linkage to dense/bottom water formation, Geosci. Lett., 3(13), https://doi.org/10.1186/s40562-016-0045-4, 2016.

Pawłowska, J., Włodarska-Kowalczuk, M., Zajączkowski, M., Nygård, H. and Berge, J.: Seasonal variability of meio- and macrobenthic standing stocks and diversity in an Arctic fjord (Adventfjorden, Spitsbergen), Polar Biol., 34(6), 833–845, https://doi.org/10.1007/s00300-010-0940-7, 2011.

Quadfasel, D., Rudels, B. and Kurz, K.: Outflow of dense water from a Svalbard fjord into the Fram Strait, Deep Sea Res. Part A, Oceanogr. Res. Pap., 35(7), 1143–1150, https://doi.org/10.1016/0198-0149(88)90006-4, 1988.

R Core Team. R: A language and environment for statistical computing. R Foundation for Statistical Computing, Vienna, Austria. https://www.R-project.org/, 2020

Rasmussen, T. L. and Thomsen, E.: Brine formation in relation to climate changes and ice retreat during the last 15,000 years in Storfjorden, Svalbard, 76 – 78°N, Paleoceanography, 29, 911–929, https://doi.org/10.1002/2014PA002643.Received, 2014.

Rasmussen, T. L. and Thomsen, E.: Palaeoceanographic development in Storfjorden, Svalbard, during the deglaciation and Holocene: Evidence from benthic foraminiferal records, Boreas, 44(1), 24–44, https://doi.org/10.1111/bor.12098, 2015.

Rasmussen, T. L., Thomsen, E., Skirbekk, K., Ślubowska-Woldengen, M., Klitgaard Kristensen, D. and Koç, N.: Spatial and temporal distribution of Holocene temperature maxima in the northern Nordic seas: Interplay of Atlantic-, Arctic- and polar water masses, Quat. Sci. Rev., 92, 280–291, https://doi.org/10.1016/j.quascirev.2013.10.034, 2014.

Ribeiro, S., Sejr, M. K., Limoges, A., Heikkilä, M., Andersen, T. J., Tallberg, P., Weckström, K., Husum, K., Forwick, M., Dalsgaard, T., Massé, G., Seidenkrantz, M. S. and Rysgaard, S.: Sea ice and primary production proxies in surface sediments from a High Arctic Greenland fjord: Spatial distribution and implications for palaeoenvironmental studies, Ambio, 46, 106–118, https://doi.org/10.1007/s13280-016-0894-2, 2017.

Ribeiro, S., Limoges, A., Massé, G., Johansen, K. L., Colgan, W., Weckström, K., Jackson, R., Georgiadis, E., Mikkelsen, N., Kuijpers, A., Olsen, J., Olsen, S. M., Nissen, M., Andersen, T. J., Strunk, A., Wetterich, S., Syväranta, J., Henderson, A. C. G., Mackay, H., Taipale, S., Jeppesen, E., Larsen, N. K., Crosta, X., Giraudeau, J., Wengrat, S., Nuttall, M., Grønnow, B., Mosbech, A. and Davidson, T. A.: Vulnerability of the North Water ecosystem to climate change, Nat. Commun., 12(1), 1–12, https://doi.org/10.1038/s41467-021-24742-0, 2021.

Rudels, B. and Quadfasel, D.: Convection and deep water formation in the Arctic Ocean-Greenland Sea System, J. Mar. Syst., 2(3–4), 435–450, https://doi.org/10.1016/0924-7963(91)90045-V, 1991.

Rysgaard, S., Bendtsen, J., Delille, B., Dieckmann, G. S., Glud, R. N., Kennedy, H., Mortensen, J., Papadimitriou, S., Thomas, D. N. and Tison, J. L.: Sea ice contribution to the air-sea CO_2 exchange in the Arctic and Southern Oceans, Tellus, Ser. B Chem. Phys. Meteorol., 63(5), 823–830, https://doi.org/10.1111/j.1600-0889.2011.00571.x, 2011.

Sanchez-Cabeza, J. A. and Ruiz-Fernández, A. C.: 210 Pb sediment radiochronology: An integrated formulation and classification of dating models, Geochim. Cosmochim. Acta, 82, 183–200, https://doi.org/10.1016/j.gca.2010.12.024, 2012.

Schauer, U. and Fahrbach, E.: A dense bottom water plume in the western Barents Sea: Downstream modification and interannual variability, Deep. Res. Part I Oceanogr. Res. Pap., 46(12), 2095–2108, https://doi.org/10.1016/S0967-0637(99)00046-1, 1999.

Schmidt, S., Tronczynski, J., Guiot, N. and Lefevre, I.: Dating of sediments in the Biscay bay: Implication for pollution chronology, Radioprotection, 40, S655–S660, https://doi.org/10.1051/radiopro:2005s1-096, 2005.

Schönfeld, J., Alve, E., Geslin, E., Jorissen, F., Korsun, S., Spezzaferri, S., Abramovich, S., Almogi-Labin, A., du Chatelet, E. A., Barras, C., Bergamin, L., Bicchi, E., Bouchet, V., Cearreta, A., Di Bella, L., Dijkstra, N., Disaro, S. T., Ferraro, L., Frontalini, F., Gennari, G., Golikova, E., Haynert, K., Hess, S., Husum, K., Martins, V., McGann, M., Oron, S., Romano, E., Sousa, S. M. and Tsujimoto, A.: The FOBIMO (FOraminiferal BIo-MOnitoring) initiative-Towards a standardised protocol for soft-bottom benthic foraminiferal monitoring studies, Mar. Micropaleontol., 94–95, 1–13, https://doi.org/10.1016/j.marmicro.2012.06.001, 2012.

Schröder, C. J.: Sunsurface preservation of agglutinated foraminifera in the northerst atlantic ocean, Abhandlungen der Geol. Bundesanstalt, 41, 325–336, 1988.

Seidenkrantz, M. S.: Benthic foraminifera as palaeo sea-ice indicators in the subarctic realm - examples from the Labrador Sea-Baffin Bay region, Quat. Sci. Rev., 79, 135–144, https://doi.org/10.1016/j.quascirev.2013.03.014, 2013.

Silverberg, N., Nguyen, H. V., Delibrias, G., Koide, M., Sundby, B., Yokoyama, Y. and Chesselet, R.: Radionuclide profiles, sedimentation rates, and bioturbation in modern sediments of the Laurentian Trough, Gulf of St. Lawrence., Oceanol. Acta, 9(3), 285–290, 1986.

Skogseth, R., Haugan, P. M. and Haarpaintner, J.: Ice and brine production in Storfjorden from four winters of satellite and in situ observations and modeling, J. Geophys. Res. C Ocean., 109(10), 1–15, https://doi.org/10.1029/2004JC002384, 2004.

Skogseth, R., Fer, I. and Haugan, P. M.: Dense-water production and overflow from an arctic coastal polynya in storfjorden, Geophys. Monogr. Ser., 158, 73–88, https://doi.org/10.1029/158GM07, 2005a.

Skogseth, R., Haugan, P. M. and Jakobsson, M.: Watermass transformations in Storfjorden, Cont. Shelf Res., 25(5–6), 667–695, https://doi.org/10.1016/j.csr.2004.10.005, 2005b.

Skogseth, R., Smedsrud, L. H., Nilsen, F. and Fer, I.: Observations of hydrography and downflow of brine-enriched shelf water in the Storfjorden polynya, Svalbard, J. Geophys. Res. Ocean., 113(8), 1–13, https://doi.org/10.1029/2007JC004452, 2008.

Smith, W. Jr & Barber, D. G.: Polynyas: Windows to the World. 474 pp. Elsevier, Amsterdam, 2007

Smedsrud, L. H., Budgell, W. P., Jenkins, A. D. and Ådlandsvik, B.: Fine-scale sea-ice modelling of the Storfjorden polynya, Svalbard, Ann. Glaciol., 44(1), 73–79, https://doi.org/10.3189/172756406781811295, 2006.

Szymańska, N., Pawłowska, J., Kucharska, M., Kujawa, A., Łącka, M. and Zajączkowski, M.: Impact of shelf-transformed waters (STW) on foraminiferal assemblages in the outwash and glacial fjords of Adventfjorden and Hornsund, Svalbard, Oceanologia, 59(4), 525–540, https://doi.org/10.1016/j.oceano.2017.04.006, 2017.

Tomašových, A., Kidwell, S. M., Alexander, C. R. and Kaufman, D. S.: Millennial-scale age offsets within fossil assemblages: result of bioturbation below the taphonomic active zone and out-of-phase production, Paleoceanogr. Paleoclimatology, 34(6), 954–977, https://doi.org/10.1029/2018PA003553, 2019.

de Vernal, A., Gersonde, R., Goosse, H., Seidenkrantz, M. S. and Wolff, E. W.: Sea ice in the paleoclimate system: The challenge of reconstructing sea ice from proxies - an introduction, Quat. Sci. Rev., 79, 1–8, https://doi.org/10.1016/j.quascirev.2013.08.009, 2013.

Vincent, R. F.: A study of the North Water polynya ice arch using four decades of satellite data, Sci. Rep., 9(1), 1–12, https://doi.org/10.1038/s41598-019-56780-6, 2019.

Vihtakari M.: PlotSvalbard: PlotSvalbard - Plot research data from Svalbard on maps. R package version 0.9.2. https://github.com/MikkoVihtakari/PlotSvalbard, 2020

Supplement Chapter 2

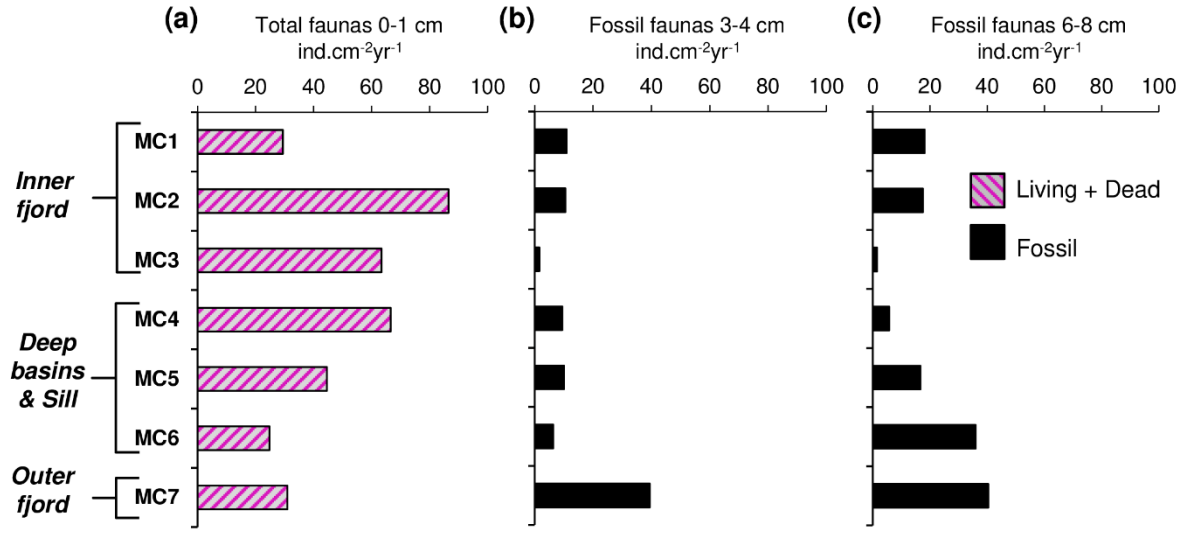

Figure S1. Benthic foraminiferal accumulation rates (BFAR) expressed in number of individuals per cm^2 per year ($ind.cm^{-2}yr^{-1}$) calculated on **(a)** total (living + dead 0-1 cm) and **(b, c)** fossil faunas (3-4 and 6-8 cm).

Chapter 3

Influence of modern environmental gradients on foraminiferal faunas in the inner Kongsfjorden (Svalbard)

Eleonora Fossile[1]*, Maria Pia Nardelli[1], Hélène Howa[1], Agnes Baltzer[2], Yohann Poprawski[1], Ilaria Baneschi[3], Marco Doveri[3], Meryem Mojtahid[1]

[1] *Laboratoire de Planétologie et Géosciences, Université d'Angers, Nantes Université, Le Mans Université, CNRS UMR 6112, Angers, France*

[2] *LETG, UMR CNRS 6554, University of Nantes, Campus du Tertre, 44312 Nantes Cedex 3, France*

[3] *Istituto di Geoscienze e Georisorse IGG-CNR, Via Moruzzi 1, 56100 Pisa, Italy*

*Corresponding author: Eleonora Fossile (eleonora.fossile@gmail.com)

An updated version of this chapter including minor revisions has been published in *Marine Micropaleontology* (https://doi.org/10.1016/j.marmicro.2022.102117).

Abstract

Kongsfjorden (Svalbard archipelago) is subjected to strong environmental gradients creating high physical and geochemical stress on benthic faunas. The present study aims at understanding the environmental drivers governing benthic foraminifera in the innermost part of the fjord. Surface sediments from 9 stations were sampled during August 2018 along a transect starting at ca. 2 km from the tidewater glacier Kronebreen and ending 12 km seaward. Three ecological groups were identified in response to physical disturbances linked to the proximity of the Kronebreen front (i.e., high water turbidity, freshwater, and sediment inputs from subglacial discharges). Close to the terminus, few stress-tolerant and glacier proximal species were present (i.e., *Capsammina bowmanni* and *Cassidulina reniforme*). At about 6-8 km from the front, reduced turbidity, and increased organic fluxes, resulted in a higher diversity, and a high abundance of the phytodetritus-indicator *Nonionellina labradorica*. Relatively high diversity persisted until 12 km from the front due to higher organic inputs and reduced stressful conditions. The outer assemblage was dominated by the Atlantic Water (AW) indicator *Adercotryma glomeratum*, in coherence with the presence of warm and salty AW detected far inside the fjord. Physical stress related to the glacier dynamics appears to favour the establishment of opportunistic species close to the terminus, whereas reduced disturbance away from the glacier induces the establishment of diverse assemblages. Our results show that benthic foraminifera may be effective bioindicators to monitor the long-term retreat of tidewater glaciers induced by climate change in Kongsfjorden.

Keywords: benthic foraminifera, bioindicators, tidewater glacier, Arctic, fjord hydrology

1. Introduction

The ongoing climate change is threatening the Arctic region at faster rate compared to lower latitudes (IPCC, 2019). In the last decades, the Arctic warming was double of the global mean, a phenomenon called Arctic amplification (AA - Dai et al., 2019; Holland and Bitz, 2003). Although the exact causes of the AA are still debated, the scientific community agrees that it is mainly the result of both local feedbacks (e.g., ice-albedo - Screen and Simmonds, 2010; Stuecker et al., 2018) and climatic/oceanographic forcing (e.g., changes in poleward heat transport - Graversen et al., 2008; Screen et al., 2012). The rapidly shrinking sea ice cover and glacier mass loss is a striking evidence of climate change in the Arctic (IPCC, 2019). The climate-change induced increase in ocean temperature and reduction in water stratification are among the causes of the sea ice decline in the Arctic Ocean (e.g., Lind et al., 2018; Polyakov et al., 2017; Yu et al., 2021). For land-terminating glaciers, the major mechanism for melting is through surface meltwaters migrating to the ice-bedrock interface (e.g., Tedstone et al., 2015; Zwally et al., 2002), whereas ocean-terminating glaciers mainly lose mass through calving at the glacial front by warming seawater temperatures (e.g., Luckman et al., 2015). Whether through rising sea temperatures or changes in freshwater and sediment inputs induced by glacier melting, these climate-change induced phenomena are having, and will continue to have, several implications for Arctic marine ecosystems, with repercussions on the benthic and pelagic realms (Meredith et al., 2019).

The Svalbard archipelago (74-81°N and 10-35°E) is largely influenced by the warm and saline Atlantic Water (AW). The AW, carried by the North Atlantic Current (NAC) and further north by the West Spitsbergen Current (WSC), flows west of the archipelago and enters the Arctic Ocean as the major source of heat, carbon, and plankton (e.g., Vernet et al., 2019) (Fig. 1). Western Svalbard fjords, located close to the WSC path, experience an increasing influence of warm and saline AW, more than any other Arctic fjords (Cottier et al., 2007; Saloranta and Svendsen, 2001). Furthermore, the mean temperature of the WSC core (20-200 m depth) has increased by 0.7°C in the last 20 years (Norwegian Polar Institute, 2021). Beside the climatic modifications, the hydrological conditions of the fjord are also subjected to extreme seasonal variations. During summer, warm AW incursions and freshwater inputs from glaciers, determine the presence of strong temperature and salinity gradients across these systems (e.g., Cottier et al., 2010; Hop et al., 2002; Hop and Wiencke, 2019; Svendsen et al., 2002). The fjords, through circulation dynamics and mixing between fjord and shelf waters (i.e. an inshore dominated by glaciers with seasonal meltwater inputs and an offshore influenced by warm

oceanic water intrusions), represent a link between the ocean and the land (Cottier et al., 2010). Therefore, these systems are subjected to combined variations of these two end-members and are thus sensitive to seasonal climatic fluctuations and to oceanographic changes (Cottier et al., 2005).

Kongsfjorden, a glacially, over-deepened valley located in the north-western coast of Spitsbergen, is influenced by the AW circulation as well as by tidewater glacier dynamics and the associated water masses at the fjord head (Hop et al., 2002; Sundfjord et al., 2017; Svendsen et al., 2002). Nowadays, this fjord is experiencing important changes. Before 2006, extensive sea ice was formed each winter in the inner fjord, but since then, the increased inflow of AW and the resulting overall increasing trend in seawater temperatures (e.g., Cottier et al., 2007; David T and K.P., 2017; Payne and Roesler, 2019; Tverberg et al., 2019) shifted the fjord system into a warmer state (Cottier et al., 2010, 2007). This resulted in a reduced sea ice cover (i.e., up to 50% decrease; Pavlova et al., 2019) and thickness (i.e., from 0.6 m to 0.2 m decrease; Pavlova et al., 2019).

In summer, it has been reported that AW intrusion in Kongsfjorden occurred during prolonged periods of time, and that AW has reached the inner part of the fjord only in the last decade (Holmes et al., 2019). This recent hydrological change strongly enhanced submarine melt and calving (i.e., frontal ablation) of tidewater glaciers (Holmes et al., 2019; Luckman et al., 2015), and consequently increased meltwater discharges and associated sediment load at the fjord head. As a result, the higher water turbidity in the vicinity of the marine termini of Kronebreen and Kongsvegen glaciers reduces local euphotic depth, disrupting phytoplankton distribution and biomass at the head of the fjord (Payne and Roesler, 2019). Furthermore, glacial meltwater runoff has a direct implication in building up steep temperature and salinity vertical gradients that lead to stable water stratification in the fjord. As a consequence primary production is even more affected with repercussions on the entire trophic chain (Pasculli et al., 2020). Knowing that marine-terminating glaciers generally sustain high productivity in arctic fjords (Meire et al., 2017), the recent seasonal processes developing in Kongsfjorden may cause persistent physical and geochemical stresses with impact on the fjord ecosystem, particularly on the benthic faunas.

The impact of increasing glacial melting on the Arctic marine ecosystems remains poorly studied (Meire et al., 2017), and a better understanding of the resilience capability of fjord ecosystems under present-day evolving conditions is needed (Hop et al., 2019). To that aim, benthic foraminifera are powerful and promising tools. Thanks to their short life cycle and specific ecological requirements, they respond quickly to environmental disturbance (e.g.,

Jorissen et al., 1995; Hald and Korsun, 1997; Alve et al., 2016; Jernas et al., 2018). Moreover, their fossilisation potential allows historical and paleoenvironmental reconstructions (e.g., Skirbekk et al., 2010; Jernas et al., 2013; Pawłowska et al., 2017) providing critical information on the evolution of a similar habitat in the recent past (e.g., tens to hundreds of years).

The present study focuses on the ecology of benthic foraminiferal faunas under current environmental conditions in the inner Kongsfjorden, with the aim of understanding the main drivers of benthic communities in fjords influenced by glacier dynamics and in a warm state. Foraminiferal distribution was analysed in response to the steep environmental gradients created by the meltwater runoff from tidewater glaciers at the fjord head and the AW inflow at the fjord mouth in summer.

2. Study area

2.1. Geographical and geological setting

Kongsfjorden is a glaciomarine fjord (20 km long and 4-10 km wide) located on the north western coast of Spitsbergen (79°N, 12° E) in the Svalbard archipelago. This fjord, elongated in the SE-NW direction, is located on a tectonic boundary between the Tertiary Fold and Thrust Belt to the south-west thrusting on the Northwestern Basement Province to the north-east (Bergh et al., 2000). Kongsfjorden has likely developed in a morphological depression linked to fractures of the bedrock, parallel to the thrust front (Husum et al., 2019; Svendsen et al., 2002).

Bedrocks of different composition are present in the fjord basement (Svendsen et al. 2002). Located on the Northwestern Basement Province, the northern bank of the fjord consists of medium-grade metamorphic (Middle Proterozoic age) marbles, mica-schists, and quartzites. The eastern part of the fjord and the islands at the fjord head (e.g., BlomstandhalvØya; Fig.1) are composed of slices of unmetamorphosed rocks (red conglomerates and sandstones) of Devonian age and marbles. Above the basal Tertiary thrust, the southern Kongsfjorden bedrock consists of sedimentary rocks of Late Palaeozoic and Tertiary Age, with some Proterozoic low- and medium-grade metamorphic rocks (mica-schists, marbles, phyllites, quartzites) (Svendsen et al., 2002).

The main source of sediment in Kongsfjorden is through subglacial discharge from tidewater glaciers (Svendsen et al., 2002; Trusel et al., 2010; D'Angelo et al., 2018). In addition, the glacial rivers of the Lovenbreen continental glaciers can provide a further supply of sediment (Bourriquen et al., 2016; 2018). Particle flux into Kongsfjorden mainly consist of siliciclastic

and detrital carbonate grains (D'Angelo et al., 2018). The bedrock geology of glacier catchments also influences the nutrient dynamics in the fjord. The sedimentary supply derived from the erosion of the surrounding bedrocks, that nourishes Kongsfjorden waters through meltwater discharge, makes this environment rich in silicon (e.g., silica-rich bedrock determines high silicic acid content in glacier meltwaters; Halbach et al., 2019) and iron (Laufer-Meiser et al., 2021). Limitation of sea life will come from a deficit of fresh organic matter with low C:N ratio (Laufer-Meiser et al, 2021). At the fjord head, high accumulation rates of detrital material (i.e., 6-8 cm yr^{-1}; Zaborska et al., 2006; Trusel et al., 2010) and low primary productivity lead to bottom sediments with low total organic carbon (TOC) content, as a result of the dilution effect of lithogenic material. Laufer-Meiser et al. (2021) found organic carbon with a very high C:N ratio (i.e., ratio of up to 70) in sediment close to the glacial source, originating from the terrestrial input of refractory petrogenic organic carbon (more resistant to microbial degradation compared to fresh marine organic carbon, Arndt et al., 2013)

2.2. Oceanographic and hydrological setting

The Svalbard archipelago (74-81°N and 10-35°E) is the eastern margin of the Fram Strait that connects the Atlantic and Arctic Oceans. Active exchanges between northern-sourced and southern-sourced water masses, that are essential for modulating the climate at various time-scales occur through this gateway (Dickson et al. 2008). The Fram Strait channels the inflow of the dominant heat source for the Arctic Ocean, the Atlantic Water (AW), via the West Spitsbergen Current (WSC), a branch of the North Atlantic Current (Schauer et al., 2004). On the western margin of Svalbard, the WSC flows northwards along the continental slope whereas the Spitsbergen Polar Current (SPC), an extension of the East Spitsbergen Current (ESC), transport Arctic Water (ArW) parallel on the continental shelf of Spitzbergen (Tverberg et al., 2019) (Fig. 1). Cold and fresh ArW carried by SPC is separated from the warm and saline AW by the Arctic front (Fig. 1).

Kongsfjorden, due to its geographical location on the western margin of Svalbard, and its open fjord configuration, i.e. without a well-defined sill (Howe et al. 2003), is strongly influenced by oceanic intrusion derived from the Fram Strait circulation and depending on the Arctic front dynamics (Svendsen et al., 2002). Water mass intrusions across this front are allowed by barotropic instabilities (Saloranta and Svendsen, 2001). Frontal instabilities, due to strong northerly winds, promote the AW upwelling from the WSC core and thus, the AW advection across the shelf into Kongsfjorden (Cottier et al., 2005, 2007; Svendsen et al., 2002).

However, the AW intrusions occur especially in summer when there is a geostrophic balance between shelf and fjord waters (Svendsen et al., 2002; Cottier et al., 2005). These cross-shelf mechanisms determine a seasonal shift between the prevailing cold and fresh ArW during winter, and the warm and saline AW during summer on the shelf and into the fjord (Svendsen et al., 2002; Cottier et al., 2005).

The spreading of AW intrusion into the fjord changes yearly, determining the distinction between "cold" and "warm" years (Cottier et al., 2005; Hop et al., 2002; Svendsen et al., 2002). Cottier et al. (2005) hypothesised that this interannual variability depends on both internal and external factors. The internal parameter would be the formation of sea ice during the preceding winter, whereas the external factor is most likely the shelf wind field creating instabilities at the shelf front during summer.

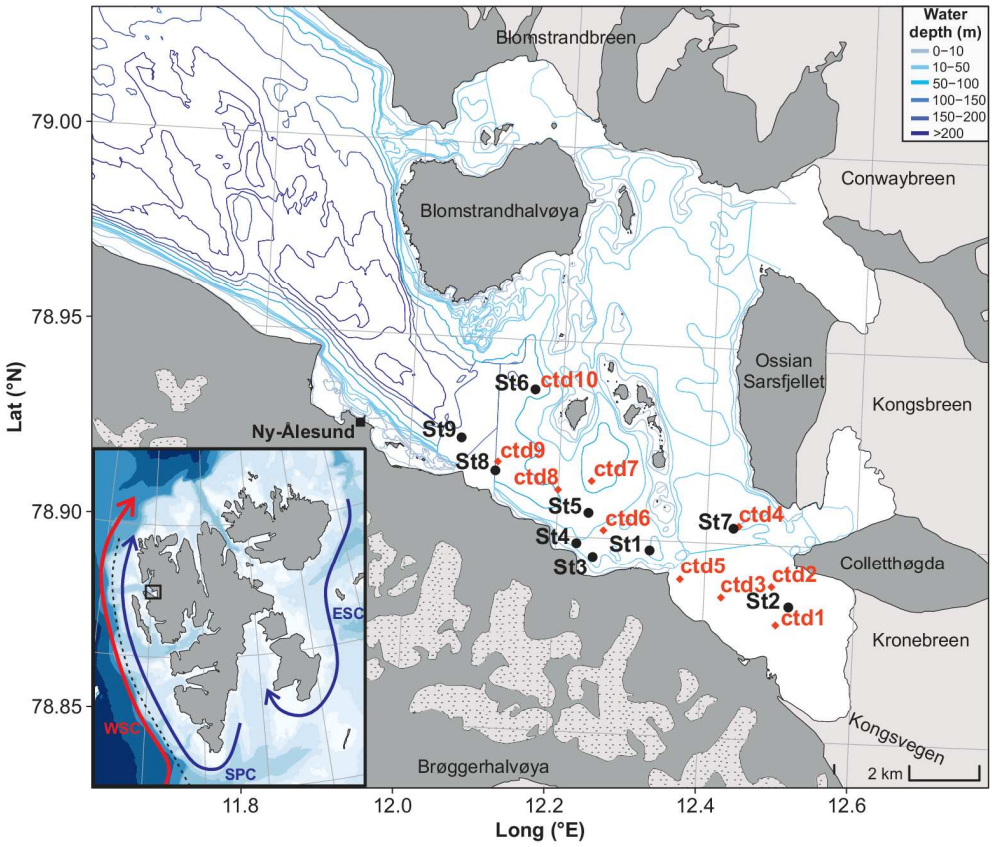

Figure 1. Map of Kongsfjorden showing, on the eastern and northern bank, the five tidewater glaciers flowing in the fjord (light grey) and on the southern bank the continental (land terminating) glaciers (dotted light grey). 'Nine stations sampled with the interface corer (black dots), and the ten locations of CTD casts (red squares) performed during August 2018 are indicated. On the bottom left of the panel, a map of Svalbard archipelago showing the main currents: Arctic waters (blue lines) carried by the East Spitsbergen Current (ESC) and Spitsbergen Polar Current (SPC), and Atlantic waters transported by the West Spitsbergen Current (WSC). The dashed black line represents the Arctic front west of Spitsbergen. The map was performed with the R package *PlotSvalbard* (Vihtakari, 2020).

Kongsfjorden is surrounded by four continental (land-terminating) glaciers (Austre Lovénbreen, Midtre Lovénbreen, Vestre Lovénbreen, and Pedersenbreen) and five tidewater (marine-terminating) glaciers (Blomstrandbreen, Conwaybreen, Kongsbreen, Kronebreen and Kongsvegen; Fig. 1). During summer, those tidewater glaciers highly contribute to the fjord dynamics with important freshwater and sediment inputs. Kronebreen, a fast-flowing tidewater glacier, has one of the highest flux rates in Svalbard (winter speed of 1.5-2 m d^{-1}, with 3-4 m d^{-1} peaks in summer; Luckman et al., 2015).

Due to the dual influence of AW inflow and freshwater inputs from glacier meltwaters, Kongsfjorden is characterised by different seasonal water masses. Cottier et al. (2005) revised the classification of these water masses based on Svendsen et al. (2002). Most of the AW entering the fjord mixes with ArW on the shelf forming Transformed Atlantic Water (TAW).

During late spring and summer, within the fjord, Surface Water (SW) forms from glacial meltwaters and this layer can mix with the underlying AW or TAW, forming Intermediate Water (IW). During autumn and winter, surface water cooling leads to the formation of Local Water (LW). Sea ice formations and consequent brine releases form cold and dense Winter Cooled Water (WCW). During spring and early summer, LW and WCW progressively warm up and decrease in salinity and so are merged in the IW.

Most of the freshwater inputs into the fjord come from glacier runoff with the major contribution coming from the fjord head (i.e., Kronebreen and Kongsvegen glaciers; Pramanik et al., 2018). Glacier meltwater exits from the bottom of the terminus through subglacial channels forming a buoyant turbulent plume (How et al., 2017). Subglacial runoff and consequent upwelling of meltwater plumes in front of the tidewater glacier front generate a strong surface outflow and consequent sub-surface inflow of warm and saline AW that promotes submarine melting at the glacier front (Cowton et al., 2015; Sundfjord et al., 2017). It was indeed observed that frontal ablation of tidewater glaciers is primarily controlled by warm sub-surface waters (Holmes et al., 2019; Luckman et al., 2015). During summer, the Kronebreen glacier is a main source of meltwaters and suspended particles which consists in a typical glacial upwelling system; this source forms a plume of fresh and turbid meltwaters spreading in the inner part of the fjord (Meslard et al., 2018). The contribution of continental glaciers to the freshwater inputs is not yet fully understood, but the changes observed in the drainage rivers network from the Lovénbreen glaciers (Bourriquen et al., 2018) reveal their important impact related to the glacier retreat.

2.3. Productivity and organic matter export in Kongsfjorden

In Arctic environments, phytoplanktonic blooms are limited by light availability and sea ice cover. Spring blooms occur after sea ice break-up and consequent light availability increase, but their timing and intensity can change yearly (Hegseth and Tverberg, 2013; Hodal et al., 2012). Also, changes in community structure in relation to water mass advection from the Fram Strait into the fjord were observed for phytoplankton (Hegseth and Tverberg, 2013; Hodal et al., 2012; Lalande et al., 2016; Piquet et al., 2014). During spring, export fluxes of biogenic matter (phytoplankton) are controlled by zooplankton grazing and sink processes (Lalande et al., 2016).

In the summer season, freshwater inputs from land-terminating glaciers do not seem to affect the euphotic depth, whereas meltwater discharges from marine-terminating glaciers have demonstrated a negative impact on the light penetration depth (Payne and Roesler, 2019). Meltwater plumes scatter high quantity of suspended matter away from the glacier front which hampers primary productivity (Hopwood et al., 2020) and increases benthic deposition processes via flocculation at the glacier fronts (Halbach et al., 2019; Payne and Roesler, 2019).

Although export fluxes of matter are reduced to high input of inorganic particles from glaciers particularly in the innermost part of the fjord (Lalande et al., 2016), meltwater turbid plumes have a fundamental role in fjord ecosystems. Surface waters are continuously supplied by meltwater at the tidewater glacier fronts and are pushed away from the coast and replaced by intermediate water rich in plankton and nutrients from the outer fjord (Lydersen et al., 2014). This upwelling system promotes the formation of foraging area (for seabirds and marine mammals) identified as “ecological hotspots” (Lydersen et al., 2014). Furthermore, water masses advected from the shelf carry Arctic and Atlantic faunas (Basedow et al., 2004; Willis et al., 2006), influencing fjord’s biodiversity.

3. Material and methods

3.1 Environmental parameters

3.1.1 CTD (conductivity-temperature-depth) profiles

In August 2018, several water column casts were performed with a conductivity-temperature-depth sensor (CTD profiler, Saiv SD204) equipped with a fluorometer. We selected ten CTD casts (Table 1) close to the sediment sampling stations (see Fig. 2a) to determine water mass characteristics at the sampling time.

The Ocean Data View software V.5.3.0 (ODV; Schlitzer, 2020) was used to produce temperature and salinity plots. Mean surface turbidity was calculated considering the uppermost 20 m of the surface column, then an interpolation plot was performed with inverse distance weighted interpolation using the function *interpolate_spatial* in the R package *PlotSvalbard* (Vihtakari, 2020).

Station	Transect line	Sampling date	Latitude (N)	Longitude (E)	Max depth (m)
CTD1	**Proximal**	21/08/2018	78°52.769'	12°29.809'	72.3
CTD2	**Proximal**	21/08/2018	78°53.353'	12°29.368'	67.9
CTD3	**Proximal**	21/08/2018	78°53.159'	12°25.378'	85
CTD4	**Proximal**	23/08/2018	78°53.413'	12°25.045'	38.7
CTD5	**Proximal**	21/08/2018	78°54.272'	12°26.560'	64
CTD6	**Medial**	21/08/2018	78°54.122'	12°15.771'	33.8
CTD7	**Medial**	21/08/2018	78°54.873'	12°14.641'	104
CTD8	**Medial**	21/08/2018	78°54.717'	12°11.992'	86.3
CTD9	**Distal**	21/08/2018	78°55.104'	12°7.082'	138
CTD10	**Distal**	21/08/2018	78°56.221'	12°9.760'	142

Table 1. Sampling date and degrees decimal minutes coordinates of the ten CTD cast location during the ISMOGLAC mission.

3.1.2 Sediment sampling

In the frame of the IPEV field campaign C3 (Coasts under Climate Change suite) organised in August 2018, within a collaboration with the Aztec Lady sailing boat, the KING18 mission allowed to sample nine stations along a SE-NW transect in Kongsfjorden, from about 2 km to 12 km off the Kronebreen and Kongsvegen tidewater glacier fronts (Table 2, Fig. 1). The order of the stations is reported based on the distance from the glacier front, determining three zones along the studied transect, i.e. proximal stations close to the glacier front margin, medial stations located in a ~75m-deep sub-basin (enclosed in shoals and small islands), and distal stations, at the fjord trench head, deeper than 100 meters. The sediment-water interface was properly sampled by use of a GeMAX corer that collected two twin sediment cores (9 cm inner diameter) at each station: the first for grain size and organic matter analyses and the second for foraminiferal analyses.

Station	Transect line	Sampling date	Latitude (N)	Longitude (E)	Sampling depth (m)	Distance from the front (km)
St2	**Proximal**	21/08/2018	78°53.053'	12°30.780'	49	1.92
St7	**Proximal**	22/08/2018	78°54.239'	12°26.142'	68	4.53
St1	**Medial**	21/08/2018	78°53.847'	12°19.520'	52	6.22
St3	**Medial**	21/08/2018	78°53.705'	12°15.006'	38	7.68
St4	**Medial**	22/08/2018	78°53.905'	12°13.657'	35.5	8.25
St5	**Medial**	22/08/2018	78°54.382'	12°14.511'	75.7	8.25
St8	**Distal**	22/08/2018	78°54.966'	12°06.917'	114	11.18
St6	**Distal**	22/08/2018	78°56.241'	12°09.806'	148	11.43
St9	**Distal**	22/08/2018	78°55.447'	12°04.086'	156	12.47

Table 2. Location along the transect, sampling date, degrees decimal minutes coordinates, sampling water depth and distance from the glacier front of the nine stations sampled during the KING18 mission.

3.1.3 Sediment grain size and carbon analysis

At each station, one core was sliced on board, collecting seven sediment layers (every 0.5 cm between 0 and 2 cm and every 1 cm from 2 down to 5 cm depth, i.e., 0-0.5, 0.5-1, 1-1.5, 1.5-2, 2-3, 3-4 and 4-5 cm), then stored at +4°C. In the laboratory, an aliquot of each slice was used for grain-size analyses and the rest was lyophilised for carbon analyses. The laser diffraction particle size analyser Malvern Mastersizer 3000 was used to obtain grain-size data. The particle size distributions were analysed with GRADISTAT 8.0 software program (Blott and Pye, 2001).

The carbon analysis was performed using a TOC-V$_{CPH}$ analyser. This instrument measures the free CO_2 gas released by the combustion of the carbon contained in the sediment sample using a non-dispersive infrared system (NDIR). The total carbon (TC) and total inorganic carbon (TIC) contents were determined on three pseudo-replicates and their values were calculated based on two calibration curves using two standards (glucose for TC and sodium bicarbonate for TIC). The combustion at 900°C of 100 mg of sediment has been used to determine the TC. The combustion at 200°C of 100 mg of sediment was conducted after the addition of 450 µl of concentrate phosphoric acid to determine the TIC. The total organic carbon (TOC) was then calculated indirectly as the difference between the TC and the TIC (Bisutti et al., 2004).

3.1.4 Correlation among environmental variables

Pearson correlations and two sided test between environmental variables were calculated and illustrated using the *ggpairs* function in the R package *GGally* (Schloerke et al., 2021). The correlations were tested for sediment-related properties measured in the 0-0.5 cm sediment layer (i.e., percentage of total carbon (TC), percentage of total inorganic carbon (TIC), percentage of total organic carbon (TOC), percentage of sand, silt and clay), sampling water depth (expressed in meters), extrapolated mean surface water turbidity (0-20 m, expressed in FTU), and distance from the glacier front (expressed in kilometers).

Mean surface water turbidity was extrapolated for sediment sampling coordinates performing inverse distance weighted interpolation on CTD cast measurements using the function *interpolate_spatial* in the R package *PlotSvalbard* (Vihtakari, 2020).

The distance of each sampling station from the front of the glacier was calculate as follow. We used the satellite image taken on the 1st of August 2018 by LANDSAT7 and LANDSAT8 (https://landsatlook.usgs.gov) as a reference for the position of the Kronebreen glacier front at the sampling time. Then, the reference point for the front position was selected along the centre-line of the glacier (calculated using the box method; Lea et al., 2014) and its coordinates (i.e., 78°52'39.19"N, 12°35'42.51"E) were obtained using the Google Earth Pro software (v 7.3.3.7786) after overlying the satellite image. The distances between the reference point and the individual sampling stations were calculated using the *distm* and *distGeo* functions in the R package *geosphere* (Hijmans, 2019).

3.2 Foraminiferal analyses

3.2.1 Sample processing

Immediately after recovery, the interface cores were sliced horizontally as for the sedimentary analysis (every 0.5 cm between 0 and 2 cm and every 1 cm from 2 down to 5 cm depth, i.e. 0–0.5, 0.5–1, 1–1.5, 1.5-2, 2-3, 3-4 and 4-5 cm). Following the FOBIMO recommendations (Schönfeld et al., 2012), each sample was stored in a 500 cm^3 bottle filled with 95% ethanol with 2 g.L^{-1} of rose bengal stain (to label living foraminifera). In the laboratory, the uppermost two sediment layers (0-0.5 and 0.5-1 cm) were sieved through 63, 100, 125 and 150 µm meshes, and all sediment layer below 1 cm depth were sieved through 63 and 150 µm meshes. All samples were then stored in 95% ethanol. All living (rose bengal-stained) specimens of the >150 µm fraction were hand-picked in water for each sediment layer. The small fraction 63-150 µm (i.e., 63-100, 100-125, 125-150 µm fractions combined) was considered to investigate

potential supplementary ecological information (i.e., presence of juveniles, elongated and/or small sized species), knowing that high abundances of small sized foraminifera are common in foraminiferal studies (e.g., Duchemin et al., 2007; Shepherd et al., 2007; Gooday and Goineau, 2019; Fossile et al., 2020). However, being extremely time-consuming, the picking of the living foraminifera from the 63-150 µm size fraction was restricted to the uppermost centimetre of the sediment. Due to high foraminiferal abundances, some samples of the small fraction were dried at 50°C, split with an Otto Microsplitter and hand-sorted to reach a minimum of 300 individuals from a whole subsample, then standardised to the entire sample.

The presence of fragments of living and dead specimens of two large tubular agglutinated species (*Hyperammina* sp. and *Archimerismus subnodosus*) was documented in some samples (St5, St6, St8 and St9). However, due to the fragility of their test and impossibility to determine the number of individuals represented by the observed fragments, they were not included in the analysis (e.g., Duros et al., 2013; Caulle et al., 2014). Scanning electron micrographs (SEM) of the major agglutinated and calcareous species are shown in Figure S4 and Figure S5, respectively. *Cassidulina* spp. and *Islandiella* spp. SEM and stereomicroscope pictures are displayed in Figure S6.

The dead assemblages from 4-5 cm were picked and analysed to highlight possible differences between living and dead assemblages due to seasonal variability. To do so, the L/(L+D) ratios (%Living / (%Living + %Dead); Jorissen and Wittling, 1999) were calculated considering the living assemblages from the 0-5 cm core top interval (merging the seven sediment layers) and the dead assemblages from the 4-5 cm sediment layer, for all species > 5% in either living or dead assemblages. A ratio ranging between 0 and 0.5 indicates that a species is relatively more abundant in the dead fauna, whereas a species is more abundant in the living assemblage when the ratio ranges between 0.5 and 1. A species is equally abundant in the living and dead assemblages when the ratio is 0.5. As it was not possible to calculate the accumulation rates at our sampling stations, we cannot ascertain whether the 4-5 cm layer a good representation of the thaphonomic loss. Therefore, the L/(L+D) ratios were only used to have a qualitative information on possible seasonal sampling bias. A ratio of 0.5 indicates that there is no discrepancy between the relative abundance of the given species sampled alive in August 2018 and its production all year along. Higher or lower ratios suggest that the sampling time (i.e., August 2018) is not representative of the given species life cycle.

3.2.2 Diversity metrics and multivariate analysis

Taxonomic diversity was estimated using three different metrics using R package *vegan* (Oksanen, 2019):

1. Species richness (S; i.e., number of species);
2. Shannon index (H') calculated as:

$$H' = -\sum_{i=1}^{S} p_i \ln p_i \quad \text{(i)}$$

where p_i is the proportion of each species i in the community;

3. Pielou's evenness (J) calculated as:

$$J = \frac{H'}{\ln S} \quad \text{(ii)}$$

All multivariate analyses were performed using the R software (v. 4.0.0; R Core Team, 2020). Hierarchical clustering analyses were performed on relative abundances considering the 0-5 cm sediment layer and the >150 µm size fraction (Bray-Curtis dissimilarity measure). The cluster on stations (complete linkage method) was performed on foraminiferal abundances considering all the species, whereas the cluster on the species (average linkage method) used only the abundances of the major species (relative abundance >5%). Dissimilarity matrices were calculated using the *vegdist* function in the R package *vegan* (Oksanen, 2019). Different linkage methods were compared among each other and cophenetic distances were computed to assess clustering consistency. Dendrograms were produced with *fviz_dend* function in the R package *factoextra* (Kassambara and Mundt, 2020).

Transformation-based redundancy analysis (tb-RDA) was performed on living foraminiferal community considering the 0-5 cm sediment layer and the >150 µm size fraction in relation to environmental parameters. Forward selection was performed on several environmental variables (bottom water depth, TOC, sand, silt, clay percentages and surface water turbidity) and only three parameters were retained (i.e., turbidity and depth, $p < 0.05$; TOC, $p < 0.1$). The significance of the model and ordination axes was tested with the *anova.cca* function in the R package *vegan* (Oksanen, 2019), applying Bonferroni correction. Hellinger transformation was applied to foraminiferal abundances, whereas environmental variables were centred and scaled. Both transformations were performed using the *decostand* function in the R package *vegan* (Oksanen, 2019). Adjusted R^2 was calculated to determine the model fit.

Differences between the two size fractions (63-150 µm and >150 µm) in the 0-1 cm sediment layer were investigated with a non-metric multidimensional scaling analysis (nMDS). The analysis was performed on foraminiferal abundances using the *metaMDS* function (which applied square root transformation and wisconsin double standardisation) in the R package *vegan* (Oksanen, 2019) using Bray-Curtis dissimilarity. A similarity of percentages (SIMPER) analysis was performed using the *simper* function in R package *vegan* (Oksanen, 2019) to investigate the relative contribution of each species to the difference between size fractions. The most influential species (i.e., $p<0.01$ and average contribution >5%) were extracted and displayed on the nMDS biplot.

4. Results

4.1 Environmental parameters

4.1.1 Water properties

During August 2018, a water stratification typical of the summer season was well established in Kongsfjorden (Fig. 2). The uppermost 10 m of the water column were relatively fresh (salinity range = 30.0-34.0) with a narrow temperature range between 3.5 and 4.0°C and thus identified as Surface Water (SW, T > 1°C and S < 34.0; Cottier et al., 2005). In the 4-10 km section of the transect, below the SW at about 10–30 m depth, waters with the highest temperature, between 4.5 and 5.5°C and salinity range between 34.1 and 34.8 were detected. Below 30 m depth an homogeneous water column (T = 3-4 °C, S = 34.8-34.9) can be identified as Atlantic Water (AW, T > 3°C and S > 34.65; Cottier et al., 2005) intruding into the fjord up to at least 4 km from the Kronebreen-Kongsvegen front. In the innermost part of the fjord (0-4 km of the section transect), below the surface layer, waters of 4-4.5°C temperature and a salinity range between 34 and 34.7 were observed and possibly correspond to Intermediate Water (IW, T > 1°C and 34.00 < S < 34.65; Cottier et al., 2005). A relatively colder layer of 1.0 to 3.0°C with a salinity of about 34.7 appeared at the bottom, likely issued from mixing between Arctic and Atlantic waters.

The surface water turbidity (average of the 0-20 m layer) displayed values above 80 FTU in front of the Kronebreen-Kongsvegen terminus and below 20 FTU in all stations located close to the southern coast or far away from the glacier front (Fig. S1).

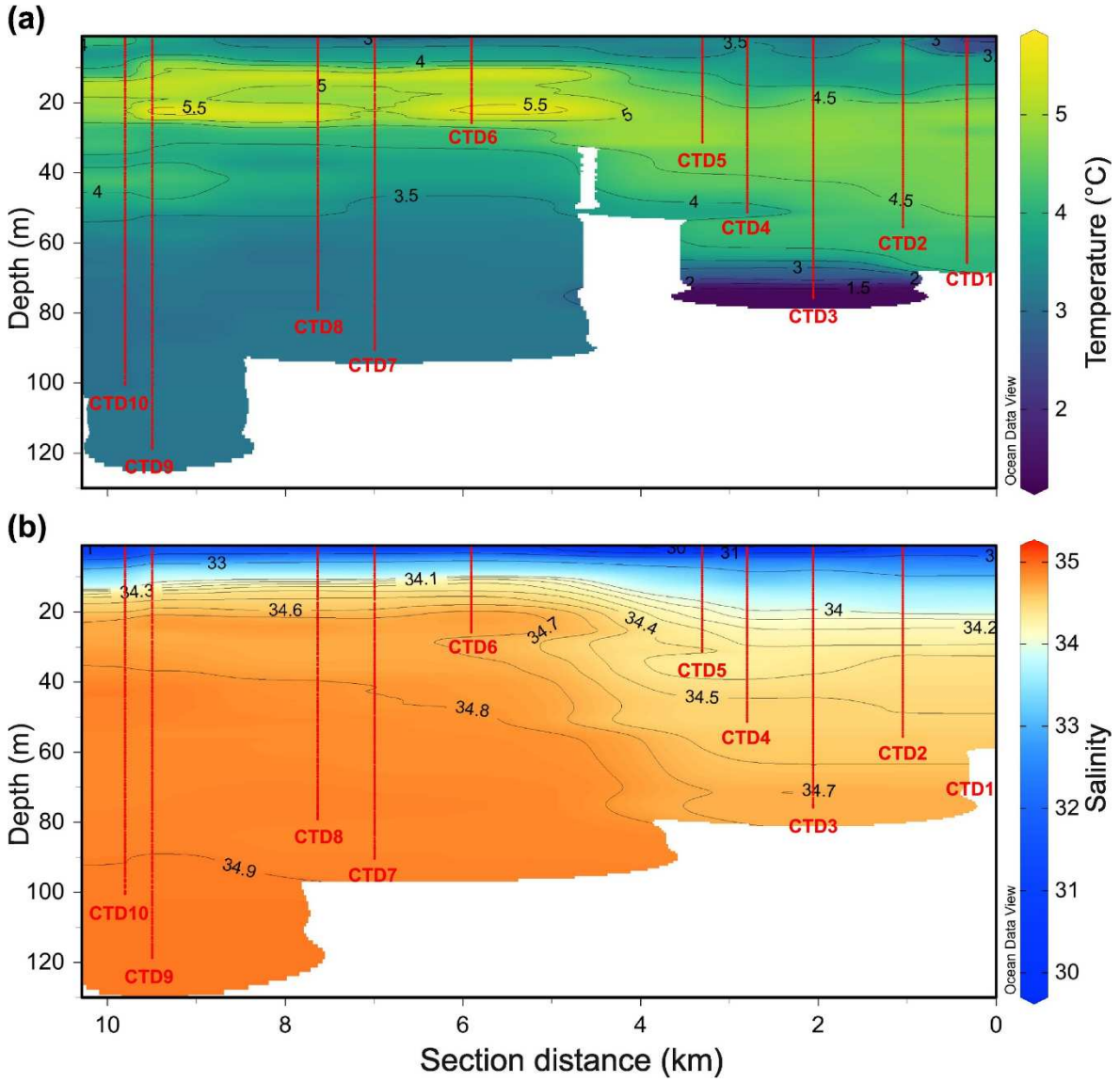

Figure 2. SE-NW 0-130 m deep sections across Kongsfjorden of the 10 CTD casts for temperature (°C) **(a)** and salinity **(b)**. Salinity data for CTD1 are not available.

4.1.2 Grain size analyses

Sediments, at all stations and both surficial (0-0.5 cm) and intermediate (2-3 cm) levels, were medium silts with mean grain sizes ranging from 6.3 to 16.3 µm (Table S1). Grain size curves mainly showed unimodal distribution with a single mode around 7-9 µm, except at the 2-3 cm level from two stations (St2 and St8) where a second mode picks at 37.7 and 62.9 µm respectively, indicating a mixture with a population of coarse silts. At all stations, the mean values slightly increased with depth, a trend more obvious at St2 and St8 (coherent with the bimodal distribution mentioned above), and at the two shallowest stations close to the southern coast of the fjord (St3 and St4) where the single mode reached 17.5 and 22.6 µm, respectively. At all stations, the percentage of sand (>63 µm) remained low, about or below 10%, except at depth at St8 where it reached almost 20% (coherent with the secondary mode of the grainsize

distribution at 62.9 µm). The percentage of clay (<2 µm) was everywhere slightly higher in the surficial sediments and ranging from around 10 to 18%.

4.1.3 Organic matter analysis

All the sampled stations were characterised by total carbon contents (TC%) between 2.68 and 3.10% in the surface sediment layer (0-0.5 cm) (Table 4). TC was mostly composed of inorganic carbon (TIC%; values between 2.07 and 2.65 %). Therefore, the total organic carbon content (TOC%) of the fjord showed values below 0.70% at all stations (Table 3). In general, TOC percentages were lower close to the terminus in the innermost fjord (St2, St7 and St1 <0.40%) than at downstream stations (between 0.40 and 0.70%). TOC percentages are significantly different among the stations (One-Way ANOVA, $p<0.001$) (Table 3).

Stations	Location	TC	TIC	TOC
St2	**Proximal**	2.78±0.03 %	2.59±0.07 %	0.20±0.04 %
St7	**Proximal**	2.84±0.05 %	2.44±0.05 %	0.40±0.04 %
St1	**Medial**	2.78±0.01 %	2.65±0.02 %	0.12±0.01 %
St3	**Medial**	2.75±0.03 %	2.26±0.08 %	0.48±0.05 %
St4	**Medial**	2.68±0.02 %	2.30±0.04 %	0.38±0.03 %
St5	**Medial**	3.10±0.01 %	2.40±0.07 %	0.70±0.04 %
St8	**Distal**	2.76±0.05 %	2.28±0.01 %	0.48±0.03 %
St6	**Distal**	3.04±0.03 %	2.39±0.02 %	0.65±0.02 %
St9	**Distal**	2.73±0.02 %	2.07±0.03 %	0.65±0.02 %

Table 3. Total carbon (TC), Total Inorganic Carbon (TIC) and Total Organic Carbon (TOC) percentages measured on the uppermost sediment layer (0-0.5 cm) at each sampling station. Data are displayed as mean ± standard deviation (n=3).

4.1.4 Correlation between environmental variables

Few significant relationships were observed between environmental variables (Fig. S2). The most significant correlations were observed between distance from the glacier front and turbidity of surface waters ($r = -0.969$, $p<0.001$) and between sampling depth and sediment clay percentage ($r = -0.90$, $p<0.001$). Distance from the front was also significantly correlated with TIC and TOC percentages in sediment ($r = -0.739$, 0.729, respectively, $p<0.05$).

4.2 Foraminiferal assemblages in the upper 5 cm sediment (>150 µm fraction)

4.2.1 Abundances and diversity

Foraminiferal absolute abundances and diversity metrics, considering the 0-5 cm sediment interval and the >150 fraction, are displayed in Table 4. Abundances were below 300

ind. 50 cm^{-2} in the three stations closest to the glacial front (proximal stations St2 and St7 and the first medial station St1). The other medial and distal stations located beyond 6 km from the terminus showed abundances between 1700 and 3500 ind. 50 cm^{-2} (except St4 with 658 ind. 50 cm^{-2}). The number of species was about or below 10 in the innermost proximal stations (St2 and St7) and almost double at the first medial station (St1), whereas all the other stations showed a species richness between 32 and 49. Low values of Shannon index H' were found at the proximal stations (below 1), a small increase in diversity was observed at St3, St6 and St8 (values between 1 and 2), whereas higher H' values (above 2) were observed at St1, St4, St5 and St9. The equitability (J, Table 4) was below 0.50 at St2, St3, St7 and St8, whereas higher values (up to 0.73) were observed at the other locations.

Stations	Transect location	Abundance (ind. 50 cm^{-2})	Richness (S)	Shannon index (H')	Equitability (J)
St2	**Proximal**	261	8	0.91	0.44
St7	**Proximal**	238	10	0.99	0.43
St1	**Medial**	263	19	2.16	0.73
St3	**Medial**	2308	34	1.12	0.32
St4	**Medial**	658	36	2.60	0.73
St5	**Medial**	1733	45	2.45	0.64
St8	**Distal**	3485	49	1.78	0.46
St6	**Distal**	1841	43	1.97	0.52
St9	**Distal**	2086	32	2.10	0.61

Table 4. Foraminiferal total abundances (in number of individuals per 50 cm^2) and diversity metrics (richness, equitability and Shannon index), considering the total living fauna (>150 µm size fraction) in the 0 to 5 cm core top sediment.

4.2.2 Assemblage composition

The first cluster analysis divided the sampling stations into four clusters: cluster 1 composed by the proximal stations (St2 and St7), cluster 2 including only the first medial St1, cluster 3 grouping the remaining medial stations (St3, St4, and St5) and cluster 4 for the distal stations (St8, St6, and St9) (Fig. 3). The second cluster analysis, performed on the most abundant species only, divided the species in two major groups: group *a* including species present in the proximal stations and first medial station, and group *b* including species present mostly in the other medial and distal stations (Fig. 3).

Foraminiferal species composition in terms of relative abundances is shown in Figure 3 and scanning electron micrographs (SEM) of the major species are displayed in Plate 1 and 2. The proximal station St2 was dominated by the agglutinated *Capsammina bowmanni* (73%) and *Saccammina* cf. *sphaerica* (15%), with a minor contribution from the miliolid *Quinqueloculina*

stalkeri. *Capsammina bowmanni* was also dominant at the other proximal station St7 (55%), together with the calcareous *Cassidulina reniforme* (39%). *Cassidulina reniforme*, *Nonionellina labradorica*, *Reophax fusiformis* and *Textularia earlandi* were the main species at the medial St1 with abundances between 15 and 20%. The medial St3 assemblage was characterised by *Nonionellina labradorica* (78%), which was also a major component in the medial and distal stations (with abundances between 13 and 33 %). *Globobulimina auriculata* made up to 13% at St4. The agglutinated *Adercotryma glomeratum* showed high relative abundances (between 35 and 57%) at the distal stations (St8, St6, St9). *Cibicidoides lobatulus* reached 11 % only in the outermost station St9.

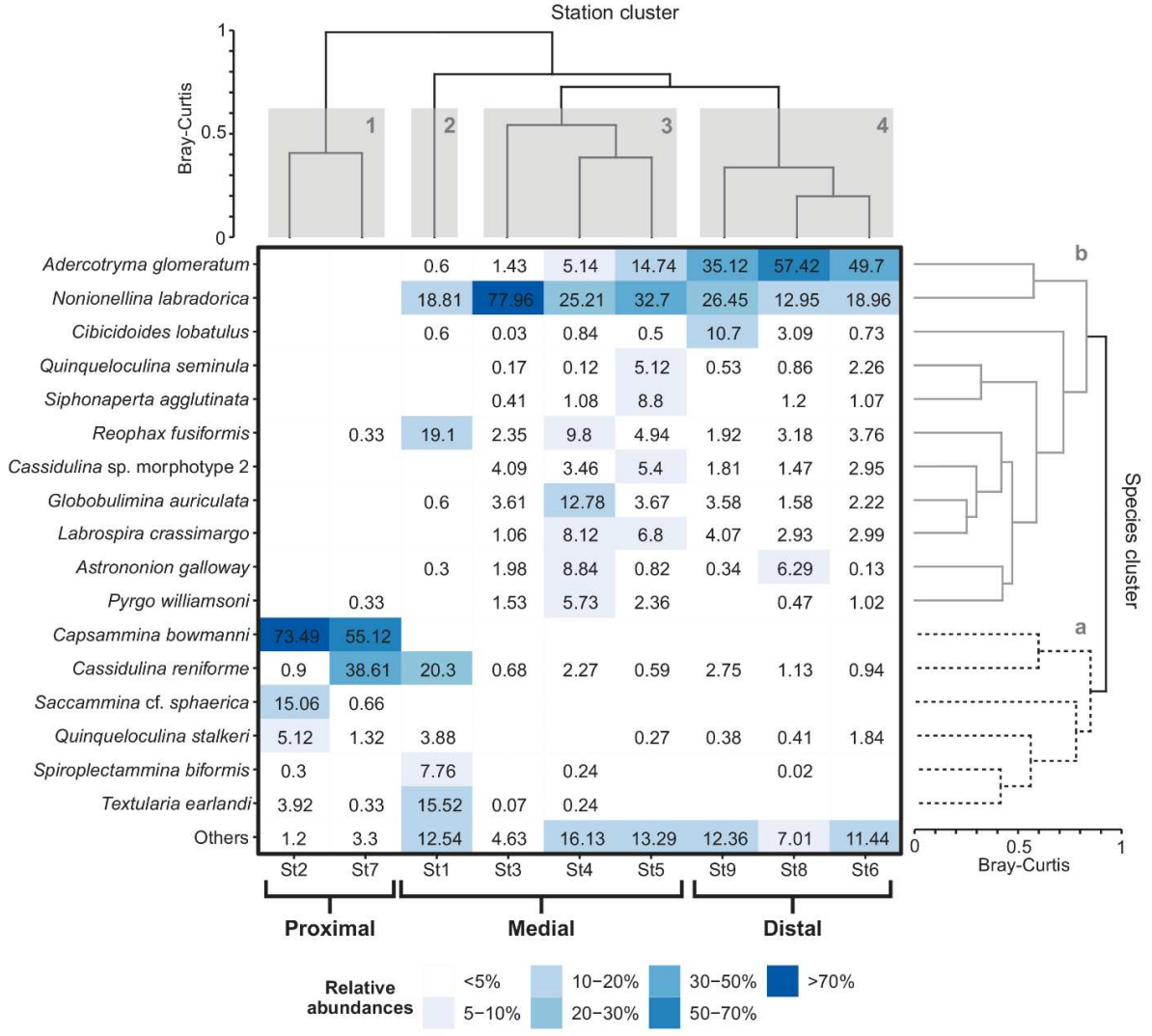

Figure 3. Heatmap showing the cluster analysis of the foraminiferal fauna based on relative abundances of the major species considering the total living faunas (>150µm size fraction) in the 0 to 5 cm core top sediment. The dichotomy clustering is based on the Bray-Curtis dissimilarity. The station cluster (complete linkage method) considers all the species whereas the species cluster (average linkage method) considers only the relative abundances of the major species (>5 %).

4.2.3 Microhabitat distribution

The foraminiferal vertical distribution profiles from the surface down to 5 cm sediment depth were heterogeneous along the fjord axis (Fig. 4). Living foraminifera were present mostly in the uppermost half centimetre of sediment, rapidly disappearing downcore at the two proximal stations (St2 and St7; cluster 1). This surface layer was dominated by *C. bowmanni* and *Saccamina* cf *sphaerica* at St2, whereas St7 was characterised by *C. bowmanni* and *C. reniforme*. Cluster 2 including only St1 shows the presence of *C. reniforme* mostly in the 0-0.5 cm layer together with other species (e.g., *N. labradorica*, *R. fusiformis* and *T. earlandi*). The three medial stations of cluster 3 (St3, St4, St5) showed the typical exponential decrease in foraminiferal abundances with sediment depth. Some species were mostly present in the uppermost centimetre (e.g., *Cassidulina* sp. morphotype 2 and *Labrospira crassimargo*). The only species abundant below the 0-0.5 cm layer were *N. labradorica*, particularly at St3, and *Globobulimina auriculata*, even more abundant at the 1-2 cm layer of St4. In the distal stations (cluster 4), deep infauna (i.e., *A. glomeratum* and/or *N. labradorica*) was encountered. Foraminiferal abundances at St6 remained similar at all layers below the 0.5 cm depth. On the contrary St9 showed a subsurface peak at 1-2 cm depth with foraminiferal abundances almost double than the uppermost centimetre due to the high abundances of *A. glomeratum* and *N. labradorica*. The intermediate and deep infaunal microhabitats showed similar species compositions than the uppermost centimetre.

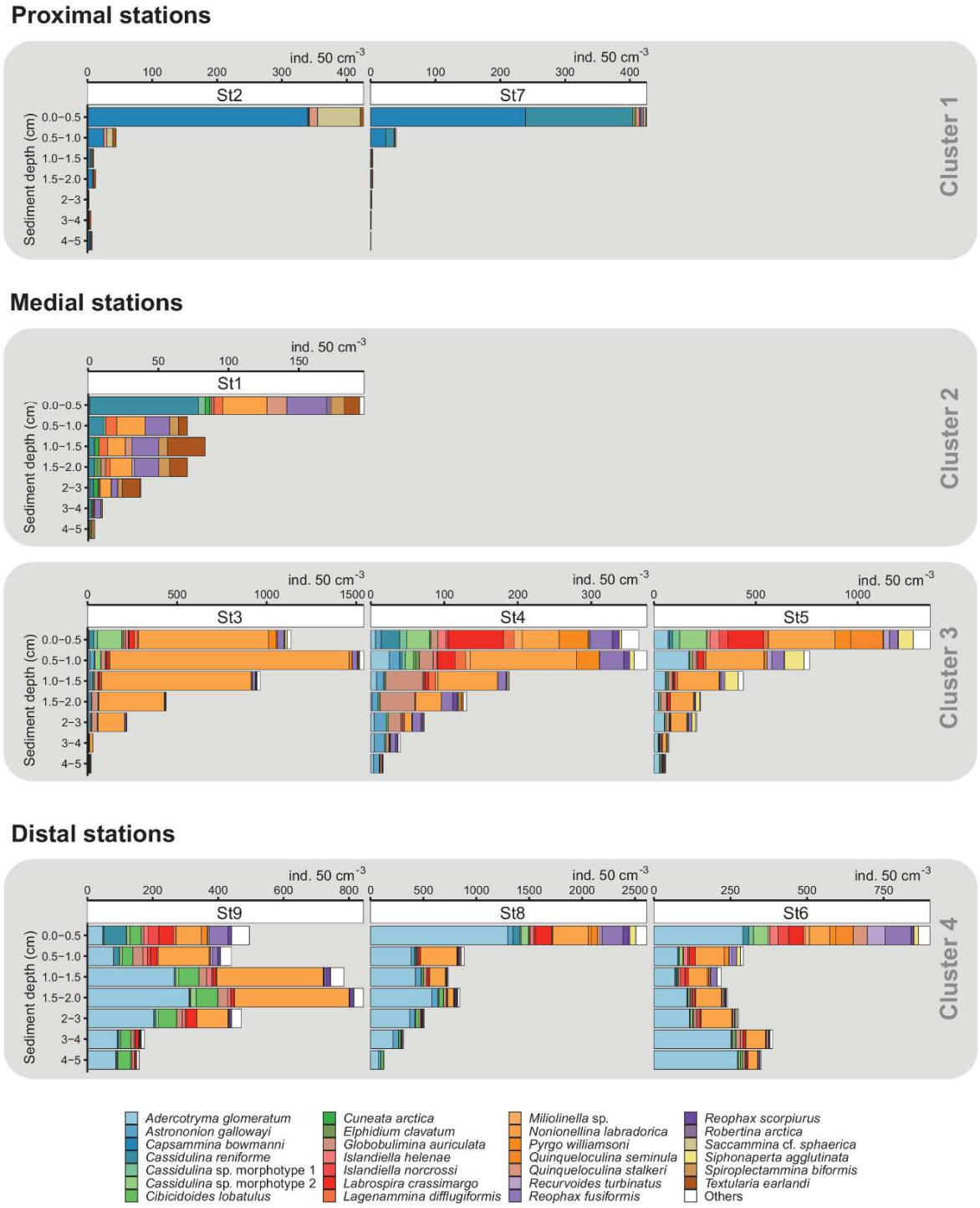

Figure 4. Foraminiferal microhabitat distribution of the most representative species (contributing with >5% in at least one sample) from the sediment surface down to 5 cm depth considering the >150 µm fraction. Note that stations are displayed based on their location (proximal, medial, distal) and on the results of the station cluster analysis displayed in Fig. 3.

4.2.3 Redundancy analysis

Three predictors of variation in species composition were identified from the redundancy analysis (turbidity and depth $p<0.05$; TOC, $p<0.1$). The first two components of the model

explained 66.4% of the total variance (r^2 adjusted = 0.59). RDA1 was positively correlated with sediment organic matter content (TOC) and water depth, and negatively with surface water turbidity. Opposite correlations were observed for the RDA2. RDA1 separates the proximal stations plus St1 from the other medial and distal stations. RDA2 separates proximal and distal stations from the medial stations. The proximal stations were positively correlated with turbidity, whereas the distal stations with TOC and depth. The three species with the highest scores are *C. bowmanni*, *N. labradorica* and *A. glomeratum*, which were the major species respectively at the proximal, medial and distal stations.

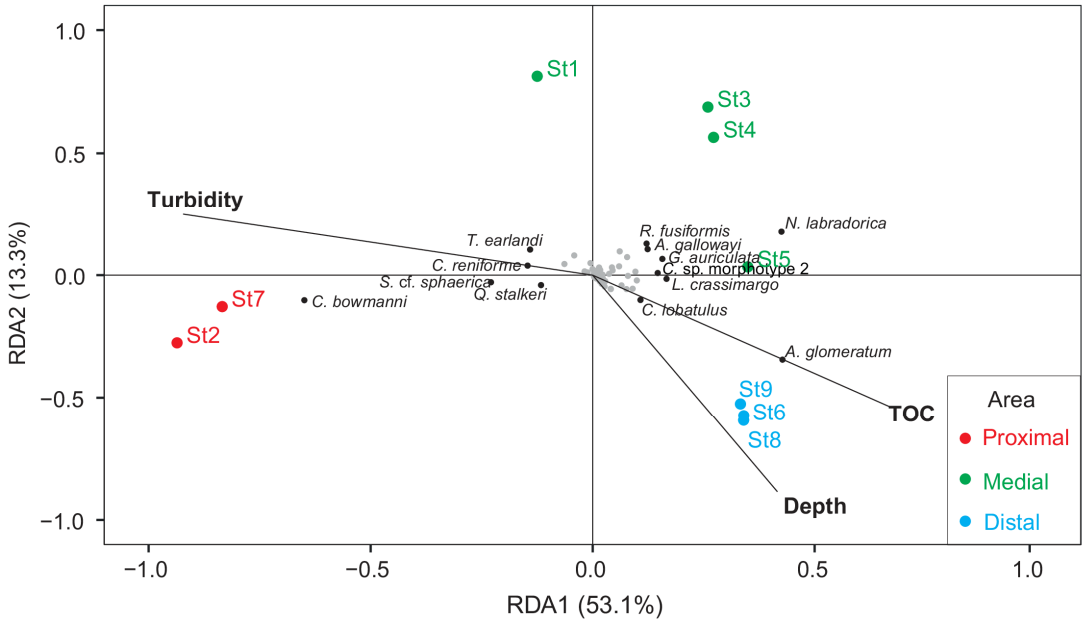

Figure 5. Transformed-based redundancy analysis (tb-RDA) performed on living foraminiferal community (total abundances in the 0-5 cm interval, >150 µm fraction) in relation to three significative environmental parameters (surface water turbidity in the 0-20 m surface layer, percentage of TOC, and sampling water depth).

4.3 Comparison between the 63-150 µm and > 150 µm size fractions (in the 1 cm core top)

4.3.1 Abundance and diversity

Foraminiferal abundances and diversity metrics were calculated considering the 63-150 µm and >150 µm fractions in the 0-1 cm sediment layer (Fig. 6). The finer fraction (63-150 µm) showed abundances always higher than the coarse fraction (>150 µm) with abundances between 1000 and 4700 ind. 50 cm^{-3}. The small fraction contributed from 72 up to 96% to the total abundances (63-150 µm + >150 µm) (Fig. 6a). Foraminiferal abundances considering the >150 µm were lower than 300 ind. 50 cm^{-3} at St2, St7 and St1, between 300 and 600 ind. 50 cm^{-3} at St4, St6 and St9 and over 1000 ind. 50 cm^{-3} at St3, St5 and St8.

Less than 20 species were observed for both size fractions in the first three stations of the transect (St2, St7 and St1), whereas values between 29 and 57 were observed further away in the transect. The number of species observed in the finer fraction was always higher than in the coarse fraction but with a similar trend along the main fjord axis (Fig.6b).

Shannon index was lower than 2 at the three innermost stations, whereas values between 2 and 3 were observed further away in the transect considering the finer fraction (63-150 µm). The >150 fraction presented values lower than 1.5 at the station St2, St7 and St3, values around 2 at St1 and St8, while the remaining stations showed values around 2.5. Equitability values for the >150 µm fraction were below 0.5 at St2, St7 and St3, whereas values between 0.5 and 0.8 were observed at all other stations. The finer fraction (63-150 µm) showed very low equitability at St2, values between 0.5 and 0.6 at St7, St1, and St3, and over 0.7 at the other stations. Shannon index and equitability diversity metrics showed more variability between the two size assemblages (Fig. 6c, d) compared to species richness (Fig. 6a), but a similar diversity increase from the inner to the outer stations was observed.

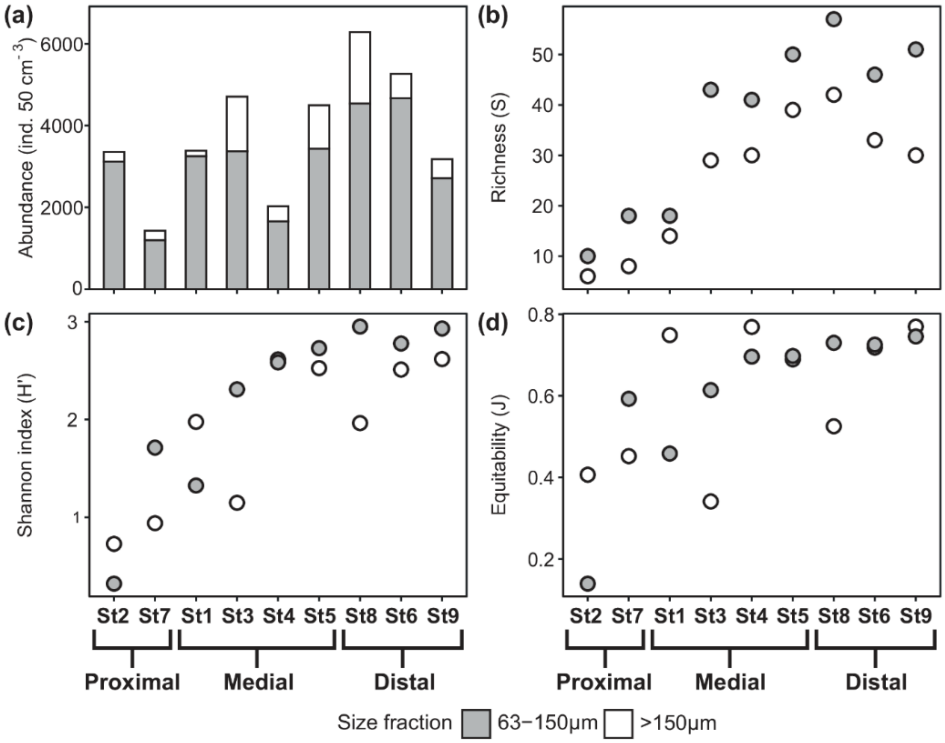

Figure 6. (a) Foraminiferal cumulative abundances (ind. 50 cm^{-3}) for two size fractions (63-150 µm and >150 µm) of the 0-1 cm sediment layer and **(b)** richness (S), **(c)** Shannon index (H'), and **(d)** equitability (J) indexes comparison among the 63–150 µm and >150µm fractions. The >150 µm fraction is represented in white and the 63-150 µm in grey.

4.3.2 Non-metric multidimensional scaling analysis

The nMDS ordination plot (stress = 0.071), based on species abundances considering the fine (63-150 µm) and coarse (>150 µm) size fractions in the 0-1 cm sediment layer, showed a similar

clustering of the stations by area (proximal, medial, distal) but differences in assemblage composition (Fig. 7). The NMDS1 axis separates the first three stations of the transect (St2, St7, and St1) from the remaining stations, whereas NMDS2 separates the two size fractions. The area of the polygon for the >150 µm size fraction is bigger than the one for the 63-150 µm, indicating lower dissimilarity among stations in the finer fraction.

Although both fractions separated the nine stations into the same stations' clusters, no overlap can be observed between convex hulls due to large differences in foraminiferal assemblages (Fig. 7). Indeed, the SIMPER analysis identified five major species (i.e., *Cassodulina reniforme*, *Textularia earlandi*, *Spiroplectammina biformis*, *Stainforthia feylingi*, *Pullenia* cf. *osloensis*) influencing this difference (average contribution >5%, p<0.01). Four of them were positively correlated with the NMDS2 axis and mostly represented in the 63-150 µm fraction. The only exception being *C. reniforme,* which was almost equally present in both fractions. The two size fractions had 50 common species. The >150 µm had 14 exclusive species, whereas the 63-150 µm presented 21 exclusive species. Species relative abundances for both size fractions are displayed as heatmaps in the supplement (Fig. S3).

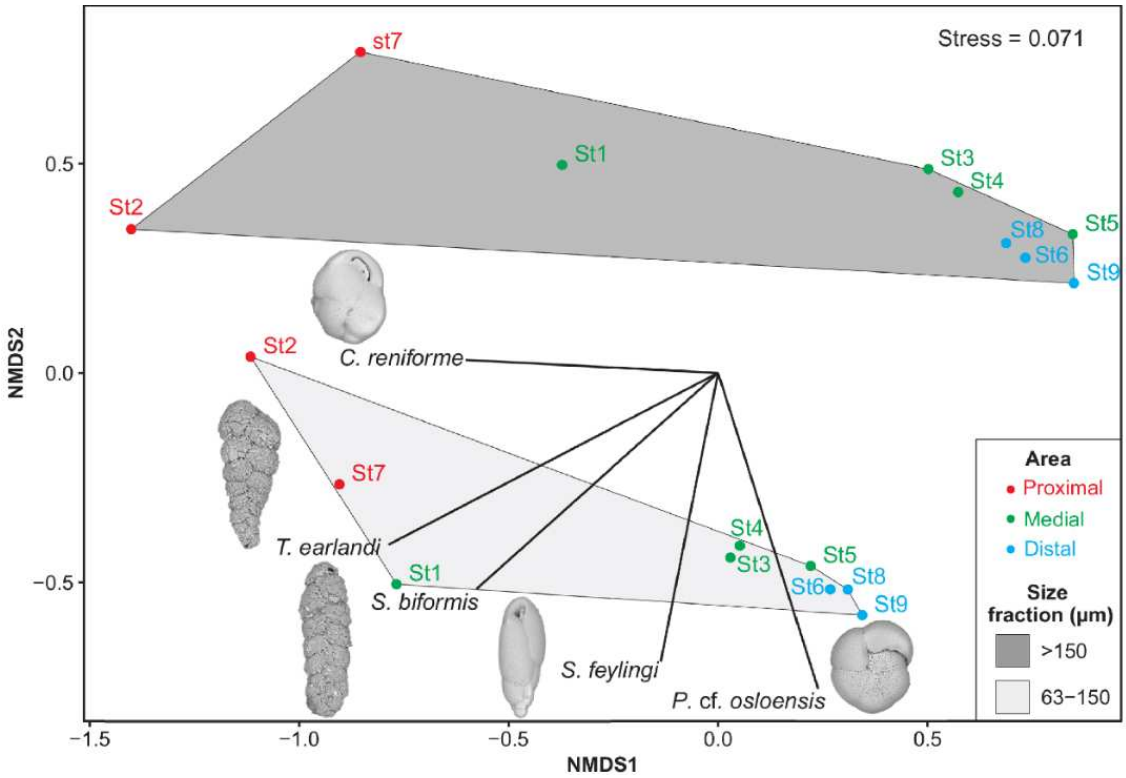

Figure 7. Non-metric multidimensional scaling (nMDS) analysis (Bray-Curtis dissimilarity) on foraminiferal abundances considering two groups corresponding to the two size fractions (63-150 µm and >150 µm) in the 0-1 cm. Station colours correspond to the sampling area (proximal, medial, distal). The convex hulls enclosed each of the groups. The displayed vectors are the species explaining significant (p<0.01) percentage of dissimilarity (>5%) between the two groups based on SIMPER analysis.

5. Discussion

The geographical position of Kongsfjorden and its geometric configuration (i.e., no entrance sill) are responsible for the build-up of steep environmental gradients developing along the short fjord axis between two contrasted end-members (Lalande et al., 2016; Meslard et al., 2018; Svendsen et al., 2002). Gradients of water salinity and temperature, turbidity, nutrient distribution, and inorganic particulate sedimentation, are determined by the concomitance of glacier dynamics at the fjord head with the AW inflow from the outer shelf. The present study, performed in August 2018, shows that benthic foraminiferal faunas respond clearly to these summer environmental gradients. Our analyses identified three biozones related to the glacier front in the inner Kongsfjorden: distal, medial and proximal.

I. Proximal biozone

During August 2018, CTD casts detected a water column typical of the summer stratification (Svendsen et al, 2002; Cottier et al. 2005) with a fresh surface layer of meltwaters overlying saltier water mass (due to mixing with AW) (Fig. 1). The surface layer also revealed high turbidity, particularly in the vicinity of the front of the tidewater glacier Kronebreen (Fig. S2). This observation confirms previous studies that identified the Kronebreen glacier as the major source of meltwater, suspended particles and sediment in Kongsfjorden (D'Angelo et al., 2018; Meslard et al., 2018; Svendsen et al., 2002; Trusel et al., 2010). Generally, Kronebreen subglacial discharges and associated sediment load eroded from the glacier basement exit from the northernmost part of the glacier front (Meslard et al., 2018; Trusel et al., 2010). Consequently, a buoyant turbid plume is formed at the tidewater glacier front and is pushed away northwards by the downfjord surface circulation at the fjord head (Sundfjord et al., 2017; Torsvik et al., 2019), implying the spreading of the plume above our sampling stations St2 and St7 (Fig. 1). The fine grained particles, transported in suspension in the plume are deposited with a high sedimentation rate estimated at about 6-9 cm y^{-1} in the vicinity of the Kronebreen front (< 0.5 km) (Trusel et al., 2010). This explains our observations at the proximal stations where unconsolidated and potentially high mobile surface sediment (i.e., low sediment stability) was composed of medium silt. Coarser particles from subglacial discharges, such as coarse silt and fine sand, can also be transported in suspension in the plume during sporadic hydrodynamic events (e.g., accelerated melting period, surge, storm), and then deposited along a decreasing size gradient off the glacier front (Torsvik et al., 2019). This process may be recorded by layers of coarse silts as observed 3 cm downcore at St2.

The proximal stations (St2 and St7), grouped into cluster 1 (Fig. 3), were positively correlated with surface water turbidity (Fig. 5). This area, directly subjected to high sedimentation from the meltwater turbid plume was characterised by low foraminiferal abundances and/or low taxonomic diversity in both size fractions (Table 3, Fig. 6). Only few species (i.e., *Capsammina bowmanni, Saccammina* cf *sphaerica, Cassidulina reniforme* and *Textularia earlandi*) that are most likely adapted to colonise soft-bottom sediments subjected to high physical disturbance, were identified in this area (Fig. 3 and Fig. 7). The agglutinated monothalamus species *C. bowmanni* completely dominated the assemblage in the immediate proximity of the glacier (St2, 1.9 km far from the glacier front). This species lives preferentially in the uppermost centimetre of the sediment (Gooday et al., 2010) and was previously reported in a temperate fjord under fluvial influence in southern Norway (e.g., Alve and Nagy, 1986). However, it has never been reported as a dominant species and its presence has not been often documented, likely due to the fragility of the test that can be lost during sample preparation. At St7, *C. bowmanni* was accompanied by *C. reniforme* and *T. earlandi*. The increased distance (about 4.5 km) from the glacier front and a consequent slightly reduced environmental stress may have favoured the coexistence of these species. *Cassidulina reniforme* is a typical glacier proximal species that has been previously observed in several Svalbard fjords from the western coast (Adventfjorden, Hornsund, Van Mijenfjorden, Isfjorden, Tempelfjorden, Krossfjorden, Smeerenburgfjorden; Hald and Korsun, 1997; Korsun and Hald, 2000; Szymańska et al., 2017) and from the southern coast (Storfjorden; Fossile et al., 2020). This species was suggested to prefer less saline waters (e.g., Hald and Korsun, 1997; Jernas et al., 2018). *Cassidulina reniforme* was also present as juveniles in the fine fraction at the proximal station St7. The presence of juveniles of this glacier-proximal species (e.g., Hald and Korsun, 1997; Korsun and Hald, 1998, 2000) may suggest an opportunistic response to the stressful conditions related to glacier dynamics (i.e., high turbidity and reduced organic flux). In other Svalbard fjords, *C. reniforme* is often accompanied by another glacier proximal opportunist, *Elphidium clavatum* (e.g., Hald and Korsun, 1997; Korsun and Hald, 1998, 2000; Fossile et al., 2020). In the studies mentioned above, it was proposed that *C. reniforme* would replace *E. clavatum* when environmental conditions ameliorate in terms of glacial physical disturbance and food supply. In our study *E. clavatum* was observed only in the dead assemblages, suggesting a potential temporal shift in the dynamics for their reproduction (Table S2). Indeed, high frequencies of *E. clavatum* and *C. reniforme* were documented in September 2015 at Kongsfjorden head (Kniazeva and Korsun, 2019). In the small size assemblage of St7 there was also the

agglutinated *T. earlandi*. This is a typical glaciomarine species usually found in fjord environments (e.g., Korsun and Hald, 2000).

The meltwater turbidity plume can spread for several kilometres from the glacier front (Meslard et al., 2018) reducing the euphotic depth to few meters (Halbach et al., 2019) and locally preventing phytoplankton growth. Moreover, glacial runoff transports old and refractory terrestrial organic carbon (Bourgeois et al., 2016; Calleja et al., 2017; Kedra et al., 2012). This generally causes the depletion of available organic matter export fluxes to the seafloor in the inner fjord (Lalande et al., 2016). Previous studies reported sediment depleted in organic carbon close to the Kronebreen terminus (TOC% < 0.25%; Bourgeois et al., 2016).

The presence of living foraminifera restricted at the sediment surface (Fig. 4) was likely due to the unconsolidated and potentially mobile sediment (i.e., low sediment stability) caused by rapid accumulation from high suspended sediment load coming from the glacier terminus. But, it can also be a response to the poor TOC concentrations lower or about 0.4% (TROX model, Jorissen et al., 1995). Deposition of massive amounts of sediments can also hamper the oxygen penetration into the sediment. It is well known that oxygen availability as well as organic matter are two limiting factors for foraminiferal microhabitat distribution (Jorissen et al., 1995). Moreover, the presence of *C. bowmanni* and *C. reniforme* restricted at the sediment surface may be the result of their microhabitat preferences. High absolutes and relative abundances and microhabitat restriction might be indicative of the pioneer character of *C. bowmanni*. The presence of opportunistic and simple agglutinated species capable of rapid colonisation after physical disturbance was previously observed in highly disturbed areas (i.e., canyons; Koho et al., 2007). This species, together with *T. earlandi* and the calcareous *C. reniforme*, may be the only species able to deal with the stressful conditions prevailing at the sampling time. Similar habitat restrictions to the sediment-water interface were observed for benthic macrofauna in some areas of Arctic fjords subjected to high disturbance (e.g., Wlodarska-Kowalczuk et al., 2005). Finally, the high availability of mica at the Kronebreen terminus originated from mica-schists (from Proterozoic low- and medium-grade metamorphic rocks; Svendsen et al., 2002), could have also played a positive role in the thriving of *C. bowmanni*. Indeed, this species appears to have an obligated use of mica flakes to build its test (Gooday et al., 2010).

II. Medial biozone

In the central part of the inner fjord, the water column was characterised by the same fresh surface layer and a clear signal of AW intrusion (Fig. 1). A reduced water turbidity compared to the proximal area was observed (Fig. S1). The increased distance from the glacier front and

a progressive dispersal of the meltwater turbid plume coming from Kronebreen can explain such a pattern (e.g., Meslard et al., 2019). Medium silts were also observed in this area, as a result of the sedimentation from the meltwater turbid plume away from the glacier front. Indeed, high sedimentation rates were previously estimated to values of about 2.5 cm yr^{-1} in the medial zone, but they are 2.5 to 3.5 times lower than the ones measured in the proximal zone (Zaborska et al., 2006). At the two shallowest stations St3 and St4, located in front of glacial sandur deltas, in the vicinity of prodeltas (Bourriquen et al., 2016) developed along the southern coast, coarse silts were observed as a secondary peak in the grainsize distribution of down core sediment layers. This relatively coarse particulate input to the fjord may be provided by meltwaters (and associated sedimentary load) derived from the sandur drainage downstream the continental glaciers (i.e., Austre Lovénbreen and Midtre Lovénbreen) located on the southern bank of the fjord (Bourriquen et al., 2018).

The medial stations grouped into cluster 2 (St1 alone) and cluster 3 (St3, St4 and St5) (Fig. 3) and do not show any strong correlation with a specific environmental variable (Fig. 5). However, foraminiferal communities showed some differences between the two identified clusters. St1 was separated from the remaining medial stations and it was composed by a transitional assemblage from the proximal to the medial biozone. Such assemblage was characterised by the presence of *C. reniforme*, *Reophax fusiformis* and *T. earlandi*. *Cassidulina reniforme*, which was also dominant in the proximal station assemblages, could indicate the persistence of the tidewater glacier disturbance, as also suggested by the presence of juveniles of this species. Moreover, the relatively high disturbance at St1 is supported by the lowest TOC content (around 0.1 %) measured along the transect. *Textularia earlandi*, was the dominant species in the small size assemblage of St1. This elongated species together with *Spiroplectammina biformis* was mostly present in the fine fraction and especially in the medial stations (Fig. 7, Fig. S3). Both species are typical of glaciomarine environments, and their relative abundances usually increase with distance from the glacier but still under glacier influence (e.g., Korsun and Hald, 2000; Forwick et al., 2010; Szymańska et al., 2017; Fossile et al., 2020). The agglutinated *R. fusiformis* was previously observed together with *T. earlandi*, in a West Greenland fjord, an Arctic fjord under the influence of Atlantic-sourced waters (Lloyd, 2006). The preference of both species for these waters is coherent with their presence in August 2018 when an AW intrusion was clearly observed in the medial area. Station St1 presented also high relative abundances of *Nonionellina labradorica*, which is in common with all the other medial stations grouped into cluster 3, underlying the transitional character of this station.

At all the stations grouped into cluster 3, the calcareous species *Nonionellina labradorica* was the major species with variable relative abundances. This is a typical glacier-distal species, of which the distribution was often related to nutrient enrichment or to the presence of AW (Hald and Korsun, 1997; Korsun and Hald, 1998). This species preferentially feeds on diatoms (e.g., Cedhagen, 1991; Jernas et al., 2018) and its location at the sediment surface may indicate the presence of fresh phytodetritus inputs, which is mostly composed of diatoms in the inner Kongsfjorden (Lalande et al., 2016). The presence of *N. labradorica* is compatible with the slightly higher organic carbon content measured in the stations of cluster 3 (0.4-0.7 % of TOC) (Table 3). Indeed, the fjord dynamics, with the deep AW intrusion, consequent subglacial-induced upwelling at the glacier terminus and downfjord surface advection, can supply nutrients (i.e., nitrate and phosphate) in this medial area enhancing primary productivity (Halbach et al., 2019). Several other minor species (e.g., *Quinqueloculina seminula*, *Labrospira crassimargo*, *Astrononion gallowayi*, *Siphonaperta agglutinata* and *Adercotryma glomeratum*) often found in Svalbard fjords (e.g., Hald and Korsun, 1997; Korsun and Hald, 2000; Forwick et al., 2010; Jernas et al., 2018; Kniazeva and Korsun, 2019) were identified in the medial stations and are the reason for the increased diversity measured in this area compared to the innermost part of the fjord (Table 3). The fine fraction at these stations was characterised by the elongated calcareous species *Stainforthia feylingi*. This species was previously found in the outer Kongsfjorden (Jernas et al, 2018), but little is known about its ecology. This species is reported as opportunist (e.g., Lloyd et al., 2007) and often associated to high primary productivity in the vicinity of sea ice in paleoenvironmental reconstructions (e.g., Seidenkrantz, 2013). In August 2018, *S. feylingi* co-occurred with a phytodetritus indicator (i.e., *N. labradorica*), which supports the speculation of its preferences for that food resource. The small fraction at station St5 was dominated by the small-sized species *Pullenia* cf. *osloensis* which presented high relative abundances also in the distal stations.

The microhabitat distribution in the >150 µm fraction showed decreased foraminiferal abundances with sediment depth. The downcore microhabitat distribution of *N. labradorica* showed subsurface peaks that demonstrate its capacity to occupy infaunal habitats. This suggests a potential ability to exploit other food resources than fresh phytodetritus (e.g., buried organic matter) or to benefit from an alternative metabolism (e.g., denitrification; Jauffrais et al., 2019). Indeed, some closely related species are capable of denitrification (e.g., *Nonionella* sp. T1 and *Nonionella* cf *stella*; Glock et al., 2019; Choquel et al., 2021) and thus can successfully occupy and exploit subsurface sediment resources. *Globobulimina auriculata* also displayed a subsurface increase at St4. This behaviour can be explained by its tolerance for low

oxygen conditions and/or denitrification capacity as other *Globobulimina* species (e.g., Risgaard-Petersen et al., 2006; Koho et al., 2011) and thus able to occupy infaunal habitats where interspecific competition is reduced. The microhabitat distribution observed in the medial stations may also result from reduced sediment deposition, increased sediment stability, increase in organic flux, and therefore the development of diverse suitable ecological niches to occupy.

III. Distal biozone

The outer part of the transect was characterised by a fresh surface layer and by an intermediate water and deep layer of AW (Fig. 1). This part of the fjord, deeper than 100 m, is directly influenced by the inflow of warm and salty AW coming from the WSC current flowing along the western coast of Svalbard. The lowest values of surface turbidity were observed in this area of the fjord (Fig. S1). The increased water transparency was the result of augmented distance from the Kronebreen front. However, we observed the same type of sediment (i.e., medium silt) as upstream. This could suggest that this area is still impacted by the sedimentation from a diluted turbid plume. At St8, which is located close to the southern coast, the coarser medium silt of the fjord sediment was observed with a secondary mode of very fine sand. This may suggest sediment inputs from continental glacier meltwaters (i.e., Midtre Lovénbreen). Unfortunately, the local sedimentation rate is unknown.

The distal stations grouped into cluster 4 (St6, St8 and St9) (Fig. 3) were positively correlated with sediment organic carbon and water depth (Fig. 5). The dominant species was the agglutinated *Adercotryma glomeratum* followed by the calcareous *N. labradorica* (Fig. 3). *Adercotryma glomeratum* was suggested to be able to exploit low food quality and/or quantity (Jernas et al., 2018), whereas *N. labradorica* is supposed to feed on fresh phytodetritus or to have different metabolism (i.e., able of denitrification; see references above). The coexistence of these two species may be explained by the occupation of different ecological niches. *Adercotryma glomeratum* was also previously related to AW influence in Kongsfjorden (Jernas et al., 2018), in other western Svalbard fjords including Isfjorden and Krossfjorden (Korsun and Hald, 1997), and in the southern fjord Storfjorden (Fossile et al., 2020). The clear dominance of this species in the distal stations and its decreasing percentage in the medial area (where represented only a minor proportion of the assemblages), suggests the decline in the AW influence upstream fjord. This is coherent with AW intrusion invading the fjord trench from the outer sea and perhaps suggests a longer persistence of AW at the distal stations. At St9,

Cibicidoides lobatulus is highly present and could indicate high-energy near-bed currents at this station (Murray, 2006).

The fine fraction (63-150 µm) of the distal stations and were characterised by the presence of the small-sized species *Pullenia* cf. *osloensis*. The ecological preferences of *P.* cf. *osloensis* have not been previously described. *Pullenia* spp. were previously reported as detritivore and typically found on the shelf-bathyal area of cold environments (Murray, 2006). Some species of this genus are often used as AW indicators in paleoenvironmental studies (e.g., Chauhan et al., 2016 and reference therein), potentially explaining the presence of this species mostly at St5 and in the distal stations that are under the inflow of AW (Fig. S3). Moreover, *Stainforthia feylingi* showed important relative abundances at the outermost station St9 suggesting increased phytodetritus inputs at this location (e.g., Lloyd et al., 2007; Seidenkrantz, 2013).

Even if foraminiferal species composition was similar among the distal stations, the microhabitat distribution displayed some differences (Fig. 5). The subsurface peaks observed at St9 (Fig. 5) was determined by the high abundances of *A. glomeratum* and *N. labradorica*. Both species may have preferred the infaunal habitat to exploit additional food resources (i.e., buried organic matter of lower quality) or use different metabolisms (i.e., denitrification) and thus reduce competition with the many species present at the sediment surface. However, *A. glomeratum* was also present with high numbers at the sediment surface and presented a deep increase in abundances at St6, that may point out to bioturbation processes at these stations (e.g., Thibault De Chanvalon et al., 2015).

6. Conclusions

Living benthic foraminiferal faunas from the inner Kongsfjorden were studied to determine the combined influence of glacier melting with AW inflow on the benthic system. To that aim, foraminiferal patterns were investigated in relation to water masses properties, sediment characteristics and organic matter inputs to the seafloor during late summer, when environmental gradients are the steepest. Benthic environmental conditions were connected to tidewater glacier dynamics and interpreted based on the glacial-related disturbances. The surface water turbidity, water depth and the organic inputs to the seafloor are the main driving factors for foraminiferal patterns in the inner Kongsfjorden, determining the establishment of three different biozones (i.e., proximal, medial and distal) summarised in the conceptual model (Fig. 8). High surface water turbidity related to freshwater and sediment inputs from subglacial discharges and surface runoff, and reduced organic flux due to reduced primary production,

were the limiting factors for the proximal biozone. This inner area was dominated by few stress-tolerant and/or opportunistic glacier proximal species restricted to the sediment surface (e.g., *Capsammina bowmanni*, *Cassidulina reniforme* and *Textularia earlandi*). A progressive reduction of the general stressful environmental conditions (i.e., reduced physical disturbance and increase organic flux) and the increased AW inflow influence in the medial and distal biozones favoured the establishment of diversified foraminiferal communities able to occupy different ecological niches and microhabitats (i.e., epifaunal and/or infaunal). In particular, the phytodetritus indicator *Nonionellina labradorica* and the AW indicator *Adercotryma glomeratum* were the representative species in the medial and distal biozone, respectively. The comparison between the two size fractions highlighted the presence of different foraminiferal assemblages in terms of species composition but similar foraminiferal patterns along the transect. The supplementary ecological information obtained from the small size assemblage was imprecise due the lack of knowledge regarding the ecological preferences for these species in modern environments. Ultimately, the variation of several environmental parameters in relation to the distance from the glacier terminus, parallelly to the appearance of different foraminiferal assemblages, suggests the potential investigation of diversity patterns in relation to the distance from the front as potential proxy for glacier retreat.

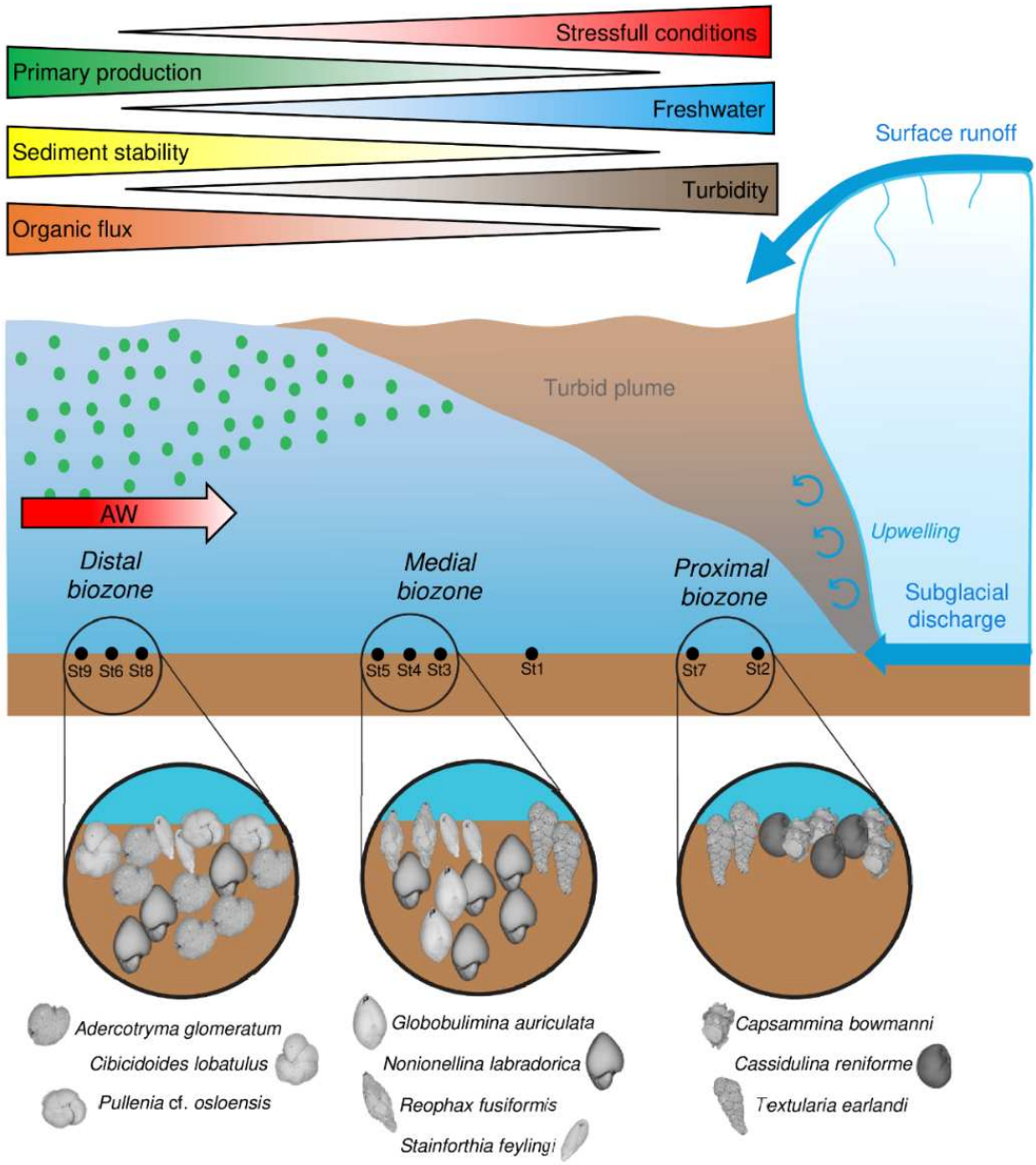

Figure 8. Conceptual model showing the environmental gradients created by tidewater glacier dynamics and, repartition of benthic foraminiferal communities and their microhabitat preferences.

Data availability. Raw data will be made available on the online repository PANGAEA upon publication of this manuscript in *Marine Micropaleontology*.

Supplement. Tables S1 and S2 and Figs. S1, S2 and S3 can be found in the Supplement section. Scanning electron micrographs (plates) of the most relevant species are shown in Figs. S4, S5, and S6 in the Supplement section.

Author contributions. EF: conceptualisation, data curation, formal analysis, investigation, methodology, validation, visualisation, writing-original draft, writing-review & editing. MM, MPN and HH: conceptualisation, funding acquisition, investigation, resources, supervision, validation, writing-review & editing. AB: funding acquisition, resources, writing-review & editing. YP: investigation, writing-review & editing. IB: methodology, writing-review & editing. MD: methodology, writing-review & editing.

Acknowledgements. We thank Alain Jadas-Hecart and Nadage Blon for technical support during sediment organic matter analysis, Francois Guillory for technical support during sediment grain size analysis, Sabine Schmidt for sedimentological investigation and Katrine Husum for taxonomical support. This project benefits from the technical support of the AWIPEV French - German Arctic Research Base at Ny-Ålesund.

Financial support. This research is part of the PhD thesis of Eleonora Fossile, which is co-funded by French National Program MOPGA (Make Our Planet Great Again) and the University of Angers. The field campaign was organised into the frame of IPEV logistic project C3 (Coasts under Climate Change3 suite) with the collaboration of the sailing boat Aztec Lady. Sediment sampling was founded by BiSMART project (University of Angers). Water column properties were measured by CTD profiling in the context of the ISMOGLAC project (*ISotopic and physicalchemical MOnitoring of GLACial drainages and sea water in the Ny-Ålesund area (Svalbard)*).

Competing interests. The authors declare that they have no conflict of interest.

References

Alboukadel K. and Mundt F.: factoextra: Extract and Visualize the Results of Multivariate Data Analyses. R package version 1.0.7. https://CRAN.R-project.org/package=factoextra, 2020.

Alve, E., Korsun, S., Schönfeld, J., Dijkstra, N., Golikova, E., Hess, S., Husum, K., Panieri, G.: Foram-AMBI: A sensitivity index based on benthic foraminiferal faunas from North-East Atlantic and Arctic fjords, continental shelves and slopes. Mar. Micropaleontol. 122, 1–12. https://doi.org/10.1016/j.marmicro.2015.11.001, 2016.

Alve, E., Nagy, J.: Estuarine foraminiferal distribution in Sandebukta, a branch of the Oslo Fjord (Norway). J. Foraminifer. Res. 16, 261–284. https://doi.org/10.2113/gsjfr.16.4.261, 1986.

Arndt, S., Jørgensen, B.B., LaRowe, D.E., Middelburg, J.J., Pancost, R.D., Regnier, P.: Quantifying the degradation of organic matter in marine sediments: A review and synthesis. Earth-Science Rev. 123, 53–86. https://doi.org/10.1016/j.earscirev.2013.02.008, 2013.

Basedow, S.L., Eiane, K., Tverberg, V., Spindler, M.: Advection of zooplankton in an Arctic fjord (Kongsfjorden, Svalbard). Estuar. Coast. Shelf Sci. 60, 113–124. https://doi.org/10.1016/j.ecss.2003.12.004, 2004.

Bisutti, I., Hilke, I., Raessler, M.: Determination of total organic carbon - An overview of current methods. TrAC - Trends Anal. Chem. 23, 716–726. https://doi.org/10.1016/j.trac.2004.09.003, 2004.

Blott, S.J., Pye, K.: GRADISTAT: a grain size distribution and statistics package for the analysis of unconsolidated sediments. Earth Surf. Process. Landforms 26, 1237–1248. https://doi.org/10.1002/esp.261, 2001.

Bourgeois, S., Kerhervé, P., Calleja, M.L., Many, G., Morata, N.: Glacier inputs influence organic matter composition and prokaryotic distribution in a high Arctic fjord (Kongsfjorden, Svalbard). J. Mar. Syst. 164, 112–127. https://doi.org/10.1016/j.jmarsys.2016.08.009, 2016.

Bourriquen, M., Baltzer, A., Mercier, D., Fournier, J., Pérez, L., Haquin, S., Bernard, E., Jensen, M.: Coastal evolution and sedimentary mobility of Brøgger Peninsula, northwest Spitsbergen. Polar Biol. 39, 1689–1698. https://doi.org/10.1007/s00300-016-1930-1, 2016.

Bourriquen, M., Mercier, D., Baltzer, A., Fournier, J., Costa, S., Roussel, E.: Paraglacial coasts responses to glacier retreat and associated shifts in river floodplains over decadal timescales (1966–2016), Kongsfjorden, Svalbard. L. Degrad. Dev. 29, 4173–4185. https://doi.org/10.1002/ldr.3149, 2018.

Calleja, M.L., Kerhervé, P., Bourgeois, S., Kędra, M., Leynaert, A., Devred, E., Babin, M., Morata, N.: Effects of increase glacier discharge on phytoplankton bloom dynamics and pelagic geochemistry in a high Arctic fjord. Prog. Oceanogr. 159, 195–210. https://doi.org/10.1016/j.pocean.2017.07.005, 2017.

Caulle, C., Koho, K.A., Mojtahid, M., Reichart, G.J., Jorissen, F.J..: Live (Rose Bengal stained) foraminiferal faunas from the northern Arabian Sea: Faunal succession within and below the OMZ. Biogeosciences 11, 1155–1175. https://doi.org/10.5194/bg-11-1155-2014, 2014.

Cedhagen, T.: Retention of chloroplasts and bathymetric distribution in the sublittoral foraminiferan *Nonionellina labradorica*. Ophelia 33, 17–30. https://doi.org/10.1080/00785326.1991.10429739, 1991.

Chauhan, T., Rasmussen, T.L., Noormets, R.: Palaeoceanography of the Barents Sea continental margin, north of Nordaustlandet, Svalbard, during the last 74 ka. Boreas 45, 76–99. https://doi.org/10.1111/bor.12135, 2016.

Choquel, C., Geslin, E., Metzger, E., Filipsson, H.L., Risgaard-Petersen, N., Launeau, P., Giraud, M., Jauffrais, T., Jesus, B., Mouret, A.: Denitrification by benthic foraminifera and their contribution to N-loss from a fjord environment. Biogeosciences 18, 327–341. https://doi.org/10.5194/bg-18-327-2021, 2021.

Corliss, B.H.: Morphology and microhabitat preferences of benthic foraminifera from the northwest Atlantic Ocean. Mar. Micropaleontol. 17, 195–236. https://doi.org/10.1016/0377-8398(91)90014-W, 1991.

Cottier, F., Tverberg, V., Inall, M., Svendsen, H., Nilsen, F., Griffiths, C.: 2005. Water mass modification in an Arctic fjord through cross-shelf exchange: The seasonal hydrography of Kongsfjorden, Svalbard. J. Geophys. Res. Ocean. 110, 1–18. https://doi.org/10.1029/2004JC002757, 2005.

Cottier, F.R., Nilsen, F., Enall, M.E., Gerland, S., Tverberg, V., Svendsen, H.: Wintertime warming of an Arctic shelf in response to large-scale atmospheric circulation. Geophys. Res. Lett. 34, 1–5. https://doi.org/10.1029/2007GL029948, 2007.

Cottier, F.R., Nilsen, F., Skogseth, R., Tverberg, V., Skarðhamar, J., Svendsen, H.: Arctic fjords: a review of the oceanographic environment and dominant physical processes. Geol. Soc. London, Spec. Publ. 344, 35–50. https://doi.org/10.1144/sp344.4, 2010.

Cowton, T., Slater, D., Sole, A., Goldberg, D., Nienow, P.: Modeling the impact of glacial runoff on fjord circulation and submarine melt rate using a new subgrid-scale parameterization for glacial plumes. J. Geophys. Res. Ocean. 796–812. https://doi.org/10.1002/2014JC010324, 2015.

D'Angelo, A., Giglio, F., Miserocchi, S., Sanchez-Vidal, A., Aliani, S., Tesi, T., Viola, A., Mazzola, M., Langone, L.: Multi-year particle fluxes in Kongsfjorden, Svalbard. Biogeosciences 15, 5343–5363. https://doi.org/10.5194/bg-15-5343-2018, 2018.

Dai, A., Luo, D., Song, M., Liu, J., 2019. Arctic amplification is caused by sea-ice loss under increasing CO_2. Nat. Commun. 10, 1–13. https://doi.org/10.1038/s41467-018-07954-9, 2019.

David T, D., K.P., K.: Recent variability in the Atlantic water intrusion and water masses in Kongsfjorden, an Arctic fjord. Polar Sci. 11, 30–41. https://doi.org/10.1016/j.polar.2016.11.004, 2017.

Dickson, B., Meincke, J., and Rhines, P.: "Arctic–subarctic ocean fluxes: defining the role of the northern seas in climate," in Arctic–Subarctic Ocean Fluxes, eds R. R. Dickson, J. Meincke, and P. Rhines (Dordrecht: Springer), 1–13. https://doi.org/10.1007/978-1-4020-6774-7_1, 2008.

Duchemin, G., Fontanier, C., Jorissen, F.J., Barras, C., Griveaud, C.: Living small-sized (63–150 µm) foraminifera from mid-shelf to mid-slope environments in the Bay of Biscay. J. Foraminifer. Res. 37, 12–32. https://doi.org/10.2113/gsjfr.37.1.12, 2007.

Duros, P., Fontanier, C., Metzger, E., Cesbron, F., Deflandre, B., Schmidt, S., Buscail, R., Zaragosi, S., Kerhervé, P., Rigaud, S., Delgard, M.L., Jorissen, F.J.: Live (stained) benthic foraminifera from the Cap-Ferret Canyon (Bay of Biscay, NE Atlantic): A comparison between the canyon axis and the surroun.ding areas. Deep. Res. Part I Oceanogr. Res. Pap. 74, 98–114. https://doi.org/10.1016/j.dsr.2013.01.004, 2013.

Forwick, M., Vorren, T.O., Hald, M., Korsun, S., Roh, Y., Vogt, C., Yoo, K.-C.: Spatial and temporal influence of glaciers and rivers on the sedimentary environment in Sassenfjorden and Tempelfjorden, Spitsbergen. Geol. Soc. London, Spec. Publ. 344, 163–193. https://doi.org/10.1144/SP344.13, 2010.

Fossile, E., Nardelli, M.P., Jouini, A., Lansard, B., Pusceddu, A., Moccia, D., Michel, E., Péron, O., Howa, H., Mojtahid, M.: Benthic foraminifera as tracers of brine production in the Storfjorden "sea ice factory." Biogeosciences 17, 1933–1953. https://doi.org/10.5194/bg-17-1933-2020, 2020.

Glock, N., Roy, A.S., Romero, D., Wein, T., Weissenbach, J., Revsbech, N.P., Høgslund, S., Clemens, D., Sommer, S., Dagan, T.: Metabolic preference of nitrate over oxygen as an electron acceptor in foraminifera from the Peruvian oxygen minimum zone. PNAS 116, 2860–2865. https://doi.org/10.1073/pnas.1813887116, 2019.

Gooday, A.J., Aranda da Silva, A., Koho, K.A., Lecroq, B., Pearce, R.B.: The "mica sandwich"; a remarkable new genus of Foraminifera (Protista , Rhizaria) from the Nazaré Canyon (Portuguese margin , NE Atlantic) 56, 345–357. http://www.jstor.org/stable/40959488, 2010.

Gooday, A.J., Goineau, A.: The contribution of fine sieve fractions (63-150 µm) to foraminiferal abundance and diversity in an area of the eastern Pacific Ocean licensed for polymetallic nodule exploration. Front. Mar. Sci. 6, 1–17. https://doi.org/10.3389/fmars.2019.00114, 2019.

Google Earth Pro V 7.3.3.7786 (July 26, 2016). Spitsbergen, Norway. 78°52'39.19"N, 12°35'42.51"E. Eye alt. 20 km. Maxar Technologies 2021. https://www.google.com/earth/index.html, [January 25, 2021].

Graversen, R.G., Mauritsen, T., Tjernström, M., Källén, E., Svensson, G.: Vertical structure of recent Arctic warming. Nature 451, 53–56. https://doi.org/10.1038/nature06502, 2008.

Halbach, L., Vihtakari, M., Duarte, P., Everett, A., Granskog, M.A., Hop, H., Kauko, H.M., Kristiansen, S., Myhre, P.I., Pavlov, A.K., Pramanik, A., Tatarek, A., Torsvik, T., Wiktor, J., Wold, A., Wulff, A., Steen, H., Assmy, P.: Tidewater Glaciers and Bedrock Characteristics Control the Phytoplankton Growth Environment in a Fjord in the Arctic. Front. Mar. Sci. 6. https://doi.org/10.3389/fmars.2019.00254, 2019.

Hald, M., Korsun, S.: Distribution of modern benthic foraminifera from fjords of Svalbard, European Arctic. J. Foraminifer. Res. 27, 101–122. https://doi.org/10.2113/gsjfr.27.2.101, 1997.

Hegseth, E.N., Tverberg, V.: Effect of Atlantic water inflow on timing of the phytoplankton spring bloom in a high Arctic fjord (Kongsfjorden, Svalbard). J. Mar. Syst. 113–114, 94–105. https://doi.org/10.1016/j.jmarsys.2013.01.003, 2013.

Hijmans, R. J.: geosphere: Spherical Trigonometry. R package version 1.5-10. https://CRAN.R-project.org/package=geosphere, 2019.

Hodal, H., Falk-Petersen, S., Hop, H., Kristiansen, S., Reigstad, M.: Spring bloom dynamics in Kongsfjorden, Svalbard: Nutrients, phytoplankton, protozoans and primary production. Polar Biol. 35, 191–203. https://doi.org/10.1007/s00300-011-1053-7, 2012.

Holland, M.M., Bitz, C.M.: Polar amplification of climate change in coupled models. Clim. Dyn. 21, 221–232. https://doi.org/10.1007/s00382-003-0332-6, 2003.

Holmes, F.A., Kirchner, N., Kuttenkeuler, J., Krützfeldt, J., Noormets, R.: Relating ocean temperatures to frontal ablation rates at Svalbard tidewater glaciers: Insights from glacier proximal datasets. Sci. Rep. 9, 1–11. https://doi.org/10.1038/s41598-019-45077-3, 2019.

Hop, H., Pearson, T., Hegseth, E.N., Kovacs, K.M., Wiencke, C., Kwasniewski, S., Eiane, K., Mehlum, F., Gulliksen, B., Wlodarska-Kowalezuk, M., Lydersen, C., Weslawski, J.M., Cochrane, S., Gabrielsen, G.W., Leakey, R.J.G., Lonne, O.J., Zajaczkowski, M., Falk-Petersen, S., Kendall, M., Wangberg, S.A., Bischof, K., Voronkov, A.Y., Kovaltchouk, N.A., Wiktor, J., Poltermann, M., di Prisco, G., Papucci, C., Gerland, S.: The marine ecosystem of Kongsfjorden, Svalbard. Polar Res. 21, 167–208. https://doi.org/10.3402/polar.v21i1.6480, 2002.

Hop, H., Wiencke, C.: The Ecosystem of Kongsfjorden, Svalbard. Alfred Wegener Institute, Helmholtz Centre for Polar and Marine Research, Bremerhaven, Germany. https://doi.org/10.1007/978-3-319-46425-1_1, 2019 .

Hopwood, M.J., Carroll, D., Dunse, T., Hodson, A., Holding, J.M., Iriarte, J.L., Ribeiro, S., Achterberg, E.P., Cantoni, C., Carlson, D.F., Chierici, M., Clarke, J.S., Cozzi, S., Fransson, A., Juul-Pedersen, T., Winding, M.H.S., Meire, L.: Review article: How does glacier discharge affect marine biogeochemistry and primary production in the Arctic? Cryosphere 14, 1347–1383. https://doi.org/10.5194/tc-14-1347-2020, 2020.

How, P., Benn, D.I., Hulton, N.R.J., Hubbard, B., Luckman, A., Sevestre, H., Pelt, W.J.J.V., Lindbäck, K., Kohler, J., Boot, W.: Rapidly changing subglacial hydrological pathways at a tidewater glacier revealed through simultaneous observations of water pressure, supraglacial lakes, meltwater plumes and surface velocities. Cryosphere 11, 2691–2710. https://doi.org/10.5194/tc-11-2691-2017, 2017.

Howe, J. A., Moreton, S. G., Morri, C. and Morris, P.: Multibeam bathymetry and depositional environments of Kongsfjorden and Krossfjorden, western Spitsbergen, Svalbard, Polar Res., 22(2), 301–316, https://doi.org/10.3402/polar.v22i2.6462, 2003.

Husum, K., Howe, J.A., Baltzer, A., Forwick, M., Jensen, M., Jernas, P., Korsun, S., Miettinen, A., Mohan, R., Morigi, C., Myhre, P.I., Prins, M.A., Skirbekk, K., Sternal, B., Boos, M., Dijkstra, N., Troelstra, S.: The marine sedimentary environments of Kongsfjorden, Svalbard: an archive of polar environmental change. Polar Res. 38, 1–16. https://doi.org/10.33265/polar.v38.3380, 2019.

IPCC Special Report on the Ocean and Cryosphere in a Changing Climate [H.-O. Pörtner, D.C. Roberts, V. Masson-Delmotte, P. Zhai, M. Tignor, E. Poloczanska, K. Mintenbeck, A. Alegría, M. Nicolai, A. Okem, J. Petzold, B. Rama, N.M. Weyer (eds.)]. In press., 2019.

Jauffrais, T., LeKieffre, C., Schweizer, M., Geslin, E., Metzger, E., Bernhard, J.M., Jesus, B., Filipsson, H.L., Maire, O., Meibom, A.: Kleptoplastidic benthic foraminifera from aphotic habitats: insights into assimilation of inorganic C, N and S studied with sub-cellular resolution. Environ. Microbiol. 21, 125–141. https://doi.org/10.1111/1462-2920.14433, 2019.

Jernas, P., Klitgaard-Kristensen, D., Husum, K., Koç, N., Tverberg, V., Loubere, P., Prins, M., Dijkstra, N., Gluchowska, M.: Annual changes in Arctic fjord environment and modern benthic foraminiferal fauna: Evidence from Kongsfjorden, Svalbard. Glob. Planet. Change 163, 119–140. https://doi.org/10.1016/j.gloplacha.2017.11.013, 2018.

Jernas, P., Klitgaard Kristensen, D., Husum, K., Wilson, L., Koç, N.: Palaeoenvironmental changes of the last two millennia on the western and northern Svalbard shelf. Boreas 42, 236–255. https://doi.org/10.1111/j.1502-3885.2012.00293.x, 2013.

Jorissen, F.J., de Stigter, H.C., Widmark, J.G. V.: A conceptual model explaining benthic foraminiferal microhabitats. Mar. Micropaleontol. 26, 3–15. https://doi.org/10.1016/0377-8398(95)00047-X, 1995.

Jorissen, F. J. and Wittling, I.: Ecological evidence from live-dead comparisons of benthic foraminiferal faunas off Cape Blanc (Northwest Africa), Palaeogeogr. Palaeoclimatol. Palaeoecol., 149(1–4), 151–170, https://doi.org/10.1016/S0031-0182(98)00198-9, 1999.

Kedra, M., Kuliński, K., Walkusz, W., Legezyńska, J.: The shallow benthic food web structure in the high Arctic does not follow seasonal changes in the surrounding environment. Estuar. Coast. Shelf Sci. 114, 183–191. https://doi.org/10.1016/j.ecss.2012.08.015, 2012.

Kniazeva, O., Korsun, S.: Seasonal data on Rose Bengal stained foraminifera in the head of Kongsfjorden, Svalbard. Data Br. 25, 104040. https://doi.org/10.1016/j.dib.2019.104040, 2019.

Koho, K.A., Kouwenhoven, T.J., de Stigter, H.C., van der Zwaan, G.J.: Benthic foraminifera in the Nazaré Canyon, Portuguese continental margin: Sedimentary environments and disturbance. Mar. Micropaleontol. 66, 27–51. https://doi.org/10.1016/j.marmicro.2007.07.005, 2007.

Koho, K.A., Piña-Ochoa, E., Geslin, E., Risgaard-Petersen, N.: Vertical migration, nitrate uptake and denitrification: Survival mechanisms of foraminifers (Globobulimina turgida) under low oxygen conditions. FEMS Microbiol. Ecol. 75, 273–283. https://doi.org/10.1111/j.1574-6941.2010.01010.x, 2011.

Korsun, S., Hald, M.: Seasonal dynamics of Benthic Foraminifera in a Glacially Fed Fjord of Svalbard, European Arctic. J. Foraminifer. Res. 30, 251–271. https://doi.org/10.2113/0300251, 2000.

Korsun, S., Hald, M.: Modern benthic foraminifera off Novaya Zemlya tidewater glaciers, Russian Arctic. Arct. Alp. Res. 30, 61–77. https://doi.org/10.2307/1551746, 1998.

Lalande, C., Moriceau, B., Leynaert, A., Morata, N.: Spatial and temporal variability in export fluxes of biogenic matter in Kongsfjorden. Polar Biol. 39, 1725–1738. https://doi.org/10.1007/s00300-016-1903-4, 2016.

Laufer-Meiser, K., Michaud, A.B., Maisch, M., Byrne, J.M., Kappler, A., Patterson, M.O., Røy, H., Jørgensen, B.B.: Potentially bioavailable iron produced through benthic cycling in glaciated Arctic fjords of Svalbard. Nat. Commun. 12, 1–13. https://doi.org/10.1038/s41467-021-21558-w, 2021.

Lea, J.M., Mair, D.W.F., Rea, B.R.: Instruments and Methods: Evaluation of existing and new methods of tracking glacier terminus change. J. Glaciol. 60, 323–332. https://doi.org/10.3189/2014JoG13J061, 2014.

Lind, S., Ingvaldsen, R.B., Furevik, T.: Arctic warming hotspot in the northern Barents Sea linked to declining sea-ice import. Nat. Clim. Chang. 8, 634–639. https://doi.org/10.1038/s41558-018-0205-y, 2018.

Lloyd, J., Kuijpers, A., Long, A., Moros, M., Park, L.A.: Foraminiferal reconstruction of mid- to late-Holocene ocean circulation and climate variability in Disko Bugt, West Greenland. The Holocene 8, 1079–1091. https://doi.org/10.1177/0959683607082548, 2007.

Lloyd, J.M.: Modern Distribution of Benthic Foraminifera From Disko Bugt, West Greenland. J. Foraminifer. Res. 36, 315–331. https://doi.org/10.2113/gsjfr.36.4.315, 2006..

Luckman, A., Benn, D.I., Cottier, F., Bevan, S., Nilsen, F., Inall, M.: Calving rates at tidewater glaciers vary strongly with ocean temperature. Nat. Commun. 6. https://doi.org/10.1038/ncomms9566, 2015.

Lydersen, C., Assmy, P., Falk-Petersen, S., Kohler, J., Kovacs, K.M., Reigstad, M., Steen, H., Strøm, H., Sundfjord, A., Varpe, Ø., Walczowski, W., Weslawski, J.M., Zajaczkowski, M.: The importance of tidewater glaciers for marine mammals and seabirds in Svalbard, Norway. J. Mar. Syst. 129, 452–471. https://doi.org/10.1016/j.jmarsys.2013.09.006, 2014.

Meire, L., Mortensen, J., Meire, P., Juul-Pedersen, T., Sejr, M.K., Rysgaard, S., Nygaard, R., Huybrechts, P., Meysman, F.J.R.: Marine-terminating glaciers sustain high productivity in Greenland fjords. Glob. Chang. Biol. 23, 5344–5357. https://doi.org/10.1111/gcb.13801, 2017.

Meredith, M., M. Sommerkorn, S. Cassotta, C. Derksen, A. Ekaykin, A. Hollowed, G. Kofinas, A. Mackintosh, J. Melbourne-Thomas, M.M.C. Muelbert, G. Ottersen, H. Pritchard, and E.A.G. Schuur.: Polar Regions. In: IPCC Special Report on the Ocean and Cryosphere in a Changing Climate [H.-O. Pörtner, D.C. Roberts, V. Masson-Delmotte, P. Zhai, M. Tignor, E. Poloczanska, K. Mintenbeck, A. Alegría, M. Nicolai, A. Okem, J. Petzold, B. Rama, N.M. Weyer (eds.)]. In press., 2019.

Meslard, F., Bourrin, F., Many, G., Kerhervé, P.: Suspended particle dynamics and fluxes in an Arctic fjord (Kongsfjorden, Svalbard). Estuar. Coast. Shelf Sci. 204, 212–224. https://doi.org/10.1016/j.ecss.2018.02.020, 2018.

Murray, J.W.: Ecology and Application of Benthic Foraminifera. Cambridge University Press, Cambridge, New York. https://doi.org/10.1017/CBO9780511535529, 2006.

Norwegian Polar Institute.: Annual maximum temperature in the West Spitsbergen Current. Environmental monitoring of Svalbard and Jan Mayen (MOSJ). http://www.mosj.no/en/climate/ocean/temperature-salinity-fram-strait.html, 2021.

Oksanen J., F., Blanchet G., Friendly M., Kindt R., Legendre P., McGlinn D., Minchin P.R., O'Hara R. B., Simpson G. L., P. Solymos, Stevens M. Henry H., Szoecs E., and Wagner H..: vegan: Community Ecology Package. R package version 2.5-6. https://CRAN.R-project.org/package=vegan, 2019.

Pasculli, L., Piermattei, V., Madonia, A., Bruzzone, G., Caccia, M., Ferretti, R., Odetti, A., Marcelli, M.: New cost-effective technologies applied to the study of the glacier melting influence on physical and biological processes in Kongsfjorden area (Svalbard). J. Mar. Sci. Eng. 8. https://doi.org/10.3390/JMSE8080593, 2020.

Pavlova O., Gerland S., Hop H.: Changes in Sea-Ice Extent and Thickness in Kongsfjorden, Svalbard (2003–2016). In: Hop H., Wiencke C. (eds) The Ecosystem of Kongsfjorden, Svalbard. Advances in Polar Ecology, vol 2. Springer, Cham. https://doi.org/10.1007/978-3-319-46425-1_4, 2019.

Pawłowska, J., Łącka, M., Kucharska, M., Szymańska, N., Koziorowska, K., Kuliński, K., Zajączkowski, M.: Benthic foraminifera contribution to fjord modern carbon pools: A seasonal study in Adventfjorden, Spitsbergen. Geobiology 15, 704–714. https://doi.org/10.1111/gbi.12242, 2017.

Payne, C.M., Roesler, C.S.: Characterizing the influence of Atlantic water intrusion on water mass formation and phytoplankton distribution in Kongsfjorden, Svalbard. Cont. Shelf Res. 191, 104005. https://doi.org/10.1016/j.csr.2019.104005, 2019.

Piquet, A.M.T., Van De Poll, W.H., Visser, R.J.W., Wiencke, C., Bolhuis, H., Buma, A.G.J.: Springtime phytoplankton dynamics in Arctic Krossfjorden and Kongsfjorden (Spitsbergen) as a function of glacier proximity. Biogeosciences 11, 2263–2279. https://doi.org/10.5194/bg-11-2263-2014, 2014.

Polyakov, I. V., Pnyushkov, A. V., Alkire, M.B., Ashik, I.M., Baumann, T.M., Carmack, E.C., Goszczko, I., Guthrie, J., Ivanov, V. V., Kanzow, T., Krishfield, R., Kwok, R., Sundfjord, A., Morison, J., Rember, R., Yulin, A.: Greater role for Atlantic inflows on sea-ice loss in the Eurasian Basin of the Arctic Ocean. Science (80-.). 356, 285–291. https://doi.org/10.1126/science.aai8204, 2017.

Pramanik, A., Van Pelt, W., Kohler, J., Schuler, T. V.: Simulating climatic mass balance, seasonal snow development and associated freshwater runoff in the Kongsfjord basin, Svalbard (1980-2016). J. Glaciol. 64, 943–956. https://doi.org/10.1017/jog.2018.80, 2018.

R Core Team. R.: A language and environment for statistical computing. R Foundation for Statistical Computing, Vienna, Austria. https://www.R-project.org/, 2020.

Risgaard-Petersen, N., Langezaal, A.M., Ingvardsen, S., Schmid, M.C., Jetten, M.S.M., Op Den Camp, H.J.M., Derksen, J.W.M., Piña-Ochoa, E., Eriksson, S.P., Nielsen, L.P., Revsbech, N.P., Cedhagen, T., Van Der Zwaan, G.J.: Evidence for complete denitrification in a benthic foraminifer. Nature 443, 93–96. https://doi.org/10.1038/nature05070, 2006.

Saloranta, T.M., Svendsen, H.: Across the Arctic front west of Spitsbergen: High-resolution CTD sections from 1998-2000. Polar Res. 20, 177–184. https://doi.org/10.3402/polar.v20i2.6515, 2001.

Schauer, U., Fahrbach, E., Osterhus, S., Rohardt, G.: Arctic warming through the Fram Strait: Oceanic heat transport from 3 years of measurements. J. Geophys. Res. C Ocean. 109, 1–14. https://doi.org/10.1029/2003JC001823, 2004.

Schlitzer, R.: Ocean Data View User's Guide Version 5.3.0, Ocean Data View. Available online at: https://odv.awi.de, 2020.

Schloerke B., Cook D, Larmarange J., Briatte F., Marbach M., Thoen E., Elberg A., and Crowley J.: GGally: Extension to 'ggplot2'. R package version 2.1.0. https://CRAN.R-project.org/package=GGally, 2021 .

Schönfeld, J., Alve, E., Geslin, E., Jorissen, F., Korsun, S., Spezzaferri, S., Abramovich, S., Almogi-Labin, A., du Chatelet, E.A., Barras, C., Bergamin, L., Bicchi, E., Bouchet, V., Cearreta, A., Di Bella, L., Dijkstra, N., Disaro, S.T., Ferraro, L., Frontalini, F., Gennari, G., Golikova, E., Haynert, K., Hess, S., Husum, K., Martins, V., McGann, M., Oron, S., Romano, E., Sousa, S.M., Tsujimoto, A.: The FOBIMO (FOraminiferal BIo-MOnitoring) initiative-Towards a standardised protocol for soft-bottom benthic foraminiferal monitoring studies. Mar. Micropaleontol. 94–95, 1–13. https://doi.org/10.1016/j.marmicro.2012.06.001, 2012.

Screen, J.A., Deser, C., Simmonds, I.: Local and remote controls on observed Arctic warming. Geophys. Res. Lett. 39, 1–5. https://doi.org/10.1029/2012GL051598, 2012.

Screen, J.A., Simmonds, I.: The central role of diminishing sea ice in recent Arctic temperature amplification. Nature 464, 1334–1337. https://doi.org/10.1038/nature09051, 2010.

Seidenkrantz, M.S.: Benthic foraminifera as palaeo sea-ice indicators in the subarctic realm - examples from the Labrador Sea-Baffin Bay region. Quat. Sci. Rev. 79, 135–144. https://doi.org/10.1016/j.quascirev.2013.03.014, 2013.

Shepherd, A.S., Rathburn, A.E., Pérez, M.E.: Living foraminiferal assemblages from the Southern California margin: A comparison of the > 150, 63-150, and > 63 μm fractions. Mar. Micropaleontol. 65, 54–77. https://doi.org/10.1016/j.marmicro.2007.06.001, 2007.

Skirbekk, K., Kristensen, D.K., Rasmussen, T.L., Koç, N., Forwick, M.: Holocene climate variations at the entrance to a warm Arctic fjord: evidence from Kongsfjorden trough, Svalbard. Geol. Soc. London, Spec. Publ. 344, 289–304. https://doi.org/10.1144/SP344.20, 2010.

Stuecker, M.F., Bitz, C.M., Armour, K.C., Proistosescu, C., Kang, S.M., Xie, S.P., Kim, D., McGregor, S., Zhang, W., Zhao, S., Cai, W., Dong, Y., Jin, F.F.: Polar amplification dominated by local forcing and feedbacks. Nat. Clim. Chang. 8, 1076–1081. https://doi.org/10.1038/s41558-018-0339-y, 2018.

Sundfjord, A., Albretsen, J., Kasajima, Y., Skogseth, R., Kohler, J., Nuth, C., Skarðhamar, J., Cottier, F., Nilsen, F., Asplin, L., Gerland, S., Torsvik, T.: Effects of glacier runoff and wind on surface layer dynamics and Atlantic Water exchange in Kongsfjorden, Svalbard; a model study. Estuar. Coast. Shelf Sci. 187, 260–272. https://doi.org/10.1016/j.ecss.2017.01.015, 2017.

Svendsen, H., Beszczynska-Møller, A., Hagen, J.O., Lefauconnier, B., Tverberg, V., Gerland, S., Ørbæk, J.B., Bischof, K., Papucci, C., Zajaczkowski, M., Azzolini, R., Bruland, O., Wiencke, C., Winther, J.-G., Dallmann, W.: The physical environment of Kongsfjorden – Krossfjorden, an Arctic fjord system in Svalbard. Polar Res. 21, 133–166. https://doi.org/10.3402/polar.v21i1.6479, 2002.

Szymańska, N., Pawłowska, J., Kucharska, M., Kujawa, A., Łącka, M., Zajączkowski, M.: Impact of shelf-transformed waters (STW) on foraminiferal assemblages in the outwash and glacial fjords of Adventfjorden and Hornsund, Svalbard. Oceanologia 59, 525–540. https://doi.org/10.1016/j.oceano.2017.04.006, 2017.

Tedstone, A.J., Nienow, P.W., Gourmelen, N., Dehecq, A., Goldberg, D., Hanna, E.: Decadal slowdown of a land-terminating sector of the Greenland Ice Sheet despite warming. Nature 526, 692–695. https://doi.org/10.1038/nature15722, 2015.

Thibault De Chanvalon, A., Metzger, E., Mouret, A., Cesbron, F., Knoery, J., Rozuel, E., Launeau, P., Nardelli, M.P., Jorissen, F.J., Geslin, E.: Two-dimensional distribution of living benthic foraminifera in anoxic sediment layers of an estuarine mudflat (Loire estuary, France). Biogeosciences 12, 6219–6234. https://doi.org/10.5194/bg-12-6219-2015, 2015.

Torsvik, T., Albretsen, J., Sundfjord, A., Kohler, J., Sandvik, A.D., Skarðhamar, J., Lindbäck, K., Everett, A.: Impact of tidewater glacier retreat on the fjord system: Modeling present and future circulation in Kongsfjorden, Svalbard. Estuar. Coast. Shelf Sci. 220, 152–165. https://doi.org/10.1016/j.ecss.2019.02.005, 2019.

Trusel, L.D., Powell, R.D., Cumpston, R.M., Brigham-Grette, J.: Modern glacimarine processes and potential future behaviour of Kronebreen and Kongsvegen polythermal tidewater glaciers, Kongsfjorden, Svalbard. Geol. Soc. Spec. Publ. 344, 89–102. https://doi.org/10.1144/SP344.9, 2010.

Vernet, M., Ellingsen, I.H., Seuthe, L., Slagstad, D., Cape, M.R., Matrai, P.A.: Influence of Phytoplankton Advection on the Productivity Along the Atlantic Water Inflow to the Arctic Ocean. Front. Mar. Sci. 6, 1–18. https://doi.org/10.3389/fmars.2019.00583, 2019.

Vihtakari M.: PlotSvalbard: PlotSvalbard - Plot research data from Svalbard on maps. R package version 0.9.2. https://github.com/MikkoVihtakari/PlotSvalbard, 2020.

Willis, K., Cottier, F., Kwasniewski, S., Wold, A., Falk-Petersen, S.: The influence of advection on zooplankton community composition in an Arctic fjord (Kongsfjorden, Svalbard). J. Mar. Syst. 61, 39–54. https://doi.org/10.1016/j.jmarsys.2005.11.013, 2006.

Wlodarska-Kowalczuk, M., Pearson, T.H., Kendall, M.A.: Benthic response to chronic natural physical disturbance by glacial sedimentation in an Arctic fjord. Mar. Ecol. Prog. Ser. 303, 31–41. https://doi.org/10.3354/meps303031, 2005.

Yu, L., Zhong, S., Vihma, T., Sun, B.: Attribution of late summer early autumn Arctic sea ice decline in recent decades. npj Clim. Atmos. Sci. 4, 1–14. https://doi.org/10.1038/s41612-020-00157-4, 2021.

Zaborska, A., Pempkowiak, J., Papucci, C., 2006. Some Sediment Characteristics and Sedimentation Rates in an Arctic Fjord (Kongsfjorden, Svalbard). Annu. Environ. Prot. 8, 79–96, 2006.

Zwally, H.J., Abdalati, W., Herring, T., Larson, K., Saba, J., Steffen, K.: Surface Melt – Induced Acceleration of Greenland Ice-Sheet Flow. Science, 297, 218–222. https://doi.org/10.1126/science.1072708, 2002.

Supplement Chapter 3

Table S1. Grain size characteristics of the uppermost sediment layer (0-0.5 cm) and of an intermediate layer (2-3 cm) to highlight the main differences among stations and sediment levels.

Stations	Area	Sediment layer (cm)	Sediment type	Mean (µm)	Mode (µm)	D_{10} (µm)	D_{50} (µm)	D_{90} (µm)	Sand (%)	Silt (%)	Clay (%)
St2	**Proximal**	**0-0.5**	Medium Silt	8.8	7.2	1.4	8.9	49.8	5.9	78.7	15.4
		2-3		10.5	37.7 9.3	1.5	11.2	57.6	8.3	78.2	13.5
St7	**Proximal**	**0-0.5**	Medium Silt	6.6	8.2	1.3	7.0	30.8	1.6	80.7	17.7
		2-3		6.9	9.3	1.3	7.4	31.5	2.2	81.0	16.8
St1	**Medial**	**0-0.5**	Medium Silt	6.5	8.2	1.2	7.0	28.9	1.1	81.3	17.6
		2-3		8.4	9.3	1.6	8.8	40.8	5.0	81.8	13.2
St3	**Medial**	**0-0.5**	Medium Silt	6.6	8.2	1.3	7.1	29.1	1.4	81.8	16.8
		2-3		11.0	17.5	2.0	11.7	50.5	6.4	83.7	9.9
St4	**Medial**	**0-0.5**	Medium Silt	6.3	8.2	1.3	6.8	27.1	1.1	81.6	17.3
		2-3		13.2	22.6	2.1	14.0	66.3	11.2	79.9	8.9
St5	**Medial**	**0-0.5**	Medium Silt	6.5	8.2	1.3	7.0	28.3	1.7	81.3	17.0
		2-3		7.7	8.2	1.5	8.0	35.9	3.6	82.3	14.1
St8	**Distal**	**0-0.5**	Medium Silt	8.3	9.3	1.5	8.4	48.9	7.4	78.4	14.3
		2-3		16.3	10.5 62.9	2.5	16.3	95.4	19.2	73.4	7.4
St6	**Distal**	**0-0.5**	Medium Silt	7.7	8.2	1.7	8.0	31.7	2.6	85.0	12.5
		2-3		7.8	8.2	1.7	8.0	33.2	3.3	84.3	12.3
St9	**Distal**	**0-0.5**	Medium Silt	8.4	8.2	1.7	8.5	40.5	5.2	83.1	11.8
		2-3		10.2	8.2	2.0	9.9	54.4	8.1	82.0	9.8

Table S2. Ratios L/(L+D) based on the living faunas from the 0-5 cm layer (>150 µm) and the dead faunas from the 4-5 cm layer (>150 µm). Ratios calculated for St2 and St7 should be evaluated carefully (only 13 and 35 specimens were picked for St2 and St7 respectively).

Stations	St2	St7	St1	St3	St4	St5	St8	St6	St9
Adercotryma glomeratum	NA	NA	NA	NA	0.82	0.47	0.90	0.64	0.59
Astrononion galloway	NA	NA	NA	NA	0.84	NA	0.63	NA	NA
Capsammina bowmanni	1.00	1.00	NA	NA	NA	NA	NA	NA	NA
Cassidulina reniforme	0.06	0.33	0.54	NA	0.25	NA	NA	0.12	NA
Cassidulina sp. morphotype 2	0.00	NA	NA	NA	NA	0.65	NA	NA	NA
Cibicidoides lobatulus	NA	NA	NA	NA	NA	NA	0.38	NA	0.71
Elphidium bartletti	NA	NA	NA	NA	NA	0.01	NA	0.00	NA
Elphidium clavatum	0.04	0.08	0.07	0.02	0.03	NA	NA	0.01	0.00
Globobulimina auriculata	NA	NA	NA	NA	0.97	NA	NA	NA	NA
Labrospira crassimargo	NA	NA	NA	0.05	0.52	0.30	0.10	NA	0.41
Nonionellina labradorica	0.00	NA	0.47	0.81	0.41	0.69	0.73	0.55	0.57
Pyrgo williamsoni	NA	NA	NA	0.21	NA	NA	NA	NA	NA
Quinqueloculina arctica	0.00	NA	NA	NA	NA	NA	NA	NA	NA
Quinqueloculina seminula	NA	NA	NA	NA	NA	1.00	NA	NA	NA
Quinqueloculina stalkeri	0.12	NA	0.32	0.00	NA	0.05	NA	0.24	NA
Recurvoides turbinatus	NA	NA	NA	NA	NA	NA	0.02	NA	NA
Reophax fusiformis	NA	NA	0.63	0.14	0.47	0.39	0.22	NA	NA
Saccammina cf. *sphaerica*	1.00	NA	NA	NA	NA	NA	NA	NA	NA
Siphonaperta agglutinata	NA	NA	NA	NA	NA	0.93	NA	NA	NA
Spiroplectammina biformis	NA	NA	1.00	NA	NA	NA	NA	NA	NA
Textularia earlandi	NA	NA	0.86	NA	NA	NA	NA	NA	NA

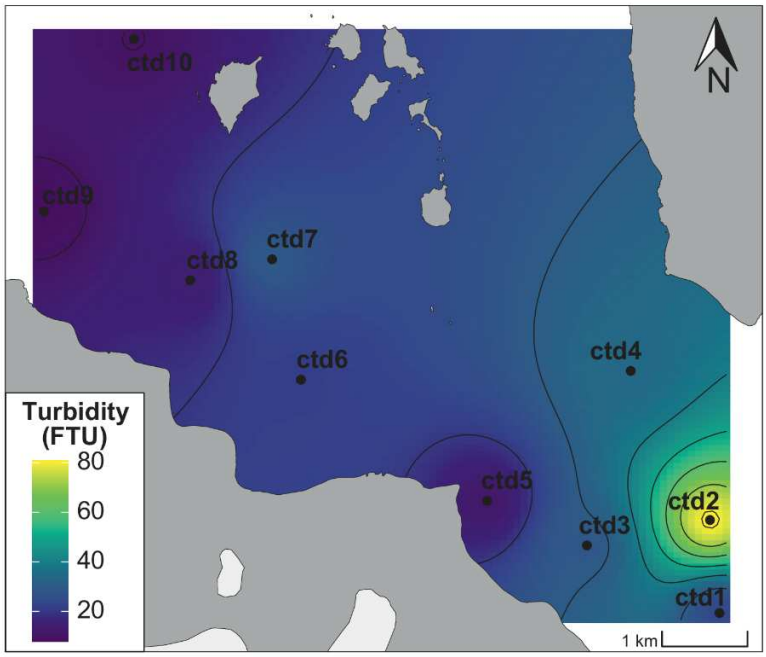

Figure S1. Interpolation map of the mean surface water turbidity (0-20 m water layer) obtained from the CTD casts.

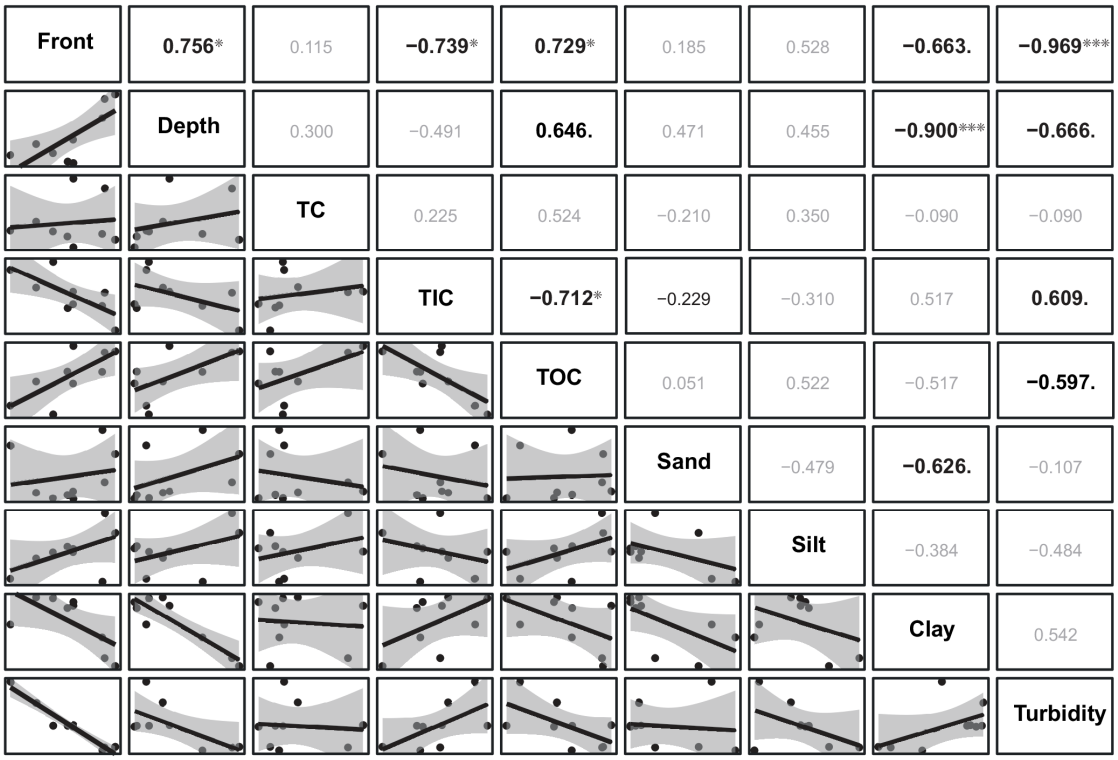

Figure S2. Distributon and correlation between environmental variables measured at each sampling station. Front = distance from the glacier front (km), Depth = sampling water depth (m), TC = Total Carbon (%), TIC = Total Inorganic Carbon (%), TOC = Total Organic Carbon (%), Sand (%), Silt (%), Clay (%), Turbidity = extrapolated mean turbidity in the 0-20 m water column. Significance of p-values is dysplayed as follow: . p<0.1; * p<0.05, p< 0.01, *** p<0.001.

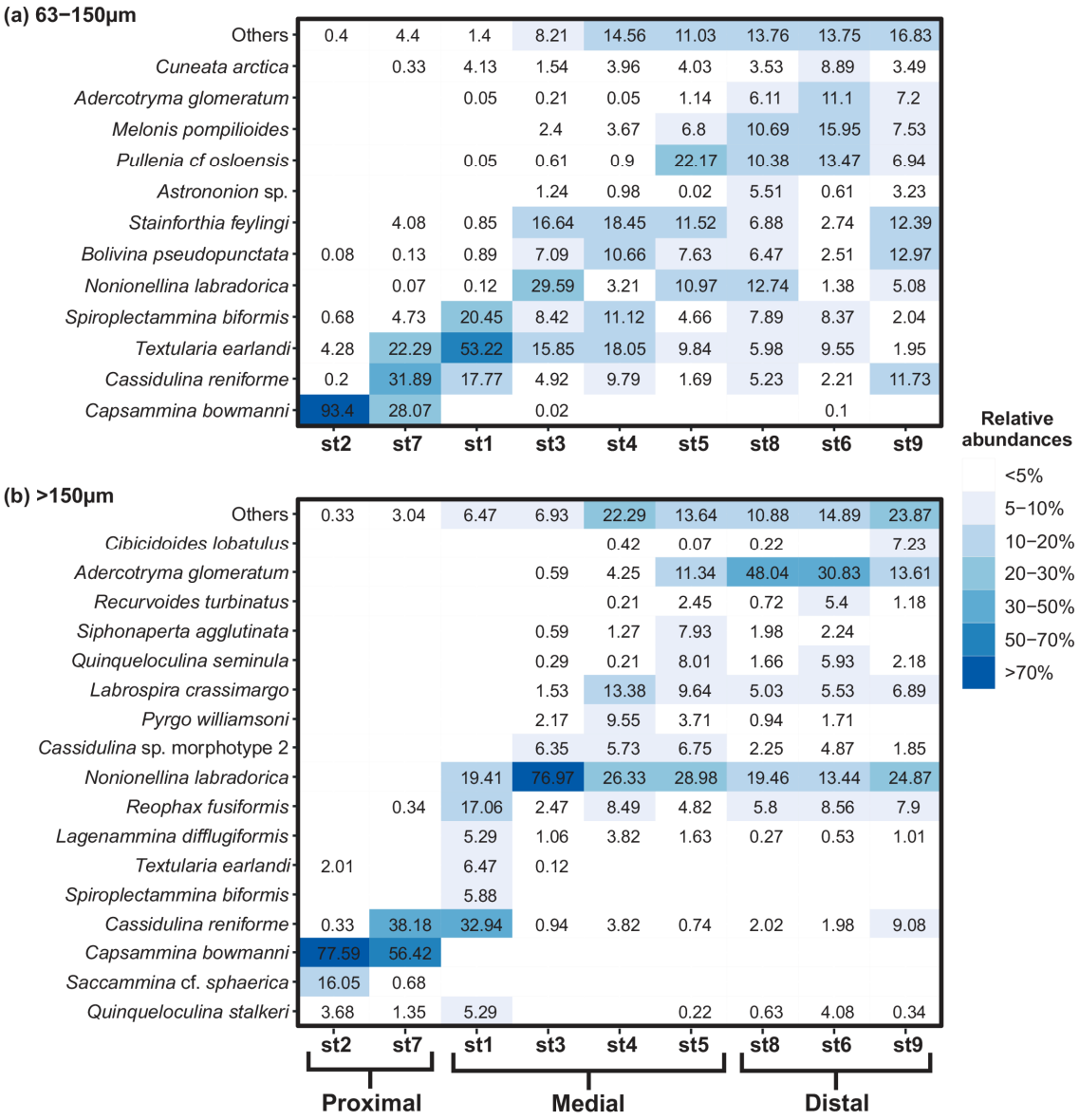

Figure S3. Heatmap showing foraminiferal relative abundances of the major species considering the total living faunas in the 0-1 cm sediment layer for the **(a)** 63-150 µm and **(b)** >150 µm size fractions.

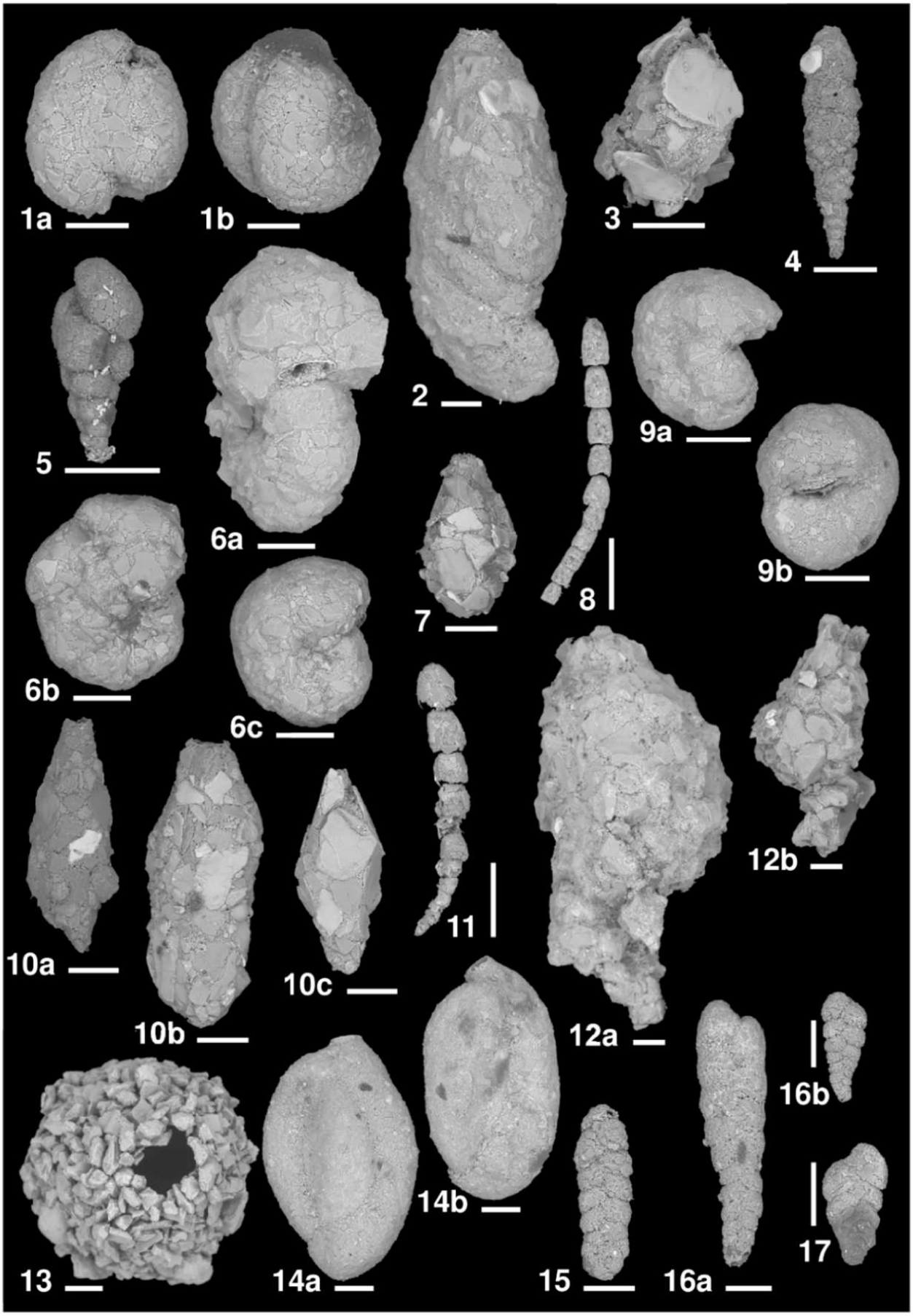

Figure S4. Please see caption in the next page.

Figure S4. Scanning electron micrographs (SEM) of the most relevant agglutinated benthic species from Kongsfjorden (scale bars = 100 μm). **1a,1b.** *Adercotryma glomeratum* (Brady, 1878). **2.** *Ammotium cassis* (Parker, 1870). **3.** *Capsammina bowmanni* (Heron-Allen & Earland, 1912). **4.** *Cuneata arctica* (Brady, 1881). **5.** *Eggerella advena* (Cushman, 1922). **6a, 6b, 6c.** *Labrospira crassimarg*o (Norman, 1892). **7.** *Lagenammina difflugiformis* (Brady, 1879). **8.** *Leptohalysis scottii* (Chaster, 1892). **9a, 9b.** *Recurvoides turbinatus* (Brady, 1881). **10a, 10b, 10c.** *Reophax fusiformis* (Williamson, 1858). **11.** *Reophax catella* Höglund, 1947. **12a, 12b.** *Reophax scorpiurus* Montfort, 1808. **13.** *Saccammina* cf. *sphaerica* Brady, 1871. **14a, 14b.** *Siphonaperta agglutinata* (Cushman, 1917). **15.** *Spiroplectammina biformis* (Parker & Jones, 1865). **16a, 16b.** *Textularia earlandi Parker, 1952.* **17.** *Textularia torquata* Parker, 1952.

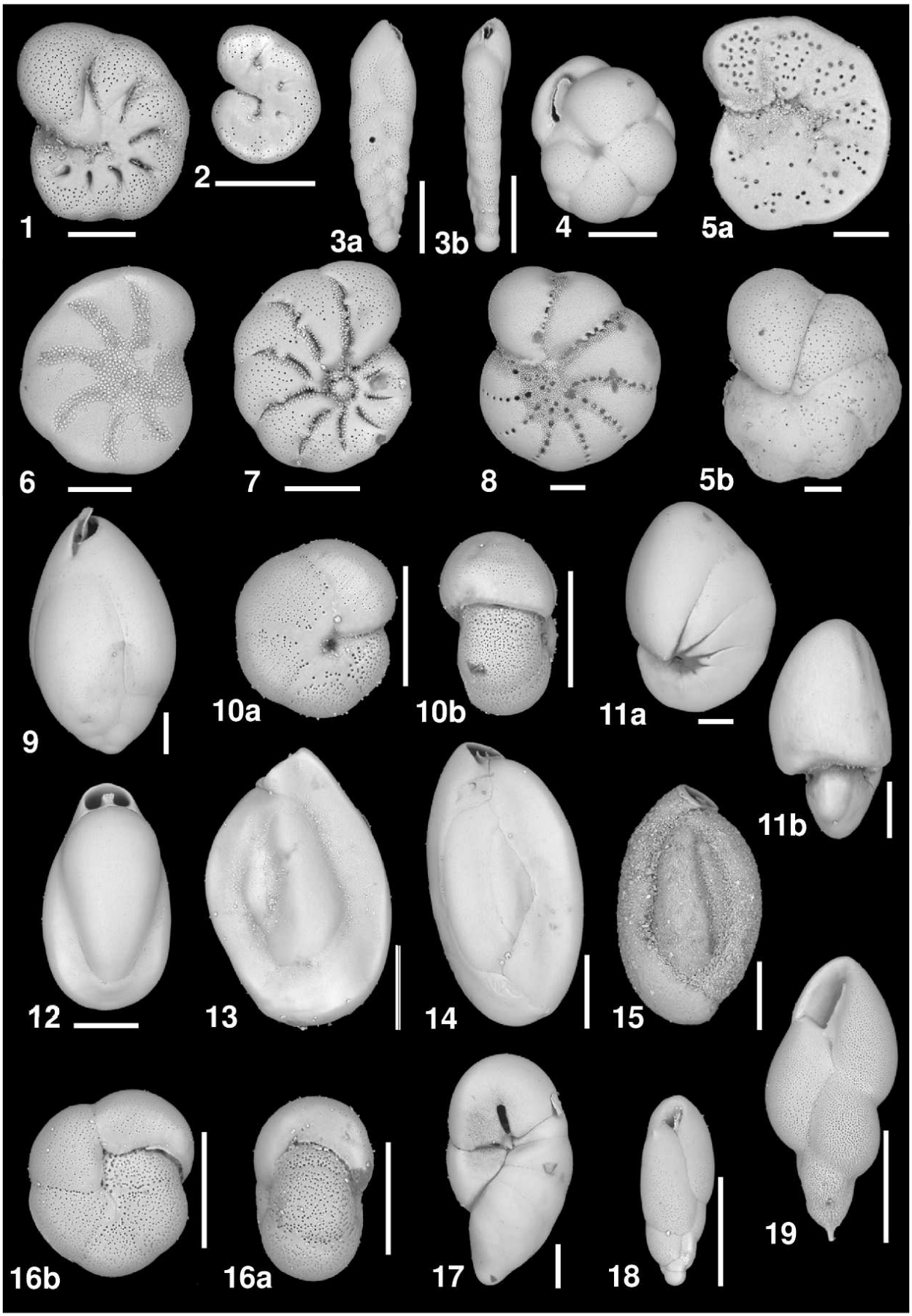

Figure S5. Please see caption in the next page.

Figure S5. Scanning electron micrographs (SEM) of the most relevant calcareous benthic species from Kongsfjorden (scale bars = 100 μm). **1a,1b.** *Astrononion gallowayi* Loeblich & Tappan, 1953. **2.** *Astrononion* sp. Cushman & Edwards, 1937**. 3.** *Bolivina pseudopunctata* Höglund, 1947. **4.** *Cassidulina reniforme* Nørvang, 1945. **5a, 5b.** *Cibicidoides lobatulus* (Walker & Jacob, 1798). **6.** *Cribroelphidium subarcticum* (Cushman, 1944). **7.** *Elphidium clavatum* Cushman, 1930. **8.** *Elphidium bartletti* Cushman, 1933. **9.** *Globobulimina auriculata* (Bailey, 1894). **10a, 10b.** *Melonis pompilioides* (Fichtel & Moll, 1798). **11a, 11b.** *Nonionellina labradorica* (Dawson, 1860). **12.** *Pyrgo williamsoni* (Silvestri, 1923). **13.** *Quinqueloculina arctica* Cushman, 1933. **14.** *Quinqueloculina seminula* (Linnaeus, 1758). **15.** *Quinqueloculina stalkeri* Loeblich & Tappan, 1953. **16a, 16b.** *Pullenia* cf. *osloensis* Feyling-Hanssen, 1954. **17.** *Robertina arctica* d'Orbigny, 1846. **18.** *Stainforthia feylingi* Knudsen & Seidenkrantz, 1994. **19.** *Stainforthia loeblichi* (Feyling-Hanssen, 1954).

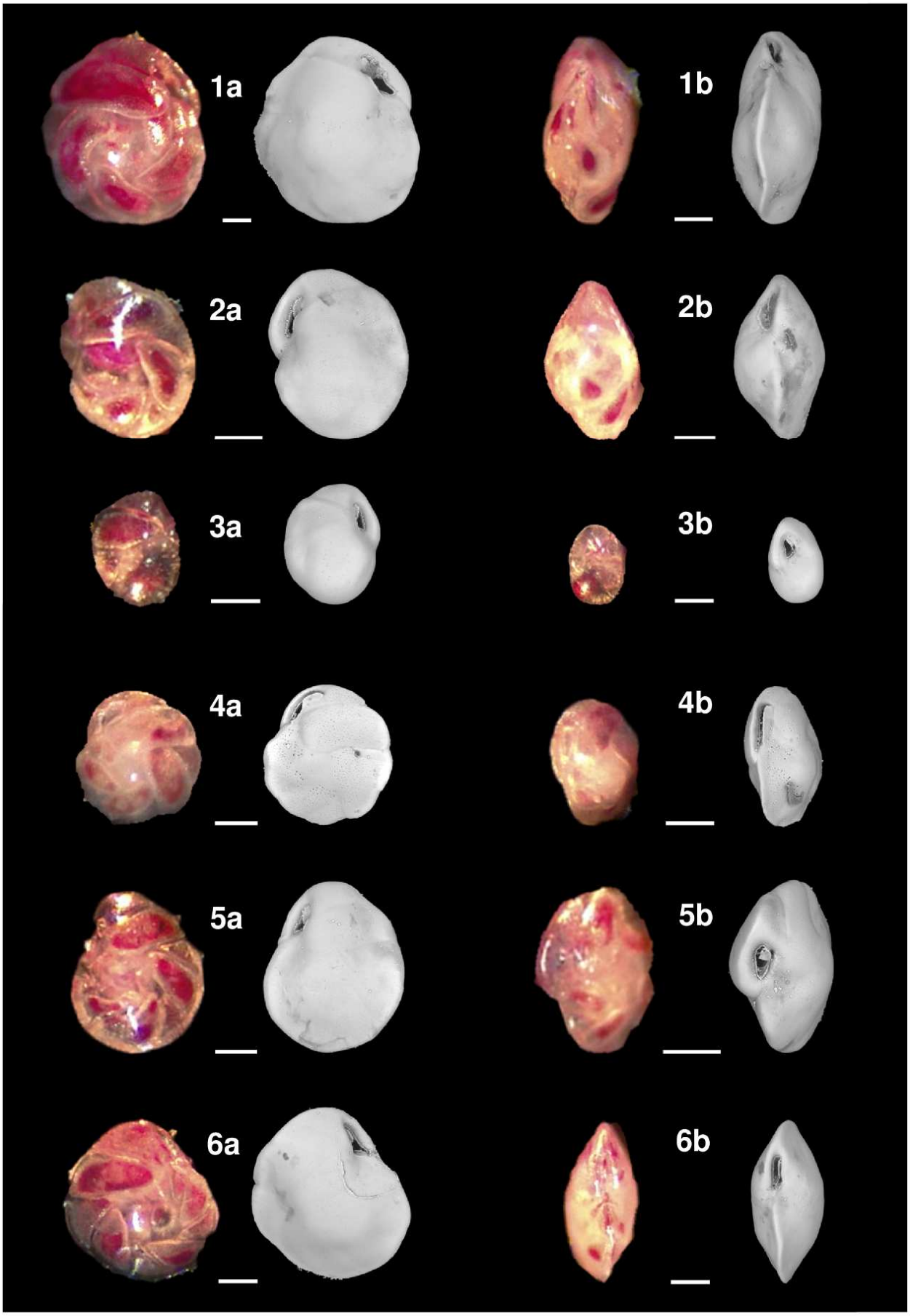

Figure S6. Please see caption in the next page.

Figure S6. Stereomicroscope pictures and scanning electron micrographs (SEM) of side **(a)** and peripheral **(b)** views of *Cassidulina* and *Islandiella* species identified in this study (scale bars = 100 μm). **1a, 1b.** *Cassidulina* sp. morphotype 1. **2a, 2b, 3a, 3b.** *Cassidulina* sp. morphotype 2. **4a, 4b.** *Cassidulina teretis*. **5a, 5b.** *Islandiella helenae.* **6a, 6b.** *Islandiella norcrossi*.

Chapter 4

Foraminiferal taxonomic and functional diversity decreases towards a tidewater glacier front: a promising proxy for glacier retreat

Eleonora Fossile[1#], Mattia Ghilardi[2,3#], Meryem Mojtahid[1], Hélène Howa[1], Agnes Baltzer[4], Maria Pia Nardelli[1]

[1] *Laboratoire de Planétologie et Géosciences, Université d'Angers, Nantes Université, Le Mans Université, CNRS UMR 6112, Angers, France*

[2] *Reef Systems Research Group, Department of Ecology, Leibniz Centre for Tropical Marine Research (ZMT), Fahrenheitstraße 6, 28359 Bremen, Germany*

[3] *Department of Marine Ecology, Faculty of Biology and Chemistry, University of Bremen, Leobener Str. UFT, 28359 Bremen, Germany*

[4] *LETG, UMR CNRS 6554, University of Nantes, Campus du Tertre, 44312 Nantes Cedex 3, France*

[#]These authors contributed equally to this work

Abstract

Benthic foraminifera, worldwide distributed single-celled protists, are widely used in biomonitoring and paleoenvironmental studies due to their prompt responses to environmental changes. However, to date, research has only relied on taxonomic diversity patterns, thus lacking a direct link to ecosystem functioning. Functional trait analysis provides a better understanding of biodiversity responses to environmental perturbations and their influence on ecosystem functions and services. Tidewater-glacier fjord systems are extremely sensitive to climate change and subjected to strong seasonal gradients (e.g., temperature, salinity, turbidity, organic inputs). As such, they are ideal for investigating diversity patterns along steep environmental gradients and developing proxies for biodiversity responses to glacier retreat. Here, we investigate benthic foraminiferal taxonomic and functional diversity along a gradient of decreased environmental stress from the Kronebreen tidewater glacier front in Kongsfjorden (Svalbard). We assessed foraminiferal biodiversity using four size assemblages (i.e., >63, >100, >125, and >150 µm) to test a potential size bias on diversity patterns. In all size assemblages, we observed a general increase in both taxonomic and functional diversity with increasing distance from the glacier front. Only the regularity component was not captured by the largest fraction (i.e., >150 µm). We hypothesise that reduced glacier-induced disturbance far from the front increases the availability of ecological niches, which in turn allow the establishment of species occupying different regions of the functional space. Few stress-tolerant and/or opportunistic species are able to exploit the "hostile" environment near the front (e.g., freshwater and sediment inputs, reduced organic fluxes), whereas the progressive development of more equilibrated and diverse communities far from the front, indicate improved environmental conditions (e.g., reduced physical disturbance, increased primary productivity). The progressive diversity loss observed towards the tidewater glacier front may be a potential ecological proxy for glacier retreat in historical reconstructions.

Keywords: benthic foraminifera, biodiversity response, functional traits, size fraction, fjord, Arctic

1. Introduction

Benthic foraminifera are protists widely distributed in all marine environments, from coastal areas to abyssal plains. Besides their ubiquity and high density in marine sediments, short life cycles and specific ecological requirements allow foraminifera to respond rapidly to environmental changes. Therefore, foraminiferal abundances, species composition, and taxonomic diversity are widely used to evaluate present environmental conditions (e.g., Hallock et al., 2003; Koukousioura et al., 2011; Bouchet et al., 2012, 2018; Hallock, 2012; Schönfeld et al., 2012; Dimiza et al., 2016; Jorissen et al., 2018) and trace past changes (e.g., Murray, 1991, 2006; Schmiedl, 2019). However, taxonomic metrics provide only an incomplete picture of biodiversity patterns (Villéger et al., 2010).

Species' roles in the ecosystem are defined by specific functional traits determining species' response to environmental conditions (Villéger et al., 2010). A functional trait includes any physiological, morphological and phenological characteristics that influence the ecological performance of an individual, or, in other words, indirectly influence the fitness by affecting growth, reproduction and survival (McGill et al., 2006; Violle et al., 2007; Dawson et al., 2021). Therefore, the investigation of trait-based diversity can help better constrain the description of environmental perturbations (Mouillot et al., 2013). The importance of functional diversity (FD; i.e., the diversity of traits between organisms; Carmona et al., 2016) in understanding community responses to environmental changes has been demonstrated for several taxonomic groups (e.g., Thuiller et al., 2006; Buisson et al., 2013; Brown et al., 2018; Marcisz et al., 2020). However, the application of trait-based approaches to foraminiferal communities remains underdeveloped (e.g., Cleary and Renema, 2007; Manasa et al., 2016; Saraswat et al., 2018) due to limited knowledge on the relationship between organismal traits and ecological functions. Nevertheless, morphological traits integrate both functional and evolutionary information (Wainwright and Reilly, 1994).

Areas with natural environmental gradients are ideal to investigate species responses to environmental changes. Fjords, as semi-enclosed marine basins characteristic of high latitude coasts, are typical examples of environments subjected to strong physical and biogeochemical gradients on relatively small (i.e., decametric to kilometric) spatial scale (Howe et al., 2010; Bianchi et al., 2020). This is particularly the case for glaciated fjords, where marine-terminating glaciers discharge high amounts of meltwater and associated sediment load at the continent-sea interface (e.g., Svendsen et al., 2002; Meslard et al., 2018). Consequently, near tidewater glacier fronts, fresh organic inputs to the seafloor are low due to high water turbidity hampering

primary production (e.g., Lalande et al., 2016; Meslard et al., 2018; Hop and Wiencke, 2019; Hopwood et al., 2020). This generates seasonal chronicle physico-chemical disturbances (e.g., high sedimentation rates, low salinity waters) affecting benthic compartments (e.g.,Włodarska-Kowalczuk et al., 2005, 2013; Cauvy-Fraunié and Dangles, 2019). Among benthic organisms, foraminifera are particularly sensitive to these perturbations. For instance, Fossile et al. (Chapter 3) observed the succession of assemblages along a gradient created by tidewater glacier dynamics which weakens with increasing distance from the front, and further suggested to investigate diversity patterns as potential proxy for glacier retreat.

The development of robust ecological proxy applicable on fossil assemblages requires a deep knowledge of present foraminiferal ecology and bias determined by different methodological approaches. Particularly, a common divergence in foraminiferal studies is the size fraction investigated. While some studies focus on the >150 µm fraction (see Schönfeld, 2012 and references therein), the FOraminiferal BIo-Monitoring (FOBIMO) protocol (Schönfeld et al., 2012) suggests the analysis of the >125 µm fraction for biomonitoring studies, and to eventually consider the 63-125 µm fraction for specific cases. However, traditionally, the >125 µm fraction is rarely used in paleoenvironmental studies determining a mismatch between living- and fossil-based studies (Lo Giudice Cappelli and Austin, 2019). For instance, in the Arctic Region, living assemblages are often reported for the >100 µm (e.g., Hald and Korsun, 1997; Ivanova et al., 2008; Husum et al., 2015; Kujawa et al., 2021), >106 µm (e.g., Jennings et al., 2004; Saher et al., 2009, 2012; Jernas et al., 2018), or >125 µm (e.g., Korsun and Hald, 1998; Rytter et al., 2002; Forwick et al., 2010) fraction, with a few studies also analysing the fraction 63-150 µm (e.g., Fossile et al., 2020, *Chapter 3*; Caridi et al., 2021), and the same inconsistency is observed in paleoenvironmental studies (e.g., >100 µm: Skirbekk et al., 2010; Rasmussen and Thomsen, 2014; Chauhan et al., 2016; Pawlowska et al., 2016; El bani Altuna et al., 2020; >106 µm: Jernas et al., 2013; >125 µm: Rasmussen et al., 2012; >150 µm: Bartels et al., 2018). However, the use of different fractions skews the analysis of foraminiferal abundances, taxonomic and morphological compositions (e.g., elongated taxa or small opportunists are not retained by larger meshes), as well as resultant taxonomic and functional diversity calculations, with potential implications on ecological interpretations. Therefore, the development of a reliable proxy requires to investigate the bias caused by the chosen size fraction.

The present study focuses on a 10 km longitudinal transect in the Artic fjord Kongsfjorden (Svalbard), starting close to the Kronebreen glacier terminus at the fjord head. In Fossile et al. (*Chapter 3*) we explored benthic foraminiferal assemblages from the surface sediment along the transect and their distribution in relation to environmental gradients forced at the inner end-

member by tidewater glacier dynamics. Here, we investigate how the abundance, size structure, community composition, taxonomic and functional diversity of living benthic foraminifera vary in relation to the distance from the glacier front. We further test whether analysing foraminiferal communities at different resolutions (i.e., different size fractions: >63, >100, >125, and >150 µm) alters the patterns observed at the highest resolution (>63 µm) and, therefore, the ecological interpretations. Thus, we identify the size fraction which represents the best trade-off between methodological effort and accuracy of results. Lastly, we propose the most suitable ecological metrics as promising proxy for glacier retreat.

2. Study area

Kongsfjorden is a glaciomarine fjord (20 km long and 4-10 km wide) located on the north western coast of Spitsbergen (79°N, 12° E) in the Svalbard archipelago (Fig. 1). The fjord is subjected to strong seasonality, and it is influenced by two major oceanographic drivers: the Atlantic Water (AW) intrusion from the shelf, and tidewater-glacier associated Arctic water masses in the innermost part (e.g., Svendsen et al., 2002; Hop and Wiencke, 2019). The geographical location of the fjord and the absence of a well-defined sill (Howe et al., 2003) allow oceanic intrusion of AW from the Fram strait (Svendsen et al., 2002). Indeed, the West Spitsbergen Current (WSC, a branch of the North Atlantic Current) flows on the western margin of the archipelago transporting the AW, which is the main heat source for the Arctic Ocean (e.g., Schauer et al., 2004).

Five tidewater (marine-terminating) glaciers (Blomstrandbreen, Conwaybreen, Kongsbreen, Kronebreen and Kongsvegen; Fig. 1) calve into the fjord. Tidewater glaciers are major sources of sedimentation and freshwater through meltwater discharges during summer, while a minor contribution comes from continental glaciers (land-terminating) covering the mountain range running along the southern coast of the fjord (Svendsen et al., 2002). In particular, the Kronebreen, a fast-flowing glacier with one of the highest flux rates in the Svalbard (winter speed of 1.5-2 m d^{-1} and 3-4 m d^{-1} peaks in summer; Luckman et al., 2015), discharges high amounts of meltwater and associated sediment into the fjord during the melting season (Svendsen et al., 2002). This forms a plume of fresh and turbid meltwaters spreading in the inner part of the fjord (Meslard et al., 2018). The meltwater turbid plume hampers primary production through light limitation, thus affecting carbon fluxes to the seafloor, and increases inorganic particle deposition at the glacier front (e.g., Lalande et al., 2016; Bischof et al., 2019; Halbach et al., 2019; Payne and Roesler, 2019). During the melting season, sediment and

freshwater discharges, combined with the warm and salty AW inflow, establish environmental gradients along the main fjord axis with great influences on the benthic environment (Hop and Wiencke, 2019).

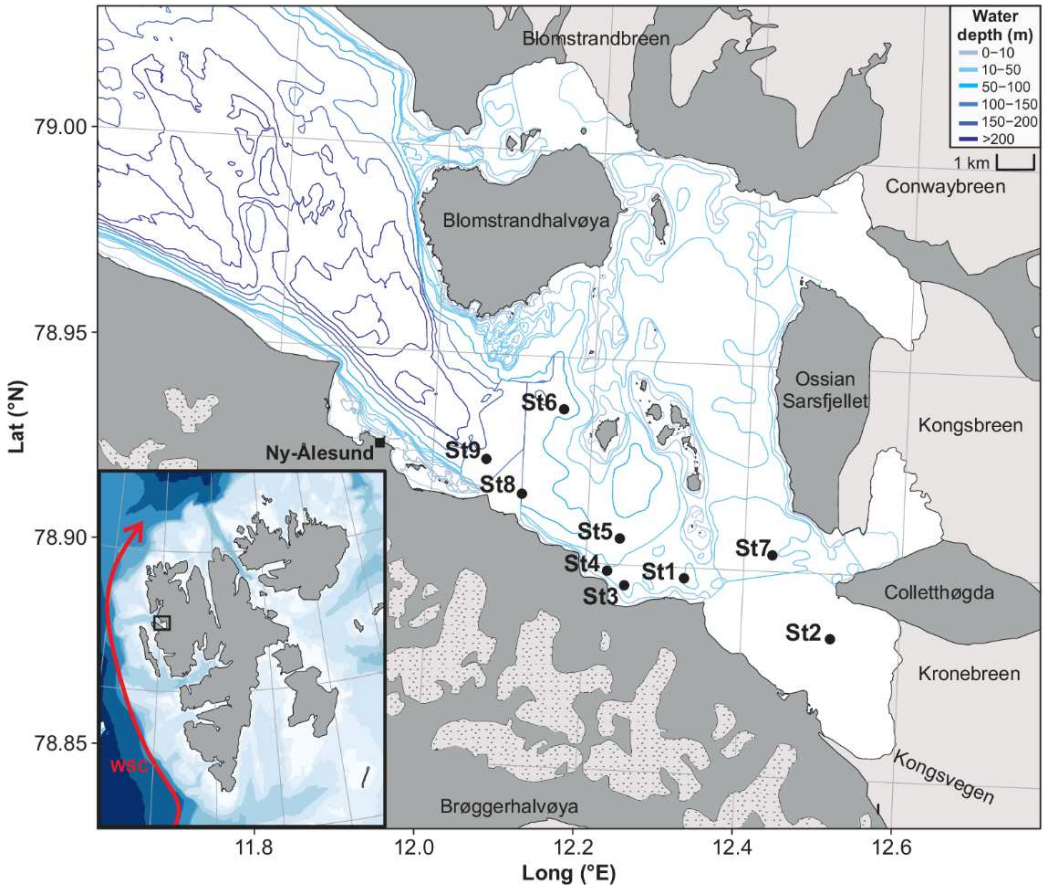

Figure 1. Kongsfjorden map showing the nine stations sampled in August 2018 along a SW-NE transect (black dots) and the five tidewater glaciers flowing in the fjord (light grey); continental (land-terminating) glaciers are represented in dotted grey. On the bottom left of the panel, a map of Svalbard archipelago showing West Spitsbergen Current (WSC) transporting Atlantic Water (AW). The map was produced with the R package *PlotSvalbard* (Vihtakari, 2020).

3. Material and methods

3.1 Sediment sampling and processing

Nine interface sediment cores (9 cm inner diameter) were sampled along a longitudinal (SE-NW) transect of about 10 km length in Kongsfjorden, starting at about 2 km from the terminus of the Kronebreen glacier (Fig. 1, Table 1) during the KING18 mission (August 2018, R/V: Aztec Lady and Teinsten) as reported in Fossile et al., (Chapter 3). For each station we calculated the linear distance from the glacier front (for detailed methodology see Fossile et al., *Chapter 3*).

Station	Sampling date	Latitude (N)	Longitude (E)	Sampling depth (m)	Distance from the front (km)
St2	21/08/2018	78°53.053'	12°30.780'	49	1.92
St7	22/08/2018	78°54.239'	12°26.142'	68	4.53
St1	21/08/2018	78°53.847'	12°19.520'	52	6.22
St3	21/08/2018	78°53.705'	12°15.006'	38	7.68
St4	22/08/2018	78°53.905'	12°13.657'	35.5	8.25
St5	22/08/2018	78°54.382'	12°14.511'	75.7	8.25
St8	22/08/2018	78°54.966'	12°06.917'	114	11.18
St6	22/08/2018	78°56.241'	12°09.806'	148	11.43
St9	22/08/2018	78°55.447'	12°04.086'	156	12.47

Table 1. Sampling date, coordinates, and sampling water depth of the nine sampling stations. Stations are displayed based on the distance from the glacier front.

As detailed in Fossile et al. (*Chapter 3*), immediately after recovery, the interface cores were sliced horizontally to collect the uppermost five centimetres of sediment (0-0.5, 0.5-1, 1-1.5, 1.5-2, 2-3, 3-4, and 4-5 cm), then stored in bottles with 95% ethanol with 2 $g.L^{-1}$ of Rose Bengal stain. In the laboratory, the uppermost two sediment layers (i.e., 0-0.5, 0.5-1 cm) were sieved through 63, 100, 125 and 150 µm meshes and the residues were stored in 95% ethanol.

Living (Rose Bengal stained) foraminifera were picked from all four different size fractions (63-100, 100-125, 125-150, and >150 µm) and identified to the highest taxonomic level. All living specimens from the >150 µm fraction were hand-picked in water. Samples with high foraminiferal abundances from the remaining fractions were dried at 50°C, split with an Otto Microsplitter, and hand-sorted to reach a minimum of 300 individuals from a whole subsample, then standardised to the entire sample.

3.2 Foraminiferal analyses

3.2.1 Foraminiferal abundance and size structure

We combined foraminiferal counts of the first two sediment layers (0-0.5, 0.5-1 cm), and calculated the total abundance for four cumulative size fractions (i.e., >63 µm = the sum of the four size fractions; >100 µm = 100-125 µm + 125-150 µm + >150 µm; >125 µm = 125-150 µm + >150 µm; >150 µm alone). Abundances were then standardised to 50 cm^3. Furthermore, to investigate the size structure of the communities, the relative contribution of each individual size fraction (i.e., 63-100, 100-125, 125-150, and >150 µm) to the total community (i.e., >63 µm) was calculated for each station.

3.2.2 Community composition

To examine how species compositions vary among stations and size fractions, a species-by-sample matrix was created indicating the abundance of each species in each of the 36 analysed samples (i.e., nine stations per four cumulative size fractions). The matrix was used to perform a non-metric multidimensional scaling (nMDS) ordination (stress = 0.085) with Bray-Curtis dissimilarity of the square root transformed data. Convex hull polygons for the four cumulative size fractions were constructed and overlayed to the ordination plot. nMDS ordination was carried out with the function *metaMDS()* in the R package *vegan* (Oksanen et al., 2019).

4. Results

4.1 Foraminiferal abundance and size structure

Total living foraminiferal abundances (i.e., >63 µm) spanned between about 1,400 ind. 50 cm^{-3} and 6,300 ind. 50 cm^{-3}. No significant relationship was detected between total abundance and distance from the glacier front for any of the four cumulative size fractions (i.e., >63, >100, >125, and >150 µm) (Fig. 2a). However, the size structure of foraminiferal communities varied across the gradient (Fig. 2b). Specifically, the relative contribution of the finest fraction (63-100 µm) increased from about 20 to 60 % with increasing distance from the glacier front (p = 0.001) to the detriment of the contribution of the 125-150 µm fraction that decreased rapidly from about 50 to 10 % (p < 0.001). Conversely, the proportions of the 100-125 and >150 µm fractions did not vary significantly (p = 0.53, p = 0.29, respectively) (Fig. 2b).

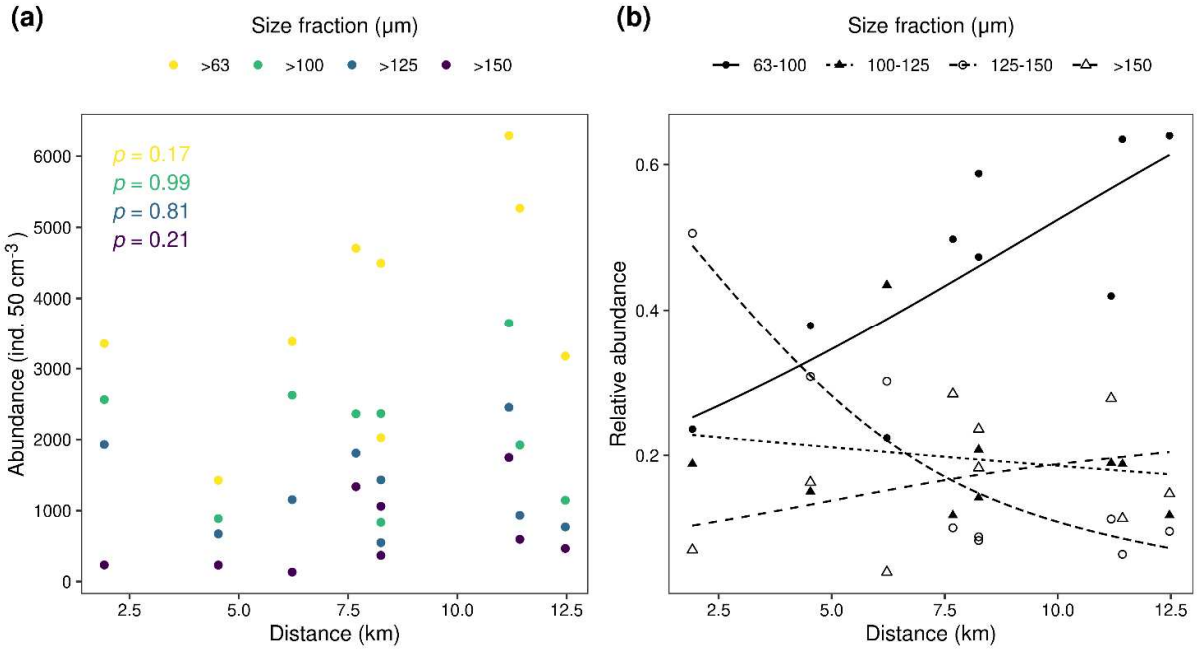

Figure 2. (a) Relationship between foraminiferal abundances (ind. 50 cm^{-3}) and distance from the glacier front for four cumulative size fractions (i.e., >63, >100, >125, and >150 µm); *p*-values refer to linear regression models. **(b)** Relationships between the relative abundance of four individual size fractions (63-100, 100-125, 125-150, and >150 µm) and distance from the glacier front.

4.2 Community composition

Dissimilarities among foraminiferal communities at different fraction resolution were investigated with a nMDS analysis (Fig. 3). The first dimension of the nMDS (NMDS1) separates the three stations closer to the glacier front (i.e., St2, St7, and St1) from all other stations, whereas the second dimension separates the cumulative size fractions of each station (Fig. 3a). Furthermore, the minimum convex hulls plotted per cumulative size fraction show decreased dissimilarity with increased fraction resolution (i.e., the area of the polygon decreases) (Fig. 3a). Foraminiferal composition was strongly related to the distance from the glacier front, as indicated by the significant linear relationship with the NMDS1, which was consistent among all cumulative size fractions (Fig. 3b).

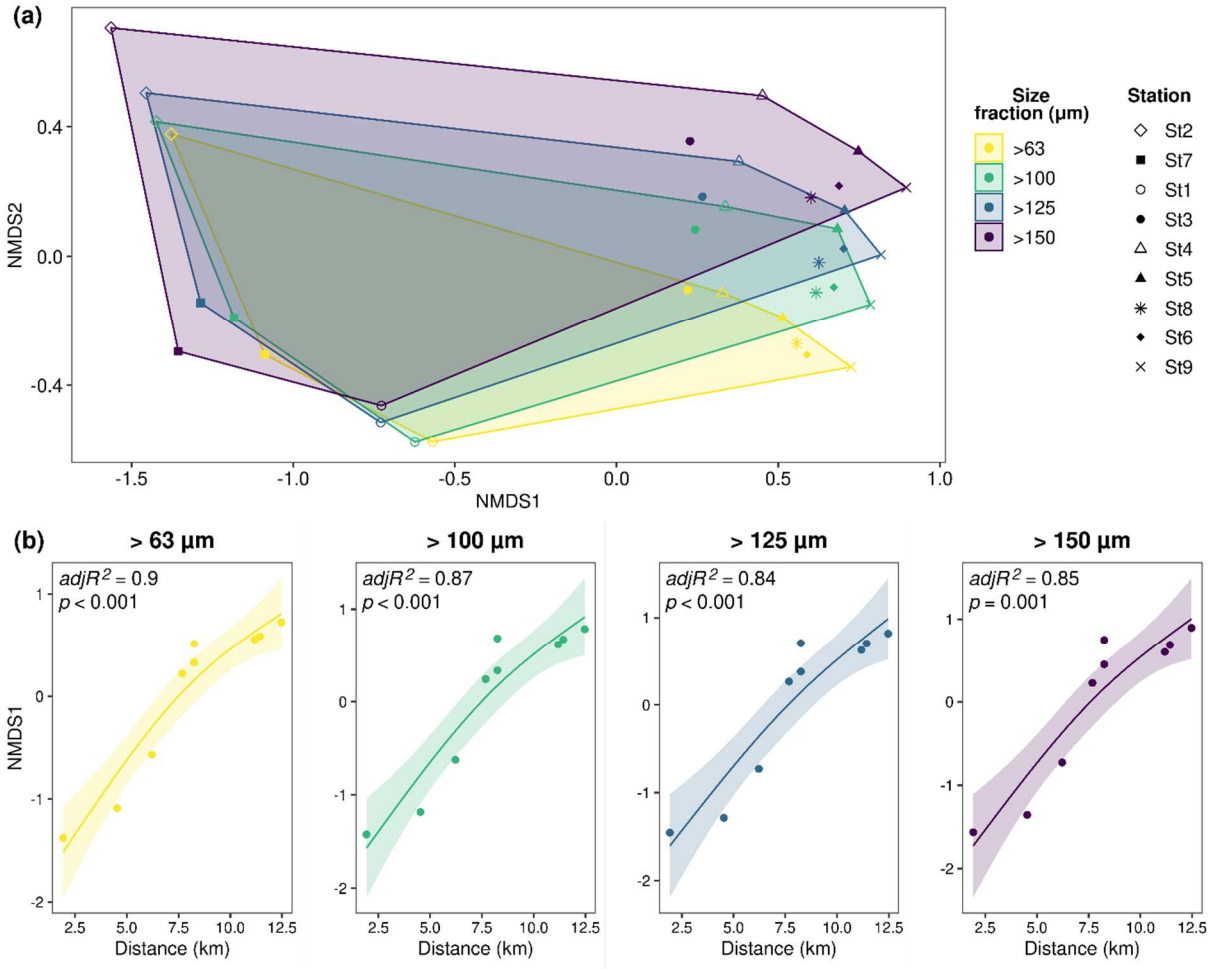

Figure 3. (a) nMDS ordination plot (stress = 0.085) based on 36 samples (i.e., 9 stations x 4 cumulative size fractions). Coloured polygons show the minimum convex hull plotted per

cumulative size fraction. **(b)** Relationship between the first dimension of the nMDS (i.e., NMDS1) and distance from the glacier front for each of the four cumulative size fractions (>63, >100, >125, and >150 µm). Dots depict the raw data, dark lines represent the average model estimate, and ribbons around the estimate represent ±2SE for the GAMs.

4.3 Correlations between diversity metrics calculated at different resolution

The correlation between diversity metrics calculated at the highest (>63 µm) and at lower (>100, >125, and >150 µm) resolution showed a progressive decreasing trend (Fig. 4). All cumulative fractions yielded values of S and F_{Ric} significantly highly correlated with those calculated with the >63 µm fraction (r = 0.984-0.999 and r = 0.987-0.997 for S and F_{Ric}, respectively). A similar result was observed for H', although values obtained with the largest fraction (>150 µm) were slightly less correlated (r = 0.815). Conversely, while comparable results were obtained using foraminiferal communities at the highest (>63 µm) and intermediate resolution (i.e., >100, >125 µm) for J, F_{Eve}, and Rao, the largest fraction (>150 µm) largely failed to obtain values of these metrics correlated with those at the highest resolution (r < 0.57 and non-significantly different from 0).

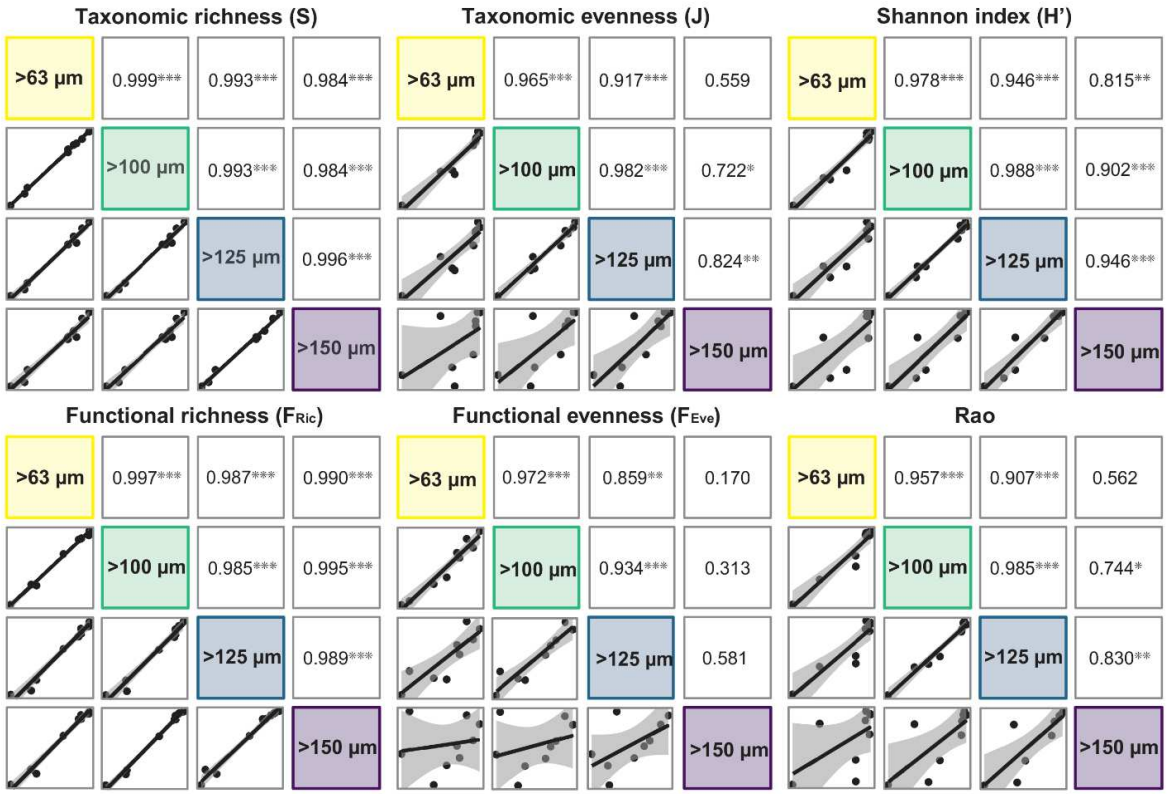

Figure 4. Pairwise Pearson's correlations among taxonomic and functional metrics calculated based on the four cumulative size fractions (>63, >100, >125, and >150 µm). Significance of p-values is displayed as follow: * p < 0.05, ** p < 0.01, *** p < 0.001.

4.4 Relationship between diversity metrics and distance from tidewater glacier front

Foraminiferal taxonomic and functional diversity increased with increasing distance from the glacier front (Fig. 5). At the highest resolution (i.e., >63 µm), a threefold linear increase along the transect was observed for J and Rao but less pronounced for F_{Eve}. On the contrary, non-linear relationships better described the patterns for S, F_{Ric}, and H' (Fig. 5, Table S3). The latter three metrics showed a steep increase between 3 and 7 km from the front and reached a plateau at approximately 8 km. For all diversity metrics similar patterns were detected by the >100 µm, and >125 µm fractions. Conversely, the >150 µm fraction compared to the highest resolution showed similar patterns for S and F_{Ric} and slight differences for H' and Rao, but completely failed to detect patterns in J and F_{Eve} ($p > 0.05$). Relative functional redundancy was generally low (<0.1) and did not show a clear pattern along the transect with the highest value at the intermediate station St1. However, results were consistent among size fractions (Fig. S1).

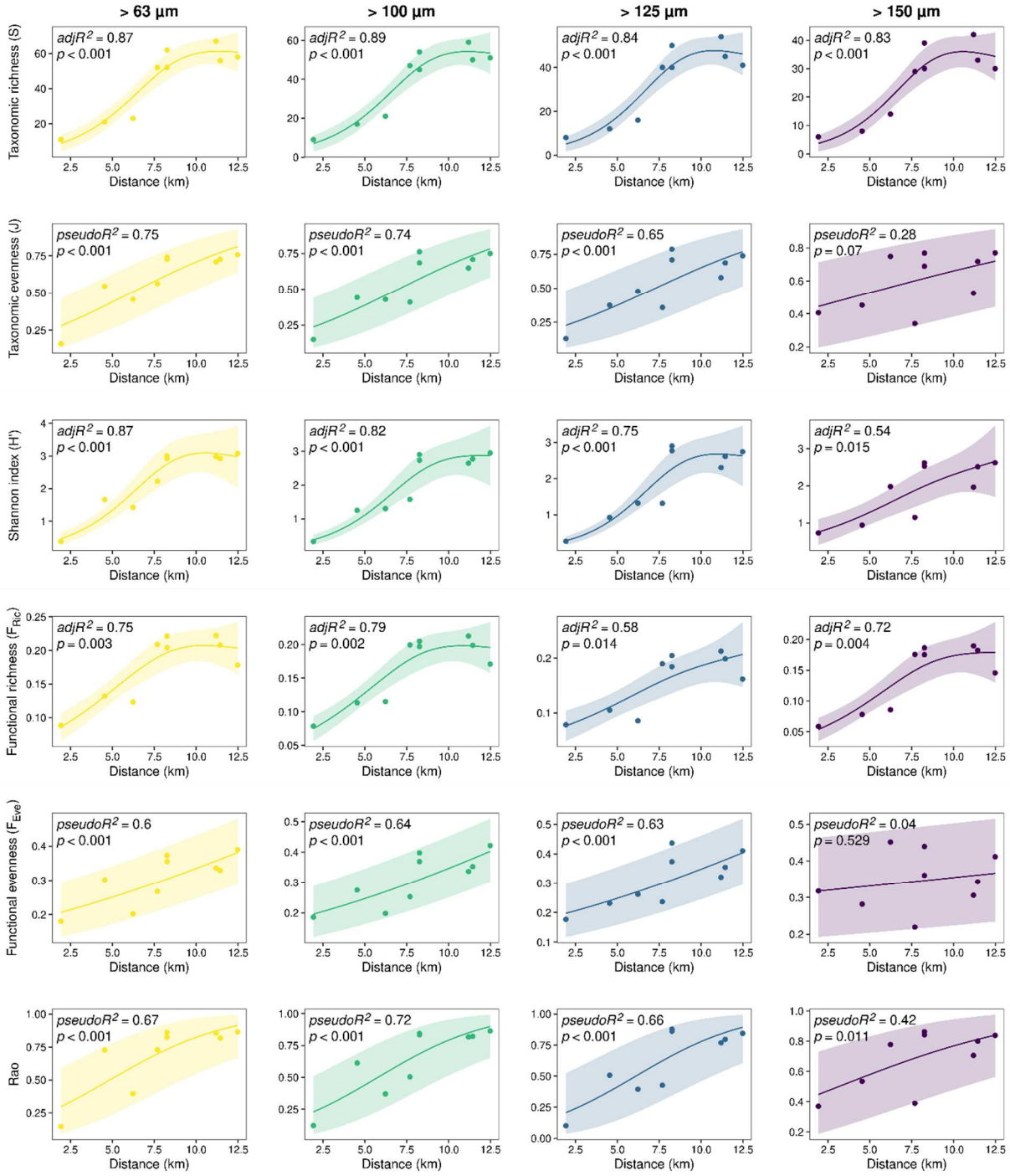

Figure 5. Relationships between taxonomic and functional diversity metrics and distance from the glacier front for each of the four cumulative size fractions (from left to right: >63, >100, >125, and >150 µm). Dots depict the raw data, while dark lines represent the average model estimate. The ribbons around the estimate represent ±2SE for GAMs, or the 2.5 and 97.5 percentiles for GLMs. In each panel the adjusted or pseudo R^2 (for GAMs and GLMs, respectively) and the *p*-value are displayed.

3.2.3 Diversity metrics

Several taxonomic and functional diversity metrics were calculated for each cumulative size fraction (i.e., >63, >100, >125, and >150 µm). Taxonomic diversity was estimated using three

metrics: 1) taxonomic richness (S; i.e., number of species); 2) Shannon Index (H') calculated as

$$H' = -\sum_{i=1}^{S} p_i \ln p_i \quad \text{(i)}$$

where p_i is the proportion of each species i in the community; and 3) taxonomic evenness (Pielou's evenness, J) calculated as

$$J = \frac{H'}{\ln S} \quad \text{(ii)}$$

To estimate foraminiferal functional diversity (FD), the functional strategy of each species was characterised using six categorical and binary traits: test material (calcareous or agglutinated), test shape (rounded, ovoid, elongated or irregular), symmetry/asymmetry of the test, presence/absence of pores, tooth (none, single tooth, teeth-like tubercles), and number of chambers (monothalamous, polythalamous). The relationship between morphological traits and ecological functions is detailed in Table S1, while the assignment of the functional traits for each species can be found in Table S2.

The Gower distance (Gower, 1971) was used to build a multi-trait dissimilarity matrix based on the six functional traits. In order to obtain a dissimilarity matrix with uniform contributions of all the traits, the R package *gawdis* was used (de Bello et al., 2020). Then, a Principal Coordinate Analysis (PCoA) was performed on the dissimilarity matrix to identify the main axes of functional trait variation. The first three axis of the PCoA (representing 79% of the total variance) were retained; this reduced space is hereinafter referred to as functional space.

Functional richness (F_{Ric}; i.e., the amount of the functional space occupied by the species in a community), functional evenness (F_{Eve}; i.e., the regularity in the distribution of species abundances in the functional space of a community), and Rao's quadratic entropy (Rao; i.e., the dissimilarity between two randomly chosen individuals from a community; Botta-Dukát, 2005) were computed using the R package *TPD* (Carmona et al., 2019a, 2019b). The distribution probability of each species in the functional space was estimated using the *TPDsMean()* function calculating a multivariate normal distribution centred in the species coordinates and bandwidth chosen using *Hpi.diag()* function in the R package *ks* (Duong, 2007; Duong, 2020). The probability density of each species was calculated separately for each of 125,000 equal-sized cells in which the three-dimensional functional space was divided (i.e., a grid 50x50x50). The combination of the individual distribution probabilities of each species in a community together with their abundances result in the trait probability density function of

that community in the functional space (Carmona et al., 2016, 2019a). The *REND()* function was then used to compute the F_{Ric} and F_{Eve} of each community (Carmona et al. 2019a, 2019b), while the dissimilarity-based index Rao was calculated using overlap-based functional dissimilarity between all pairs of species in a community with the help of the *dissim()* and *Rao()* functions (Carmona et al., 2016, 2019a). Moreover, to evaluate vulnerability to species loss the functional redundancy of each community (i.e., the average number of species that could be removed from a community without reducing its functional volume) was calculated using the *redundancy()* function. Functional redundancy was then expressed in relative terms by dividing it by the maximum possible value (i.e., number of species minus one), which represents the proportion of the community that could be removed without reducing its functional volume (Carmona et al., 2016, 2019a; Galland et al., 2020).

3.3 Statistical analyses

The relationships between all foraminiferal descriptors (i.e., abundances, size structure, species composition, taxonomic and functional diversity) and the distance from the glacier front were investigated. For each cumulative abundance (i.e., >63, >100, >125, and >150 µm), a linear model (LM) and a generalised additive model (GAM) with *Gaussian* error distribution were fitted to investigate linear and non-linear responses to distance from the glacier front. Models were then compared using Akaike's Information Criterion corrected for small sample size (AIC_c) with the R package *MuMIn* (Bartoń, 2020), where the best fit had the lowest AIC_c score. When LM and GAM were equally supported (i.e., $\Delta AIC_c < 2$; Burnham and Anderson, 2004) model selection was performed by visual inspection of goodness of fit plots. To investigate how foraminiferal size structure changes in relation to the distance from the glacier front, a GAM with *Beta* error distribution was performed using the relative proportion of each individual size fraction as response variable. Both the intercept and smooth terms were allowed to vary among fractions.

Then, the relationship between the first dimension of the nMDS and the distance from the glacier front was analysed to assess the variation in species composition along the gradient. As for species abundances, a LM and GAM with *Gaussian* error distribution were fitted for each cumulative size fraction and the best models were selected based on AIC_c scores and visual inspection of goodness of fit plots.

To investigate whether measuring biodiversity using communities at different resolutions yield similar results, we analysed the Pearson's correlation between the values of each diversity

metric (taxonomic and functional) calculated with different cumulative size fractions. Then, the relationships between each diversity metric calculated for the four cumulative size fractions and the distance from the glacier front were investigated. For each metric, a generalised linear model (GLM) and a GAM were fitted and compared using AIC_c. We modelled S using a *Poisson* error distribution with log link function, while we used a *Beta* distribution with logit link function for J, F_{eve}, and Rao, and a *Gamma* distribution with log link function for H' and F_{Ric}.

All LMs and GLMs were fitted using the R packages *stats* (R Core Team, 2020) and *betareg* (Cribari-Neto and Zeileis, 2010), whereas GAMs were fitted with the R package *mgcv* (Wood, 2017) using cubic regression splines with the minimum basis dimension (i.e., k = 3) to avoid overfitting. All analyses were performed with the software R (version 4.0.0; R core team, 2020), relying heavily on the packages within the *tidyverse* ecosystem (Wickam et al., 2019) for data wrangling and plotting.

5. Discussion

5.1 Foraminiferal responses to glacier induced disturbance

The disturbance created by tidewater glaciers in fjords generally affects the abundance and diversity of multiple taxonomic groups, such as annelids, echinoderms, cnidarians, arthropods and foraminifers (Cauvy-Fraunié and Dangles, 2019). In the present study, the absence of trend in the overall foraminiferal abundances in surface sediments from the inner Kongsfjorden (Svalbard) would suggest that the standing stocks are not influenced by the glacier-induced disturbance (GID; Włodarska-Kowalczuk et al., 2005). However, the decreasing intensity of the GID with distance from the Kronebreen front resulted in clear patterns in size structure, species composition, taxonomic and functional diversity of benthic foraminiferal faunas. Indeed, as distance from the glacier front increased, the foraminiferal smallest size fraction (i.e., 63-100 µm) dominated, and community compositions changed. In parallel, taxonomic and functional richness, and Shannon index increased rapidly within a few kilometres from the front and remained stable from about 8 km distance. Conversely, taxonomic and functional evenness, and Rao increased more linearly. This suggests that the progressively reduced disturbance along the gradient favoured the establishment of more diverse and equilibrated communities. This is coherent with the observation of a succession of different foraminiferal communities, with few stress-tolerant and/or opportunistic species restricted to the sediment surface in the glacier proximal area, and more diversified assemblages with complex microhabitats further away (Fig. S2; Fossile et al., *Chapter 3*). Similar patterns in taxonomic diversity, with values decreasing

towards glacier fronts, were observed for benthic foraminiferal assemblages in other Arctic fjords (e.g., Korsun et al., 1995; Korsun and Hald, 2000; Włodarska-Kowalczuk et al., 2013). Furthermore, other benthic organisms, such as macrofauna, displayed similar diversity trends which were attributed to the GID (e.g., Włodarska-Kowalczuk and Pearson, 2004; Włodarska-Kowalczuk et al., 2005, 2013, 2016; Kedra et al., 2010; Nandan et al., 2016).

The threefold increase in the occupied functional space volume along the environmental gradient suggests that the total niche space available to the community increased as GID decreases. This allowed the establishment of functionally diverse species which occupy different regions of the functional space. However, taxonomic and functional richness were strongly positively correlated ($r = 0.96$), indicating that the number of functional entities (i.e., unique combinations of traits) increased linearly with the number of species. This means that a few redundant species were present (Micheli and Halpern, 2005). Indeed, relative functional redundancy was generally low along the gradient (<0.1; Fig. S1), suggesting that each cell of the functional space grid is occupied by a single or few species (Carmona et al. 2016). Therefore, despite an increase in ecological functions performed by benthic foraminifera away from the glacier front, these functions are weakly represented and thus likely vulnerable to species loss.

The low taxonomic evenness in proximity of the Kronebreen front reiterates the fact that a few stress-tolerant and/or opportunistic species dominate in this highly disturbed domain, characterised by high sedimentation rate and low primary productivity (e.g., Meslard et al., 2018; Hopwood et al., 2020). Moreover, the low functional evenness suggests that these dominant species occupy a restricted area of the functional space (mainly characterised by agglutinated, monothalamous, rounded, asymmetrical foraminifera without teeth and pores; Fig. S3), while the majority of the niche space is occupied by rare species (Mason et al., 2005). Although rare species increase the niche space of the communities in proximity of the front, potentially increasing the functions supported by benthic foraminifera, they are unlikely to support such functions due to their very low abundances. On the contrary, the higher taxonomic and functional evenness at increased distance from the front, suggests that the communities in this area are not only more diverse but also more homogeneous, both in terms of species abundance and their distribution in the functional space. Indeed, the strong increase in Rao with decreasing GID highlights a higher average trait dissimilarity between individuals (de Bello et al., 2016) and, therefore, an increased probability to encounter individuals occupying different part of the functional space.

5.2 Effect of sampling resolution on biodiversity patterns

The spatial patterns in foraminiferal abundance and community composition observed at the highest resolution (i.e., >63 µm) were consistently detected regardless of the resolution at which the analysis was carried out. Particularly, foraminiferal communities at lower resolutions displayed increased dissimilarity while maintaining the relationships with the distance from the glacier front (Fig. 3). On the contrary, patterns in biodiversity were not always identified when the analysis was performed at the lowest resolution (i.e., >150 µm). Specifically, taxonomic and functional evenness, and Rao measured at the lowest resolution were not correlated with those measured at the highest resolution. This resulted in a failure to capture the spatial patterns in taxonomic and functional evenness and, partially, in Shannon index and Rao, which showed more linear relationships than those observed at the highest resolution. Therefore, our results show that analysing foraminifera at the >150 µm fraction may lead to distort patterns in some metrics of taxonomic and functional diversity and misinterpretation of the ecological patterns. Nevertheless, both the >100 and >125 µm fractions were able to capture the spatial variability in all considered diversity metrics.

Other studies have compared foraminiferal communities and taxonomic diversity among size fractions (e.g., Weinkauf and Milker, 2018; Lo Giudice Cappelli and Austin, 2019; Fossile et al., 2020; Klootwijk and Alve, 2022). The general conclusion was that results and trends were similar between small and large fractions, supporting the use of the large fraction (either >125 or >150 µm depending on the study) in comparable studies. In comparison, our detailed analysis (i.e., based on four cumulative size fractions and including a range of taxonomic and functional diversity metrics) allowed us to detect important size effects on biodiversity metrics and conclusions drawn about environmental patterns. However, these effects were limited to the lowest resolution analysed here. This suggests that, although an increased resolution can give a more holistic view of biodiversity across time or space, the >125 µm fraction can provide correct ecological interpretations of foraminiferal composition and diversity along environmental gradients while containing the required analytical effort. Thus, we suggest the use of this size fraction to study benthic foraminiferal distribution in Arctic fjord environments. This work adds to an increasing body of literature (Weinkauf and Milker, 2018; Lo Giudice Cappelli and Austin, 2019; Klootwijk and Alve, 2022) to suggest the use of the >125 µm fraction in both biomonitoring and paleoenvironmental studies, thus extending recommendations of the FOBIMO group (Schönfeld et al., 2012).

5.3 Foraminiferal biodiversity as potential proxy for glacier retreat

Our findings have important implications in reconstructing past tidewater glacier retreat and thus improve related future predictions (e.g., Slater et al., 2019). In this regard, we show that several taxonomic and functional diversity metrics are strongly related to the distance from the glacier front. Therefore, they can potentially be used in reconstructing past tidewater glacier front positions and, consequently, glacier retreat. As the investigated metrics provide complementary information on benthic foraminiferal responses to glacier distance, it is advisable to use multiple diversity metrics to reconstruct glacier retreat. Specifically, we suggest focusing on both taxonomic and functional diversity and on both metrics which do or do not account for species abundance. This is particularly important along historical archives where taphonomic processes may alter the observed biodiversity patterns in living benthic foraminifera.

While past environmental conditions are often inferred using indicator species (e.g., Jackson et al., 2021; Tesi et al., 2021), the application of diversity metrics has the advantage of considering the whole community, including minor species, and being independent of species identity, which can vary in space and time. This also facilitates their use by less experienced researchers as potential taxonomic misidentification would not affect the results. Nevertheless, taxonomic composition can be investigated in parallel to the diversity analysis as it may provide additional support to the interpretation of glacier retreat (e.g., glacier proximal indicator).

As both biodiversity and GID intensity vary seasonally and among fjords (e.g., Hopwood et al., 2020), the use of biodiversity metrics as proxy for glacier retreat remains, at present, mainly applicable in a qualitative way through the identification of trends. However, the observation of periods of steep increase in biodiversity (mainly taxonomic and functional diversity, and Shannon Index) followed by stable values, may allow a more semi-quantitative estimation of glacier front position (i.e., about 5-7 km from the sampling site at the time in which the inflection point is observed, and about 8-10 km at the time in which biodiversity stabilises). Further investigation of foraminiferal biodiversity patterns in other fjords influenced by tidewater glaciers is necessary to build more robust models with direct quantitative application.

Although the proposed ecological proxy is promising, the spatial range of our data is relatively limited (i.e., 1.9-12.5 km). Therefore, future studies should aim to enlarge it and increase the sampling resolution, particularly where the gradient is the steepest, to improve models' predictions. Nevertheless, we covered the area with the greatest variability in GID (Fossile et al., *Chapter 3*). Furthermore, the biodiversity patterns presented here are

representative of the summer season when the GID is at its peak. However, the communities present throughout the year are recorded in historical archives, thus potentially altering the patterns observed. A validation of the proposed ecological proxy and its robustness to taphonomic processes is therefore required.

6. Conclusions

In this study we explored benthic foraminiferal biodiversity along a natural environmental gradient created by tidewater glacier dynamics in Kongsfjorden. Benthic foraminiferal biodiversity and the bias introduced by the selected size fraction were analysed to find the best ecological proxy to reconstruct past tidewater glacier retreat. Clear biodiversity patterns were established in response to glacier-induced disturbance (GID). Foraminiferal taxonomic and functional diversity increased with increasing distance from the glacier front. Few stress-tolerant and/or opportunistic species characterised by a specific combination of traits (i.e., agglutinated, monothalamous, rounded, asymmetrical foraminifera without teeth and pores) were able to occupy the glacier proximal environment. Conversely, ameliorated conditions allowed the development of more equilibrated and diversified foraminiferal communities away from the front. These results were generally consistent among four different cumulative size fractions investigated. However, some patterns were not, or only partially, captured by the largest size fraction (i.e., >150 µm). Based on our findings the >125 µm appears as the best compromise between accuracy in ecological interpretation and analytical effort. Taxonomic and functional diversity metrics are promising indicators of distance from tidewater glacier front and, therefore, as ecological proxy to reconstruct glacier retreat along historical and paleoenvironmental time scales. We thus suggest testing the effectiveness of the proposed proxy on an historical record in front of a tidewater glacier front to validate our findings. Lastly, our study paves the way to the use of functional diversity in parallel to classical taxonomic metrics in foraminiferal studies. This would allow to obtain a comprehensive view of diversity without neglecting the ecosystem functioning.

Data availability. Raw data are from Fossile et al. (*Chapter 3*) and will be published in the online repository PANGAEA upon acceptance of the manuscript. Values of foraminiferal diversity metrics computed for four cumulative size fractions are reported in the Supplement section (Table S4).

Supplement. Tables S1, S2, S3 and Figures S1, S2 and S3 can be find in the Supplement section.

Author contributions. EF, MG: conceptualisation, data curation, formal analysis, investigation, methodology, validation, visualisation, writing-original draft, writing-review & editing. MM, MPN and HH: funding acquisition, investigation, resources, supervision, validation, writing-review & editing. AB: funding acquisition, resources.

Acknowledgements. This project benefits from the technical support of the AWIPEV French - German Arctic Research *Base at Ny-Ålesund*.

Financial support. The field campaign was organised into the frame of IPEV logistic project C3 (Coasts under Climate Change3). The authors sincerely thank the crew and tourists of the sailing boat Aztec Lady and Hugues De Lauzon for the precious technical support during sampling. Sediment sampling and analyses were funded by BiSMART project (University of Angers). This research is part of the PhD thesis of Eleonora Fossile, which is co-funded by French National Program MOPGA (Make Our Planet Great Again) and the University of Angers.

Competing interests. The authors declare that they have no conflict of interest.

References

Austin, H. A., Austin, W. E. N. and Paterson, D. M.: Extracellular cracking and content removal of the benthic diatom Pleurosigma angulatum (Quekett) by the benthic foraminifera Haynesina germanica (Ehrenberg), Mar. Micropaleontol., 57(3–4), 68–73, https://doi.org/10.1016/j.marmicro.2005.07.002, 2005.

Bartels, M., Titschack, J., Fahl, K., Stein, R. and Hebbeln, D.: Wahlenbergfjord, eastern Svalbard: a glacier-surrounded fjord reflecting regional hydrographic variability during the Holocene?, Boreas, 47(4), 1003–1021, https://doi.org/10.1111/bor.12325, 2018.

Bartoń, K.: MuMIn: Multi-Model Inference. R package version 1.43.17, https://CRAN.R-project.org/package=MuMIn, 2020

Bianchi, T. S., Arndt, S., Austin, W. E. N., Benn, D. I., Bertrand, S., Cui, X., Faust, J. C., Koziorowska-Makuch, K., Moy, C. M., Savage, C., Smeaton, C., Smith, R. W. and Syvitski, J.: Fjords as Aquatic Critical Zones (ACZs), Earth-Science Rev., 203(February), 103145, https://doi.org/10.1016/j.earscirev.2020.103145, 2020.

Bischof K., Convey P., Duarte P., Gattuso J.-P., Granberg M., Hop H., Hoppe C., Jiménez C., Lisitsyn L., Martinez B., Roleda M.Y., Thor P., Wiktor J.M., Gabrielsen G.W.: Chapter 14: Kongsfjorden as harbinger of the future Arctic: knowns, unknowns and research priorities. In: Hop H, Wiencke C (eds) The ecosystem of Kongsfjorden, Svalbard, pp. 537-562. Springer Nature Switzerland AG, 2019

Botta-Dukát, Z.: Rao's quadratic entropy as a measure of functional diversity based on multiple traits, J. Veg. Sci., 16(5), 533, https://doi.org/10.1658/1100-9233(2005)16[533:rqeaam]2.0.co;2, 2005.

Bouchet, V. M. P., Alve, E., Rygg, B. and Telford, R. J.: Benthic foraminifera provide a promising tool for ecological quality assessment of marine waters, Ecol. Indic., 23(2012), 66–75, https://doi.org/10.1016/j.ecolind.2012.03.011, 2012.

Bouchet, V. M. P., Goberville, E. and Frontalini, F.: Benthic foraminifera to assess Ecological Quality Statuses in Italian transitional waters, Ecol. Indic., 84(January 2017), 130–139, https://doi.org/10.1016/j.ecolind.2017.07.055, 2018.

Bowser, S. S., Gooday, A. J., Alexander, S. P. and Bernhard, J. M.: Larger agglutinated foraminifera of McMurdo Sound, Antarctica: Are Astrammina rara and Notodendrodes antarctikos allogromiids incognito?, Mar. Micropaleontol., 26(1–4), 75–88, https://doi.org/10.1016/0377-8398(95)00024-0, 1995.

Brown, L. E., Khamis, K., Wilkes, M., Blaen, P., Brittain, J. E., Carrivick, J. L., Fell, S., Friberg, N., Füreder, L., Gislason, G. M., Hainie, S., Hannah, D. M., James, W. H. M., Lencioni, V., Olafsson, J. S., Robinson, C. T., Saltveit, S. J., Thompson, C. and Milner, A. M.: Functional diversity and community assembly of river invertebrates show globally consistent responses to decreasing glacier cover, Nat. Ecol. Evol., 2(2), 325–333, https://doi.org/10.1038/s41559-017-0426-x, 2018.

Buisson, L., Grenouillet, G., Villéger, S., Canal, J. and Laffaille, P.: Toward a loss of functional diversity in stream fish assemblages under climate change, Glob. Chang. Biol., 19(2), 387–400, https://doi.org/10.1111/gcb.12056, 2013.

Burnham, K. P. and Anderson, D. R.: Multimodel inference: Understanding AIC and BIC in model selection, Sociol. Methods Res., 33(2), 261–304, https://doi.org/10.1177/0049124104268644, 2004.

Caridi, F., Sabbatini, A., Bensi, M., Kovačević, V., Lucchi, R. G., Morigi, C., Povea, P. and Negri, A.: Benthic foraminiferal assemblages and environmental drivers along the Kveithola Trough (NW Barents Sea), J. Mar. Syst., 224(August), https://doi.org/10.1016/j.jmarsys.2021.103616, 2021.

Carmona, C. P., de Bello, F., Mason, N. W. H. and Lepš, J.: Traits Without Borders: Integrating Functional Diversity Across Scales, Trends Ecol. Evol., 31(5), 382–394, https://doi.org/10.1016/j.tree.2016.02.003, 2016.

Carmona, C. P., de Bello, F., Mason, N. W. H. and Lepš, J.: Trait probability density (TPD): measuring functional diversity across scales based on TPD with R, Ecology, 100(12), 1–8, https://doi.org/10.1002/ecy.2876, 2019a.

Carmona, C. P.: TPD: Methods for Measuring Functional Diversity Based on Trait Probability Density. R package version 1.1.0. https://CRAN.R-project.org/package=TPD, 2019b.

Cauvy-Fraunié, S. and Dangles, O.: A global synthesis of biodiversity responses to glacier retreat, Nat. Ecol. Evol., 3(12), 1675–1685, https://doi.org/10.1038/s41559-019-1042-8, 2019.

Chauhan, T., Rasmussen, T. L. and Noormets, R.: Palaeoceanography of the Barents Sea continental margin, north of Nordaustlandet, Svalbard, during the last 74 ka, Boreas, 45(1), 76–99, https://doi.org/10.1111/bor.12135, 2016.

Cleary, D. F. R. and Renema, W.: Relating species traits of foraminifera to environmental variables in the Spermonde Archipelago, Indonesia, Mar. Ecol. Prog. Ser., 334, 73–82, https://doi.org/10.3354/meps334073, 2007.

Corliss, B. H.: Morphology and microhabitat preferences of benthic foraminifera from the northwest Atlantic Ocean, Mar. Micropaleontol., 17(3–4), 195–236, https://doi.org/10.1016/0377-8398(91)90014-W, 1991.

Cribari-Neto F., Zeileis A : Beta Regression in R."Journal of Statistical Software_,*34*(2), 1-24, https://doi.org/10.18637/jss.v034.i02, 2010.

Dawson, S. K., Carmona, C. P., González-Suárez, M., Jönsson, M., Chichorro, F., Mallen-Cooper, M., Melero, Y., Moor, H., Simaika, J. P. and Duthie, A. B.: The traits of "trait ecologists": An analysis of the use of trait and functional trait terminology, Ecol. Evol., 11(23), 16434–16445, https://doi.org/10.1002/ece3.8321, 2021.

de Bello, F., Carmona, C. P., Lepš, J., Szava-Kovats, R. and Pärtel, M.: Functional diversity through the mean trait dissimilarity: resolving shortcomings with existing paradigms and algorithms, Oecologia, 180(4), 933–940, https://doi.org/10.1007/s00442-016-3546-0, 2016.

Dimiza, M. D., Triantaphyllou, M. V., Koukousioura, O., Hallock, P., Simboura, N., Karageorgis, A. P. and Papathanasiou, E.: The Foram Stress Index: A new tool for environmental assessment of soft-bottom environments using benthic foraminifera. A case study from the Saronikos Gulf, Greece, Eastern Mediterranean, Ecol. Indic., 60, 611–621, https://doi.org/10.1016/j.ecolind.2015.07.030, 2016.

Dubicka, Z., Złotnik, M. and Borszcz, T.: Test morphology as a function of behavioral strategies - Inferences from benthic foraminifera, Mar. Micropaleontol., 116, 38–49, https://doi.org/10.1016/j.marmicro.2015.01.003, 2015.

Duong, T.: Ks: Kernel density estimation and kernel discriminant analysis for multivariate data in R, J. Stat. Softw., 21(7), 1–16, https://doi.org/10.18637/jss.v021.i07, 2007.

Duong T.: ks: Kernel Smoothing. R package version 1.11.7. https://CRAN.R-project.org/package=ks, 2020.

El bani Altuna, N., Ezat, M. M., Greaves, M. and Rasmussen, T. L.: Millennial-scale changes in bottom water temperature and water mass exchange through the Fram Strait 79oN, 63–13 ka, Paleoceanogr. Paleoclimatology, 1–21, https://doi.org/10.1029/2020pa004061, 2020.

Forwick, M., Vorren, T. O., Hald, M., Korsun, S., Roh, Y., Vogt, C. and Yoo, K.-C.: Spatial and temporal influence of glaciers and rivers on the sedimentary environment in Sassenfjorden and Tempelfjorden, Spitsbergen, Geol. Soc. London, Spec. Publ., 344, 163–193, https://doi.org/10.1144/SP344.13, 2010.

Fossile, E., Nardelli, M. P., Jouini, A., Lansard, B., Pusceddu, A., Moccia, D., Michel, E., Péron, O., Howa, H. and Mojtahid, M.: Benthic foraminifera as tracers of brine production in the Storfjorden "sea ice factory," Biogeosciences, 17(7), 1933–1953, https://doi.org/10.5194/bg-17-1933-2020, 2020.

Galland, T., Pérez Carmona, C., Götzenberger, L., Valencia, E. and de Bello, F.: Are redundancy indices redundant? An evaluation based on parameterized simulations, Ecol. Indic., 116(April), 106488, https://doi.org/10.1016/j.ecolind.2020.106488, 2020.

Lo Giudice Cappelli, E. and Austin, W. E. N.: Size Matters: Analyses of Benthic Foraminiferal Assemblages Across Differing Size Fractions, Front. Mar. Sci., 6(December), 1–8, https://doi.org/10.3389/fmars.2019.00752, 2019.

Gower, A. J. C.: A General Coefficient of Similarity and Some of Its Properties, Int. Biometric Soc., 27(4), 857–871, https://doi.org/10.2307/2528823, 1971.

Halbach, L., Vihtakari, M., Duarte, P., Everett, A., Granskog, M. A., Hop, H., Kauko, H. M., Kristiansen, S., Myhre, P. I., Pavlov, A. K., Pramanik, A., Tatarek, A., Torsvik, T., Wiktor, J., Wold, A., Wulff, A., Steen, H. and Assmy, P.: Tidewater Glaciers and Bedrock Characteristics Control the Phytoplankton Growth Environment in a Fjord in the Arctic, Front. Mar. Sci., 6(254), https://doi.org/10.3389/fmars.2019.00254, 2019.

Hald, M. and Korsun, S.: Distribution of modern benthic foraminifera from fjords of Svalbard, European Arctic, J. Foraminifer. Res., 27(2), 101–122, https://doi.org/10.2113/gsjfr.27.2.101, 1997.

Hallock, P.: The FoRAM Index revisited: uses, challenges, and limitations, Proc. 12th Int. Coral Reef …, (July), 9–13 http://www.icrs2012.com/proceedings/manuscripts/ICRS2012_15F_2.pdf, 2012.

Hallock, P., Lidz, B. H., Cockey-Burkhard, E. M. and Donnelly, K. B.: Foraminifera as bioindicators in coral reef assessment and monitoring: The foram index, Environ. Monit. Assess., 81(1–3), 221–238, https://doi.org/10.1023/A:1021337310386, 2003.

Hijmans, R. J.: geosphere: Spherical Trigonometry. R package version 1.5-10. https://CRAN.R-project.org/package=geosphere, 2019

Hohenegger, J.: Foraminiferal growth and test development, Earth-Science Rev., 185(June), 140–162, https://doi.org/10.1016/j.earscirev.2018.06.001, 2018.

Hop, H. and Wiencke, C.: The Ecosystem of Kongsfjorden, Svalbard, edited by Springer, Alfred Wegener Institute, Helmholtz Centre for Polar and Marine Research, Bremerhaven, Germany., 2019.

Hopwood, M. J., Carroll, D., Dunse, T., Hodson, A., Holding, J. M., Iriarte, J. L., Ribeiro, S., Achterberg, E. P., Cantoni, C., Carlson, D. F., Chierici, M., Clarke, J. S., Cozzi, S., Fransson, A., Juul-Pedersen, T., Winding, M. H. S. and Meire, L.: Review article: How does glacier discharge affect marine biogeochemistry and primary production in the Arctic?, Cryosphere, 14(4), 1347–1383, https://doi.org/10.5194/tc-14-1347-2020, 2020.

Hottinger, L. C.: Functional morphology of benthic foraminiferal shells, envelopes of cells beyond measure, Micropaleontology, 46(SUPPLEMENT 1), 57–86, 2000.

Howe, J. A., Moreton, S. G., Morri, C. and Morris, P.: Multibeam bathymetry and depositional environments of Kongsfjorden and Krossfjorden, western Spitsbergen, Svalbard, Polar Res., 22(2), 301–316, 2003.

Howe, J. A., Austin, W. E. N., Forwick, M., Paetzel, M., Harland, R. E. X. and Cage, A. G.: Fjord systems and archives : a review, Fjord Syst. Arch., 5–15, https://doi.org/10.1144/SP344.2, 2010.

Husum, K., Hald, M., Stein, R. and Weißschnur, M.: Recent benthic foraminifera in the Arctic Ocean and Kara Sea continental margin, Arktos, 1(1), 5, https://doi.org/10.1007/s41063-015-0005-9, 2015.

Ivanova, E. V., Ovsepyan, E. A., Risebrobakken, B. and Vetrov, A. A.: Downcore distribution of living calcareous foraminifera and stable isotopes in the Western Barents Sea, J. Foraminifer. Res., 38(4), 337–356, https://doi.org/10.2113/gsjfr.38.4.337, 2008.

Jackson, R., Kvorning, A. B., Limoges, A., Georgiadis, E., Olsen, S. M., Tallberg, P., Andersen, T. J., Mikkelsen, N., Giraudeau, J., Massé, G., Wacker, L. and Ribeiro, S.: Holocene polynya dynamics and their interaction with oceanic heat transport in northernmost Baffin Bay, Sci. Rep., 11(1), https://doi.org/10.1038/s41598-021-88517-9, 2021.

Jennings, A. E., Weiner, N. J., Helgadottir, G. and Andrews, J. T.: Modern Foraminiferal Faunas of the Southwestern To Northern Iceland Shelf: Oceanographic and Environmental Controls, J. Foraminifer. Res., 34(3), 180–207, https://doi.org/10.2113/34.3.180, 2004.

Jernas, P., Klitgaard Kristensen, D., Husum, K., Wilson, L. and Koç, N.: Palaeoenvironmental changes of the last two millennia on the western and northern Svalbard shelf, Boreas, 42(1), 236–255, https://doi.org/10.1111/j.1502-3885.2012.00293.x, 2013.

Jernas, P., Klitgaard-Kristensen, D., Husum, K., Koç, N., Tverberg, V., Loubere, P., Prins, M., Dijkstra, N. and Gluchowska, M.: Annual changes in Arctic fjord environment and modern benthic foraminiferal fauna: Evidence from Kongsfjorden, Svalbard, Glob. Planet. Change, 163(November 2017), 119–140, https://doi.org/10.1016/j.gloplacha.2017.11.013, 2018.

Jorissen, F., Nardelli, M. P., Almogi-Labin, A., Barras, C., Bergamin, L., Bicchi, E., El Kateb, A., Ferraro, L., McGann, M., Morigi, C., Romano, E., Sabbatini, A., Schweizer, M. and Spezzaferri, S.: Developing Foram-AMBI for biomonitoring in the Mediterranean: Species assignments to ecological categories, Mar. Micropaleontol., 140(January), https://doi.org/10.1016/j.marmicro.2017.12.006, 2018.

Kedra, M., Włodarska-Kowalczuk, M. and Wesławski, J. M.: Decadal change in macrobenthic soft-bottom community structure in a high Arctic fjord (Kongsfjorden, Svalbard), Polar Biol., 33(1), 1–11, https://doi.org/10.1007/s00300-009-0679-1, 2010.

Klootwijk, A. T. and Alve, E.: Does the analysed size fraction of benthic foraminifera influence the ecological quality status and the interpretation of environmental conditions? Indications from two northern Norwegian fjords, Ecol. Indic., 135(September 2021), 108423, https://doi.org/10.1016/j.ecolind.2021.108423, 2022.

Korsun, S. and Hald, M.: Modern benthic foraminifera off Novaya Zemlya tidewater glaciers, Russian Arctic, Arct. Alp. Res., 30(1), 61–77, https://doi.org/10.2307/1551746, 1998.

Korsun, S. and Hald, M.: Seasonal dynamics of Benthic Foraminifera in a Glacially Fed Fjord of Svalbard, European Arctic, J. Foraminifer. Res., 30(4), 251–271, https://doi.org/10.2113/0300251, 2000.

Korsun, S. A., Pogodina, I. A., Forman, S. L. and Lubinski, D. J.: Recent foraminifera in glaciomarine sediments from three arctic fjords of Novaja Zemlja and Svalbard, Polar Res., 14(1), 15–32, https://doi.org/10.3402/polar.v14i1.6648, 1995.

Koukousioura, O., Dimiza, M. D., Triantaphyllou, M. V. and Hallock, P.: Living benthic foraminifera as an environmental proxy in coastal ecosystems: A case study from the Aegean Sea (Greece, NE Mediterranean), J. Mar. Syst., 88(4), 489–501, https://doi.org/10.1016/j.jmarsys.2011.06.004, 2011.

Kujawa, A., Łącka, M., Szymańska, N., Pawłowska, J., Telesiński, M. M. and Zajączkowski, M.: Could Norwegian fjords serve as an analogue for the future of the Svalbard fjords? State and fate of high latitude fjords in the face of progressive "atlantification," Polar Biol., (2016), https://doi.org/https://doi.org/10.1007/s00300-021-02951-z, 2021.

Lalande, C., Moriceau, B., Leynaert, A. and Morata, N.: Spatial and temporal variability in export fluxes of biogenic matter in Kongsfjorden, Polar Biol., 39(10), 1725–1738, https://doi.org/10.1007/s00300-016-1903-4, 2016.

Leutenegger, S. and Hansen, H. J.: Ultrastructural and radiotracer studies of pore function in foraminifera, Mar. Biol., 54(1), 11–16, https://doi.org/10.1007/BF00387046, 1979.

Luckman, A., Benn, D. I., Cottier, F., Bevan, S., Nilsen, F. and Inall, M.: Calving rates at tidewater glaciers vary strongly with ocean temperature, Nat. Commun., 6, https://doi.org/10.1038/ncomms9566, 2015.

Manasa, M., Saraswat, R. and Nigam, R.: Assessing the suitability of benthic foraminiferal morpho-groups to reconstruct paleomonsoon from Bay of Bengal, J. Earth Syst. Sci., 125(3), 571–584, https://doi.org/10.1007/s12040-016-0677-y, 2016.

Marcisz, K., Jassey, V. E. J., Kosakyan, A., Krashevska, V., Lahr, D. J. G., Lara, E., Lamentowicz, Ł., Lamentowicz, M., Macumber, A., Mazei, Y., Mitchell, E. A. D., Nasser, N. A., Patterson, R. T., Roe, H. M., Singer, D., Tsyganov, A. N. and Fournier, B.: Testate Amoeba Functional Traits and Their Use in Paleoecology, Front. Ecol. Evol., 8(October), https://doi.org/10.3389/fevo.2020.575966, 2020.

Marszalek, D. S., Wright, R. C. and Hay, W. W.: Function of the Test in Foraminifera, Trans. Gulf Coast Assoc. Geol. Soc., 19, 341–352, 1969.

Mason, N. W. H., Mouillot, D., Lee, W. G. and Wilson, J. B.: Functional richness, functional evenness and functional divergence: The primary components of functional diversity, Oikos, 111(1), 112–118, https://doi.org/10.1111/j.0030-1299.2005.13886.x, 2005.

McGill, B. J., Enquist, B. J., Weiher, E. and Westoby, M.: Rebuilding community ecology from functional traits, Trends Ecol. Evol., 21(4), 178–185, https://doi.org/10.1016/j.tree.2006.02.002, 2006.

Meslard, F., Bourrin, F., Many, G. and Kerhervé, P.: Suspended particle dynamics and fluxes in an Arctic fjord (Kongsfjorden, Svalbard), Estuar. Coast. Shelf Sci., 204, 212–224, https://doi.org/10.1016/j.ecss.2018.02.020, 2018.

Micheli, F. and Halpern, B. S.: Low functional redundancy in coastal marine assemblages, Ecol. Lett., 8(4), 391–400, https://doi.org/10.1111/j.1461-0248.2005.00731.x, 2005.

Moodley, L. and Hess, C.: Tolerance of infaunal benthic foraminifera for low and high oxygen concentrations, Biol. Bull., 183(1), 94–98, https://doi.org/10.2307/1542410, 1992.

Mouillot, D., Graham, N. A. J., Villéger, S., Mason, N. W. H. and Bellwood, D. R.: A functional approach reveals community responses to disturbances, Trends Ecol. Evol., 28(3), 167–177, https://doi.org/10.1016/j.tree.2012.10.004, 2013.

Murray, J. W.: Ecology and Palaeoecology of Benthic Foraminifera, Taylor & Francis, New York., 1991.

Murray, J. W.: Ecology and Application of Benthic Foraminifera, Cambridge University Press, Cambridge, New York., 2006.

Nandan, S. B., P. P., K., Vijay, A., C. V., A., P. R., J. and Krishnan, K. P.: Benthic Faunal Assemblage of the Arctic Kongsfjorden System, Norway, Int. J. Mar. Sci., 6(54), 1–8, https://doi.org/10.5376/ijms.2016.06.0054, 2016.

Oksanen, J., Blanchet, F. G., Friendly M., Kindt R., Legendre P., McGlinn D., Minchin P.R., O'Hara R. B.,. Simpson G. L, Solymos P., Stevens M. H. H., Szoecs E., and Wagner H: vegan: Community Ecology Package. R package version 2.5-6. https://CRAN.R-project.org/package=vegan, 2019

Pawlowska, J., Zajaczkowski, M., Lacka, M., Lejzerowicz, F., Esling, P. and Pawlowski, J.: Palaeoceanographic changes in Hornsund Fjord (Spitsbergen, Svalbard) over the last millennium: new insights from ancient DNA, Clim. Past, 12(7), 1459–1472, https://doi.org/10.5194/cp-12-1459-2016, 2016.

Payne, C. M. and Roesler, C. S.: Characterizing the influence of Atlantic water intrusion on water mass formation and phytoplankton distribution in Kongsfjorden, Svalbard, Cont. Shelf Res., 191, 104005, https://doi.org/10.1016/j.csr.2019.104005, 2019.

R Core Team: R: A language and environment for statistical computing. R Foundation for Statistical Computing, Vienna, Austria. URL https://www.R-project.org/, 2020.

Rasmussen, T. L. and Thomsen, E.: Brine formation in relation to climate changes and ice retreat during the last 15,000 years in Storfjorden, Svalbard, 76 – 78°N, Paleoceanography, 29, 911–929, https://doi.org/10.1002/2014PA002643.Received, 2014.

Rasmussen, T. L., Forwick, M. and Mackensen, A.: Reconstruction of inflow of Atlantic Water to Isfjorden, Svalbard during the Holocene: Correlation to climate and seasonality, Mar. Micropaleontol., 94–95, 80–90, https://doi.org/10.1016/j.marmicro.2012.06.008, 2012.

Richirt, J., Champmartin, S., Schweizer, M., Mouret, A., Petersen, J., Ambari, A. and Jorissen, F. J.: Scaling laws explain foraminiferal pore patterns, Sci. Rep., 9(1), 1–11, https://doi.org/10.1038/s41598-019-45617-x, 2019.

Rytter, F., Knudsen, K. L., Seidenkrantz, M. S. and Eiríksson, J.: Modern Distribution of Benthic Foraminifera on the North Iceland Shelf and Slope, , (3), 217–244, 2002.

Saher, M., Kristensen, D. K., Hald, M., Korsun, S. and Jørgensen, L. L.: Benthic foraminifera assemblages in the Central Barents Sea: An evaluation of the effect of combining live and total fauna studies in tracking environmental change, Nor. Geol. Tidsskr., 89(1–2), 149–161, 2009.

Saher, M., Kristensen, D. K., Hald, M., Pavlova, O. and Jørgensen, L. L.: Changes in distribution of calcareous benthic foraminifera in the central Barents Sea between the periods 1965-1992 and 2005-2006, Glob. Planet. Change, 98–99, 81–96, https://doi.org/10.1016/j.gloplacha.2012.08.006, 2012.

Saraswat, R., Roy, C., Khare, N., Saalim, S. M. and Kurtarkar, S. R.: Assessing the environmental significance of benthic foraminiferal morpho-groups from the northern high latitudinal regions, Polar Sci., 18(August), 28–38, https://doi.org/10.1016/j.polar.2018.08.002, 2018.

Schauer, U., Fahrbach, E., Osterhus, S. and Rohardt, G.: Arctic warming through the Fram Strait: Oceanic heat transport from 3 years of measurements, J. Geophys. Res. C Ocean., 109(6), 1–14, https://doi.org/10.1029/2003JC001823, 2004.

Schmiedl, G.: Use of Foraminifera in Climate Science., 2019.

Schönfeld, J.: History and development of methods in Recent benthic foraminiferal studies, J. Micropalaeontology, 31(1), 53–72, https://doi.org/10.1144/0262-821x11-008, 2012.

Schönfeld, J., Alve, E., Geslin, E., Jorissen, F., Korsun, S., Spezzaferri, S., Abramovich, S., Almogi-Labin, A., du Chatelet, E. A., Barras, C., Bergamin, L., Bicchi, E., Bouchet, V., Cearreta, A., Di Bella, L., Dijkstra, N., Disaro, S. T., Ferraro, L., Frontalini, F., Gennari, G., Golikova, E., Haynert, K., Hess, S., Husum, K., Martins, V., McGann, M., Oron, S., Romano, E., Sousa, S. M. and Tsujimoto, A.: The FOBIMO (FOraminiferal BIo-MOnitoring) initiative-Towards a standardised protocol for soft-bottom benthic foraminiferal monitoring studies, Mar. Micropaleontol., 94–95, 1–13, https://doi.org/10.1016/j.marmicro.2012.06.001, 2012.

Skirbekk, K., Kristensen, D. K., Rasmussen, T. L., Koç, N. and Forwick, M.: Holocene climate variations at the entrance to a warm Arctic fjord: evidence from Kongsfjorden trough, Svalbard, Geol. Soc. London, Spec. Publ., 344(1), 289–304, https://doi.org/10.1144/SP344.20, 2010.

Slater, D. A., Straneo, F., Felikson, D., Little, C. M., Goelzer, H., Fettweis, X. and Holte, J.: Estimating Greenland tidewater glacier retreat driven by submarine melting, Cryosphere, 13(9), 2489–2509, https://doi.org/10.5194/tc-13-2489-2019, 2019.

Svendsen, H., Beszczynska-Møller, A., Hagen, J. O., Lefauconnier, B., Tverberg, V., Gerland, S., Ørbæk, J. B., Bischof, K., Papucci, C., Zajaczkowski, M., Azzolini, R., Bruland, O., Wiencke, C., Winther, J.-G. and Dallmann, W.: The physical environment of Kongsfjorden – Krossfjorden, an Arctic fjord system in Svalbard, Polar Res., 21(1), 133–166, https://doi.org/10.3402/polar.v21i1.6479, 2002.

Tesi, T., Muschitiello, F., Mollenhauer, G., Miserocchi, S., Langone, L., Ceccarelli, C., Panieri, G., Chiggiato, J., Nogarotto, A., Hefter, J., Ingrosso, G., Giglio, F., Giordano, P. and Capotondi, L.: Rapid Atlantification along the Fram Strait at the beginning of the 20th century, Sci. Adv., 7(48), https://doi.org/10.1126/sciadv.abj2946, 2021.

Thuiller, W., Lavorel, S., Sykes, M. T. and Araújo, M. B.: Using niche-based modelling to assess the impact of climate change on tree functional diversity in Europe, Divers. Distrib., 12(1), 49–60, https://doi.org/10.1111/j.1366-9516.2006.00216.x, 2006.

Vihtakari M.: PlotSvalbard: PlotSvalbard - Plot research data from Svalbard on maps. R package version 0.9.2. https://github.com/MikkoVihtakari/PlotSvalbard, 2020

Villéger, S., Miranda, J. R., Hernández, D. F. and Mouillot, D.: Contrasting changes in taxonomie vs. functional diversity of tropical fish communities after habitat degradation, Ecol. Appl., 20(6), 1512–1522, https://doi.org/10.1890/09-1310.1, 2010.

Violle, C., Navas, M.-L., Vile, D., Kazakou, E., Fortunel, C., Hummel, I. and Garnier, E.: Let the concept of trait be functional!, Oikos, 116(5), 882–892, https://doi.org/10.1111/j.2007.0030-1299.15559.x, 2007.

Wainwright, P. C.*, and* Reilly S. M.: Ecological morphology: integrative organismal biology. *University of Chicago Press,* Chicago, Illinois, USA*, 1994.*

Weinkauf, M. F. G. and Milker, Y.: The effect of size fraction in analyses of benthic foraminiferal assemblages: A case study comparing assemblages from the >125 and >150µm size fractions, Front. Earth Sci., 6(May), 1–10, https://doi.org/10.3389/feart.2018.00037, 2018.

Wetmore, K. L.: Correlations between test strength, morphology and habitat in some benthic foraminifera from the coast of Washington (USA)., J. Foraminifer. Res., 17(1), 1–13, https://doi.org/10.2113/gsjfr.17.1.1, 1987.

Wickham, H., Averick, M., Bryan, J., Chang, W., McGowan, L., François, R., Grolemund, G., Hayes, A., Henry, L., Hester, J., Kuhn, M., Pedersen, T., Miller, E., Bache, S., Müller, K., Ooms, J., Robinson, D., Seidel, D., Spinu, V., Takahashi, K., Vaughan, D., Wilke, C., Woo, K. and Yutani, H.: Welcome to the Tidyverse, J. Open Source Softw., 4(43), 1686, https://doi.org/10.21105/joss.01686, 2019.

Włodarska-Kowalczuk, M. and Pearson, T. H.: Soft-bottom macrobenthic faunal associations and factors affecting species distributions in an Arctic glacial fjord (Kongsfjord, Spitsbergen), Polar Biol., 27(3), 155–167, https://doi.org/10.1007/s00300-003-0568-y, 2004.

Włodarska-Kowalczuk, M., Pearson, T. H. and Kendall, M. A.: Benthic response to chronic natural physical disturbance by glacial sedimentation in an Arctic fjord, Mar. Ecol. Prog. Ser., 303, 31–41, 2005.

Włodarska-Kowalczuk, M., Pawłowska, J. and Zajaczkowski, M.: Do foraminifera mirror diversity and distribution patterns of macrobenthic fauna in an Arctic glacial fjord?, Mar. Micropaleontol., 103, 30–39, https://doi.org/10.1016/j.marmicro.2013.07.002, 2013.

Włodarska-Kowalczuk, M., Górska, B., Deja, K. and Morata, N.: Do benthic meiofaunal and macrofaunal communities respond to seasonality in pelagial processes in an Arctic fjord (Kongsfjorden, Spitsbergen)?, Polar Biol., 39(11), 2115–2129, https://doi.org/10.1007/s00300-016-1982-2, 2016.

Wood, S.N.: Generalized Additive Models: An Introduction with R (2nd edition). Chapman and Hall/CRC, 2017.

Supplement Chapter 4

Table S1. List of foraminiferal functional traits and correspondent function for each trait based on previous publications.

Functional trait	Hypothesized link to performance and fitness	References
Test material	Adaptations to specific ecological niches; habitat preferences	Marszalek et al., 1969 Murray, 1991, 2006
Test shape	Adaptations to specific ecological niches or microhabitats; test strength and survival	Marszalek et al., 1969 Wetmore, 1987 Corliss, 1991
Test symmetry	Motion (e.g., bilateral pseudopodial extrusion); habitat preferences (e.g., trochospiral-asymmetrical, or planispiral-symmetrical)	Hottinger, 2000; Dubicka et al., 2015
Pores	Gas exchanges	Leutenegger and Hansen, 1979; Moodley and Hess, 1992; Richirt et al., 2019
Tooth presence	Assistance in feeding (i.e., break up aggregates of food and detritus, or diatoms frustuls)	Austin et al., 2005; Murray, 2006
Chamber number	Growth investment	Bowser et al., 1995; Hohenegger, 2018

Table S2. Functional trait values for each species. Binary traits are identified as follow: test material, 1 = calcareous, 0 = agglutinated; test symmetry, 1 = symmetrical, 0 = asymmetrical; pores, 1 = presence, 0 = absence; chamber number, 1 = polythalamus, 0 = monothalamus. Categorical traits are: test shape (rounded, ovoid, elongated, irregular); tooth presence (none, tooth, tubercles)

Species	***Test material***	***Test shape***	***Test symmetry***	***Pores***	***Tooth presence***	***Chamber number***
Adercotryma glomeratum	0	rounded	0	0	none	1
Ammodiscus sp.	0	rounded	1	0	none	0
Ammonia sp.	1	rounded	0	1	none	1
Ammotium cassis	0	elongated	1	0	none	1
Astrononion galloway	1	rounded	1	1	none	1
Astrononion sp.	1	rounded	1	1	none	1
Baculogypsinoides sp.	1	irregular	0	1	none	1
Bolivina pseudopunctata	1	elongated	0	1	single-tooth	1
Buccella frigida	1	rounded	0	1	tubercles	1
Buccella sp.	1	rounded	0	1	tubercles	1
Capsammina bowmanni	0	rounded	0	0	none	0
Cassidulina neoteretis	1	rounded	0	1	single-tooth	1
Cassidulina reniforme	1	rounded	0	1	single-tooth	1
Cassidulina sp.	1	rounded	0	1	single-tooth	1
Cassidulina sp. morphotype 1	1	rounded	0	1	single-tooth	1
Cassidulina sp. morphotype 2	1	rounded	0	1	single-tooth	1
Cibicides bertheloti	1	rounded	0	1	none	1
Cibicidoides lobatulus	1	rounded	0	1	none	1
Cornuspira foliacea	1	rounded	1	0	none	0
Cornuspira involvens	1	rounded	1	0	none	0
Cornuspira sp.	1	rounded	1	0	none	0
Cuneata arctica	0	elongated	1	0	none	1
Dentalina ittai	1	elongated	1	1	none	1
Discorbina sp.	1	rounded	0	1	none	1
Eggerella advena	0	elongated	0	0	none	1
Elphidium bartletti	1	rounded	1	1	tubercles	1
Elphidium clavatum	1	rounded	1	1	tubercles	1
Elphidium sp.	1	rounded	1	1	tubercles	1
Epistominella exigua	1	rounded	0	1	none	1
Eponides sp.	1	rounded	0	1	none	1
Fissurina sp.	1	ovoid	1	1	none	0
Globobulimina auriculata	1	ovoid	0	1	single-tooth	1
Globobulimina sp.	1	ovoid	0	1	single-tooth	1
Globocassidulina sp.	1	rounded	0	1	single-tooth	1
Glomospira sp.	0	rounded	0	0	none	0
Haplophragmoides sp.	0	rounded	0	0	none	1
Hippocrepina sp.	0	elongated	1	0	none	0
Hormosina globulifera	0	elongated	1	0	none	0
Hyalinonetrion sp.	1	elongated	1	1	none	0
Islandiella helenae	1	rounded	0	1	single-tooth	1
Islandiella norcrossi	1	rounded	0	1	single-tooth	1
Islandiella sp.	1	rounded	0	1	single-tooth	1

Species	*Test material*	*Test shape*	*Test symmetry*	*Pores*	*Tooth presence*	*Chamber number*
Labrospira crassimargo	0	rounded	1	0	none	1
Lagena striata	1	elongated	1	1	none	0
Lagenammina difflugiformis	0	ovoid	1	0	none	0
Leptohalysis scottii	0	elongated	1	0	none	1
Lotostomoides calomorphum	1	elongated	1	1	none	1
Melonis pompilioides	1	rounded	1	1	none	1
Miliolinella circularis	1	rounded	0	0	single-tooth	1
Miliolinella sp.	1	rounded	0	0	single-tooth	1
Miliolinella sp. juvenile	1	rounded	0	0	single-tooth	1
Nonion commune	1	rounded	1	1	none	1
Nonion sp.	1	rounded	1	1	none	1
Nonionella digitata	1	rounded	0	1	none	1
Nonionella turgida	1	rounded	0	1	none	1
Nonionellina labradorica	1	rounded	1	1	tubercles	1
Paratrochammina sp.	0	rounded	0	0	none	1
Procerolagena gracilis	1	elongated	1	1	none	0
Psammosphaera fusca	0	rounded	1	0	none	0
Pullenia cf osloensis	1	rounded	1	1	none	1
Pyrgo williamsoni	1	rounded	1	0	single-tooth	1
Pyrulina cilindroides	1	elongated	0	1	none	1
Pyrulina sp.	1	elongated	0	1	none	1
Quinqueloculina arctica	1	ovoid	0	0	single-tooth	1
Quinqueloculina seminula	1	ovoid	0	0	single-tooth	1
Quinqueloculina stalkeri	1	ovoid	0	0	single-tooth	1
Recurvoides turbinatus	0	rounded	0	0	none	1
Reophax catella	0	elongated	1	0	none	1
Reophax fusiformis	0	elongated	0	0	none	1
Reophax scorpiurus	0	elongated	1	0	none	1
Reophax sp.	0	elongated	1	0	none	1
Robertina arctica	1	ovoid	0	1	none	1
Saccammina cf. *sphaerica*	0	rounded	1	0	none	0
Silicosigmoilina groenlandica	0	ovoid	0	0	none	1
Siphonaperta agglutinata	0	ovoid	0	0	none	1
Spiroplectammina biformis	0	elongated	1	0	none	1
Stainforthia feylingi	1	elongated	0	1	single-tooth	1
Stainforthia loeblichi	1	elongated	0	1	single-tooth	1
Textularia earlandi	0	elongated	1	0	none	1
Textularia torquata	0	elongated	1	0	none	1
Trifarina fluens	1	elongated	0	1	none	1
Triloculina oblonga	1	elongated	0	0	single-tooth	1
Triloculina trihedra	1	ovoid	0	0	single-tooth	1
Trochammina inflata	0	rounded	0	0	none	1
Trochammina sp.	0	rounded	0	0	none	1

Table S2 (continued)

Table S3. Akaike's Information Criterion corrected for small sample size (AIC_c) for each model, and difference in AIC_c (ΔAIC_c) relative to the model with the lowest AIC_c for each diversity metric (S = Taxonomic richness, J = Taxonomic evenness, H' = Shannon index, F_{Ric} = Functional richness, F_{Eve} = Functional evenness, Rao = Rao's quadratic entropy) and cumulative size fraction (>63, >100, 125, and >150 µm). GLM = Generalised Linear Model; GAM = Generalised Additive Model.

Diversity metric	Size fraction	Model	df	AICc	ΔAICc
S	>63 µm	GLM	2.00	81.92	13.40
		GAM	2.94	68.51	0.00
	>100 µm	GLM	2.00	78.33	13.03
		GAM	2.94	65.30	0.00
	>125 µm	GLM	2.00	81.59	14.21
		GAM	2.94	67.37	0.00
	>150 µm	GLM	2.00	73.47	11.18
		GAM	2.93	62.28	0.00
J	>63 µm	GLM	3.00	-7.66	0.00
		GAM	3.95	-5.21	2.45
	>100 µm	GLM	3.00	-5.86	0.00
		GAM	3.70	-2.43	3.43
	>125 µm	GLM	3.00	-2.18	0.00
		GAM	3.82	1.57	3.75
	>150 µm	GLM	3.00	-0.57	0.00
		GAM	3.00	-0.39	0.18
H'	>63 µm	GLM	3.00	28.43	3.14
		GAM	3.94	25.29	0.00
	>100 µm	GLM	3.00	25.74	2.94
		GAM	3.93	22.80	0.00
	>125 µm	GLM	3.00	26.36	4.43
		GAM	3.94	21.93	0.00
	>150 µm	GLM	3.00	22.95	0.00
		GAM	3.59	24.63	1.68
F_{Ric}	>63 µm	GLM	3.00	-26.22	1.30
		GAM	3.89	-27.53	0.00
	>100 µm	GLM	3.00	-26.83	1.75
		GAM	3.90	-28.58	0.00
	>125 µm	GLM	3.00	-24.78	0.00
		GAM	3.60	-23.21	1.56
	>150 µm	GLM	3.00	-25.75	0.02
		GAM	3.83	-25.76	0.00
Feve	>63 µm	GLM	3.00	-19.41	0.00
		GAM	3.00	-19.17	0.25
	>100 µm	GLM	3.00	-17.94	0.00
		GAM	3.00	-17.70	0.24
	>125 µm	GLM	3.00	-16.62	0.00
		GAM	3.00	-16.38	0.24
	>150 µm	GLM	3.00	-11.33	0.00
		GAM	3.00	-11.10	0.23
Rao	>63 µm	GLM	3.00	-2.67	0.00
		GAM	3.70	0.67	3.34
	>100 µm	GLM	3.00	-2.69	0.00
		GAM	3.00	-2.56	0.13
	>125 µm	GLM	3.00	-0.61	0.00
		GAM	3.63	2.46	3.08
	>150 µm	GLM	3.00	-1.28	0.00
		GAM	3.00	-1.13	0.15

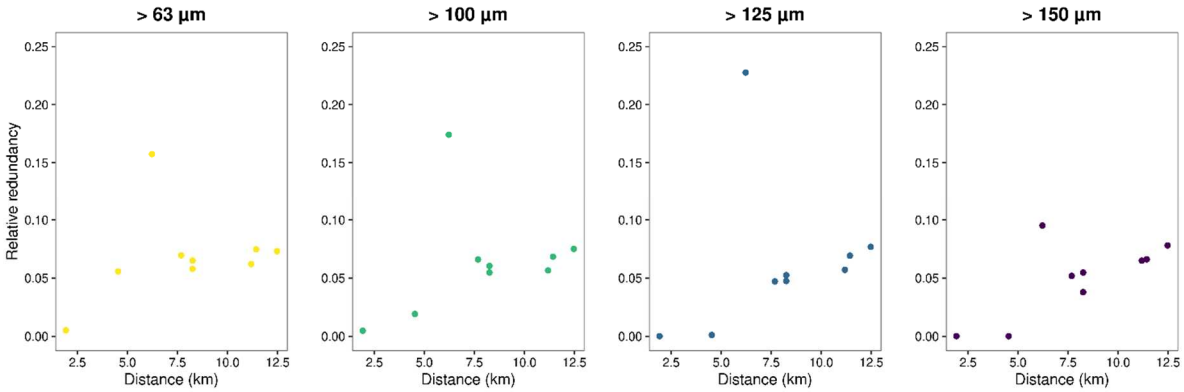

Figure S1. Relative redundancy considering the four cumulative size fractions (>63, >100, 125, and >150 µm).

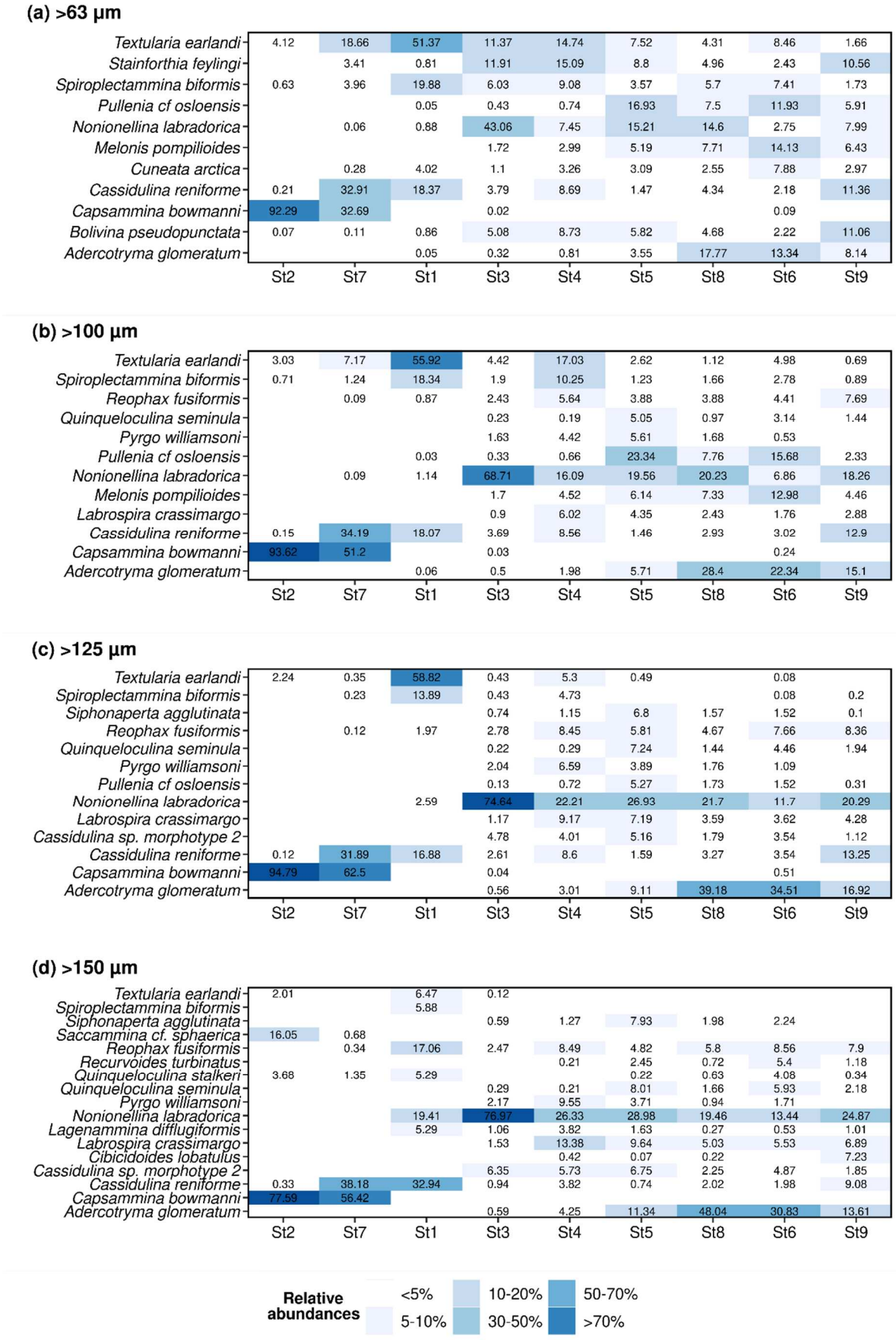

Figure S2. Heatmaps showing the relative abundance of the major species (>5 %) for four cumulative size fraction: **(a)** >63 µm, **(b)** >100 µm, **(c)** 125 µm and **(d)** >150 µm.

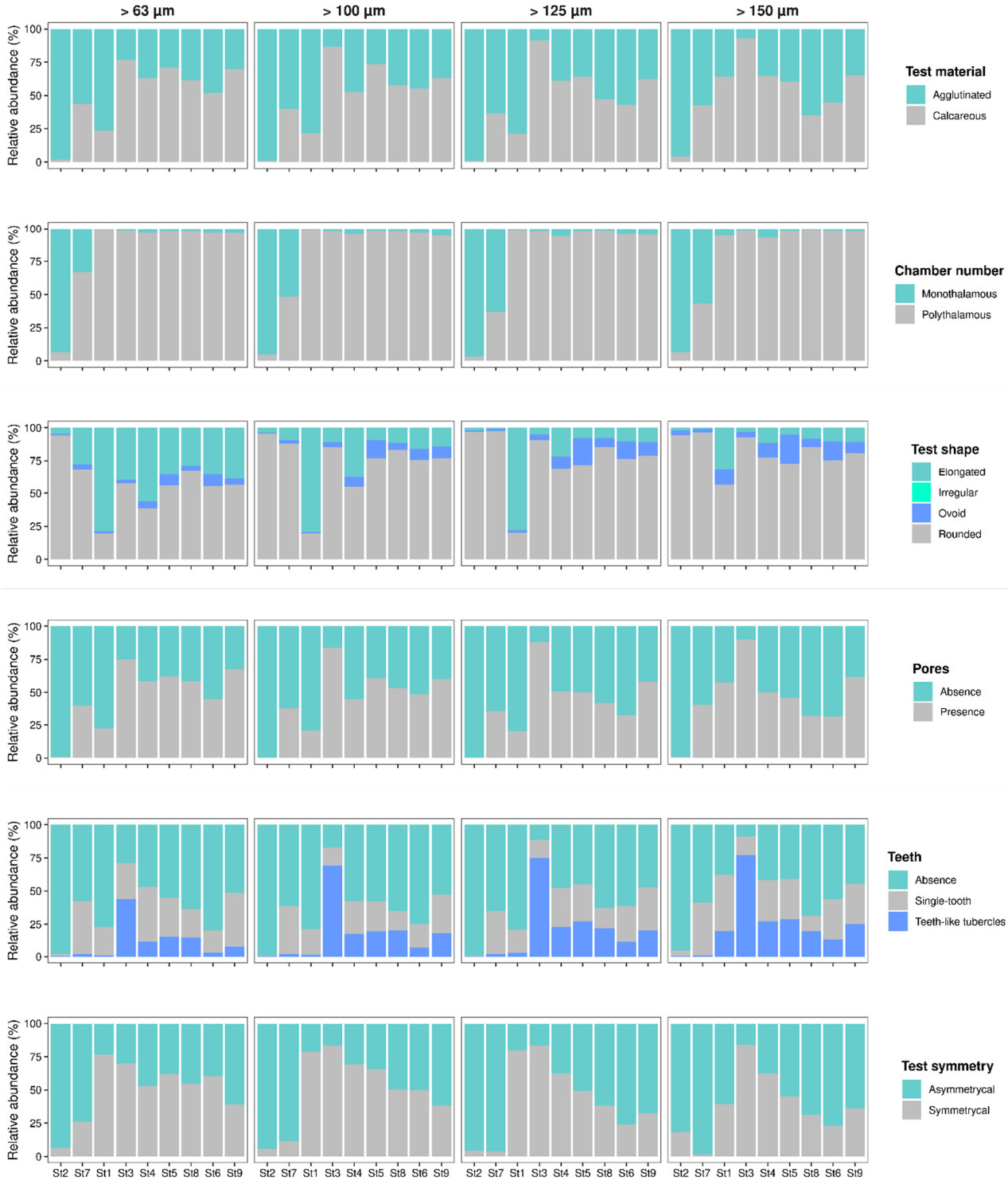

Figure S3. Relative contribution of different functional strategies for each trait considering the foraminiferal assemblages from the four cumulative size fractions (>63, >100, 125, and >150 µm).

Table S4. Values of taxonomic (S = Taxonomic richness, J = Taxonomic evenness, H' = Shannon index) and functional (F_{Ric} = Functional richness, F_{Eve} = Functional evenness, Rao = Rao's quadratic entropy) diversity metrics for each station and four cumulative size fractions (>63, >100, 125, and >150 µm). Stations are displayed from left to right following the distance from the glacier front.

Size fraction	Diversity metric	St2	St7	St1	St3	St4	St5	St8	St6	St9
>63 µm	S	11	21	23	52	52	62	67	56	58
	J	0.16	0.55	0.46	0.56	0.74	0.73	0.71	0.73	0.76
	H'	0.38	1.66	1.43	2.23	2.93	3.00	2.98	2.92	3.08
	F_{Ric}	0.09	0.13	0.12	0.21	0.20	0.22	0.22	0.21	0.18
	F_{Eve}	0.18	0.30	0.20	0.27	0.36	0.37	0.34	0.33	0.39
	Rao	0.15	0.73	0.40	0.73	0.82	0.86	0.86	0.82	0.87
>100 µm	S	9	17	21	47	45	54	59	50	51
	J	0.15	0.44	0.43	0.41	0.76	0.68	0.65	0.71	0.75
	H'	0.33	1.25	1.30	1.57	2.90	2.73	2.64	2.77	2.95
	F_{Ric}	0.08	0.11	0.11	0.20	0.20	0.20	0.21	0.20	0.17
	F_{Eve}	0.19	0.27	0.20	0.25	0.40	0.37	0.34	0.35	0.42
	Rao	0.12	0.61	0.37	0.50	0.84	0.83	0.82	0.82	0.86
>125 µm	S	8	12	16	40	40	50	54	45	41
	J	0.13	0.37	0.48	0.36	0.79	0.71	0.58	0.69	0.74
	H'	0.27	0.93	1.32	1.32	2.90	2.77	2.30	2.61	2.74
	F_{Ric}	0.08	0.11	0.09	0.19	0.18	0.20	0.21	0.20	0.16
	F_{Eve}	0.18	0.23	0.26	0.24	0.44	0.37	0.32	0.35	0.41
	Rao	0.10	0.51	0.39	0.43	0.88	0.86	0.77	0.80	0.84
>150 µm	S	6	8	14	29	30	39	42	33	30
	J	0.41	0.45	0.75	0.34	0.77	0.69	0.53	0.72	0.77
	H'	0.73	0.94	1.98	1.15	2.61	2.53	1.96	2.51	2.62
	F_{Ric}	0.06	0.08	0.09	0.18	0.18	0.19	0.19	0.18	0.15
	F_{Eve}	0.32	0.28	0.45	0.22	0.44	0.36	0.31	0.34	0.41
	Rao	0.37	0.54	0.78	0.39	0.86	0.84	0.71	0.80	0.84

Chapter 5

Foraminifera as tool to reconstruct tidewater glacier retreat: A case study from Kongsfjorden (Svalbard)

Eleonora Fossile[1], Meryem Mojtahid[1], Katrine Husum[2], Christine Barras[1], Katharina Streuff[3], Hélène Howa[1] and Maria Pia Nardelli[1]

[1] *Laboratoire de Planétologie et Géosciences, Université d'Angers, Nantes Université, Le Mans Université, CNRS UMR 6112, Angers, France*

[2] *Norwegian Polar Institute, Fram Centre, N-9296 Tromsø, Norway*

[3] *MARUM, University of Bremen, Klagenfurterstr. 4, 28359 Bremen, Germany*

Abstract

Mass loss and retreat of glaciers are striking evidence of climate change. Tidewater glaciers, as marine terminating, are particularly sensitive to these changes and their seasonal disturbance on the benthic system evolves through time. Future predictions of glacier retreat rely on solid historical reconstructions. Benthic foraminifera, as marine microorganisms capable of quick turnover and fossilisation potential, may be powerful tools in this regard. We analysed foraminiferal assemblages along a sedimentary core collected in 2010 in front of a surge-type tidewater glacier (Kronebreen complex) in the inner Kongsfjorden (Svalbard). The last surge occurred in 1948 and the glacier complex has retreated rapidly in about half century. Thanks to previously reconstructed front positions through time, we could test if foraminiferal diversity metrics can be valuable proxy for glacier retreat. Specifically, we tested relationships between taxonomic and functional diversity metrics and the distance from the glacier front across 60 years. We observed a general increase in foraminiferal fluxes and diversity with the progressive glacier retreat, confirming a positive benthic response to reduced glacier-induced disturbance through time. Such response includes the gradual replacement of opportunist glacier proximal species (e.g., *Cassidulina reniforme*) by more diversified communities, thanks to new several ecological niches available further away from the glacier front. This study assesses the use of taxonomic and functional diversity metrics as promising proxies for tidewater glacier retreat and paves the way for a potential application in paleoreconstructions across thousand years.

Keywords: proxy, taxonomic diversity, functional diversity, Arctic, climate change.

1. Introduction

The cryosphere is severely threatened by current global warming. In general, glaciers are particularly sensitive to climate and the anthropogenic impact is affecting those systems irreversibly. Glacier mass loss and rapid retreat are among the major consequences of climate change with large ecological implications (IPCC, 2019). The processes causing these modifications and the effects of these abrupt changes vary based on the nature of the glacier. Glaciers can typically terminate on the land (land-terminating) or at the sea (marine-terminating) and they are respectively called continental and tidewater glaciers. The mass-balance of continental and tidewater glaciers is controlled by different processes atmospheric- and/or marine- related and thus with different sensitivity to climate change. Continental glaciers lose mass through surface melting under atmospheric temperature forcing (e.g., Zwally et al., 2002; Tedstone et al., 2015), whereas tidewater glaciers lose mass additionally through calving and submarine melting as frontal ablation (Cogley et al., 2011). Directly located at the interface between the terrestrial and marine environment, tidewater glaciers are more sensitive to climate-induced modifications. Cumulative effects of increasing air and ocean temperatures with Arctic amplification phenomenon accentuate tidewater glacier mass loss and front retreat in the Arctic (e.g., Luckman et al., 2015; Meredith et al., 2019).

Besides, glacier dynamics is also driven by internal forcing. Glacier ice forms through the accumulation, compression, and compaction of snow for several years. The ice flow processes result from the interplay of the physical mechanism causing a glacier to move downhill (gravity) and forces resisting this movement (friction, substratum topography). Glaciers' flow and its subsequent frontal retreat or advance depends on their mass-balance (i.e., difference between the snow accumulated in the winter and the snow and ice melted over the summer). When the flow speed is not constant, but periodically subjected to flow instabilities, they are called surging glaciers. Surge-type glaciers are naturally subjected to advance (active), retreat (passive) or stagnate (quiescent) phases. Glacier surges are related to internal changes in the glacial system, but the recurrence interval of the surge can depend on climate change (Dowdeswell et al., 1995). In a changing climate, it is difficult to understand if the glacier is retreating because of negative mass-balance or because it is in quiescent state (Hansen, 2003).

The Svalbard archipelago, located above the Arctic Circle (74-81°N and 10-35°E), is ice-covered at 60% (Hagen et al., 1993; Dowdeswell et al., 1995; König et al., 2014) and the majority of the glaciers are surge-type (Sund et al., 2009). Surge events in Svalbard are generally longer compared to other places: the active phases span between 3 and 10 years,

whereas the quiescent phases between 50 and 500 years (Dowdeswell et al., 1991; Murray et al., 1998). Due to its geographical location, the Svalbard archipelago is under the influence of the warm and saline Atlantic Water (AW) carried north by the West Spitsbergen Current (WSC; the northernmost extension of the North Atlantic Current). In particular, western Svalbard fjords experience important AW influence making them particularly sensitive to ocean heat transport modulations (e.g., Cottier et al., 2007; Pavlov et al., 2013).

Kongsfjorden, among the Atlantic-influenced western Svalbard fjords, is located in the north-western coast of Spitsbergen and is under the influence of tidewater glacier dynamics and the associated water masses at the fjord head (Hop et al., 2002; Svendsen et al., 2002; Sundfjord et al., 2017). Some of these tidewater glaciers are of surge-type with cyclical velocity fluctuations and subsequent front position changes that reflect internal changes rather than climatic fluctuations (e.g., Hagen et al., 2003; Sund et al., 2009). Since tidewater glacier retreat is linked to both warming ocean temperatures (Luckman et al., 2015) and internal instabilities (i.e. surge cycles), it is difficult to disentangle the cause of retreat of a surge-type glacier in an evolving climate.

Independently of the causes of tidewater glacier retreat, seasonal glacier dynamics create steep environmental gradients affecting in a similar way the pelagic and the benthic systems (e.g., Hop et al., 2002; Włodarska-Kowalczuk et al., 2005; Hopwood et al., 2020). The glacier-induced disturbance (GID) (e.g., high sediment and freshwater discharges, substrate instability, low organic fluxes) creates persistent physical and geochemical stress on fjord ecosystems. Glaciers and their retreat can have either a positive or negative effect on abundances and biodiversity depending on the considered taxon (Cauvy-Fraunié and Dangles, 2019). Important consequences on the biosphere and taxon-specific responses would occur if the retreat would involve a shift from marine- to land-terminating glacier (Meredith et al., 2019).

To understand ongoing changes and to build reliable predictions about glacier retreat, there is the need of robust glacier terminus reconstructions back to the preindustrial era to better distinguish between natural or human-induced changes. However, direct reconstructions of glacier terminus from satellite images are limited to the last decades (i.e., since the ‘80s). Benthic organisms living near the tidewater glacier are directly affected by GID and may reflect the distance from the glacier front. Benthic foraminifera, thanks to their short life cycle, their prompt response to environmental changes and their fossilisation potential, are promising tools to reconstruct glacier front position back when direct measurements were not yet developed. Several studies observed an increased foraminiferal taxonomic richness with increased distance from tidewater glacier fronts due to reduced disturbance (e.g., Korsun et al., 1995; Korsun and

Hald, 1998; Forwick et al., 2010; Włodarska-Kowalczuk et al., 2013). In *Chapter 4*, we proposed some foraminiferal taxonomic and functional diversity metrics as potential proxies to reconstruct tidewater glacier retreat.

The present study aims at validating the use of the proposed ecological proxies to reconstruct tidewater glacier retreat. In this scope, foraminiferal assemblages are investigated along a sedimentary core from the inner Kongsfjorden which recorded the retreat of the well-known tidewater glacier complex Kronebreen over the last six decades. We test the relationships between taxonomic and functional diversity metrics and the changing distance from the glacier front as potential proxy for glacier retreat.

2. Study area

Kongsfjorden is a glacial fjord located along the north-western coast of Spitsbergen (79°N, 12°E; Svalbard). It is about 20 km long and 4-10 km wide, shallow in the inner part (<100 m) and deeper in the central and outer parts (reaching about 350 m depth). The fjord hydrology is subjected to strong seasonal variations, and it is largely influenced by the warm and saline Atlantic Water (AW) carried by the continuum of the Gulf Stream, the West Spitsbergen Current (WSC) all year round (Cottier et al., 2005; Hop and Wiencke, 2019a).

During summer, strong temperature and salinity gradients caused by AW inflow and freshwater inputs from glaciers, are established in the fjord (e.g. Cottier et al., 2010; Hop et al., 2002; Hop and Wiencke, 2019; Svendsen et al., 2002). These intrusions play an important role in frontal ablation of tidewater glaciers enhancing submarine melting and calving (Luckman et al., 2015; Holmes et al., 2019). Meltwater turbid plumes reduce light penetration depth (Payne and Roesler, 2019) hampering primary productivity (Hopwood et al., 2020), thus limiting fresh organic matter fluxes to the seafloor.

Several tidewater glaciers flow into Kongsfjorden including two surge-types: Kronebreen (about 390 km^2) from east and Kongsvegen (165 km^2) from south-east (Fig. 1), both constituting a glacier complex (Darlington, 2015). Kongsvegen joins Kronebreen at about 5 km from their shared terminus (together with the confluent Infantfonna, a glacier of 85 km^2) and they are separated by a medial moraine (Darlington, 2015). Kronebreen occupies most of the shared front entering the fjord (70 %; Sund et al., 2011) whereas the majority of Kongsvegen terminates on land.

Darlington (2015) gives a complete overview of the historical change of the glacier complex. Briefly, the maximum extension of the complex Kronebreen-Kongsvegen was during the Little

Ice Age (Liestøl, 1988). After, the glacier complex retreated and it undergone two surge events: in 1869 (Kronebreen; Hagen et al., 1993) and 1948 (Konsgsvegen; Bennett et al., 1999). The front of the glacier complex has retreated 10 km between 1869 and 1988 (Liestøl, 1988), and about half retreat occurred after 1948 (Trusel et al., 2010). Kronebreen ice velocity significantly slowed down after 1990 (post surge quiescent-phase conditions; Trusel et al., 2010). The surge events of the Kronebreen-Kongsvegen tidewater glacier left typical landform assemblages on the fjord seafloor (e.g., glacial lineations produced during the advancing phase and terminal moraines at the maximum ice extent) as described by Streuff et al. (2015).

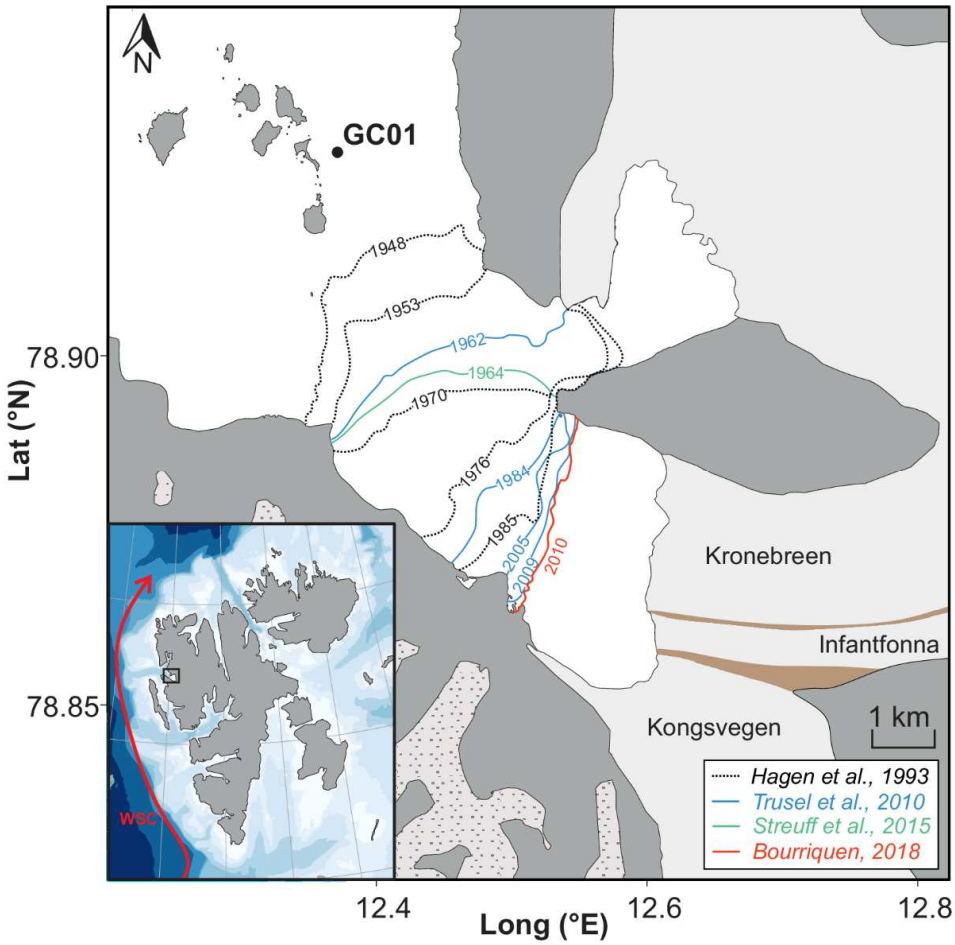

Figure 1. Map of Svalbard showing the main path of the West Spitsbergen Current (WSC) transporting Atlantic Water. Map of the inner Kongsfjorden showing the Kronebreen-Kongsvegen glacier complex (including the Infantfonna) and location of the 10JM-GLACIBAR-GC01 core site sampled in 2010 (indicated as GC01 in the figure). Different colour lines represent the evolution of the front positions since 1948 based on previous publications (Hagen et al., 1993; Trusel et al., 2010; Streuff et al., 2015; Bourriquen, 2018). The base map was performed with the R package *PlotSvalbard* (Vihtakari, 2020). The brownish landforms on the glaciers represent the moraines. Continental glaciers are shown with a pointed texture whereas tidewater glaciers are displayed in light grey.

At present, Kronebreen, as fast-flowing glacier, has one of the highest flux rates in Svalbard (winter speed of 1.5-2 m d^{-1}, with 3-4 m d^{-1} peaks in summer; Luckman et al., 2015) and is the

major source of meltwater and suspended particles in Kongsfjorden (Meslard et al., 2018; Pramanik et al., 2018). The seasonal dynamics related to the glacier creates a multi-factorial disturbance on the biota, especially on the benthic compartment. Specifically, during the warm season, glacial meltwater and sediment discharges from the terminus are responsible for the creation of buoyant meltwater turbid plume spreading on the sea surface far from the front (D'Angelo et al., 2018; Meslard et al., 2018).

Consequently, in the proximity of the glacier front, the sea bottom stability is compromised by sediment burial. Water turbidity reduces light penetration depth (Payne and Roesler, 2019) and as such, hampers primary productivity (PP) leading to scarce organic fluxes to the seafloor (e.g., Lalande et al., 2016; Hopwood et al., 2020). The intensity of these limiting environmental factors is reduced as the distance from the glacier front increases. The impacts of these steep gradients on the benthic biota have been observed for several groups of organisms, including foraminifera in a global meta-analysis (Cauvy-Fraunié and Dangles, 2019). In particular, a negative influence of the glacier activity was observed for benthic diversity for macrofauna and meiofauna (e.g., Włodarska-Kowalczuk and Pearson, 2004; Włodarska-Kowalczuk et al., 2005, 2013, 2016; Kedra et al., 2010; Nandan et al., 2016).

3. Material and methods

3.1 Core sampling

Sediment core 10JM-GLACIBAR-GC01, 286 cm long, was collected in Autumn 2010 with R/V Jan Mayen (now called R/V Helmer Hanssen) using a gravity corer. The core site was located at 50 m water depth in the innermost Kongsfjorden (78°55'50''N, 12°20'49''E; Fig. 1). Immediately after collection, the core was divided into sections (up to 1 m long) and stored at +4°C.

Previous investigations conducted on this core (Streuff et al., 2015) demonstrated that the core is composed of two sedimentological units: unit 2 (286-165 cm) which is a diamict with abundant clasts distributed in a clayey matrix, and unit 1 (165-0 cm) which contains stratified clayey silt with clasts occurring in concentrated layers or as randomly distributed lonestones. The results of the ^{137}Cs activity measurements indicate that the upper 110 cm have likely been deposited after 1950. Streuff et al., (2015) then inferred that the uppermost part of the core was deposited after the Kongsvegen surge in 1948 and reflects an increasingly ice distal environment during glacier retreat.

Considering the aim of this study, we focused our analyses on sediments deposited after the last glacial surge in 1948, i.e. the 0-112 cm top interval of the 10JM-GLACIBAR-GC01 core that will be refereed hereinafter as "the study core".

3.2 Sedimentological analyses and age model

The following sedimentological analyses were conducted on the entire core (as described in Streuff et al. 2015) but will be presented here only for the upper 112 cm.

Before the core opening, p-wave velocity, density, magnetic susceptibility, acoustic impedance, and fractional porosity were measured each centimetre using a GEOTEK multi-sensor core logger (MSCL) at the UiT-The Arctic University of Norway. The lithological log presented in this manuscript was reproduced based on the draw published by Streuff et al. (2015) which was based on visual descriptions of the sediment surface and X-radiographs (colour images of the core can be found in the same publication). Grain size analyses were performed with a Beckman Coulter LS13320 Laser Diffraction Particle Size Analyzer every 10 cm on ~1 gram of sediment sample.

Wet sediment samples were weighted, then dried in the oven at 50°C and weighted again to obtain the dry weight. The dry weight was corrected for the content of salt (dry weight salt corrected, M_s) and the mass using the following formula (Dadey et al., 1992):

$$M_s = \frac{M_d - s\,M}{1 - s} \qquad \text{(i)}$$

where M_d is the dry mass of the sediment, M is the wet mass of the sediment and s is the salinity (expressed as decimal; a salinity of 35 was used and expressed as 0.035 in the formula). The dry bulk density of the sediment was calculated following (Dadey et al., 1992):

$$\rho_d = \frac{M_s}{V} \qquad \text{(ii)}$$

Where V is the total volume of the wet sediment. V was calculated from the wet mass of the sediment and the sediment density measured with the core logger.

The sediment accumulation rates (SAR; centimetres of sediment deposited in a certain period, here expressed as cm yr^{-1}) were determined using ^{210}Pb and ^{137}Cs analyses as detailed in Streuff et al. (2015). Briefly, 20 grams of sediment samples were taken from 10 cm thick intervals, dried and ground. A decay-correction for the sampling date was performed for ^{210}Pb and ^{137}Cs activities. SAR were calculated from the decrease of ^{210}Pb excess activities with sediment depth. In parallel, the first detection of ^{137}Cs was approximated as 1952, the maximum peak of activity as 1962 (both peaks are related to atmospheric nuclear testing in the 1950s and

1960s), and the most recent peak as 1986 (peak Chernobyl related) (Appleby, 2008). The presented SAR should be considered carefully because of possible sampling bias (i.e., loss of top core sediment during coring) and sediment mixing.

3.3 Foraminiferal analyses

The following faunal analyses were conducted on the upper 112 cm of the 10JM-GLACIBAR-GC01 core, thanks to 47 sediment samples made available to us by the Norwegian Polar Institute.

3.3.1 Sample processing

Faunal analyses were performed on sediment samples of one centimetre thickness, corresponding to a mean sampling resolution of 1.4 ± 0.6 years (following the age model described in Streuff et al., 2015). Sediment samples were washed through 125, 100 and 63 µm mesh size sieves. All foraminifera were picked from the 100-125 µm and >125 µm size fractions. Due to very low foraminiferal abundances, foraminiferal counts from the two size fractions were summed, and the >100 µm fraction was considered for further analyses.

The raw foraminiferal counts were standardised as densities, i.e. number of individuals per gram of dry sediment (*No*, ind. g^{-1}). The Benthic Foraminifera Accumulation Rates (BFAR) were calculated using the following formula and expressed as number of individuals per cm^2 per year (ind. cm^{-2} yr^{-1}):

$$BFAR = No \,.\, \rho_d \,.\, SAR \qquad \text{(iii)}$$

3.3.2 Diversity analysis

Taxonomic and functional diversity metrics were investigated for the 47 samples considering the >100 size µm fraction. For the taxonomic diversity estimation, we calculated: 1) the taxonomic richness (S; i.e., number of species) and 2) Shannon index (H') calculated as:

$$H' = -\sum_{i=1}^{S} p_i \ln p_i \qquad \text{(iv)}$$

where p_i is the proportion of each species i in the community.

To estimate foraminiferal functional diversity (FD; Carmona et al., 2016), the functional strategy of each species was characterised using six categorical and binary traits (i.e., test material, test shape, pores, test symmetry, chamber number, and tooth) as detailed in Fossile et al. (*Chapter 4*). The assignment of the functional traits for each species can be found in Table

S1. A multi-trait dissimilarity matrix based on the six functional traits was built using the Gower distance (Gower, 1971) with the R package *gawdis* (de Bello et al., 2020). The dissimilarity matrix was used to compute a Principal Coordinate Analysis (PCoA) to identify the main axes of functional trait variation and the first two axis (63% of the total variance) were retained. This space is hereinafter referred to as functional space.

Two FD indices were used, Functional richness (F_{Ric}) and Rao's quadratic entropy (Rao), which were calculated as detailed in Fossile et al. (*Chapter 4*). F_{Ric} represents the amount of the functional space occupied by the species in a community (Villéger et al., 2008), whereas Rao represents the dissimilarity between two randomly chosen individuals from a community (Botta-Dukát, 2005). These two indices were computed using the R package *TPD* (Carmona et al., 2019a, 2019b). The distribution probability of each species in the functional space was estimated using the *TPDsMean* function. The *REND()* function was then used to compute the F_{Ric} of each community (Carmona et al., 2019a, 2019b). The dissimilarity-based index Rao's quadratic entropy (Botta-Dukát, 2005) was calculated using the *dissim()* and *Rao()* functions (Carmona et al., 2016, 2019a).

3.4 Laser ablation analysis

3.4.1 Cleaning methods

Specimens of *Cassidulina reniforme* and *Elphidium clavatum* were picked from each of the 40 selected sediment layers, rich enough in foraminiferal abundances. Depending on foraminiferal density in each layer, an average of 6 specimens of *C. reniforme* and 8 of *E. clavatum* were prepared for Laser Ablation-Inductively Coupled Plasma-Mass Spectrometry (LA-ICP-MS) analyses, for a total of 590 specimens.

The cleaning procedure was divided in two main steps: the first to remove clay particles and the second to remove organic matter (oxidative-cleaning). The procedure for clay-removal cleaning was modified after Glock et al., (2016) and Mayk et al., (2020). Foraminiferal specimens from each sample were transferred into PFA vials (1.5 ml), rinsed with ethanol (500 µl) and placed in ultrasonic bath (80 kHz, 50 % power, degas mode) for 20 s. This step was repeated three times, after which the vials were rinsed three times with Milli-Q water (1 ml) to remove any residue of ethanol from foraminiferal test. The procedure for oxidative cleaning was adapted from Barker et al., (2003) following previous studies (e.g., Van Dijk et al., 2017, 2019; Mayk et al., 2020). The milli-Q water from the first cleaning phase was removed from the vials and 350 µl of oxidative solution (fresh 1% H_2O_2 buffered with 0.1 M NH_4OH) was

added to each vial. The vials were placed in a water bath at 80°C for 10 min, put in an ultrasonic bath (80 kHz, 50 % power, degas mode) for 30 s, and then the oxidizing reagent was removed. These oxidative-cleaning steps were repeated three times, after which any residual of oxidising reagent was removed by rinsing three times with Milli-Q water (1 ml). The vials were then put in the oven at 50°C to dry. Dried foraminifera (a total of 317 specimens of *C. reniforme* and 232 of *E. clavatum*) were placed on double-sided tape on slides for LA-ICP-MS analyses.

3.4.2 LA-ICP-MS operating conditions and calibration

LA-ICP-MS analyses were performed at the LPG-Nantes, University of Nantes (France) using an ArF excimer laser (193 nm, Analyte G2, Teledyne Photon Machines) coupled with a quadrupole ICP-MS (Varian Bruker 820-MS). Ablations were conducted in a helium atmosphere. The pulse repetition rate was 5 Hz and the laser energy density was set at 0.91 Jcm^{-2} (10% of the laser energy output).

The size of ablation spots was adapted to the test and/or chamber size of each specimen varying between 65 and 85 µm diameter. Due to the complex organization of *Cassidulina reniforme* and the fragility of the test, the specimens of *C. reniforme* were preferentially ablated in the central part instead of targeting a precise chamber. The surface of *C. reniforme* is smooth and flat, conditions that are essential to obtain a uniform ablation spot. The central part of *Elphidium clavatum* was not targeted because it is not flat and uniform as it is for *C. reniforme*. Therefore, individuals of *Elphidium clavatum* were preferentially ablated between two older successive chambers, most often between *n*-4 and *n*-5, where *n* is the last chamber.

The isotope mass analysed were ^{23}Na, ^{24}Mg, ^{25}Mg, ^{27}Al, ^{43}Ca, ^{44}Ca, ^{55}Mn, ^{57}Fe, ^{66}Zn, ^{88}Sr and ^{137}Ba. Calibration of all (except ^{23}Na) trace element concentration was performed against NIST SRM 610 (National Institute of Science and Technology Standard Reference Materials) glass standard (Jochum et al., 2011). Due to signal saturation of ^{23}Na with NIST SRM 610 standard, the calibration for this element was performed against MACS-3 which is a pressed powder carbonate (synthetic calcium) standard (Jochum et al., 2012). In both cases ^{43}Ca isotope was used as internal standard, and 40 wt.% (weight percentage) for $CaCO_3$ were assumed to calculate element concentrations.

Similar ablation conditions were used to measure standards (NIST SRM 610 and MACS-3) and foraminiferal samples. One and two measurements of MACS-3 and NIST SRM 610, respectively, were performed every 15 foraminiferal measurements. A series of standards (NIST SRM 610, NIST SRM 612 glass standard and MACS-3) were measured in duplicate at the beginning and end of each session of analysis. Precision and accuracy for each element and

for the three standards is reported in Table 1. The limit of detection (LOD = background signal + 3.3σ; σ = SD calculated on the background signal) was calculated for each element and data below LOD were discarded (e.g., Petersen et al., 2018).

In total 590 measurements on foraminiferal samples were performed of which 322 on specimens of *Cassidulina reniforme* and 268 on specimens of *Elphidium clavatum*. Only some specimens (33 in total) were ablated 2 or 3 times for sediment layer with very low foraminiferal abundances.

Element	**MACS-3** (*n* = 93)		**NIST 610** (*n* = 96)		**NIST 612** (*n* = 18)	
	Precision (RSD %)	**Accuracy** (%)	**Precision** (RSD %)	**Accuracy** (%)	**Precision** (RSD %)	**Accuracy** (%)
^{137}Ba	13.9	105.6	4.4	95.3	7.5	98.8
^{24}Mg	9.0	91.5	3.9	105.4	4.3	84.9
^{25}Mg	9.7	92.1	5.6	104.6	9.4	83.5
^{55}Mn	8.8	104.3	3.8	94.6	4.5	103.1
^{88}Sr	11.8	108.1	8.2	94.3	17.9	102.2
^{23}Na	3.38	NA	NA	NA	NA	NA

Table 1. Precision (RSD % of *n* measurements) and accuracy (% of reference value) of three standards (accuracy was calculated against NIST 610 for MACS-3 and NIST 612, whereas accuracy for NIST 610 was calculated against NIST 610).

3.4.3 Data treatment

All profiles for each element and sample were analysed using the GLITTER software (GEMOC ARC National Key Centre and CSIRO) to select the ablation interval and convert raw counts to element concentrations. The selection within each profile (integration interval) was based on constant raw counts of ^{43}Ca and ^{44}Ca indicative of calcite ablation, and absence of peaks in elements indicative of surface contamination (^{27}Al, ^{57}Fe, ^{66}Zn). The selection within the profile was carefully placed where most of the element profiles were stable to obtain a good integration interval for all elements. A total of 170 foraminiferal profiles were discarded immediately because of short ablation time (due to foraminifera breaking) and/or excessive contamination along the profile (i.e., 29% of the conducted measurements).

Once obtained the element concentrations from the raw counts, the data treatment was performed using R software (R Core Team, 2020). The element concentrations obtained from GLITTER software, expressed in ppm, were converted to mmol dividing by the molar mass (mg mmol^{-1}) of each element respectively. Elemental calcium ratios (El/Ca) were calculated for each measurement. For each sediment layer and species, the mean El/Ca was calculated after removing extreme outliers based on 1.5*interquartile range (i.e., ratio values < Q1-1.5*IQR or >Q3+1.5*IQR, where Q1= 25th percentile, Q3=75th percentile, and IQR=Q3-Q1).

3.5 Reconstruction of the distance from the glacier front

The aim was to reconstruct the distance separating the GC01 core site from the glacier front through time (Fig. 1), on the basis of the front position shift known by means of old maps and descriptions, seafloor landform assemblages, or recent satellite images (Hagen et al., 1993; Trusel et al., 2010; Streuff et al., 2015; Bourriquen, 2018). Firstly, we calculated the distance between the core site and the successive known positions of the glacier front as follows. A reference point for each front position was selected along the centre-line of the glacier (calculated using the box method as shown in Figure S1; Lea et al., 2014) and its coordinates were obtained using the Google Earth Pro software (v7.3.3.7786) after overlying the reconstructed image. The linear distances between the core site and the median points on the front positions (i.e., 11 points listed in Table S2) were calculated using the *distm* and *distGeo* functions in the R package *geosphere* (Hijmans, 2019). Then we predicted the distances along the entire time series as follow. A generalised additive model (GAM) was fitted on the time series using the known distances as response variable and the years as predictor (Fig. 2). The GAM was fitted using the R package *mgcv* (Wood, 2017) using thin plate regression spline with the minimum basis dimension (i.e., k = 3) to avoid overfitting. The distance between the core site and the reconstructed position of the Kronebreen glacier front increased almost linearly between 1948 and approximately 1985 passing from 1.5 to 6 km of distance, and then it strongly slowed down to reach 6.5 km in 2010. Lastly, using this model we were able to predict the distance from the front for each year along the sediment core.

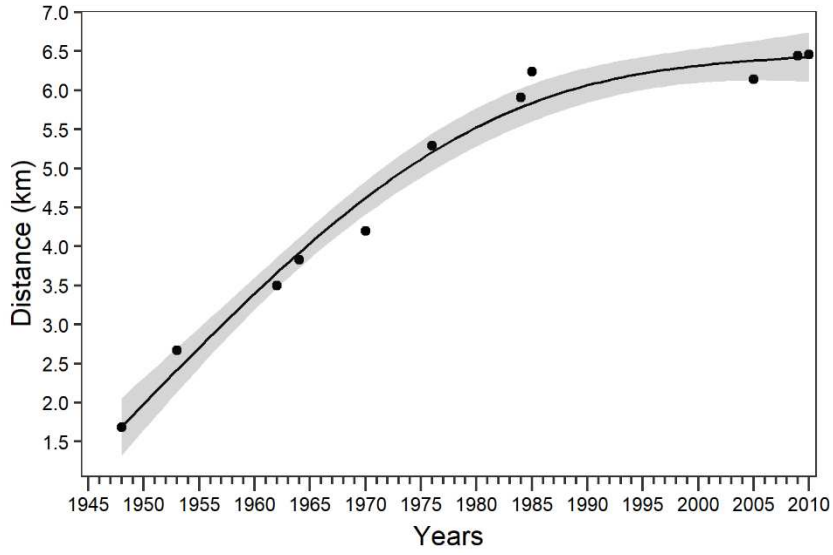

Figure 2. Relationship between distance from the front and time. Dots represent distances calculated for the known positions of the front (Table S2) and the dark line represents the average model estimate. The ribbon around the estimate represents ±2SE.

3.6 Relationship between diversity metrics and distance from tidewater glacier front

For each diversity metric a GAM was fitted with the distance from the glacier front as predictor using the R package *mgcv* (Wood, 2017). Each model was fitted using thin plate regression splines and ten basis dimensions. Taxonomic richness was modelled using Poisson error distribution with log-link function, Rao using beta distribution with logit-link function, while Shannon index and functional richness using gamma distribution with log-link function.

Due to very low foraminiferal abundances in some samples, we used only the sediment layers with > 20 picked individuals to fit the models. This threshold was selected as a compromise between the retained number of samples, the homogeneity of their distribution on the predicting variable, and the accuracy of the measured diversity metrics. To support the selected threshold, all models were fitted also using the samples containing ≥ 30 picked individuals.

3.7 Foraminiferal communities in relation to the distance from the front

A principal component analysis (PCA) was performed on foraminiferal relative abundances using the R package *vegan* (Oksanen et al., 2019). The first two axis of the PCA (explaining about 88% of the total variance) were retained. Then, to test if species composition varies in relation to the distance from the glacier front, GAMs were fitted on PCA scores using the sample coordinates along the PC1 and PC2 component as the response variables, and the distance from the glacier front as predictor using the R package *mgcv* (Wood, 2017). Both models were fitted using cubic regression splines with ten basis dimension (Wood, 2017).

4. Results

4.1 Sedimentological parameters

Figure 3 shows the lithologic log of the uppermost 112 cm of the core, and other physical parameters measured with the GEOTEK multi-sensor core logger (MSCL). The core is mostly characterised by clayey silts, with silt contents measured at about 80% throughout the core and clay contents between 16 and 19% (Table S3). Some layers rich in clasts, layered or isolated, reaching 74% of sand (level 91-92 cm), were observed between 101 and 82 cm depth, i.e. before 1962, when the glacier front was about 2.5 km away. Lonestones were observed all along the core. Magnetic susceptibility is low all along the core, varying between 5 and 8 10^{-8} m^3kg^{-1} and

sediment dry bulk density varies between 1.2 and 1.5 g cm^{-3}. Supplementary sedimentological parameters are reported in Figure S2.

Data of ^{137}Cs activity for the study core and a twin core sampled at the same time, 50 m apart from this GC01 (i.e., core GC02), are reported in Figure 3b, modified from Streuff et al., (2015). ^{137}Cs activity was found from the 110 cm level to the core top, and the maximum activity was recorder at 85 cm depth. A secondary peak of ^{137}Cs was observed at 15 cm depth, better pronounced in the twin core CG02. Based on ^{137}Cs activity, three dates were used for the final age model (i.e., 1950 at 105 cm, 1962 at 85 cm, and 1986 at 15 cm depth). Then, SAR were approximately estimated by Streuff et al. (2015) at ~1.67 $cm.yr^{-1}$ before 1962, ~2.92 $cm.yr^{-1}$ between 1962 and 1986 and 0.63 $cm.yr^{-1}$ since 1986. This later low SAR measured in the uppermost 15 cm of the core is likely due to core top lost during sampling (see details in Streuff et al., 2015).

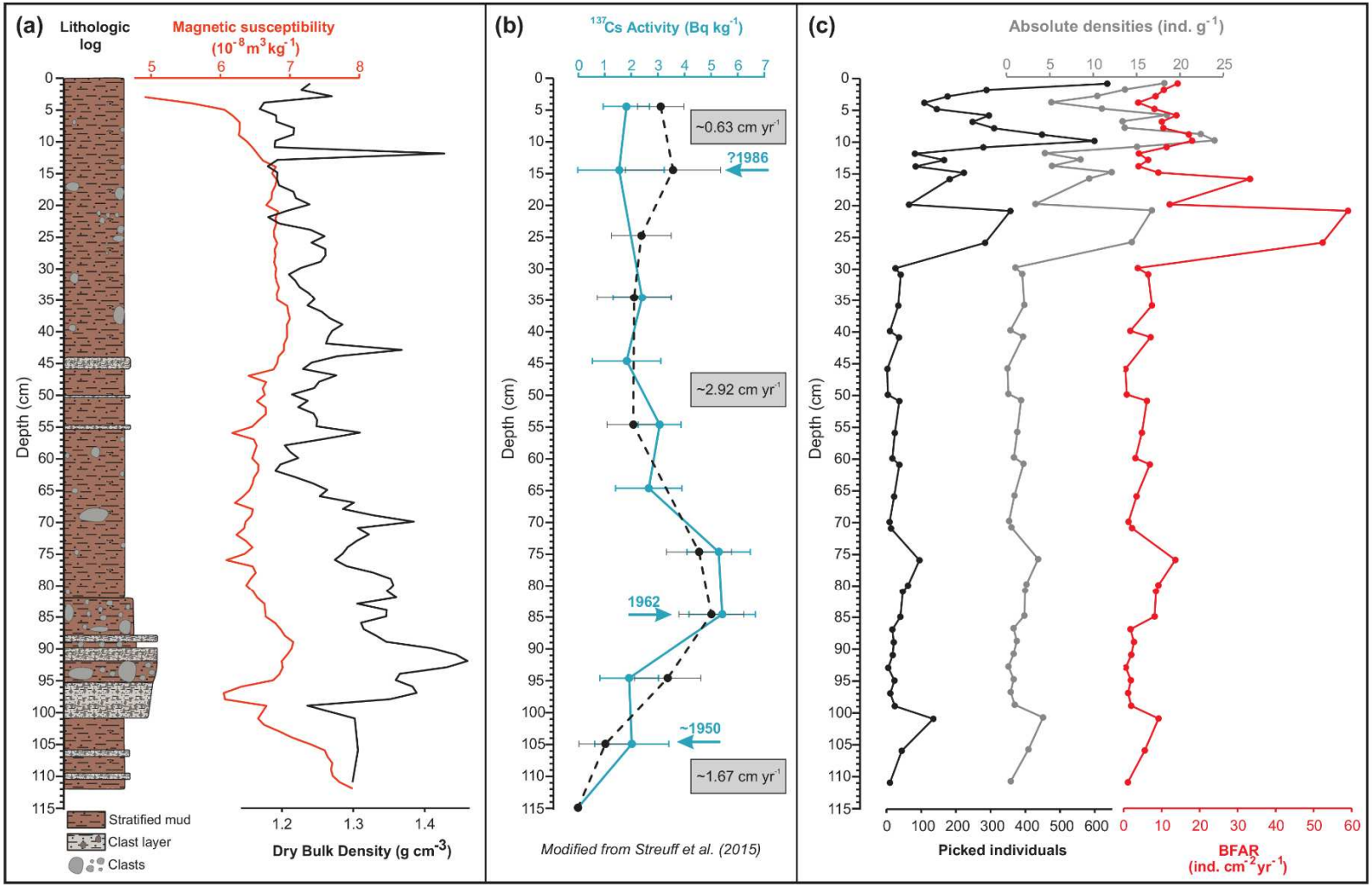

Figure 3. (a) Lithologic log (modified from Streuff et al., 2015) accompanied by magnetic susceptibility, and dry bulk density of the studied core. **(b)** Excess ^{137}Cs activity profiles for the study core GC01 (continued blue line) and its twin core GC02 (dashed black line), error bars represent 2σ uncertainties; SARs expressed in cm yr^{-1}are indicated in in grey rectangles; modified from Streuff et al. (2015). **(c)** Raw number of picked foraminifera (black line), standardised per gram of dry sediment (grey line) and Benthic Foraminiferal Accumulation Rates (red line) along the core (all considering the >100 µm fraction).

4.2 Foraminiferal changes through time

4.2.1 Foraminiferal densities and fluxes

The number of picked foraminifera together with absolute densities per gram of dry sediment and BFAR values are reported in Figure 3c in function of the core depth. The number of picked foraminifera is <50 picked individuals in the interval 112-30 cm with two exceptions (i.e., layers 101, 80-76 cm). Higher number of individuals (i.e., varying between 65 and about 650) with a large variability is observed in the uppermost part (30-0 cm). The same trend is observed for the absolute densities with densities < 4 ind. g^{-1} in the 112-30 cm interval and much variable densities in the 30-0 cm interval (i.e., between 3 and 23 ind. g^{-1}). BFAR spans between 2 and 20 ind. $cm^{-2}yr^{-1}$ all along the core except at 16 cm (about 33 ind. $cm^{-2}yr^{-1}$) and at 26 and 21 cm where the BFAR reaches 50-60 ind. cm^{-2} yr^{-1}. Thus, both absolute densities and BFAR become highly variable from the 30-26 cm level to the core top, corresponding to the ~1982-2010 period, when the glacier retreat started to slow down, and the front took position from about 5.5 to 6.5 km from the core site.

4.2.2 Diversity metrics versus distance from the front

Taxonomic and functional richness remained constant when the glacier front was closer to the core site than 4.5 km, and started to exponentially increase afterwards (Fig. 4a, 4b). From about 5.5 km, a twofold increase is observed for taxonomic richness, going from an average of 5 to 15 species, whereas an increase of about one third was observed for functional richness from 0.6 to 0.8. Shannon index (H') and Rao's quadratic entropy display a linear increase with the distance from the glacier front (Fig. 4c, 4d). Results were consistent when the models were fitted with samples containing >30 picked individuals (Fig. S3).

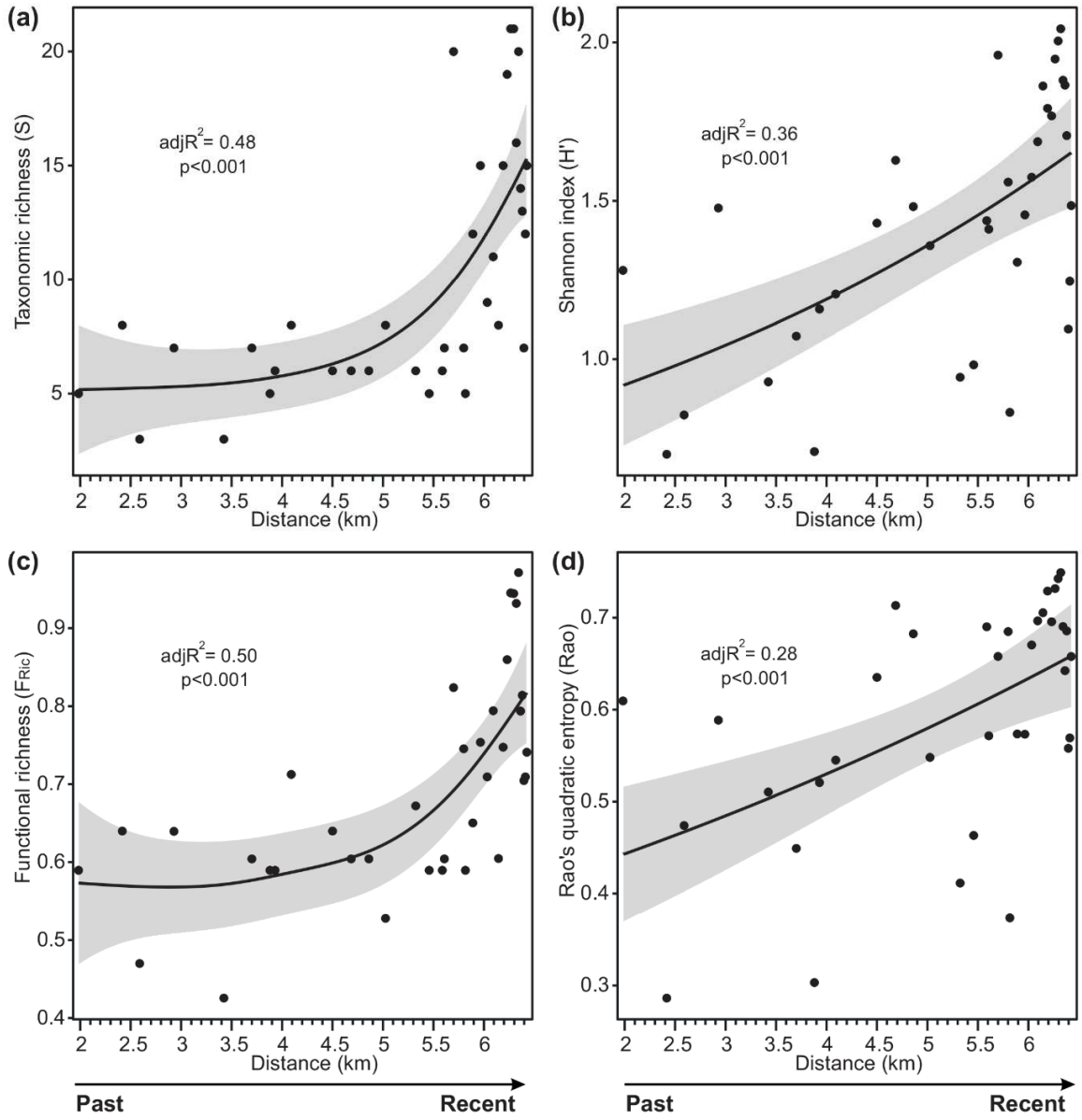

Figure 4. Relationship between distance from the glacier front and taxonomic richness **(a)**, Shannon index **(b)**, functional richness **(c)**, and Rao's quadratic entropy **(d)**. Dots represent the raw data points including samples with > 20 picked individuals, while dark lines represent the average model estimates. The ribbon around the estimates represents ±2SE.

4.2.3 Foraminiferal communities versus distance from the front

A PCA analysis was performed on foraminiferal communities to detect community changes through time as a function of the distance from the glacier front. The first two axis (explaining about 88% of the total variance) were retained from the principal component analysis (PCA; Fig. 5a). The PC1 is mainly driven by *Cassidulina reniforme* and *Quinqueloculina stalkeri*, PC2 is essentially driven by *Elphidium clavatum* and *Q. stalkeri*. The models of the Principal Component (PC) axis in relation to the distance from the glaciers front show that when the glacier front was closer to the core site than 4.5 km, the assemblages were dominated by *C.*

reniforme, followed by a dominance of *Q. stalkeri* at about 5 km and *E. clavatum* at 6 km (Fig. 5b, 5c). Then, the assemblages living at about 6.5 km were more diversified. Foraminiferal relative abundances for the major species in relation to time and distance from the front can be find in supplementary material (Fig. S4).

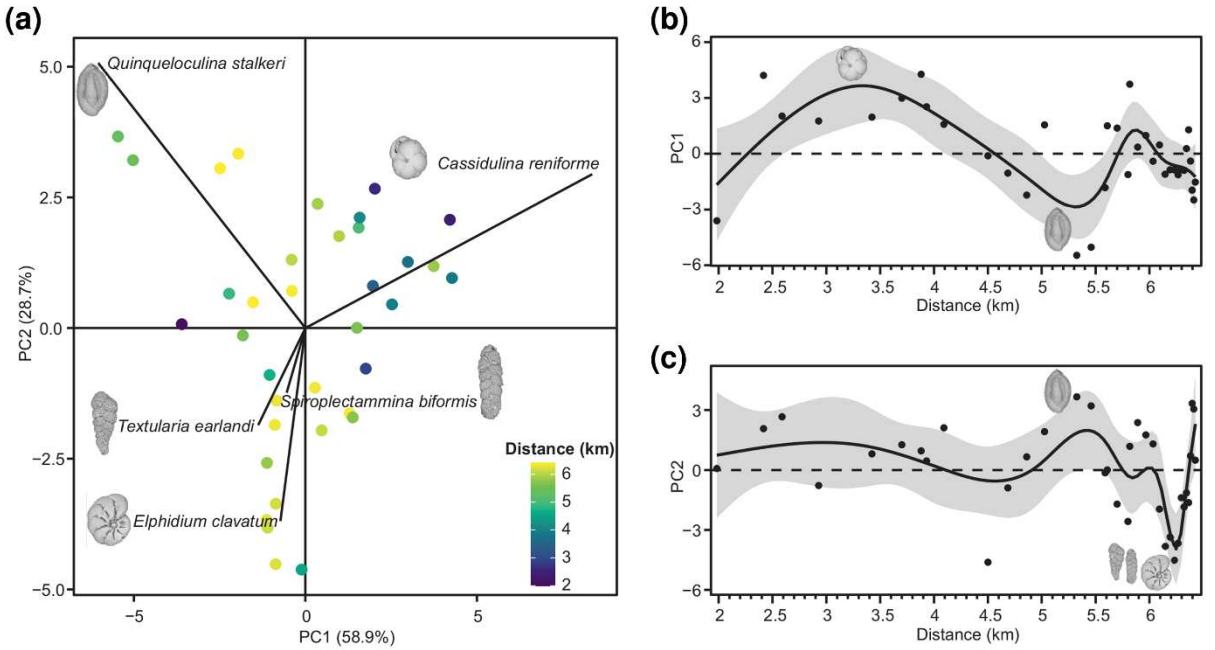

Figure 5. (a) Principal component analysis (PCA) performed on relative abundances of foraminiferal communities considering the entire assemblages (i.e., all species including minor ones). Species vectors are displayed only for the species explaining the majority of the variance. The scale colour corresponds to the distance from the glacier front. **(b)** GAMs predicting PC1 and **(c)** PC2 based on the distance from the glacier front. Dots represent the raw data points and dark lines represent the average model estimate. The ribbon around the estimate represents ±2SE.

4.2.4 Elemental ratios on foraminifera

The ratios of five elements (i.e., Ba/Ca, Mg/Ca, Mn/Ca, Na/Ca, and Sr/Ca) expressed in mmol mol^{-1} for the two species *Cassidulina reniforme* and *Elphidium clavatum* along the core are reported in supplementary material (Fig. S5). In general, the signals for both species and all five ratios did not show any clear pattern, and vary in a limited interval of concentrations along the core. The mean Ba/Ca ratio for both species varies between 0.003 and 0.010 mmol mol^{-1}. The mean Mg/Ca values for *C. reniforme* varies between 0.66 and 2.07 mmol mol^{-1}, while for *E. clavatum* the mean varies between 0.71 and 1.82 mmol mol^{-1}. The Mn/Ca ratio varies in the 0.02-0.19 mmol mol^{-1} interval for *C. reniforme* and in the 0.03-0.23 mmol mol^{-1} interval for *E. clavatum*. The Sr/Ca ratio varies from 1.02 to 1.25 mmol mol^{-1} for *C. reniforme* and from 1.34 to 1.88 mmol mol^{-1} for *E. clavatum*. The Na/Ca ratio varies from 4.44 to 8.20 mmol mol^{-1} for *C. reniforme* and from 5.85 to7.67 mmol mol^{-1} for *E. clavatum*. In general, *Elphidium clavatum*

shows a more stable signal since 1990, when the terminus was about 6 km away from the core site.

5. Discussion

5.1 Glacier retreat and foraminiferal fluxes

The study core covers the time interval between ~1950 and 2010, i.e. recording the period of a general glacier front retreat from the last intense glacier surge (and advance) of 1948 until the present-day position. Our results show lower foraminiferal densities and fluxes before year ~1982 (i.e., from ~110 to 30 cm depth in the core) compared to the higher values found in the more recent layers (Fig. 3). The low foraminiferal densities recorded at the deepest sediment section can be explained by *(i)* high SARs, *(ii)* physical disturbance, and *(iii)* non-fossilizing species.

(i) High SARs. High sedimentation rates dilute the signal of the foraminiferal production resulting in artificial low foraminiferal densities, as we observed before ~1982, whereas low SARs may concentrate organisms. Historical reconstructions of the movements of the Kronebreen glacier complex and the associated SARs are reported in the study of Streuff et al., (2015). The active phase of the glacier surge (i.e., maximum ice extent by front advance) was identified through the terminal moraine, dated at 1948, and located in the proximity of the CG01 core site. Unit 1 of the sedimentary record (as described by Streuff et al., 2015 in core CG01) started with the deposit of a massive diamict (10 cm of coarse sediment observed at 165-155cm depth in the CG01 core) due to this glacier surge in 1948, followed by 60 cm of sediment deposited between 1948 and 1950. This very high SAR of 30 cm yr^{-1} is in accordance with previous estimations of sediment supply in the immediate proximity of a glacier front (e.g., Trusel et al., 2010). After a surge event, a fast retreat of the glacier terminus generally occurs and is accompanied by a high calving flux (Mansell et al., 2012). During this retreat phase, the glacier slides, abrading the bedrock and charging in sediment the surrounding environment (e.g., Powell, 1991). In the historical record of Kronebreen glacier complex, the fast retreat phase has lasted about 30 years, and provoked high sedimentary supply, typical of the proximal front environment. High sedimentation rates between 1.67 and 2.92 cm yr^{-1} were recorded before ~1982 (i.e., below 30 cm depth in the core) whereas later, SARs decreased to reach 0.63 cm yr^{-1} (Streuff et al., 2015). Based on our reconstitution of the distance between the glacier front and the core site, we note that the change at ~1982 coincides with the onset of the slowing down of the glacier front retreat (Fig. 2), leading to reduced SARs.

(ii) Disturbance. Physical disturbance on the seafloor is mainly associated with high sediment supply and the consequent burying of the benthic habitat. After the 1948 surge event and during the fast 30-year long retreat of the Kronebreen glacier complex, sediment typical of glacier-proximal environments is deposited at the core site, i.e. fine sediments from the buoyant meltwater turbid plume originated from subglacial discharges, and the coarse clasts deposited in layers, from ice rafting (Streuff et al., 2015). As such, the fast glacier retreat leading to a continuous and high supply of sediment may have hampered the settlement of diverse and abundant benthic foraminiferal communities, even several kilometres away from the terminus and can be an additional cause for low foraminiferal densities.

(iii) Species loss. Sedimentary archives may not preserve some species, so called non-fossilizing species, especially from the agglutinated group. These build organic-cemented tests that are potentially destroyed almost immediately after their death. As such, the low foraminiferal densities recorded here may be due, at least partly, to this taphonomic process. This hypothesis is supported by the living and dead assemblage compositions observed at the present sea-sediment interface (cf. Fossile et al., *Chapter 3*). Indeed, between 2 to 5 km from the glacier terminus, the living assemblages in the inner Kongsfjorden are largely dominated by two agglutinated opportunistic species *Capsammina bowmanni* and *Saccammina* cf. *sphaerica* (cf. Fossile et al., *Chapter 3*) whereas these two species are almost absent in the dead assemblages. Because the test of the two cited species is extremely fragile (*C. bowmanni* has a very delicate, flexible test composed of mica flakes agglutinated by fine grained white material; Gooday et al., 2010) they are typical non-fossilizing species. Other agglutinated species however, such as *Textularia earlandi* and *Spiroplectammina biformis*, are well preserved in today Arctic environments and are found in high abundances along sedimentary archives (e.g., (e.g., Lloyd, 2006; Rasmussen and Thomsen, 2015; Jackson et al., 2021). They were observed as well along the study core with more than 30 % relative to calcareous specimens (cf. Fig. S6).

Since ~1982 (from 30 cm depth up to the core top), when the glacier retreat started to slow down (Fig. 2), we observe, besides the overall increasing trend, a great variability in foraminiferal densities and BFAR, with the presence of several successive peaks. Based on the age model, between 30 and 15 cm depth, each sample would correspond to approximately 4 months, whereas each sample in the topmost 15 cm would correspond to about 1.6 years. Therefore, the measured variability may be related to *(i)* seasonality and/or *(ii)* interannual variability.

(i) Seasonality. The Arctic is characterised by a strong seasonality due to light limitation, which implies reduced organic fluxes to the seafloor during winter (e.g., Wassmann and

Reigstad, 2011). This seasonality is also observed in the glacier dynamics itself. Specifically, a seasonal cycle is normally observed for tidewater glacier in quiescent phase: enhanced retreat in summer (related to surface melting, subglacial discharges and calving) and reduced retreat in winter (Mansell et al., 2012). These processes differently influence benthic foraminiferal assemblages during the warm and cold seasons with also possible effects on foraminiferal densities (e.g., Korsun and Hald, 2000; Pawłowska et al., 2017). During winter, sea ice can form in the fjord, and it promotes local primary production (PP) in late spring (e.g., Hodal et al., 2012). During summer, glacial discharges of turbid meltwaters spread from the glacier terminus creating water turbidity gradients (e.g., D'Angelo et al., 2018; Meslard et al., 2018). These meltwater turbid plumes reduce light penetration depths (e.g., Payne and Roesler, 2019) limiting PP near the terminus (i.e., hundreds of meters to 10 Km; Hopwood et al., 2020) and carbon fluxes to the seafloor.

(i) Interannual variability. Calving rates at tidewater glacier fronts are strictly related to ocean temperatures (Luckman et al., 2015). In Kongsfjorden, the frontal ablation of Kronebreen glacier complex is influenced by the AW inflow which also contributes to the formation of strong temperature and salinity gradients (e.g., Hop et al., 2002; Svendsen et al., 2002; Cottier et al., 2010; Hop and Wiencke, 2019). However, the AW intrusion in the fjord is not constant. The intrusions are linked to the geostrophic balance between shelf and fjord waters (Svendsen et al., 2002; Cottier et al., 2005), and are subjected to interannual variability (Hop et al., 2002; Svendsen et al., 2002; Cottier et al., 2005) depending on internal and external factors (e.g., formation of sea ice during the preceding winter as internal, and the shelf wind field creating instabilities at the shelf front during summer as external; Cottier et al., 2005). This interannual variability of AW intrusion into the fjord may have an influence on the frontal ablation of the glaciers. Consequently, the glacier induced disturbance (GID) on the benthic environment would undergo an interannual variability potentially causing the observed variations in foraminiferal densities. It is also possible that the variable intrusion of AW had a direct influence on foraminiferal faunas, promoting or not their development.

5.2 Foraminiferal diversity patterns

Our data show positive relationships between diversity metrics and the reconstructed distance from the glacier front. The patterns observed for taxonomic (S) and functional (F_{Ric}) richness were similar and characterised by a stable estimate between 2 and 5.5 km from the glacier front (i.e., between ~1950 and ~1982), followed by an exponential increase after 5.5 km (i.e., years

~1982 - 2010) (Fig. 4a, c). Conversely, Shannon index (H') and Rao's quadratic entropy (Rao) increased linearly since the beginning of the glacier retreat (Fig. 4b, d). This suggests that in the first retreat phase, while the number of species and functional space volume occupied remained stable, the community became more equilibrated in term of species and functional composition. It is possible that the disturbance (GID) caused by a progressively reduced glacier favoured at first a reduced competition among the species already present, and only afterwards triggered the establishment of other species and functional entities.

The general increase in taxonomic richness observed when moving far from the glacier front is coherent with previous observations on living foraminiferal assemblages in other Arctic fjords (e.g., Korsun et al., 1995; Korsun and Hald, 1998; Forwick et al., 2010; Włodarska-Kowalczuk et al., 2013). Furthermore, the recorded trends across six decades (in response to a glacier retreat of about 4.5 km) seem to confirm a recently published global meta-analysis suggesting that glacier retreat has a positive local influence on several taxa including benthic foraminifera (Cauvy-Fraunié and Dangles, 2019). They observed that taxonomic richness increases at lower glacial influence, but with a variability in species responses to the retreat (i.e., winners and losers). In particular, species adapted and restricted to the glacier-influenced area were identified among the loser populations of glacier-retreat, whereas generalist/invasive species colonising from downfjord were identified as winners. Glacial-influenced areas, such as Arctic fjords, are subjected to strong environmental gradients contributing to the heterogeneity of the region, thus favouring the establishment of specialised species with positive influence on the regional diversity (i.e., ɣ-level biodiversity; Willig and Presley, 2017). The retreat of glaciers and their transition from marine- to land-terminating would reduce the environmental gradients and habitat heterogeneity. This would lead to loss of specialised species restricted to the glacier-influenced area as well as loss of ecological functions performed only by those species and a consequent decrease in regional diversity.

5.3 Validation of diversity metrics as proxies for glacier retreat

The diversity patterns observed for the fossil faunas along a temporal scale, as a function of the distance from the glacier front, are generally congruent with those observed for the living faunas along a spatial scale in the same fjord (Fossile et al., *Chapter 4*). Specifically, the four diversity metrics considered here increased with glacier retreat, as previously observed along a transect going away from the glacier front (Fig. 6). Although the number of species in fossil faunas was about half that in the living faunas, a threefold increase in taxonomic richness is observed for

both fossil and living faunas between 2 and 6.5 km distance from the front (Fig. 6a). However, this increase resulted from slightly different patterns, with a more exponential increase observed in the fossil record. Conversely, Shannon index increased more rapidly in the living compared to the fossil faunas, while reaching a similar value at the greatest distance (Fig. 6b). Unlike taxonomic richness, the threefold increase in functional richness observed in the living faunas was only partially detected in the fossil faunas (Fig. 6c). Instead, Rao showed a similar pattern between fossil and living faunas despite generally higher values in the former (Fig. 6d).

The observed differences in diversity patterns between living and fossil faunas may be the result of *(i)* the different sampling resolution (i.e., n=9 and n=36 for living and fossil, respectively) and/or *(ii)* the presence of abundant, non-fossilizing species in the living faunas not observed in the archive (i.e., *Capsammina bowmanni*, *Saccammina* cf. *sphaerica*). Indeed, when the models on the living faunas are recomputed after excluding the two extremely fragile species with no fossilisation potential, the results are much closer to that of the fossil faunas for Shannon and Rao (Fig. 6b, d). However, this is not observed for taxonomic and functional richness, for which differences are maintained beside the exclusion of these species and are therefore possibly linked to the sampling resolution.

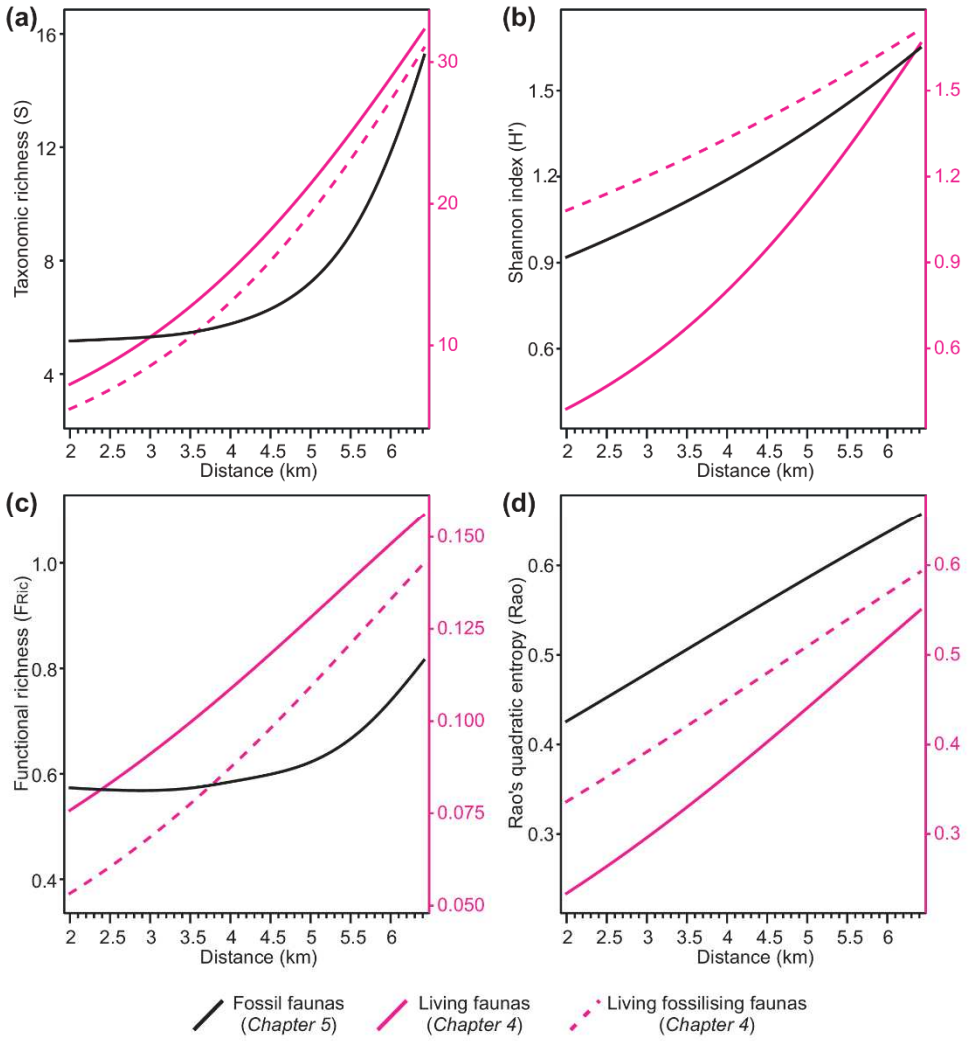

Figure 6. Relationship between distance from the glacier front and **(a)** taxonomic richness, **(b)** Shannon index, **(c)** functional richness, and **(d)** Rao's quadratic entropy. Black lines represent the average model estimate for the fossil faunas (this study) while pink lines represent the estimates for the living faunas. Total living faunas are represented by the continuous lines, while fossilising faunas are represented through dashed pink lines.

The documented diversity patterns across six decades reflect the changes that have occurred in about 4.5 km of glacier retreat in Kongsfjorden in response to a gradient of glacier induced disturbance (GID). A general diversity increase with increased distance from the glacier front is detected by all diversity metrics, suggesting that they can be simultaneously used to reconstruct tidewater glacier retreat. Furthermore, our results demonstrate that Shannon index and Rao better detect the progressive glacier distal environment. Indeed, both metrics consider the proportions of the species or those of the functional entities, thus being able to better represent community changes through time.

Altogether, our results support the use of diversity metrics (especially H' and Rao) as potential proxies for glacier retreat as previously proposed (Fossile et al., *Chapter 4*). These

diversity metrics can qualitatively reconstruct glacier retreat through the observation of a general diversity increase in other fjords. Furthermore, Shannon and Rao can be applied semi-quantitatively by analysing relative changes in these metrics through time in comparison to relative changes through space shown in Fossile et al. (*Chapter 4*). This semi-quantitative application can only be performed on sediment archives for which at least one reference point is available (i.e., the distance of the sampling site from the glacier front at a certain sediment depth). This generally corresponds to the sediment surface of the core sampled at a known time for which the distance from the front can be retrieved (either from satellite images or from previously reconstructed front). A more quantitative application could be achieved if the analysis conducted by Fossile et al., (*Chapter 4*) is replicated in other fjords subjected to different GID intensities.

The proposed proxies can be applied on historical archives (i.e., hundreds of years) collected from similar environments in front of present tidewater glaciers as well as in front of past tidewater glacier that now are land-terminating. While applying the proxy, it should be considered that it was developed along a limited spatial scale (i.e., about 2-12 km distance from the glacier front; Fossile et al., *Chapter 4*) and therefore reconstructing glacier retreat on greater distances may not be reliable. Future investigations should focus on enlarging this spatial scale and increasing the sampling resolution in the glacier proximity where the steepness of environmental gradients is greatest.

Furthermore, these proxies may help to enlarge the window of the instrumental period used in predictions of future glacier retreat. The ability of these metrics to detect ice-sheets changes across longer time scales (i.e., thousands of years) needs to be considered carefully. Further investigations along paleo-environmental archives are needed because there are potential limitations linked to taphonomic loss which could affect the observed diversity patterns.

5.4 Foraminiferal community changes through time

Foraminiferal communities evolve through time in relation to the distance from the glacier front. At less than 4.5 km from the front, the assemblages were dominated by *Cassidulina reniforme*, followed by an alternative increase in relative abundances of *Quinqueloculina stalkeri* or *Elphidium clavatum*, and by more diversified and homogeneous communities in site located further than 6 km (Fig. 5, Fig. S4).

The dominance of *C. reniforme* occurred during the fast retreat of the glacier after the surge in 1948 and continued until the front reached about 4.5 km of distance from the core site. This

pattern is in accordance with previous studies identifying *C. reniforme* as a glacier proximal species (e.g., Hald and Korsun, 1997; Korsun and Hald, 2000; Szymańska et al., 2017; Fossile et al., 2020, *Chapter 3*; Jima et al., 2021). This suggests its opportunistic response to the stressful conditions related to GID and supports the observation that *C. reniforme* is a loser species from glacier retreat (cf. Cauvy-Fraunié and Dangles, 2019). Indeed, its specialisation for the glacier-influenced area is linked to the presence of gradients created by tidewater glaciers and therefore affected by their retreat.

The subsequent increase of *Q. stalkeri* and *E. clavatum* suggests that the ability of these two species to compete with *C. reniforme* increases in ameliorated conditions (e.g., reduce glacial physical disturbance, increase organic flux). *Quinqueloculina stalkeri* is considered as an opportunist species commonly found in glaciated fjords heads and previously linked to the presence of glaciomarine clay (e.g., Korsun and Hald, 1998).. Also, *E. clavatum* usually shows an opportunistic behaviour and is commonly found together with *C. reniforme* in glacial influenced areas (e.g., Łącka and Zajączkowski, 2016; Szymańska et al., 2017). Furthermore, the two agglutinated species *Textularia earlandi* and *Spiroplectammina biformis*, are generally associated with *E. clavatum* once reached 6 km of distance from the glacier front. This is in accordance with previous observations on the living faunas from Kongsfjorden at a comparable distance from the glacier front (cf. station St1 in Fossile et al., *Chapter 3*). These species are typical of glaciomarine habitats but potentially less competitive than *Q. stalkeri* and *E. clavatum*. In particular, *T. earlandi* is a shallow infaunal species (Murray, 2006) and therefore potentially dependent on an increased sediment stability which is found at about 6 km from the glacier front (Fossile et al., *Chapter 3*).

6. Conclusions

In the present study we assessed the use of benthic foraminifera in reconstructing glacier retreat. For this purpose, we analysed sedimentological characteristics and foraminiferal patterns along a sedimentary core (10JM-GLACIBAR-GC01) collected in 2010 in front of the Kronebreen glacier complex in Kongsfjorden (Svalbard). The archive, covering a period of about six decades registered a progressive glacial distal environment after the last event of surge in 1948. Foraminiferal fluxes were influenced by the glacier retreat and consequent intense disturbance in the period following the surge event. Taxonomic and functional diversity metrics increased as a function of the distance from the glacier terminus, with patterns consistent with previous observations on living faunas in the same fjord. Further, foraminiferal communities evolve in

relation to a progressive glacier distal environment, with few opportunistic species preferring and/or tolerating the GID (i.e., *Cassidulina reniforme*) gradually replaced by more equilibrated and diversified assemblages. Altogether these observations validate the use of multiple diversity metrics, and in particular of Shannon and Rao indices, as proxies for glacier retreat in glaciated coastal environments and their application in historical reconstructions. At present the proxies can be applied qualitatively or semi-quantitatively, and additional investigations along longer spatial scales or in other fjords, may improve their applicability.

Data availability. Raw data will be made available online upon submission and acceptance of this manuscript.

Supplement. Tables S1, S2 and S3 and Figs. S1, S2, S3, S4 and S5 can be found in the Supplement section.

Author contributions. EF: conceptualisation, data curation, formal analysis, investigation, methodology, validation, visualisation, writing-original draft, writing-review and editing. MPN, MM, HH: conceptualisation, funding acquisition, resources, project administration, supervision, validation, writing-review and editing. KH: investigation, resources. CB: investigation, writing-review and editing. KS: investigation.

Acknowledgements. We acknowledge the efficient technical help provided by Juliette Tessier, Anaëlle Kocher and Corentin Guilhermic.

Financial support. The research was funded by the ABBA (Observatoire des Sciences de l'Univers de Nantes Atlantique), Bi-SMART (University of Angers) and TANDEM (Région Pays de la Loire) projects. This research is part of the PhD thesis of Eleonora Fossile, which is co-funded by French National Program MOPGA (Make Our Planet Great Again) and the University of Angers.

Competing interests. The authors declare that they have no conflict of interest.

References

Appleby P.: Decades of dating recent sediments by fallout radionuclides: a review. Holocene 18:83–93, 2008

Barker, S., Greaves, M. and Elderfield, H.: A study of cleaning procedures used for foraminiferal Mg/Ca paleothermometry, Geochemistry, Geophys. Geosystems, 4(9), 1–20, https://doi.org/10.1029/2003GC000559, 2003.

Barras, C., Mouret, A., Nardelli, M. P., Metzger, E., Petersen, J., La, C., Filipsson, H. L. and Jorissen, F.: Experimental calibration of manganese incorporation in foraminiferal calcite, Geochim. Cosmochim. Acta, 237, 49–64, https://doi.org/10.1016/j.gca.2018.06.009, 2018.

Bennett, M. R., Hambrey, M. J., Huddart, D., Glasser, N. F. and Crawford, K.: The landform and sediment assemblage produced by a tidewater glacier surge in Kongsfjorden, Svalbard, Quat. Sci. Rev., 18(10–11), 1213–1246, https://doi.org/10.1016/S0277-3791(98)90041-5, 1999.

Botta-Dukát, Z.: Rao's quadratic entropy as a measure of functional diversity based on multiple traits, J. Veg. Sci., 16(5), 533, https://doi.org/10.1658/1100-9233(2005)16[533:rqeaam]2.0.co;2, 2005.

Bourriquen, M.: Evolution du littoral de la presqu'île de Brøgger dans le contexte du changement climatique contemporain, Spitsberg nord-occidental, 2018.

Carmona, C. P., de Bello, F., Mason, N. W. H. and Lepš, J.: Traits Without Borders: Integrating Functional Diversity Across Scales, Trends Ecol. Evol., 31(5), 382–394, https://doi.org/10.1016/j.tree.2016.02.003, 2016.

Carmona, C. P., de Bello, F., Mason, N. W. H. and Lepš, J.: Trait probability density (TPD): measuring functional diversity across scales based on TPD with R, Ecology, 100(12), 1–8, https://doi.org/10.1002/ecy.2876, 2019a.

Carmona, C. P.: TPD: Methods for Measuring Functional Diversity Based on Trait Probability Density. R package version 1.1.0. https://CRAN.R-project.org/package=TPD, 2019b

Cauvy-Fraunié, S. and Dangles, O.: A global synthesis of biodiversity responses to glacier retreat, Nat. Ecol. Evol., 3(12), 1675–1685, https://doi.org/10.1038/s41559-019-1042-8, 2019.

Cogley, J. G., Hock, R., Rasmussen, L. A., Arendt, A. A., Bauder, A., Braithwaite, R. J., Jansson, P., Kaser, G., Möller, M., Nicholson, L. and Zemp, M.: Glossary of glacier mass balance and related terms, UNESCO/IHP, Paris., 2011.

Cottier, F., Tverberg, V., Inall, M., Svendsen, H., Nilsen, F. and Griffiths, C.: Water mass modification in an Arctic fjord through cross-shelf exchange: The seasonal hydrography of Kongsfjorden, Svalbard, J. Geophys. Res. Ocean., 110(12), 1–18, https://doi.org/10.1029/2004JC002757, 2005.

Cottier, F. R., Nilsen, F., Enall, M. E., Gerland, S., Tverberg, V. and Svendsen, H.: Wintertime warming of an Arctic shelf in response to large-scale atmospheric circulation, Geophys. Res. Lett., 34(10), 1–5, https://doi.org/10.1029/2007GL029948, 2007.

Cottier, F. R., Nilsen, F., Skogseth, R., Tverberg, V., Skarðhamar, J. and Svendsen, H.: Arctic fjords: a review of the oceanographic environment and dominant physical processes, Geol. Soc. London, Spec. Publ., 344, 35–50, https://doi.org/10.1144/sp344.4, 2010.

D'Angelo, A., Giglio, F., Miserocchi, S., Sanchez-Vidal, A., Aliani, S., Tesi, T., Viola, A., Mazzola, M. and Langone, L.: Multi-year particle fluxes in Kongsfjorden, Svalbard, Biogeosciences, 15(17), 5343–5363, https://doi.org/10.5194/bg-15-5343-2018, 2018.

Dadey, K. A., Janecek, T. and Klaus, A.: Dry-bulk density: its use and determination, Proc., Sci. results, ODP, Leg 126, Bonin Arc/Trench Syst., 126, 551–554, https://doi.org/10.2973/odp.proc.sr.126.157.1992, 1992.

Darlington, E.: Kronebreen to Kongsfjorden , Svalbard ; insights from in situ and remote-sensing analyses of sediment plumes by, 2015.

de Bello, F., Botta-Dukát, Z., Lepš, J. and Fibich, P.: Towards a more balanced combination of multiple traits when computing functional differences between species, Methods Ecol. Evol., 2020(May), 1–6, https://doi.org/10.1111/2041-210X.13537, 2020.

de Nooijer, L., Brombacher, A., Mewes, A., Langer, G., Nehrke, G., Bijma, J. and Reichart, G.-J.: Ba incorporation in benthic foraminifera, Biogeosciences Discuss., 1–35, https://doi.org/10.5194/bg-2017-45, 2017.

Dowdeswell, A., Hamilton, G. S. and Hagen, O. V. E.: The duration of the active phase on surge-type glaciers: contrasts between Svalbard and other regions, J. Glaciol., 37(127), 388–400, https://doi.org/https://doi.org/10.3189/S0022143000005827, 1991.

Dowdeswell, J. A., Hodgkins, R., Nuttall, A. -M, Hagen, J. O. and Hamilton, G. S.: Mass balance change as a control on the frequency and occurrence of glacier surges in Svalbard, Norwegian High Arctic, Geophys. Res. Lett., 22(21), 2909–2912, https://doi.org/10.1029/95GL02821, 1995.

Forwick, M., Vorren, T. O., Hald, M., Korsun, S., Roh, Y., Vogt, C. and Yoo, K.-C.: Spatial and temporal influence of glaciers and rivers on the sedimentary environment in Sassenfjorden and Tempelfjorden, Spitsbergen, Geol. Soc. London, Spec. Publ., 344, 163–193, https://doi.org/10.1144/SP344.13, 2010.

Fossile, E., Nardelli, M. P., Jouini, A., Lansard, B., Pusceddu, A., Moccia, D., Michel, E., Péron, O., Howa, H. and Mojtahid, M.: Benthic foraminifera as tracers of brine production in the Storfjorden "sea ice factory," Biogeosciences, 17(7), 1933–1953, https://doi.org/10.5194/bg-17-1933-2020, 2020.

Glock, N., Liebetrau, V., Eisenhauer, A. and Rocholl, A.: High resolution I/Ca ratios of benthic foraminifera from the Peruvian oxygen-minimum-zone: A SIMS derived assessment of a potential redox proxy, Chem. Geol., 447, 40–53, https://doi.org/10.1016/j.chemgeo.2016.10.025, 2016.

Gooday, A. J., Aranda da Silva, A., Koho, K. A., Lecroq, B. and Pearce, R. B.: The "mica sandwich"; a remarkable new genus of Foraminifera (Protista , Rhizaria) from the Nazaré Canyon (Portuguese margin , NE Atlantic), , 56(3/4), 345–357, 2010.

Gower, A. J. C.: A General Coefficient of Similarity and Some of Its Properties, Int. Biometric Soc., 27(4), 857–871, https://doi.org/10.2307/2528823, 1971.

Hagen, J. O., Liestøl, O., Roland, E. and Jørgensen, T.: Glacier Atlas of Svalbard and Jan Mayen., 1993.

Hagen, J. O., Kohler, J., Melvold, K. and Winther, J. G.: Glaciers in Svalbard: Mass balance, runoff and freshwater flux, Polar Res., 22(2), 145–159, https://doi.org/10.1111/j.1751-8369.2003.tb00104.x, 2003.

Hald, M. and Korsun, S.: Distribution of modern benthic foraminifera from fjords of Svalbard, European Arctic, J. Foraminifer. Res., 27(2), 101–122, https://doi.org/10.2113/gsjfr.27.2.101, 1997.

Hansen, S.: From surge-type to non-surge-type glacier behaviour: Midre Lovénbreen, Svalbard, Ann. Glaciol., 36, 97–102, https://doi.org/10.3189/172756403781816383, 2003.

Hijmans, R. J.: geosphere: Spherical Trigonometry. R package version 1.5-10. https://CRAN.R-project.org/package=geosphere, 2019

Hodal, H., Falk-Petersen, S., Hop, H., Kristiansen, S. and Reigstad, M.: Spring bloom dynamics in Kongsfjorden, Svalbard: Nutrients, phytoplankton, protozoans and primary production, Polar Biol., 35(2), 191–203, https://doi.org/10.1007/s00300-011-1053-7, 2012.

Holmes, F. A., Kirchner, N., Kuttenkeuler, J., Krützfeldt, J. and Noormets, R.: Relating ocean temperatures to frontal ablation rates at Svalbard tidewater glaciers: Insights from glacier proximal datasets, Sci. Rep., 9(1), 1–11, https://doi.org/10.1038/s41598-019-45077-3, 2019.

Hop, H. and Wiencke, C.: The Ecosystem of Kongsfjorden, Svalbard, in The Ecosystem of Kongsfjorden, pp. 1–20, https://doi.org/10.1007/978-3-319-46425-1_1, , 2019a.

Hop, H. and Wiencke, C.: The Ecosystem of Kongsfjorden, Svalbard, edited by Springer, Alfred Wegener

Institute, Helmholtz Centre for Polar and Marine Research, Bremerhaven, Germany., 2019b.

Hop, H., Pearson, T., Hegseth, E. N., Kovacs, K. M., Wiencke, C., Kwasniewski, S., Eiane, K., Mehlum, F., Gulliksen, B., Wlodarska-Kowalezuk, M., Lydersen, C., Weslawski, J. M., Cochrane, S., Gabrielsen, G. W., Leakey, R. J. G., Lonne, O. J., Zajaczkowski, M., Falk-Petersen, S., Kendall, M., Wangberg, S. A., Bischof, K., Voronkov, A. Y., Kovaltchouk, N. A., Wiktor, J., Poltermann, M., di Prisco, G., Papucci, C. and Gerland, S.: The marine ecosystem of Kongsfjorden, Svalbard, Polar Res., 21(1), 167–208, https://doi.org/https://doi.org/10.3402/polar.v21i1.6480, 2002.

Hopwood, M. J., Carroll, D., Dunse, T., Hodson, A., Holding, J. M., Iriarte, J. L., Ribeiro, S., Achterberg, E. P., Cantoni, C., Carlson, D. F., Chierici, M., Clarke, J. S., Cozzi, S., Fransson, A., Juul-Pedersen, T., Winding, M. H. S. and Meire, L.: Review article: How does glacier discharge affect marine biogeochemistry and primary production in the Arctic?, Cryosphere, 14(4), 1347–1383, https://doi.org/10.5194/tc-14-1347-2020, 2020.

Jackson, R., Kvorning, A. B., Limoges, A., Georgiadis, E., Olsen, S. M., Tallberg, P., Andersen, T. J., Mikkelsen, N., Giraudeau, J., Massé, G., Wacker, L. and Ribeiro, S.: Holocene polynya dynamics and their interaction with oceanic heat transport in northernmost Baffin Bay, Sci. Rep., 11(1), https://doi.org/10.1038/s41598-021-88517-9, 2021.

Jima, M., Jayachandran, P. R. and Nandan, S. B.: Modern Benthic Foraminiferal Diversity Along the Fjords of Svalbard Archipelago : Diversity Evaluation, Thalass. An Int. J. Mar. Sci., https://doi.org/10.1007/s41208-021-00356-7, 2021.

Kedra, M., Włodarska-Kowalczuk, M. and Wesławski, J. M.: Decadal change in macrobenthic soft-bottom community structure in a high Arctic fjord (Kongsfjorden, Svalbard), Polar Biol., 33(1), 1–11, https://doi.org/10.1007/s00300-009-0679-1, 2010.

König, M., Nuth, C., Kohler, J., Moholdt, G. and Pettersen, R.: A digital glacier database for svalbard, Glob. L. Ice Meas. from Sp., 229–239, https://doi.org/10.1007/978-3-540-79818-7_10, 2014.

Korsun, S. and Hald, M.: Modern benthic foraminifera off Novaya Zemlya tidewater glaciers, Russian Arctic, Arct. Alp. Res., 30(1), 61–77, https://doi.org/10.2307/1551746, 1998.

Korsun, S. and Hald, M.: Seasonal dynamics of Benthic Foraminifera in a Glacially Fed Fjord of Svalbard, European Arctic, J. Foraminifer. Res., 30(4), 251–271, https://doi.org/10.2113/0300251, 2000.

Korsun, S. A., Pogodina, I. A., Forman, S. L. and Lubinski, D. J.: Recent foraminifera in glaciomarine sediments from three arctic fjords of Novaja Zemlja and Svalbard, Polar Res., 14(1), 15–32, https://doi.org/10.3402/polar.v14i1.6648, 1995.

Łącka, M. and Zajączkowski, M.: Does the recent pool of benthic foraminiferal tests in fjordic surface sediments reflect interannual environmental changes? The resolution limit of the foraminiferal record, Ann. Soc. Geol. Pol., 86, 59–71, https://doi.org/10.14241/asgp.2015.019, 2016.

Lalande, C., Moriceau, B., Leynaert, A. and Morata, N.: Spatial and temporal variability in export fluxes of biogenic matter in Kongsfjorden, Polar Biol., 39(10), 1725–1738, https://doi.org/10.1007/s00300-016-1903-4, 2016.

Lea, J. M., Mair, D. W. F. and Rea, B. R.: Instruments and Methods :Evaluation of existing and new methods of tracking glacier terminus change, J. Glaciol., 60(220), 323–332, https://doi.org/10.3189/2014JoG13J061, 2014.

Liestøl, O.: The glaciers in the Kongsfjorden area, spitsbergen, Nor. Geogr. Tidsskr., 42(4), 231–238, https://doi.org/10.1080/00291958808552205, 1988.

Lloyd, J.: Late Holocene environmental change in Disko Bugt, west Greenland: interaction between climate, ocean circulation and Jakobshavn Isbrae, Boreas, 35(1), 35–49, https://doi.org/10.1080/03009480500359061, 2006.

Luckman, A., Benn, D. I., Cottier, F., Bevan, S., Nilsen, F. and Inall, M.: Calving rates at tidewater glaciers vary strongly with ocean temperature, Nat. Commun., 6, https://doi.org/10.1038/ncomms9566, 2015.

Mansell, D., Luckman, A. and Murray, T.: Dynamics of tidewater surge-type glaciers in northwest Svalbard, J. Glaciol., 58(207), 110–118, https://doi.org/10.3189/2012JoG11J058, 2012.

Mayk, D., Fietzke, J., Anagnostou, E. and Paytan, A.: LA-MC-ICP-MS study of boron isotopes in individual planktonic foraminifera: A novel approach to obtain seasonal variability patterns, Chem. Geol., 531(March 2019), 119351, https://doi.org/10.1016/j.chemgeo.2019.119351, 2020.

Meredith, M., Sommerkorn, M., Cassotta, S., Derksen, C., Ekaykin, A., Hollowed, A., Kofinas, G., Mackintosh, A., Melbourne-Thomas, J., Muelbert, M. M. C., Ottersen, G., Pritchard, H. and Schuur, E. A. G.: Polar Regions, in IPCC Special Report on the Ocean and Cryosphere in a Changing Climate, pp. 203–320, , 2019.

Meslard, F., Bourrin, F., Many, G. and Kerhervé, P.: Suspended particle dynamics and fluxes in an Arctic fjord (Kongsfjorden, Svalbard), Estuar. Coast. Shelf Sci., 204, 212–224, https://doi.org/10.1016/j.ecss.2018.02.020, 2018.

Murray, T., Dowdeswell, J. A., Drewry, D. J. and Frearson, I.: Geometric evolution and ice dynamics during a surge of Bakaninbreen, Svalbard, J. Glaciol., 44(147), 263–272, https://doi.org/10.1017/S0022143000002604, 1998.

Nandan, S. B., P. P., K., Vijay, A., C. V., A., P. R., J. and Krishnan, K. P.: Benthic Faunal Assemblage of the Arctic Kongsfjorden System, Norway, Int. J. Mar. Sci., 6(54), 1–8, https://doi.org/10.5376/ijms.2016.06.0054, 2016.

Oksanen, J., Blanchet, F. G., Friendly M., Kindt R., Legendre P., McGlinn D., Minchin P.R., O'Hara R. B.,. Simpson G. L, Solymos P., Stevens M. H. H., Szoecs E., and Wagner H: vegan: Community Ecology Package. R package version 2.5-6. https://CRAN.R-project.org/package=vegan, 2019

Pavlov, A. K., Tverberg, V., Ivanov, B. V., Nilsen, F., Falk-Petersen, S. and Granskog, M. A.: Warming of Atlantic water in two west Spitsbergen fjords over the last century (1912-2009), Polar Res., 32(SUPPL.), 1–14, https://doi.org/10.3402/polar.v32i0.11206, 2013.

Pawłowska, J., Łącka, M., Kucharska, M., Szymańska, N., Koziorowska, K., Kuliński, K. and Zajączkowski, M.: Benthic foraminifera contribution to fjord modern carbon pools: A seasonal study in Adventfjorden, Spitsbergen, Geobiology, 15(5), 704–714, https://doi.org/10.1111/gbi.12242, 2017.

Payne, C. M. and Roesler, C. S.: Characterizing the influence of Atlantic water intrusion on water mass formation and phytoplankton distribution in Kongsfjorden, Svalbard, Cont. Shelf Res., 191, 104005, https://doi.org/10.1016/j.csr.2019.104005, 2019.

Petersen, J., Barras, C., Bézos, A., La, C., De Nooijer, L. J., Meysman, F. J. R., Mouret, A., Slomp, C. P. and Jorissen, F. J.: Mn/Ca intra- and inter-test variability in the benthic foraminifer Ammonia tepida, Biogeosciences, 15(1), 331–348, https://doi.org/10.5194/bg-15-331-2018, 2018.

Powell, R. D.: Grounding-line systems as second-order controls on fluctuations of tidewater termini of temperate glaciers, Geol. Soc. Am., (261), 75–94, https://doi.org/10.1130/SPE261-p75, 1991.

Pramanik, A., Van Pelt, W., Kohler, J. and Schuler, T. V.: Simulating climatic mass balance, seasonal snow development and associated freshwater runoff in the Kongsfjord basin, Svalbard (1980-2016), J. Glaciol., 64(248), 943–956, https://doi.org/10.1017/jog.2018.80, 2018.

R Core Team: R: A language and environment for statistical computing. R Foundation for Statistical Computing, Vienna, Austria. URL https://www.R-project.org/, 2020.

Rasmussen, T. L. and Thomsen, E.: Palaeoceanographic development in Storfjorden, Svalbard, during the deglaciation and Holocene: Evidence from benthic foraminiferal records, Boreas, 44(1), 24–44, https://doi.org/10.1111/bor.12098, 2015.

Scherer R.: PropCIs: Various Confidence Interval Methods for Proportions. R package version 0.3-0. https://CRAN.R-project.org/package=PropCIs, 2018

Skirbekk, K., Hald, M., Marchitto, T. M., Junttila, J., Kristensen, D. K. and Sørensen, S. A.: Benthic foraminiferal growth seasons implied from Mg/Ca-temperature correlations for three Arctic species, Geochemistry, Geophys. Geosystems, 17, 4684–4704, https://doi.org/doi:10.1002/2016GC006505, 2016.

Streuff, K., Forwick, M., Szczuciński, W., Andreassen, K. and Ó Cofaigh, C.: Submarine landform assemblages and sedimentary processes related to glacier surging in Kongsfjorden, Svalbard, Arktos, 1(1), 14, https://doi.org/10.1007/s41063-015-0003-y, 2015.

Suchéras-Marx, B., Escarguel, G., Ferreira, J. and Hammer, Ø.: Statistical confidence intervals for relative abundances and abundance-based ratios: Simple practical solutions for an old overlooked question, Mar. Micropaleontol., 151(February), 101751, https://doi.org/10.1016/j.marmicro.2019.101751, 2019.

Sund, M., Eiken, T., Hagen, J. O. and Kääb, A.: Svalbard surge dynamics derived from geometric changes, Ann. Glaciol., 50(52), 50–60, https://doi.org/10.3189/172756409789624265, 2009.

Sund, M., Eiken, T. and Rolstad Denby, C.: Velocity structure, front position changes and calving of the tidewater glacier Kronebreen, Svalbard, Cryosph. Discuss., 5, 41–73, https://doi.org/10.5194/tcd-5-41-2011, 2011.

Sundfjord, A., Albretsen, J., Kasajima, Y., Skogseth, R., Kohler, J., Nuth, C., Skarðhamar, J., Cottier, F., Nilsen, F., Asplin, L., Gerland, S. and Torsvik, T.: Effects of glacier runoff and wind on surface layer dynamics and Atlantic Water exchange in Kongsfjorden, Svalbard; a model study, Estuar. Coast. Shelf Sci., 187, 260–272, https://doi.org/10.1016/j.ecss.2017.01.015, 2017.

Svendsen, H., Beszczynska-Møller, A., Hagen, J. O., Lefauconnier, B., Tverberg, V., Gerland, S., Ørbæk, J. B., Bischof, K., Papucci, C., Zajaczkowski, M., Azzolini, R., Bruland, O., Wiencke, C., Winther, J.-G. and Dallmann, W.: The physical environment of Kongsfjorden – Krossfjorden, an Arctic fjord system in Svalbard, Polar Res., 21(1), 133–166, https://doi.org/10.3402/polar.v21i1.6479, 2002.

Szymańska, N., Pawłowska, J., Kucharska, M., Kujawa, A., Łącka, M. and Zajączkowski, M.: Impact of shelf-transformed waters (STW) on foraminiferal assemblages in the outwash and glacial fjords of Adventfjorden and Hornsund, Svalbard, Oceanologia, 59(4), 525–540, https://doi.org/10.1016/j.oceano.2017.04.006, 2017.

Tedstone, A. J., Nienow, P. W., Gourmelen, N., Dehecq, A., Goldberg, D. and Hanna, E.: Decadal slowdown of a land-terminating sector of the Greenland Ice Sheet despite warming, Nature, 526(7575), 692–695, https://doi.org/10.1038/nature15722, 2015.

Toyofuku, T., Suzuki, M., Suga, H., Sakai, S., Suzuki, A., Ishikawa, T., de Nooijer, L. J., Schiebel, R., Kawahata, H. and Kitazato, H.: Mg/Ca and δ18O in the brackish shallow-water benthic foraminifer Ammonia "beccarii," Mar. Micropaleontol., 78(3–4), 113–120, https://doi.org/10.1016/j.marmicro.2010.11.003, 2011.

Trusel, L. D., Powell, R. D., Cumpston, R. M. and Brigham-Grette, J.: Modern glacimarine processes and potential future behaviour of Kronebreen and Kongsvegen polythermal tidewater glaciers, Kongsfjorden, Svalbard, Geol. Soc. Spec. Publ., 344(Powell 1984), 89–102, https://doi.org/10.1144/SP344.9, 2010.

Van Dijk, I., Nooijer De, L. J. and Reichart, G. J.: Trends in element incorporation in hyaline and porcelaneous foraminifera as a function of pCO_2, Biogeosciences, 14(3), 497–510, https://doi.org/10.5194/bg-14-497-2017, 2017.

Van Dijk, I., Barras, C., De Nooijer, L. J., Mouret, A., Geerken, E., Oron, S. and Reichart, G. J.: Coupled calcium and inorganic carbon uptake suggested by magnesium and sulfur incorporation in foraminiferal calcite, Biogeosciences, 16(10), 2115–2130, https://doi.org/10.5194/bg-16-2115-2019, 2019.

Vihtakari M.: PlotSvalbard: PlotSvalbard - Plot research data from Svalbard on maps. R package version 0.9.2. https://github.com/MikkoVihtakari/PlotSvalbard, 2020

Villéger, S., Mason, N. W. H. and Mouillot, D.: New multidimensional functional diversity indices for a multifaceted framework in functional ecology, Ecology, 89(8), 2290–2301, https://doi.org/10.1890/07-1206.1, 2008.

Wit, J. C., De Nooijer, L. J., Wolthers, M. and Reichart, G. J.: A novel salinity proxy based on na incorporation

into foraminiferal calcite, Biogeosciences, 10(10), 6375–6387, https://doi.org/10.5194/bg-10-6375-2013, 2013.

Wassmann, P. and Reigstad, M.: Future Arctic Ocean seasonal ice zones and implications for pelagic-benthic coupling, Oceanography, 24(3), 220–231, https://doi.org/10.5670/oceanog.2011.74, 2011.

Willig, M. R. and Presley, S. J.: Biodiversity and disturbance, Elsevier Inc., 2017.

Włodarska-Kowalczuk, M. and Pearson, T. H.: Soft-bottom macrobenthic faunal associations and factors affecting species distributions in an Arctic glacial fjord (Kongsfjord, Spitsbergen), Polar Biol., 27(3), 155–167, https://doi.org/10.1007/s00300-003-0568-y, 2004.

Włodarska-Kowalczuk, M., Pearson, T. H. and Kendall, M. A.: Benthic response to chronic natural physical disturbance by glacial sedimentation in an Arctic fjord, Mar. Ecol. Prog. Ser., 303, 31–41, 2005.

Włodarska-Kowalczuk, M., Pawłowska, J. and Zajaczkowski, M.: Do foraminifera mirror diversity and distribution patterns of macrobenthic fauna in an Arctic glacial fjord?, Mar. Micropaleontol., 103, 30–39, https://doi.org/10.1016/j.marmicro.2013.07.002, 2013.

Włodarska-Kowalczuk, M., Górska, B., Deja, K. and Morata, N.: Do benthic meiofaunal and macrofaunal communities respond to seasonality in pelagial processes in an Arctic fjord (Kongsfjorden, Spitsbergen)?, Polar Biol., 39(11), 2115–2129, https://doi.org/10.1007/s00300-016-1982-2, 2016.

Wood, S.N.: Generalized Additive Models: An Introduction with R (2nd edition). Chapman and Hall/CRC, 2017.

Zwally, H. J., Abdalati, W., Herring, T., Larson, K., Saba, J. and Steffen, K.: Surface Melt – Induced Acceleration of Greenland Ice-Sheet Flow, Science (80-.)., 297(5579), 218–222, https://doi.org/10.1126/science.1072708, 2002.

Supplement Chapter 5

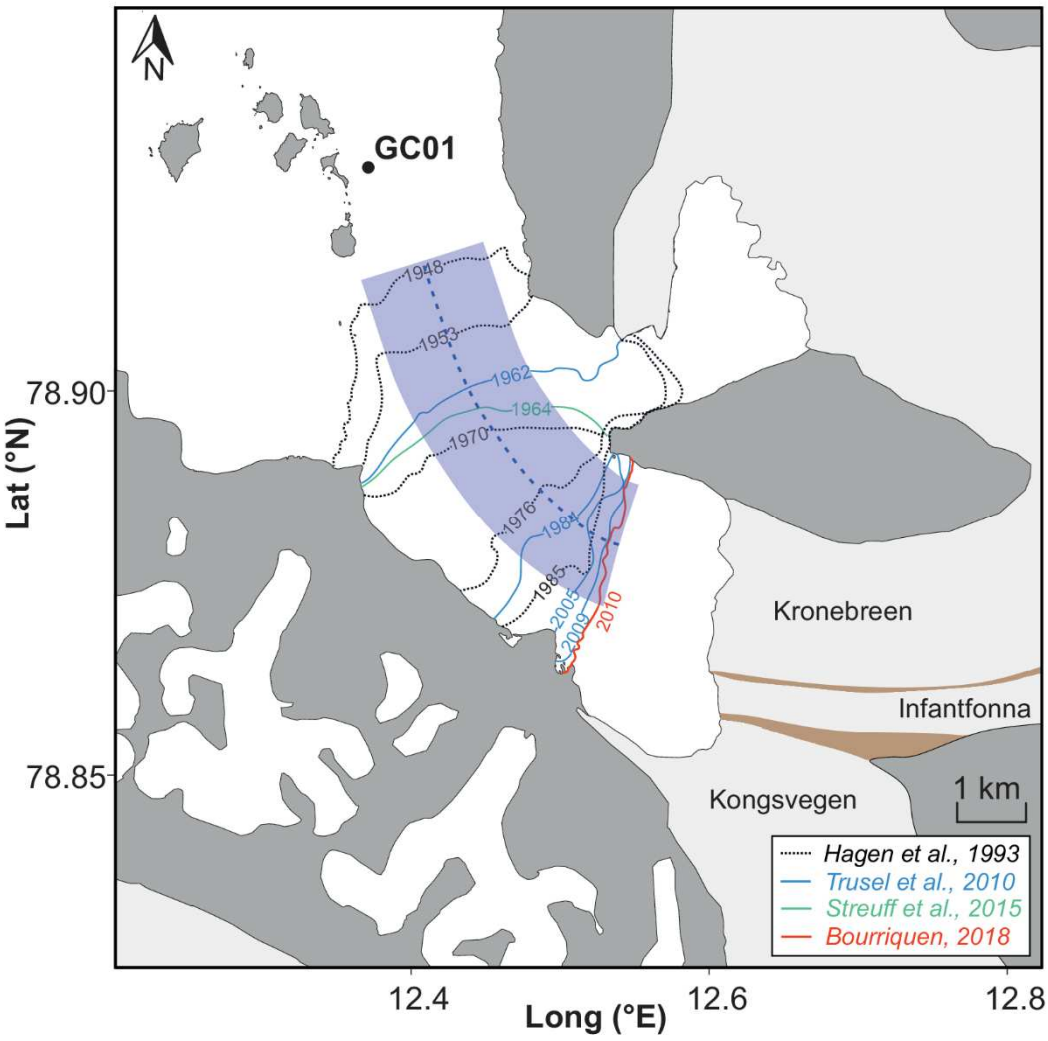

Figure S1. Map of the inner Kongsfjorden showing the Kronebreen-Kongsvegen glacier complex (including the Infantfonna) and the 10JM-GLACIBAR-GC01 core site sampled in 2010. On the map is presented the centre-line (blue dashed line) of the Kronebreen glacier reconstructed using the box method (blue box; Lea et al., 2014). Different colour lines represent the evolution of the front positions since 1948 based on previous publications (Hagen et al., 1993; Trusel et al., 2010; Streuff et al., 2015; Bourriquen, 2018). The base map was performed with the R package *PlotSvalbard* (Vihtakari, 2020). The brownish landforms on the glaciers represent the lateral moraines.

Table S1. List of the six functional traits for each species. Binary traits are identified as follow: Test material, 1 = calcareous, 0 = agglutinated; Test symmetry, 1 = symmetrical, 0 = asymmetrical; Pores, 1 = presence, 0 = absence; Chamber number, 1 = polythalamus, 0 = monothalamus. Categorical traits are: test shape (rounded, ovoid, elongated, irregular); tooth presence (none, single-tooth, tubercles).

Species	*Test material*	*Test shape*	*Test symmetry*	*Pores*	*Tooth presence*	*Chamber number*
Astrononion gallowayi	1	rounded	1	1	none	1
Buccella frigida	1	rounded	0	1	tubercles	1
Buccella sp.	1	rounded	0	1	tubercles	1
Cassidulina neoteretis	1	rounded	0	1	single-tooth	1
Cassidulina reniforme	1	rounded	0	1	single-tooth	1
Cassidulina sp. morphotype 1	1	rounded	0	1	single-tooth	1
Cassidulina sp. morphotype 2	1	rounded	0	1	single-tooth	1
Cassidulinoides sp.	1	rounded	0	1	single-tooth	1
Cibicidoides lobatulus	1	rounded	0	1	none	1
Cornuspira involvens	1	rounded	1	0	none	0
Cornuspira sp.	1	rounded	1	0	none	0
Cuneata arctica	0	elongated	1	0	none	1
Dentalina ittai	1	elongated	1	1	none	1
Dentalina sp.	1	elongated	1	1	none	1
Discorbina sp.	1	rounded	0	1	none	1
Elphidium clavatum	1	rounded	1	1	tubercles	1
Elphidium sp.	1	rounded	1	1	tubercles	1
Elphidium subarcticum	1	rounded	1	1	tubercles	1
Epistominella exigua	1	rounded	0	1	none	1
Fissurina sp.	1	ovoid	1	1	none	0
Globocassidulina sp.	1	rounded	0	1	single-tooth	1
Globulina sp.	1	rounded	1	1	none	0
Guttulina sp.	1	ovoid	0	1	none	1
Islandiella helenae	1	rounded	0	1	single-tooth	1
Islandiella norcrossi	1	rounded	0	1	single-tooth	1
Labrospira crassimargo	0	rounded	1	0	none	1
Lenticulina sp.	1	rounded	1	1	none	1
Melonis barleanuum	1	rounded	1	1	none	1
Miliolinella circularis	1	rounded	0	0	single-tooth	1
Miliolinella sp.	1	rounded	0	0	single-tooth	1
Nonionellina labradorica	1	rounded	1	1	tubercles	1
Procerolagena gracilis	1	elongated	1	1	none	0
Pullenia cf *osloensis*	1	rounded	1	1	none	1
Pyrgo williamsoni	1	rounded	1	0	single-tooth	1
Pyrulina cilindroides	1	elongated	0	1	none	1
Quinqueloculina seminulum	1	ovoid	0	0	single-tooth	1
Quinqueloculina stalkeri	1	ovoid	0	0	single-tooth	1
Recurvoides turbinatus	0	rounded	0	0	none	1
Reophax fusiformis	0	elongated	0	0	none	1
Reophax scorpiurus	0	elongated	1	0	none	1
Reophax sp.	0	elongated	1	0	none	1
Robertina arctica	1	ovoid	0	1	none	1
Silicosigmoilina groenlandica	0	ovoid	0	0	none	1
Spiroplectammina biformis	0	elongated	1	0	none	1
Stainforthia feylingi	1	elongated	0	1	single-tooth	1
Stainforthia fusiformis	1	elongated	0	1	single-tooth	1
Stainforthia loeblichi	1	elongated	0	1	single-tooth	1
Textularia earlandi	0	elongated	1	0	none	1
Triloculina oblonga	1	elongated	0	0	single-tooth	1
Triloculina trihedra	1	ovoid	0	0	single-tooth	1

Table S2. Degrees decimal minutes coordinates for each glacier front positions and distance (expressed in km) of each median point from the study core GC01.

Years	Latitude (°N)	Longitude (°E)	Distance (km)
1948	78° 55.0632'	12° 23.2652'	1.68
1953	78° 54.5538'	12° 24.1805'	2.67
1962	78° 54.1483'	12° 25.159'	3.50
1964	78° 53.9953'	12° 25.6278'	3.83
1970	78° 53.8347'	12° 26.2725'	4.20
1976	78° 53.3772'	12° 28.2798'	5.29
1984	78° 53.1612'	12° 29.721'	5.91
1985	78° 53.0435'	12° 30.4628'	6.24
2005	78° 53.0733'	12° 30.236'	6.14
2009	78° 52.9885'	12° 31.0613'	6.44
2010	78° 52.9832'	12° 31.1237'	6.46

Table S3. Percentages of clay (< 2 µm), silt (2 µm - 63 µm) and sand (63 µm - 2 mm) and correspondent sediment depth along the study core GC01.

Depth (cm)	Clay (%)	Silt (%)	Sand (%)
12	16.6	80.1	3.3
22	19.3	76.4	4.3
32	18.6	77.7	3.8
42	16.2	79.2	4.6
52	17.2	81.2	1.6
62	18.9	76.8	4.3
72	18.7	77.5	3.8
82	16.7	79.7	3.6
92	3.8	22.7	73.5
102	16.5	78.7	4.7
112	18.5	77.5	4.0

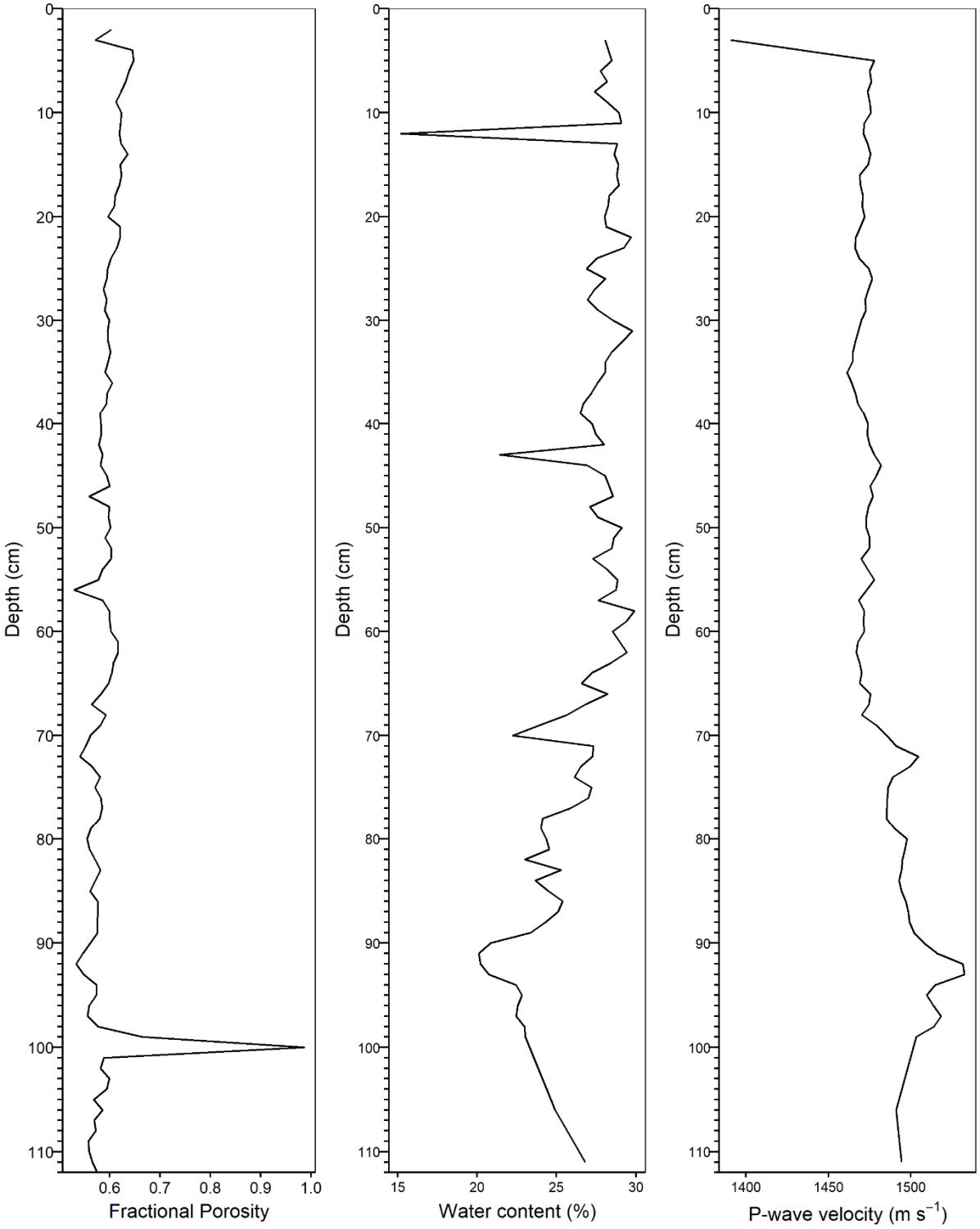

Figure S2. Supplementary sedimentological parameters measured by Streuff et al., (2015), on the core 10JM-GLACIBAR-GC01. From left to right: fractional porosity, percentage of water content and p-wave velocity (expressed in m s^{-1}).

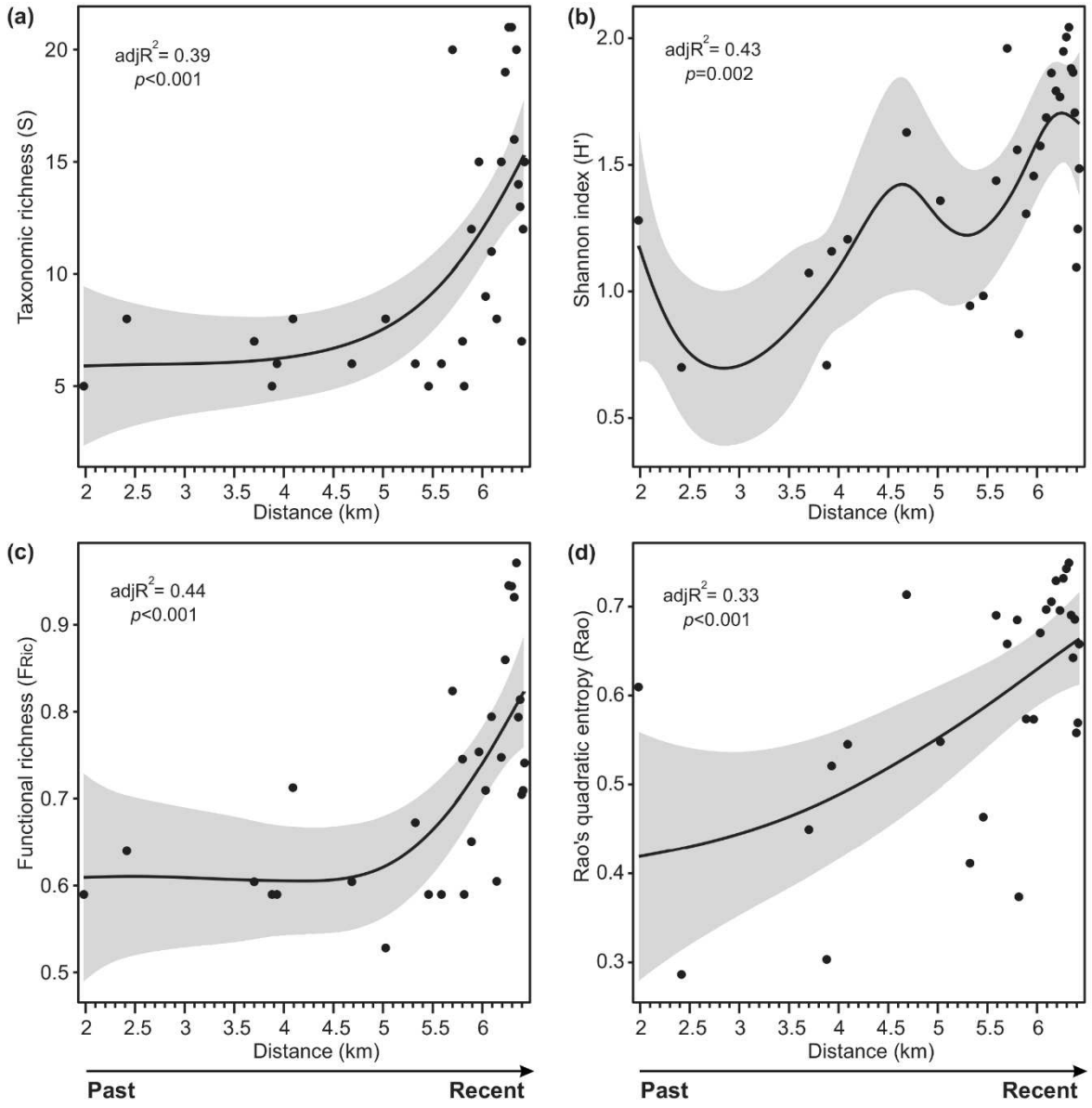

Figure S3. Relationship between distance from the glacier front and taxonomic richness **(a)**, Shannon index **(b)**, functional richness **(c)**, and Rao's quadratic entropy **(d)**. Dots represent the raw data points including samples with > 30 picked individuals, while dark lines represent the average model estimates. The ribbon around the estimates represents ±2SE.

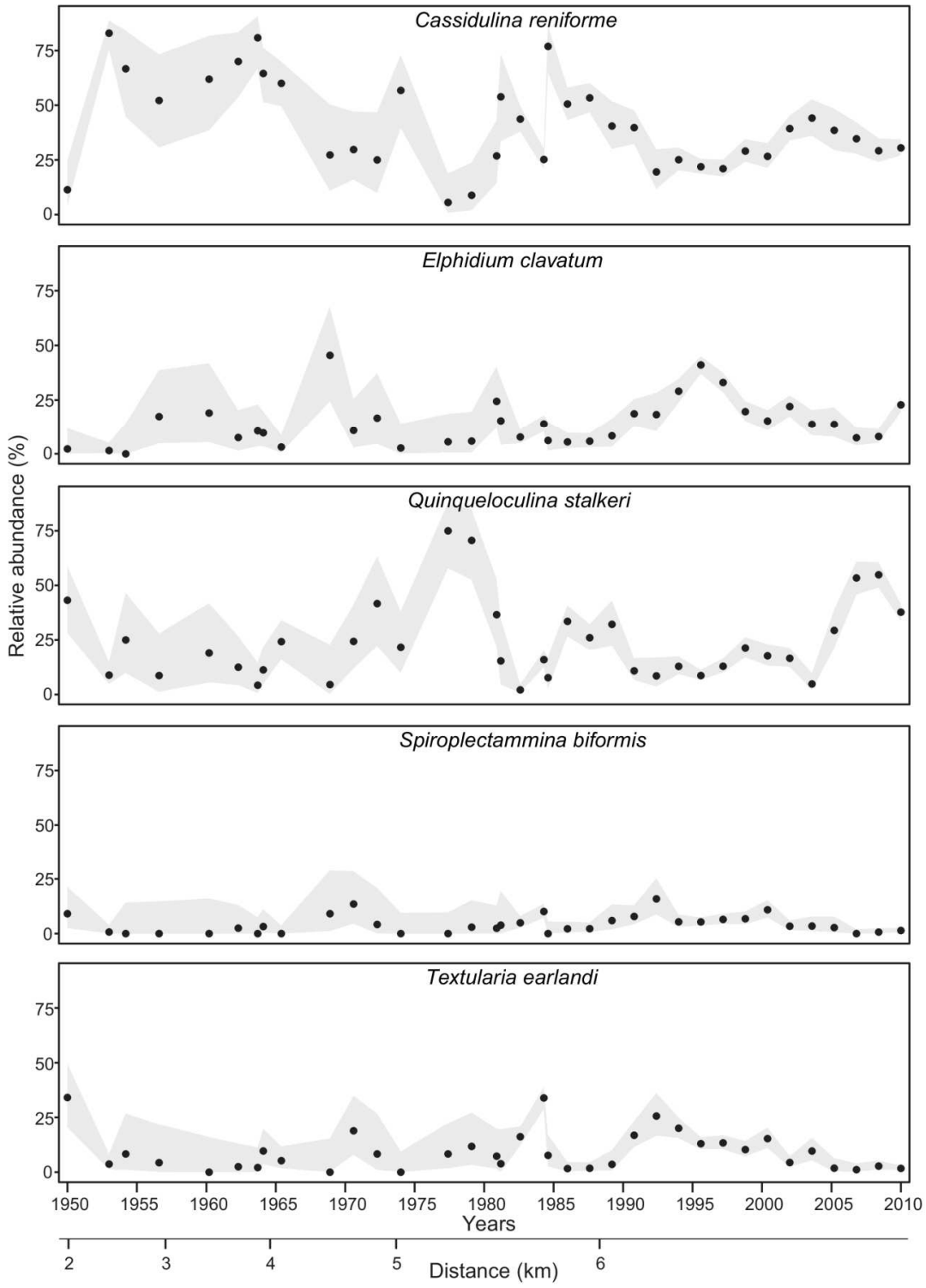

Figure S4. Relative abundances of the major species along the core 10JM-GLACIBAR-GC01 in function of time and distance from the glacier front. In the figure are reported only the samples with ≥ 20 picked individuals (considering the >100 µm) and the species contributing with ≥ 15% because considered statistically significant (i.e., probability of failure to detect the presence of a species is less than 5%; Fatela and Taborda, 2000). Black dots represent the data, the grey interval represents the confidence interval (CI) (Suchéras-Marx et al., 2019). The binomial proportion CIs was calculated with the *exactci* function in the R package *PropCIs* (Scherer, 2018) which uses the Clopper-Pearson method using a confidence level of 95%.

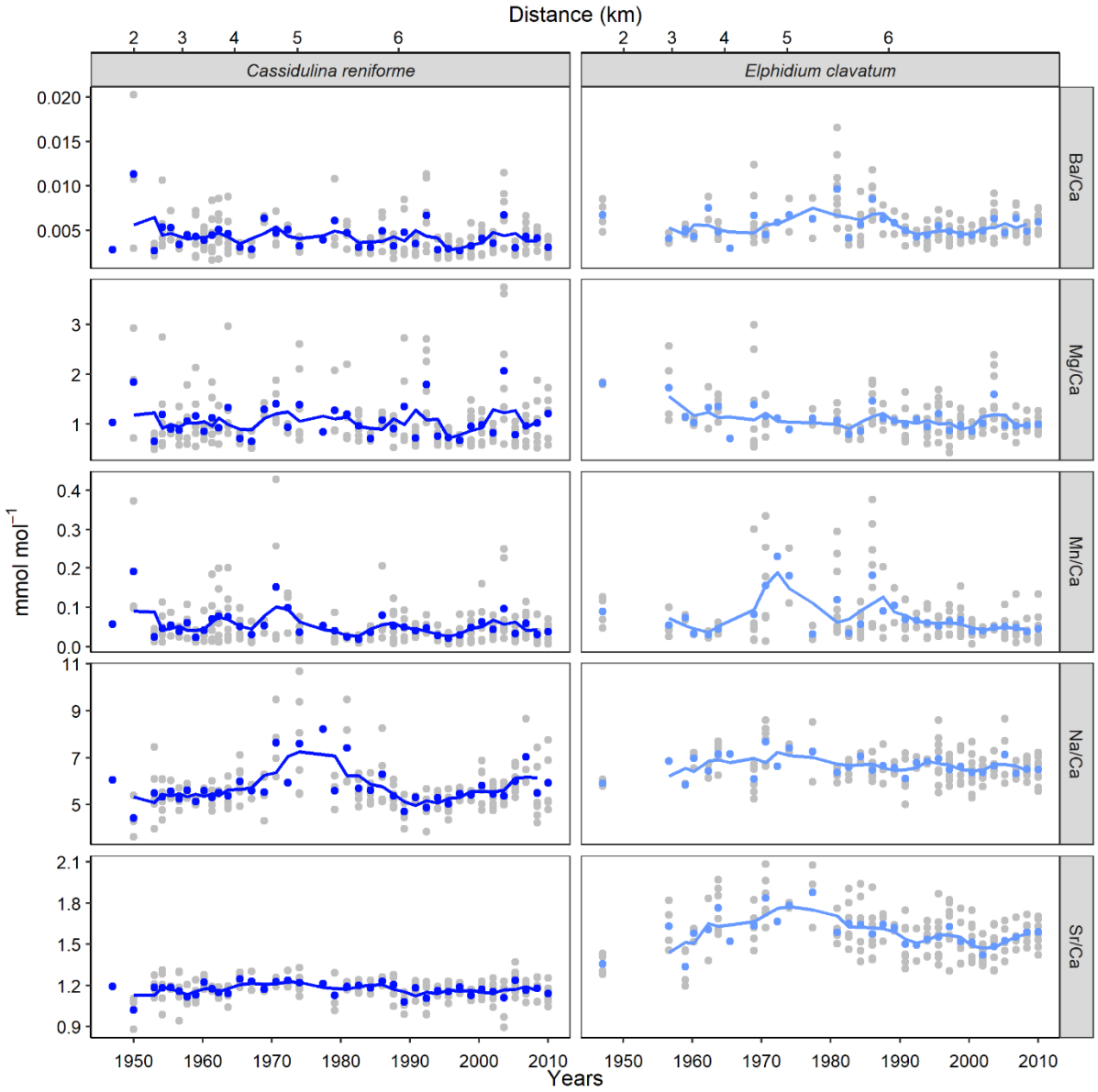

Figure S5. Element/Calcium ratios reported in mmol mol^{-1} for five ratios (Ba/Ca, Mg/Ca, Mn/Ca, Na/Ca, Sr/Ca) and two species. The coloured dots represent the mean ratio, the lines represent the rolling mean (n=3), and the grey dots represent all the measurements.

The laser ablation anayses on two different foraminiferal species did not show any clear pattern along the core for all ratios. It can only be observed an increase in the Na/Ca ratios in the 1970-1985 period for *Cassidulina reniorme*, and an increase in the Sr/Ca over the same period for *Elphidium clavatum* which also showed an increase in the Mn/Ca ratio before that period. Moreover, the stability of the geochemical signal for *Elphidium clavatum* increased after 1990. Back this year, the terminus was about 6 km far from the core site and the glacier retreat was slowing down, suggesting a reduced GID on the benthic environment. Altogether, the variability of the investigated ratios may be linked to the glacier proximity as they are related to melwater dischages, primary productivity, water temperature and salinity, and bottom water

oxygenation (e.g., Toyofuku et al., 2011; Wit et al., 2013; de Nooijer et al., 2017; Barras et al., 2018), all parameters being greatly influenced by seasonal glacier dynamics. A previous study in Kongsfjorden, analysed the Mg/Ca ratios from other Arctic species sampled at different seasons concluding that they reproduce more seasonal temperatures rather than annual year average (Skirbekk et al., 2016). Therefore, the absence of a clear pattern along six decades in our study core may be due to the registration of the seasonal variability, which is potentially greater or comparable than the annual variability recorded along the study core.

Further investigations are needeed to understand if the variation observed for Na/Ca ratios in the 1970-1985 could be linked to an increased infleunce of the AW during these years at the core site. It is interesting that when it registered this variation in the Na/Ca by *C. reniforme*, another species (*Quinqueloculina stalkeri*) became dominant in the assemblage, possibly in response to an important environmental change.

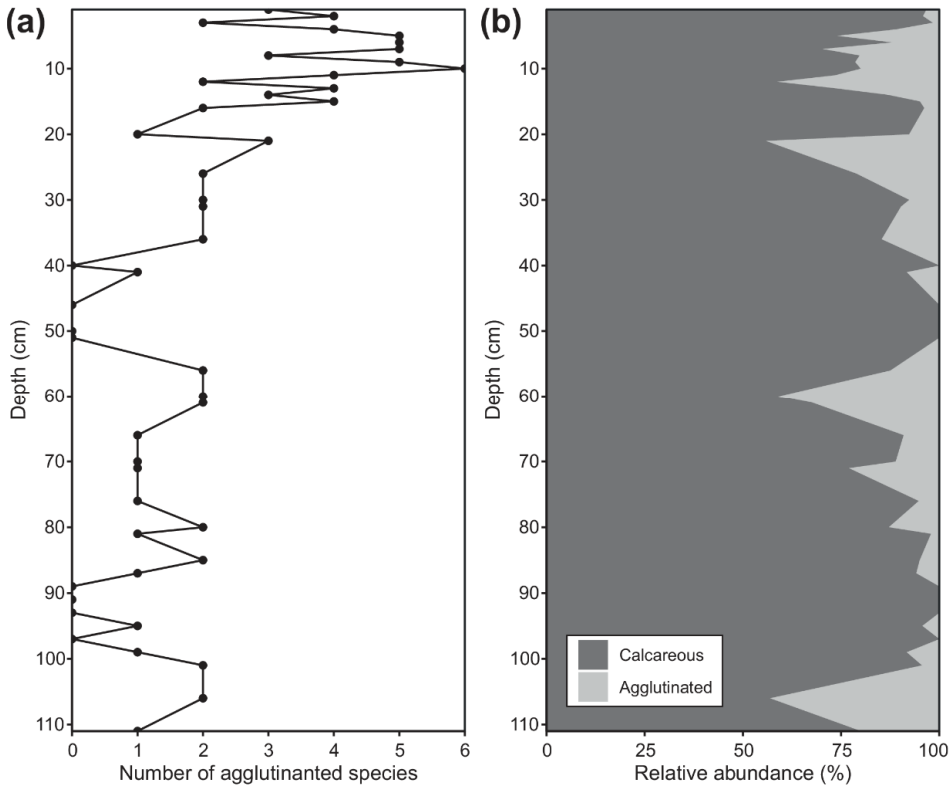

Figure S6. (a) Number of agglutinated species and **(b)** relative abundances of agglutinated vs calcareous species along the study core.

Synthesis & Perspectives

1. Chapters' overview

The major scientific goal of this PhD thesis was to investigate and understand the effect of ice-related phenomena on benthic foraminiferal communities in Arctic fjords, and further propose and test reliable proxies for specific dynamics. Benthic foraminifera were used as indicators to estimate the influence of sea ice cycles and glacier melting on the benthic ecosystems. Measurable ecological responses (i.e., ecological proxies) were proposed and their effectiveness was tested. This thesis focused on two contrasting fjords, in terms of ice-related dynamics, from the Svalbard archipelago:

- **Storfjorden:** a fjord affected by strong **brine cascading** (i.e., cold, salty, and corrosive waters) during first-year sea ice production phases. These brine-enriched waters persist all year long in bottom waters of some locations. This fjord is the subject of Chapters 1 and 2;
- **Kongsfjorden:** a fjord affected by **massive releases of sediments and freshwater** from tidewater glaciers during the melting season. This fjord is the subject of the Chapters 3, 4, and 5.

The objectives of this thesis were addressed through five chapters of which the main findings are described in the following and summarised in Figure 1.

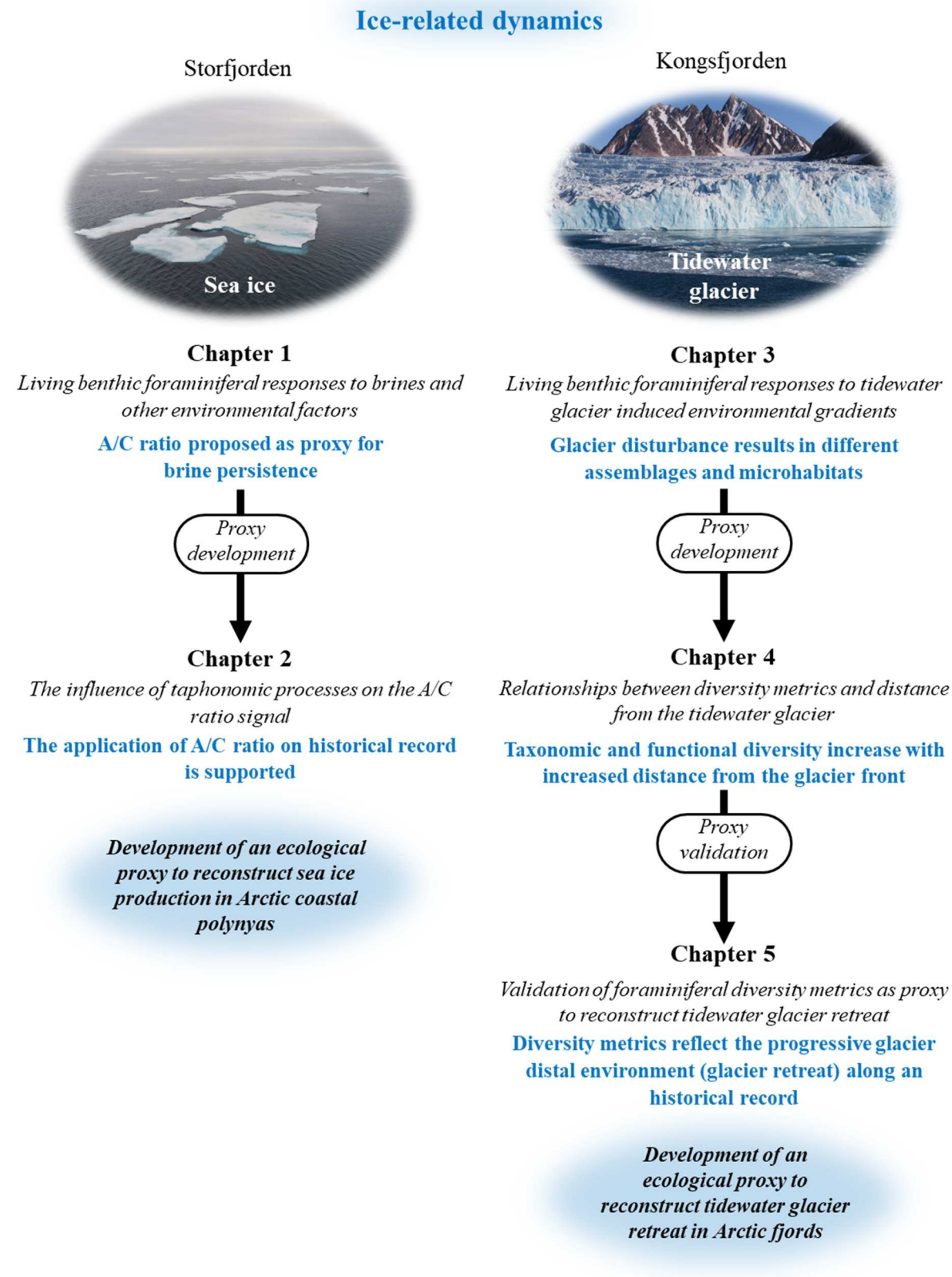

Figure 1. Conceptual synthesis of this PhD thesis indicating the concluding remarks of each chapter (blue text) and the main achievements of this work (black text in the blue clouds).

1.1 Living benthic foraminiferal responses to brines and other environmental factors

In July 2016, the STeP (Storfjorden Polynya Multidisciplinary Study) cruise was organised in the biggest Svalbard fjord, Storfjorden, better known as the "sea ice factory". Storfjorden is characterised by the recurrent formation of a latent-heat polynya (e.g., Haarpaintner, 1999) contributing to dense water formation in the Arctic region (e.g., Cavalieri and Martin, 1994). **Chapter 1** aimed at investigating living foraminiferal responses to multiple environmental parameters (e.g., sediment characteristics, organic matter quantity and composition, sediment oxygen and pH microprofiles), to understand if and how their distribution along the fjord is affected by brine-enriched shelf waters (BSW), and suggest a potential proxy related to brines production.

To achieve this aim, seven stations were sampled along a N-S transect following the topography of the fjord: *(i)* three stations were placed in the inner fjord zone, close to the polynya open waters and possibly only intermittently affected by brines cascading, *(ii)* two stations in the deep basins, where brines are supposed to be trapped and persist all year long, *(iii)* one on top of the sill, influenced by brine overflow during sea ice production season and iv) the last in the outer fjord zone, potentially only episodically touched by BSW outflowing from the fjord.

The results of living benthic foraminifera sampled in the warm season show three major biozones. In the "inner fjord" zone, glacier proximal calcareous species (i.e., *Cassidulina reniforme* and *Elphidium clavatum*) dominated the assemblages in the surface sediment, and they were accompanied by *Nonionellina labradorica* especially in the shallow and intermediate infaunal habitat. These species did not show severe dissolution marks which may indicate the influence of corrosive waters. The presence of juveniles of the same species, indicative of recent reproductive events, and the high concentration of fresh organic matter in the area led us to suggest that *C. reniforme* and *E. clavatum* opportunistically responded to fresh organic matter inputs derived from the summer algal bloom. This was further supported by the abundance of the phytodetritus-feeder *Nonionellina labradorica*. The latter species was especially dominant in the intermediate microhabitat, possibly because of reduced competition through exploitation of different metabolic pathways (e.g., N and S assimilation; Jauffrais et al., 2019). The "outer fjord" zone was characterised by a mix of typical Atlantic species (e.g., *Melonis barleeanus*, *Globobulimina auriculata*) promoted by the intrusion of the North Atlantic water in the Storfjordrenna, and polar species, due to the occasional outflow of Arctic water from the fjord. Between these two zones, the "deep basins and sill" zone was mostly characterised by glacier

distal agglutinated taxa (e.g., *Reophax scorpiurus*, *Reophax fusiformis*, *Recurvoides turbinatus*, and *Spiroplectammina biformis*) tolerating a wide range of conditions and probably more competitive when refractory organic matter is present. The sill station showed a similar species composition to that at the deep basins, although additional species, such as *Adercotryma glomeratum* and *Textularia torquata*, presented relatively large abundances due most likely to the higher Atlantic Water influence in this area of the fjord. The dominance of agglutinated faunas in the "deep basins and sill" zone was accompanied by the observation of several degrees of dissolution of calcareous foraminifera, especially in the deep basins. We suppose that the persistence of old corrosive waters (i.e., BSW) promotes agglutinated taxa by hampering the development of calcareous species and by being associated to aged and refractory organic matter. Based on these results, we proposed the use of the agglutinated / calcareous (A/C) ratio as a proxy for brine persistence and/or overflow in historical sedimentary archives.

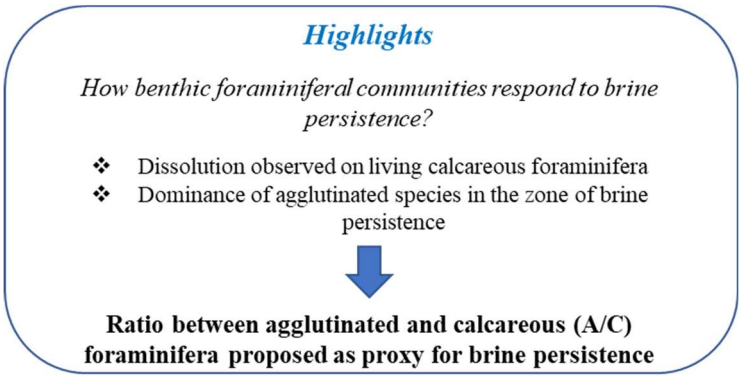

1.2 The influence of taphonomic processes on the A/C ratio signal

In Chapter 1, the A/C ratio was suggested as a potential proxy for brine persistence and overflow in Storfjorden. The proportion of agglutinated species was previously suggested to be a possible (uncalibrated) signal of BSW presence in Storfjorden. This was used, with other proxies, for paleoenvironmental reconstruction from the last post-glacial due to a surprisingly high preservation of agglutinated foraminifera in the fossil record of the fjord (Rasmussen and Thomsen, 2014, 2015). **Chapter 2** aimed at investigating the potential effects of early taphonomy on the A/C proxy and therefore testing its reliability on fossil faunas in sedimentary archives. To this aim, foraminiferal living assemblages from Chapter 1 were compared with fossil faunas found below the taphonomically active zone (TAZ) from the same cores, to highlight the potential selectivity of taphonomic loss against certain species. Furthermore, the A/C ratio of fossil faunas from the seven stations was compared to the A/C ratio of living faunas to estimate the extent of taphonomic loss and its effect on the reliability of the A/C proxy.

The internal part of the fjord (i.e., "inner fjord", "deep basins and sill" zones) was characterised by lower densities of dead foraminifera from the surface sediment as well as fossil faunas below the TAZ, compared to the living faunas, underlining a strong taphonomic filter in the entire area of the fjord. However, in the inner fjord, similar species composition between living dead and fossil faunas (i.e., *Elphidium clavatum*, *Cassidulina reniforme*, and *Nonionellina labradorica*) are found, suggesting that the taphonomic loss is not selective. In the "deep basins and sill" zone, a shift between the living and fossil faunas was observed, with a selective taphonomic loss against some more fragile agglutinated taxa (e.g., *Reophax* spp.) accompanied with the increased presence of some calcareous species (i.e., *E. clavatum*, *Cibicidoides lobatulus*). These latter species possibly indicate a transport from the inner fjord via the brine outflow. These changes in the fossil faunas and selective taphonomic loss resulted in increased proportions of calcareous foraminifera compared to living faunas. In the "outer fjord", some differences in species composition were observed with the disappearance of the fragile *G. auriculata* and the increased relative abundances of other calcareous species (e.g., *Buccella frigida*, *E. clavatum*) but the taphonomic loss is much lower than inside the fjord and is not selective against calcareous or agglutinated taxa.

Despite the faunal changes due to taphonomic loss inside the fjord, the differences in A/C ratios between the zone of the fjord only periodically influenced by brines (i.e., the inner fjord) and the zone persistently affected by brines (i.e., deep basins) or overflow (i.e., the sill) is still clearly visible, with values of ratios up to three times higher. These findings support the use of the A/C ratio in sedimentary archives to investigate the presence-absence of BSW at the seafloor and as indirect proxy for sea ice production in Arctic coastal polynyas.

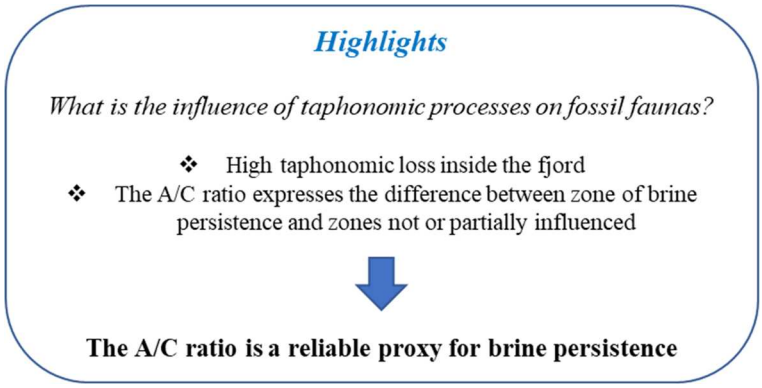

1.3 Living benthic foraminiferal responses to tidewater glacier induced environmental gradients

In August 2018, the mission KING18 was conducted in Kongsfjorden, a Svalbard fjord located in the northwestern coast of Spitsbergen. This fjord, as well as other western Svalbard fjords, is largely influenced by the warm and saline Atlantic water (AW) transported northwards (Saloranta and Svendsen, 2001; Cottier et al., 2007), and it is recently experiencing an excessive warming (e.g., Cottier et al., 2007; Hop and Wiencke, 2019). During summer, the inflow of AW from the shelf enhances tidewater glaciers melting. Meltwater discharges and the associated sediment supply from these glaciers located at the fjord head create steep salinity and turbidity gradients on relatively small spatial scales (less than 10 km). Besides the direct environmental effects, these discharges also influence primary production and organic fluxes to the seafloor. In **Chapter 3** we investigated the foraminiferal distribution along these gradients in the innermost part of Kongsfjorden, at the peak of the melting season. At this scope, interface cores from nine stations were sampled along an axial transect of about 10 km starting close to the Kronebreen tidewater glacier front, at the SE head of the fjord.

Results showed that foraminiferal faunas responded to the environmental gradients created by the tidewater glacier dynamics and AW inflow by establishing different foraminiferal assemblages identified as proximal, medial, and distal biozones. The proximal biozone was largely influenced by tidewater glaciers dynamics and therefore subjected to strong sedimentation from the meltwater turbid plume. This resulted in assemblages composed of few species mostly restricted to the sediment surface (e.g., *Capsammina bowmanni*, *Cassidulina reniforme* and *Textularia earlandi*) opportunistically responding to the stressful conditions. The microhabitat preferences of these species may be the result of low organic inputs as well as their rapid colonisation after physical disturbance.

The medial biozone included a transitional assemblage with some species in common with the proximal biozone as well as several other species including indicators of fresh organic matter input, such as *Nonionellina labradorica* and *Stainforthia feylingi*. These observations matched with the reduced water turbidity in this area at about 6-8 km from the glacier front, favouring local primary productivity. Foraminifera were not restricted to the sediment surface and some species showed typical infaunal microhabitat distribution (e.g., *N. labradorica*, *G. auriculata*) suggesting a more stable environment and a higher availability of diverse functional niches.

In the distal biozone, the AW-associated agglutinated species *Adercotryma glomeratum* is the most abundant species, accompanied with *N. labradorica*. In the surface sediment, however, a large diversity was observed and the occupation of the infaunal microhabitats by these two species, as also observed in the medial zone, is the result of the exploitation of different ecological niches. The increased diversity observed in the distal biozone was attributed to the further reduction of the stressful environmental conditions related to the tidewater glacier dynamics and the strong influence of AW inflow in this part of the fjord.

The measured environmental gradients mainly correlated with the distance from the glacier front and were mostly interpreted as directly or indirectly driven by this parameter. In parallel, a remarkable increase in foraminiferal diversity from the proximal to the distal biozones was observed suggesting the investigation of diversity metrics as potential proxy for glacier retreat.

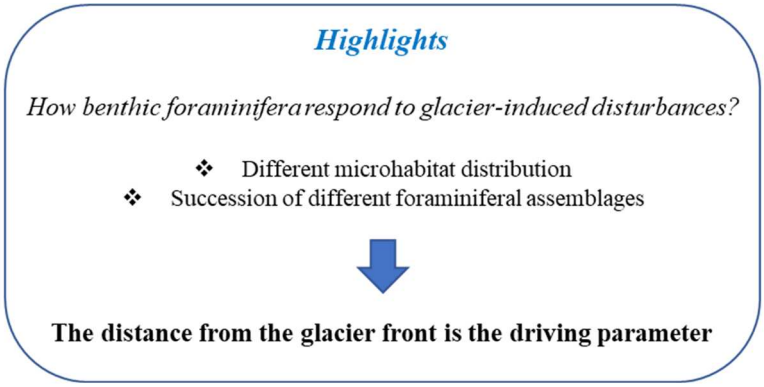

1.4 Relationships between diversity metrics and distance from the tidewater glacier

In **Chapter 4** we investigated how different biodiversity descriptors of living benthic foraminifera (i.e., abundance, size structure, community composition, taxonomic and functional diversity) vary in relation to the distance from the glacier front.

Apart from the foraminiferal abundance and partially the size structure that were not affected by the glacier-induced disturbances (GID), all the foraminiferal descriptors correlated with the distance from the glacier front. An overall biodiversity increase was observed when moving away from the front. Taxonomic and functional richness together with the Shannon index showed a rapid increase within few kilometres until reaching a plateau at about 8 km distance. Differently, taxonomic, and functional evenness and Rao's quadratic entropy showed a linear increase with glacier distance. The progressive reduction of the GID most likely triggers the establishment of more diversified and equilibrated communities. The increasing occupation of the functional space along the gradient is possible because of the increased availability of ecological niches as a result of reduced GID. Near the front, the low value of regularity metrics

suggested the dominance of few opportunistic species able to occupy only a restricted region of the functional space. The increased regularity further away from the front, together with increased Rao's quadratic entropy, resulted in higher probability to encounter individual occupying different niches.

All biodiversity patterns were investigated at different size resolution (i.e., size fractions: >63, >100, >125, and >150 µm) to find the best compromise between analytical effort and ecological information. We observed that spatial patterns of abundances and community composition are maintained at every resolution. However, some biodiversity patterns were not completely captured by the lowest resolution (i.e., >150 µm). Specifically, the regularity components (taxonomic and functional evenness) failed to capture biodiversity patterns, whereas Shannon index and Rao partially captured the trends observed at higher resolution.

The final aim of this study was to identify and propose a potential proxy for glacier retreat based on benthic foraminifera. Based on our findings, we suggested the use of four taxonomic and functional diversity metrics (i.e., taxonomic and functional richness, Shannon index, and Rao) as qualitative and semi-quantitative indicators of distance from the glacier front and, therefore, as proxy for glacier retreat in historical and paleoenvironmental reconstructions. Furthermore, we suggested to apply these proxies using the >125 µm foraminiferal size fraction as the best compromise to obtain a representative overview of biodiversity patterns while maintaining the minimal analytic effort.

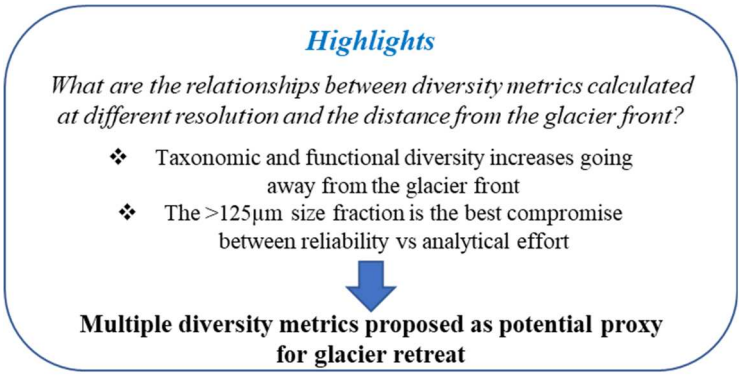

1.5 Validation of foraminiferal diversity metrics as a proxy to reconstruct tidewater glacier retreat

Based on the response of living benthic foraminiferal faunas to the distance from the glacier front analysed in Chapter 4, multiple diversity metrics were proposed as potential proxy for glacier retreat. In **Chapter 5**, we tested the validity of the proposed proxy along a sedimentary archive influenced by a rapid glacier retreat. The sediment core, sampled in Kongsfjorden in 2010, registered the retreat of the Kronebreen glacier complex across six decades after the last

surge event in 1948. We used the 11 known positions of the glacier front since 1948 (obtained from previous publications (i.e., Hagen et al., 1993; Trusel et al., 2010; Streuff et al., 2015; Bourriquen, 2018) to calculate the increasing of the linear distance between the glacier front and the core site, all along the time series. Patterns of foraminiferal communities and multiple diversity metrics in function of the distance from the glacier front were investigated. In parallel, different geochemical proxies (elemental calcium ratio) were measured on two foraminiferal species.

Lower foraminiferal abundances were observed downcore compared to the uppermost part of the core. This is possibly the consequence of high accumulation rates and high physical disturbance on the seafloor, related to the rapid retreat during ~30 years after the surge event in 1948. In the most recent deposit, after 1982, some variations in foraminiferal fluxes were observed and attributed to seasonal or interannual variability. Geochemical proxies measured on foraminiferal calcite did not show clear patterns in function of the distance from the front, but a generally more stable signal was observed for a fauna living far from the glacier front.

Positive relationships between diversity metrics and distance from the glacier front were observed. More specifically, taxonomic and functional richness remained low between 2 and 5 km from the front, and increased exponentially afterwards, while Shannon index and Rao showed a linear increase with increased distance from the front. These observations are coherent with the patterns observed for the living assemblages along a spatial gradient as detailed in Chapter 4. The measured increase in diversity is linked to the reduced GID at the core site with progressive distancing of the glacier front. When the core site was close to the front, the typical stress tolerant glacier-proximal species *Cassidulina reniforme* dominated and as the GID decreased it left space for *Elphidium clavatum* and *Quinqueloculina stalkeri* as well as to other minor species in the most recent assemblages. These results seem to validate the use of patterns of diversities as qualitative and semi-quantitative indicators of progressive glacier retreat along a kilometric spatial scale.

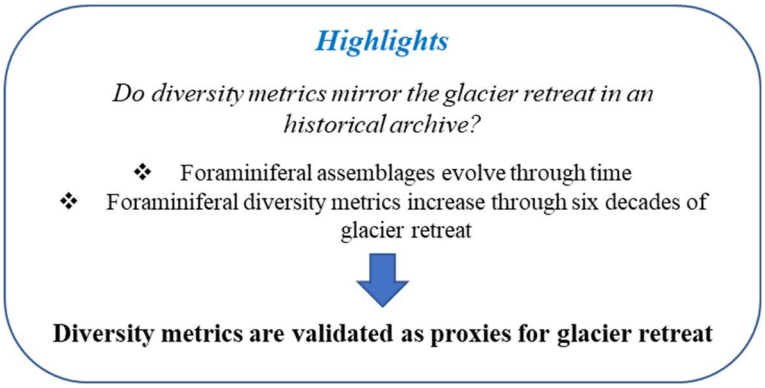

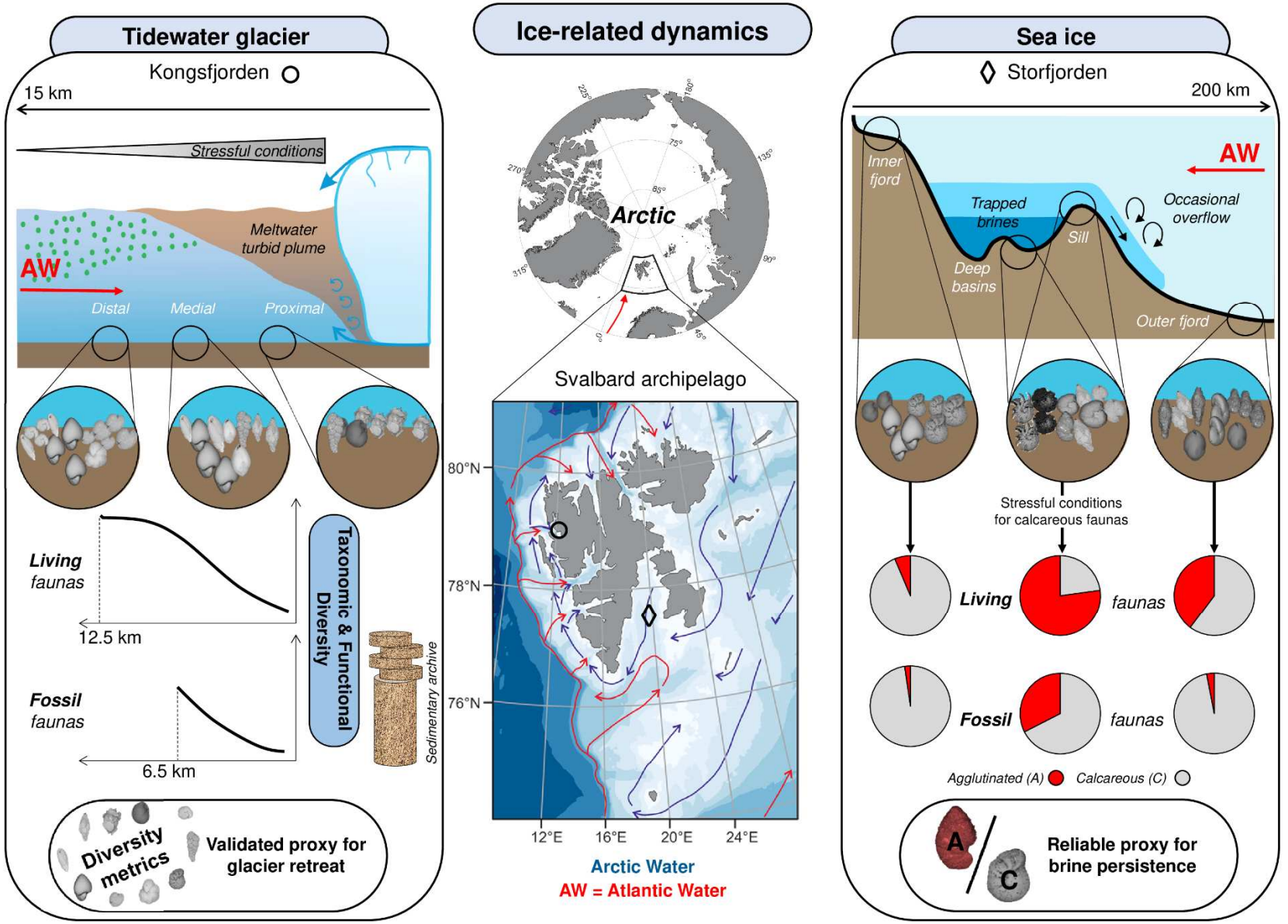

Figure 2. Sketch highlighting the main findings of this PhD thesis.

2. Two contrasted glaciated fjords

2.1 Environmental differences and major ice-related dynamics

Located at the interface between terrestrial and marine systems, high latitude glaciated fjords are sensitive spots to current climate change (e.g., Meredith et al., 2019; Bianchi et al., 2020). Furthermore, the two fjords investigated in this thesis are located on a particularly sensitive spot in the Arctic region: the Svalbard archipelago. The archipelago is indeed located at the gateway between the Atlantic and Arctic Ocean, where warm waters enter the Arctic Ocean as the principal source of heat and nutrients (e.g., Rudels et al., 2005; Vernet et al., 2019). These two fjords present some analogies, but also substantial differences which result in different sensitivity and responses to climate-induced modifications.

Storfjorden, located in the southern part of the archipelago, is the biggest Svalbard fjord (about 190 km length) characterised by the presence of a sill at the entrance that separates the central deep basins from the outer part. It is defined as "sea ice factory" because of the presence of a recurrent coastal polynya responsible to produce brines during winter-early spring. Due to the fjord topography, brines are retained in the deep basins for the entire year by the sill.

Conversely, Kongsfjorden, located on the western part of the Svalbard archipelago, is ten times smaller than Storfjorden (about 20 km length) and it does not have a well-defined sill. Its location on the western Svalbard and its shallow topography result in a strong influence of warm intermediate Atlantic water (AW) that inflows into the fjord in the opposite direction of the glacial discharges produced at the fjord-head, creating steep environmental gradients.

Storfjorden, as located just above the Polar Front, is subjected to interannual variability in seasonal water masses (Loeng, 1991; Haarpaintner et al., 2001b). Arctic waters are imported in the fjord by the East Spitsbergen Current (ESC) from its entrance and two sounds (Heleysundet and Freemansundet) next to the fjord head in the northeast (see Fig. 1 *Chapter 1*) (Haarpaintner et al., 2001b). During winter-early spring the freezing of these Arctic waters (ArW) at the surface produce cold, saline, downwelling dense waters, which fill the deeper part of the fjord. In summer, three main layer characterised the water column: a dense brine-enriched layer at the bottom trapped by the sill (120 m depth), an Arctic intermediate layer, and the Storfjorden Surface Water (about 60 m thick) (Haarpaintner et al., 2001b). Inflow of warm and saline AW has been observed in Storfjorden at intermediate depth in autumn, but the amount of AW entering Storfjorden varies interannually and seasonally depending on the Polar Front location (Skogseth et al., 2005a, 2005b). Furthermore, also the extension and location of the Storfjorden

coastal polynya is influenced by atmospheric factors (i.e., northerly winds) and it is therefore subjected to strong interannual variability (e.g., Haarpaintner et al., 2001). Nevertheless, the rapid changes undergoing in the Arctic are expected to strongly affect polynya dynamics (variations in occurrence and size) with consequent feedbacks on dense water production and water mass stratification, PP, and potential drastic changes in biological processes (Smith and Barber, 2007).

Kongsfjorden, due to its geographical location and its open fjord configuration, is largely influenced by the inflow of AW which occurs especially during summer due to geostrophic balance between shelf and fjord waters (Svendsen et al., 2002; Cottier et al., 2005, 2007). This determines a seasonal shift between prevailing cold and fresh ArW in winter, and warm and saline AW in summer (Svendsen et al., 2002; Cottier et al., 2005). The AW inflow is amplified by the presence of tidewater glaciers which discharge high amounts of freshwaters into the fjord during summer. The upwelling of subglacial waters from marine-terminating glaciers generates a surface outflow compensated by the subsurface inflow of AW (Cowton et al., 2015; Sundfjord et al., 2017) which in turn promotes frontal ablation (e.g., Holmes et al., 2019; Luckman et al., 2015). In general the AW inflow in Kongsfjorden is subjected to interannual variability (Hop et al., 2002; Svendsen et al., 2002; Cottier et al., 2005). Currently, Kongsfjorden is experiencing important changes. Since 2006 the fjord faced an increased inflow of AW and an overall increase in seawater temperatures (e.g., Cottier et al., 2007; David T and K.P., 2017; Payne and Roesler, 2019; Tverberg et al., 2019). This has shifted the fjord system into a warmer state (Cottier et al., 2007, 2010) which resulted in reduced sea ice cover (i.e., up to 50% decrease; Pavlova et al., 2019) and thickness (i.e., from 0.6 m to 0.2 m decrease; Pavlova et al., 2019). An increased residence time of AW, as well as their further intrusion far inside the innermost part of the fjord has been documented in the last decade (e.g., Holmes et al., 2019). This recent hydrological change strongly enhanced frontal ablation of tidewater glaciers (Luckman et al., 2015; Holmes et al., 2019), and as a consequence, meltwater discharges and associated sediment load at Kongsfjorden head. The landward progression of tidewater glaciers and the potential transition from marine- to land-terminating glaciers would have consequences on the fjord stratification, PP, and related biological process (e.g., Meredith et al., 2019).

2.2 Analogies in ecological responses of benthic foraminifera

In these two contrasted Svalbard fjords, living benthic foraminiferal distributions were analysed and interpreted in relation to several environmental parameters which are supposed to be linked

to the targeted dynamics for proxy development. Storfjorden was selected to calibrate a proxy related to sea ice formation, whereas Kongsfjorden was selected to calibrate a proxy for tidewater glacier retreat. To build a proxy based on the foraminiferal responses to different environmental dynamics, there is the need to know all drivers of foraminiferal distribution on a regional and on a micro spatial scale (i.e., microhabitat distribution). Living foraminiferal assemblages were investigated in two Svalbard fjords during the summer season, precisely in July 2016 for Storfjorden and August 2018 for Kongsfjorden. Besides the important physico-chemical differences and different perturbations characterising the two fjords, some analogies can be identified in foraminiferal assemblages.

The inner part of Storfjorden was inhabited by the commonly defined "glacier proximal" species *Elphidium clavatum* accompanied in the innermost station by *Cassidulina reniforme*. Both species showed high densities of juveniles in the surface sediment suggesting summer reproductive events, possibly as a response to fresh organic inputs. This hypothesis was supported by the presence of the fresh phytodetritus-feeder *N. labradorica* especially in the infaunal habitats. Adults and juveniles of *Cassidulina reniforme* were also found as dominant species in the proximal part of Kongsfjorden but this time accompanied by the fragile *Capsammina bowmanni*. Both species were restricted to the sediment surface (topmost half centimetre) with almost bare sediment below. The pattern distribution of these species was interpreted as an opportunistic response to the stressful conditions induced by the high proximity of the tidewater glacier Kronebreen.

In Kongsfjorden, *N. labradorica* dominated the medial area of the fjord, where reduced turbidity and increased organic fluxes could have favoured its development. In both fjords, *N. labradorica* appeared at the surface but high densities were observed as well below the surface sediment. This suggests a higher competitivity of this species in infaunal microhabitats, maybe favoured by alternative metabolisms, as previously suggested in the literature (e.g., denitrification, Risgaard-Petersen et al., 2006; Piña-Ochoa et al., 2010; pathways involving ammonium and sulphur assimilation, Jauffrais et al., 2019). When competition at the surface is strong it is moving in the infaunal microhabitats.

A mixture of agglutinated species often reported as "glacier distal" species was found in the Storfjorden deep basins and sill as well as in the medial and distal areas of Kongsfjorden (e.g., *Reophax* spp., *Recurvoides turbinatus*, *Labrospira crassimargo*). These species are believed to tolerate a wide range of conditions and to prefer more refractory organic matter. Their ecological preferences as well as the effect of brines on calcareous faunas were given as the explanation for the agglutinated dominance in the deep basins and sill of Storfjorden. In

Kongsfjorden, these species shared their habitats with several other calcareous species with different ecological preferences. For examples their coexistence with fresh phytodetritus feeders (e.g., *N. labradorica* and *S. feylingi*) would suggest that they occupy different ecological niches, e.g., feeding on more refractory organic matter as supposed for the Storfjorden faunas.

Another analogy observed between the two fjords was the presence of the agglutinated *Adercotryma glomeratum* at the Storfjorden sill and at the distal zone of Kongsfjorden. This species is often reported as AW or Transformed Atlantic Water (TAW) indicator and its presence at outer areas of both fjords supports this hypothesis. Indeed, the Storfjorden sill is influenced by the AW carried by the WSC, but the rest of the fjord is much less influenced due to the presence of the sill and the dominance of Arctic Waters, which limit the presence of *A. glomeratum*. Conversely, Kongsfjorden without a well-defined sill and located on the WSC path, is subjected to a strong inflow of AW far inside the fjord thus supporting the establishment of *A. glomeratum*.

In this section we underlined some analogies between the two investigated fjords in species composition and regional distribution from fjord-head to fjord-mouth. Our work supplements the knowledge on foraminiferal diversity along Svalbard fjords described by Jima et al., (2021). We highlight that the response to a combination of environmental factors and stressors (e.g., water masses, sediment inputs, glacial discharges, carbon fluxes) can result in similar benthic foraminiferal communities. Therefore, it is important to deeply investigate the major environmental dynamics occurring in a specific area to correctly interpret species-specific responses in that area.

3. Proxies for ice-related dynamics

3.1 Proxy development

Species-specific foraminiferal ecological preferences are often inferred from correlations between their abundances and measured environmental parameters. Ecological proxies can be based on individual indicator species (i.e., species that are dominant under certain specific conditions) or on communities (i.e., variation of different biodiversity measures such as abundances, size, biomass, taxonomic and functional diversity metrics). In this thesis we proposed proxy focused on overall responses of foraminiferal communities to specific phenomenon.

- **Proxy for brines.** We first observed that brine persistence had a physico-chemical effect on calcareous foraminifera causing their dissolution or hampering their growth. This, in

parallel to potential adaptability to more refractory organic matter in the persistence zone of the fjord, resulted in the dominance of agglutinated foraminifera. These observations resulted in the proposition of the ratio between agglutinated and calcareous foraminifera (A/C) as proxy for brine persistence and indirectly for sea ice formation.

- **Proxy for glacier retreat.** We first observed that the dynamics linked to tidewater glacier were responsible of several effects of environmental disturbance at different levels (i.e., physical, chemical, biological) globally defined as glacier-induced disturbance (GID). The GID impacted foraminiferal microhabitats and drove the establishment of different foraminiferal assemblages along Kongsfjorden. Most of identified drivers of foraminiferal distribution were linked to the distance from the glacier front suggesting the use this unique parameter to develop a proxy related to this dynamic. Multiple taxonomic and functional diversity metrics showed clear positive relationships with the distance from the glacier front and were proposed as proxy for glacier retreat.

3.2 Proxy application

The proposed proxies for brine persistence and glacier retreat were developed in specific Arctic environments. At the present state of knowledge, the proxies seem to be reliable and useful in the fjords where they were developed, but their use could be easily extended to other areas characterised (or possibly having been characterised) by similar environmental conditions. Our validation and applicability tests were limited to quite recent fossil faunas, corresponding to an historical time (<100 years). Therefore, at present, we recommend their application on comparable time scales. The reliability of the proxies can be further challenged by their application on existing reconstructions based on other indicators.

3.2.1 Proxy for brine persistence

Based on our results, the proxy for brine persistence is adapted for application in environments characterised by coastal polynyas and the presence of a basin of retention. At present, several coastal polynyas are found around the Arctic region (see Fig. 8 from the *Introduction*) and over-deepened basins behind a sill are common topographic features in Arctic glaciated fjords (Howe et al., 2010; Bianchi et al., 2020). Therefore, the proposed proxy may be applied to multiple areas around the Arctic. Moreover, the A/C proxy presents several advantages, including an easy application by non-experts in foraminiferal taxonomy and the consideration of the entire foraminiferal community (without overlooking for minor species). Indeed, being based only on

the distinction between agglutinated and calcareous foraminifera, it can be easily applied in future studies wishing to use a multiproxy approach.

Furthermore, it seems that the application of the A/C proxy on more than historical time scales is promising. A recent study from the Baffin Bay (West Greenland) successfully used our A/C proxy (as the proportion of agglutinated foraminifera) to reconstruct the dynamics of the North Water Polynya (NOW) during the Holocene (Jackson et al., 2021). The A/C proxy was used in combination to other sea ice related proxies including IP_{25}, lipids, diatoms, and foraminiferal indicator species (Jackson et al., 2021). With such multi-proxy reconstruction, they observed that the NOW activity had a great influence on the seafloor bottom water conditions since about 4.4 kyr BP. In two sediment cores collected below the NOW polynya, Jackson et al. (2021) observed the dominance of agglutinated species (nearly 100 %) since 4.4 kyr BP in one core and more variable proportions during the same period in a second core (10-30 % between 3.8 kyr and 1.8 kyr and 40-85% after 1.8 kyr BP). Hence, the A/C proxy can be used in multiproxy approaches as demonstrated by Jackson et al. (2021) to have a qualitative idea of the intensity of polynya activity. Furthermore, based on the conclusions of this recent study (Jackson et al., 2021), it seems that the A/C proxy is suitable for paleoenvironmental reconstructions from other Arctic areas.

3.2.2 Proxy for glacier retreat

The proxy for glacier retreat is adapted for the reconstruction of the historical evolution of benthic system located close to existent tidewater glaciers and/or for the documentation of the retreat of past tidewater glaciers that are currently land-terminating. The proposed proxy (i.e., diversity metrics) could be used in parallel to the observation of seafloor morphology (e.g., glacial lineation, moraines) to reconstruct glacial movements in fjord environments. The proxy proposed here could also help reconstructing the ice sheet variations together with Ice Rafted Debris during the Younger Dryas for example. Indeed, several sedimentary cores around Svalbard were used to reconstruct the retreat of the ice sheet during the deglaciation (e.g., Skirbekk et al., 2010; Bartels, 2017). Furthermore, West Spitsbergen fjords are all located close to the path of the WSC and thus periodically influenced by inflow of warm Atlantic waters and presence of several tidewater glaciers. The proxy proposed for glacier retreat could be applied in addition to present, historical and paleoenvironmental records existing from these fjords (see Bartels, 2017) to detect possible diversity patterns that are potentially correlated to an increased glacial influence. At this regard, a study focusing on a sedimentary archive covering the last

3000 years from the central Kongsfjorden is in progress to reconstruct the AW inflow (cf. *Perspectives*).

The diversity multi-metrics proxy has several advantages. Firstly, it does not use a species-specific composition to reconstruct the retreat but the diversity of the entire community. This has the advantage to include minor species, often neglected, which could have important ecological functions in the analysis. Therefore, it is suitable for use in parallel to the variation of foraminiferal species composition to spot diversity patterns along the sedimentary archives. Secondly, there is no need to assign a specific name to foraminiferal species but only separate them based on their morphological characteristics. This has the advantage that also non-foraminiferal experts can apply the proposed proxy.

4. Concluding remarks

Rapid climate modifications are underway in the Arctic and its associated ecosystems. Sea ice cover loss and modification in brine production together with retreat of glaciers, are major consequences of recent/current environmental changes and provide strong feedbacks on internal climatic forcings (i.e., radiative forcing/surface albedo, CO_2 budget/acid brine production, oceanic thermohaline circulation/dense water production). Indeed, complex dynamics are associated to sea ice and glaciers and different biotic marine compartments and trophic levels are influenced and rely on them. Therefore, rapid climate-induced modifications imply responses by the biosphere on a short period of time. Predictions about sea ice and glacier changes rely on paleoenvironmental reconstructions to extend the knowledge based on the instrumental period, and thus reduce the uncertainties characterising climate modelling. Such reconstructions are based on the use of proxies. In this PhD thesis we focused on the marine benthic compartment and on specific microorganism as powerful bioindicators: benthic foraminifera. At first, we explored benthic foraminiferal responses to the chronical influence of brines (linked to sea ice formation) and tidewater glacier. Then, we proposed reliable ecological proxies to chronicle recent changes in benthic environments related to ice dynamics. Specifically, we identified the ratio between agglutinated and calcareous (A/C) foraminifera as proxy for brine persistence due to the brine-induced dissolution on calcareous test, and the variation of taxonomic and functional diversity metrics as proxy for glacier retreat due to the glacier-induced disturbance on the diversity. Further investigations on the influence of taphonomic processes on the A/C ratio supported its use. We also tested the effectiveness of diversity metrics in recording the progressive retreat of a tidewater glacier on an historical

record and we confirmed its use as proxy for glacier retreat. The two proposed proxies in this PhD thesis are based on characteristics of the entire foraminiferal communities thus recording a wide ecological signal without overlooking or neglecting minor species. A major advantage of these proxies is that they do not rely on species identity which could vary depending on the area of study, thus avoiding potential bias linked to the sampling area and could be more easily used by non-experts in foraminiferal taxonomy.

5. Perspectives

The results of this PhD thesis will certainly contribute to a better understanding of the response of benthic ecosystems to environmental constraints related to glacier dynamics. Despite this, several limitations stand out and will require more investigation in the future.

5.1 Overcoming the spatial scale limitations

Several questions arise from the limitations of the developed proxies as regards to their effective inclusion in future predictions and application on longer time scales (i.e., thousands of years). From our study based on two Arctic fjords, the proposed proxies can only be applied qualitatively or semi-quantitatively, but further studies in other Arctic fjords can help to generalise the observed relationships and potentially apply these proxies in a more quantitative way. Future predictions about sea ice cover and glacier retreat are based on measurements obtained during the instrumental period. This results in high uncertainties in the predictions of future climate, but proxies can extend this small window of observations and help obtaining more robust models.

5.2 Improving the trait-function relationship in foraminifera

This thesis highlights the great potential of using functional metrics for understanding the community responses to perturbations. However, functional metrics are often overlooked because it is complicated to know the exact functions of certain morphological characteristics in small microorganisms. Even though the functions of some morphological traits are limited, the consideration of functional diversity metrics can still give a complementary view of the community responses to ice-related perturbations. There is also the need to deeply investigate the relationship between trait and function in foraminifera. The trait-based approaches should be used more extensively as it is already done for several other taxonomic groups instead of limiting the analyses only to taxonomic approaches.

5.3 Disentangling the environmental factors

Most of the ecological interpretations from the major foraminiferal species encountered here were inferred from correlation between their relative abundances and their ambient environment, as a combination of multiple environmental parameters. However, mesocosm experiments under controlled laboratory conditions could give a great contribution in understanding foraminiferal responses to specific physical disturbances. At this regard, a PhD student (Corentin Guilhermic) in our research team at LPG (University of Angers) is contributing to this topic by investigating foraminiferal responses to the physical perturbations determined by massive deposits of sediments or intermittent sediment pulses simulating the glacier-induced disturbance on the benthic environments.

5.4 Linking the recent observed changes to past climatic periods

Throughout the five main chapters of this manuscript, we focused on living and recent fossil (less than 100 years) foraminiferal faunas. The following step will be to apply and test a multiproxy approach based on the combination of "classic" proxies, such as benthic foraminiferal assemblages and geochemical proxies (elemental ratio on foraminiferal calcite), together with the proxies proposed in this PhD (i.e., taxonomic and functional diversity metrics, A/C ratio) on long sedimentary archives. For this purpose, a study of a long core, collected in the central Kongsfjorden and covering the last three millennia, was initiated to reconstruct the two end-members relationship between AW inflow and glacier retreat in western Svalbard fjords during the Late Holocene. In the following paragraphs, we report the very preliminary results, issued from the Master thesis of Serena Santoni, that need to be deepened and supplemented before publication.

5.4.1 Materials and methods in brief

In 2007, Core NP07-13/58-GC (NP07 in the following) of 370 cm length was collected in Kongsfjorden (Fig. 3a) with a gravity corer during a cruise onboard R/V LANCE organised by the Norwegian Polar Institute (NPI). Thanks to a collaboration with Katrine Husum (Senior Research Scientist at NPI), we had the opportunity to subsample this core to investigate foraminiferal assemblages at high time resolution (i.e., 31 ± 12 yrs in the 175-1047 yrs BP interval, and 110 ± 31 yrs in the 1130-3023 yrs BP interval). A total of 47 sediment samples were analysed for benthic foraminiferal assemblages. Some environmental parameters (i.e., sediment grain size and organic matter content) were also kindly provided by Matthias Forwick

(UiT, The Arctic University of Norway). Part of the data reported below were part of the master's thesis of Serena Santoni, who I co-supervised during my second year of PhD.

A total of 3 AMS ^{14}C radiocarbon dates (from bivalves; performed at Aarhus AMS Centre, Aarhus University, Denmark) and 8 based on bulk measures of the benthic foraminifera *Nonionellina labradorica* (performed at LSCE by the GEOTRAC team, Gif-sur-Yvette, France) were obtained to be included in the age model. AMS ^{14}C dates were converted to calendar ages (years before present, BP) using the R package *Bchron* (Haslett and Parnell, 2008) in R Software (R Core Team, 2020) with the marine calibration curve Marine13 (Reimer et al., 2013). A regional reservoir age of 105±24 was applied (Mangerud et al., 2006). Of the 11 AMS ^{14}C dates (i.e., 3+8), three were identified as outliers and thus removed from the final age model which was therefore based on a total of 8 AMS ^{14}C dates (Fig. 3b).

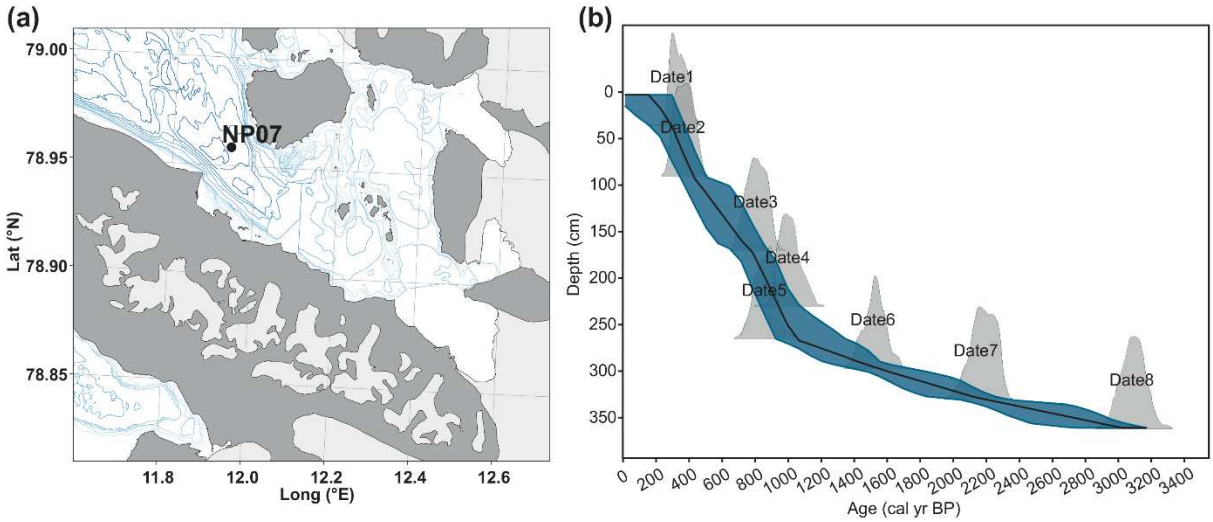

Figure 3. (a) Location of core NP07 in Kongsfjorden; **(b)** age depth profile used as age model of the studied core.

5.4.2 Preliminary results and discussion

The investigated sedimentary archive covers the period between ~3000 yrs cal BP and 200 yrs cal BP. Figure 4 reports three taxonomic diversity metrics and the relative abundances of some major species. All along the investigated period, taxonomic richness ranged between 15 and 38 species, taxonomic evenness varied between 0.5 and 0.8, and Shannon index between 1.6 and 2.5.

The beginning of the Neoglaciation (until 2.7 kyrs cal BP; NEO) was characterised by a general low diversity and high relative abundances of the two glacier proximal species, *Cassidulina reniforme* and *Elphidium clavatum*. Similar patterns were observed through the Roman Warm Period (RWP; 2.7-1.6 kyrs BP). This would suggest that the glacial influence on the core site remained generally stable across the NEO and RWP periods. Comparison with the

diversity metrics models presented in *Chapter 4*, and *Chapter 5*, would suggest that the glacier grounding line/ice sheet was advanced during the NEO and RWP periods compared to its position during the mid *XX*th century. During the Dark Ages Cold Period (1.6-1.2 kyrs cal BP) and Medieval Warm Period (MWP; 1.2-0.8 kyrs cal BP), taxonomic diversity increased. A correspondent slight decrease in the relative abundance of the two glacier proximal species (i.e., *C. reniforme* and *E. clavatum*) was observed. This would suggest decreased glacial influence over approximately 800 yrs period, and possibly an increased influence of Atlantic Water in the fjord.

At the beginning of the Little Ice Age (LIA), between 800 yrs cal BP and about 500 yrs cal BP, taxonomic diversity measured an abrupt decrease. This may suggest an increased glacial influence over this short period and therefore a possible advance of the ice sheet at the beginning of this cold period. The most recent part of our core, between 500 yrs cal BP and about 200 yrs cal BP, recorded an important increase in biodiversity, and a concomitant marked decrease of the stress-tolerant glacier proximal species *C. reniforme*. In parallel, a greater variability in *E. clavatum* and *N. labradorica* was detected and an increased relative abundance of the AW indicator *Adercotryma glomeratum* was observed. Even though the trend observed for this last agglutinated species may seem the result of selective taphonomic loss, the numbers of individuals per gram of dry sediment remained variable all along the archive and did not show any abrupt change along the core. The observed results seem to indicate a progressive reduction of the glacier influence (possible retreat of glaciers) and an increased influence of the Atlantic Water carried by the West Spitsbergen Current that would have triggered the increased diversity. The increase in diversity observed in the most recent period recorded by our archive, seems congruent with a recent study focused on a sediment core just few kilometres away from our archive (Tesi et al., 2021). Using a multiproxy approach including organic biomarkers and foraminiferal data, they documented an increased influence of the AW inflow in the fjord since 50 yrs cal BP (i.e., 1900 AD). In particular, Tesi et al., (2021) documented a decrease in relative abundances of the two glacier proximal species (*C. reniforme* and *E. clavatum*) and an increased in the proportion of *A. glomeratum* since the beginning of the *XX*th century and they explained these patterns as a response as an increased influence in warmer and saltier water masses in the fjord.

These ecological observations need further investigations and comparison with published studies from Kongsfjorden (e.g., Skirbekk et al., 2010; Jernas et al., 2013; Tesi et al., 2021) and other Svalbard fjords. Further investigations with multivariate analyses and Generalised Additive Models could help better interpret the patterns observed in term of species

composition and general diversity. Furthermore, the integration of our results with geochemical proxies (elemental calcium ratios) measured on *N. labradorica* and *E. clavatum* could help reconstruct changes in water masses influences, as well as on carbon fluxes to the seafloor.

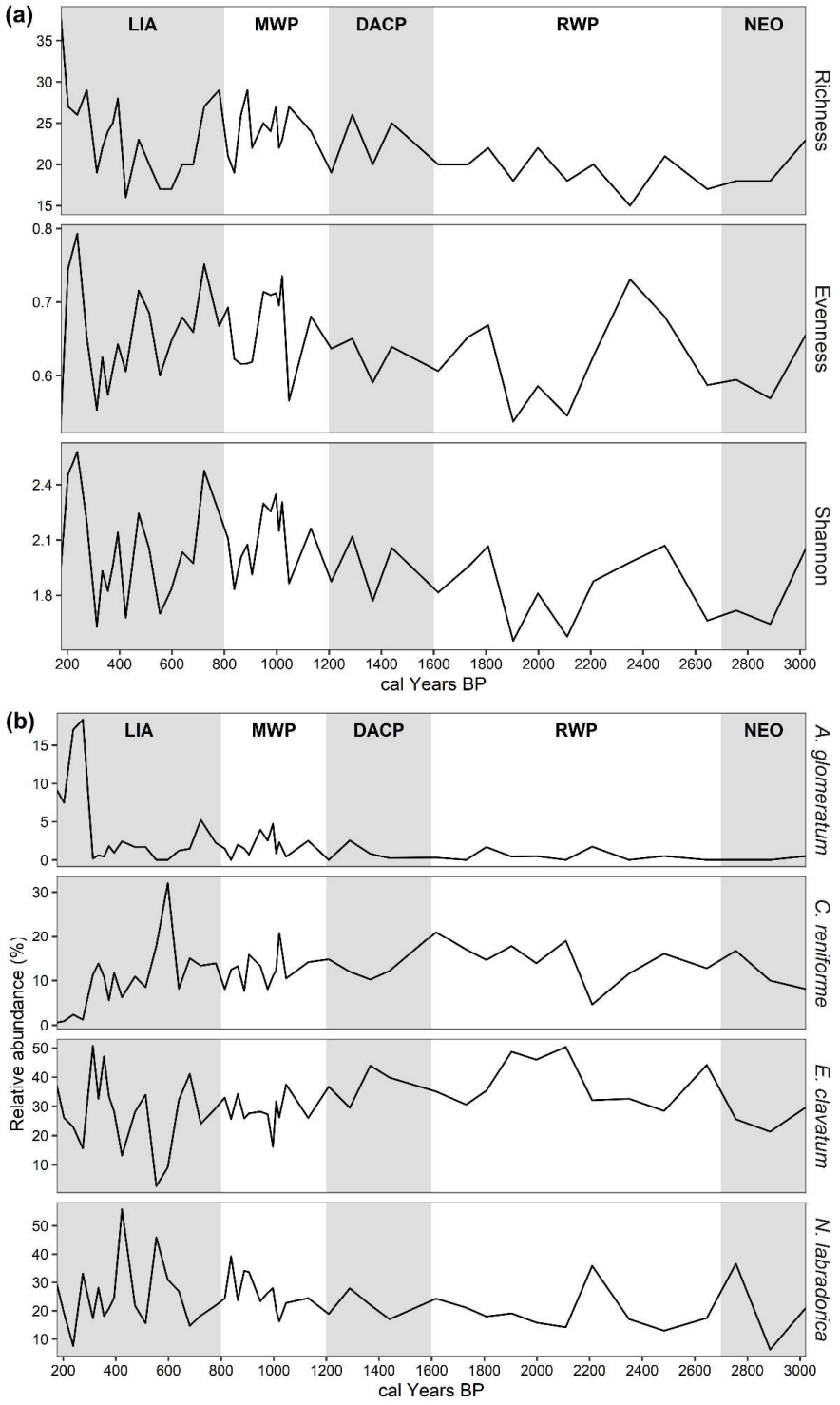

Figure 4. **(a)** Taxonomic diversity metrics and **(b)** relative abundances of some major species along the core NP07. Periods are indicated as follow: NEO = the beginning of the Neoglaciation, RWP = Roman Warm Period, DACP = Dark Ages Cold Period, MWP =Medieval Warm Period, LIA = Little Ice Age. Cold periods are indicated in grey.

References

Bartels, M.: Atlantic Water advection and glacier responses at the margins of Svalbard since the deglaciation, 2017.

Bianchi, T. S., Arndt, S., Austin, W. E. N., Benn, D. I., Bertrand, S., Cui, X., Faust, J. C., Koziorowska-Makuch, K., Moy, C. M., Savage, C., Smeaton, C., Smith, R. W. and Syvitski, J.: Fjords as Aquatic Critical Zones (ACZs), Earth-Science Rev., 203(February), 103145, https://doi.org/10.1016/j.earscirev.2020.103145, 2020.

Bourriquen, M.: Evolution du littoral de la presqu'île de Brøgger dans le contexte du changement climatique contemporain, Spitsberg nord-occidental, 2018.

Cavalieri, D. J. and Martin, S.: The contribution of Alaskan, Siberian, and Canadian coastal polynyas to the cold halocline layer of the Arctic Ocean, J. Geophys. Res., 99(C9), 18,343-18,362, https://doi.org/https://doi.org/10.1029/94JC01169, 1994.

Cottier, F., Tverberg, V., Inall, M., Svendsen, H., Nilsen, F. and Griffiths, C.: Water mass modification in an Arctic fjord through cross-shelf exchange: The seasonal hydrography of Kongsfjorden, Svalbard, J. Geophys. Res. Ocean., 110(12), 1–18, https://doi.org/10.1029/2004JC002757, 2005.

Cottier, F. R., Nilsen, F., Enall, M. E., Gerland, S., Tverberg, V. and Svendsen, H.: Wintertime warming of an Arctic shelf in response to large-scale atmospheric circulation, Geophys. Res. Lett., 34(10), 1–5, https://doi.org/10.1029/2007GL029948, 2007.

Cottier, F. R., Nilsen, F., Skogseth, R., Tverberg, V., Skarðhamar, J. and Svendsen, H.: Arctic fjords: a review of the oceanographic environment and dominant physical processes, Geol. Soc. London, Spec. Publ., 344, 35–50, https://doi.org/10.1144/sp344.4, 2010.

Cowton, T., Slater, D., Sole, A., Goldberg, D. and Nienow, P.: Modeling the impact of glacial runoff on fjord circulation and submarine melt rate using a new subgrid-scale parameterization for glacial plumes, J. Geophys. Res. Ocean., 796–812, https://doi.org/10.1002/2014JC010324, 2015.

David T, D. and K.P., K.: Recent variability in the Atlantic water intrusion and water masses in Kongsfjorden, an Arctic fjord, Polar Sci., 11, 30–41, https://doi.org/10.1016/j.polar.2016.11.004, 2017.

Haarpaintner, J.: The Storfjorden polynya: ERS-2 SAR observations and overview, Polar Res., 18(2), 175–182, https://doi.org/10.3402/polar.v18i2.6571, 1999.

Haarpaintner, J., Haugan, P. M. and Gascard, J. C.: Interannual variability of the Storfjorden (Svalbard) ice cover and ice production observed by ERS-2 SAR, Ann. Glaciol., 33, 430–436, 2001a.

Haarpaintner, J., O'Downer, J., Gascard, J. C., Haugan, P. M., Schauer, U. and Øterhus, S.: Seasonal transformation of water masses, circulation and brine formation observed in Storfjorden, Svalbard, Ann. Glaciol., 33, 437–443, https://doi.org/doi:10.3189/172756401781818635, 2001b.

Hagen, J. O., Liestøl, O., Roland, E. and Jørgensen, T.: Glacier Atlas of Svalbard and Jan Mayen., 1993.

Haslett, J., & Parnell, A.C.: A simple monotone process with application to radiocarbon-dated depth chronologies. Journal of the Royal Statistical Society: Series C (Applied Statistics), 57(4), 399-418, 2008.

Holmes, F. A., Kirchner, N., Kuttenkeuler, J., Krützfeldt, J. and Noormets, R.: Relating ocean temperatures to frontal ablation rates at Svalbard tidewater glaciers: Insights from glacier proximal datasets, Sci. Rep., 9(1), 1–11, https://doi.org/10.1038/s41598-019-45077-3, 2019.

Hop, H. and Wiencke, C.: The Ecosystem of Kongsfjorden, Svalbard, in The Ecosystem of Kongsfjorden, pp. 1–20, https://doi.org/10.1007/978-3-319-46425-1_1, , 2019.

Hop, H., Pearson, T., Hegseth, E. N., Kovacs, K. M., Wiencke, C., Kwasniewski, S., Eiane, K., Mehlum, F., Gulliksen, B., Wlodarska-Kowalezuk, M., Lydersen, C., Weslawski, J. M., Cochrane, S., Gabrielsen, G. W., Leakey, R. J. G., Lonne, O. J., Zajaczkowski, M., Falk-Petersen, S., Kendall, M., Wangberg, S. A., Bischof, K., Voronkov, A. Y., Kovaltchouk, N. A., Wiktor, J., Poltermann, M., di Prisco, G., Papucci, C. and Gerland, S.: The marine ecosystem of Kongsfjorden, Svalbard, Polar Res., 21(1), 167–208, https://doi.org/https://doi.org/10.3402/polar.v21i1.6480, 2002.

Howe, J. A., Austin, W. E. N., Forwick, M., Paetzel, M., Harland, R. E. X. and Cage, A. G.: Fjord systems and archives : a review, Fjord Syst. Arch., 5–15, https://doi.org/10.1144/SP344.2, 2010.

Jackson, R., Kvorning, A. B., Limoges, A., Georgiadis, E., Olsen, S. M., Tallberg, P., Andersen, T. J., Mikkelsen, N., Giraudeau, J., Massé, G., Wacker, L. and Ribeiro, S.: Holocene polynya dynamics and their interaction with oceanic heat transport in northernmost Baffin Bay, Sci. Rep., 11(1), https://doi.org/10.1038/s41598-021-88517-9, 2021.

Jauffrais, T., LeKieffre, C., Schweizer, M., Geslin, E., Metzger, E., Bernhard, J. M., Jesus, B., Filipsson, H. L., Maire, O. and Meibom, A.: Kleptoplastidic benthic foraminifera from aphotic habitats: insights into assimilation of inorganic C, N and S studied with sub-cellular resolution, Environ. Microbiol., 21(1), 125–141, https://doi.org/10.1111/1462-2920.14433, 2019.

Jernas, P., Klitgaard Kristensen, D., Husum, K., Wilson, L. and Koç, N.: Palaeoenvironmental changes of the last two millennia on the western and northern Svalbard shelf, Boreas, 42(1), 236–255, https://doi.org/10.1111/j.1502-3885.2012.00293.x, 2013.

Jima, M., Jayachandran, P. R. and Nandan, S. B.: Modern Benthic Foraminiferal Diversity Along the Fjords of Svalbard Archipelago : Diversity Evaluation, Thalass. An Int. J. Mar. Sci., https://doi.org/10.1007/s41208-021-00356-7, 2021.

Koerner, K. A., Limoges, A., Van Nieuwenhove, N., Richerol, T., Massé, G. and Ribeiro, S.: Late Holocene sea-surface changes in the North Water polynya reveal freshening of northern Baffin Bay in the 21st century, Glob. Planet. Change, 206, https://doi.org/10.1016/j.gloplacha.2021.103642, 2021.

Loeng, H.: Features of the physical oceanographic conditions of the Barents Sea, Polar Res., 10(1), 5–18, https://doi.org/10.3402/polar.v10i1.6723, 1991.

Luckman, A., Benn, D. I., Cottier, F., Bevan, S., Nilsen, F. and Inall, M.: Calving rates at tidewater glaciers vary strongly with ocean temperature, Nat. Commun., 6, https://doi.org/10.1038/ncomms9566, 2015.

Mangerud, J., Bondevik, S., Gulliksen, S., Karin Hufthammer, A. and Høisæter, T.: Marine 14C reservoir ages for 19th century whales and molluscs from the North Atlantic, Quat. Sci. Rev., 25(23–24), 3228–3245, https://doi.org/10.1016/j.quascirev.2006.03.010, 2006.

Meredith, M., Sommerkorn, M., Cassotta, S., Derksen, C., Ekaykin, A., Hollowed, A., Kofinas, G., Mackintosh, A., Melbourne-Thomas, J., Muelbert, M. M. C., Ottersen, G., Pritchard, H. and Schuur, E. A. G.: Polar Regions, in IPCC Special Report on the Ocean and Cryosphere in a Changing Climate, pp. 203–320, , 2019.

Payne, C. M. and Roesler, C. S.: Characterizing the influence of Atlantic water intrusion on water mass formation and phytoplankton distribution in Kongsfjorden, Svalbard, Cont. Shelf Res., 191, 104005, https://doi.org/10.1016/j.csr.2019.104005, 2019.

Piña-Ochoa, E., Høgslund, S., Geslin, E., Cedhagen, T., Revsbech, N. P., Nielsen, L. P., Schweizer, M., Jorissen,

F., Rysgaard, S. and Risgaard-Petersen, N.: Widespread occurrence of nitrate storage and denitrification among Foraminifera and Gromiida, Proc. Natl. Acad. Sci. U. S. A., 107(3), 1148–1153, https://doi.org/10.1073/pnas.0908440107, 2010.

R Core Team: R: A language and environment for statistical computing. R Foundation for Statistical Computing, Vienna, Austria. URL https://www.R-project.org/, 2020.

Rasmussen, T. L. and Thomsen, E.: Brine formation in relation to climate changes and ice retreat during the last 15,000 years in Storfjorden, Svalbard, 76 – 78°N, Paleoceanography, 29, 911–929, https://doi.org/10.1002/2014PA002643.Received, 2014.

Rasmussen, T. L. and Thomsen, E.: Palaeoceanographic development in Storfjorden, Svalbard, during the deglaciation and Holocene: Evidence from benthic foraminiferal records, Boreas, 44(1), 24–44, https://doi.org/10.1111/bor.12098, 2015.

Reimer, P. J., Edouard Bard, B., Alex Bayliss, B., Warren Beck, B. J., Paul Blackwell, B. G. and Christopher Bronk Ramsey, B.: Intcal13 and Marine13 Radiocarbon Age Calibration Curves 0–50,000 Years Cal Bp, Radiocarbon, 55(4), 1869–1887, 2013.

Risgaard-Petersen, N., Langezaal, A. M., Ingvardsen, S., Schmid, M. C., Jetten, M. S. M., Op Den Camp, H. J. M., Derksen, J. W. M., Piña-Ochoa, E., Eriksson, S. P., Nielsen, L. P., Revsbech, N. P., Cedhagen, T. and Van Der Zwaan, G. J.: Evidence for complete denitrification in a benthic foraminifer, Nature, 443(7107), 93–96, https://doi.org/10.1038/nature05070, 2006.

Rudels, B., Björk, G., Nilsson, J., Winsor, P., Lake, I. and Nohr, C.: The interaction between waters from the Arctic Ocean and the Nordic Seas north of Fram Strait and along the East Greenland Current: Results from the Arctic Ocean-02 Oden expedition, J. Mar. Syst., 55(1–2), 1–30, https://doi.org/10.1016/j.jmarsys.2004.06.008, 2005.

Saloranta, T. M. and Svendsen, H.: Across the Arctic front west of Spitsbergen: High-resolution CTD sections from 1998-2000, Polar Res., 20(2), 177–184, https://doi.org/https://doi.org/10.3402/polar.v20i2.6515, 2001.

Skirbekk, K., Kristensen, D. K., Rasmussen, T. L., Koç, N. and Forwick, M.: Holocene climate variations at the entrance to a warm Arctic fjord: evidence from Kongsfjorden trough, Svalbard, Geol. Soc. London, Spec. Publ., 344(1), 289–304, https://doi.org/10.1144/SP344.20, 2010.

Skogseth, R., Fer, I. and Haugan, P. M.: Dense-water production and overflow from an arctic coastal polynya in storfjorden, Geophys. Monogr. Ser., 158, 73–88, https://doi.org/10.1029/158GM07, 2005a.

Skogseth, R., Haugan, P. M. and Jakobsson, M.: Watermass transformations in Storfjorden, Cont. Shelf Res., 25(5–6), 667–695, https://doi.org/10.1016/j.csr.2004.10.005, 2005b.

Smith, W. O. and Barber, D. G.: Chapter 13 Polynyas and Climate Change: A View to the Future, Elsevier Oceanogr. Ser., 74(06), 411–419, https://doi.org/10.1016/S0422-9894(06)74013-2, 2007.

Streuff, K., Forwick, M., Szczuciński, W., Andreassen, K. and Ó Cofaigh, C.: Submarine landform assemblages and sedimentary processes related to glacier surging in Kongsfjorden, Svalbard, Arktos, 1(1), 14, https://doi.org/10.1007/s41063-015-0003-y, 2015.

Sundfjord, A., Albretsen, J., Kasajima, Y., Skogseth, R., Kohler, J., Nuth, C., Skarðhamar, J., Cottier, F., Nilsen, F., Asplin, L., Gerland, S. and Torsvik, T.: Effects of glacier runoff and wind on surface layer dynamics and Atlantic Water exchange in Kongsfjorden, Svalbard; a model study, Estuar. Coast. Shelf Sci., 187, 260–272, https://doi.org/10.1016/j.ecss.2017.01.015, 2017.

Svendsen, H., Beszczynska-Møller, A., Hagen, J. O., Lefauconnier, B., Tverberg, V., Gerland, S., Ørbæk, J. B., Bischof, K., Papucci, C., Zajaczkowski, M., Azzolini, R., Bruland, O., Wiencke, C., Winther, J.-G. and Dallmann, W.: The physical environment of Kongsfjorden – Krossfjorden, an Arctic fjord system in Svalbard, Polar Res., 21(1), 133–166, https://doi.org/10.3402/polar.v21i1.6479, 2002.

Tesi, T., Muschitiello, F., Mollenhauer, G., Miserocchi, S., Langone, L., Ceccarelli, C., Panieri, G., Chiggiato, J., Nogarotto, A., Hefter, J., Ingrosso, G., Giglio, F., Giordano, P. and Capotondi, L.: Rapid Atlantification along the Fram Strait at the beginning of the 20th century, Sci. Adv., 7(48), https://doi.org/10.1126/sciadv.abj2946, 2021.

Trusel, L. D., Powell, R. D., Cumpston, R. M. and Brigham-Grette, J.: Modern glacimarine processes and potential future behaviour of Kronebreen and Kongsvegen polythermal tidewater glaciers, Kongsfjorden, Svalbard, Geol. Soc. Spec. Publ., 344(Powell 1984), 89–102, https://doi.org/10.1144/SP344.9, 2010.

Vernet, M., Ellingsen, I. H., Seuthe, L., Slagstad, D., Cape, M. R. and Matrai, P. A.: Influence of Phytoplankton Advection on the Productivity Along the Atlantic Water Inflow to the Arctic Ocean, Front. Mar. Sci., 6(September), 1–18, https://doi.org/10.3389/fmars.2019.00583, 2019.

Besides Research

1. Field work experiences

1.1 Teaching cruise

23rd July – 1st August 2019: Marine geology and geophysics cruise (GEO-8144) organised by The Arctic University of Norway (UiT).

A detailed report (20 pages including data presentation, analyses and interpretations) of the cruise was written and evaluated by the cruise leader Tom Arne Rydningen (Associate professor at UiT).

The prioritized study area for the cruise was the northwestern part of the Svalbard margin, in proximity to the Yermak Plateau. The purpose was to focus on the Woodfjorden Trough in order to increase the data coverage. The aim of the scientific cruise were:

1. Map and constrain the age of the Woodfjorden Trough Mouth Fan (TMF).
2. Study the variability of the ocean currents in order to understand their influence on the deposition and/or erosion in relation to glacienic input to the continental slope.
3. Study the continental shelf morphology to reconstruct the dynamics of the Svalbard Ice Sheet during the Last Glacial Maximum and through the final deglaciation.
4. Recover material for ^{14}C-dating to constrain the chronology of deglacial events.

In addition to the scientific aims, the course provided a detailed training in Arctic marine research including the planning and execution of a scientific cruise in the Arctic Ocean.

To achieve the scientific aims four main types of data acquisition were used:

1. Multibeam bathymetrical seabed mapping to study the morphology of the trough and the past and present sedimentary processes in the deglaciation period.
2. High-resolution seismic (Chirp) to identify possible coring sites.
3. Sub-seabed mapping (airgun seismic) to study past sedimentary processes and correlate to ODP drill sites.
4. Sediment coring (gravity and box cores) to study the past and present sedimentary processes and constrain the chronology.

1.2 Oceanographic cruise

31st July – 16th August 2021: IMPEC-2021 scientific cruise aboard the N/O L'EUROPE (Ifremer) in the Gulf of Lion (Mediterranean Sea).

I helped with the preparation of the materials for the field campaign, and I prepare beforehand

The IMPEC (IMpact de la PEChe sur les écosystèmes benthiques du large) project concerns the assessment of the benthic habitats of the offshore circalittoral in the Gulf of Lion concerning pressures from demersal fishing trawling activities using a multi-indicators approach.
The following sampling techniques were used during the cruise: Octopus interface corer, Van Veen grab, SPI, Kullenberg gravity corer, Pagure. Sediment samples from the interface cores were collected to analyse environmental parameters (i.e., sediment grain size, organic matter content, sedimentation rates, porewater geochemistry, oxygen profiling), benthic organisms (i.e., foraminifera, meiofauna, diatoms) and environmental DNA. Van Veen grab was used to collet sediment surface samples for macrofauna. The SPI was used to take pictures at the sediment interface. The Pagure was used to record videos on the bottom sediment along a linear transect. The Kullenberg gravity corer was used to collect long sediment cores.

2. Research mobility

2nd – 24th September 2019: Norwegian Polar Institute (NPI) Tromso (Norway) in collaboration with the research scientist Katrine Husum.
Thanks to the collaboration with Katrine Husum, I had the opportunity to subsample sediment samples from two long cores (collected several years before) from the Kongsfjorden (Svalbard). One core is the 10JM-GLACIBAR-GC01, collected in 2010 from the innermost fjord (see *Chapter 5*), and the second core is the NP07-13/58-GC, collected in 2007 form the outermost part of the fjord (see *Perspectives*).

3. Student supervision

- Co-supervision of L3 student (Juliette Tessier) from the University Paris VII (13/01/2020-21/02/2020). She helped me analysing 10 samples from the long core GC01 (Kongsfjorden). I followed her in the preparation of the samples, foraminiferal picking, foraminiferal taxonomy, basic analysis of the assemblages and interpretation of the data.
- Co-supervision of a M2 student (Serena Santoni) from the University of Rennes (13/01/2020-15/06/2020). She analysed 47 samples from the long core NP07 (Kongsfjorden) and she wrote her master thesis about these data. I was strongly implicated in the preparation of the samples, foraminiferal picking, foraminiferal taxonomy, analysis of the assemblages, interpretation of the data and writing of the manuscript.
- Co-supervision of a L2 student (Anaëlle Kocher) from the University of Angers (15/11/2020-10/12/2020). She helped me analysing 10 samples from the long core GC01

(Kongsfjorden). I followed her in the preparation of the samples, foraminiferal picking, foraminiferal taxonomy, basic analysis of the assemblages and interpretation of the data.

4. Teaching experience

I had the opportunity to experience few hours of teaching at University of Angers. Specifically, I had courses for a total of **32 hours** during the first and second semester of the academic year 2019/2020 (second year of PhD). The courses were taught in French.

- Licence 1 semestre 1 : Géosciences fondamentales (Travaux dirigés (TD) en Géomorphologie).
- Licence 1 semestre 2 : Histoire de la terre et de la vie (Travaux pratique (TP) en Stratigraphie).

5. Credit acquisition

PhD students at the SML doctoral school need to follow at least 100 hours of professional and scientific courses. Below are listed part of the courses I followed during my PhD (for a total of 151 hours).

- Introduction à l'éthique de la recherche et à l'intégrité scientifique **3h**
- La communication scientifique affichée : poster **10h**
- Comprendre le fonctionnement d'une entreprise **4h**
- Ways and means from one's PHD to a career out of academic world **6h**
- Identifier et valoriser ses compétences **4h**
- Modes d'accès à l'information scientifique **3h**
- How to write and publish your paper **18h**
- Science communication **18h**
- Atelier pédagogique **14h**
- Cours de langue française niveau B2 **20h**
- Comprendre les fondamentaux des réseaux professionnels **4h**
- How to pitch ? **3h**
- Stage ile de Bailleron (Golfe du Morbihan) **30h**
- Marine geology and geophysics cruise (Svalbard, UiT) **7h**
- Oceanographic cruise IMPEC **7h**

Poster and oral communications at national and international conferences and participation in oceanographic cruises are accounted as scientific courses and supplementary credits were also attributed to those.

6. Scientific communications

Poster presentation at Atelier Climat et Impact 2018

Fossile E., Mojtahid M., Howa H., Lansard B., Michel E., Peron O., Nardelli M.P.: Benthic Foraminifera as Proxies of Brine Shelf Waters (Svalbard, Norway). **Poster**, *Atelier Climat et Impact* 29-30 November 2018 (Université de Paris-Sud, Orsay, France).

Abstract

The Storfjorden is a zone of sea-ice formation characterized by a strong production of brines (salty and acid dense waters). In order to reconstruct past dynamics of brine formation in link with past and recent climatic scenarios, we need reliable fossilizing marine bio-indicators in addition to physico-chemical proxies. Foraminifera are very abundant protists in marine benthic environments, including in the Storfjorden. Because of their short life cycles, high biodiversity and specific ecological requirements of individual species, foraminifera react quickly to environmental disturbance, and can be successfully employed as bio-indicators of environmental changes, such as those brought by brine water formation (i.e. salinity, oxygen and pH changes). The additional advantage, especially for paleoclimatologists, is that many foraminiferal taxa secrete mineralized shells that leave an excellent fossil record. Consequently, the identification of benthic foraminiferal species sensitive to brine waters' physico-chemical characteristics would allow the reconstruction of the extent and the temporal variability of Arctic sea-ice cover, and therefore a better understanding of the ongoing climatic change on historical time scales (hundred to thousand years). In order to do so, our study aims at calibrating the ecological response of living benthic foraminifera to sinking brine waters, and estimating the taphonomic loss during early stages of test fossilization.

Superficial sediments from 7 interface cores sampled along a N-S transect across the Storfjorden were analyzed for living and modern dead foraminiferal assemblages. Results from the living fauna show two major biozones: an "inner-basin" characterized by the dominance of calcareous species, with more or less dissolved tests (fig. 1); and an "outer-basin" characterized by a strong dominance of agglutinated species, potentially due to persistent low pH conditions hampering the development of calcareous species. Down-core dead faunas from the inner-basin show low amplitude temporal changes, while in the outer-basin some abrupt changes in agglutinated/calcareous ratios suggest high brine production and stagnation periods (more agglutinated). These latter might correspond with alternating low to no sea-ice cover periods due to warmer and organic enriched Atlantic water incursions into the fjord (more calcareous).

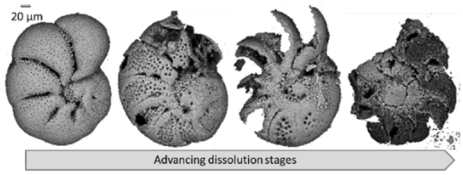

Figure 3 Different dissolution stages of calcareous species in the fjord

Indeed, the ratio between agglutinated and calcareous benthic foraminiferal species is potentially a good bio-indicator of brine seawater circulation in Arctic shelf areas. However, in such extreme environments, the fossil record may suffer from deterioration (e.g., dissolution of calcareous tests). One way to assess the resulting taphonomical loss during early stages of test fossilization is to evaluate the preservation state of the shells. In this study, four stages of dissolution (fig. 1) were determined for the calcareous species *Elphidium excavatum* subsp *clavata,* which is dominant in the modern sediments of the Storfjorden.

Benthic foraminifera as proxies of brine shelf waters

FOSSILE Eleonora[1], Mojtahid Meryem[1], Howa Hélène[1], Lansard Bruno[2], Michel Elisabeth[2], Péron Olivier[3], Nardelli Maria Pia[1]

Corresponding author: eleonora.fossile@etud.univ-angers.fr

1 LPG-BIAF UMR-CNRS 6112, University of Angers, UFR Sciences, 2 bd Lavoisier 49045, Angers Cedex 01, France; 2 Laboratoire des Sciences du Climat et de l'Environnement (LSCE-IPSL), Domaine du CNRS, Bat.12, 91198 Gif-sur-Yvette, France; 3 UMR 6457 Laboratoire de Physique Subatomique et des Technologies Associées SUBATECH IMT Atlantique, University of Nantes 4 rue Alfred Kastler La Chantrerie CS 20722 44307 Nantes cedex

Scientific context and objective

The Storfjorden is a zone of sea-ice formation characterized by a strong production and cascading of Brine-enriched Shelf Waters. In order to reconstruct past dynamics of brine formation in link with past and recent climatic scenarios, we need reliable fossilizing marine bio-indicators in addition to physico-chemical proxies.

Our study aims at calibrating the ecological response of living benthic foraminifera to sinking brine waters and estimating the taphonomic loss during early stages of test fossilization. This would allow to understand the ongoing climate change on historical time scales (hundreds of years).

Sampling Stations

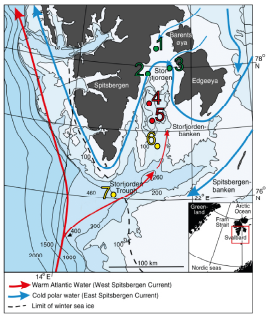

Modified from Rasmussen & Thomsen (2015)

Scheme of seasonal influence of brines in relation to the topography of the fjord

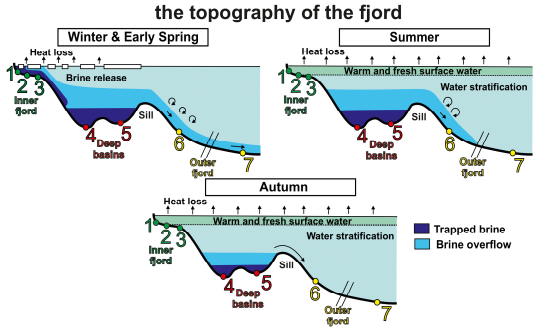

Modified from Rasmussen & Thomsen (2015) and Skogseth et al. (2005)

CTD salinity distribution (STEP16, September 2016)

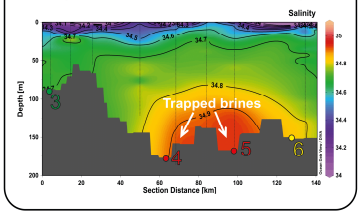

Calcareous VS Agglutinated

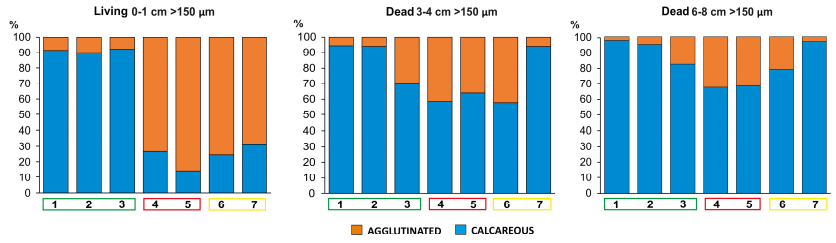

Living foraminifera assemblages are dominated by **CALCAREOUS** species in the **inner fjord** (**1**-**3**) and by **AGGLUTINATED** species in the **deep basins** and in the **outer fjord** (**4**-**7**) ⇒ **Signal of brines influence**

The signal is still visible in deep basins (**4**, **5**) and over the sill (**6**) in dead faunas ⇒ **Lower relative abundances of agglutinated possibly explained by taphonomic loss**

This signal is not visible in dead faunas at station **7** ⇒ **Wider seasonal changes in water masses (better preservation and/or more calcareous species)**

Taphonomic Loss Estimation

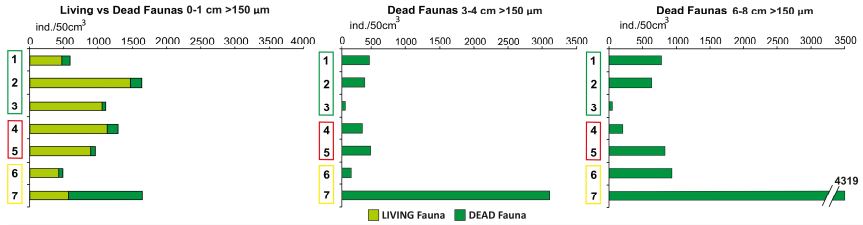

Inner fjord (**1**-**6**) ⇒ **Dominance living fauna**

Outer fjord (**7**) ⇒ **Dominance dead fauna**

Poor preservation of dead faunas in the stations inside the fjord (3-4 and 6-8 cm) ⇒ **More important taphonomic loss**

Calcareous Test Dissolution

The relationship between the higher agglutinated/calcareous ratio and the presence of brines seems associated with weak to strong dissolution stages observed on many living calcareous species.

Stage I: No sign of dissolution, transparent tests and smooth surfaces.
Stage II: Whitish tests with visible pores, and frequently, the last chamber is lost as well as the first calcite layers.
Stage III: Several chambers are dissolved and the remaining ones present opaque wall tests.
Stage IV: Nearly complete dissolution of the tests and only the organic material remains.

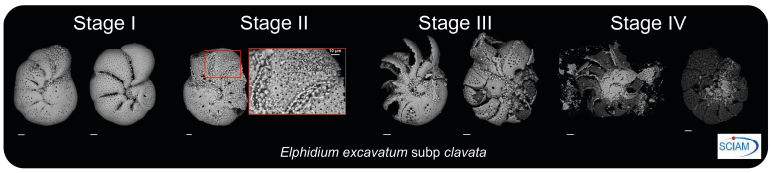

Conclusions

- Calcareous species are dominant in the shallow stations of the inner fjord as they are affected only by a seasonal brine flow, however they present different stages of test preservation including strong dissolution.
- The dominance of agglutinated foraminifera over the calcareous species in the stations influenced by brines (4-6) is consistent with Rasmussen & Thomsen (2015).
- Despite quite high taphonomic loss, **the agglutinated/calcareous ratio can trace Brine-enriched Shelf Water persistance in the deep basins and their seasonal outflow over the sill.**
- This signal seems to be diluted at station 7 because the assemblages could be influenced by more seasonal changes in water masses thanks to the presence of Atlantic Water, especially in summer.
- The degree of dissolution of calcareous species could be an additional proxy for brines.

References

Gonzales, M.V., Almeida, F.K.D., Costa, K.B., Santarosa, A.C.A., Camillo, E., Quadros, J.P. de, Toledo, F.A.L., 2017. Help Index: Hoeglundina Elegans Preservation Index For Marine Sediments in the Western South Atlantic. J. Foraminifer. Res. 47, 56–69. https://doi.org/10.2113/gsjfr.47.1.56
Rasmussen, T.L., Thomsen, E., 2015. Palaeoceanographic development in Storfjorden, Svalbard, during the deglaciation and Holocene: evidence from benthic foraminiferal records. Boreas 44, 24–44. https://doi.org/10.1111/bor.12098
Rasmussen, T.L., Thomsen, E., 2014. Brine formation in relation to climate changes and ice retreat during the last 15,000 years in Storfjorden, Svalbard, 76 – 78°N. Paleoceanography, 911–929. https://doi.org/10.1002/2014PA002643
Skogseth, R., Fer, I., Haugan, P.M., 2005. Dense-Water Production and Overflow from an Arctic Coastal Polynya in Storfjorden, in: Helgeange, Dokken, T., Furevik, T., Gerdes, R., Berger, W. (Eds.), The Nordic Seas: An Integrated Perspective. American Geophysical Union, pp. 73–88. https://doi.org/10.1029/158GM07

Acknowledgements

We thank Romain Maillet from the SCIAM (SFR4208, Univ Angers) platform for SEM images and Frédéric Vivier from LOCEAN (UMR 7159) for his major role in the success of the oceanographic campaigns. STEP project is realised thanks to INSU, IFREMER, OSUNA and University of Angers foundings.

Oral communication at *TMS Meeting 2019*

Fossile E., Nardelli M.P., Jouini A., Lansard B., Pusceddu A., Michel E., Peron O., Howa H. and Mojtahid M.: Benthic foraminifera as tracers of brine production in the Storfjorden "sea-ice factory". **Oral communication**, *TMS Meeting* 1-4 July 2019 (Fribourg, Switzerland).

Abstract

The Storfjorden (Svalbard archipelago) is an area of intense sea-ice formation characterised by the production of Brine-enriched Shelf Waters (BSW) as a result of a recurrent latent-heat polynya. The rapid response of living benthic foraminifera to environmental factors (e.g. water salinity, oxygenation, nutrient concentrations), and their high fossilisation potential, make them promising bio-indicators for intensity and recurrence of brine formation. Additionally, the high sedimentation rate occurring in the fjord (~3mm/yr) allows to trace recent changes in brine formation at high time resolution. Such approach requires to study the modern benthic foraminiferal ecology in different Arctic domains. To this aim, seven stations along a N-S transect across the Storfjorden have been sampled using an interface corer. In the top five centimetres of the sediment, living (Rose Bengal stained) foraminiferal assemblages were analysed together with geochemical and sedimentological parameters. Three major ecoregions were distinguished: i) an "inner-fjord" characterised by the dominance of calcareous species and fresh organic matter inputs; ii) a "deep-central-basin" dominated by agglutinated species potentially resulting from brine persistence that hampers the growth of calcareous species and/or causes their dissolution; iii) an "outer-fjord" characterised by typical North Atlantic species. Our results suggest the possible use of agglutinated/calcareous ratio (A/C) in the living foraminiferal faunas as a proxy for BSW intensity and persistence in the Storfjorden. Furthermore, thanks to the good sedimentary archives in the fjord, the A/C proxy will be tested on historical records in order to precisely follow the course of the quickly ongoing climate warming in the Arctic.

Oral communication at *Arctic Week 2019*

Fossile E., Nardelli M.P., Jouini A., Lansard B., Pusceddu A., Michel E., Peron O., Howa H. and Mojtahid M.: Benthic foraminifera as tracers of brine production in the Storfjorden "sea-ice factory". **Oral communication**, *Arctic Week 2019,* 9-13 December 2019 (Minister of Europe and Foreign Affairs, Paris, France).

Abstract

The Storfjorden (Svalbard) is a recurrent latent-heat polynya, with an intense sea-ice formation and associated production of Brine-enriched Shelf Waters (BSW). The ongoing climate warming in the Arctic is quickly impacting the cycles of production and melting of sea-ice and this could have heavy consequences on marine faunas and indirectly on Arctic society and economy. It is therefore crucial to understand how deep and rapid these changes are in comparison to long term (hundreds of years) natural cycles of sea-ice production. With this aim our research aims to find good indicators of past sea-ice cycles to trace the past activity of the Storfjorden polynya. The rapid response of living benthic foraminifera to environmental factors and their high fossilisation potential, make them promising bio-indicators for intensity and recurrence of brine formation. The calibration of the ecological response of these organisms to sea-ice production derived BSW we performed suggest that two different communities (calcareous- and agglutinated-dominated) can respectively represent the production of

first-year thin sea-ice and the cascading and persistence of BSW to the seafloor. Thanks to the good sedimentary archives in the fjord, these communities can be used to precisely reconstruct the course of the sea-ice cycles of the last 500 years.

Oral communication at *Journées Climat et Impacts 2020*

Fossile E., Mojtahid M., Baltzer A., Husum K., Schmidt S., Howa H. and Nardelli M.P.: Influence of modern environmental gradients on foraminiferal distribution in the Inner Kongsfjorden (Svalbard). **Oral communication**, *Journées Climat et Impacts 2020,* 23-25 November 2020 (online videoconference).

Abstract

Kongsfjorden, a 20 km-long fjord in the north-western Svalbard archipelago, is influenced by the Atlantic Water (AW) circulation as well as by tidewater glacier dynamics and the associated water masses at the fjord head. This generates a strong environmental gradient across the fjord, which continuously evolves in response to ongoing climate change. In recent years, the AW is more and more present inside the fjord both in terms of frequency and residence time, resulting in enhanced tidewater glacier calving and the consequent increase in meltwater and sediment discharges. These processes may cause persistent physical (and geochemical) stress for the benthic faunas inhabiting the fjord.

Our study focuses on the ecology of benthic foraminiferal faunas under present-day environmental conditions with the aim at obtaining useful proxies to reconstruct the hydrography of the fjord in the historical past (i.e., hundreds of years). We analysed living assemblages in the inner Kongsfjorden, and specifically their response to the gradient resulting from freshwater input, sediment and terrestrial organic matter supplies. Superficial sediments were sampled at 9 stations in summer 2018 along a SE-NW transect, starting close to the Kronebreen and Kongsvegen tidewater glacier fronts and ending about 10 km away from the fronts, at mid-length of the fjord.

Tidewater glacier melting and the subsequent run-off seem to influence the species distribution patterns. At the fjord head, close to the glacial fronts, foraminiferal abundance and diversity are low, probably because of high sediment supplies coming from the glacial system. The assemblages are dominated by non-fossilizing monothalamous agglutinated species and by *Cassidulina reniforme,* which is generally considered as a glacier proximal species. Away from the tidewater glacier fronts, foraminiferal abundance and diversity increase. At mid-transect, the assemblages are composed of species typical for Svalbard fjords, especially *Nonionellina labradorica*. At the end of the transect, 10 km away from the glacier fronts, assemblages are dominated by the agglutinated *Adercotryma glomeratum*. This species has previously been associated to transformed AW, in combination with reduced food quantity/quality. Its occurrence in the inner fjord demonstrates the influence of warm AW far inside Kongsfjorden.

The very high sedimentation rates in the inner fjord (~1-3 cm/yr) allow high resolution reconstructions of the recent history of its hydrology. Our results suggest that the physical stress related to the glacier fronts hampers the development of an equilibrated foraminiferal community, at least during summer. Therefore, when studying historical records from West Svalbard fjords, a low abundance or absence of foraminiferal faunas may be indicative of a proximity of tidewater glacier fronts, whereas the relative contribution of typical Arctic and Atlantic species could help reconstructing past changes in the pathways of Arctic and Atlantic water masses.

7. Vulgarisation scientifique

Présentation poster à la Nuit Européenne des chercheur.e.s 2019

Participation à la Nuit Européenne des chercheur.e.s pour expliquer mon sujet de recherche au grand public et présenter le poster suivante.

Fossile E. Le challenge du changement climatique en Arctique: comment les foraminifères peuvent-ils nous aider? *Nuit Européenne des chercheur.e.s*, 27 septembre 2019, Angers (France). Voir page suivante pour le poster.

Journées porte-ouvertes de l'UA 2020

Participation à la journée porte ouvertes de l'Université d'Angers le 25 janvier 2020 pour présenter le parcours géosciences et environnement.

Discussion autour du thème « La nature et le climat comme défis : on mène l'enquête et on agit ! »

Participation à une rencontre avec des élèves réunies en éco-parlement des jeunes à Montrevault sur Evre avec mon encadrante Pr. Hélène Howa le 13 Juillet 2020. La rencontre a été organisée par l'association « Les petits débrouillards Grand Ouest ». Nous avons discuté avec les élèves et répondu aux plusieurs questions autour du climat. Nous avons ensuite expliqué le travail de recherche à l'Université. Enfin nous avons montré une loupe binoculaire et des foraminifères.

Témoignage pour « French-Italian day for early career researchers »

J'ai partagé mon expérience en tant que doctorante pour le programme MOPGA (Make Our Planet Great Again) lors des journées Franco-Italiennes pour les jeunes chercheurs le 28 Octobre 2021 (webinaire).

Ma thèse en 180'

Présentation en français de ma thèse en en 180 seconds aux journées de l'école doctorale SML le 17 novembre 2021. Cette présentation a gagné le second prix du jury.

Le challenge du changement climatique en Arctique: comment les foraminifères peuvent-ils nous aider?

FOSSILE Eleonora

Encadrement: Howa Hélène, Nardelli Maria Pia, Mojtahid Meryem

LPG BIAF UMR CNRS 6112, Université d'Angers, UFR Sciences, 2 bd Lavoisier 49045, Angers Cedex 01, France

CHANGEMENT CLIMATIQUE

A partir des années 50… +0.6°C

mais pas de la même manière partout !

«Amplification de l'Arctique»

POURQUOI?

1. Réduction de l'albédo

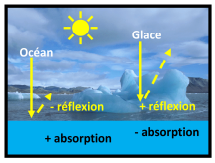

2. Transport de chaleur par les orages

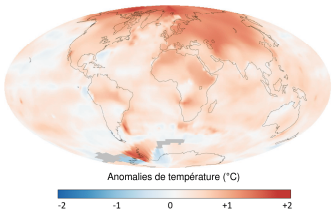

Anomalies de température moyenne de 2000 à 2009

C'est la comparaison du réchauffement (ou refroidissement) avec la température moyenne calculée entre 1951 et 1980.

Constat: Augmentation globale des températures d'environ 0.6°C.

L'Arctique est environ 2°C plus chaud.

NASA image by Robert Simmon, based on GISS surface temperature analysis data including ship and buoy data from the Hadley Centre. Caption by Adam Voiland. https://earthobservatory.nasa.gov/images/81514/arctic-amplification

QUESTION

Comment et avec quelle intensité les changements climatiques influencent les deux types de glace présents dans l'Arctique.

1. GLACE DE MER: gel de l'eau de mer de surface. Les eaux sous la banquise se chargent en sel, devenues lourdes elles s'enfoncent dans les fonds marins

2. GLACE CONTINENTALE: les glaciers, dont l'étendue varie avec les saisons, glissent jusqu'à la mer. En été, leur fonte provoque un écoulement d'eau douce et de d'alluvions glaciaires vers la mer.

FORAMINIFÈRES

…des petits organismes qui sont apparus sur Terre il y a plus de 500 millions d'années.

Ces organismes, même formés d'une seule cellule, ont l'extraordinaire capacité de construire une coquille:

- soit en carbonate de calcium;
- soit en utilisant minéraux et grains trouvés dans les sédiments marins.

Grâce à cette particularité, nous pouvons trouver leur coquille à de grandes profondeurs dans les vases marines: FORAMINIFÈRES FOSSILES

Une communauté est composée de plusieurs espèces avec des abondances variables.

En effet, chaque espèce "préfère" vivre dans un environnement qui lui convient le mieux.

Différentes communautés reflètent différents environnements

ÉCHANTILLONNAGE

Lorsque nous allons échantillonner les fonds marins pour étudier les communautés de foraminifères vivantes, nous sommes aussi capables de mesurer les nombreux paramètres de leur milieu de vie.

... Mais, à ce jour, nous sommes incapables de mesurer les paramètres en temps réel dans le passé

Comment les foraminifères peuvent nous aider à reconstruire le passé?

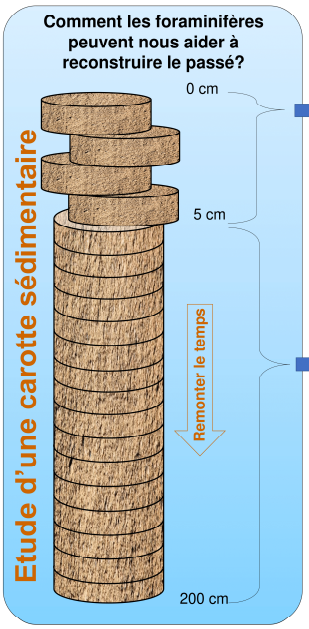

1° ÉTAPE

Dans la partie superficielle des sédiments, nous étudions les communautés de foraminifères actuelles

Nous savons dans quelles conditions environnementales ils vivent maintenant

Nous essayons de comprendre leur écologie

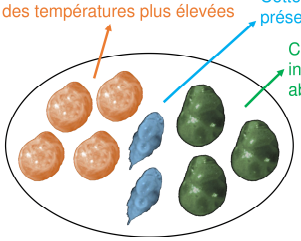

...observation microscopique de nos échantillons pour identifier les espèces présentes

2° ÉTAPE

Nous examinons les sédiments en profondeur et identifions les espèces de foraminifères fossiles à chaque niveau

Plus on s'enfonce dans les sédiments, plus on remonte dans le temps

Sur la base des communautés de foraminifères fossiles nous pouvons comprendre quelles conditions environnementales étaient présentes quand ils vivaient

Nous essayons de comprendre:

1. La formation de glace de mer a-t-elle changé ?
2. L'extension de la glace continentale est-elle plus réduite ?

Nous étudions le présent pour comprendre le passé et, j'espère, avoir des idées sur l'avenir

DOCTORAT SCIENCES BRETAGNE DE LA MER LOIRE ET DU LITTORAL

université angers

Titre : Changements environnementaux liés à la dynamique de la glace dans les fjords de l'Arctique : nouvelles connaissances apportées par les foraminifères benthiques

Mots clés : glace de mer, polynie, glacier côtier, bioindicateurs, proxy, Svalbard

Résumé: Le changement climatique menace les régions polaires avec des conséquences majeures sur la dynamique des glaces et les écosystèmes associés. Les simulations de fonte glaciaire reposent sur des reconstitutions paléo-environnementales, qui complètent les mesures directes sur la période actuelle pour réduire l'incertitude des prévisions. Des proxies basés sur l'écologie des foraminifères benthiques (FB) sont développés dans cette thèse pour suivre la dynamique des glaces de mer et le retrait des glaciers côtiers. Dans le Storfjorden, les FB montrent une réponse aux eaux enrichies en CO_2 (saumures) libérées pendant les processus de formation de glace de mer. Le rapport entre les FB agglutinés et calcaires (A/C) est proposé comme proxy de la persistance sur les fonds de ces saumures qui provoquent la dissolution des tests calcaires des FB. Bien que le signal A/C soit affecté par des processus taphonomiques, il permet de souligner les différences entre les zones affectées par la persistance de saumures et celles sous influence intermittente. Dans le Kongsfjorden, des gradients environnementaux abrupts (e.g., salinité, turbidité de l'eau, flux organiques) sont provoqués par la dynamique des glaciers côtiers. En été, différents assemblages de FB s'installent en fonction de l'éloignement au front du glacier, avec une augmentation vers le large de la diversité taxonomique et fonctionnelle. Un indicateur combinant plusieurs mesures de diversité a été proposé comme proxy du recul des glaciers côtiers, et son efficacité a été testée sur une archive sédimentaire des 60 dernières années. Les deux proxies proposés ici sont donc applicables dans tout environnement arctique similaire.

Title: Ice-related environmental changes in Arctic fjords: new insights from benthic foraminifera

Keywords: sea ice, polynya, tidewater glacier, bioindicators, proxy, Svalbard

Abstract: Climate change threatens polar regions with major consequences on ice-related dynamics and linked ecosystems. Predictions of future sea ice cover and glacier retreat rely on paleoenvironmental reconstructions (through proxies' application) to extend the instrumental period and thus reduce models' uncertainty. This PhD thesis aimed to develop and test ecological proxies for sea ice formation and glacier melting using benthic foraminifera. In the Storfjorden "sea ice factory", foraminiferal responses to brine presence (i.e., CO_2-enriched waters released during sea ice formation processes) were investigated. The ratio between Agglutinated and Calcareous (A/C) foraminifera was proposed as potential proxy for brine persistence, because of the brine-induced dissolution on calcareous foraminiferal shells. Although the A/C signal was affected by taphonomic processes, the differences between areas of brine persistence and those with intermittent influence was preserved, thus supporting the proxy. Likewise, foraminiferal responses to steep environmental gradients (e.g., water salinity and turbidity, organic fluxes) created by tidewater glacier dynamics in summer, were investigated in Kongsfjorden. The glacier induced disturbance resulted in the establishment of different foraminiferal assemblages and increased taxonomic and functional diversity with increased distance from the glacier front. A combination of diversity metrics was proposed as potential proxy for glacier retreat and its effectiveness was tested on a sedimentary archive covering the last 60 years. The two proxies proposed here are therefore applicable in any similar Arctic environments.